

JPL NO. 9950-519

**BOEING
ENGINEERING &
CONSTRUCTION**
*THE BOEING ENERGY
AND ENVIRONMENT DIVISION*

Report No. DOE/JPL 954833-81/3
Distribution Category UC-63b

(NASA-CR-164454) WIND LOADS ON FLAT PLATE N81-25431
PHOTOVOLTAIC ARRAY FIELDS Final Report
(Boeing Engineering and Construction) 384 p
HC A17/MF A01 CACL 20K Unclas
G3/39 26604

WIND LOADS ON FLAT PLATE PHOTOVOLTAIC ARRAY FIELDS

JPL CONTRACT NO. 954833

LOW COST SOLAR ARRAY PROJECT
ENGINEERING AREA

Phase III Final Report

April 1981

Ronald D. Miller
Donald K. Zimmerman



The JPL Low Cost Solar Array Project is sponsored by the U.S. Department of Energy and forms part of the Solar Photovoltaic Conversion Program to initiate a major effort toward the development of low-cost solar arrays. This work was performed for the Jet Propulsion Laboratory, California Institute of Technology by agreement between NASA and DOE.

Prepared for
Jet Propulsion Laboratory
4800 Oak Grove Drive
Pasadena, California 91103

By the
Boeing Engineering and Construction Company
(A Division of The Boeing Company)
Seattle, Washington 98124

**WIND LOADS ON
FLAT PLATE PHOTOVOLTAIC ARRAY FIELDS**

JPL Contract No. 954833

**Low Cost Solar Array Project
Engineering Area**

Phase III Final Report

April, 1981

**Ronald D. Miller
Donald K. Zimmerman**

"The JPL Low Cost Solar Array Project is sponsored by the U.S. Department of Energy and forms part of the Solar Photovoltaic Conversion Program to initiate a major effort toward the development of low-cost solar arrays. This work was performed for the Jet Propulsion Laboratory, California Institute of Technology by agreement between NASA and DOE."

Prepared for

**Jet Propulsion Laboratory
4800 Oak Grove Drive
Pasadena, California 91103**

By the

**Boeing Engineering and Construction Company
(A Division of The Boeing Company)
Seattle, Washington**

"This report was prepared as an account of work sponsored by the United States Government. Neither the United States nor the United States Department of Energy, nor any of their employees, nor any of their contractors, subcontractors, or their employees makes any warranty, express or implied, or assumes any legal liability or responsibility for the accuracy, completeness or usefulness of any information, apparatus, product or process disclosed, or represents that its use would not infringe privately owned rights."

Acknowledgements

Management and engineering on this project was provided by the Solar Systems organization of the Boeing Engineering and Construction Company (a Division of The Boeing Company). Dr. Ronald Ross and Mr. Robert Weaver, Manager and technical monitor, respectively, in the Engineering area of the Low Cost Solar Array Project, Jet Propulsion Laboratory, California Institute of Technology, contributed many helpful suggestions during the program, particularly in the preparation of the wind tunnel test plan. The wind tunnel test was performed by the Fluid Dynamics Laboratory staff of Colorado State University, Fort Collins, Colorado. The responsible Manager for the testing was Dr. Jack E. Cermak, the Project Director was Dr. Jon A. Peterka, and Principal Investigators were N. Hosoya and Dr. Mike Poreh.

Table of Contents

1.0	SUMMARY	1
2.0	INTRODUCTION	5
2.1	Study Objectives	5
2.2	Discussion and Background	6
2.3	Study Requirements	7
2.4	Report Organization	8
3.0	BASIC AERODYNAMIC EQUATIONS AND DEFINITIONS	13
3.1	Analysis Definitions and Nomenclature	13
3.2	Solar Energy-Aerodynamic Synonyms	16
3.3	Aerodynamic Sign Convention and Basic Equations	17
4.0	WIND TUNNEL TEST PROGRAM AND RESULTS	19
4.1	Uniform Wind Velocity Profile	20
4.2	1/7 Power Law Wind Velocity Profile	22
4.2.1	Array Mid-Span Wind Loads Without a Protective Wind Barrier (Fence)	22
4.2.2	Array Mid-Span Wind Loads With a Protective Wind Barrier (Fence)	23
4.2.3	Array Edge Wind Loads for Straight-On Winds	24
4.2.4	Array Edge Wind Loads for Oblique Winds	25
4.3	Comparison of Wind Tunnel Test Results for Uniform Wind Profile and 1/7 Power Law Wind Profile	28
4.4	Test Results Summary	29
5.0	THEORETICAL - EXPERIMENTAL RESULTS COMPARISON	73
6.0	DISCUSSION AND CONCLUSIONS	83
7.0	STEADY STATE WIND LOADS DESIGN GUIDELINES	87
7.1	Wind Loads on Arrays Behind a Protective Wind Barrier	87
7.2	Wind Loads on Arrays Without a Protective Wind Barrier	91
7.3	Array Edge Wind Loads	92
8.0	NEW TECHNOLOGY	101
9.0	REFERENCES	103
	APPENDIX A	1A
	APPENDIX B	1B
	APPENDIX C	1C

PRECEDING PAGE BLANK NOT FILMED

Figures

No.		Page
1-1	Steady State Wind Normal Force and Normalized Pressure Coefficient Envelope for Arrays Behind a Protective Wind Barrier	3
2-1	Array Variables Used to Study Aerodynamic Loads	10
2-2	Photovoltaic Array Field	11
2-3	Definition of an Array	11
4-1a	Array Chordwise Pressure Coefficient Distribution in Uniform Wind Velocity Profile (Tilt Angle = 20°, Wind from Front).	30
4-1b	Array Chordwise Pressure Coefficient Distribution in Uniform Wind Velocity Profile (Tilt Angle = 20° Wind from Rear)	31
4-1c	Array Chordwise Pressure Coefficient Distribution in Uniform Wind Velocity Profile (Tilt Angle = 35°, Wind from Front)	32
4-1d	Array Chordwise Pressure Coefficient Distribution in Uniform Wind Velocity Profile (Tilt Angle = 35°, Wind from Rear)	33
4-1e	Array Chordwise Pressure Coefficient Distribution in Uniform Wind Velocity Profile (Tilt Angle = 60°, Wind from Front)	34
4-1f	Array Chordwise Pressure Coefficient Distribution in Uniform Wind Velocity Profile (Tilt Angle = 60°, Wind from Rear)	35
4-1g	Array Chordwise Pressure Coefficient Distribution in Uniform Wind Velocity Profile (Tilt Angle = 90°)	36
4-2	1/7 Power Law Wind Velocity Profile	37

PRECEDING PAGE BLANK NOT FILMED

	Page
4-3a	38
Array Chordwise Pressure Coefficient Distribution in Boundary Layer Wind (Tilt Angle = 20°, Wind from Front)	
4-3b	39
Array Chordwise Pressure Coefficient Distribution in Boundary Layer Wind (Tilt Angle = 20°, Wind from Rear)	
4-3c	40
Array Chordwise Pressure Coefficient Distribution in Boundary Layer Wind (Tilt Angle = 35°, Wind from Front)	
4-3d	41
Array Chordwise Pressure Coefficient Distribution in Boundary Layer Wind (Tilt Angle = 35°, Wind from Rear)	
4-3e	42
Array Chordwise Pressure Coefficient Distribution in Boundary Layer Wind (Tilt Angle = 60°, Wind from Front)	
4-3f	43
Array Chordwise Pressure Coefficient Distribution in Boundary Layer Wind (Tilt Angle = 60°, Wind from Rear)	
4-3g	44
Array Chordwise Pressure Coefficient Distribution in Boundary Layer Wind (Tilt Angle = 90°)	
4-4	45
Effect of Head-On and Rearward Winds on Array Normal Force Coefficients (No Fence)	
4-5	46
Effect of a Fence on Array Chordwise Pressure Coefficient Distribution for Head-On and Rearward Winds	
4-6	47
Effect of a Fence on Array Normal Force Coefficients for Head-On and Rearward Winds	
4-7	48
Array Chordwise Pressure Coefficient Distribution Located .15 Chord Lengths from Side Edge for Head-On and Rearward Winds (No Fence)	
4-8	49
Effect of Fence on Array Chordwise Pressure Coefficient Distribution Located .15 Chord Lengths from Side Edge for Head-On and Rearward Winds	
4-9	50
Comparison Between Array Edge and Center of Span Normal Force Coefficients for Head-On and Rearward Winds (No Fence)	

	Page	
4-10	Effect of Fence on Array Edge Normal Force Coefficients for Head-On and Rearward Winds	50
4-11a	Effect of Oblique Winds on Array Edge Pressure Distribution (No Fence, Wind from Front)	51
4-11b	Effect of Oblique Winds on Array Edge Pressure Distribution (No Fence, Wind from Rear)	53
4-11c	Effect of Oblique Winds on Array Edge Pressure Distribution (Conventional Fence, Wind from Front)	54
4-11d	Effect of Oblique Winds on Array Edge Pressure Distribution (Conventional Fence, Wind from Rear)	55
4-11e	Effect of Oblique Winds on Array Edge Pressure Distribution (Conventional Fence, Endplated Arrays, Wind from Front)	56
4-11f	Effect of Oblique Winds on Array Edge Pressure Distribution (Conventional Fence, Endplated Arrays, Wind from Rear)	57
4-11g	Effect of Oblique Winds on Array Edge Pressure Distribution (Modified Fence Corner, Wind from Front)	58
4-11h	Effect of Oblique Winds on Array Edge Pressure Distribution (Modified Fence Corner, Wind from Rear)	59
4-12	Effect of Oblique Winds on Array Normal Force Coefficients at Array Edge	60
4-13	Maximum Pressure Coefficient at Array Side Edge Due to Oblique Winds	61
4-14a	Array Pressure Coefficient Comparison Between Uniform and Boundary Layer Wind Profiles (Tilt Angle = 20°, Wind from Front)	62
4-14b	Array Pressure Coefficient Comparison Between Uniform and Boundary Layer Wind Profiles (Tilt Angle = 20°, Wind from Rear)	63
4-14c	Array Pressure Coefficient Comparison Between Uniform and Boundary Layer Wind Profiles (Tilt Angle = 35°, Wind from Front)	64
4-14d	Array Pressure Coefficient Comparison Between Uniform and Boundary Layer Wind Profiles (Tilt Angle = 35°, Wind from Rear)	65
4-14e	Array Pressure Coefficient Comparison Between Uniform and Boundary Layer Wind Profiles (Tilt Angle = 60°, Wind from Front)	66

		<u>Page</u>
4-14f	Array Pressure Coefficient Comparison Between Uniform and Boundary Layer Wind Profiles (Tilt Angle = 60°, Wind from Rear)	67
4-14g	Array Pressure Coefficient Comparison Between Uniform and Boundary Layer Wind Profiles (Tilt Angle = 90°)	68
4-15	Array Normal Force Coefficient Comparison Between Uniform and Boundary Layer Wind Profiles	69
4-16	Configurations for Edge Load Reduction Study	71
5-1	Array Pressure Coefficient Distribution Comparison Between Wind Tunnel Test and Theoretical Methods in Free Air	76
5-2a	Array Pressure Coefficient Distribution Comparison Between Wind Tunnel Test and Theoretical Methods in Close Ground Proximity (Tilt Angle = 20°)	77
5-2b	Array Pressure Coefficient Distribution Comparison Between Wind Tunnel Test and Theoretical Methods in Close Ground Proximity (Tilt Angle = 35°)	78
5-2c	Array Pressure Coefficient Distribution Comparison Between Wind Tunnel Test and Theoretical Methods in Close Ground Proximity (Tilt Angle = 60°)	79
5-3	Effect of Ground Clearance on Front and Back Array Pressures in Uniform Flow (Tilt Angle = 60°, Wind from Back)	80
5-4	Array Normal Force Coefficient Comparison Between Wind Tunnel Test and Theoretical Methods	81
5-5	Theoretical Key Wind Loads Parameters and Their Sensitivity in Separated Flow analyses (Reference 5)	82
7-1a	Steady State Wind Normal Force Coefficient Envelope for Arrays Within an Array Field or Behind a Protective Wind Barrier	94
7-1b	Steady State Wind Normalized Pressure Coefficient Envelope for Arrays Within an Array Field or Behind a Protective Wind Barrier	95
7-2a	Steady State Wind Normal Force Coefficient Envelope for the Two Outer Boundary Array Rows in an Array Field Unprotected from the Wind	96
7-2b	Steady State Wind Normalized Pressure Coefficient Envelope for the Two Outer Boundary Array Rows in an Array Field Unprotected from the Wind	97

7-3a	Steady State Wind Pressure Coefficient and Normal Force Coefficient Guidelines for Edge Arrays in an Array Field (No Fence)	98
7-3b.	Steady State Wind Pressure Coefficient and Normal Force Coefficient Guidelines for Edge Arrays in an Array Field (Fence)	99
7-3c	Steady State Wind Pressure Coefficient and Normal Force Coefficient Guidelines for Edge Arrays in an Array Field (Fence with Modified Corners)	100

Tables

No.		Page
4-1	Array Test Conditions	22
5-1	Example of Average Normal Wind Forces on Arrays Behind Protective Fences by Theoretical and Wind Tunnel Test Methods	75

1.0 SUMMARY

This report presents the results of an experimental analysis (boundary layer wind tunnel test) of the aerodynamic forces resulting from winds acting on flat plate photovoltaic arrays. Local pressure coefficient distributions and normal force coefficients on the arrays are shown and compared to theoretical results. Parameters that were varied when determining the aerodynamic forces included tilt angle, array separation, ground clearance, protective wind barriers, and the effect of the wind velocity profile. Recommended design wind forces and pressures are presented, which envelop the test results for winds perpendicular to the array's longitudinal axis. This wind direction produces the maximum wind loads on the arrays except at the array edge where oblique winds produce larger edge pressure loads.

The arrays located at the outer boundary of an array field have a protective influence on the interior arrays of the field. A significant decrease of the array wind loads were recorded in the wind tunnel test on array panels located behind a fence and/or interior to the array field compared to the arrays on the boundary and unprotected from the wind. The magnitude of this decrease was the same whether caused by a fence or upwind arrays. Figure 1-1 shows typical envelopes of the wind loads on arrays that are presented in this report. This figure is for arrays interior to an array field or on the boundary of a field when a fence exists to protect the front arrays. Since these loads envelop the measured wind tunnel results, they can be used as guideline design steady-state wind loads on photovoltaic arrays with wind protection. Similar guideline wind loads are given in the report for arrays unprotected from the wind.

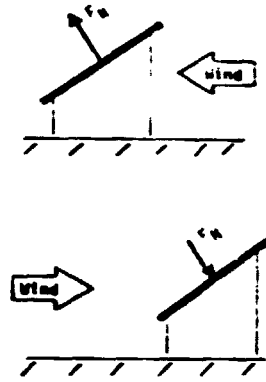
The wind loads on the arrays within two slant heights from the side edges are considerably different from the remainder of the array field. Vortices are produced by the array corners and at the fence corner if a fence exists. These vortices cause local high pressure loads on or near the array edges. Several methods to reduce the strength of the vortices and resulting pressures were tried with limited success. Endplating the arrays (completely enclosing the ends of the arrays with a 50% porosity plate to simulate shrubs or gates at the array ends) was the most successful in reducing the wind loads on the array side edges, decreasing these loads by approximately 50%. Modifying the fence corner was also successful but to a lesser extent than endplating the arrays.

However, the edge pressures are, at best, several times larger than the pressure several slant heights away from the side edge.

Theoretically calculated steady state wind loads were larger in magnitude than wind tunnel determined wind loads. Wind tunnel determined wind loads using a uniform wind profile and a 1/7 boundary layer wind profile were similar in shape and magnitude. The magnitude of the wind loads for the uniform wind profile, although similar to the boundary layer profile, were not consistently larger or smaller than the boundary layer profile results and thus could not be used reliably for design purposes in preference to the boundary layer results.



• C_N based on wind reference velocity at 10 meters



exception: not valid within two siant heights from the side edges

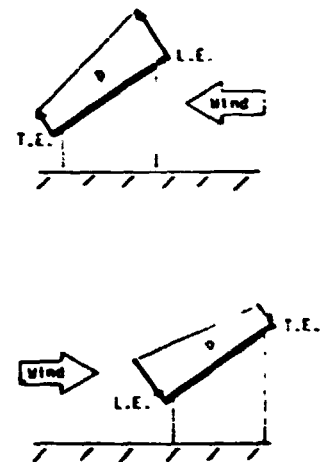
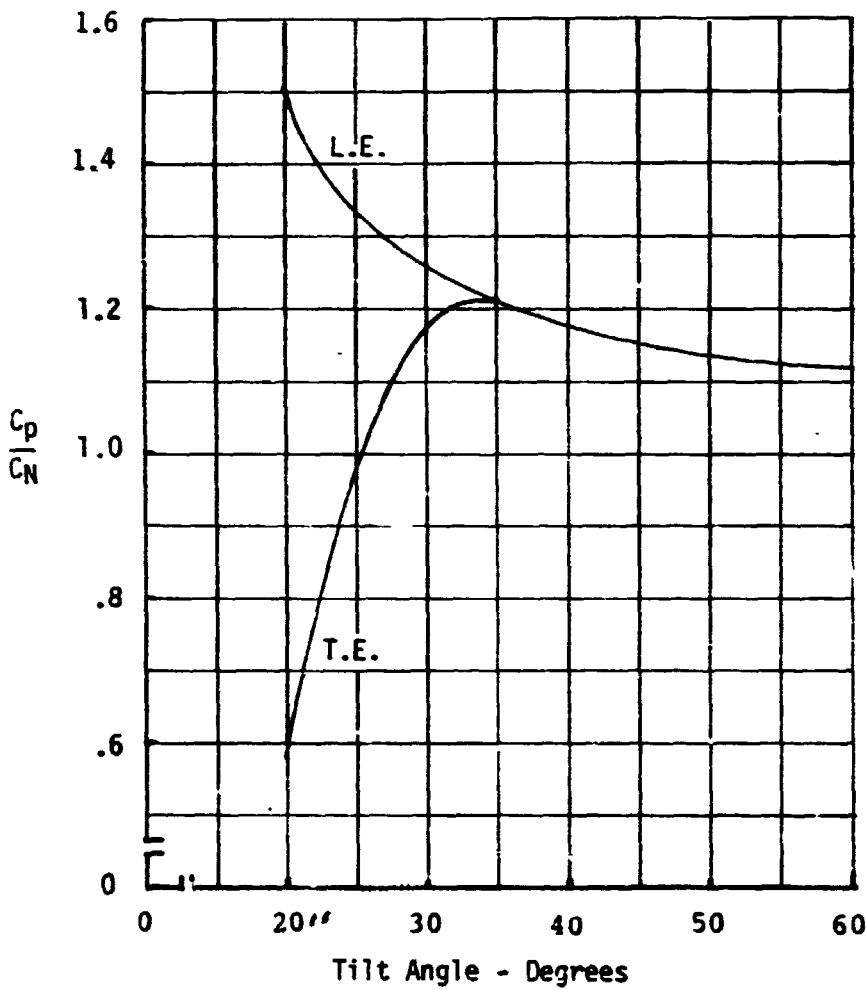


Figure 1-1. Steady State Wind Normal Force and Normalized Pressure Coefficient Envelope for Arrays Behind a Protective Wind Barrier

2.0 INTRODUCTION

This report summarizes an experimental analysis (wind tunnel test) of the aerodynamic loading on long, flat plate photovoltaic arrays resulting from exposure to the wind environments, evaluates and compares test results to theoretical results, and presents guidelines for aerodynamic loads to be used in the design of specific photovoltaic arrays. This report is an extension to the theoretical analysis reported in DOE/JPL 954833-79/2. The study was performed under contract number 954833 to the Jet Propulsion Laboratory as part of the Engineering Area Task of the Low-Cost Solar Array (LSA) Project. This project is being managed by JPL for the Department of Energy, Division of Solar Technology.

2.1 Study Objectives

The Department of Energy (DOE) photovoltaic program¹ has the overall objective to ensure that photovoltaic conversion systems will contribute significantly (50 Gwe) to the nation's energy supply by the year 2000. The cost associated with the design and construction of solar photovoltaic arrays to produce electric energy from sunlight is an important factor in the acceptance and use of solar energy. DOE has established specific price goals to produce energy at 55-92 mills/KW-h by 1986 (expressed in constant 1980 dollars) which are deemed necessary to achieve the desired industry growth and market penetration. Therefore, it is necessary in the trade-off phase of system design to ensure that the design requirements are realistic. The objective of this study was to establish wind load guidelines for flat plate photovoltaic arrays with various configurations in relation to chord lengths, array spacings, height of arrays from the ground, wind direction, array angles of attack, and with and without protective fences used to reduce the wind loading (see Figure 2-1). The guidelines were to be established by theoretical aerodynamic methods and experimental techniques. Wind tunnel testing was to be used to verify the theoretical results reported in reference 5 and to determine steady state wind loads on arrays for conditions that cannot presently be obtained by theoretical methods. These loads are required to ensure realistic design requirements.

PRECEDING PAGE BLANK NOT FILMED

2.2 Discussion and Background

The load due to wind on an array and on its support structure strongly influences the design and ultimately the cost of the photovoltaic panels, panel and array support structure and foundations of the arrays. A previous design study of flat plate array support structure showed that the arrays (structural framework and foundation) costs were of the same order of magnitude as the photovoltaic module costs. Furthermore, the array costs were strongly dependent on the assumed wind loading for loading in the range of 35 to 75 psf. Another study, using transparent inflated enclosures to protect the modules³, predicted wind loadings on the enclosures near the low end of the range compared to those used in reference 2, and showed significant cost savings compared to conventional arrays with similar wind loading criteria. It is, therefore, essential to determine the true maximum wind load that the array will experience during its lifetime in order to minimize the structure cost.

Three factors affect the amount of wind loading on a body: the flow field in which the body is placed, the aerodynamic characteristics of the body itself, and the dynamic response of the body due to the wind loading. Although the structural loads resulting from this latter factor are not totally composed of aerodynamic forces (they also include inertia forces), these structural loads do result from the wind loading, or more precisely, the fluctuations in wind loading.

A flow field of the type that would be found around arrays in an array field situated in an open terrain, as depicted in Figure 2-2, has three aspects: 1) the steady state flow before it encounters any obstacles, 2) atmospheric gusts, and 3) turbulence. The steady state flow consists of a shear layer adjacent to the ground whose shearing effects decrease with elevation above the ground until a uniform flow is attained. The shear layer for most open flatlands can be modeled as a 1/7 power law⁴. Gusting is the result of velocity variations and changes in the direction of the prevailing wind due to atmospheric instabilities. Turbulence may be caused by several factors. Gusting can cause turbulence when adjacent volumes of air are moving at different velocities, thus producing a shearing effect. The roughness of the land causes turbulence because of shearing effects. An obstacle in the path of the flow can also create turbulence by upsetting the flow and thus causing eddies and vortices to

form. In addition, the shape of the body will affect the characteristics of the turbulence. Turbulent flow is highly complex, with varying frequencies and intensities occurring in a random manner.

The body in the case of a photovoltaic array consists of modules assembled on a framework that is mounted on a support structure (Fig. 2-3). The aerodynamic characteristics of an array are the same as those of a flat plate when only steady state flow is considered. When gusting and turbulence are introduced, these characteristics are not as well defined; however, the aerodynamics for a flat plate are a good approximation in lieu of a more detailed structural design. The effect on the array forces due to the flow field are a function of the type of impingement and the resulting pressure distribution over the array. When the flow is turbulent, the pressure distribution and, consequently, the forces exerted on the array are nonuniform in frequency and intensity. These forces may cause vibrations in the structure resulting in additional structural dynamic forces on the array. Since turbulence varies in frequency and intensity, the resulting loading will also vary as a function of the frequency and intensity.

2.3 Study Requirements

The requirements of this study involve analysis and test within five specific areas. They are:

1. Wind tunnel test plan.
2. Wind tunnel test.
3. Test and theoretical results analysis and comparison.
4. Modification of theoretical results to reflect empirical results.
5. Establishment of design guidelines for estimating wind loads on photovoltaic arrays.

The following is a summary of the statement of work for Phase III.

- o Verify the analytic results obtained in Phase II and expand the effort to establish wind load and pressure distributions that can be used

as module and support structure design guidelines by performing the following four tasks.

1) Task 1 - Pre-Test Planning

Review the data requirements from the Phase II work for meeting Phase III objectives and optimize the wind tunnel test conditions and configurations that will meet the data requirements.

2) Task 2 - Wind Tunnel Testing

Based on the requirements determined in Task 1, perform the required wind tunnel tests. Review the preliminary data during the test program and modify the test plan as required to ensure that the data requirements are met.

3) Task 3 - Data Analysis

- a) Compare the wind tunnel results with the results of Phase II and determine the validity of the analytically identified key load parameters.
- b) Modify the results of Phase II to reflect the empirical results.

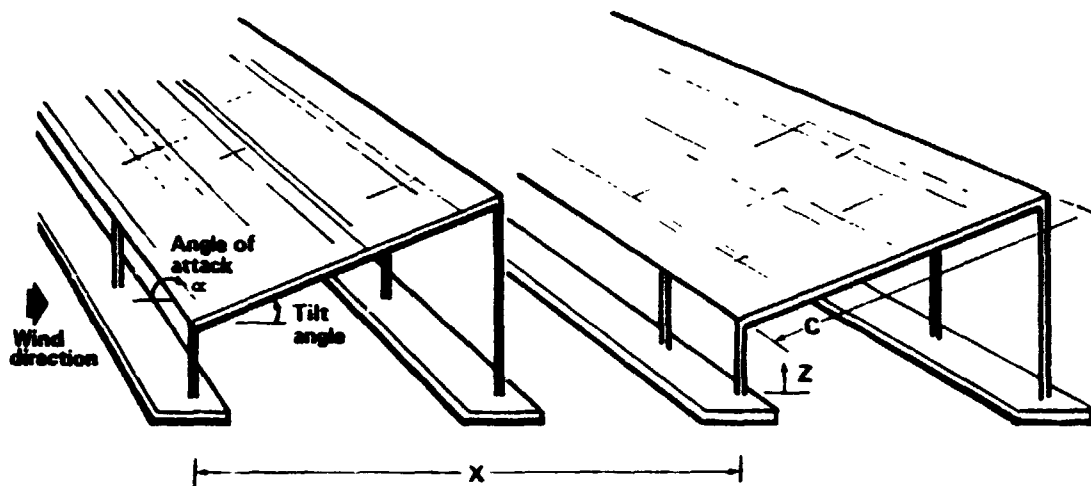
4) Task 4 - Design Guidelines

- a) Establish design guidelines for estimating the wind loads on the support structure as a function of the wind velocity and array field configuration.
- b) Establish design guidelines for estimating the pressure distribution on flat plate modules for varying wind velocities and array field configurations.

2.4 Report Organization

The remainder of this report presents the results of the wind tunnel test and its comparison to the theoretical results presented in reference 5 and the proposed design wind loads and conclusions. Section 3.0 presents basic

aerodynamic equations, definitions, and nomenclature for use in understanding the results. Section 4.0 presents the wind tunnel program and results. A comparison of theoretical results to experimental results is presented in Section 5.0. A discussion of the results of Sections 4.0 and 5.0 is included in Section 6.0 together with conclusions obtained from the results. Section 7.0 presents array wind load envelopes that may be used for design guidelines. New technology and References are outlined in Sections 8.0 and 9.0, respectively. The wind tunnel test report which includes test description and data from the tests conducted at Colorado State University in their Meteorological Wind Tunnel Facility is presented in the Appendix.



Ground clearance (Z)
 Array spacing (X)
 Tilt angle
 Wind direction

Figure 2-1. Array Variables Used to Study Aerodynamic Loads

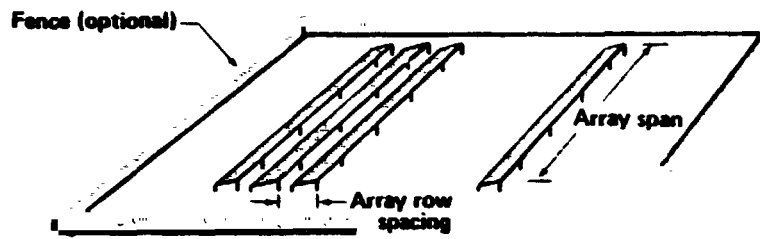


Figure 2-2. Photovoltaic Array Field

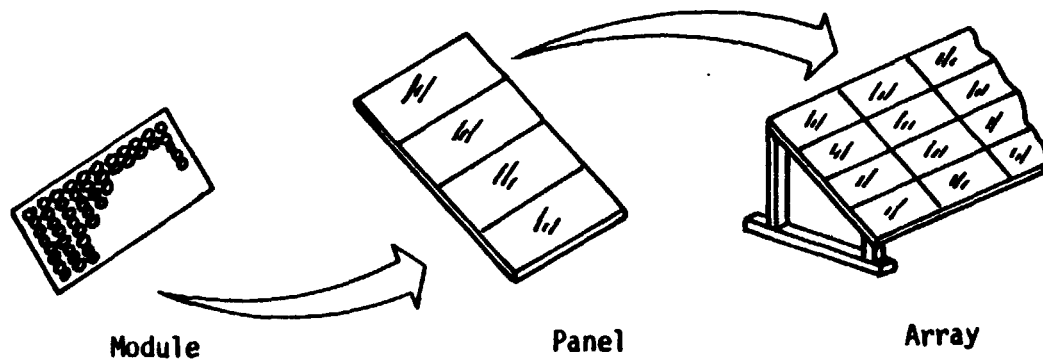


Figure 2-3. Definition of an Array

3.0 BASIC AERODYNAMIC EQUATIONS AND DEFINITIONS

The analyses used in this report required the use of aerodynamic results that were calculated in aerodynamic terms. Since these terms may be unfamiliar to designers of photovoltaic arrays, this section explains the basic aerodynamic terms and nomenclature and defines basic aerodynamic equations to assist those without an aerodynamic background to understand the results. In addition, synonyms between aerodynamic and solar energy terms are given where applicable.

3.1 Analysis Definitions and Nomenclature

Aerodynamic coefficients:	non-dimensional coefficients.
pressure coefficient (C_p):	relates lifting surface pressure to reference freestream dynamic pressure, $C_p = p/q$.
$C_{p\alpha}$	slope of the pressure coefficient curve; relates pressure coefficient to angle of attack, $C_p = C_{p\alpha}\alpha$.
ΔC_p	net pressure coefficient on lifting surface = windward face pressure coefficient minus base pressure coefficient.
normal force (F_n, F_N):	force normal to the lifting surface (positive out of base pressure face).
normal force coefficient (C_n, C_N):	relates lifting surface normal force to reference freestream dynamic pressure and reference area, $C_N = F_N/qA$.
$C_{N\alpha}$	slope of the normal force coefficient curve, relates normal force coefficient to angle of attack, $C_N = C_{N\alpha}\alpha$.

lift (L)	force on the lifting surface perpendicular to the freestream velocity (positive up).
lift coefficient (C_L)	relates lift to reference freestream dynamic pressure and reference area, $C_L = L/qA$.
drag (D)	force on the lifting surface parallel to the freestream velocity (positive in the wind direction).
drag coefficient (C_D)	relates drag to reference freestream dynamic pressure and reference area, $C_D = D/qA$.
center of pressure (X)	location of total force on lifting surface measured from the leading edge.
Angle of attack:	angle measured from the wind vector to the plane of the lifting surface.
Array:	a mechanically integrated assembly of panels together with support structure (including foundations).
Array field:	the aggregate of all arrays.
Array spacing:	horizontal distance measured from one array to the identical location on the next array.
Aspect ratio (AR):	aerodynamic geometric parameter (span/chord for a rectangular array).
Base pressure face:	downwind side of lifting surface.

Bluff body:	a nonstreamline body that causes airflow about itself to become separated and turbulent.
Chord (C):	distance of array between leading and trailing edges and perpendicular to the edges, i.e.: slant height of array.
Dynamic pressure (q):	pressure due to freestream velocity at a reference height ($q = .5\rho V^2$).
Ground clearance (Z):	distance between the ground and the lowest point on the panels forming the array.
Inviscid:	frictionless flow.
Leading edge (L.E.):	windward edge of the array.
Module:	the smallest complete environmentally protected assembly of solar cells.
Normal wash, downwash:	flow of air perpendicular to the lifting surface plane.
Panel:	a collection of one or more modules fastened together forming a field installable unit.
Plate:	thin rectangular shaped structure that acts as a lifting surface.
Pressure (p):	force per unit area.
Span (b):	distance of an array between the two side edges i.e.: length of array.

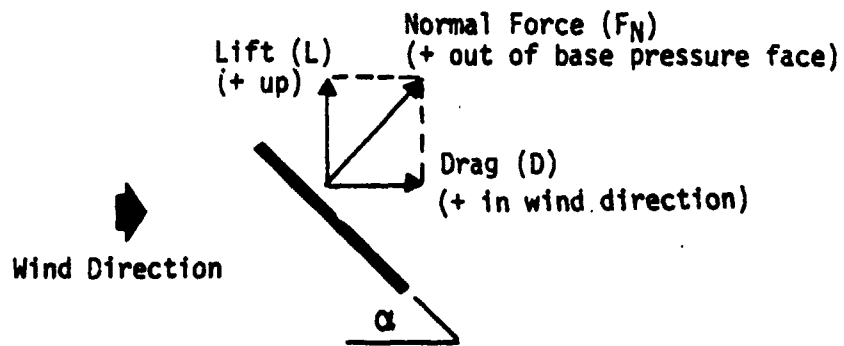
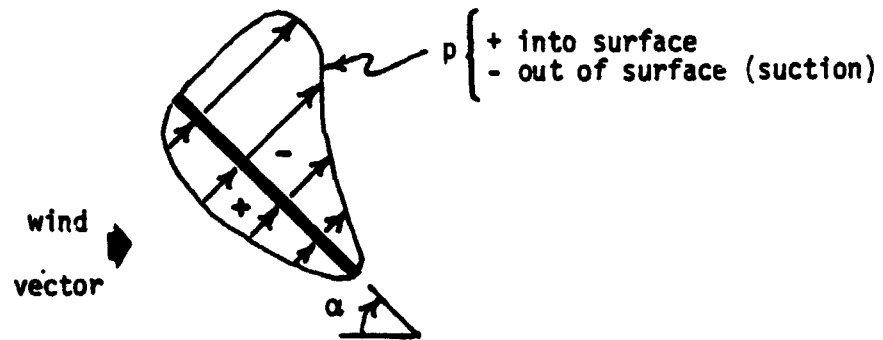
Tilt Angle:	angle measured from the horizontal to the plane of the array panels.
Trailing Edge (TE):	downwind edge of the array
Viscous:	flow that has friction.
Windward face:	windward side of lifting surface.
Yaw angle:	angle measured from wind direction to the normal of the array leading edge.
A:	reference area of array or portion of the array
l :	length
V:	velocity.
ρ :	air density.
μ :	coefficient of viscosity.
S :	area of lifting surface.
S:	distance measured along the chord from a reference point.

3.2 Solar Energy - Aerodynamic Synonyms

<u>Solar Energy</u>	<u>Aerodynamics</u>	<u>Comments</u>
Tilt angle and wind direction	Angle of attack, symbol is α	Restricted to horizontal winds
Slant height	Chord	
Wind angle	Yaw angle	

3.3 Aerodynamic Sign Convention and Basic Equations

Sign Convention:



Aerodynamic Equations:

1. Pressures and pressure coefficients are related by:

$$p = q C_p$$

2. Normal forces and normal force coefficients are related by:

$$F_N = q S C_n$$

3. When the pressure coefficients and normal force coefficients are linear with respect to angle of attack, the above expressions can be changed to:

$$p = q C_{p\alpha} \alpha$$

$$F_n = q S C_{n\alpha} \alpha$$

4. Normal force coefficient for chordwise strips can be obtained from the pressure coefficients by integrating the pressure coefficient along the chord and is expressed by:

$$C_n = \frac{1}{c} \int_c C_p$$

or for a surface as:

$$C_n = -\frac{1}{S} \int_s C_p$$

5. Lift and drag coefficients are related to the normal force coefficient by the angle of attack as:

$$C_L = C_n \cos \alpha$$

$$C_D = C_n \sin \alpha$$

6. Lift and drag forces are given by:

$$L = q S C_L$$

$$D = q S C_D$$

4.0 WIND TUNNEL TEST PROGRAM AND RESULTS

A wind tunnel test program was developed to verify the theoretical results in reference 5 and to obtain test data for conditions not presently suitable for theoretical analysis. The test plan included the testing of wind loads on single arrays, arrays within an array field, the effect of fences on arrays in an array field, and the effect of wind velocity profiles (uniform and 1/7 power law). The emphasis of the program was the testing of arrays in an array field with a boundary layer wind having a 1/7 power law velocity profile referenced at 10 meters. This wind profile was used to represent the winds found in nature in open flat terrain. The array parameters varied using this wind profile were: (1) array separation (1.5, 2.0, and 3.0C), (2) tilt angle (20°, 35°, 60°, and 90°), (3) wind direction (front, rear, and oblique winds of 45° and 135° from the front), (4) fence (with and without), (5) fence porosity (0% and 30%), and (6) fence-array separation (1.25, 2.5, and 5.0C). The array parameters not varied were the slant height (C) and the array ground clearance of .25C. Several modifications to the fence corner and array edges were tested with oblique winds in an attempt to reduce the array edge loads. A complete list of the test configurations is listed in Table 18, Appendix A. The fence corner modifications are detailed in Table 17, Appendix A, and the array edge modifications are shown in Figure 24, Appendix A.

A number of test runs were conducted utilizing a uniform velocity profile. These tests did not include any fence effects or effects of oblique winds. The tests included variations of tilt angle and array separation in an array field. Single arrays were also tested varying the tilt angle and the array ground clearance. Corresponding single array tests were performed with a 1/7 power law velocity profile for comparison to the uniform velocity profile results.

The wind tunnel testing was conducted in the Meteorological Wind Tunnel at Colorado State University (see Figure 1, Appendix A). This tunnel is characterized by a long (96 ft.) test section that is 6 ft. 8 in. wide by 6 ft. high. The long test section is required to properly develop and stabilize the boundary layer velocity profile used in the tests. Testing in a boundary layer wind profile is performed at the rear of the test section whereas testing in a uniform wind velocity profile is performed at the front of the test section.

The array model tested was a 1:24 scale of an eight ft. chord full size array. Pressure taps were located at the mid-span and edge locations as shown in Figure 10, Appendix A. Ten pressure taps were located on each of the front and rear faces of the array and at each span location. The spacing of the taps were varied such as to have more taps near the leading and trailing edges of the array. Pressures at each tap were recorded digitally for 16 seconds by means of a pressure switch to a Setra differential transducer which was sampled at 250 times per second. The test data acquisition, data reduction as well as the testing procedures are detailed in Appendix A. The recorded test data in its entirety is presented in Appendix B and the computer plotted test data in Appendix C.

The following sections present significant findings from the test results. Section 4.1 details the results from the uniform wind velocity profile for an array field. Section 4.2 presents the results from the 1/7 power law wind profile and section 4.3 shows the comparison of the wind loads on a single array due to a uniform and a boundary layer wind. Section 4.4 summarizes the significant test results.

4.1 Uniform Wind Velocity Profile

Figures 4-1a through 4-1g, show the net or delta pressure coefficient distribution (the windward face pressure coefficient minus the base pressure coefficient) along the chord for an array field positioned at four tilt angles and with a uniform velocity profile wind from both front and rearward directions. In all of these cases, the arrays are .25 slant heights above the ground and separated by a distance of two slant heights. Other array separation distances (1.5 and 3.0 slant heights) were tested. Since the results from the three array separations are similar, only the results of the 2.0 slant height separation tests are used to discuss significant findings. The pressures on the arrays, each recorded in the test for sixteen seconds, were used to calculate average and rms pressure coefficients. The rms pressures are an indication of the pressures to be expected from the turbulence generated by the arrays. However, the rms pressures do not reveal any characteristics of the flow such as the phase angle of the pressure between locations or the frequency content of the pressures. These parameters are very important to predict dynamic pressures and forces on the structure and will be reported in a future report.

The first windward array in the array field experiences by far the highest mean pressure coefficients and resulting normal forces for all tilt angles. In contrast to the mean pressures, the rms values of the unsteady pressure coefficients caused by the array induced wind turbulence is the smallest on the first windward array. The turbulence in the wind tunnel for the free stream wind prior to the array field is essentially zero.

The first array behind the windward array (2nd array) experiences considerably lower mean pressures than the first array but the rms pressures caused by the array induced wind turbulence are greatly increased. This is caused primarily by the turbulence created in the wind by the first array. In addition, the pressure distribution on the second array is significantly changed by the effects from the first array, especially when the wind is from the front. For this wind condition, the pressures on the windward array face become negative over a portion of the chord for several tilt angles, and $\Delta\ddot{u}_p$ may be negative over part of the chord for several tilt angles as shown for the 35° tilt angle case. In this condition, if only normal forces were recorded on the array, they would indicate essentially zero force. From the pressure coefficient distribution shown in Figure 4-1c to 4-1f, it can be seen that there are varying pressures on the array and a significant pitching moment is felt by the array.

The loads on the fifth array downwind from the edge of the array field experience larger fluctuating pressure coefficients than the first array, but smaller than the second array. Although the fluctuating pressure coefficients are of the same order as the steady state pressures on the fifth array, the total of these pressures is much smaller than only the steady state pressures on the first array. Another noteworthy aspect of the loads on the fifth array is the flatness of the pressure distribution along the chord. The pressure distribution is essentially constant over the chord for each tilt angle considered. An exception is the 20° tilt angle configuration with the wind approaching the array from the back, where the pressure distribution along the chord linearly increases from the trailing edge to the leading edge.

4.2 1/7 Power Law Wind Velocity Profile

The major portion of the wind tunnel test program was devoted to the wind loading on the arrays in a boundary layer wind of 1/7 power law velocity profile shown in Figure 4-2. This section presents and discusses the significant findings of the wind tunnel test results performed in the boundary layer wind. The array test configuration, pressure measurement locations and wind direction are given in Table 4.1.

Table 4-1. Array Test Conditions

Array Configuration (Tilt Angle)	Fence	Pressure Measurement Location	Wind Direction
20°, 35°, 60°, 90°	No	Center of Span	0° (Head-On), 180°
20°, 35°, 60°, 90°	Yes	Center of Span	0° (Head-On), 180°
35°	No	Edge of Span	0° (Head-On), 180°
35°	Yes	Edge of Span	0° (Head-On), 180°
35°	No	Edge of Span	45°, 225°
35°	Yes	Edge of Span	45°, 225°

4.2.1 Array Mid-Span Wind Loads Without a Protective Wind Barrier (Fence)

Figure 4-3 presents the mean and rms delta pressure coefficient distributions on the arrays in an array field with an identical configuration as in Figure 4-1, except for the wind profile. The pressure coefficients are based on the freestream reference velocity located at a height of ten meters. The results for the mean and rms ΔC_p chordwise distributions are very similar in shape to those from the uniform wind profile test results presented in Section 4.1. Because the magnitude of the coefficients are a function of the reference velocity that varies with elevation above the ground in a boundary layer wind, a direct magnitude comparison with the uniform flow results cannot be made with the boundary layer results referenced to the freestream velocity at 10 meters. The trends of the results plotted in Figure 4-3 are the same as those for the uniform velocity profile results shown in Figure 4-1. That is, the highest

steady state or mean pressures are on the first array. The downwind arrays have lower steady state pressure than the front array because of the protection afforded by the upwind arrays, but the rms pressures are slightly higher within the array field than for the front array. In addition, with increasing tilt angle, the greater the amount of protection from the wind is received by the downwind arrays from the upwind arrays.

The effect that the upwind arrays have on reducing the resulting forces on downwind arrays is shown by examining the normal force coefficients presented in Figure 4-4. The normal force coefficients were obtained by integrating the delta pressure coefficients along the chord for each array and array configuration for the steady state wind. The maximum normal force coefficient on the array is due to a wind from the rear and on the first windward array for all tilt angles. Regardless of the wind direction, the first windward array acts as a barrier to the wind for the downwind arrays and removes most of the wind energy. Consequently, the steady state wind load on the second array is significantly reduced, and the steady state wind load on succeeding arrays beyond the second array are only slightly reduced from that of the second array.

4.2.2 Array Mid-Span Loads with a Protective Wind Barrier (Fence)

The protective influence on the high aspect ratio photovoltaic arrays by a fence is presented in Figure 4-5 and 4-6. Figure 4-5 shows the ΔC_p on the first array behind a six foot fence (.75C). The corresponding normal force coefficients for the first, second and fifth arrays are shown in Figure 4-6, with the results without a fence for comparison. With a fence to protect the arrays from the wind, the wind-caused normal force coefficients are approximately the same on the first and succeeding arrays except for the arrays with tilt angles of 60°. The top of the array at a tilt angle of 60° is approximately .375 chord lengths above the top of the fence, so the upper portion of the first array is exposed to the freestream velocity resulting in increased loads. Of significant conclusion from Figure 4-6 is that the normal force on arrays several rows into the array field are the same with or without a fence. Thus, the fence only protects the first couple of rows of arrays and the remaining arrays are protected by the windward arrays.

4.2.3 Array Edge Wind Loads for Straight-On Winds

Figure 4-7 and 4-8 presents the pressure distribution at a location .15 chord lengths from the side edge for arrays having a tilt angle of 35° and for an array field without and with a protective fence respectively. Figures 4-9 and 4-10 show the normal force coefficients for the same conditions and compare the normal force coefficients at the array edge location to the mid-span location. Figure 10 of the Appendix A shows the location of the edge and center of span pressure taps on the model used in the test.) Without a fence to protect the arrays, the first windward array pressure distribution at the edge is essentially the same as at the center of the array (compare Figure 4-7 to Figure 4-3c and d). The arrays downwind from the first array have an edge pressure coefficient distribution whose magnitude is reduced from the first array but not nearly as much as for the mid-span pressure coefficients at similar conditions. The edge pressures are affected by the formation of vortices resulting from the array corners. This can be seen by the significant increase in the rms pressure coefficient levels between mid-span and edge locations and by the increased steady state pressure coefficient at the array corners, especially for winds approaching from the rear. The normal force coefficients shown in Figure 4-9 also show this trend.

The fence reduces the wind by such an amount that no large differences occur in pressure coefficient distributions at the edges compared to the mid-span pressure locations as seen by comparing Figure 4-8 to Figure 4-5 for identical array positions. One aspect of Figure 4-8 that is important is that the pressure coefficients for the fifth array downwind are larger than the first array. It is conceivable that the array edge pressures behind a protective fence will approach those without a protective fence for downward arrays when the wind is straight-on to the arrays. This results because the side fence has no effect on the straight-on wind and the fence perpendicular to the wind has a decreasing effect on the wind with increasing distance downwind from the fence. Extrapolating the normal force coefficients in Figure 4-10 further downwind supports this conclusion and suggests that loads on the arrays with a fence will approach those without a fence further downstream than five arrays.

4.2.4 Array Edge Wind Loads for Oblique Winds

Downwind effects of vortices formed at the array corners can cause large pressure coefficients near the array edges when the winds are at an angle to the arrays, because of increased vortex strength. Several wind tunnel test runs were performed with oblique winds at 45° approaching the arrays from the front and the rear directions. The array configurations were: tilt angle of 35° , array separation = $2C$ and array ground clearance = $.25C$. Large local pressures on the array edges due to oblique winds were measured as shown by the pressure coefficient distributions located $.15$ chord lengths from the array edge in Figures 4-11, a through d, for an array field without and with a protective fence.

The leading edge pressure coefficients, especially for unobstructed winds approaching from the front, were very large and can result in pressures at the leading edge approaching 45 psf for a 90 mph wind, based on the pressure coefficients in Figures 4-11a and 4-11b. When no fence exists, the array edges for arrays downwind from the first array do not receive any protection from the upwind arrays; therefore, their edge pressure distribution is essentially the same as the first array, as shown in Figures 4-11a and b. Figure 4-11a also shows the pressure distribution located $.9$ chord lengths from the edge on the first array. The trend implies that the magnitude of the pressure coefficients are decreasing with distance away from the side edge.

Even when the arrays are protected by a fence, the edge pressure coefficients due to an oblique wind are much larger than for straight-on winds as shown by comparing Figures 4-11c and d to Figure 4-8. The fence does give some protection to the arrays because the overall array edge pressure coefficient distribution is somewhat lower in magnitude than the corresponding conditions without a fence. This can be seen more easily by comparing the normal force coefficients at the edge with and without a fence as shown in Figure 4-12. Figure 4-12 also shows the reduction in normal force coefficients from $.15$ chord lengths to $.9$ chord lengths from the edge with and without a fence. The combination of a fence corner and an oblique wind causes a strong vortex to be generated at the fence corner which sweeps downwind and causes localized high pressure loadings. The high pressure loading caused by this vortex can be seen by the twin large humps in the pressure coefficient distribution shown on the first array in Figure 4-11c and by the large pressure coefficients at the

leading edge in Figure 4-11d. Figures 4-12 and 4-13 also show the effect of the vortex. Although the normal force coefficient for an array behind a fence is lower than without a fence (Figure 4-12), the corresponding maximum pressure coefficient is higher (Figure 4-13) on the first windward array when the wind approaches from the rear. This maximum pressure coefficient is at the leading edge which is directly downwind and in the vortex from the fence.

Because of the high edge pressures on the arrays, several modified configurations were tested in the wind tunnel in an attempt to reduce these pressures. The modifications (described in more detail in the Appendix) are as follows:

- 1) A short fence of the same porosity and height as the protective fence placed in front of the corner of the protective fence and at 45° to each side. This short fence would be perpendicular to a oblique wind that is at 45° to the protective fence and array field (See Figure 4-16, Configuration 1)
- 2) Three short fences overlapping each other and placed in front of the corner of the protective fence as in (1) (see Figure 4-16, Configuration 2)
- 3) Additional eight foot length added to the array with the added length having 50% porosity (See Figure 4-16, Configuration 3)
- 4) Endplating of the array ends completely closing the rows of the arrays with a 50% porosity end plate. This is to simulate shrubs etc., at the ends of the arrays (see Figure 4-16, Configuration 4)
- 5) Addition of a 50% porosity extension to the top of the array at the corner of the existing protective fence (see Figure 4-16, Configuration 5 and Figure 4-11g).

The data from the wind tunnel test for all of these configurations is given in Appendix B, and plots of the data are presented in Appendix C. The results from the configurations in (1) through (3) are not presented in the main body of the report for the following reasons. Configuration (3) did not produce any reduction in edge pressures. Configurations (1) and (2) did show reductions in the pressure coefficient distributions for the pressure taps on the model. However, this configuration would require more pressure readings over the total

array area near the edge to adequately define this reduction. It is believed, and somewhat supported by the data, that the vortex caused by the main fence corner is significantly reduced, but that other vortices are being generated at the corners of the smaller fences, thus pushing the location of the high pressure loading points inwards from the array side edge.

Configuration (4), endplating of the arrays, produced the smallest edge pressure coefficients of the configurations tested. The edge pressure coefficient distributions for the endplating effect is shown in Figures 4-11e and f. Unfortunately, this method of reducing the loads may be impractical for several reasons: (1) the endplating would cause varying amounts of shadowing on the arrays depending upon the time of day, (2) if mechanized equipment is required to be moved down each row of the arrays, a gate would be required at the end of each row.

The addition of a 50% porosity extension to the fence corner is shown with the results in Figures 4-11g and h. This extension does significantly reduce the edge pressure coefficient distributions from those of just a regular protective fence. It appears that the increased porosity and height at the corner reduces the tightness and strength of the corner vortex. Additional benefits may be realized by increased porosity and/or height of this corner addition. However, these parameters were not varied to optimize the reduction in the array edge pressure loadings.

In summary, the array and fence corners produce vortices whose strength is increased from a straight on wind to an oblique wind. The wind loads on the areas affected by the corner vortices are considerably larger than the loads at the non-affected areas. In order to reduce the corner vortex induced loads, it is necessary to reduce the strength of the corner vortex. This is best accomplished by lowering the wind velocity prior to reaching the arrays by utilizing a fence and by modifying the fence corner to reduce the vortex generated by it. From the modifications investigated in the test, the most practical modification is that of increasing the height of the fence at the corner and by varying the local fence porosity in this area as shown by the figure insert in Figure 4-11g.

4.3 Comparison of Wind Tunnel Test Results for Uniform Wind Profile and 1/7 Power Law Wind Profile

In order to compare the test results between the uniform wind profile and the 1/7 power law wind profile, it is necessary to select a reference height above the ground for defining the reference velocity in the 1/7 power law wind profile. In Phase II, reference 5, the velocity at the highest edge of the array was recommended as the reference velocity when using data obtained by a uniform velocity profile because the base pressure (the major contribution to total pressure in most cases) is affected predominately by the velocity at the array edge. The mean ΔC_p was calculated with this reference velocity for the 1/7 power law wind profile results and compared in Figure 4-14 to the ΔC_p obtained by the uniform wind profile test. The comparison of the shape of the ΔC_p distribution from the two wind profile tests is very close, the magnitude is also close except for a few configurations, such as the windward array with the wind from the rear for the 20° tilt angle configuration and the wind from the front for the 60° tilt angle configuration, where the magnitudes differ by as much as .25. The second array with a tilt angle of 35° and the wind from the rear also compares poorly; the loads from the 1/7 power law wind profile are approximately half the loads from the uniform wind profile.

Integration of the ΔC_p values over the chord to obtain normal force coefficients produced the results presented in Figure 4-15. The comparison of the normal force coefficients between the uniform wind profile and the 1/7 power law wind profile is much closer than the pressure distribution, primarily because the integration of large pressure differences over a small fraction of the total area does not have a pronounced effect on the total normal force coefficient.

From the results shown in Figure 4-14 and 4-15, the uniform velocity profile normal force coefficients results would be satisfactory for use in performing preliminary design studies and in most cases for use in the final design of array structural supports. The pressure coefficient distribution results are not as definitive; the uniform velocity profile results would be satisfactory for use in preliminary design studies but are probably not accurate enough for final design of the photovoltaic panels. However, from the results, it is certainly apparent that a uniform velocity wind tunnel can be used to evaluate parameter studies for photovoltaic arrays such as load alleviation devices.

Since environmental wind tunnels (required to model the boundary layer wind) are few in number, and sometimes difficult to obtain time in their use, the close comparison in the results between the two wind profiles is important in allowing more flexibility in the testing of array models and configuration changes.

4.4 Test Results Summary

The use of a fence to protect the arrays from the wind significantly reduces the mid-span loads on the first windward array compared to the loads on an unprotected first array. The arrays located downwind from the first array are protected by the upwind arrays and the mid-span loads are approximately the same as the first array when protected by a fence. Localized array edge loads, caused by corner vortices, are considerably larger than the array mid-span loads. These edge loads can be reduced by using a fence to protect the arrays and by appropriate modifications to the fence corners shown previously in this section. To optimize the fence corner modifications or other modifications to the arrays for minimum wind loads would require an extensive test program. Since the large wind loads are a localized effect caused by the corner vortices, the arrays could be designed for higher strength in the edge areas to withstand the high vortex induced loads.

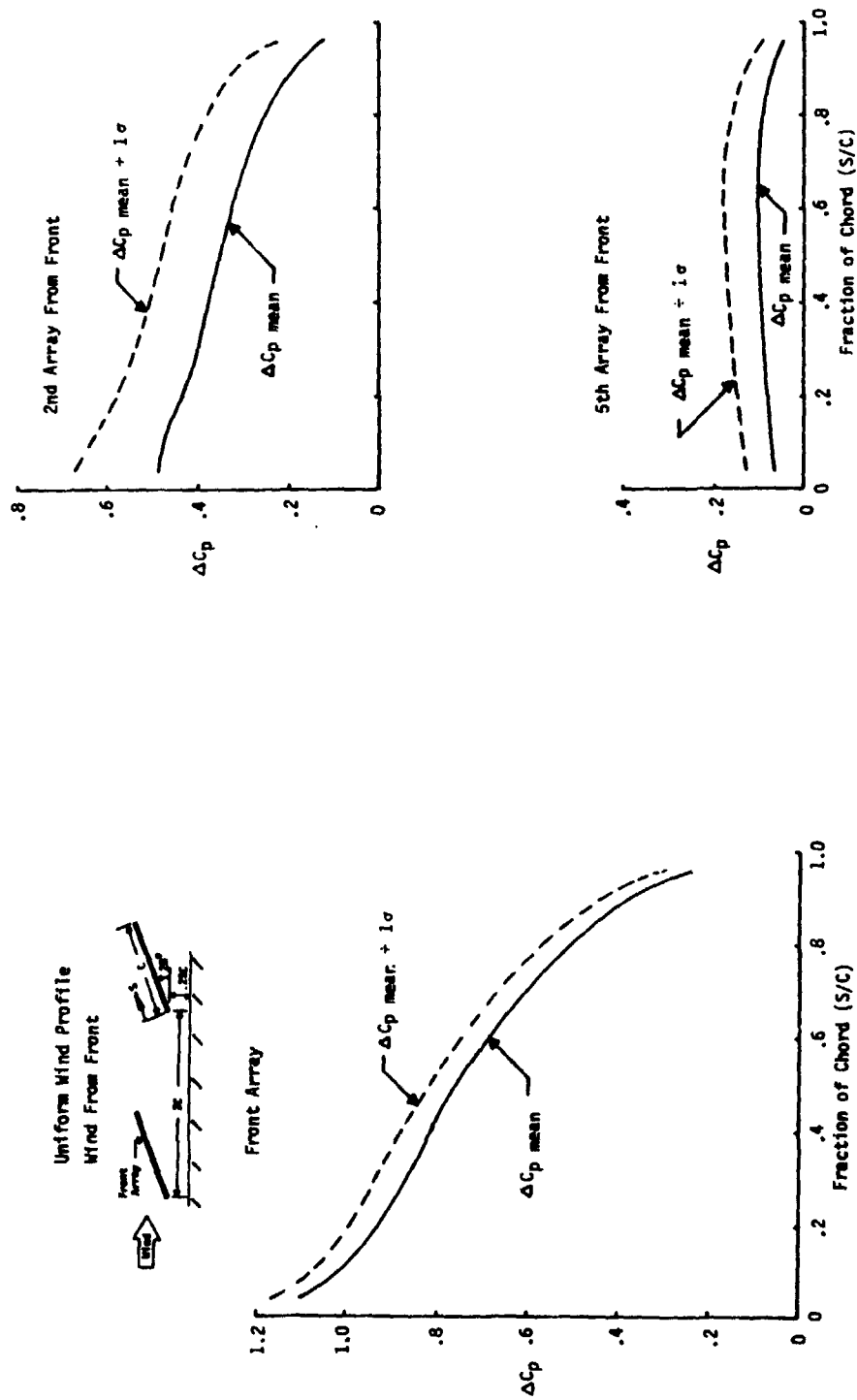


Figure 4-1a. Array Chordwise Pressure Coefficient Distribution in Uniform Wind Velocity Profile (Tilt Angle = 20° , Wind from Front).

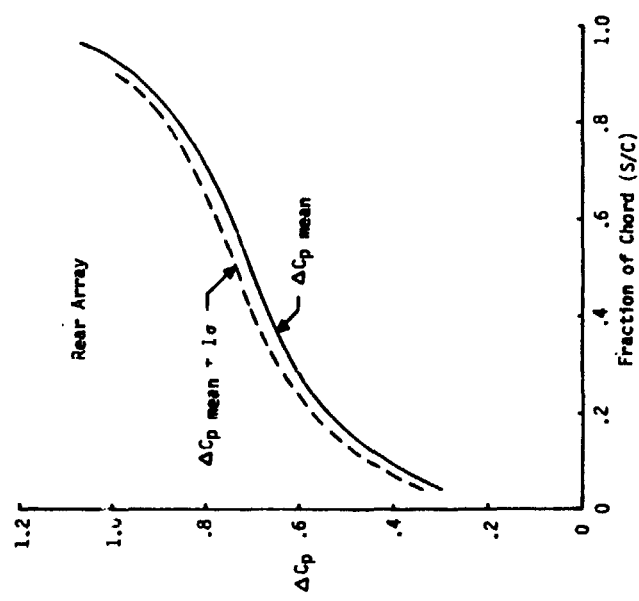
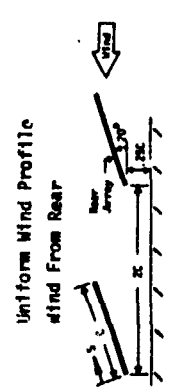
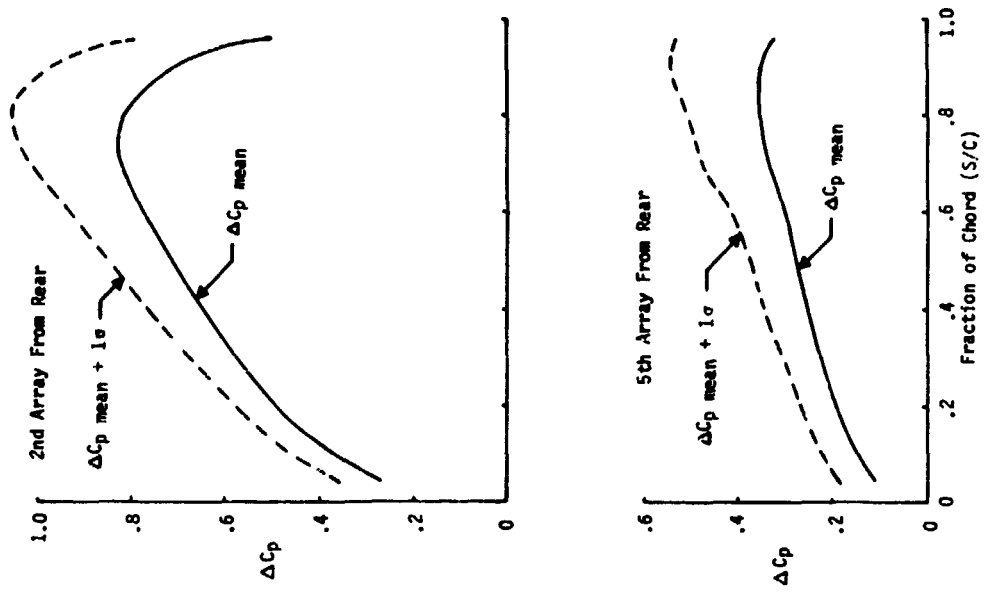


Figure 4-1b. Array Chordwise Pressure Coefficient Distribution in Uniform Wind Velocity Profile (Tilt Angle = 20°, Wind from Rear).

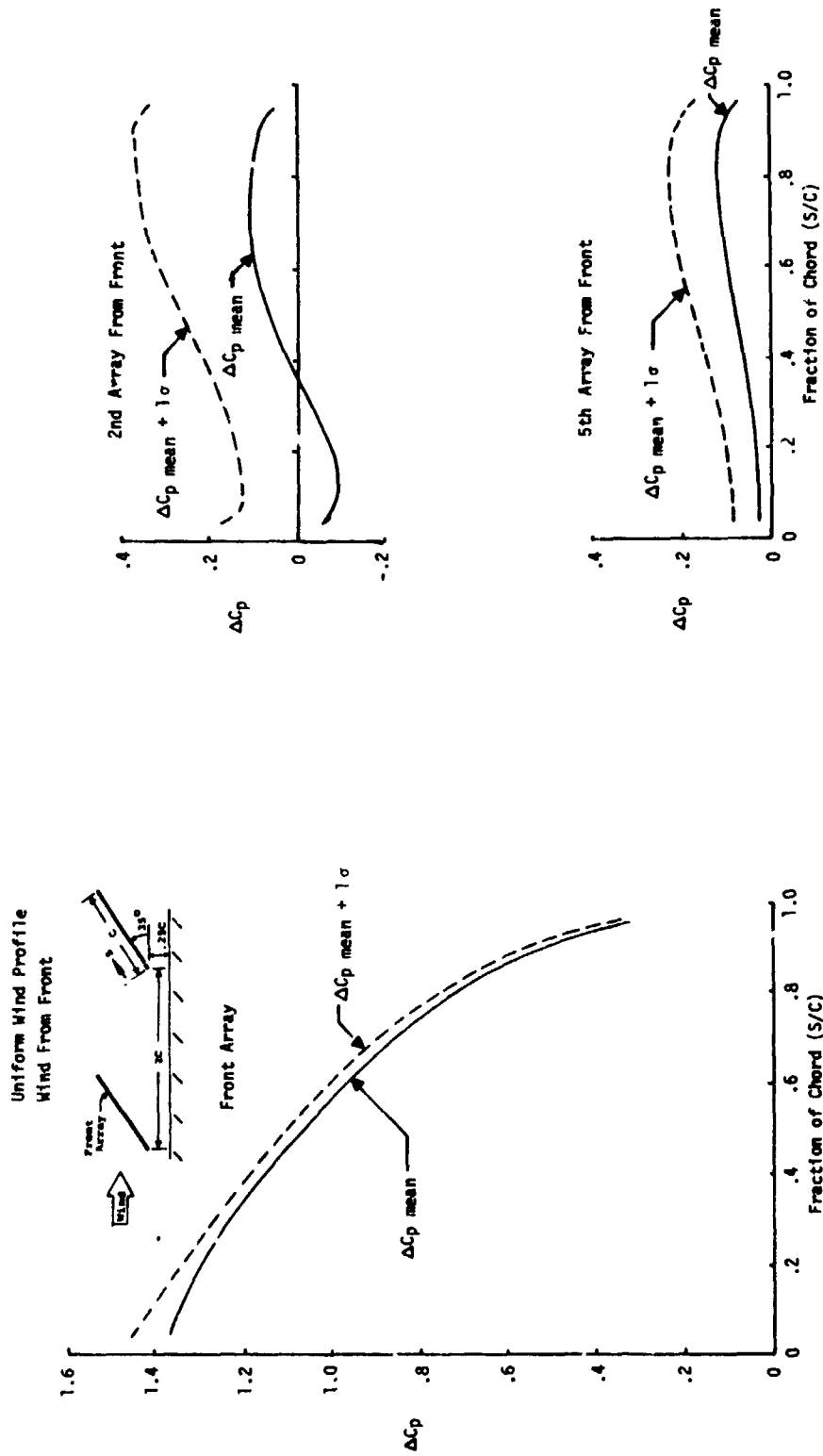


Figure 4-1c. Array Chordwise Pressure Coefficient Distribution in Uniform Wind Velocity Profile (Tilt Angle = 35°, Wind from Front!)

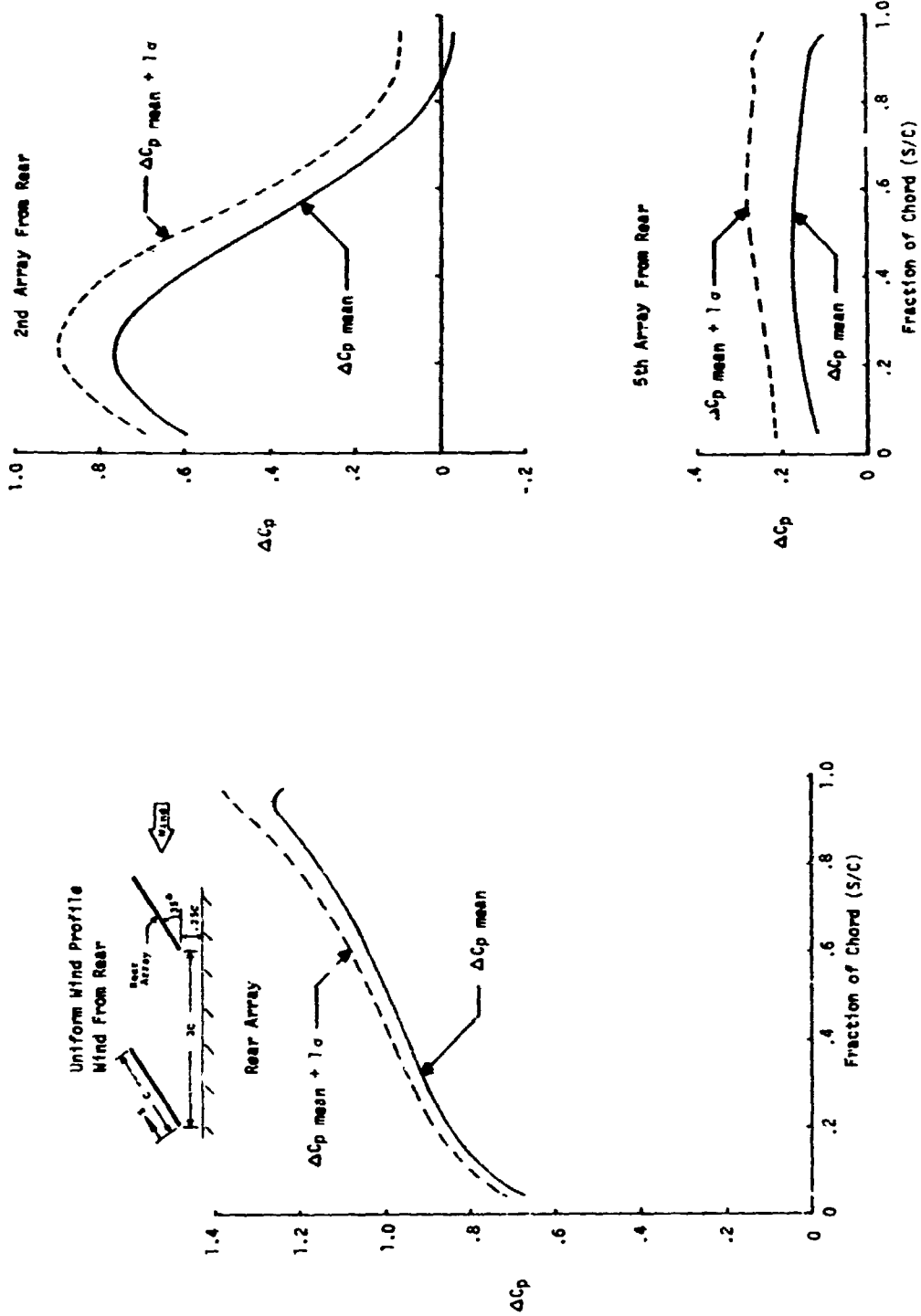


Figure 4-1d. Array Chordwise Pressure Coefficient Distribution in Uniform Wind Velocity Profile (Tilt Angle = 36° , Wind from Rear)

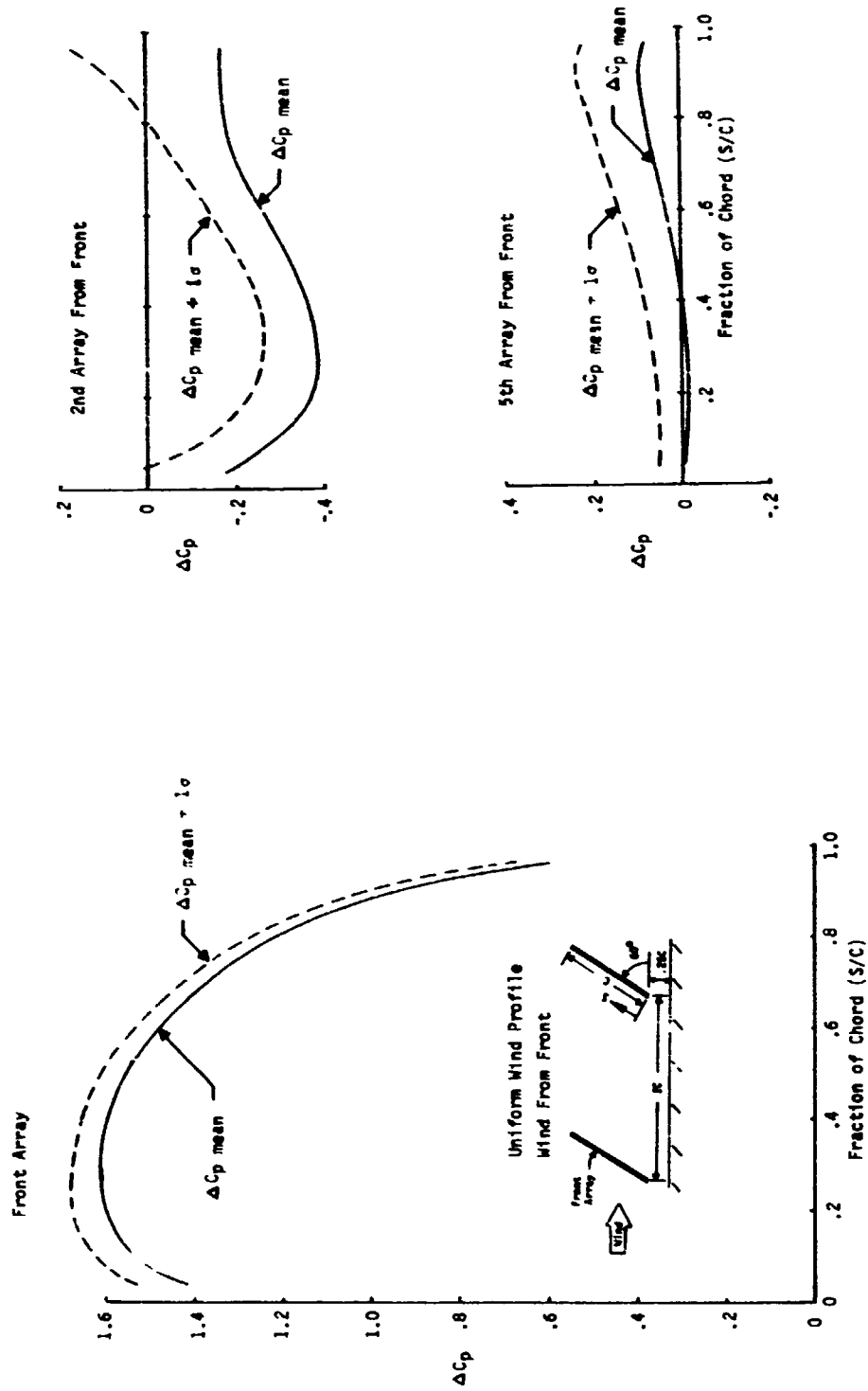


Figure 4-1e. Array Chordwise Pressure Coefficient Distribution in Uniform Wind Velocity Profile (Tilt Angle = 60° , Wind from Front)

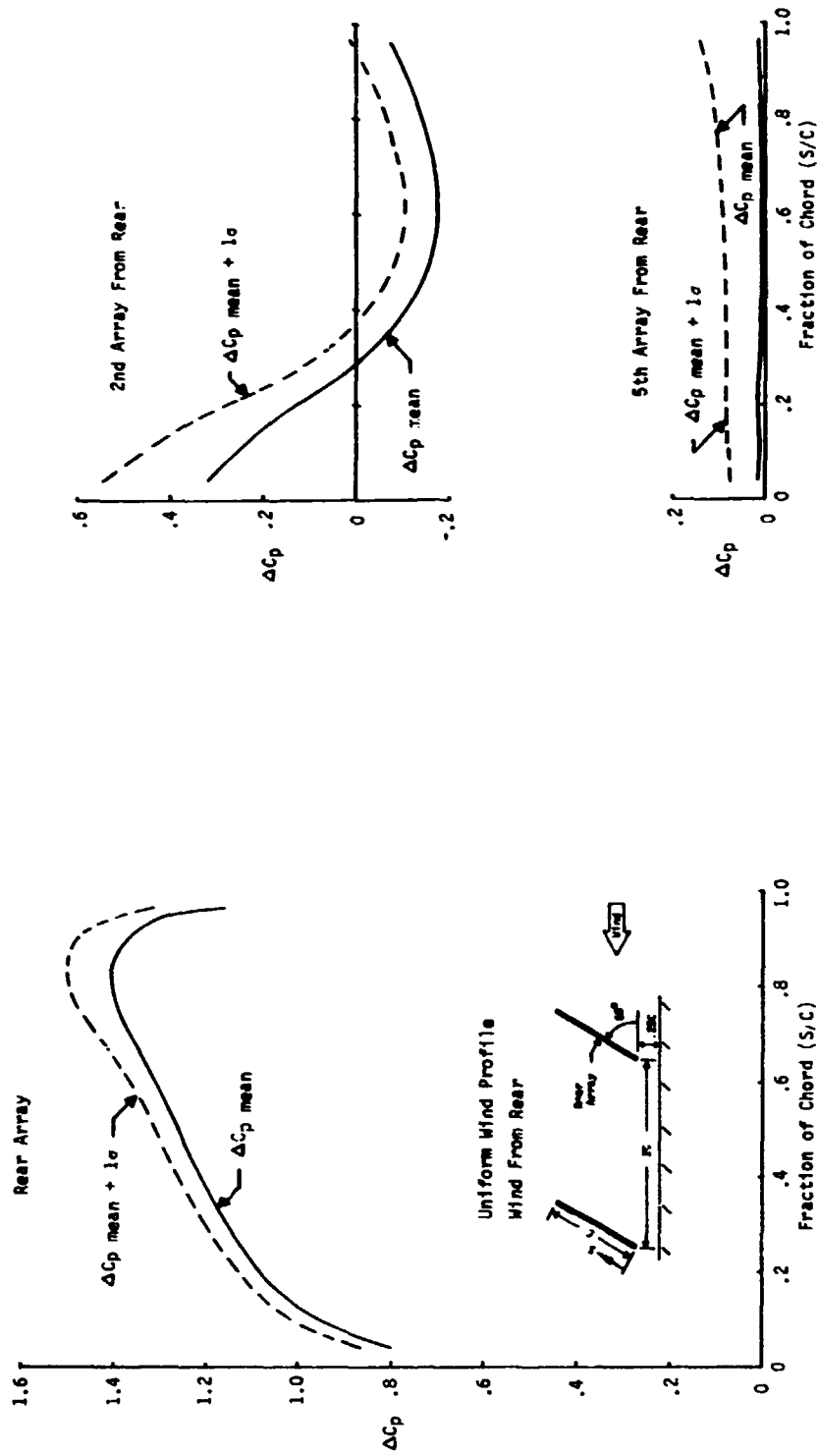


Figure 4-11. Array Chordwise Pressure Coefficient Distribution in Uniform Wind Velocity Profile (Tilt Angle = 60°, Wind from Rear)

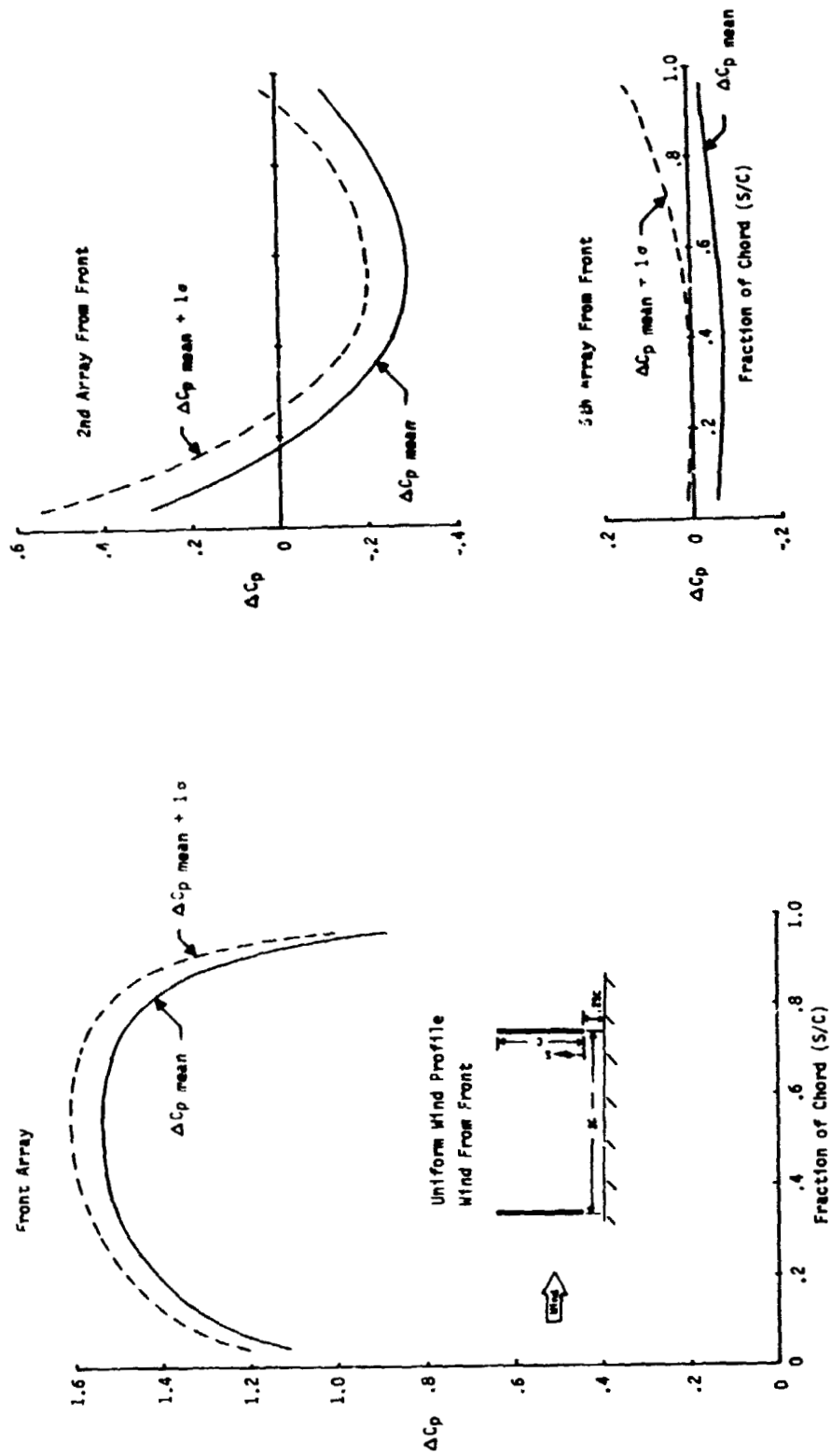


Figure 4-1g. Array Chordwise Pressure Coefficient Distribution in Uniform Wind Velocity Profile (Tilt Angle = 90°)

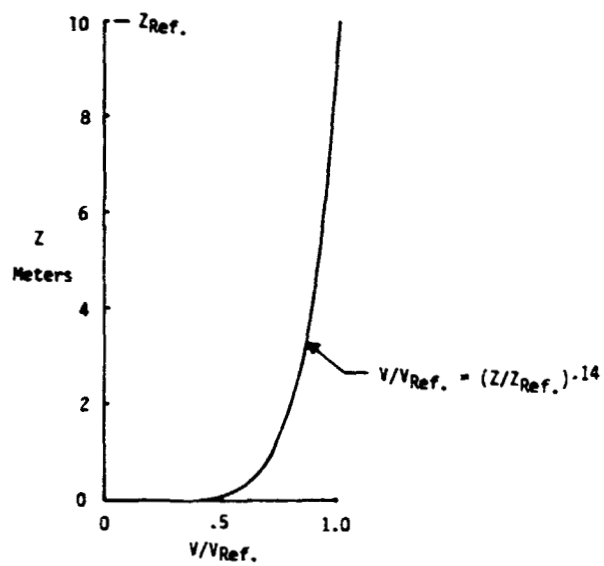


Figure 4-2. 1/7 Power Law Wind Velocity Profile

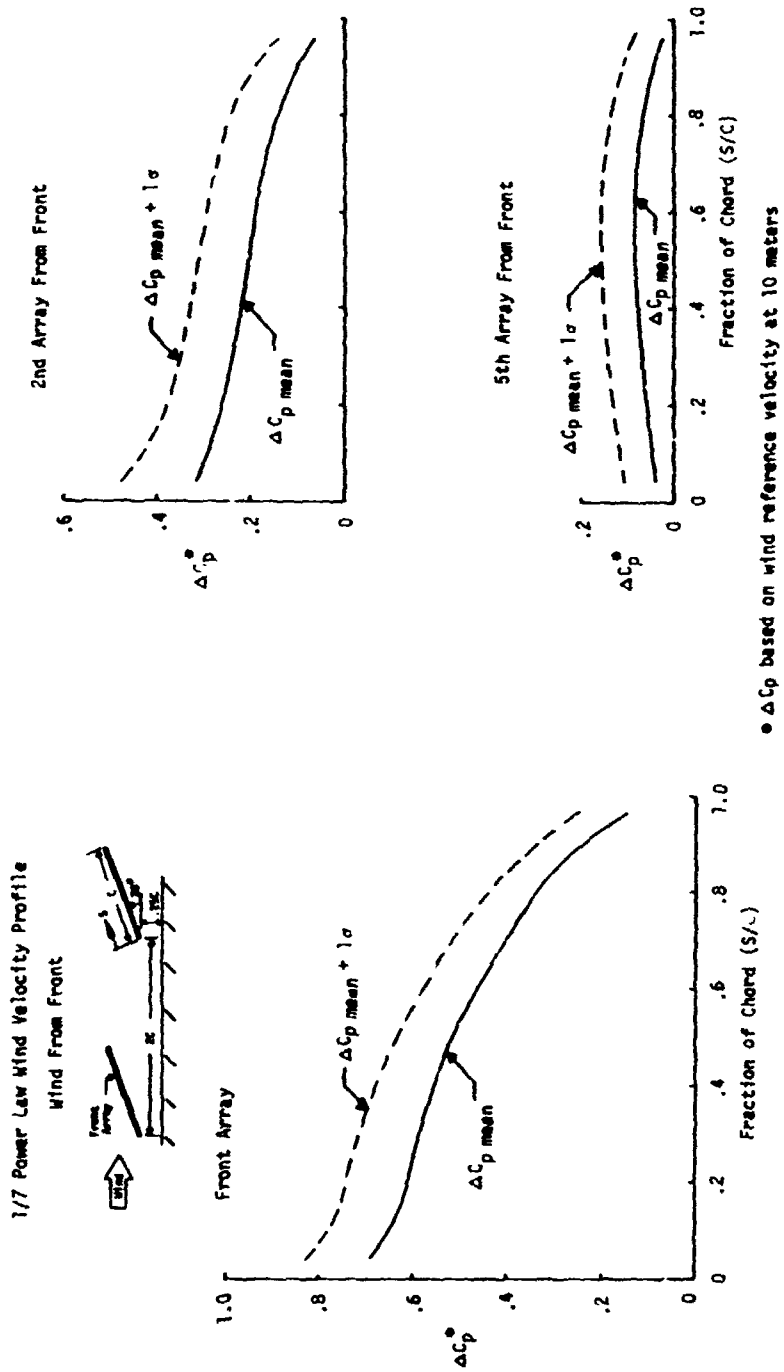
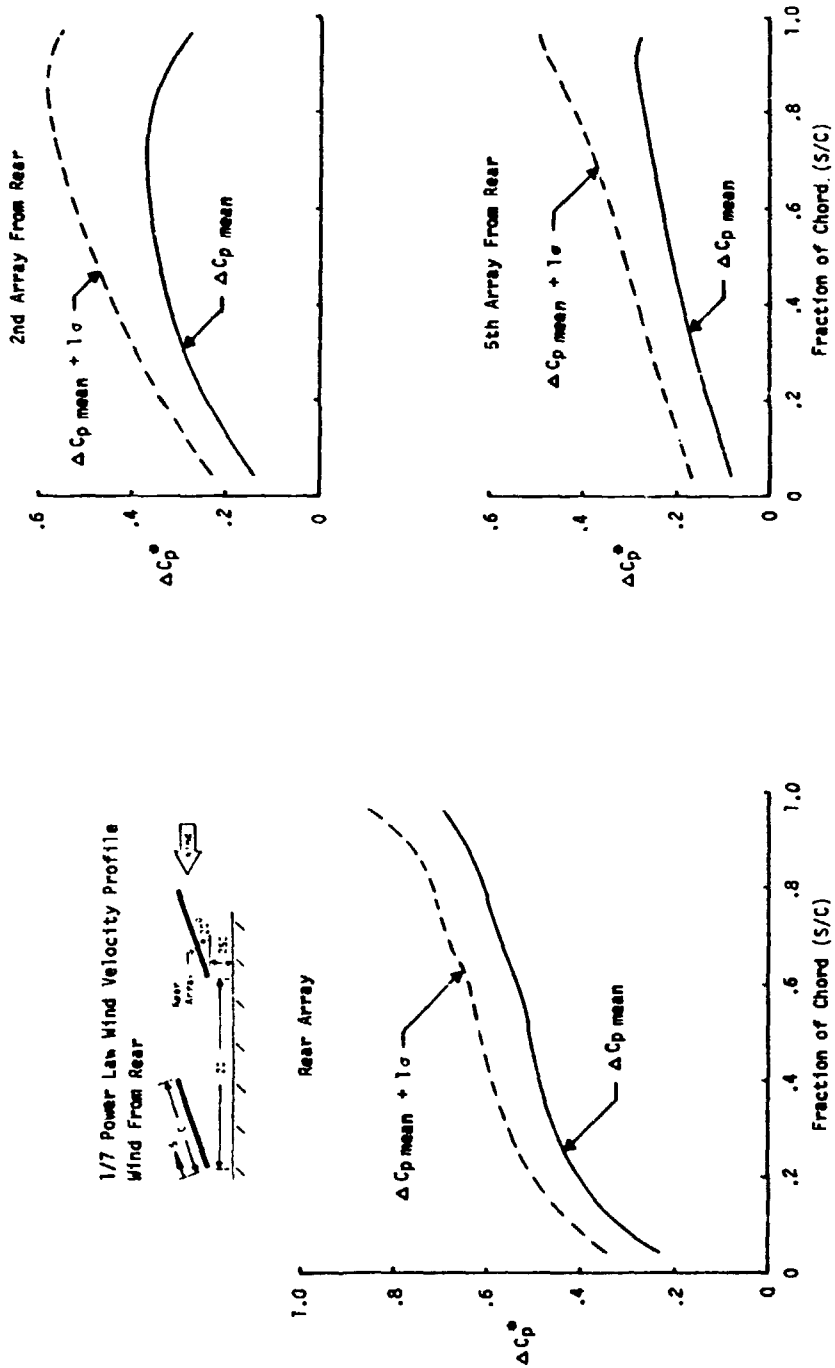


Figure 4-3a. Array Chordwise Pressure Coefficient Distribution in Boundary Layer
Wind (Tilt Angle = 20°, Wind from Front)



• ΔC_p based on wind reference velocity at 10 meters

Figure 4-3b. Array Chordwise Pressure Coefficient Distribution In Boundary Layer Wind (Tilt Angle = 20°, Wind from Rear)

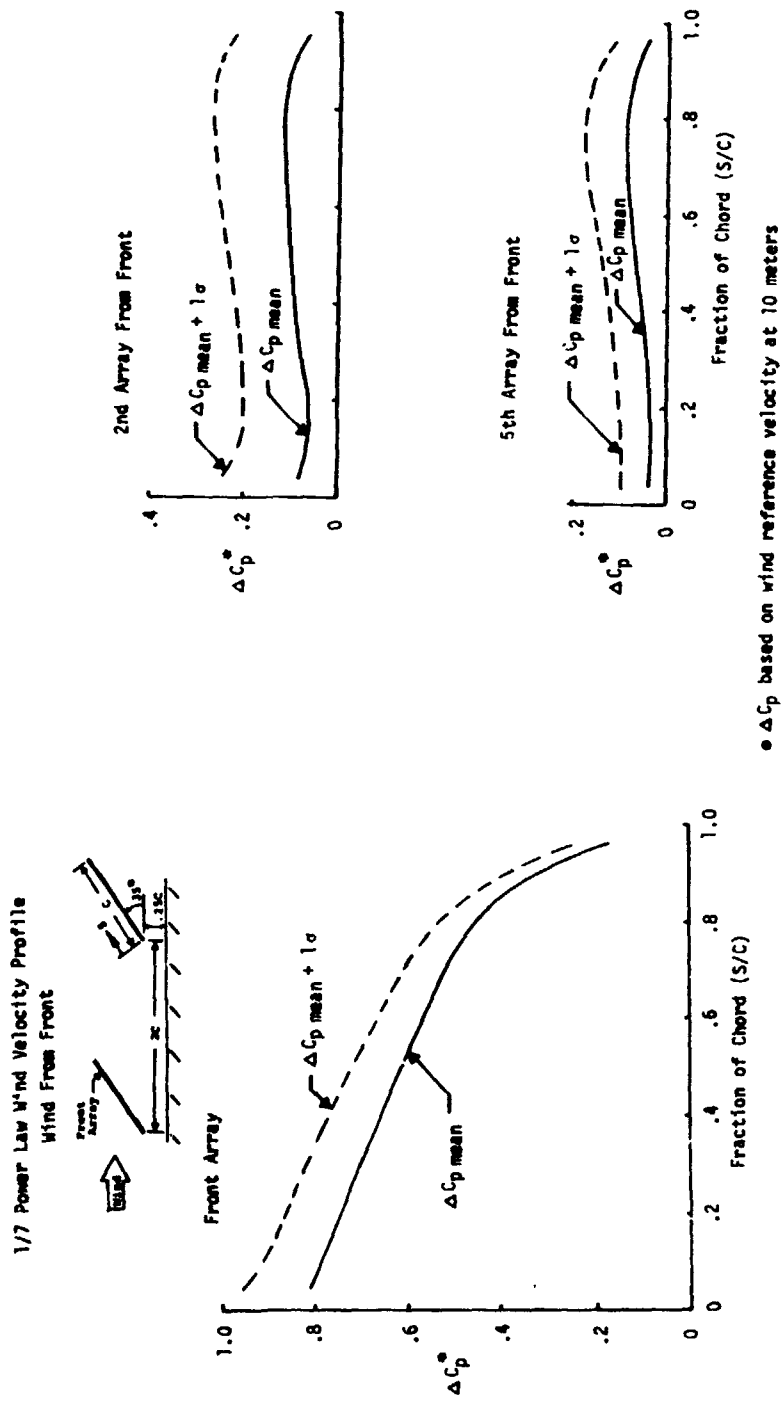
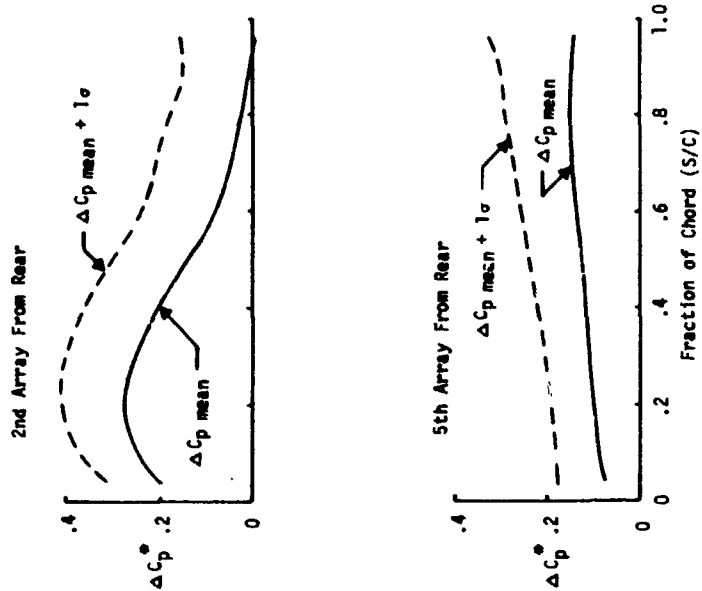
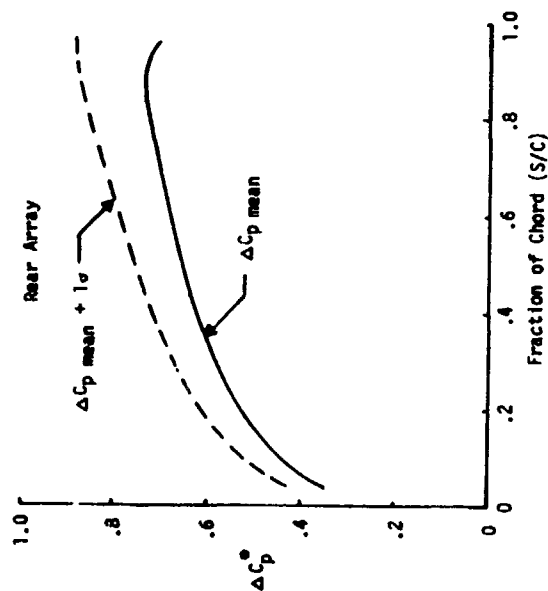


Figure 4-3c. Array Chordwise Pressure Coefficient Distribution in Boundary Layer
Wind (Tilt Angle = 35°, Wind from Front)

1/7 Power Law Wind Velocity Profile
Wind From Rear



• ΔC_p based on wind reference velocity at 10 meters

Figure 4-3d. Array Chordwise Pressure Coefficient Distribution in Boundary Layer
Wind (Tilt Angle = 35°, Wind from Rear)

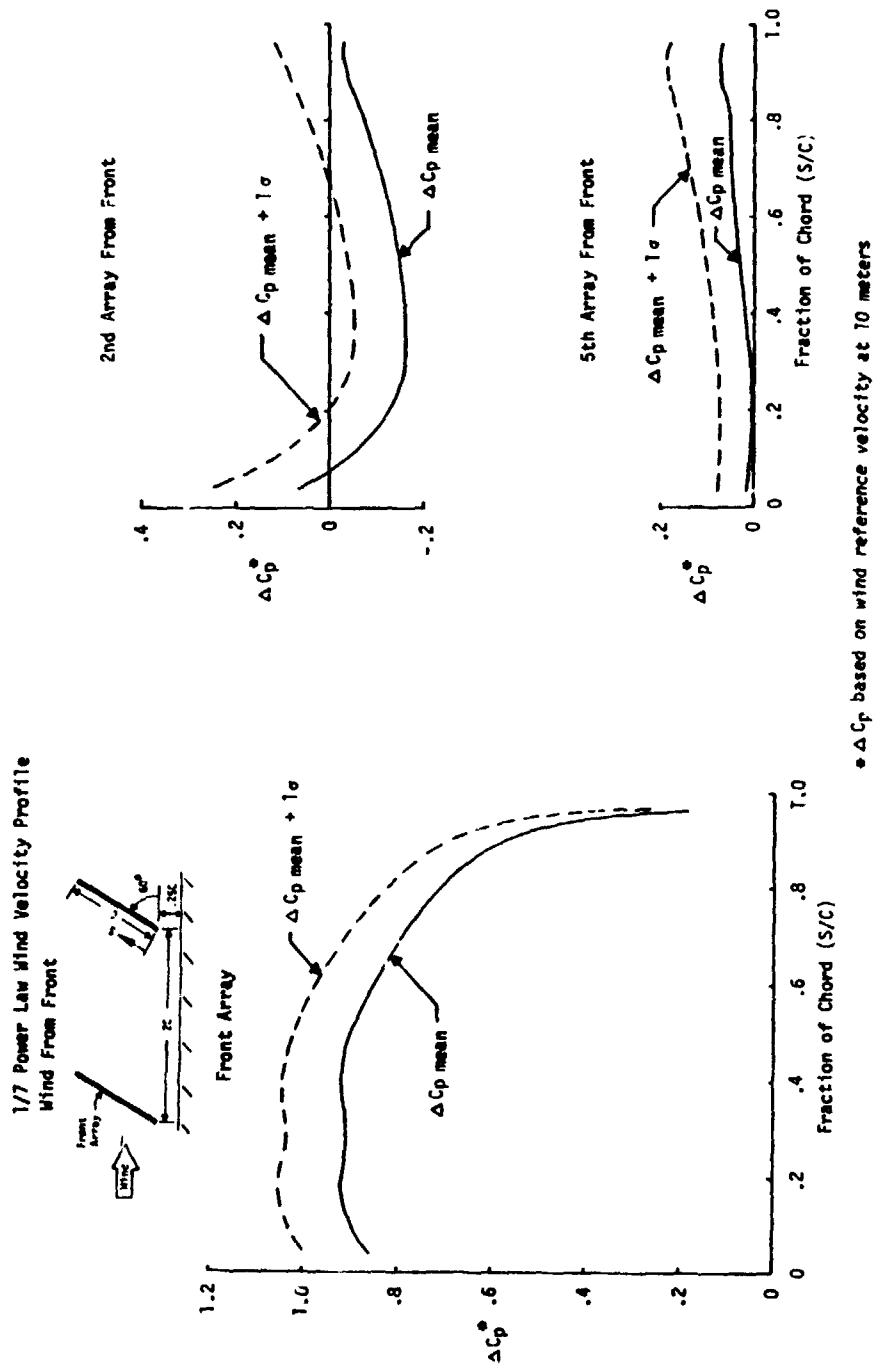


Figure 4-3e. Array Chordwise Pressure Coefficient Distribution in Boundary Layer
Wind (Tilt Angle = 60°, Wind from Front)

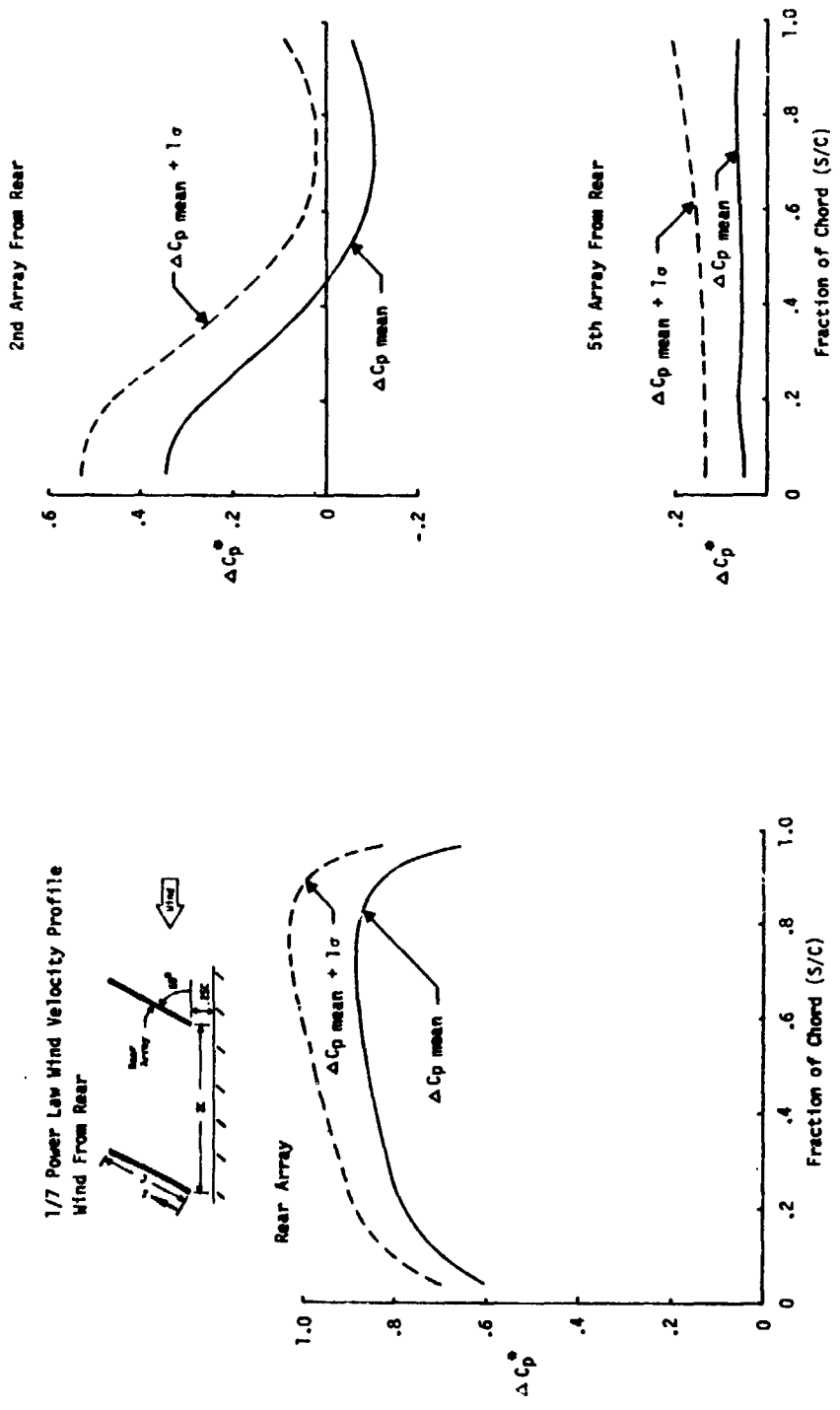


Figure 4-31. Array Chordwise Pressure Coefficient Distribution in Boundary Layer
Wind (Tilt Angle = 60°, Wind from Rear)

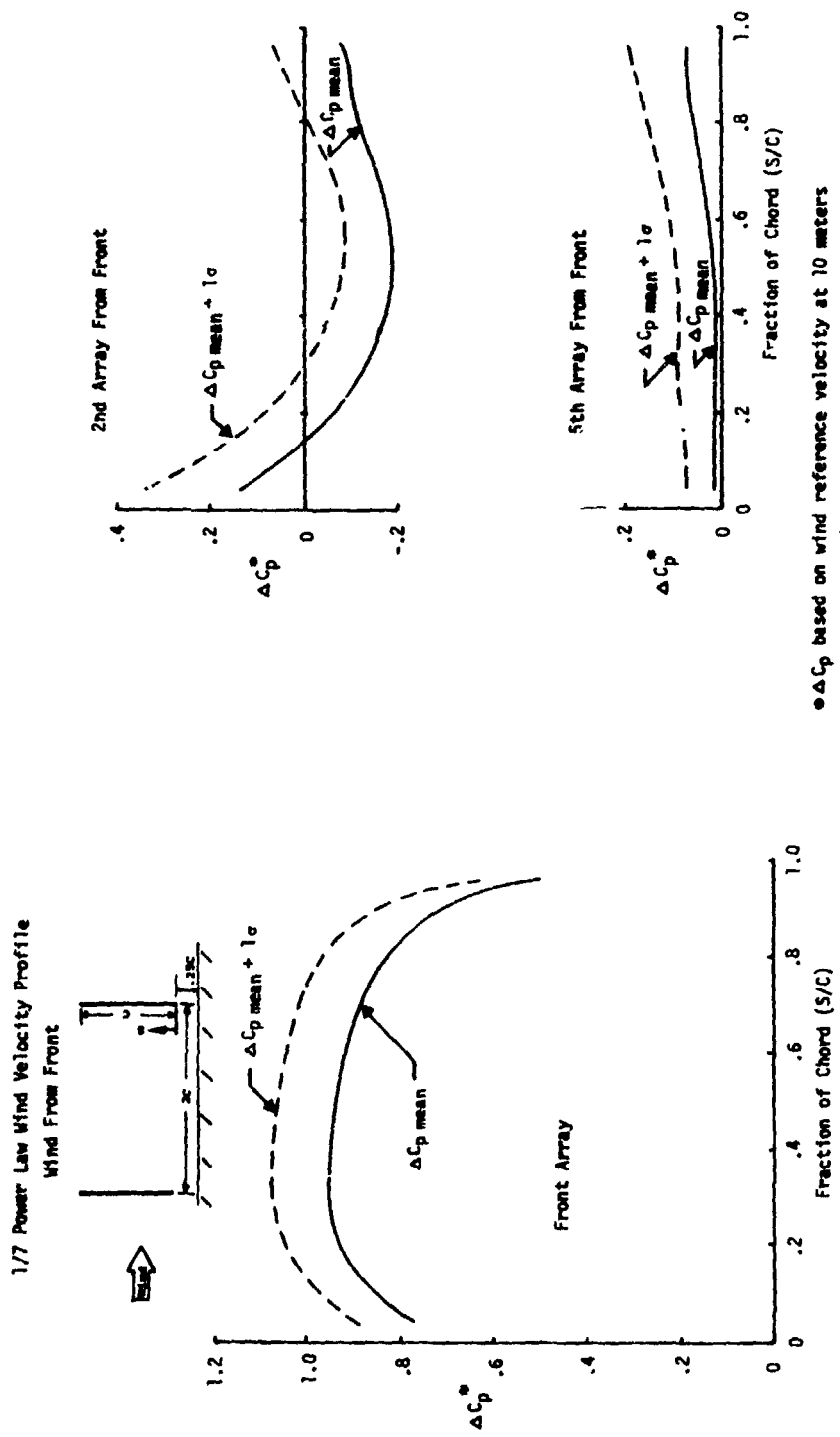
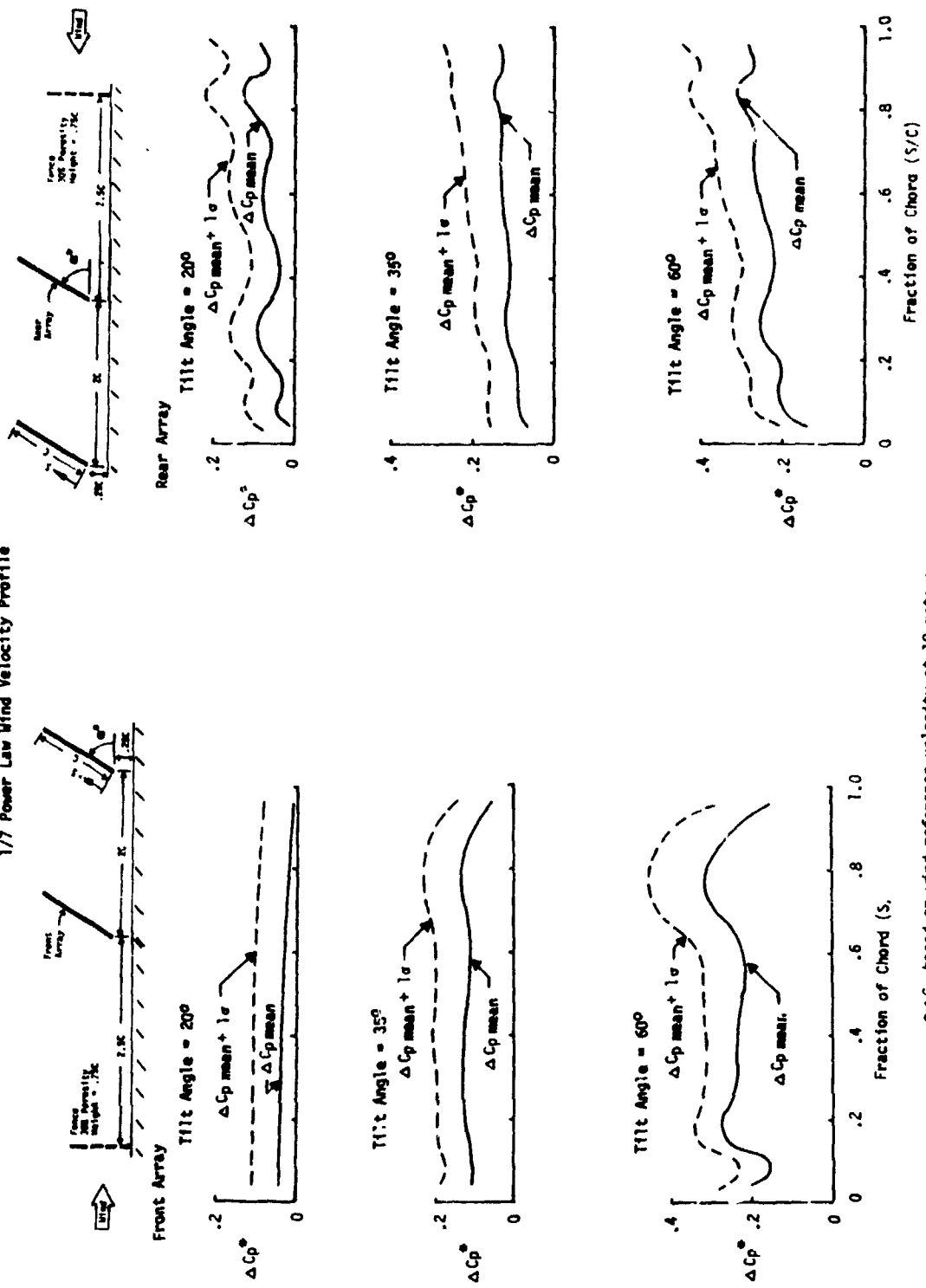


Figure 4-3g. Array Chordwise Pressure Coefficient Distribution in Boundary Layer
Wind (Tilt Angle = 90°)

1/7 Power Law Wind Velocity Profile



ΔC_p based on wind reference velocity at 10 meters

Figure 4-5. Effect of a Fence on Array Chordwise Pressure Coefficient Distribution for Head-On and Rearward Winds.

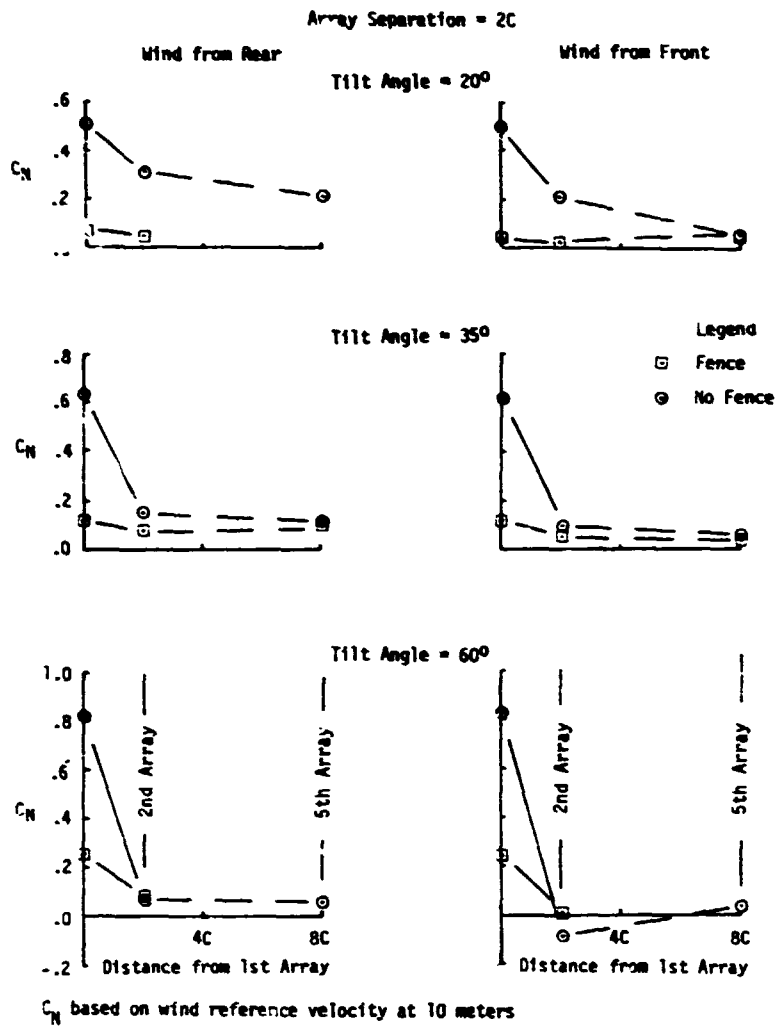


Figure 4-6. Effect of a Fence on Array Normal Force Coefficients for Head-On and Rearward Winds.

1/7 Power Law Wind Velocity Profile

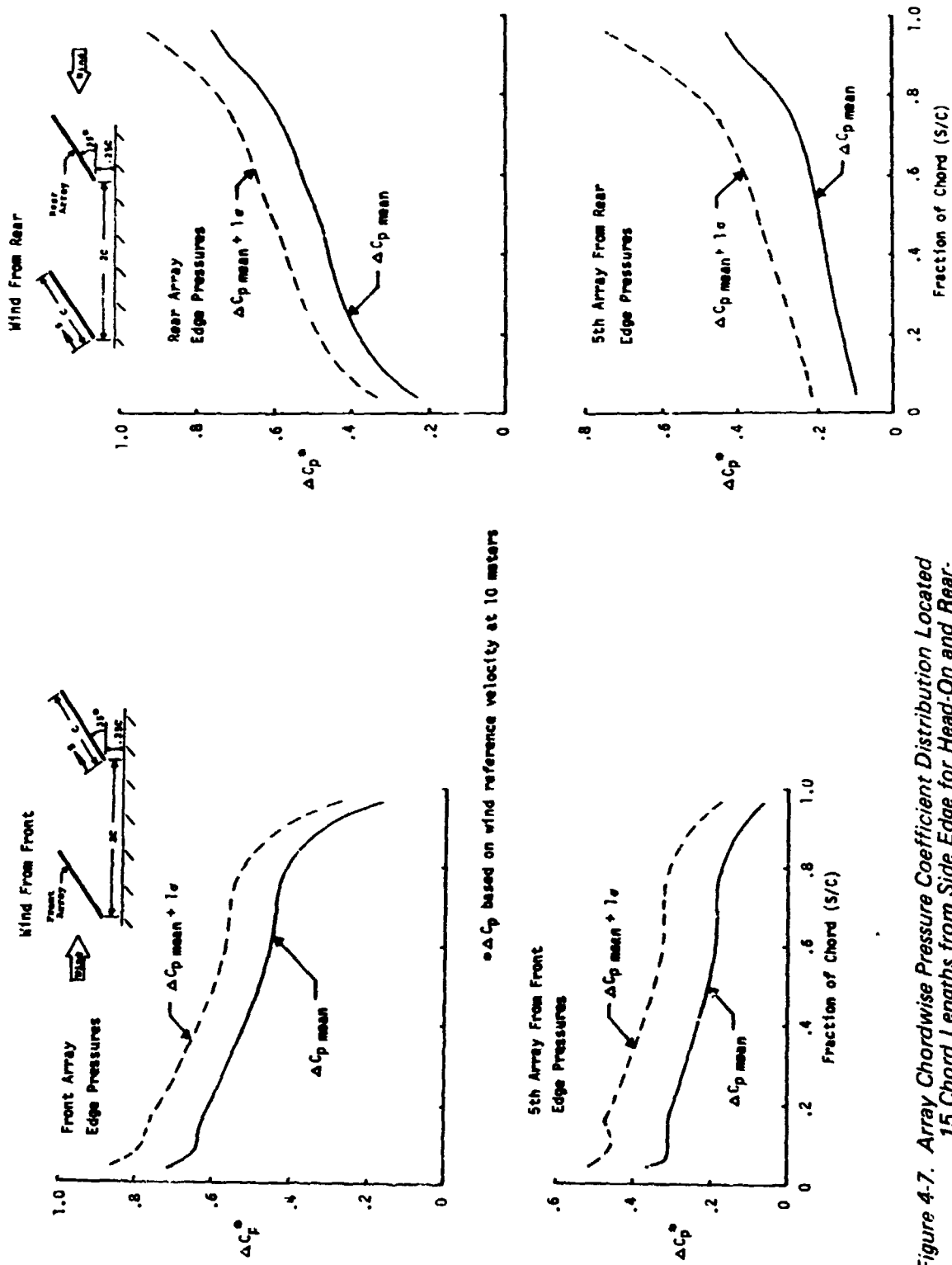
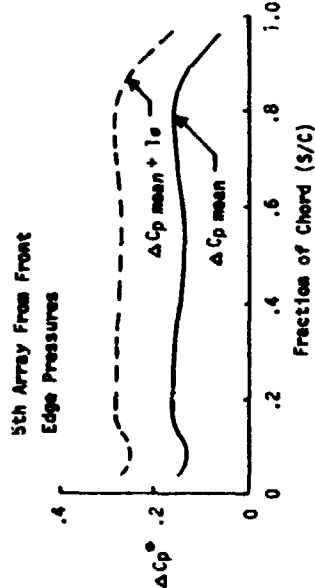
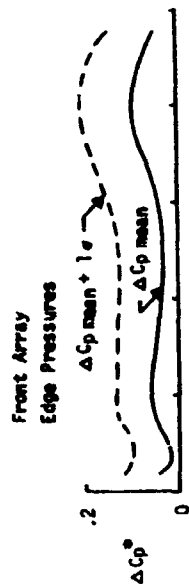
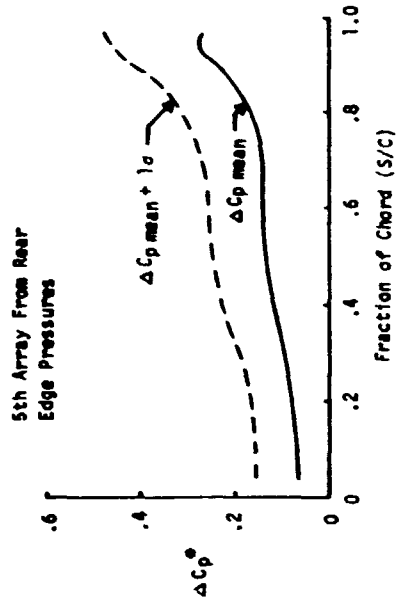
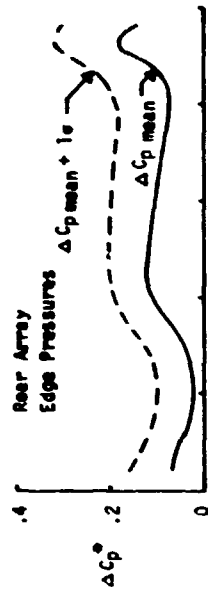


Figure 4-7. Array Chordwise Pressure Coefficient Distribution Located .15 Chord Lengths from Side Edge for Head-On and Rearward Winds (No Ferrel)

1/7 Power Law Wind Velocity Profile



• ΔC_p based on wind reference velocity at 10 meters

Figure 4-8. Effect of Fence on Array Chordwise Pressure Coefficient Distribution Located .15 Chord Lengths from Side Edge for Head-On and Rearward Winds

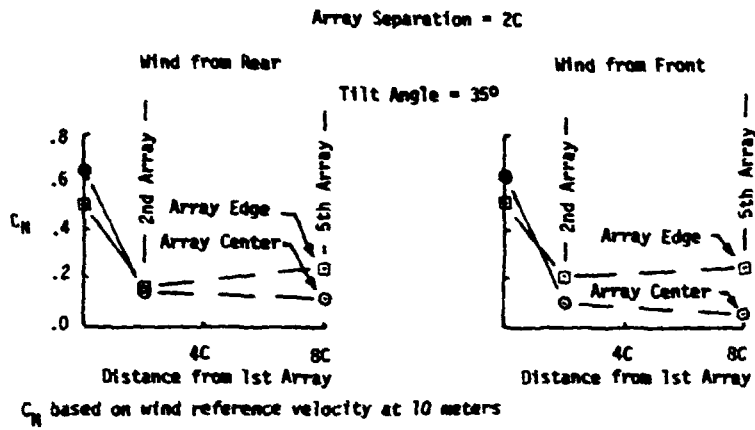


Figure 4-9. Comparison Between Array Edge and Center of Span Normal Force Coefficients for Head-On and Rearward Winds (No Fence)

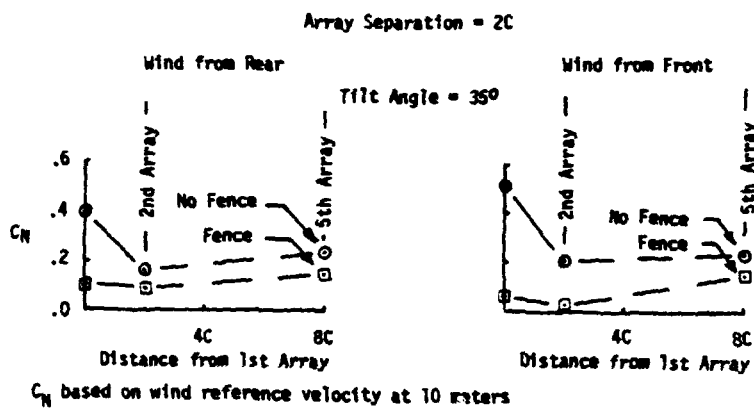
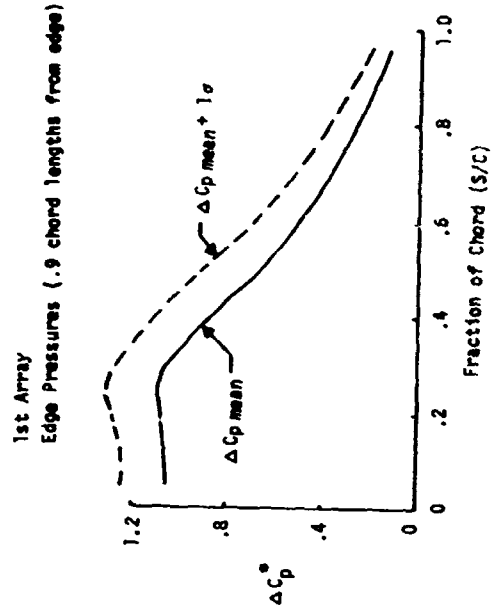
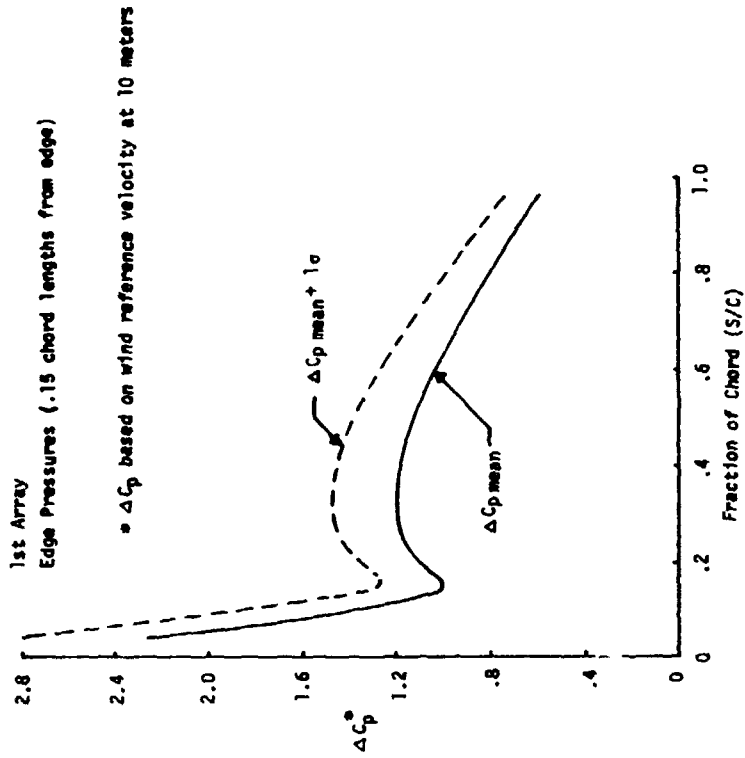
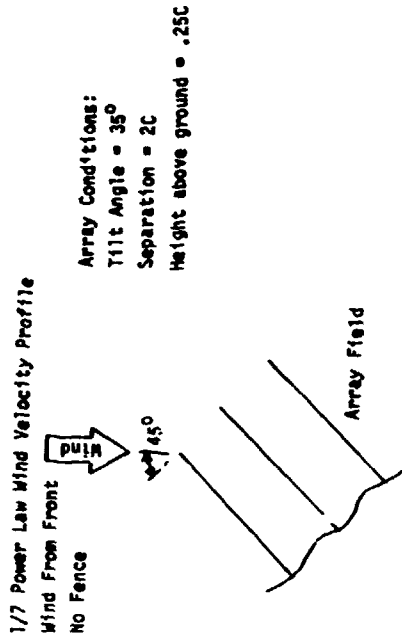


Figure 4-10. Effect of Fence on Array Edge Normal Force Coefficients for Head-On and Rearward Winds



ΔC_p based on wind reference velocity at 10 meters

Figure 4-11a Effect of Oblique Winds on Array Edge Pressure Distribution
 (No Fence, Wind from Front)

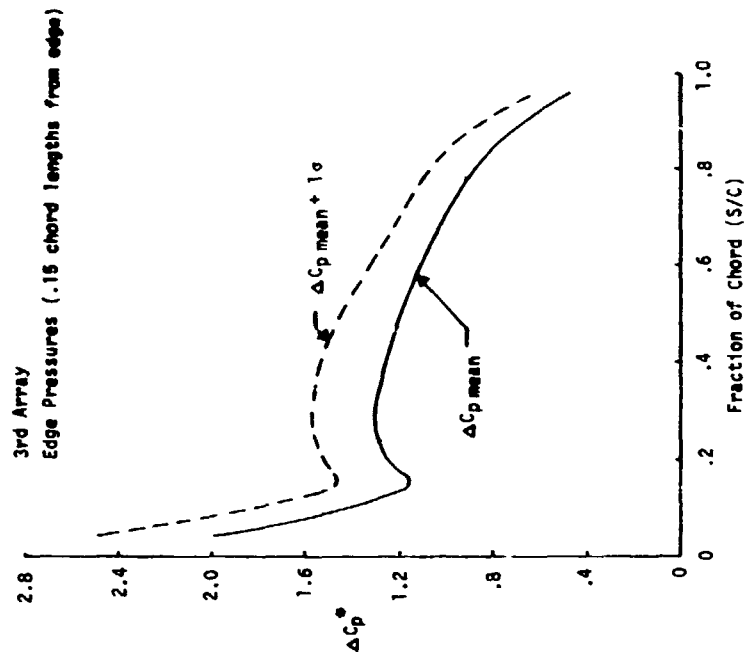
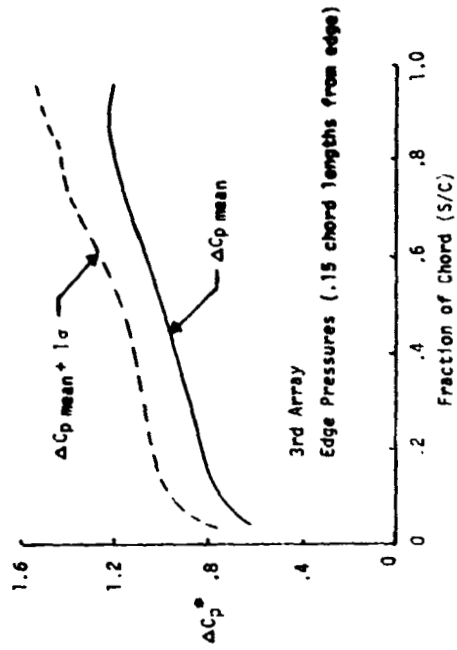
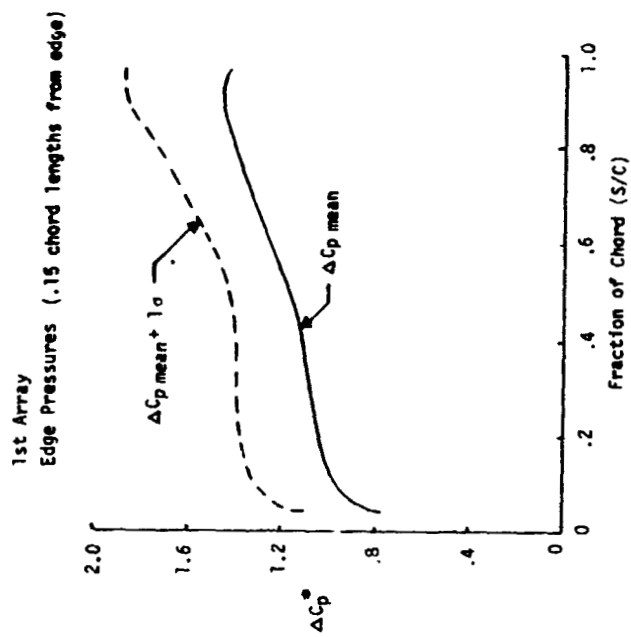
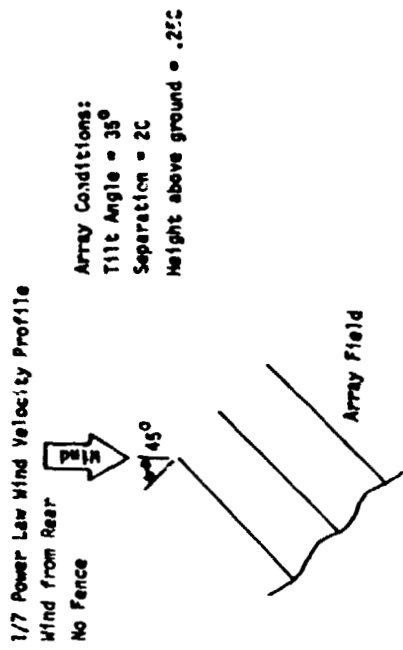


Figure 4-11a. Concluded



* ΔC_p based on wind reference velocity at 10 meters

Figure 4-11b. Effect of Oblique Winds on Array Edge Pressure Distribution
 (No Fence, Wind from Rear)

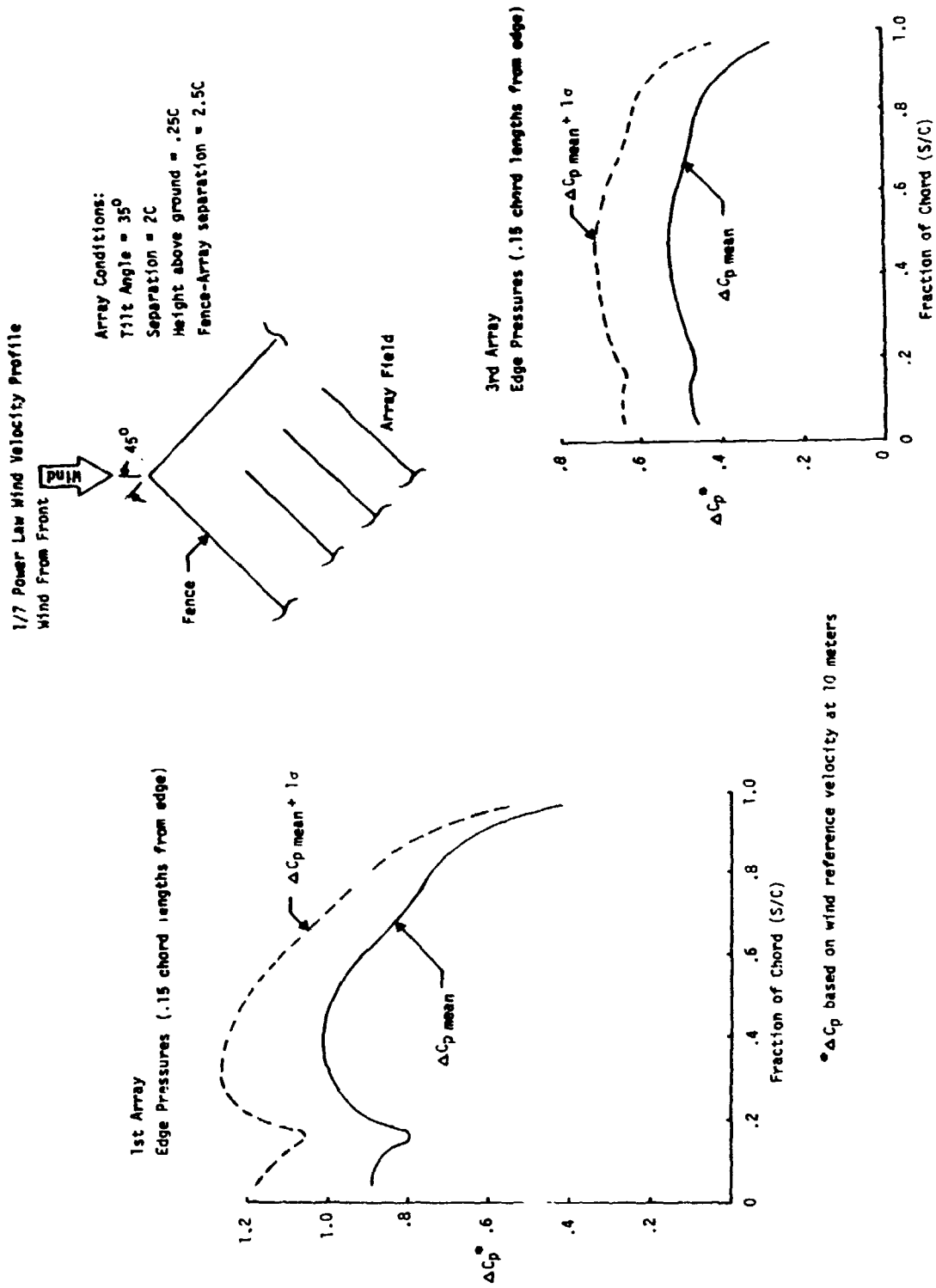


Figure 4-11c. Effect of Oblique Winds on Array Edge Pressure Distribution
(Conventional Fence, Wind from Front)

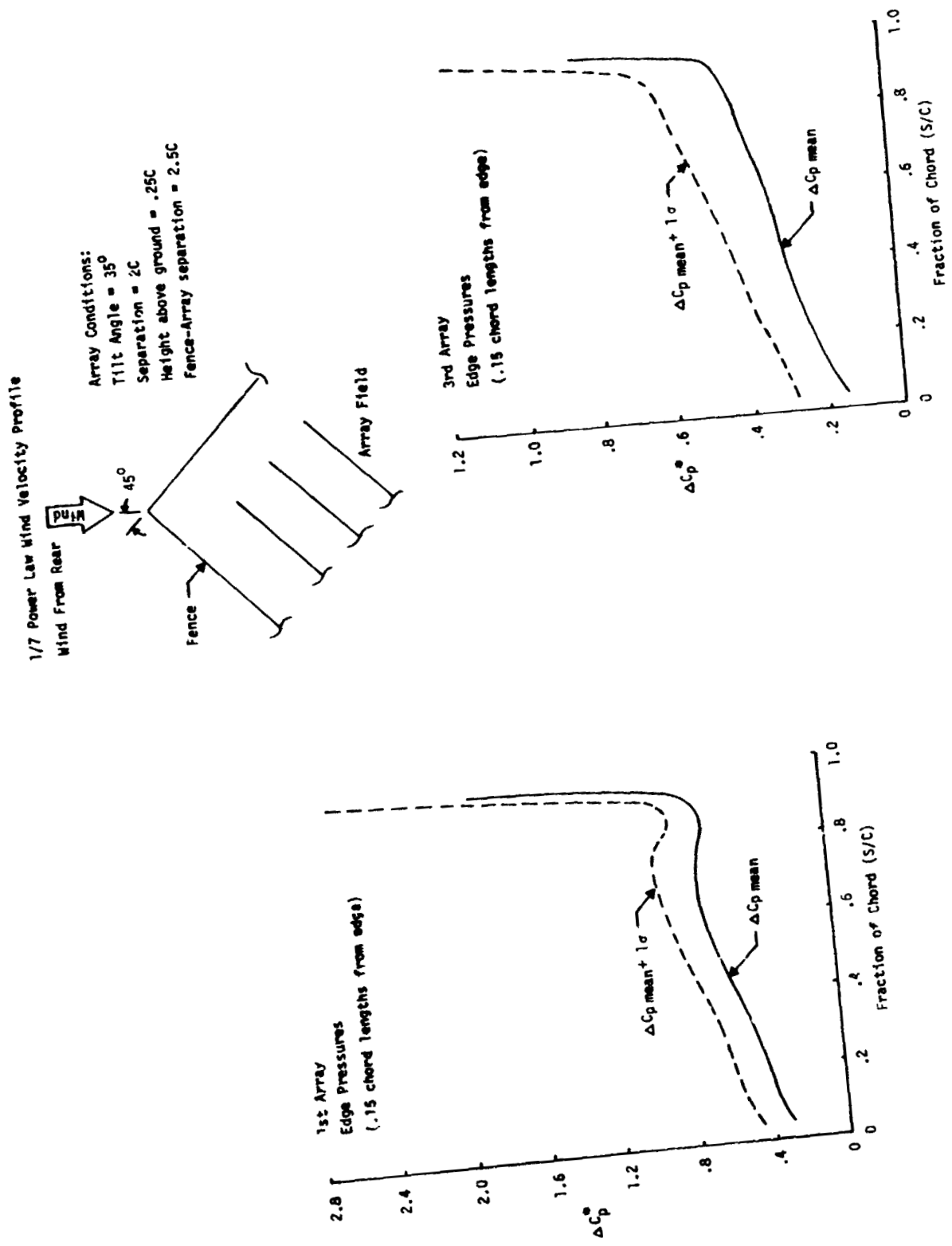
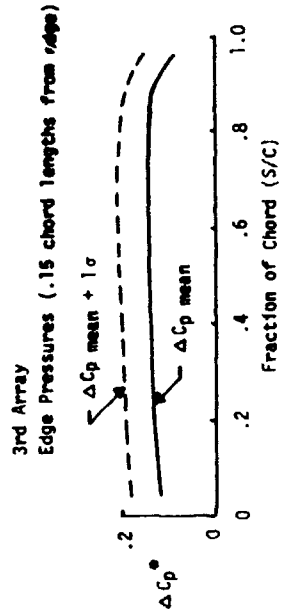
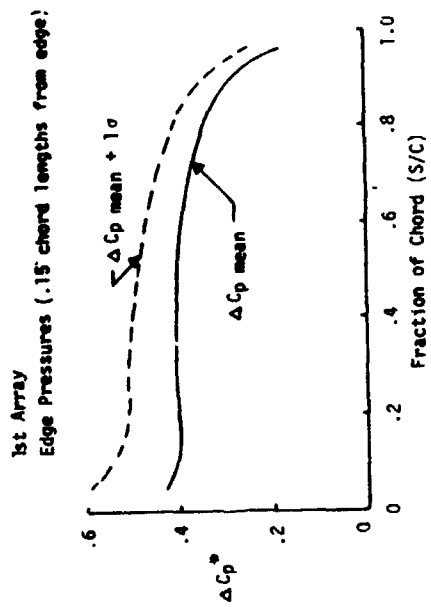
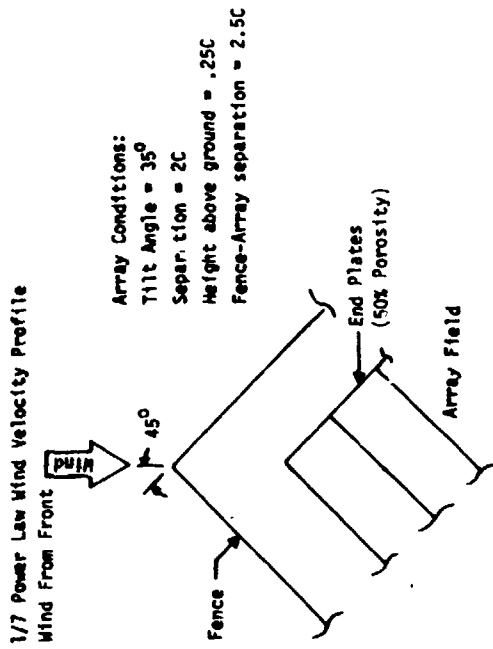
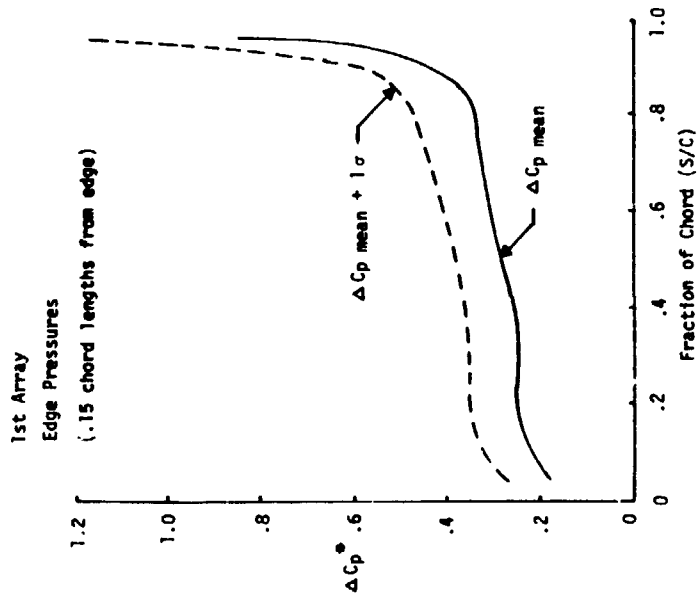
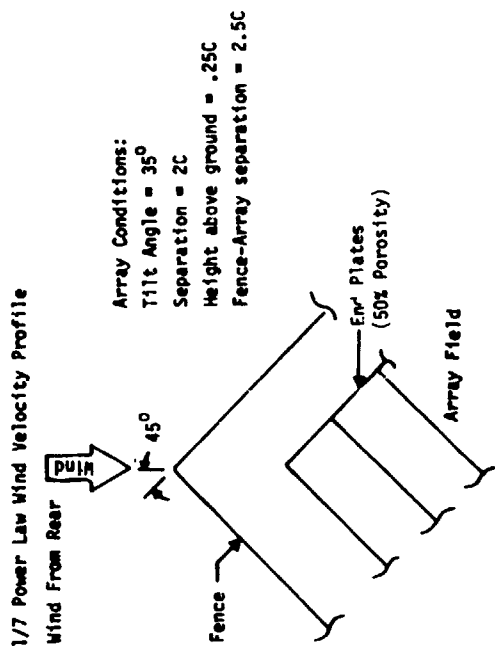


Figure 4-11d. Effect of Oblique Winds on Array Edge Pressure Distribution (Conventional Fence, Wind from Rear)



* ΔC_p based on wind reference velocity at 10 meters

Figure 4-11e. Effect of Oblique Winds on Array Edge Pressure Distribution (Conventional Fence, Endplated Arrays, Wind from Front)



* ΔC_p based on wind reference velocity at 10 meters

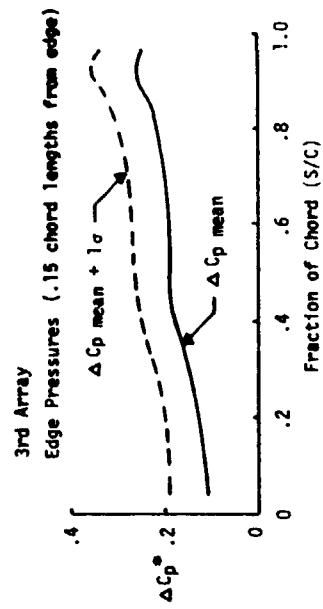
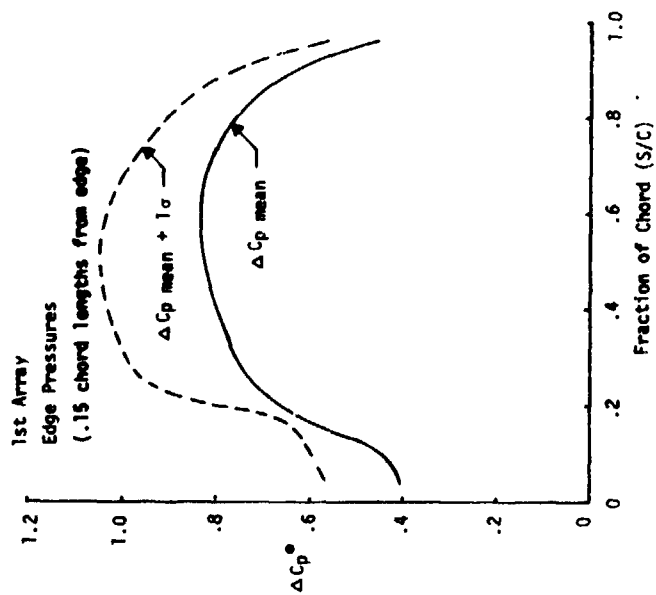
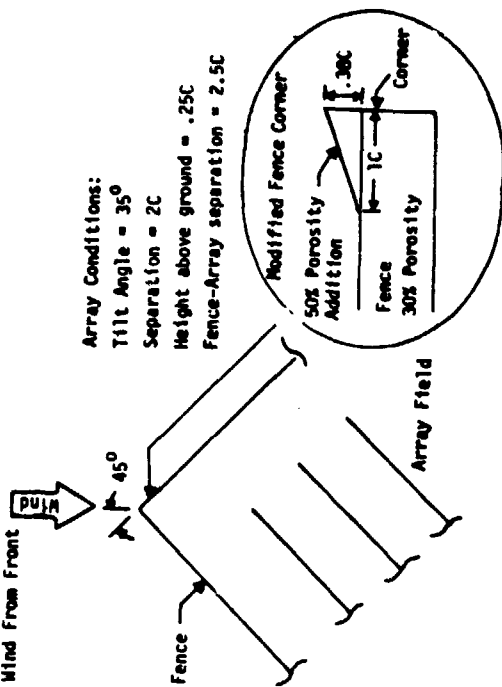


Figure 4-11f. Effect of Oblique Winds on Array Edge Pressure Distribution (Conventional Fence, Endplated Arrays, Wind from Rear)

1/7 Power Law Wind Velocity Profile
Wind From Front



* ΔC_p based on wind reference velocity at 10 meters

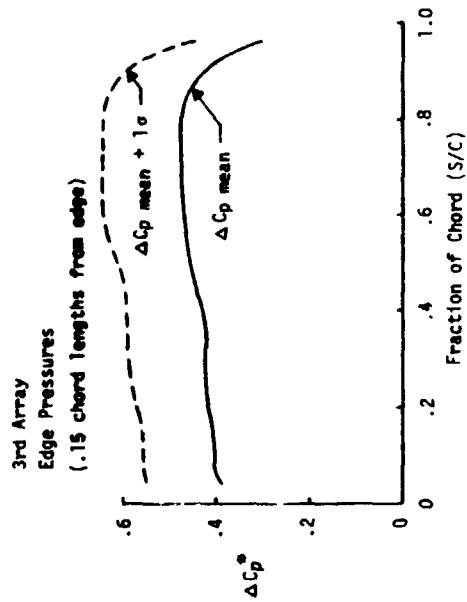


Figure 4-11g. Effect of Oblique Winds on Array Edge Pressure Distribution (Modified Fence Corner, Wind from Front)

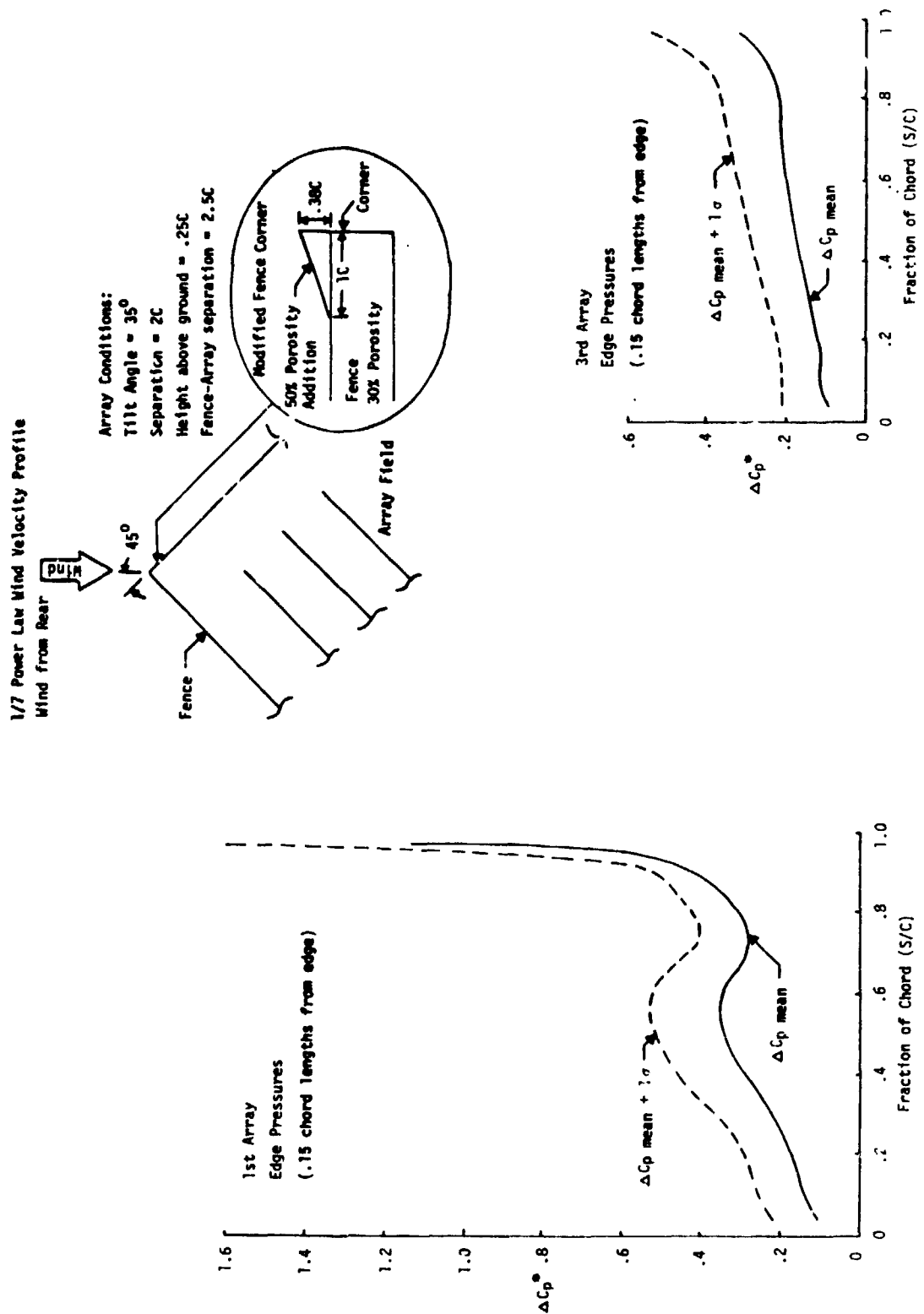


Figure 4-11h. Effect of Oblique Winds on Array Edge Pressure Distribution (Modified Fence Corner, Wind from Rear)

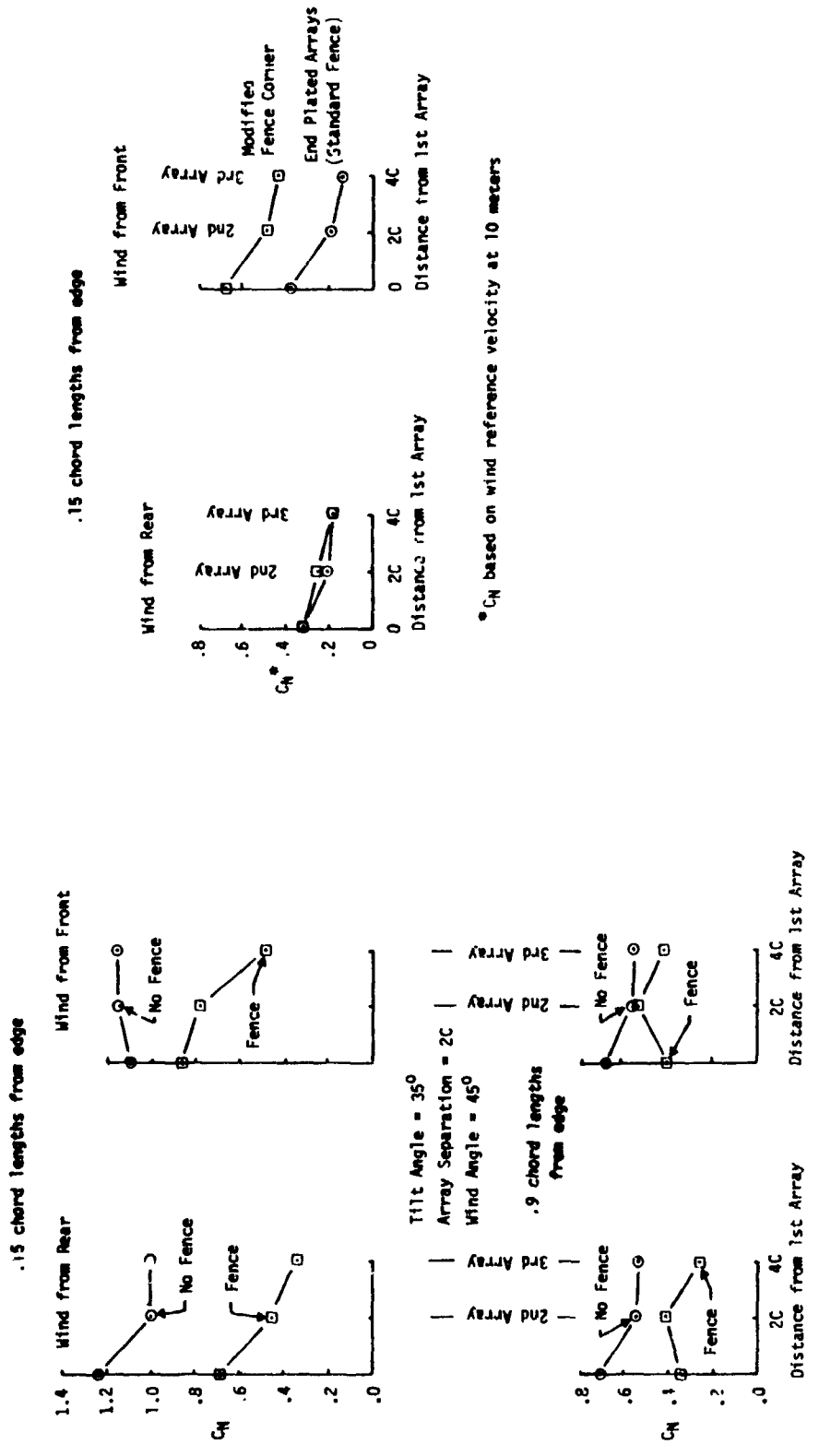


Figure 4-12. Effect of Oblique Winds on Array Normal Force Coefficients at Array Edge

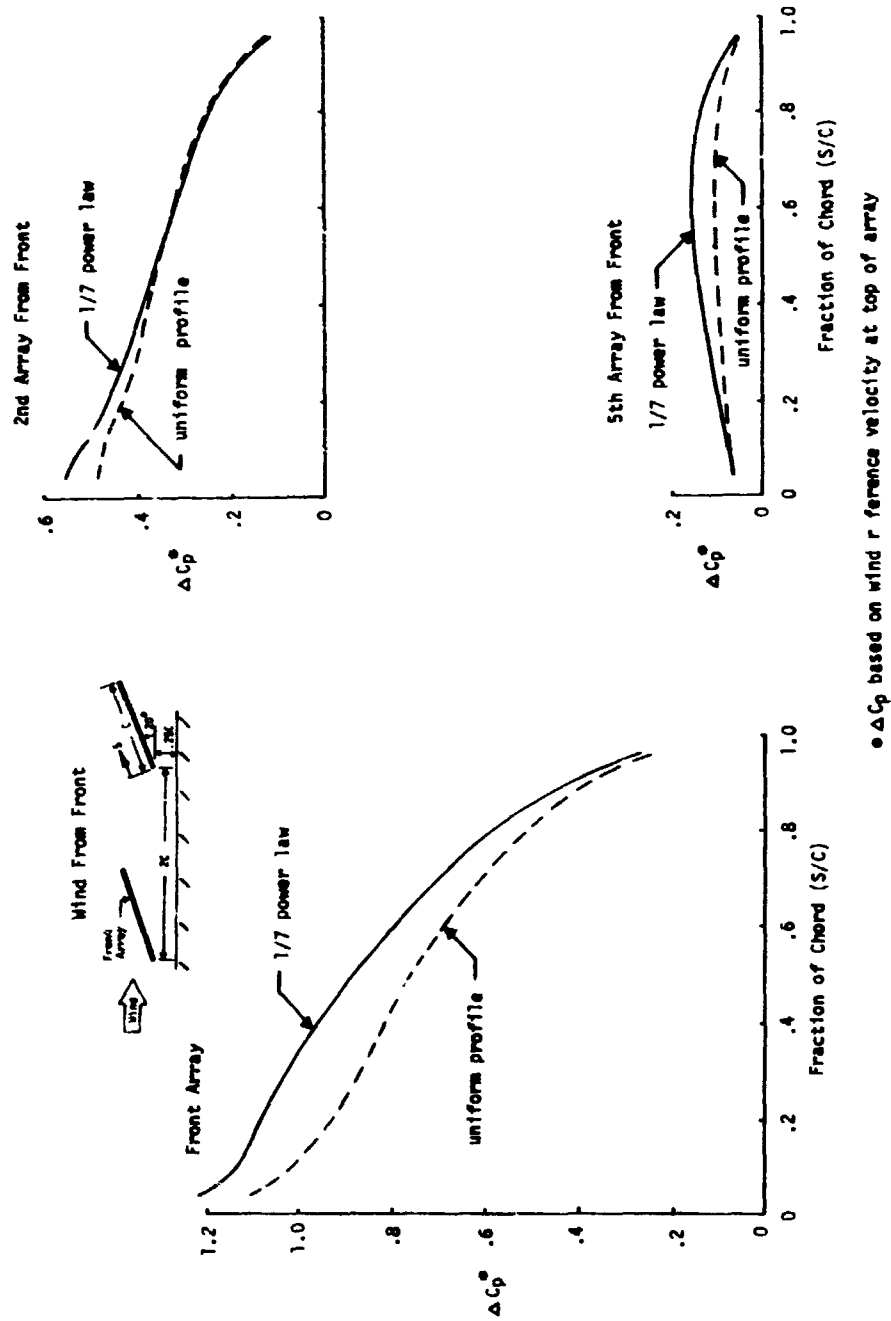
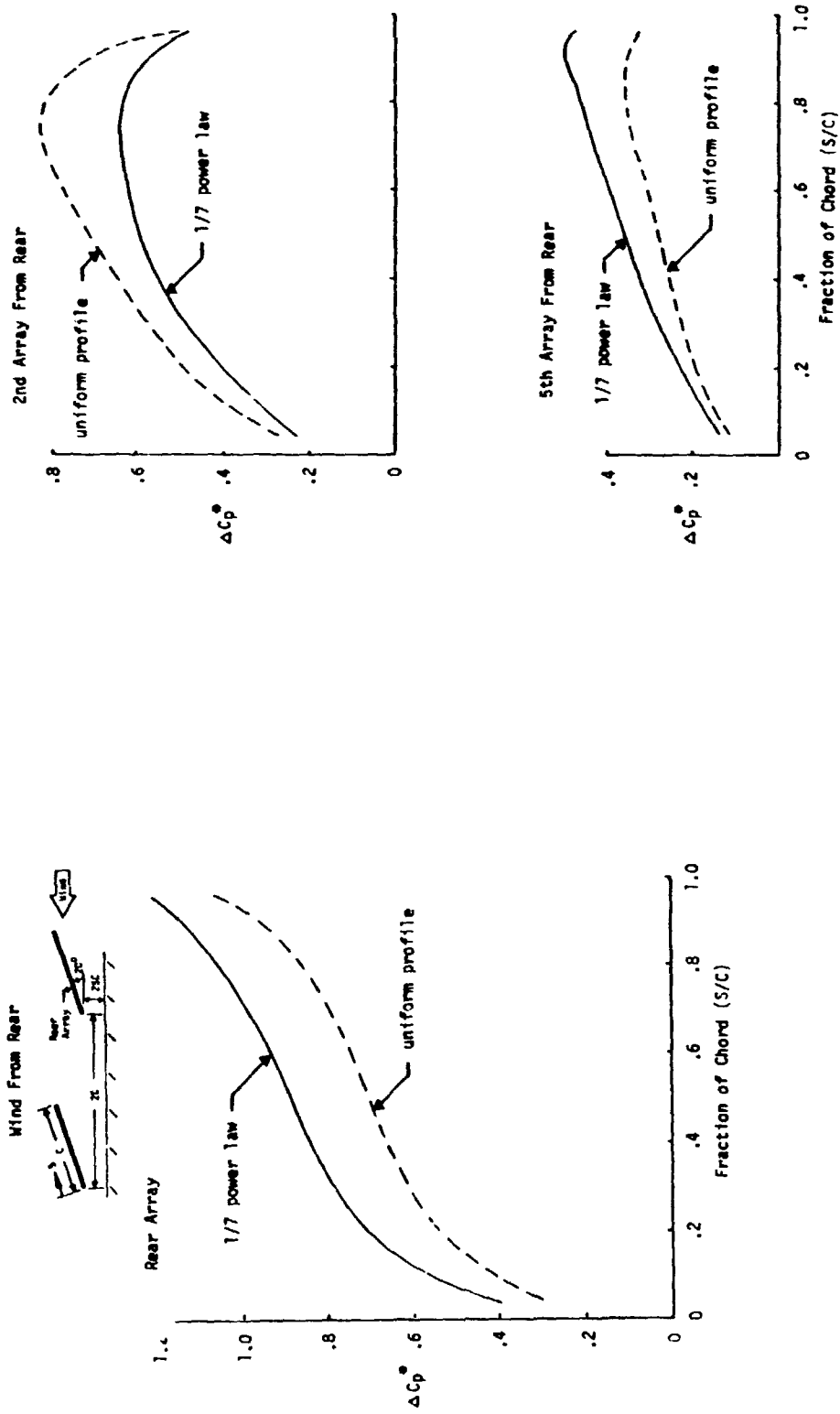


Figure 4-14a. Array Pressure Coefficient Comparison Between Uniform and Boundary Layer Wind Profiles (Tilt Angle = 20°, Wind from Front)



* ΔC_p based on wind reference velocity at top of array

Figure 4-14b. Array Pressure Coefficient Comparison Between Uniform and Boundary Layer Wind Profiles (Tilt Angle = 20°, Wind from Rear)

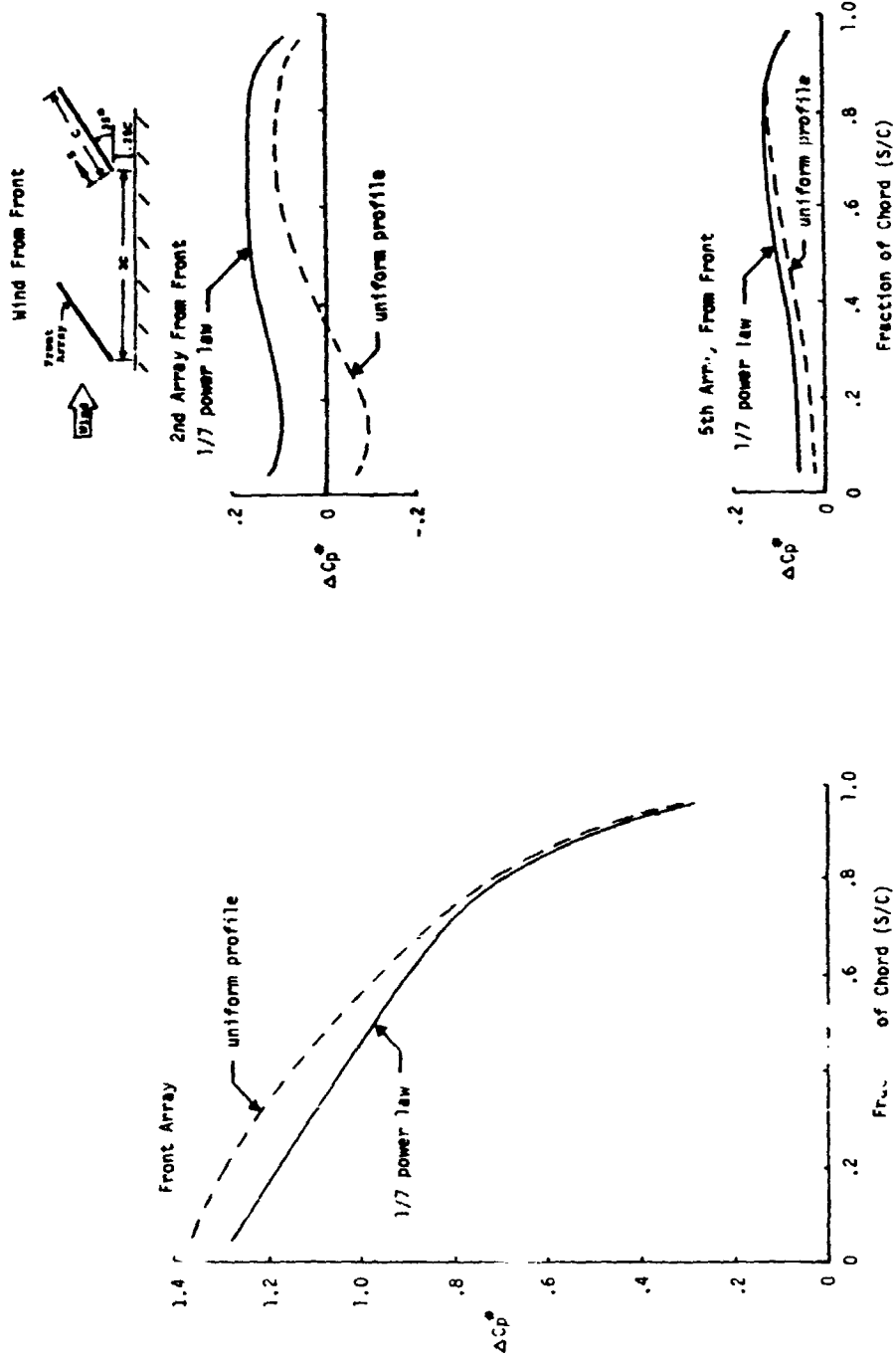


Figure 4-14c. Array Pressure Coefficient Comparison Between Uniform and Boundary Layer Wind Profiles (Tilt Angle = 35°, Wind from Front)

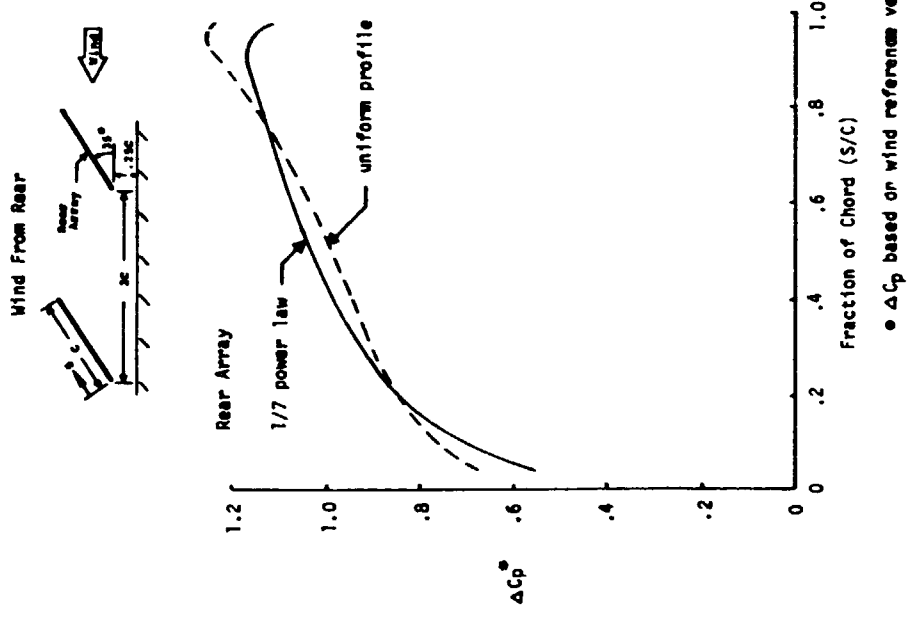
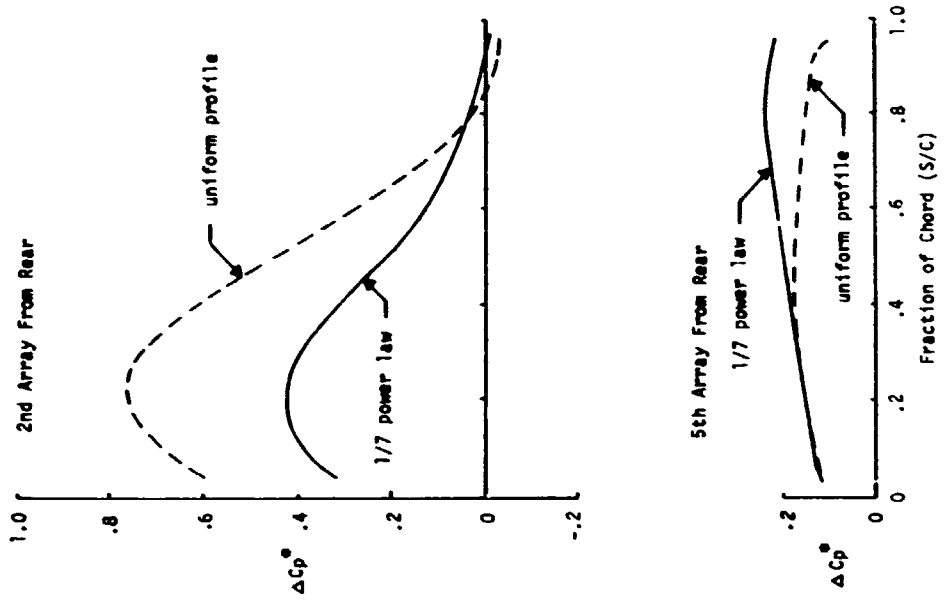


Figure 4-14d. Array Pressure Coefficient Comparison Between Uniform and Boundary Layer Wind Profiles (Tilt Angle=35°, Wind from Rear)

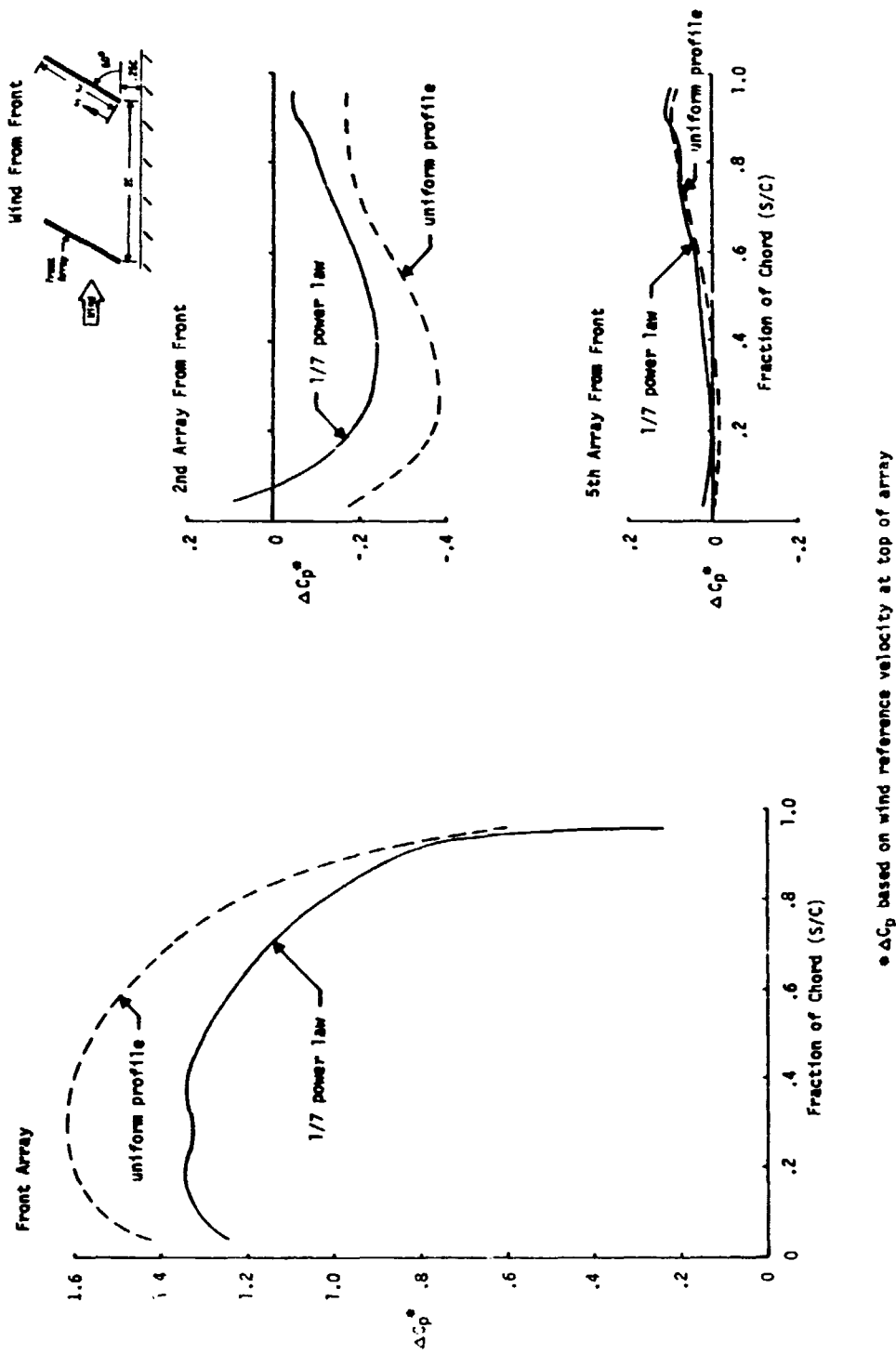
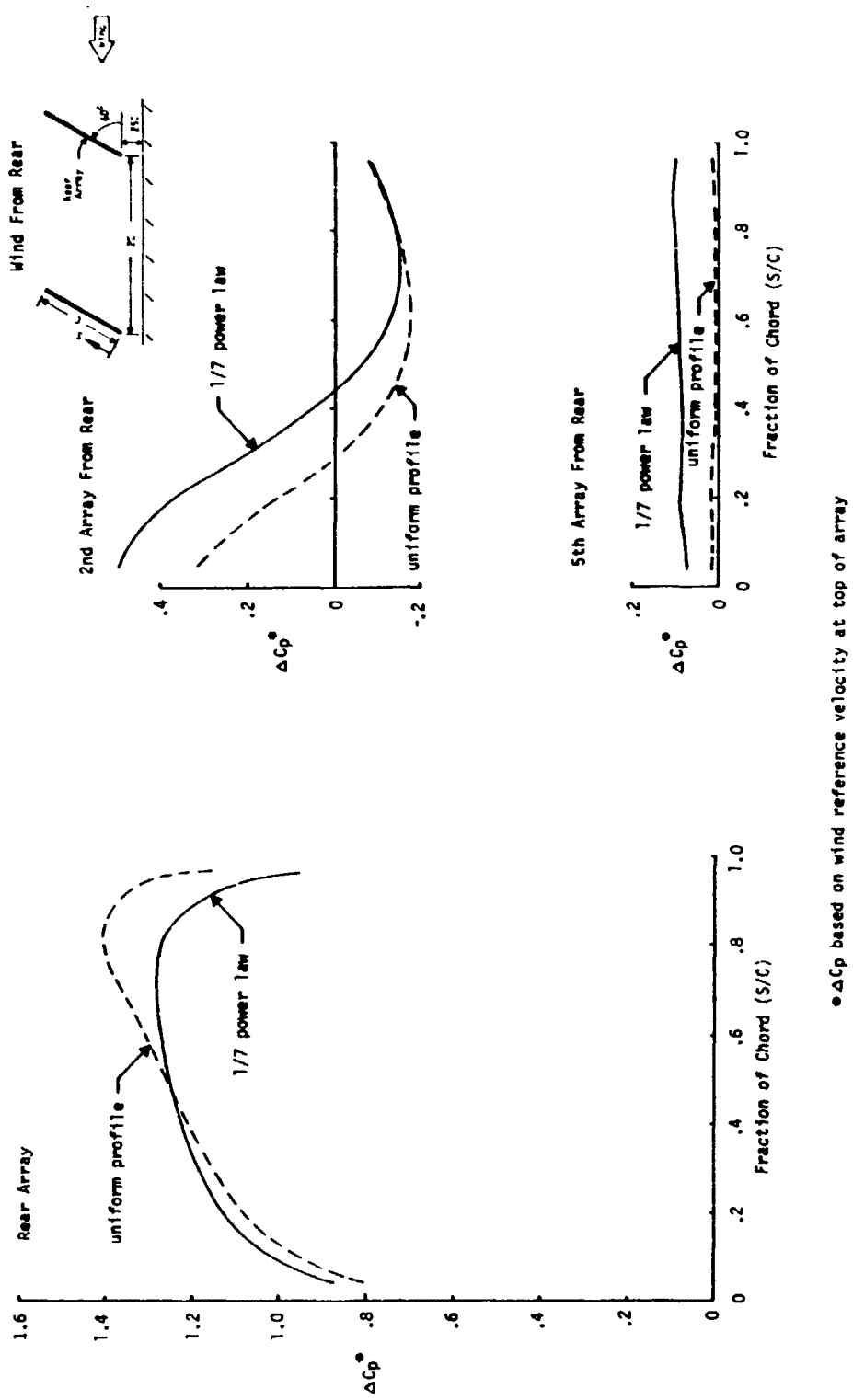
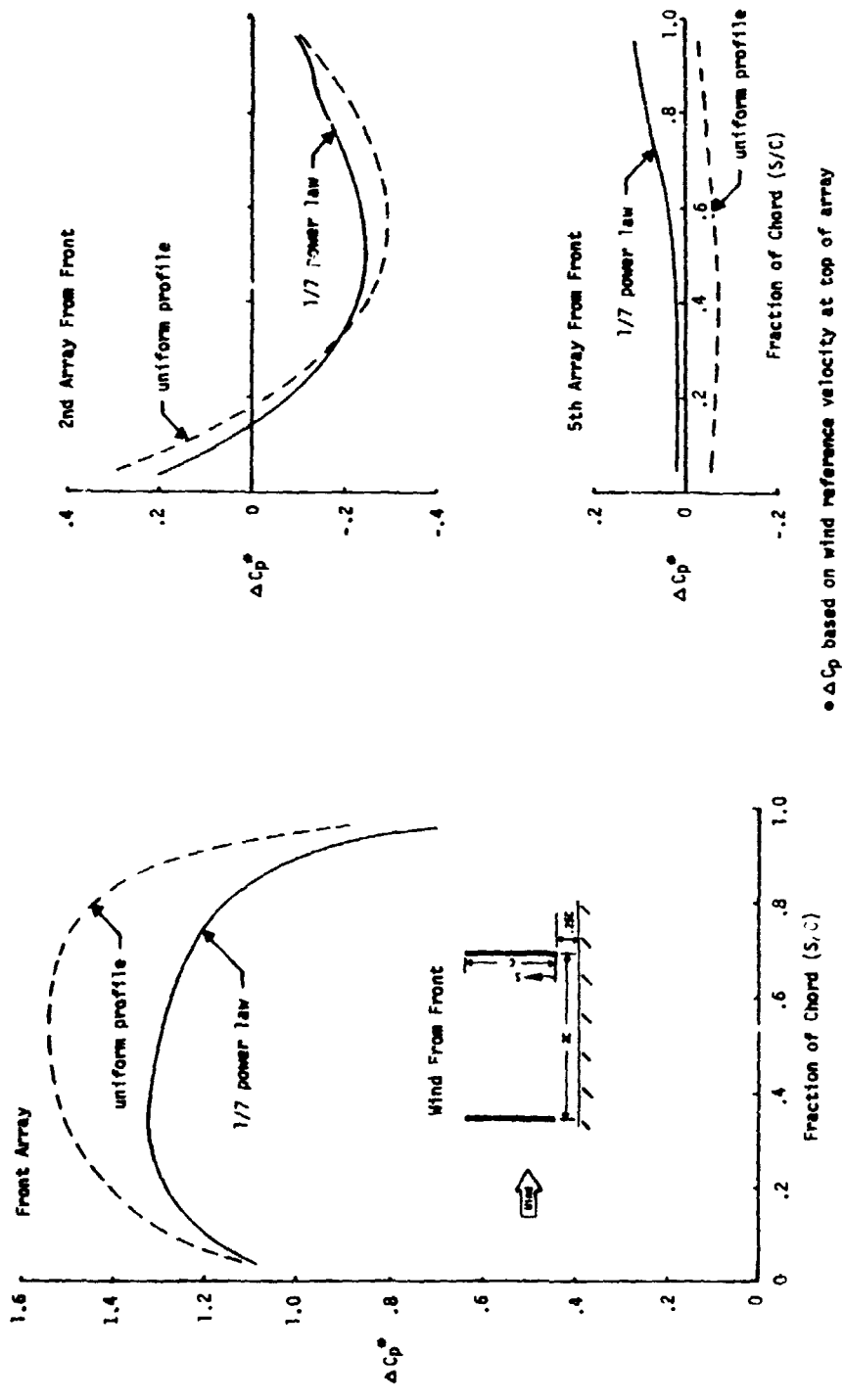


Figure 4-14e. Array Pressure Coefficient Comparison Between Uniform and Boundary Layer Wind Profiles (Tilt Angle = 60°, Wind from Front)



• ΔC_p based on wind reference velocity at top of array

Figure 4-14f. Array Pressure Coefficient Comparison Between Uniform and Boundary Layer Wind Profiles (Tilt Angle = 60° , Wind from Rear)



• ΔC_p based on wind reference velocity at top of array

Figure 4-14g. Array Pressure Coefficient Comparison Between Uniform and Boundary Layer Wind Profiles (Tilt Angle = 90°)

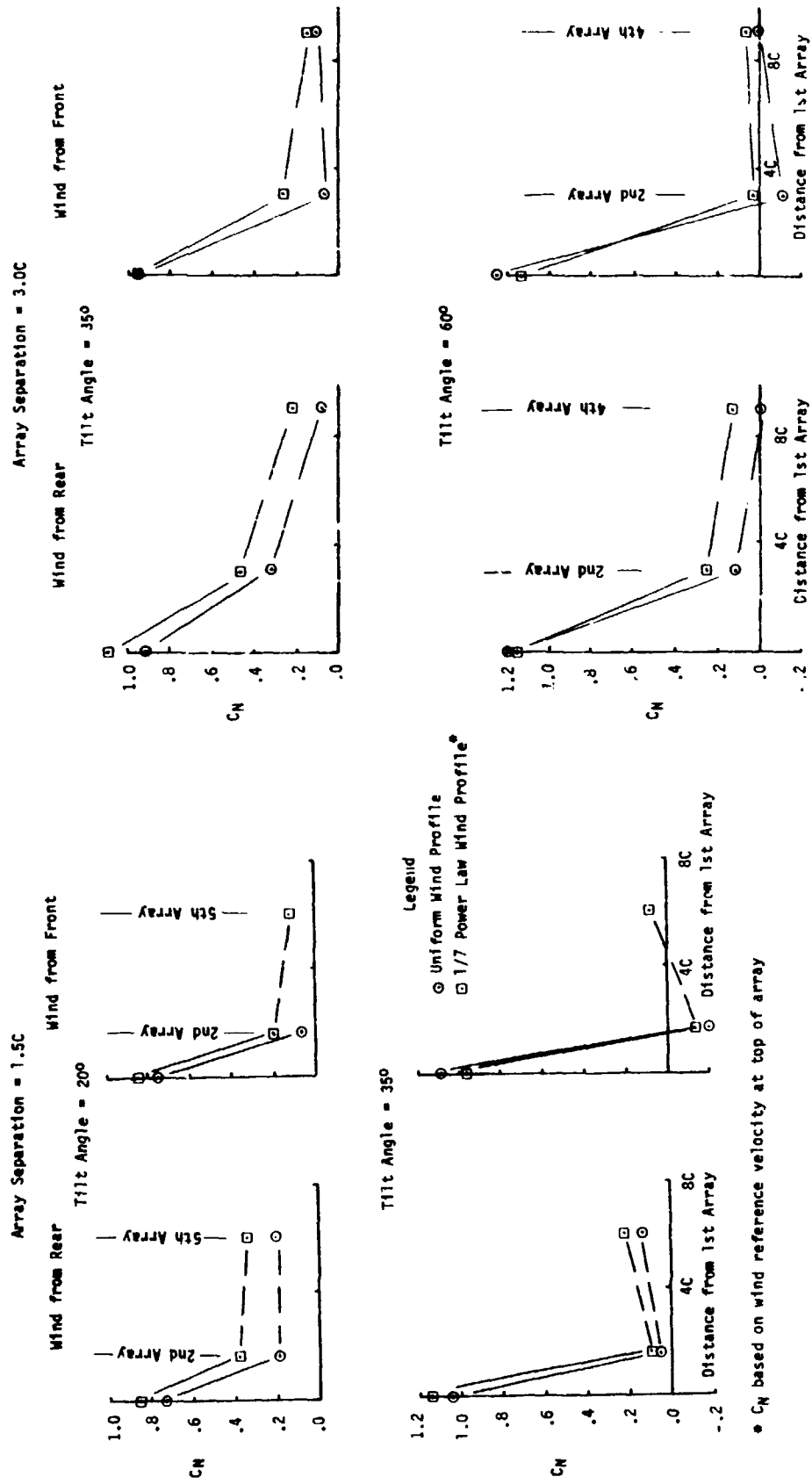


Figure 4-15. Array Normal Force Coefficient Comparison Between Uniform and Boundary Layer Wind Profiles.

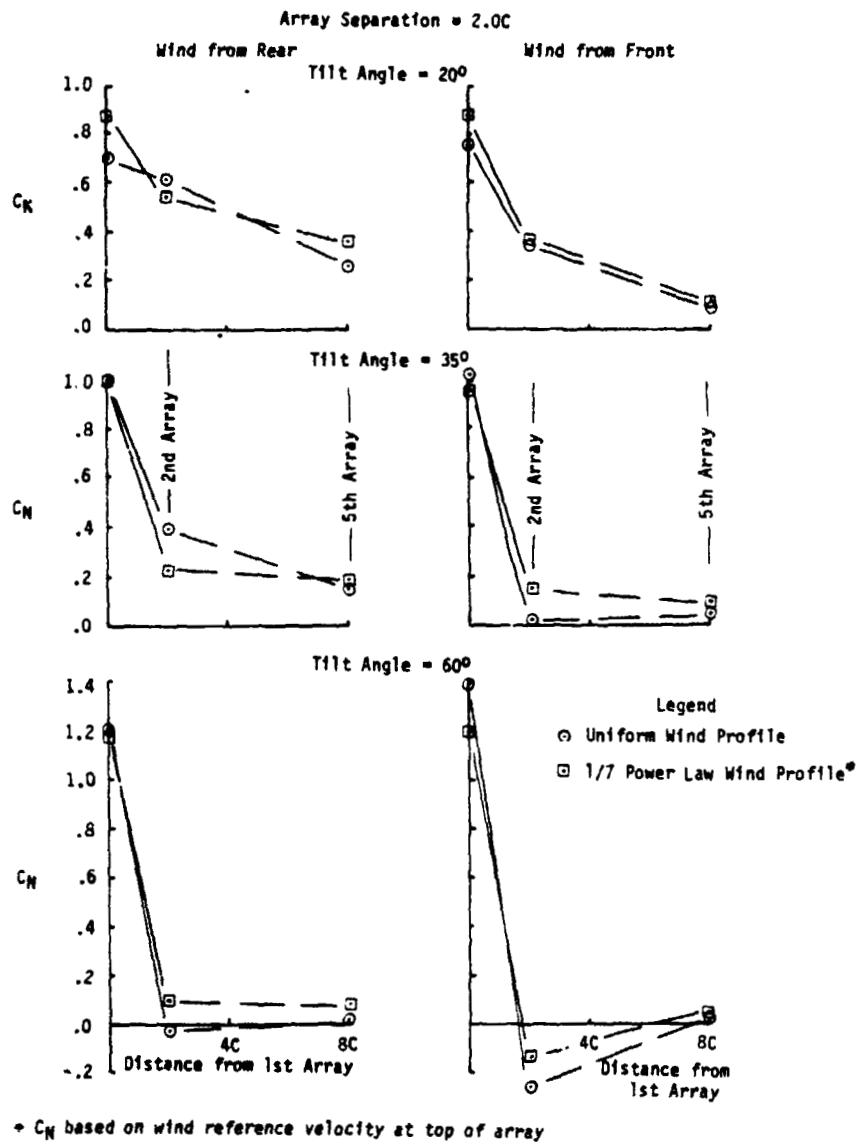


Figure 4-15. Concluded

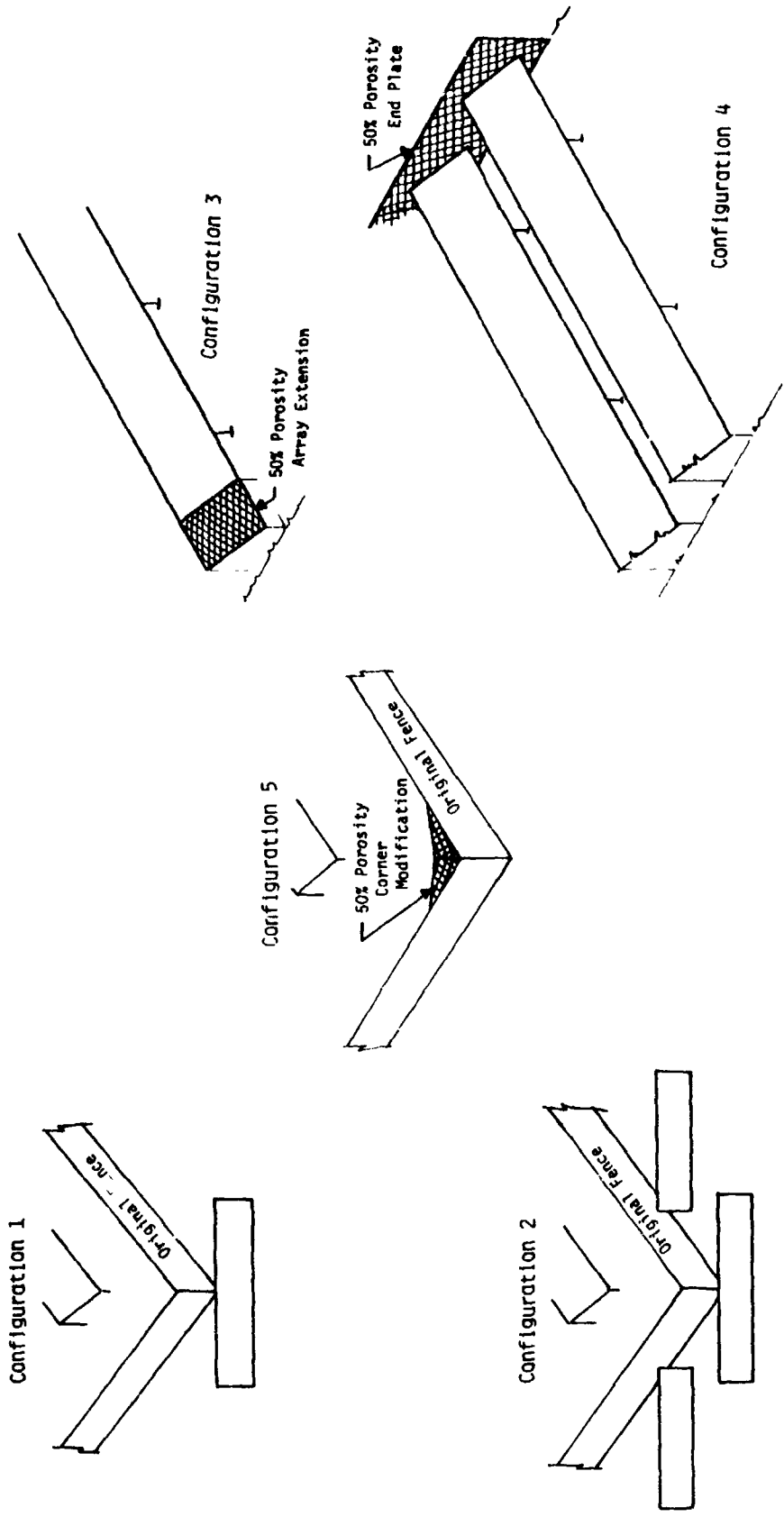


Figure 4-16. Configurations for Edge Load Reduction Study

5.0 THEORETICAL - EXPERIMENTAL RESULTS COMPARISON

The theoretical results developed in Phase II and presented in reference 5 were calculated based on a uniform velocity profile and were then adjusted to reflect the boundary layer velocity profile. Figure 5-1 shows the comparison of the theoretical results to the wind tunnel test results for the net pressure coefficient distribution along the chord of a single array located out of the influence of the ground and in a uniform velocity profile for three angles of attack (20°, 35°, and 60°). (Since the theoretical results were based on an infinite aspect ratio array, all theoretical-experimental comparisons utilize the mid-span test results.) The results differ by approximately 5% to 10% except for very low pressure coefficients; this comparison is considered very good and demonstrates that theoretical methods can be used to accurately predict the aerodynamic loads on an array located sufficiently far from the ground so that ground effects are not a consideration.

When the array is located in close ground proximity, the theoretical method tends to overpredict the pressure coefficients as compared to the wind tunnel test; this is shown in Figure 5-2. When the tilt angle of the array is small (20°), the theoretical results match the wind tunnel test results within approximately 20% or less. However, as the tilt angle increases (35° and 60°), the theoretical-experimental results become increasingly farther apart. The difference is due (at least in part, to the blockage effect that occurs to the air flow because of the restricted area between the ground and the lower edge of the array and the effects of air viscosity (not considered in the theoretical model) in this restricted flow regime. From the test results, of which Figure 5-3 is a typical example, flow blockage is seen to occur because of the ground-to-array gap. Figure 5-3 indicates that the flow is blocked and decreases in velocity as the gap is reduced in value from $H/C = \infty$ to .25 as evidenced by the increase in pressure on the lower edge ($S/C = 0$) on the windward face of the array and by the smaller negative pressure on the base pressure face. Because of the flow restriction at the gap, the flow in front of the windward face of the array is also affected, and the windward face pressure distribution is modified across the total face depending on the amount of restriction of the flow. In contrast to the test results, the theoretical separated inviscid flow method predicts that the air flow increases in velocity to allow a given mass of air to flow through the gap to compensate for the restricted gap area. This increase in velocity is further intensified as the

array presents a more bluff configuration to the wind at increasing tilt angles. Consequently, because of the inviscid flow assumptions in the theoretical method, there is an increasing spread with tilt angle between theoretical and test results as the tilt angle is increased from 20°.

In the Phase II study, reference 5, it was recommended that the theoretical normal force and pressure coefficients for all downwind arrays be calculated as 60% of the windward array. The amount of protection afforded to the downwind arrays in an array field is more complex than can be covered by a blanket percent reduction as shown in Figure 5-4; it is a function of the tilt angle and to a lesser extent, the wind direction. In general, the larger the tilt angle, the greater is the protection afforded to the downwind arrays by the windward array and the greater the load reduction. From the theoretical - experimental data comparison, the theoretical results presented in reference 5 are conservative for steady state wind loads on arrays without protective fences and can be used for design studies of photovoltaic flat plate arrays in lieu of specific test data relating to the design. However, the design would be penalized in terms of structural costs by the conservative loads.

When a fence is used as a protective wind barrier for the arrays, reference 5 recommended using the velocity isotachs behind a fence to calculate the dynamic pressure. Using this dynamic pressure with the theoretical normal force coefficients, the average normal forces per unit area were calculated and presented in reference 5 as Table 6-2 for various tilt angles and for an 8.2 foot fence. The appropriate results were extracted and are presented in Table 5-1 of this document, together with the results from the wind tunnel test for arrays positioned behind a 6 foot fence and in a boundary layer wind. The comparison is reasonably satisfactory at the 20° tilt angle, less so at 35°, and poor at 60°. Thus, the technique suggested in reference 5 should only be used for the smaller tilt angles and only when more reliable results are not available.

Table 5-1. Example of Average Normal Wind Forces on Arrays behind Protective Fences by Theoretical and Wind Tunnel Test Methods (Behind)

Wind from Front			
	Average Normal Wind Forces per unit area (psf)		
Tilt Angle	20°	35°	60°
Theory *	1.06	1.63	9.62
W.T. Test	1.03	2.46	4.92
Wind from Rear			
Theory *	1.63	2.22	11.21
W.T. Test	1.44	2.46	5.13

* Dynamic factor of 1.5 removed from Table 6-2, reference 5

The array key wind parameters detailed in reference 5 are also shown in Figure 5-5. These parameters were verified by the wind tunnel test except for the dynamic pressure which is a fundamental parameter used in both test and theoretical methods. In general, the trends of all parameters, except ground clearance, were verified. However, the test results show that the parameters are all interrelated and cannot be separated as in Figure 5-5. As an example, angle of attack, ground clearance, and array spacing, are all affected by each other. Consequently, to predict the sensitivity precisely, a family of curves would be required varying only one parameter at a time. This would require an enormous amount of test data and results.

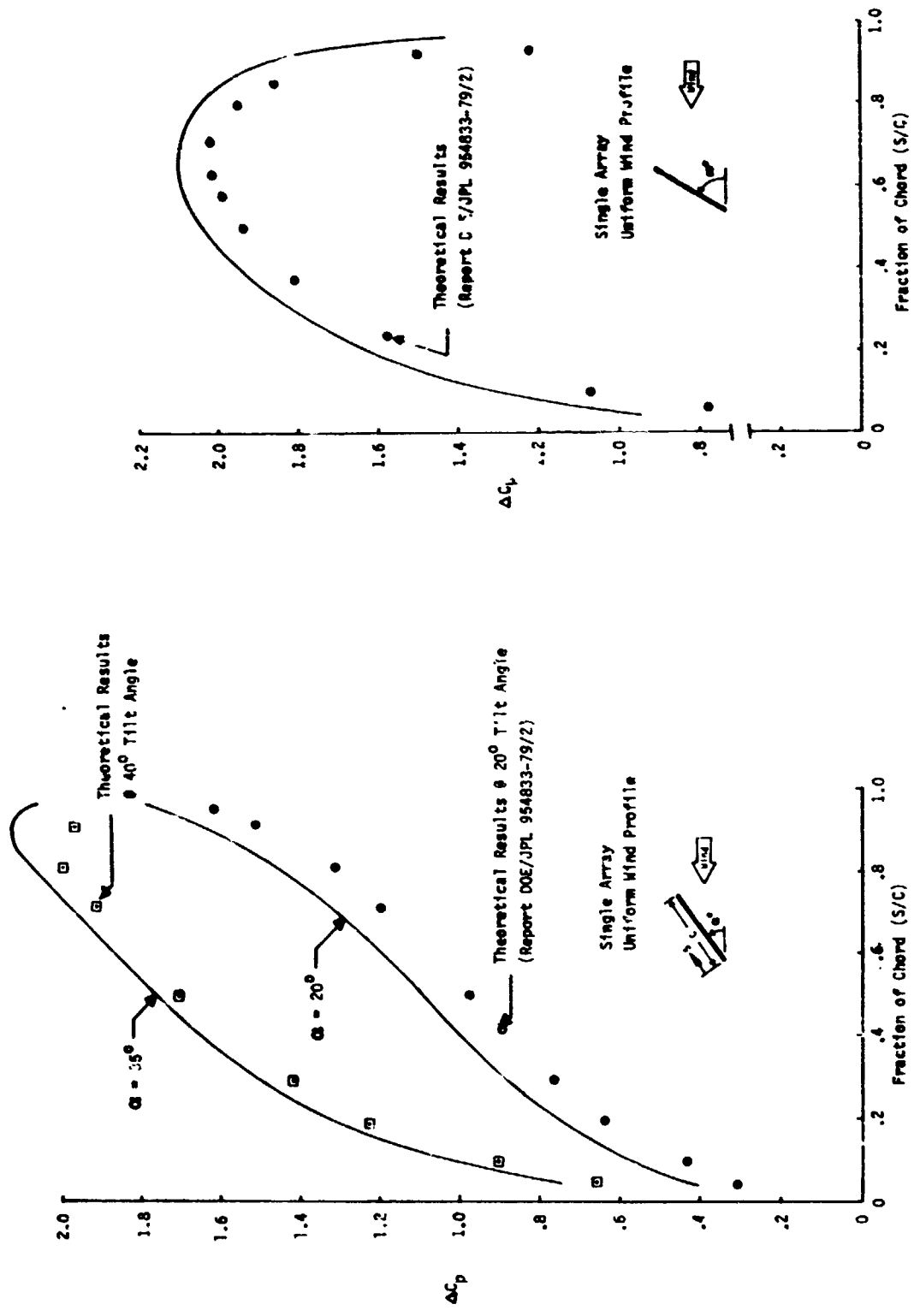


Figure 5-1. Array Pressure Coefficient Distribution Comparison Between Wind Tunnel Test and Theoretical Methods in Free Air

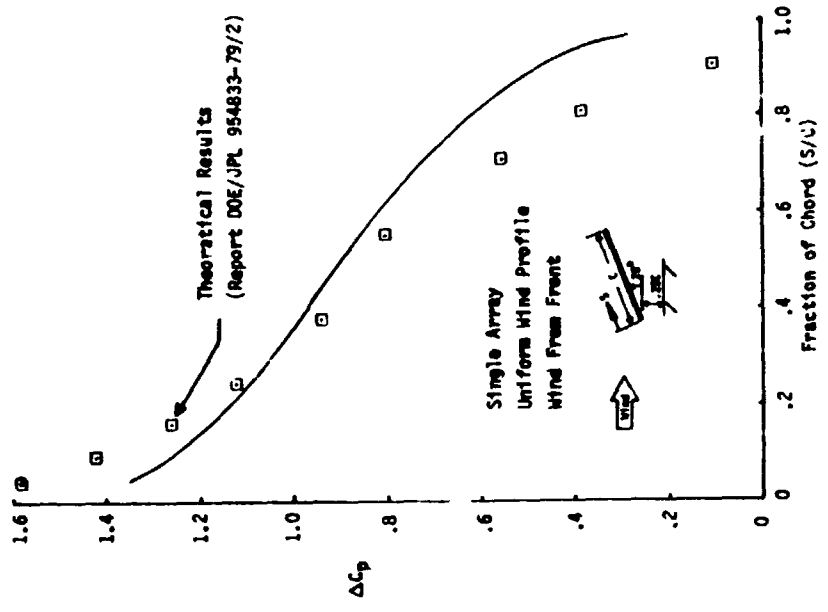
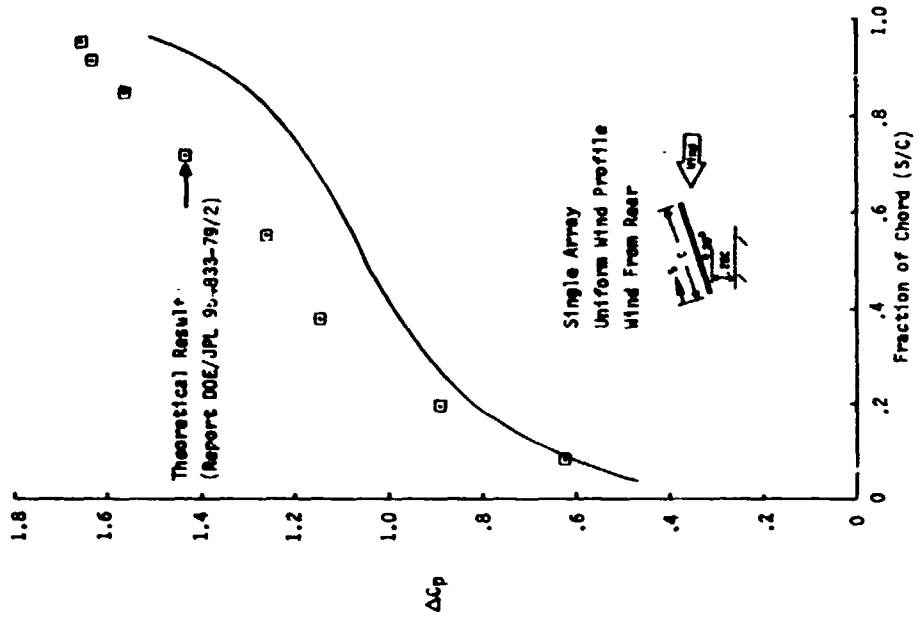


Figure 5-2a. Array Pressure Coefficient Distribution Comparison Between Wind Tunnel Test and Theoretical Methods in Close Ground Proximity (Tilt Angle = 20°)

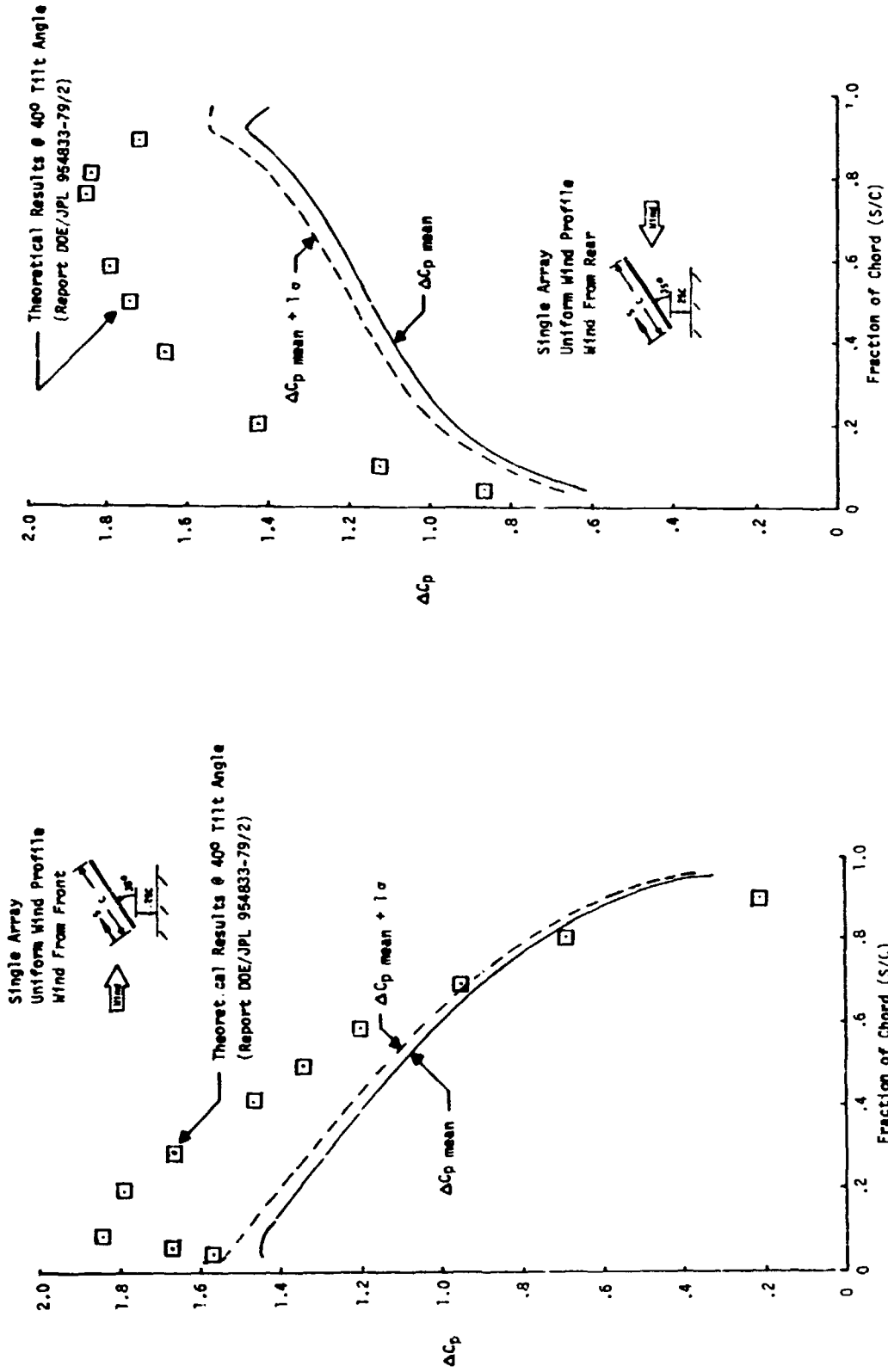


Figure 5-2b. Array Pressure Coefficient Distribution Comparison Between Wind Tunnel Test and Theoretical Methods In Close Ground Proximity (Tilt Angle = 35°)

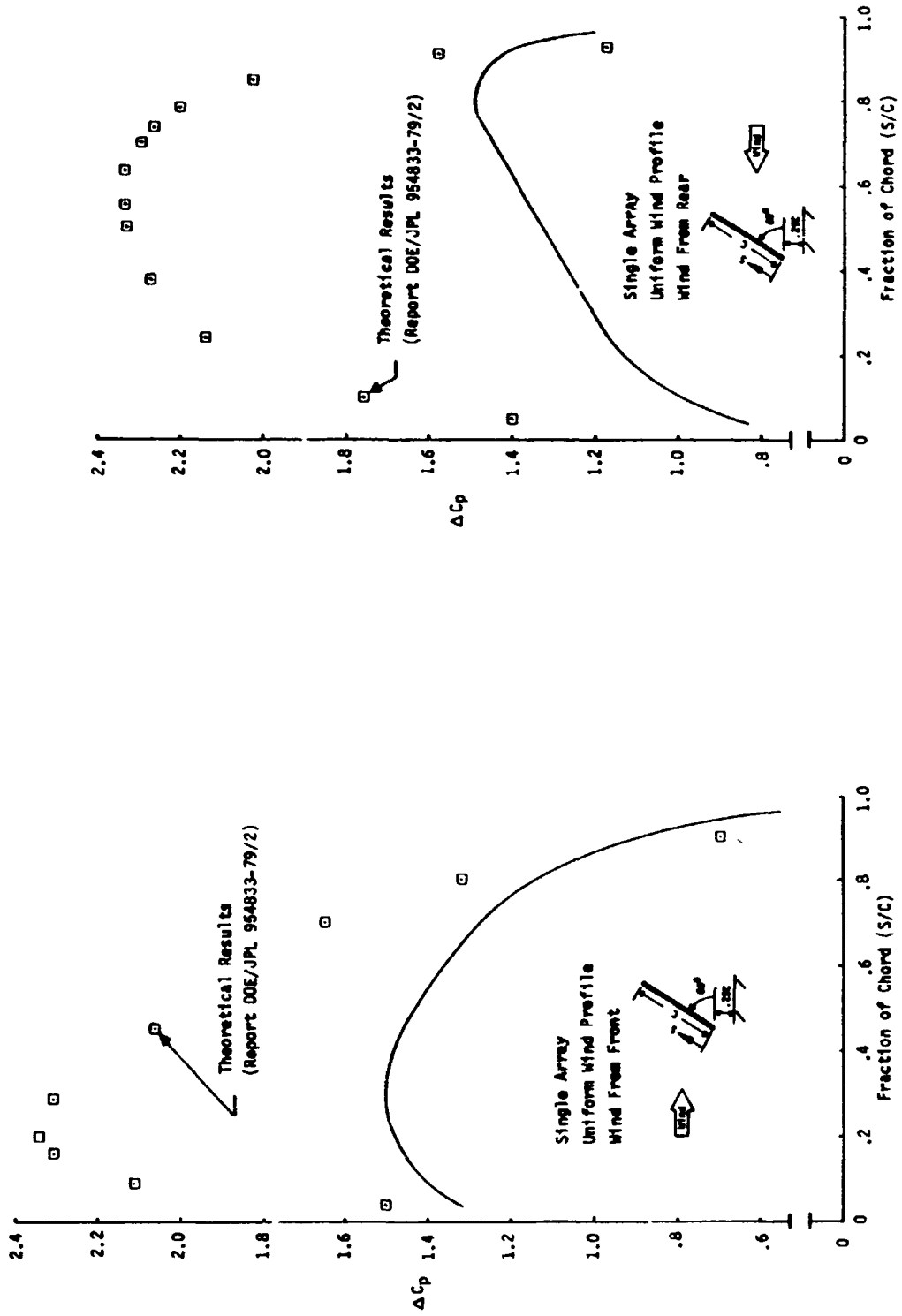
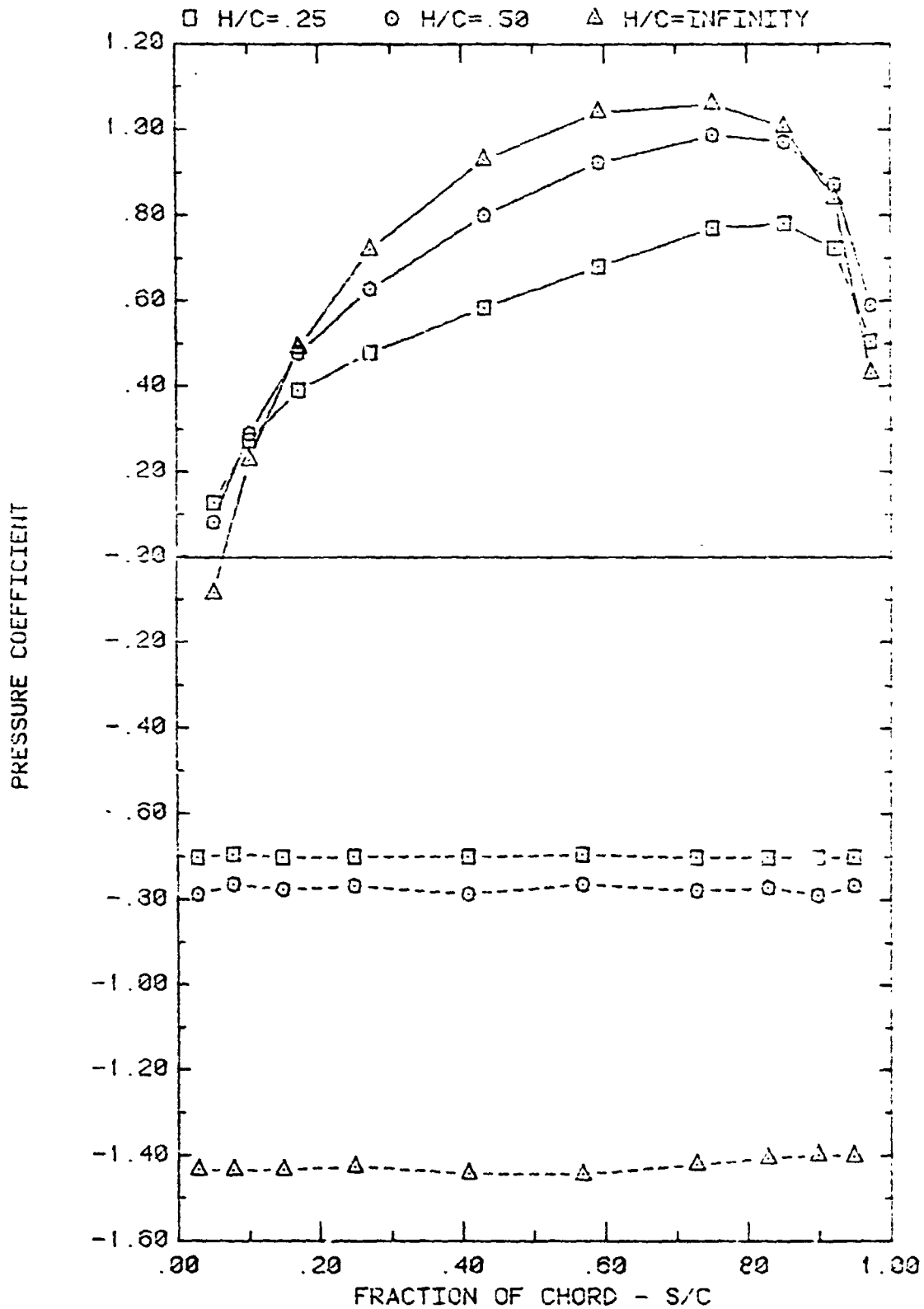


Figure 5-2c. Array Pressure Coefficient Distribution Comparison Between Wind Tunnel Test and Theoretical Methods in Close Ground Proximity (Tilt Angle = 60°)



FRONT AND BACK PRESSURES ON A SINGLE ARRAY IN UNIFORM FLOW
 EFFECT OF GROUND CLEARANCE FOR ATTACK ANGLE, ALPHA = 60

Figure 5-3. Effect of Ground Clearance on Front and Back Array Pressures in Uniform Flow (Tilt Angle = 60°, Wind from Back)

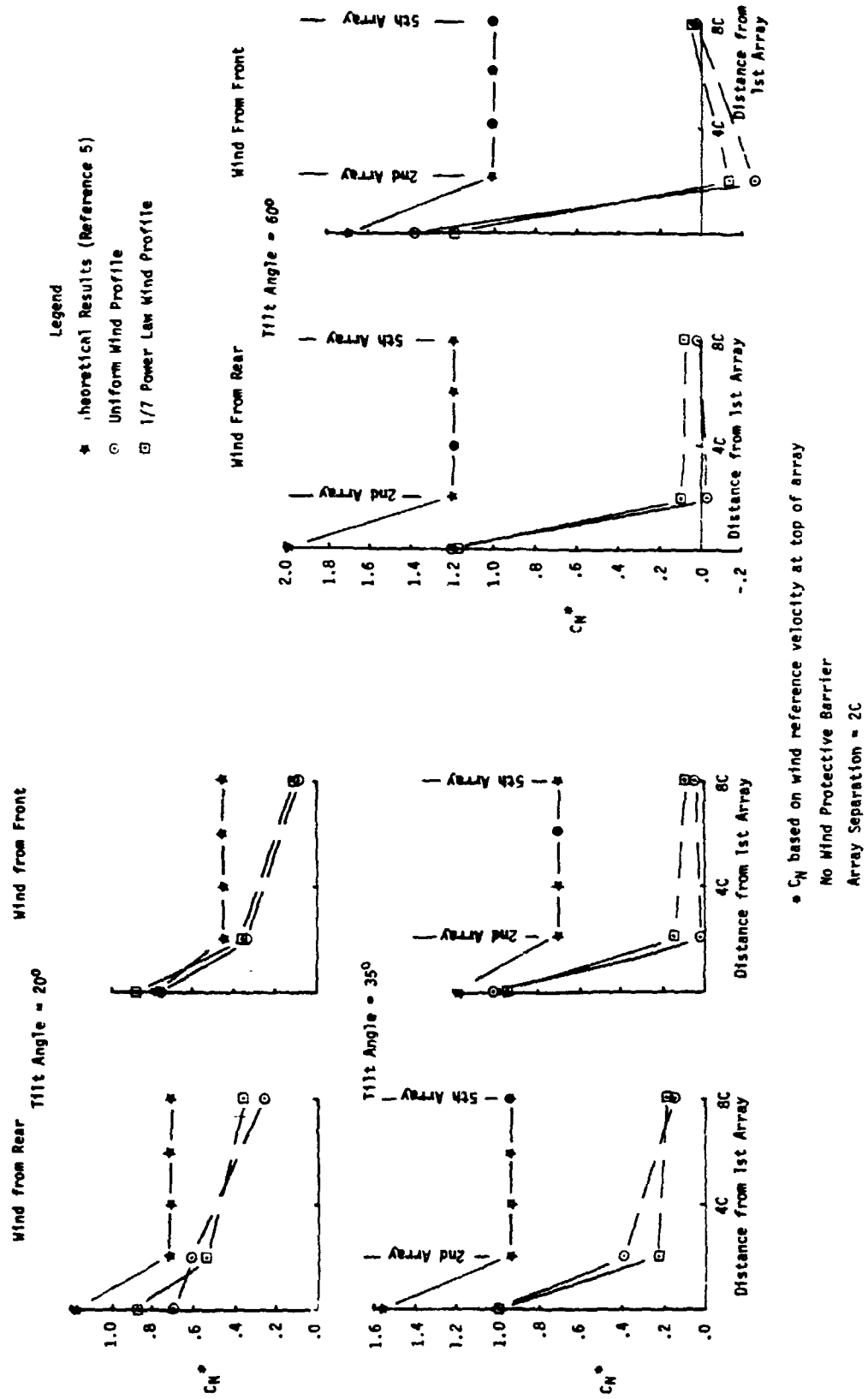


Figure 5-4. Array Normal Force Coefficient Comparison Between Wind Tunnel Test and Theoretical Methods

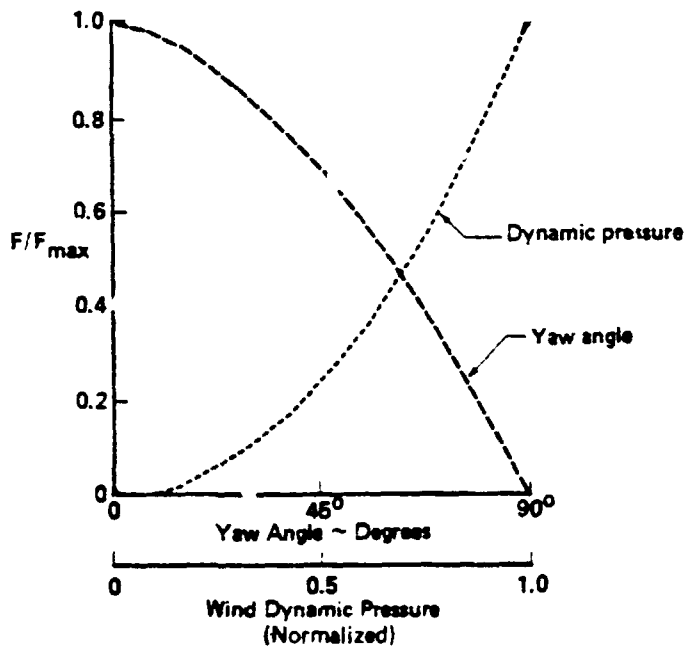
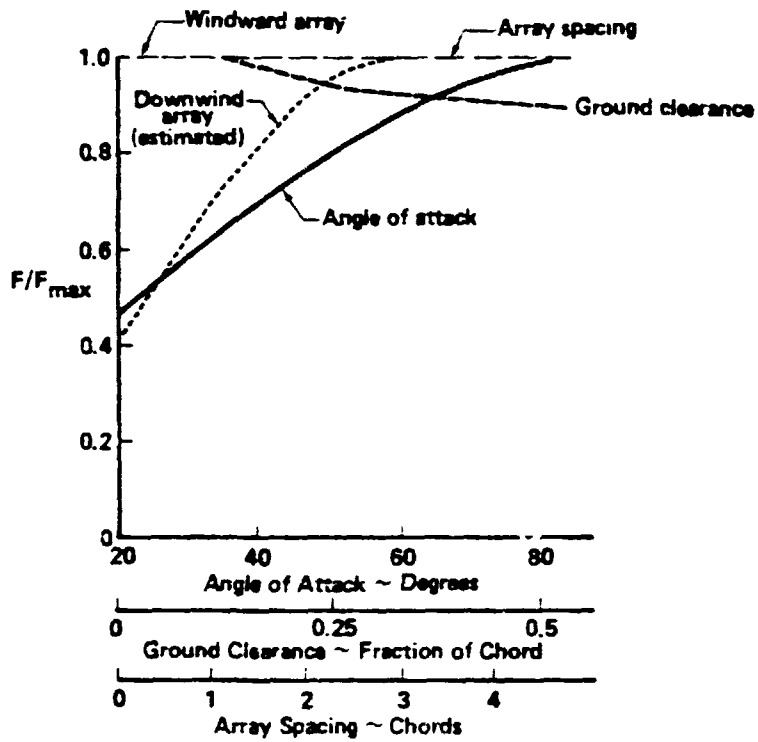


Figure 5-5. Theoretical Key Wind Loads Parameters and Their Sensitivity in Separated Flow Analyses (Reference 5)

6.0 DISCUSSION AND CONCLUSIONS

Currently, there are no known published data or results of wind loads from full sized photovoltaic arrays placed in the natural environment. The wind tunnel test utilizing the Meteorological Wind Tunnel and simulating the natural boundary layer wind as a $1/7$ power law wind profile is the closest simulation compared to theoretical methods or uniform wind tunnel simulations of arrays placed in the natural environment. Therefore, all results from the different analyses were compared to the results obtained from the wind tunnel test that simulated the wind boundary layer.

Theoretical methods to calculate pressures and forces on arrays positioned at tilt angles greater than fifteen to twenty degrees require the use of separated flow analysis techniques that are directly applicable only to single arrays with infinite aspect ratios. Thus, the results must be extrapolated or modified for the array edges, arrays positioned behind fences, and interior arrays in an array field as performed in reference 5. The theoretical array pressure distribution and normal force results for the windward array and interior arrays were shown to be conservative (over designed) compared to the boundary layer wind tunnel test. The theoretical normal force results for arrays positioned behind fences are fairly close but conservative for tilt angles less than 35° and become much more conservative for tilt angles near 60° . As a result, if theoretical means are used for determining steady state wind loads on photovoltaic arrays and for sizing the array structural members, the arrays will be overstrength for steady state wind loading.

Most previous wind tunnel tests have been conducted for various shapes of structure in uniform wind profiles and out of the ground effect. Normal force coefficients for flat plates, cylinders, and spheres are readily available in the literature for this condition. If the flat plate coefficients for plates out of the ground effect are used for arrays close to the ground, they will yield normal wind forces that are ultra conservative. If test results are obtained for flat plate arrays in an array field and in a uniform flow wind tunnel with the influence of the ground effect, the results are variable, some conditions are conservative and others unconservative. Consequently, the results from a uniform flow wind tunnel for flat plate arrays would require a factor of safety to be applied to assure that the results are conservative if

used in an absolute sense for design values. However, the results are adequate to be used for trade studies in preliminary design such as using load alleviation devices, etc.

The boundary layer wind tunnel test for the flat plate photovoltaic array field produced some interesting results and conclusions. A fence (or the first windward array, if no fence exists) protects the downwind arrays except near the array edges from the wind. The wind normal forces and pressures of these downwind arrays are several times smaller than the first windward array when no fence protects it. In addition, as the tilt angles of the arrays increase, the greater the wind protection received by the downwind arrays and the smaller the normal forces and pressures on the arrays. Wind direction (frontal or rearward) does not significantly affect the results. The normal forces and pressures on arrays positioned as close as three to four rows from the front have the same magnitude whether a fence protects the field or not. A fence will significantly lower the loads on the first array and can even lower the first array loads below the loads on the arrays within the field. Thus, a fence can actually overprotect the arrays close to the fence. If the fence to protect the arrays from wind is properly designed, all arrays could be designed for the wind loads experienced by the interior arrays.

The pressure distribution on arrays protected by a fence and/or within the array field are essentially flat, resulting in no pitching moment on the array. In contrast to this, the first and second array without a protective fence have varying pressure distributions. The first array has a pressure distribution typical of a single flat plate. The second array is affected considerably by the downwash and turbulence of the first array and may have a pressure distribution along a chord that changes from positive to negative pressures. Another noteworthy observation is that the pressure on the base pressure side is flat for all conditions except near the edges.

The wind loads on the array edges are considerably different from the remainder of the array field. Vortices are produced by array corners and fence corners and can produce very high wind loads at and near the array edges, depending on the wind direction. Pressure coefficients tend to be especially high in the localized leading edge-side edge area of the array. The high wind loads diminish to the loads within the array field at approximately two slant height distances from the edge, again depending on the wind direction. Several means

to alleviate the wind loads at the edges were presented in Section 4 but even the reduced edge loads are still several times the array mid-span loads.

In the wind tunnel test, the fluctuating pressures were recorded for a finite time, averaged to obtain the steady state loads and the rms value of the variable loads calculated to obtain indications of the level of the pressures produced by the array generated turbulence. The actual rms values will be larger than those recorded because of the damping inherent in the data acquisition. However, the rms load values do give an indication of the turbulence. In general, from the test results, the front arrays received the most turbulence induced loads when a fence existed and the second arrays received the most when no fence existed.

For design purposes, envelopes of the normal force and pressure coefficients were developed, where applicable, to encompass the steady state loads for all tilt angles and wind directions. These design envelope loads are explained and presented in total in Section 7.0.

7.0 STEADY STATE WIND LOAD DESIGN GUIDELINES

Based on the results of the boundary layer wind tunnel test and the results of the theoretical study documented in reference 5, the following design guidelines are given for determining wind loading on photovoltaic flat plate arrays. The normal force and pressure coefficient guidelines were obtained by enveloping the results from the wind tunnel test and are valid for arrays with separations from 1.5C to 3.0C. Wind tunnel tests with the winds normal to the spanwise axis of the arrays were used for the guidelines. From the theoretical study and aerodynamic principles, winds normal to the spanwise axis will produce the maximum pressure loading on the arrays at locations at least two slant heights from the array side edges.

7.1 Wind Loads on Arrays Behind a Protective Wind Barrier

If a fence is used to protect the arrays in an array field, the steady state wind loading on the first arrays will be the same or less than the arrays within the field if the fence* is properly designed for wind protection. Figure 7-1a presents normal force coefficients for conditions where the first array is protected from wind loading at least as well as the arrays interior to the field. This figure can be used to calculate steady state wind forces on arrays and array supporting structure in an array field. These loads are not applicable for the structure within two slant heights from the edge. The steady state normal wind force on the array is calculated by the equation:

$$F_N = q S C_{N1} \quad - - - (1)$$

*The fence used in this study had a porosity of 30% and a height equal to three-quarters of the array slant height. Since this study did not investigate other fence configurations, it is the designer's responsibility to assure that his fence design produces as much wind protection as the fence used in this study. There are several papers referred to in reference 5 that investigate the effects of fence porosity on the wind velocity behind the fence. In general, a porosity of from 30% to 50% produces the best wind protection. A solid fence tends to increase the turbulence compared to a higher porosity fence and also causes reversed flow behind the fence. The height of the fence is less critical than fence porosity on array loads provided that the height of the fence is near or above the array height.

where:

F_N = Steady state normal force (lbs)

q = Dynamic pressure (psf) for reference design velocity at 10 meters

S = Area of array (ft²)

$$C_{N1} = K_1 C_N$$

= Corrected normal force coefficient

C_N = Normal force coefficient from figure 7-1a

K_1 = Scale factor to correct for array size

$$= \left(\frac{C \sin \alpha + H_0}{8 \sin \alpha + 2} \right)^{.28}$$

C = Array slant height (ft)

H_0 = Ground clearance (ft)

α = Tilt angle (degrees)

The scale factor (K_1) corrects (in an approximate manner) the wind forces for arrays whose slant height and ground clearance are different than the test array baseline size of 8 ft. slant height and 2 ft. ground clearance. This scale factor considers the difference in the wind velocity at the top of an array whose size and position is different from the baseline array relative to the wind velocity at the top of the baseline array.

Figure 7-1b presents steady state pressure coefficients normalized to the normal force coefficients at corresponding tilt angles. The steady state pressure distributions on the arrays behind a fence are essentially constant or vary linearly (increasing from the trailing edge to the leading edge) for all tilt angles. The pressures can be calculated by the equation:

$$P = qC_{p1} \text{ - - - - (2)}$$

where:

p = Steady state local pressure loading (psf)

q = Dynamic pressure (psf) for reference design velocity at 10 meters

$$C_{p1} = K_1 C_p$$

= Corrected pressure coefficient

K_1 = Scale factor to correct for array size and ground clearance

$$= \left(\frac{C \sin \alpha + H_0}{8 \sin \alpha + 2} \right)^{.27}$$

C = Array slant height (ft)

H_0 = Ground clearance (ft)

α = Tilt angle (degrees)

$\frac{C_p}{C_N}$ = Normalized pressure coefficient from figure 7-1b

C_N = Normal force coefficient from figure 7-1a

The steady state pressure loading is valid for all flat plate array panels in an array field except for panels within two slant heights from the edge. Where leading edge (L.E.) and trailing edge (T.E.) are given, the pressure loading is assumed as linearly increasing from the trailing edge value to the leading edge value. It should be noted that some conservatism is designed into the panel pressure loading by assuming a flat or linearly varying pressure coefficient. This conservatism can be seen in the normalized pressure coefficient shown in Figure 7-1. If the pressure coefficient distribution was matched exactly, the C_p/C_N curve would be equal to 1.0. Thus, conservatism of from 10 to 20% is built into the pressure loading by simplifying the distribution.

The use of these design guidelines can best be illustrated by the following example:

1. Determine the design normal force and pressure distribution on an array interior to an array field for a 90 mph wind approaching the front of the array and at sea level. The array slant height is 8 feet, ground clearance is 2 feet, span is 10 feet, and the tilt angle is 30 degrees.

q = wind dynamic pressure at 10 meter height

$$= .5 \rho v^2$$

$$= .5 (.002378)(131.23)^2$$

$$= 20.5 \text{ psf}$$

S = area of array

$$= 8 \times 10$$

$$= 80 \text{ ft}^2.$$

$$\begin{aligned}
K_1 &= \text{Scale factor} \\
&= \left(\frac{8 \sin(30^\circ) + 2}{8 \sin(30^\circ) + 2} \right) \cdot 28 \\
&= 1.0
\end{aligned}$$

$$C_N = .16 \text{ from figure 7-1a}$$

$$\begin{aligned}
C_{N1} &= K_1 C_N \\
&= .16
\end{aligned}$$

To calculate the normal force

$$\begin{aligned}
F_N &= q S C_{N1} \\
&= 20.5 \times 80 \times .16 \\
&= 262.4 \text{ lbs. force normal to the array (30}^\circ \text{ from vertical) and in downward} \\
&\quad \text{direction per figure 7-1a}
\end{aligned}$$

To calculate the pressure distribution along the chord

$$p = q C_{p1}$$

$$C_{p1} = K_1 \frac{C_p}{C_N} C_N$$

From figure 7-1b

$$\frac{C_p}{C_N} = 1.18 \text{ at trailing edge (top edge for wind from front)}$$

$$= 1.26 \text{ at leading edge (bottom edge for wind from front)}$$

$$C_N = .16 \text{ from figure 7-1a}$$

$$K_1 = 1.0$$

therefore

$$\begin{aligned}
C_{p1} &= 1.18 \times .16 \\
&= .19 \text{ trailing edge}
\end{aligned}$$

$$\begin{aligned}
\text{and } C_{p1} &= 1.26 \times .16 \\
&= .20 \text{ leading edge}
\end{aligned}$$

The local pressure is

$$\begin{aligned}
p &= 20.5 (.19) \\
&= 3.9 \text{ psf at trailing edge (downward direction per figure 7-1b)} \\
p &= 20.5 (.20) \\
&= 4.1 \text{ psf at leading edge (downward direction per figure 7-1b)}
\end{aligned}$$

Therefore, the pressure varies on the panel from 4.1 psf at the leading edge (lower edge) to 3.9 psf at the trailing edge (upper edge) for a 90 mph wind approaching the front of the array field.

7.2 Wind Loads on Arrays Without a Protective Wind Barrier

If an array field is to be designed without a protective fence, the first two arrays from the front and back need to be designed for larger wind loads than in Section 7.1. All remaining arrays interior to these two front arrays can be designed to withstand wind loads given in Figure 7-1. The maximum normal wind forces on the first two arrays from the front and back of the array field can be calculated similarly to those in Section 7.1 using the normal force coefficient envelope and the delta pressure coefficient presented in Figure 7-2a and b. As an example:

- Calculate the normal force and pressure on the first array for the same conditions as in the example in 7.1.

To calculate the normal force:

From before

$$q = 20.5 \text{ psf}$$

$$S = 80. \text{ ft}^2$$

$$K_1 = 1.0$$

From figure 7-2a

$$C_N = .65$$

Therefore the normal force on the array is

$$F_N = 20.5 \times 80 \times .65$$

$$= 1066 \text{ lbs in downward direction per figure 7-2a}$$

C-2

To calculate the panel pressure

$$\begin{aligned} \frac{C_p}{C_N} &= 0.8 \text{ at trailing edge} \\ &= 1.28 \text{ at leading edge} \\ C_N &= .65 \\ p &= 20.5 \times 0.8 \times .65 \\ &= 10.7 \text{ psf at trailing edge} \\ &= 20.5 \times 1.28 \times .65 \\ &= 17.1 \text{ psf at leading edge} \end{aligned}$$

Therefore, the pressure varies from 17.1 psf at the leading edge to 10.7 psf at the trailing edge with the pressure in downward direction per figure 7-2b.

7.3 Array Edge Wind Loads

The wind loads within two slant heights from the side edges have a different character than those within the array field because of the corner vortices. This test program was primarily directed towards the wind loads within an array field and only a limited amount of testing was devoted to the edge loads. Consequently, a comprehensive set of wind load guidelines for the edge loads cannot be detailed from the test data. However, the following normal force coefficients and pressure coefficients are given as guidelines and can be used in the design of the edge arrays if the following design conditions are satisfied.

Array tilt angle $\approx 35^\circ$

Fence design details, if applicable, as footnoted in Section 7.1

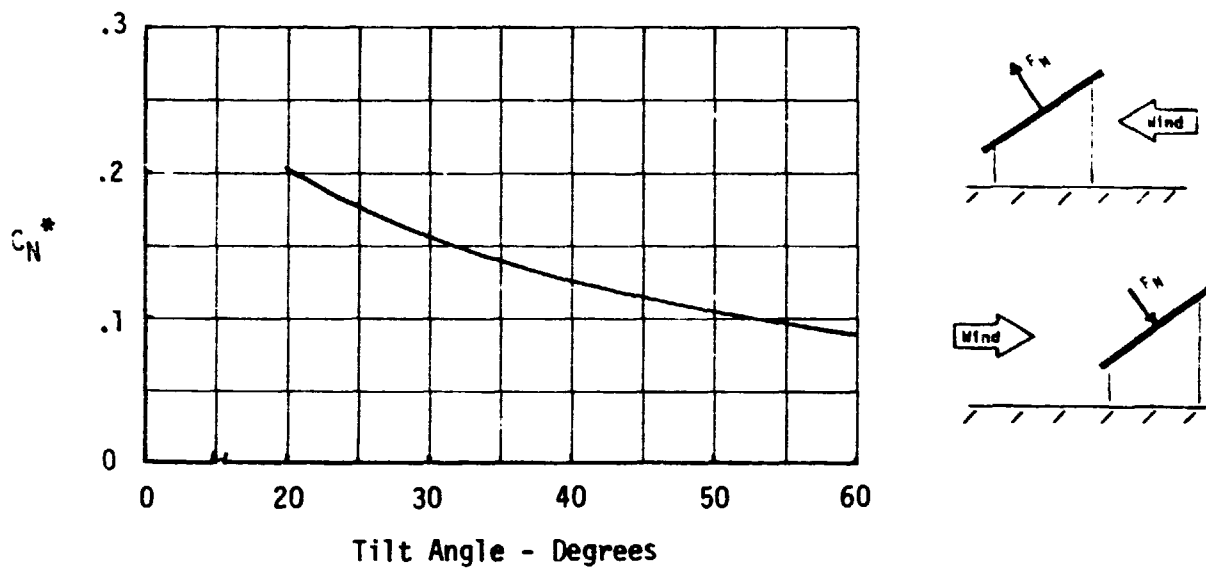
Fence corner modifications, if applicable, as shown in configuration 5,

Figure 4-16

The normal force coefficients and delta pressure coefficients for arrays within two slant heights from the side edge of the array field and for three field configurations - no fence, fence, and fence with the corners modified - are shown

in Figures 7-3a to 7-3c. These coefficients are based on the test data located .15 chord lengths from the side edge. Since the loads decrease with distance in from the edge, these coefficients are conservative if used over the two slant heights from the side edge. In addition, the pressure distributions show high pressure coefficients located within 5% to 10% from the upper edge. Since a structural support is likely to be located on the leading and trailing edges to support the arrays, these high pressure loads, within 10% of the top edge, may not be critical to the design of the panels and may not need to be considered in their design. The effect of this high pressure loading is in the normal force coefficient calculation which is a parameter used to size the supporting structure.

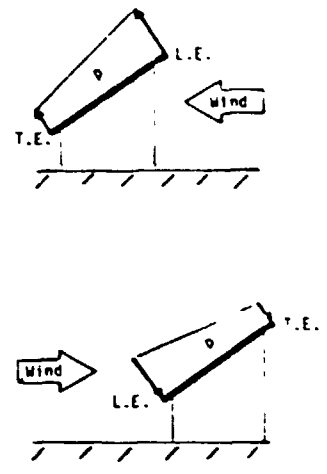
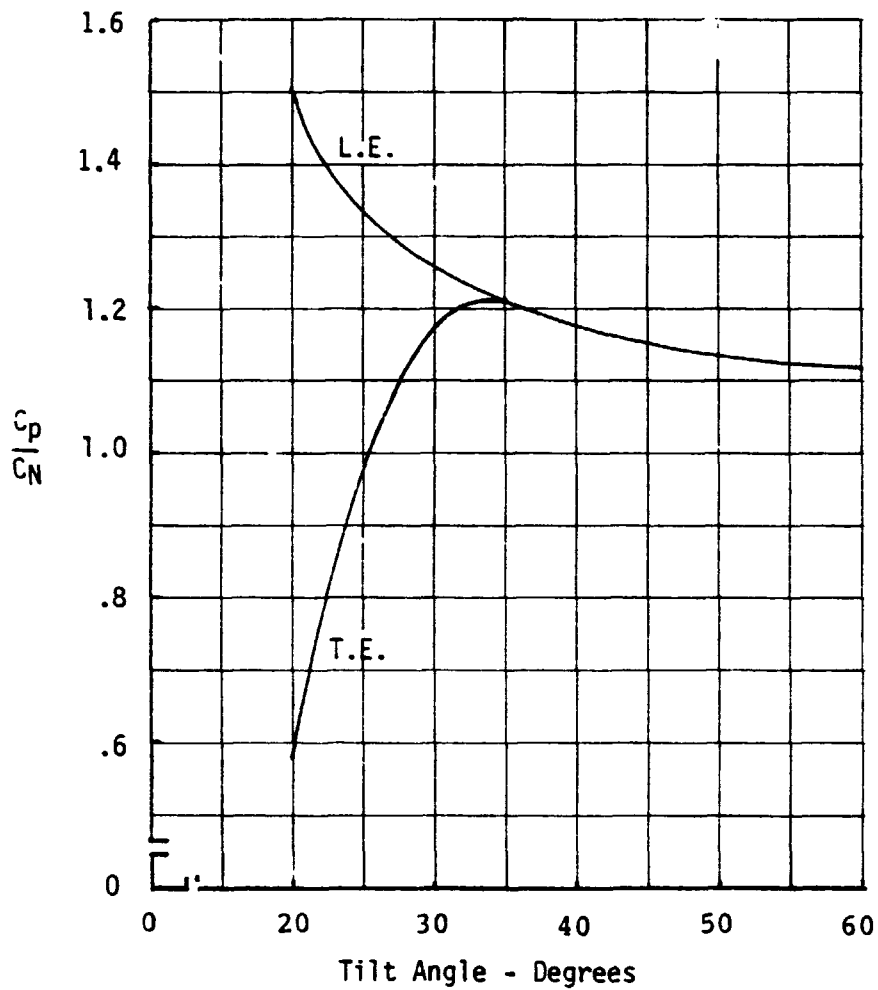
The application of these coefficients is similar to the examples shown in Section 7.1 and 7.2, except that C_p replaces $\left(\frac{C_p}{C_N}\right)(C_N)$ in the examples.



• C_N based on wind reference velocity at 10 meters

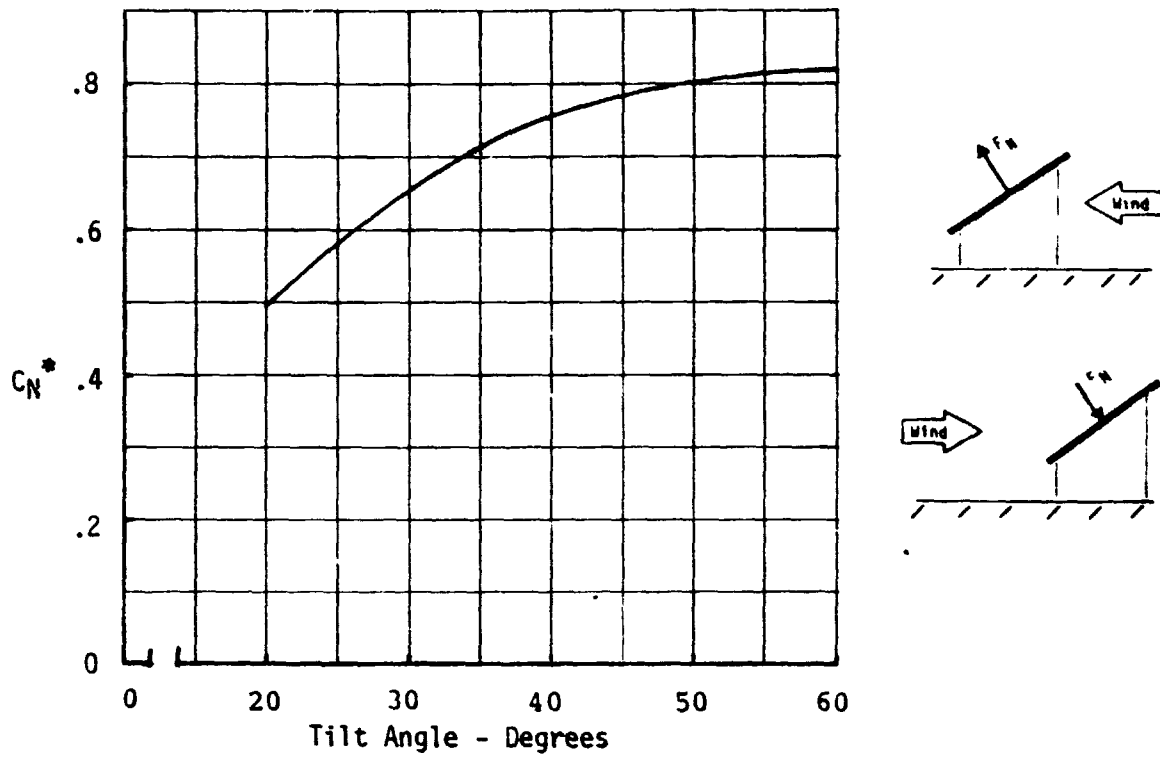
exception: not valid within two slant heights from the side edges

Figure 7-1a. Steady State Wind Normal Force Coefficient Envelope for Arrays Within an Array Field or Behind a Protective Wind Barrier.



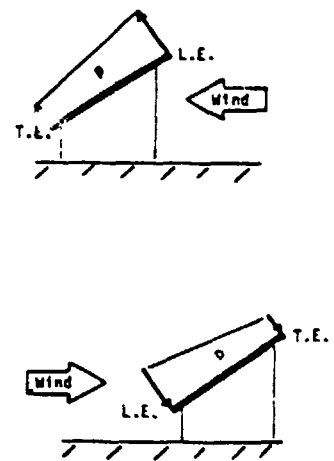
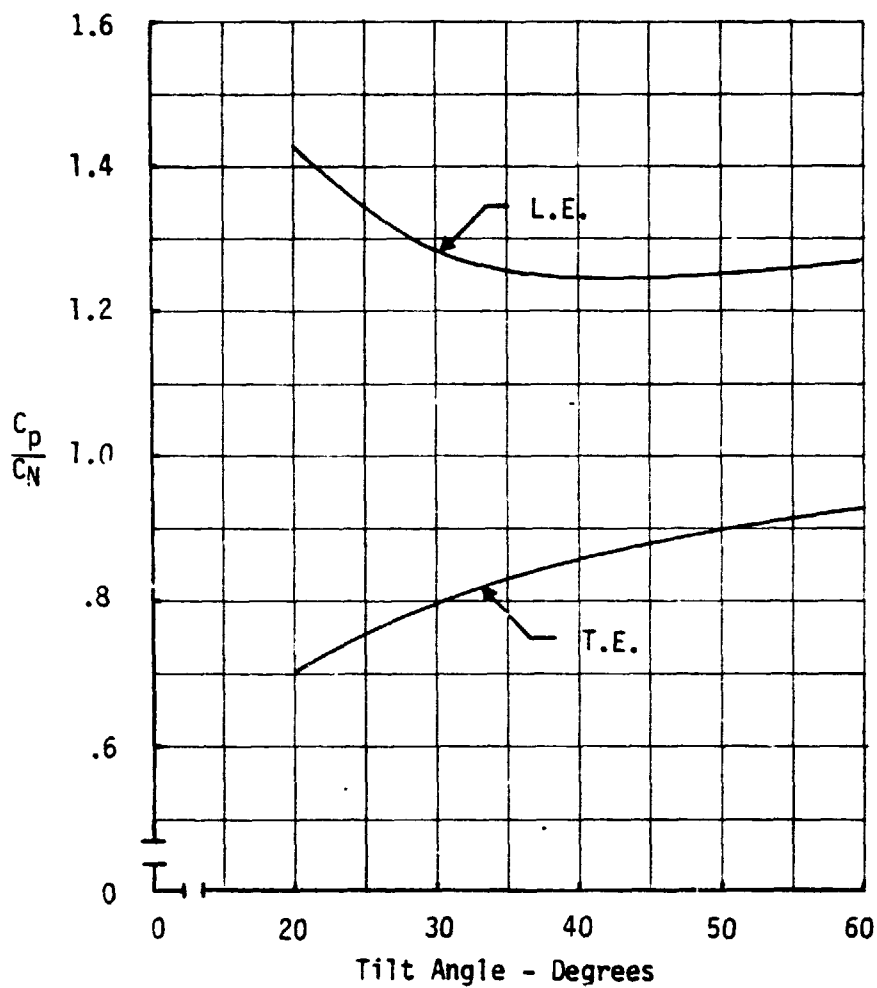
exception: not valid within two slant heights from the side edges

figure 7-1b. Steady State Wind Normalized Pressure Coefficient Envelope for Arrays Within an Array Field or Behind a Protective Wind Barrier



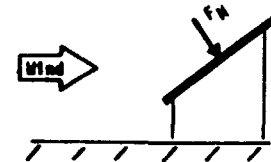
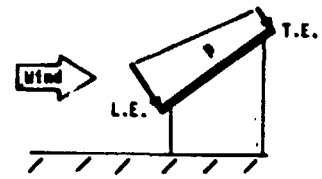
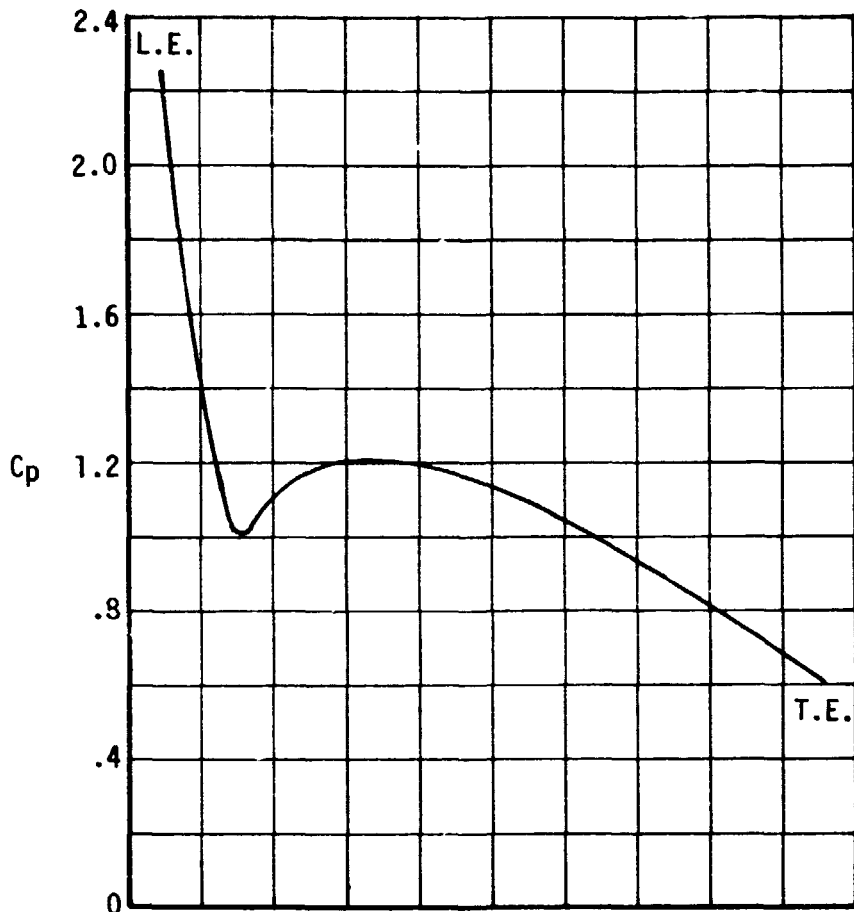
- C_N based on wind reference velocity at 10 meters
 exception: not valid within two slant heights from the side edges

Figure 7-2a. Steady State Wind Normal Force Coefficient Envelope for the Two Outer Boundary Array Rows in an Array Field Unprotected from the Wind



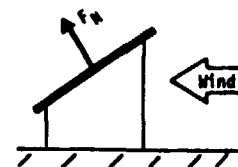
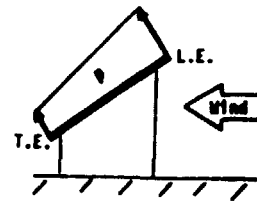
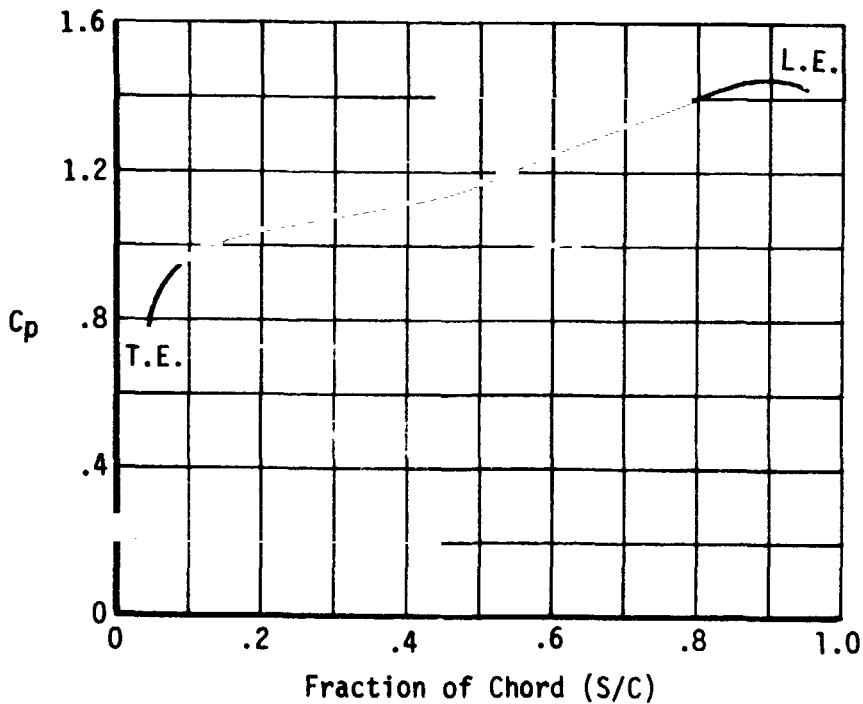
exception: not valid within two slant heights from the side edges

Figure 7-2b. Steady State Wind Normalized Pressure Coefficient Envelope for the Two Outer Boundary Array Rows in an Array Field Unprotected from the Wind



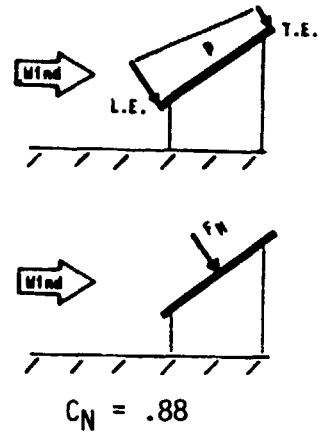
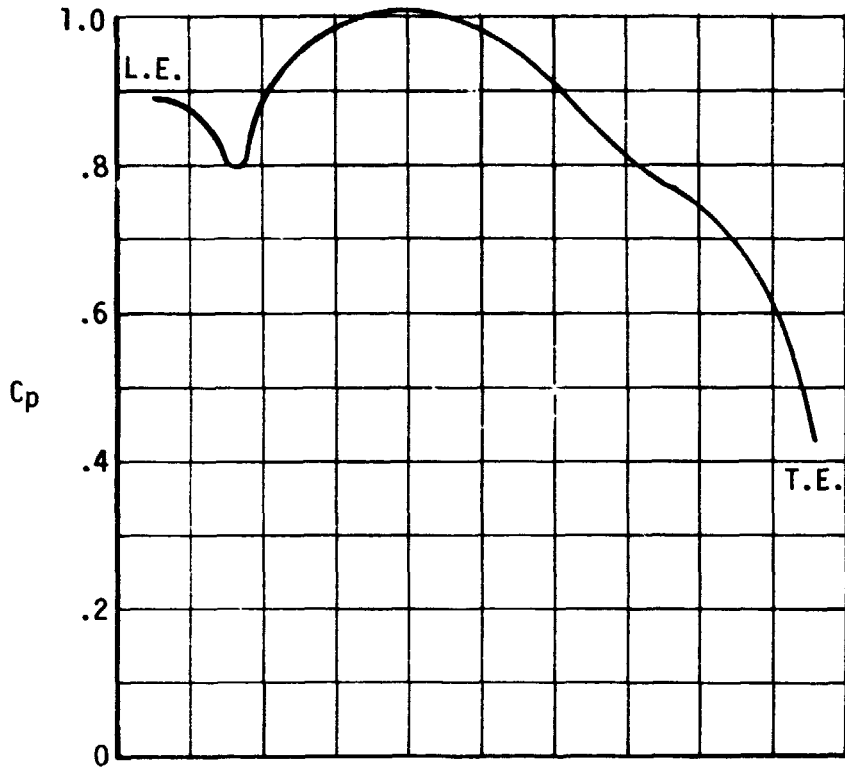
$$C_N = 1.12$$

Based on:
Tilt Angle = 35°
Wind reference velocity
at 10 meters



$$C_N = 1.29$$

Figure 7-3a. Steady State Wind Pressure Coefficient and Normal Force Coefficient Guidelines for Edge Arrays in an Array Field (No Fence)



Based on:
 Tilt Angle = 35°
 Wind reference velocity
 at 10 meters

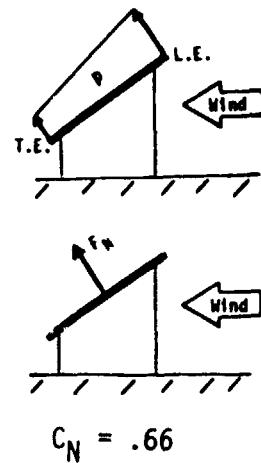
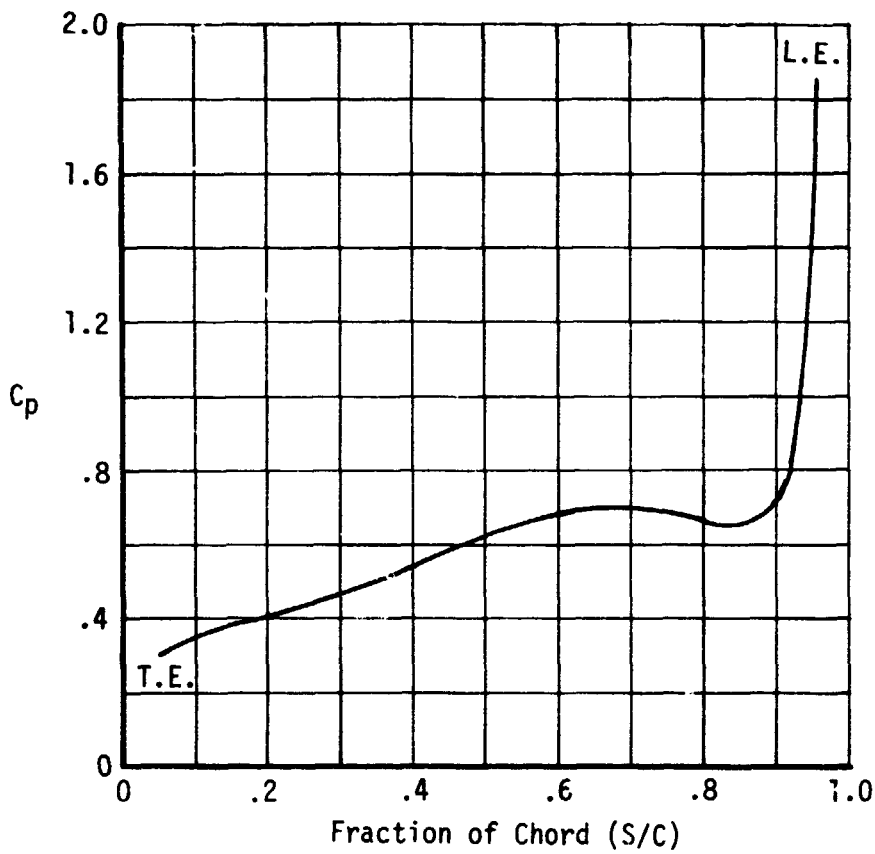
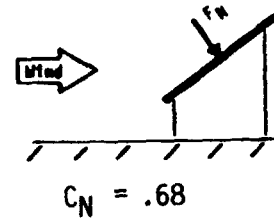
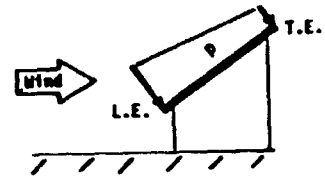
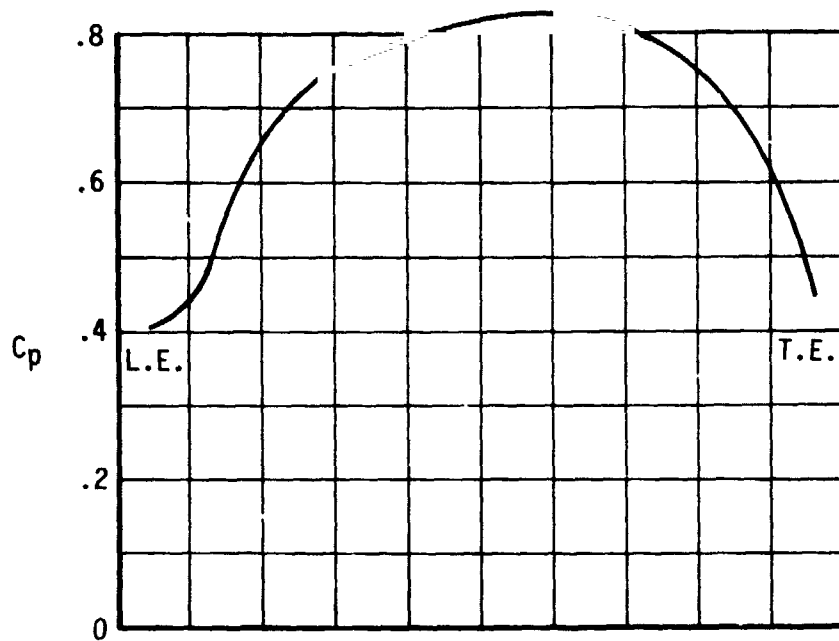


Figure 7-3b. Steady State Wind Pressure Coefficient and Normal Force Coefficient Guidelines for Edge Arrays in an Array Field (Fence)



Based on:
Tilt Angle = 35°
Wind reference velocity
at 10 meters

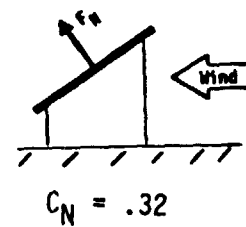
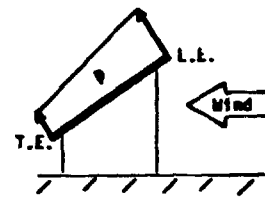
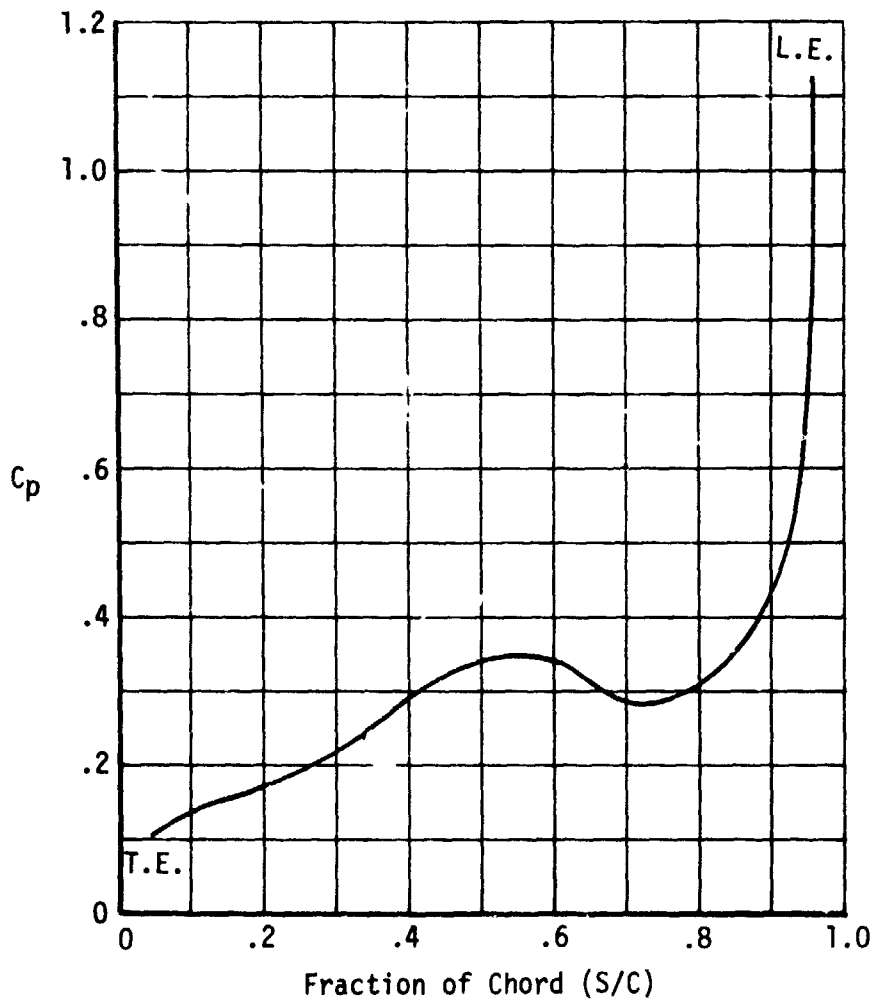


Figure 7-3c. Steady State Wind Pressure Coefficient and Normal Force Coefficient Guidelines for Edge Arrays in an Array Field (Fence with Modified Corners)

8.0 NEW TECHNOLOGY

No reportable items of new technology have been identified by Boeing during the contract of this work.

~~TOP SECRET~~

9.0 REFERENCES

1. National Photovoltaic Program, Program Plan, February 3, 1978, U.S. Department of Energy, Division of Solar Technology.
2. "Module/Array Interface Study," DOE/JPL-No. 954698-78/1, Bechtel National, Inc., Research and Engineering Operation, August, 1978.
3. "Feasibility Study of Solar Dome Encapsulation of Photovoltaic Arrays," DOE/JPL-No. 954833-78/1, Boeing Engineering and Construction Company, December, 1978.
4. A. G. Davenport, "Rationale for Determining Design Wind Velocities," Proceedings of the American Society of Civil Engineers, Vol. 86, No. ST5, May, 1960.
5. "Wind Loads on Flat Plate Photovoltaic Array Fields," DOE/JPL-No. 954833-79/2, Boeing Engineering and Construction, September, 1979.

PRECEDING PAGE BLANK NOT FILMED

PAGE _____ INTENDOMMUNE DES

APPENDIX

**WIND LOADS ON FLAT PLATE
PHOTOVOLTAIC ARRAY FIELDS**

PHASE III - FINAL REPORT

WIND TUNNEL TEST REPORT

**Prepared for Jet Propulsion Laboratory
under Contract No. 9654833**

**Boeing Engineering and Construction Company
A Division of The Boeing Company)
Seattle, Washigton 98124**

PRECEDING PAGE BLANK NOT FILMED

~~CONFIDENTIAL~~ INTELLIGENCE REPORT

WIND PRESSURES AND FORCES ON
FLAT-PLATE PHOTOVOLTAIC SOLAR ARRAYS

by

N. Hosoya,* J. A. Peterka,** M. Poreh,***
and J. E. Cermak****

for

Boeing Engineering and Construction Company
P. O. Box 3707
Seattle, Washington 98124

Fluid Dynamics and Diffusion Laboratory
Civil Engineering Department
Colorado State University
Fort Collins, Colorado 80523

September 1980

*Graduate Research Assistant

**Associate Professor

***Professor

****Professor-in-Charge, Fluid Mechanics
and Wind Engineering Program

CER80-81NH-JAP-MP-JEC13

PRECEDING PAGE BLANK NOT FILMED

~~CONFIDENTIAL~~ UNRECORDED COPY

TABLE OF CONTENTS

	<u>Page</u>
LIST OF FIGURES	v
LIST OF TABLES	viii
LIST OF SYMBOLS	x
1. INTRODUCTION	A-1
2. EXPERIMENTAL CONFIGURATION	A-3
2.1 Wind Tunnel	A-3
2.2 Flow Simulation	A-3
2.3 The Models	A-6
3. INSTRUMENTATION AND DATA ACQUISITION	A-8
3.1 Measurements of Flow Characteristics	A-8
3.2 Pressure Measurements	A-9
3.3 Normal Force Calculations	A-9
4. PRESENTATION AND ANALYSIS OF THE EXPERIMENTAL DATA	A-11
4.1 Single Array Tests	A-11
4.2 Array Field Tests	A-13
4.3 Flow Visualization	A-14
5. CONCLUSIONS	A-16
6. REFERENCES	A-17
FIGURES	A-18
TABLES	A-58

PRECEDING PAGE BLANK NOT FILMED

~~CONFIDENTIAL~~ ~~CONFIDENTIAL~~

LIST OF FIGURES

<u>Figure</u>		<u>Page</u>
1	Meteorological Wind Tunnel	A-19
2	Array Field Models in Meteorological Wind Tunnel	A-20
3	Mean Velocity and Turbulence Distribution in Nonuniform Flow	A-21
4	One Dimensional Velocity Spectra in Nonuniform Flow	A-22
5	Turbulence Spectra in Nonuniform Flow (BL1) Compared to Atmospheric Spectra	A-23
6	Mean Velocity and Turbulence Distribution in Uniform Flow	A-24
7	Typical Horizontal Velocity Distribution across Meteorological Wind Tunnel	A-25
8	1:12 Scale Models in Meteorological Wind Tunnel	A-26
9	Photograph of Standard Corner Fence	A-27
10	Position of Pressure Taps on Instrumented Model	A-28
11	Schematic Description of Array Field	A-29
12	Front and Back Pressures on a Single Array in Uniform Flow, $WD = 0^\circ$, $H/c = 0.25$, $\alpha = 20^\circ$, 35° , 60° and 90°	A-30
13	Front and Back Pressures on a Single Array in Uniform Flow, $WD = 0^\circ$, $H/c = 0.25$, $\alpha = 120^\circ$, 145° and 160°	A-31
14	Front and Back Pressures on a Single Array in Uniform Flow, $WD = 0^\circ$, $H/c = \text{infinity}$, $\alpha = 20^\circ$, 30° , 60° and 90°	A-32
15	Absolute Values of Normal Force Coefficients on a Single Array in Uniform Flow, $WD = 0^\circ$	A-33
16	Front and Back Pressures on a Single Array in Nonuniform Flow, $WD = 0^\circ$, $H/c = 0.25$, $\alpha = 20^\circ$, 35° , 60° , and 90°	A-34

PRECEDING PAGE BLANK NOT FILMED

LIST OF FIGURES (Cont.)

<u>Figure</u>		<u>Page</u>
17	Front and Back Pressures on a Single Array in Nonuniform Flow, $WD = 0^\circ$, $H/c = 0.25$, $\alpha = 120^\circ$, 145° and 160°	A-35
18	Absolute Values of Normal Force Coefficient on a Single Array in Nonuniform and Uniform Flows, $WD = 0^\circ$, $H/c = 0.25$	A-36
19	Normal Force Coefficients for an Array Field in Uniform Flow, $WD = 0$, $x/c = 2.0$, $H/c = 0.25$, No Fence	A-37
20	Normal Force Coefficients for an Array Field with a Fence of Various Height and Porosity, $WD = 0^\circ$, $x/c = 2.0$, $H/c = 0.25$, $\alpha = 35^\circ$	A-38
21	Normal Force Coefficients for an Array Field with a Fence of Various Height and Porosity, $WD = 0^\circ$, $x/c = 2.0$, $H/c = 0.25$, $\alpha = 145^\circ$	A-39
22	Corner Fence Configurations	A-40
23	Normal Force Coefficients for an Array Field with Various Fence Configurations, $WD = 45^\circ$, $x/c = 2.0$, $H/c = 0.25$, $MC = 0$	A-41
24	Model Configurations	A-42
25	Normal Force Coefficients for an Array Field with Various Model Configurations, $WD = 45^\circ$, $x/c = 2.0$, $H/c = 0.25$, $FC = 1$	A-43
26	Normal Force Coefficients for an Array Field in Nonuniform Flow, No Fence, $WD = 0^\circ$, $H/c = 0.25$, $\alpha = 20^\circ$, 35° , 60° and 90°	A-44
27	Normal Force Coefficients for an Array Field in Nonuniform Flow, No Fence, $WD = 0^\circ$, $H/C = 0.25$, $\alpha = 120^\circ$, 145° and 160°	A-45
28	Normal Force Coefficients for an Array Field with Various Fences, $WD = 0^\circ$, $x/c = 2.0$, $H/c = 0.25$, Nonuniform Flow	A-46
29	Normal Force Coefficients for an Array Field, Edge and Corner Studies, $x/c = 2.0$, $H/c = 0.25$, Nonuniform Flow	A-50

LIST OF FIGURES (Cont.)

<u>Figure</u>		<u>Page</u>
30	Normal Force Coefficients for an Array Field, Corner Study with Various Fence and Model Configurations, $x/c = 2.0$, $H/c = 0.25$, Nonuniform Flow	A-52
31	Flow Visualization for an Array Field, $WD = 0^\circ$	A-54
32	Flow Visualization for an Array Field, $WD = 45^\circ$	A-57

LIST OF TABLES

<u>Table</u>		<u>Page</u>
1	Normal Force and Maximum Pressure Difference for a Single Array in Uniform Flow	A-59
2	Normal Force and Maximum Pressure Difference for an Array Field in Uniform Flow, $x/c = 2.0$	A-60
3	Normal Force and Maximum Pressure Difference for an Array Field in Uniform Flow, $x/c = 1.5$ and 3.0	A-61
4	Normal Force and Maximum Pressure Difference for a Single Array in Nonuniform Flow	A-62
5	Normal Force and Maximum Pressure Difference for an Array Field in Nonuniform Flow, $x/c = 2.0$	A-63
6	Normal Force and Maximum Pressure Difference for an Array Field in Nonuniform Flow, $x/c = 1.5$ and 3.0	A-64
7	Normal Force and Maximum Pressure Difference for an Array Field with a Fence, $H_f/c = 0.75$, $P_f = 30\%$, $x_f/c = 1.25$	A-65
8	Normal Force and Maximum Pressure Difference for an Array Field with a Fence, $H_f/c = 0.75$, $P_f = 30\%$, $x_f/c = 2.5$	A-66
9	Normal Force and Maximum Pressure Difference for an Array Field with a Fence, $H_f/c = 0.75$, $P_f = 30\%$, $x_f/c = 5.0$	A-67
10	Normal Force and Maximum Pressure Difference for an Array Field with a Fence of Various Height and Porosity	A-68
11	Normal Force and Maximum Pressure Difference for an Array Field, Edge Study	A-69
12	Normal Force and Maximum Pressure Difference for an Array Field, No Fence, Corner Study	A-70
13	Normal Force and Maximum Pressure Difference for an Array Field with Various Fences, Corner Study	A-71

LIST OF TABLES (continued)

<u>Table</u>	<u>Page</u>
14	Normal Force and Maximum Pressure Difference for an Array Field with Various Fences, MC = 1, Corner Study A-72
15	Normal Force and Maximum Pressure Difference for an Array Field with Various Models, FC = 1 and 4, Corner Study A-73
16	Normal Force and Maximum Pressure Difference for an Array Field with a Fence, $H_f/c = 1.0$, $\alpha = 60^\circ$ and 120° A-74
17	Fence Configurations A-75
18	List of Test Configurations A-76

LIST OF SYMBOLS

<u>Symbol</u>	<u>Definition</u>
c	chord length of solar array
C_N	normal force coefficient
C_p	pressure coefficient
ΔC_{pmax}	maximum pressure difference
D	characteristic length in Reynolds number
FC	fence configuration
$F(N)$	velocity spectrum
H	ground clearance of solar array
H_{af}	height of additional fence
H_f	height of fence
H_s	height of spoiler
MC	model configuration
N	frequency
P	pressure
P_{af}	porosity of additional fence
P_f	porosity of spoiler
q_∞	dynamic pressure measured outside simulated boundary layer
q_{ref}	reference dynamic pressure
s	chordwise position--the edge where $s = 0$ corresponds to the leading edge for $\alpha \geq 90^\circ$ and the trailing edge for $\alpha < 90^\circ$
s_{max}	chordwise position where maximum pressure difference is observed
U	velocity of wind
U_{ref}	reference velocity of wind
U_{rms}	variance of fluctuating velocity

LIST OF SYMBOLS (Cont.)

<u>Symbol</u>	<u>Definition</u>
U_{δ}	velocity of wind at simulated boundary layer height
U_{∞}	velocity of wind measured outside simulated boundary layer
x	separation distance of solar array
x_f	separation distance between fence and solar array
α	angle of attack of solar array
δ	height of simulated boundary layer
ν	kinematic viscosity of air
ρ	density of air

1. INTRODUCTION

An important factor influencing the design and subsequently cost of large photovoltaic power generating systems, which involve a large number of simple structural elements and supports, is the magnitude of wind-induced loads. It has been recognized that usual design procedures, like the ANSI code (A58.1 - 1972) for example [1], are not adequate for accurate wind design of these repetitive, photovoltaic arrays with their distinctive configuration, orientation and limited height. In fact, the information presently available in the technical literature is not sufficient even for an optimum design of the structure for supporting a single photovoltaic array. Wind loads on individual arrays at different locations in a large array field are more difficult to determine as they vary according to the array location in the field and wind direction in a complicated manner. Higher loads are expected to exist at the edges of the field, but those can be reduced by carefully designed fences or barriers.

A theoretical study of the aerodynamics of flat plate arrays was recently made by Ronald D. Miller and Donald Zimmerman [2] at the Boeing Engineering and Construction Company (BECC). The study identified the basic features of the flat plate array loading which can be used for design purposes. It has been recognized by the authors, however, that theoretically derived design criteria are conservative and a wind-tunnel study of the wind loadings of such arrays was therefore recommended.

This report describes the experimental study of wind loading on flat plate photovoltaic arrays and array fields performed in the Meteorological Wind Tunnel of the Fluid Dynamics and Diffusion Laboratory at Colorado State University for BECC. The experimental program was developed in cooperation with Ronald D. Miller (BECC). The program's objectives were to determine the pressure distribution and forces acting on photovoltaic arrays for different angles of attack, two wind directions, head on winds and cornering winds ($WD = 0^\circ$ and 45° as defined in Figure 11) and two velocity profiles, as well as to investigate the effect of different fences and barriers on the wind loading at the edges and corners of an array field.

The wind-tunnel results were analyzed and the effect of the various parameters are presented in a form permitting calculation of the wind loading on prototype photovoltaic structures.

In view of the large number of data points collected in the report, it was found convenient to present most of the pressure measurements in a separate Appendix. The main report includes, however, a full description of the various runs and the calculated values of the normal force coefficient, the maximum local pressure coefficient and its location for each run in a tabulated form (Table 1 to 16) as well as a graphical representation of these data.

2. EXPERIMENTAL CONFIGURATION

2.1 Wind Tunnel

The Meteorological Wind Tunnel of the Fluid Dynamics and Diffusion Laboratory at Colorado State University (Figure 1) is characterized by a long (96 ft), slightly diverging test section, 6 ft-8 in. wide (at the turntable) and 6 ft high. The ceiling is adjustable to avoid pressure gradient along the test section. This facility is driven by a 400 HP variable pitch propeller with air flow velocity varying continuously from 0.5 fps up to 100 fps.

2.2 Flow Simulation

The primary consideration in modeling wind forces on structures in a wind tunnel is that the wind characteristics in the tunnel simulate natural boundary-layer winds at the actual site. In general this requires that the vertical distribution of mean velocity and turbulence in the wind tunnel boundary layer match those at the site and that the Reynolds numbers of the model and the prototype be equal. In addition, the small-scale model must be geometrically similar to its prototype. A detailed discussion of these requirements and their implementation in the wind-tunnel environment can be found in references 3, 4, and 5.

The construction of a 1:24 scale model of a prototype structure and its immediate surroundings (in this case, a flat, open area), submerged in a turbulent boundary layer of the Meteorological Wind Tunnel, shown in Figure 1, satisfies all the above criteria except those of equal Reynolds numbers and similarity of turbulence intensity and scale.

The kinematic viscosity ν appearing in the Reynolds number UD/ν is the same for both the tunnel and the full-scale structure. Because of this, the wind-tunnel air speed, U , would have to be 24 times the full-scale value if the model and prototype Reynolds numbers are to be equal. Testing at such high wind speeds is not feasible. However, for Reynolds numbers larger than 2×10^4 for sharp-edged structures where the flow separation point is fixed, there is no significant change in the values of aerodynamic coefficients as the Reynolds number increases. Since typical Reynolds number values are 10^6 - 10^7 for high-wind, full-scale flow and about 5×10^4 for wind-tunnel flows, acceptable flow similarity is achieved without equality of Reynolds numbers.

At a model scale of 1:24, the larger scales of turbulence in the atmospheric boundary layer are not simulated in the wind-tunnel flow. However, because the integral scale of the turbulence in the wind tunnel was 2 to 3 times the largest dimension of the model collector, the influence of the scale of turbulence is not expected to be significant [6]. Evidence exists which demonstrates some influence of turbulence intensity on drag of flat plates [6,7,8]. Because the turbulence intensity difference between the current simulation and a simulation with complete similarity of turbulent structure is not large, the effects due to turbulence intensity should be small. For cases where an upstream collector disturbs the approach flow, turbulence characteristics are dominated by the wake characteristics of the upstream object and possible differences due to turbulence intensity should further decrease.

An important factor which affects the wind loadings is the structure of the atmospheric boundary layer near the ground. The boundary layer which develops over a flat terrain is usually characterized by a non-uniform velocity profile which is closely described by a 1/7th power law mean velocity distribution. It is impossible to simulate in a wind tunnel the entire atmospheric boundary layer at the desired model scale for this study (1:24). One can, however, simulate the lower part of the atmospheric boundary layer in a 45 in. deep wind tunnel boundary layer [3-5].

The shape of the 1/7th power law boundary layer, which will be referred to as the Nonuniform flow 1 was obtained by means of selected roughness on the wind-tunnel floor upstream of the model. Forty ft of test section length were covered with 1 in. cubes followed by a 40 ft length of pegboard with 0.25 in. diameter pegs projecting 0.5 in. above the pegboard base (see Figure 2). In addition to the floor roughness, four triangular spires were installed at the test section entrance in order to get a thicker boundary layer than would otherwise be obtained. The normalized velocity and turbulence profiles of this boundary layer are shown in Figure 3 and data is tabulated in the Appendix. Turbulence intensity is the root-mean-square of the longitudinal fluctuating velocity divided by the local mean velocity. The turbulence intensity reached values of 20 percent in the boundary layer.

The spectrum of longitudinal velocity fluctuations is shown in Figures 4 and 5, including two suggested analytical models of velocity spectra for the atmosphere by Harris (9) and Davenport (10).

The spectra were obtained at 4 and 8 in. above the wind-tunnel floor. In this plot N is frequency, $F(N)$ is the velocity spectrum, U_{rms}^2 is the variance of the fluctuating velocity, δ is the simulated boundary layer height (900 ft full-scale), and U_δ is the velocity at δ . The region where turbulence structure may be important to the determination of mean loading ranges upward from abscissa values of about 20 for wind speeds up to about 30 mph at 30 ft. Thus, the simulation has a turbulence intensity somewhat too high in the frequency range affecting mean wind loading on the model and too low in the low-frequency gusts.

The "Uniform Flow" velocity profile was obtained by placing the model at the upstream end of the test section. The measured velocity profile at that station, shown in Figure 6, indicates that a very thin boundary layer has developed along the short upstream section. Its effect on the wind loading on elevated panels is expected, however, to be small. A typical velocity distribution across the tunnel is shown in Figure 7.

2.3 The Models

Aluminum models of the flat photovoltaic array field having a geometrical scaling of 1:24 (Figure 2) and 1:12 (Figure 8) were constructed. (The 1:12 model was used in a limited number of tests only).

The chord size of the 1:24 model was $c = 4$ in., corresponding to a prototype value of 8 ft. Rows of pressure taps were drilled on each face of the array as shown in Figure 10. Each pressure tap represents the average pressure along a small section of the chord. The row at the edge of the array was used to study the wind loading at the side edge of the field.

To study the wind loadings on an array located in an array field, 1:24 scale models of array rows were constructed, which could be placed on the wind tunnel floor at desired locations to simulate the relative position in the field on the array with the pressure taps on which the wind loading was measured. Figure 2 shows a photograph of a 1:24 model of a photovoltaic array field in the wind tunnel. Figure 8 shows a photograph of the 1:12 model.

The fence was simulated in the model by perforated sheet metal, with holes of 3/16 in. diameter, having the same porosity (about 30 percent) as the prototype fence (see Figure 9).

3. INSTRUMENTATION AND DATA ACQUISITION

3.1 Measurements of Flow Characteristics

Velocity and turbulence intensity profiles for the approach flow under test conditions were made at the locations of the model in the tunnel (turntable) with the model removed.

The measurements were made with a Thermosystems Model 1050 constant-temperature anemometer with a 0.001 in. diameter platinum film sensing element 0.02 in. long. The sensing probe was attached to a vertical traverse to measure velocities and turbulent intensities at different heights. Output was processed through the Laboratory on-line digital data acquisition system.

Tests were made at only one wind speed in the tunnel around 50 ft/sec. This wind was sufficiently high to ensure Reynolds number similarity between the model and prototype.

The reference velocity at each test was measured using a pitot-static tube which was connected to a Setra differential pressure transducer. The pitot tube was placed outside the simulated boundary layer and recorded the value of $q_{\infty} = \rho U_{\infty}^2 / 2$, where ρ is the mass density of the air. The ratio of the reference velocity U_{ref} , at a prototype height of 10 m above the ground, to U_{∞} was determined from the velocity distribution of the boundary layer according to the scale of the model. The value

$$q_{\text{ref}} = \frac{\rho U_{\text{ref}}^2}{2} = \frac{\rho U_{\infty}^2}{2} \left(\frac{U_{\text{ref}}}{U_{\infty}} \right)^2 \quad (1)$$

at the height corresponding to 10 m above ground in the prototype was later used in calculating the dimensionless force and moment coefficients of the array, so that it was not necessary to measure the density of the air.

3.2 Pressure Measurements

Each pressure tap was connected through a pressure switch to a calibrated Setra differential transducer which measured the value of the local pressure above the ambient pressure at the test section away from the model. The output from the pressure transducers was recorded for 16 seconds at a 250 sample per second rate. The data was then analyzed by a Hewlett-Packard System 1000 minicomputer under program control and recorded. The minicomputer calculated the local pressure coefficients and using the reference total value q_{ref} , at 30 ft prototype height,

$$C_p = \frac{P}{q_{ref}} \quad (2)$$

3.3 Normal Force Calculations

The local force per unit area acting on each section of the array is equal to the difference in the pressures measured at the center of that section on the opposite faces of the array. The magnitude of this pressure difference is

$$\Delta p(s) = P(s)_{\text{lower face of array}} - P(s)_{\text{upper face of array}} \quad (3)$$

where s designates the position of the section as defined in Figure 11. A positive value of $\Delta p(s)$ will thus correspond to a

normal net force per unit area with an upward component as shown schematically in Figure 11.

The dimensionless local pressure difference is defined as

$$\Delta C_p = \frac{\Delta P}{q_{\text{ref}}} . \quad (4)$$

The maximum value of this coefficient, $\Delta C_{p_{\text{max}}}$ is of particular interest. The normal force N acting on the entire array can be calculated by integrating the value of $\Delta p(s)$ over the cord. Similarly, the normal force coefficient C_N is given by

$$C_N = \frac{N}{c} = \frac{1}{c} \int_0^c \Delta C_p(s) ds \quad (5)$$

The direction of a positive normal force is shown in Figure 11. In most cases one would expect to find negative values of C_N for $\alpha > 90^\circ$.

4. PRESENTATION AND ANALYSIS OF THE EXPERIMENTAL DATA

4.1 Single Array Tests

Typical records of the pressure distribution on a single photovoltaic array for head-on winds ($WD = 0^\circ$) in the uniform flow are shown in Figures 12-14.* The solid lines in Figure 12 show the local pressure coefficient distributions on the upstream face of the panel. Positive values are usually recorded on the upstream face. The pressure coefficients on the downstream face, marked by dashed lines, are negative and hardly vary across the panel, indicating a flow separation, which was observed in the flow visualization study for both the single array and many of the arrays in an array field, see for example Figure 31. The shape of the pressure distribution curves on the upstream face of the panel is almost symmetric for $\alpha = 90^\circ$, but it becomes more and more skewed as the angle of attack decreases (Figure 12) or increases (Figure 13). Figure 14 shows the same data but for a large ground clearance, $H/c = \infty$ (actually measured at $H/c = 1.7$).

Comparing Figures 12 and 14 one finds that the pressure distribution on the upstream face of the panel is not affected to a large extent by the ground clearance. The back pressure, on the other hand, appears to change significantly. A value of $C_p \approx -1.35$ was recorded for $\alpha = 90^\circ$, $H/c = \infty$, whereas a value of $C_p = -0.75$ was recorded for the same angle of attack with a ground clearance of $H/c = 0.25$. This reduction of the back pressure reduces significantly the normal force acting on the plate. Figure 15 shows the absolute values of

*Unless explicitly stated, the data refers to the measurements at the center of the array (see Figure 10).

the normal force for all the single array tests in a uniform flow. Evidently, the same effect is apparent at all angles of attack.

The reduced drag at small ground clearances may be due to the changes in the wakes caused by the reduction in the eddy size downstream of the panel. It should be recalled that the approach velocities in these tests are independent of height. The complicated nature of the interaction between these eddies and the flow, which determine the base pressure, makes it difficult to predict the value of these pressures theoretically.

The pressure distributions on a single array ($H/c = 0.25$) in a nonuniform flow are shown in Figures 16 and 17. A clear reduction of the pressure coefficients relative to those in the uniform flow is observed. The corresponding absolute values of the normal force for the two cases are shown in Figure 18. The average ratio $C_N(\text{uniform})/C_N(\text{nonuniform})$ is $1.43 \pm 5\%$ for these tests. This large reduction is primarily due to the relatively small wind speeds at the height of the array for the nonuniform velocity profile. It should be recalled that q_{ref} is measured at the height of 10 m above the ground whereas the center of the panel, for this value of ground clearance, varies from 3.36 ft for $\alpha = 20^\circ$ to 6 ft for $\alpha = 90^\circ$. The corresponding ratios of $q_{\text{ref}}/q_{\text{center of panel}}$ for these cases in a 1/7th power law velocity distribution are 1.89 and 1.61 respectively. Obviously, the difference in the dynamic pressure of the free stream at the height of the panel alone cannot fully explain the observed changes. Comparing the ratio of the back pressures in the two cases, for example, one finds an average ratio

of almost 2, whereas the ratio of the pressure coefficients on the upstream face of the panel is only around 1.5. The shape of the corresponding pressure distribution curves is also different for the two cases.

4.2 Array Field Tests

A wide field of photovoltaic arrays is characterized by the separation distance, x/c , between the array (see Figure 11) and their angle of attack. The value of the normal force acting on each array depends, of course, on its position in the field. Figure 19 shows the values of C_N for the 1st, 2nd and 5th arrays (from the upstream edge of the field) for head-on uniform winds. The magnitudes of the normal force on array No. 1 are approximately equal to their values in a single array. A drastic reduction in the magnitude of the normal forces on the 2nd and 5th arrays is observed. In some cases the direction of the normal force is reversed.

The magnitude of the forces acting on the 1st array can be reduced by building a fence or a barrier (zero porosity fence) upstream of the field. The effect of the fence depends on its porosity, height and distance. Figure 20 shows the effect of a 30 percent porosity fence and a zero porosity fence on the magnitude of the normal forces acting on the 1st and 2nd rows for different fence heights, and for an angle of attack $\alpha = 35^\circ$. Similar results are obtained at different angles of attacks (see Figure 21).

The magnitude of the normal forces at the edge of an array, in case of head-on winds, is expected to be smaller than that of the forces acting on the center of the array. In case of side winds, however, the edges of the field and particularly the upstream corner will be exposed to higher loads. These forces can be reduced by a side fence and/or by different corner fence configurations. Figure 22 shows the corner fence configurations tested in this study. Their effect on the magnitude of the normal force for cornering winds is shown in Figure 23, which clearly exhibits the effect of properly designed fences on the normal forces at the field edges and corners.

Another way to reduce forces at the edge of the array field is to extend the array by an inexpensive stronger structure or by modifying the shape of the array edges. Several configurations, shown in Figure 24, have been studied. The fence configurations are also tabulated in Table 17. Their effect on the normal forces at the corner for $WD = 45^\circ$ is shown in Figure 25 for $\alpha = 35^\circ$ and $\alpha = 145^\circ$.

An overall view of the results and the effect of the various parameters on the normal forces is shown in Figures 26-30. Figures 26 and 27 show the effect of the distance between the arrays for different angles of attack. Figure 28 summarizes the fence study for head-on winds. Figures 29-30 show the effect of the corner fences and the modifications of the array edges. All test configurations investigated for this study are listed in Table 18.

4.3 Flow Visualization

Flow visualization was used in this study to explore the structure of the flow in the array field and to obtain a better understanding of the force and pressure measurements.

Figure 31a shows the wake behind the first array in the field and behind an array in the center of the field. Clear flow separation is observed for this angle of attack and spacing. Figures 31b and 31c show the structure and the nature of the flow at different points between the arrays.

Figure 32 shows two corner fence configurations and their effect on the flow structure near the fence.

5. CONCLUSIONS

Wind loadings on photovoltaic arrays in a large array field were measured on 1:24 and 1:12 scale wind-tunnel models. The dimensionless pressure and force coefficients measured are independent of the Reynolds number and can therefore be used for the design of prototype arrays.

Considerable differences were found between the normal force coefficients for uniform and nonuniform velocity fields. The arrays at the edges and corners of the field will usually be exposed to much larger forces than the arrays in the interior of the field. These forces can be considerably reduced, however, by fences and barriers. Data is presented which make it possible to design the prototype array field and fences for given atmospheric winds.

6. REFERENCES

1. American National Standards Institute, American National Standard Building Code Requirements for Minimum Design Loads in Buildings and Other Structures, ANSI Standard A58.1, 1972.
2. Miller, R. D. and Zimmerman, D., Wind Loads on Flat Plate Photovoltaic Array Fields, Boeing Engineering and Construction Report No. DOE/JPLG54833-79/2, Seattle, Washington 98124, September 1979.
3. Cermak, J. E., Aerodynamics of Buildings, Annual Review of Fluid Mechanics, Vol. 8, 1976.
4. Cermak, J. E., Laboratory Simulation of the Atmospheric Boundary Layer, AIAA J1., Vol. 9, September 1971.
5. Cermak, J. E., Applications of Fluid Mechanics to Wind Engineering, A Freeman Scholar Lecture, ASME J1. of Fluids Engineering, Vol. 97, No. 1, March 1975.
6. Bearman, P. W., Turbulence Effects on Bluff Body Mean Flow, Third U.S. National Conference on Wind Engineering Research, pp. 265-272, 1978.
7. Bearman, P. W., An Investigation of the Forces on Flat Plates Normal to a Turbulent Flow, J1. Fluid Mechanics, Vol. 46, pp. 177-198, 1971.
8. Nakamura, Y. and Tomonari, Y., The Effect of Turbulence on the Drag of Rectangular Prisms, Transactions Japan Society of Aeronautical and Space Science, Vol. 19, pp. 81-86, 1976.
9. Harris, R. I., The Nature of the Wind, Modern Design for Wind Sensitive Structures, Paper 3, 1971.
10. Davenport, A. G., The Spectrum of Horizontal Gustiness Near the Ground, Quarterly J1., Royal Meteorological Society, Vol. 81, pp. 194-211, 1961.

A-18

FIGURES

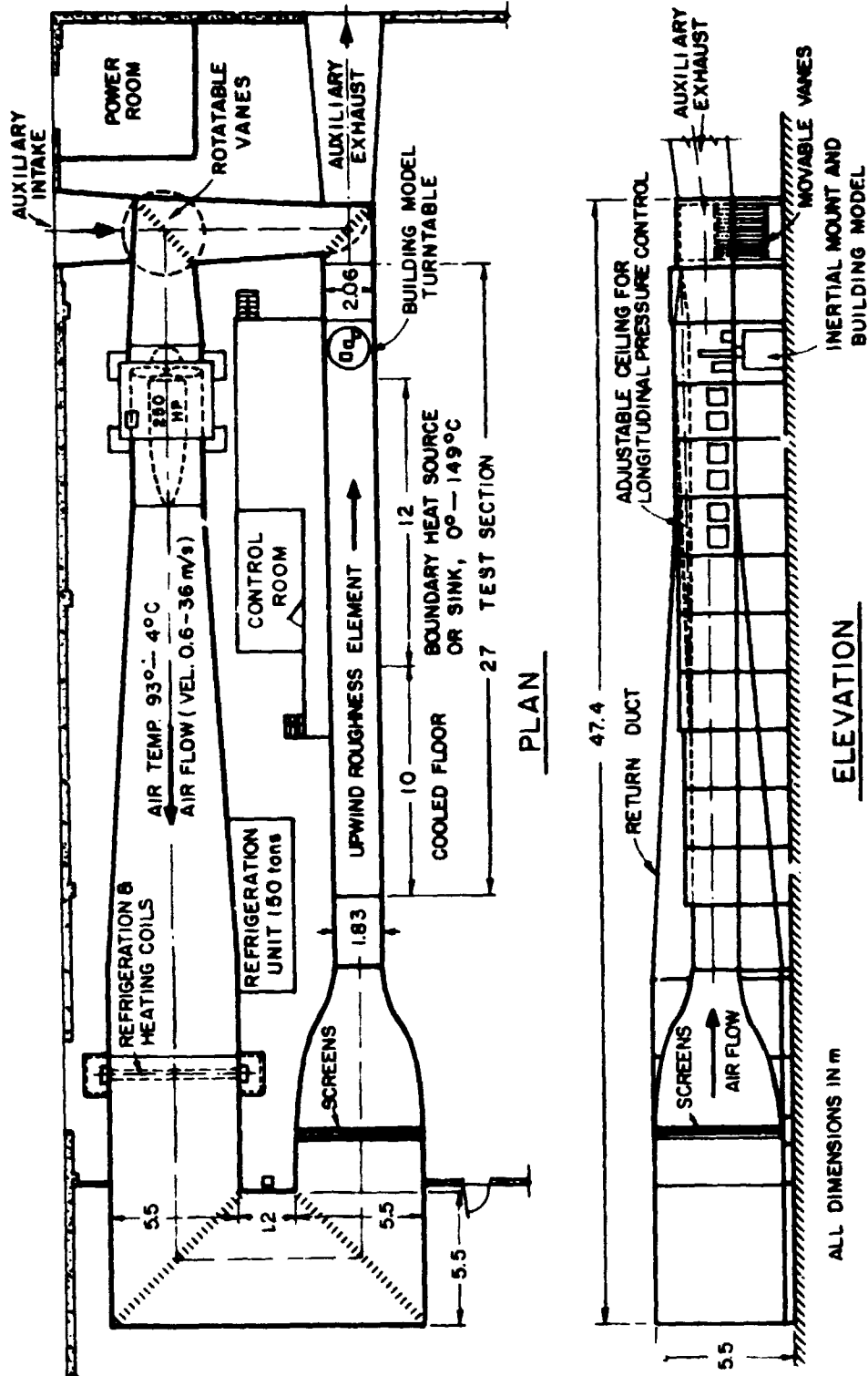


Figure 1. Meteorological Wind Tunnel

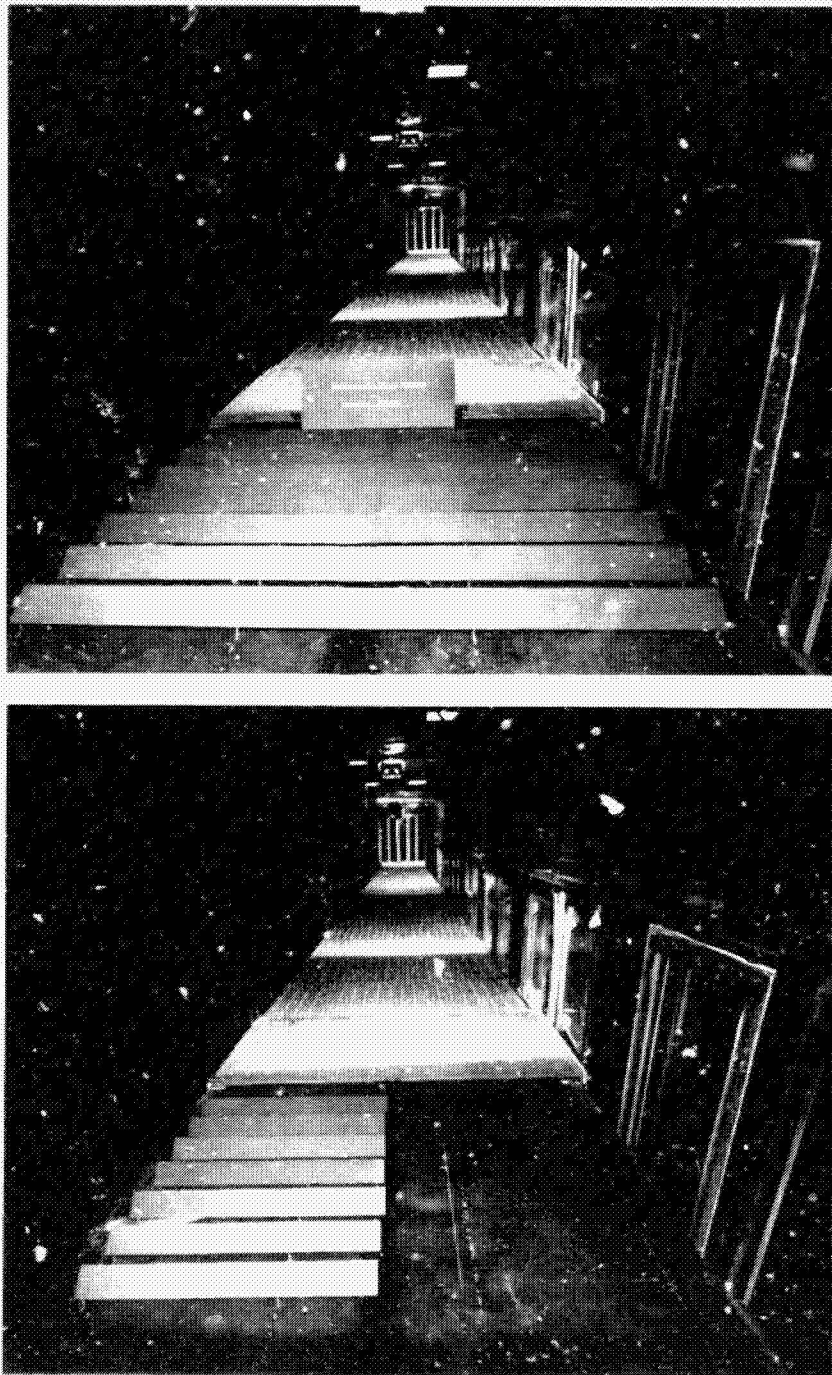


Figure 2. Array Field Models in Meteorological Wind Tunnel

ORIGINAL PAGE IS
OF POOR QUALITY

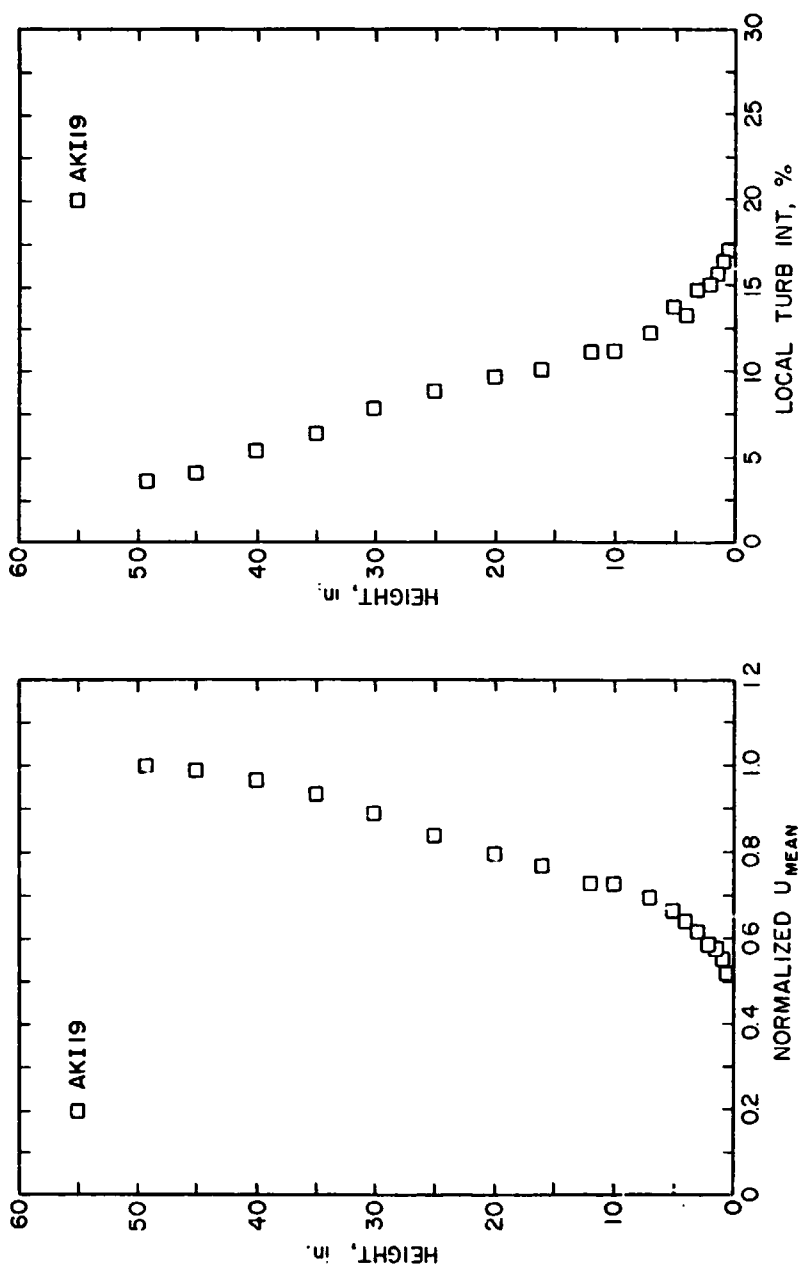


Figure 3. Mean Velocity and Turbulence Distribution in Nonuniform Flow

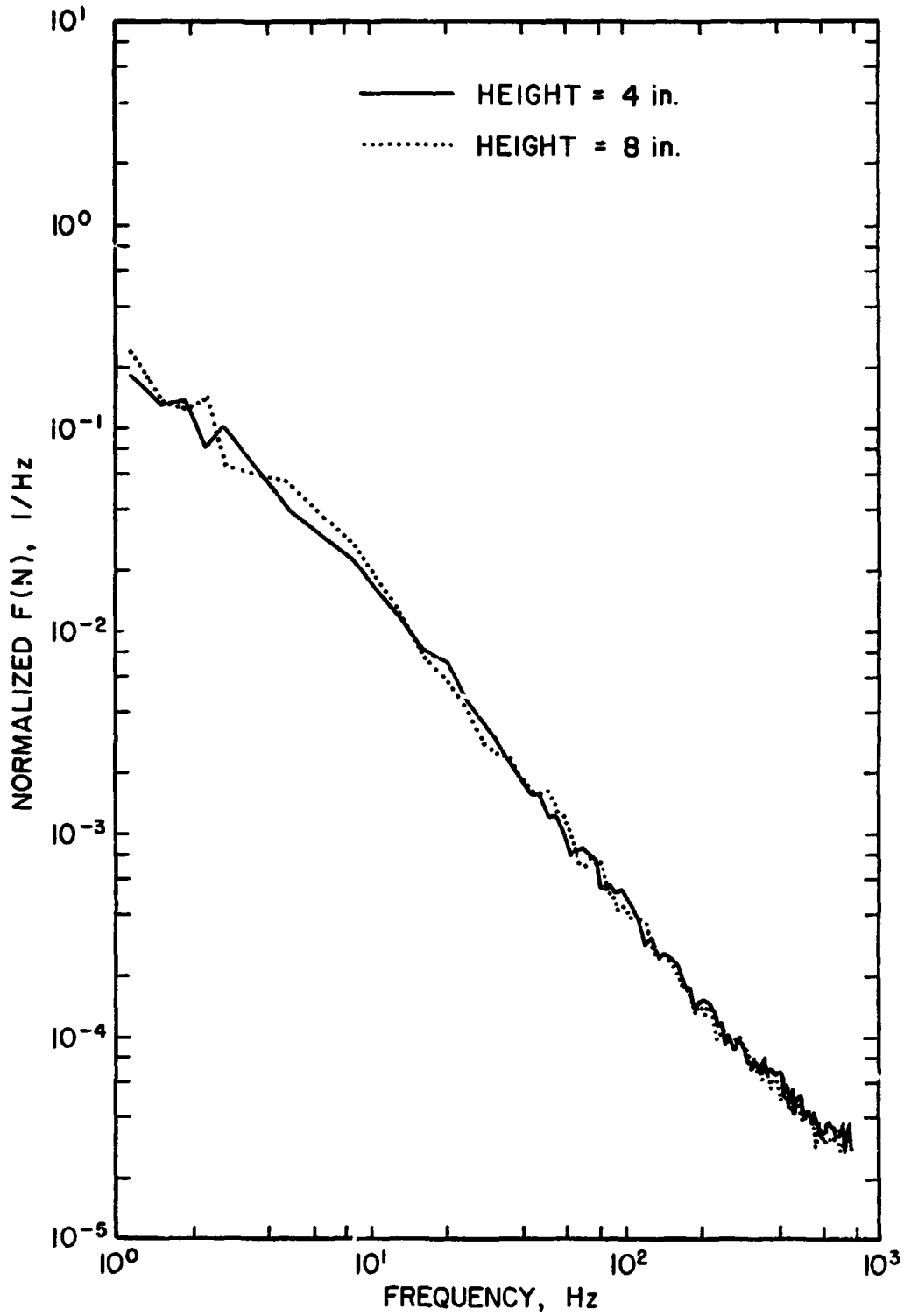


Figure 4. One Dimensional Velocity Spectra in Nonuniform Flow

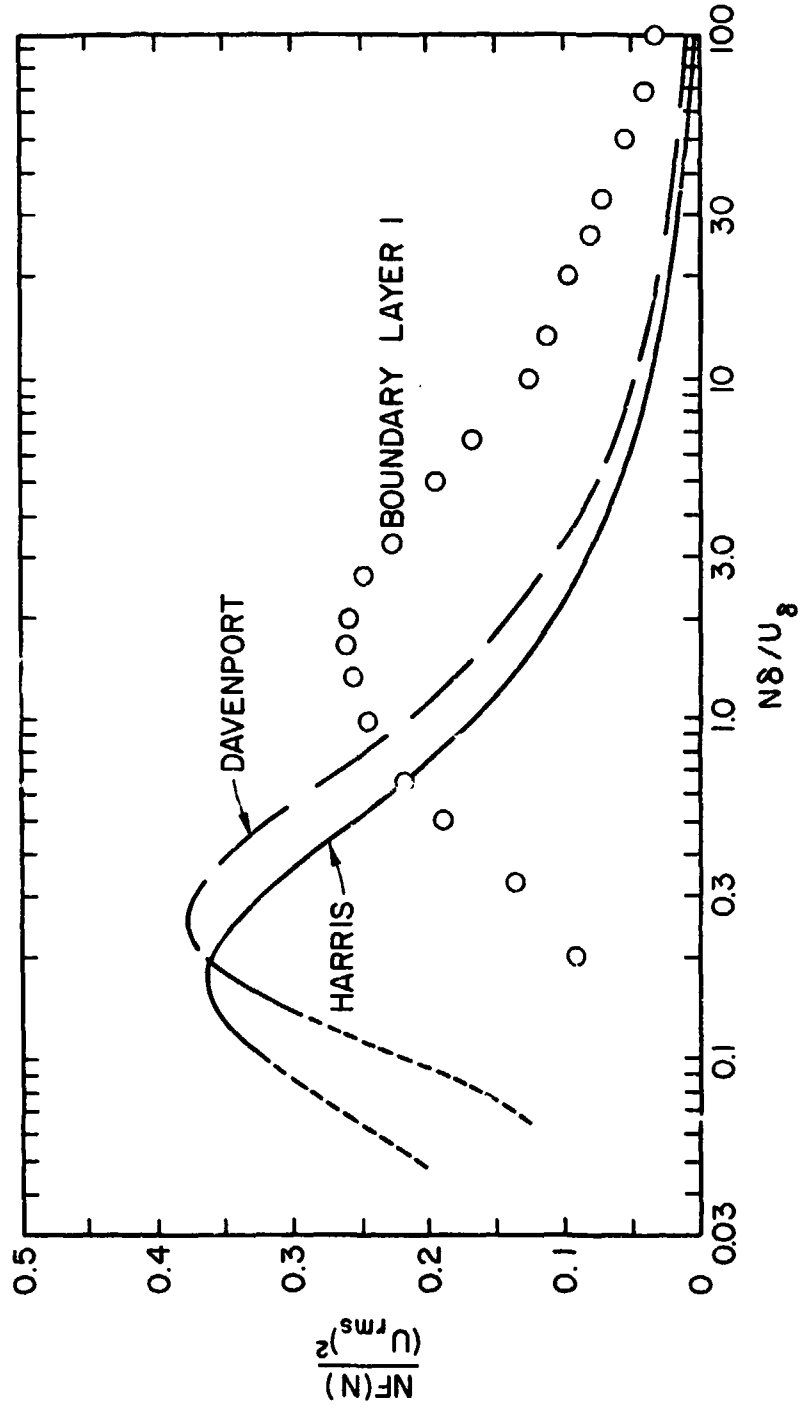


Figure 5. Turbulence Spectra in Nonuniform Flow (BL1) Compared to Atmospheric Spectra

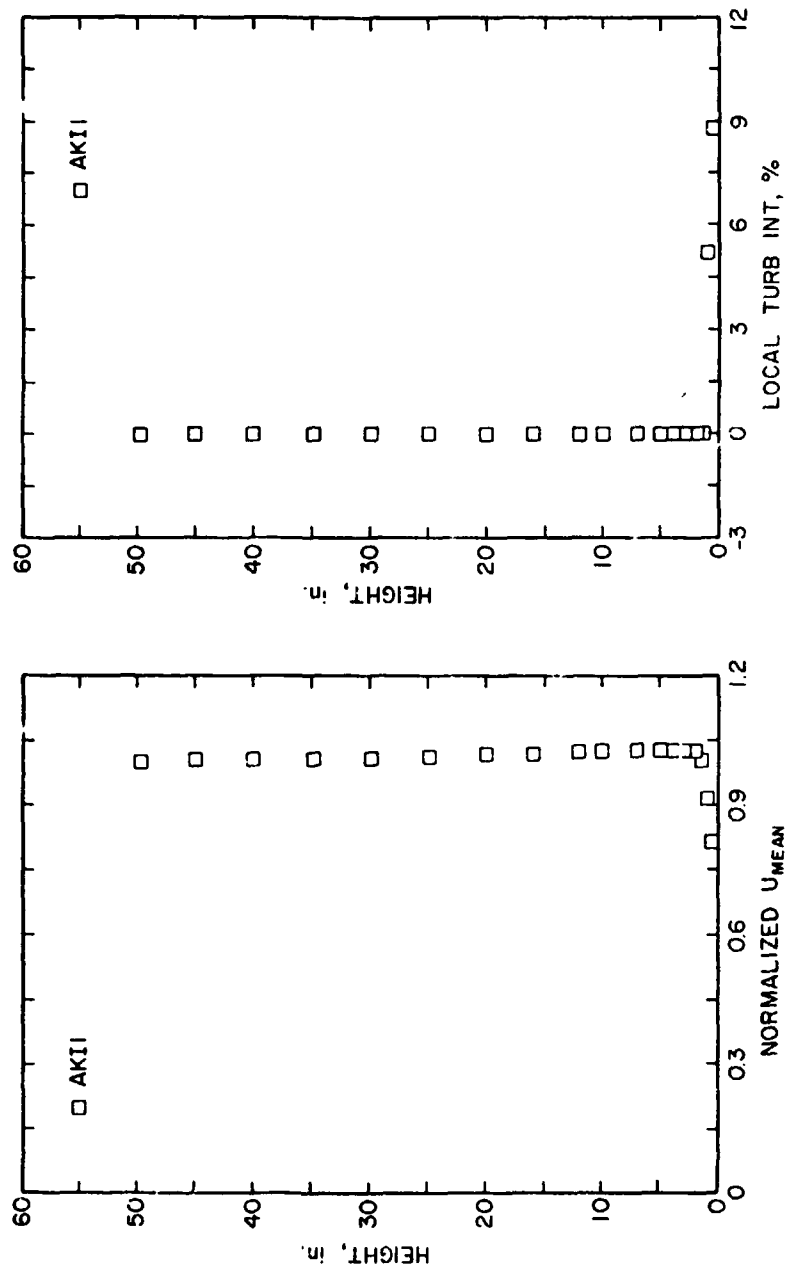


Figure 6. Mean Velocity and Turbulence Distribution in Uniform Flow

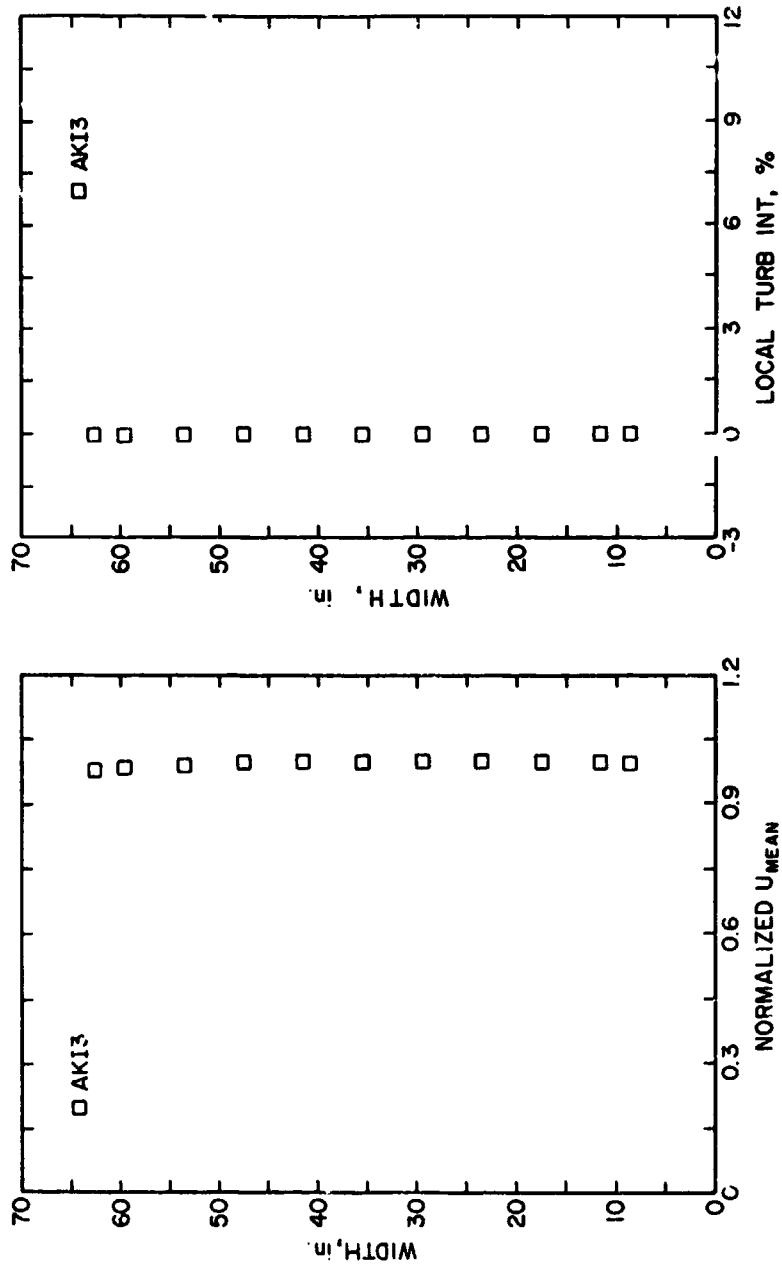


Figure 7. Typical Horizontal Velocity Distribution across Meteorological Wind Tunnel

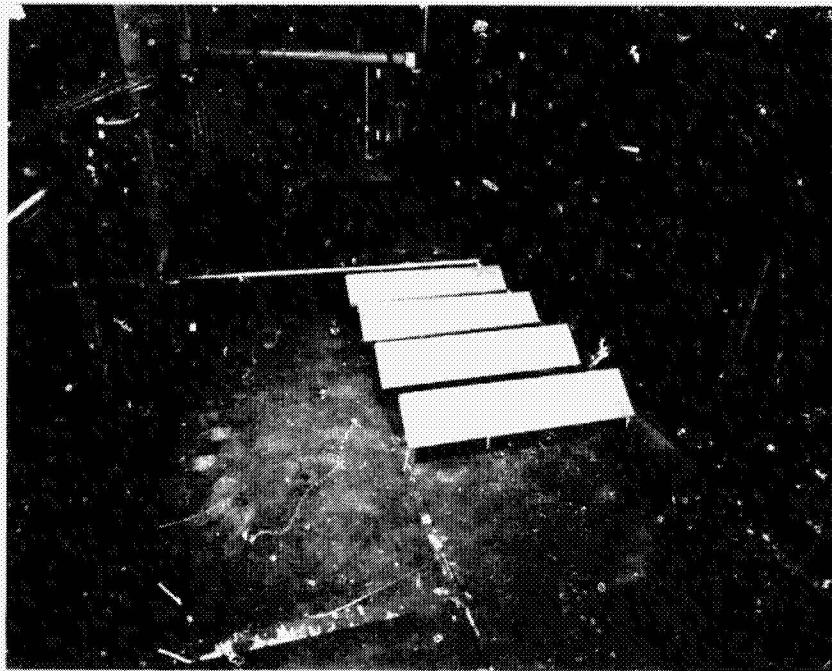


Figure 8. 1:12 Scale Models in Meteorological Wind Tunnel

ORIGINAL PAGE IS
OF POOR QUALITY

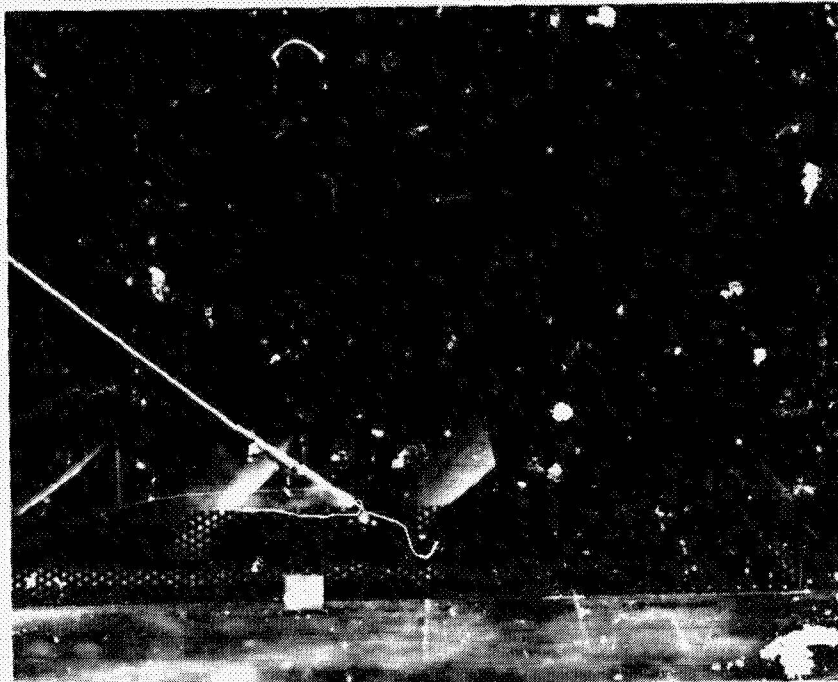
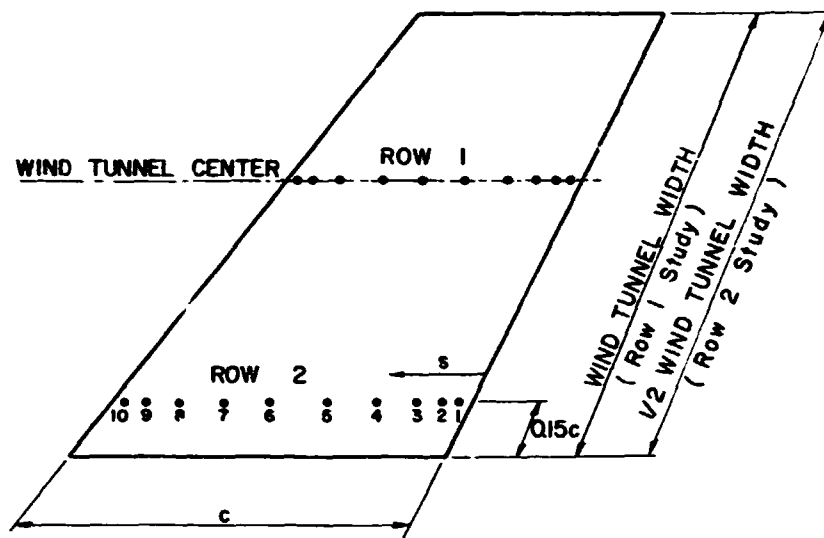


Figure 9. Photograph of Standard Corner Fence

ORIGINAL PAGE IS
OF FOUR QUALITY



TAP LOCATIONS - FRACTION OF CHORD s/c

	1	2	3	4	5	6	7	8	9	10
UPSTREAM SURFACE	0.052	0.102	0.172	0.272	0.432	0.592	0.752	0.852	0.922	0.972
DOWNSTREAM SURFACE	0.028	0.078	0.148	0.248	0.408	0.568	0.728	0.828	0.898	0.948

Figure 10. Position of Pressure Taps on Instrumented Model

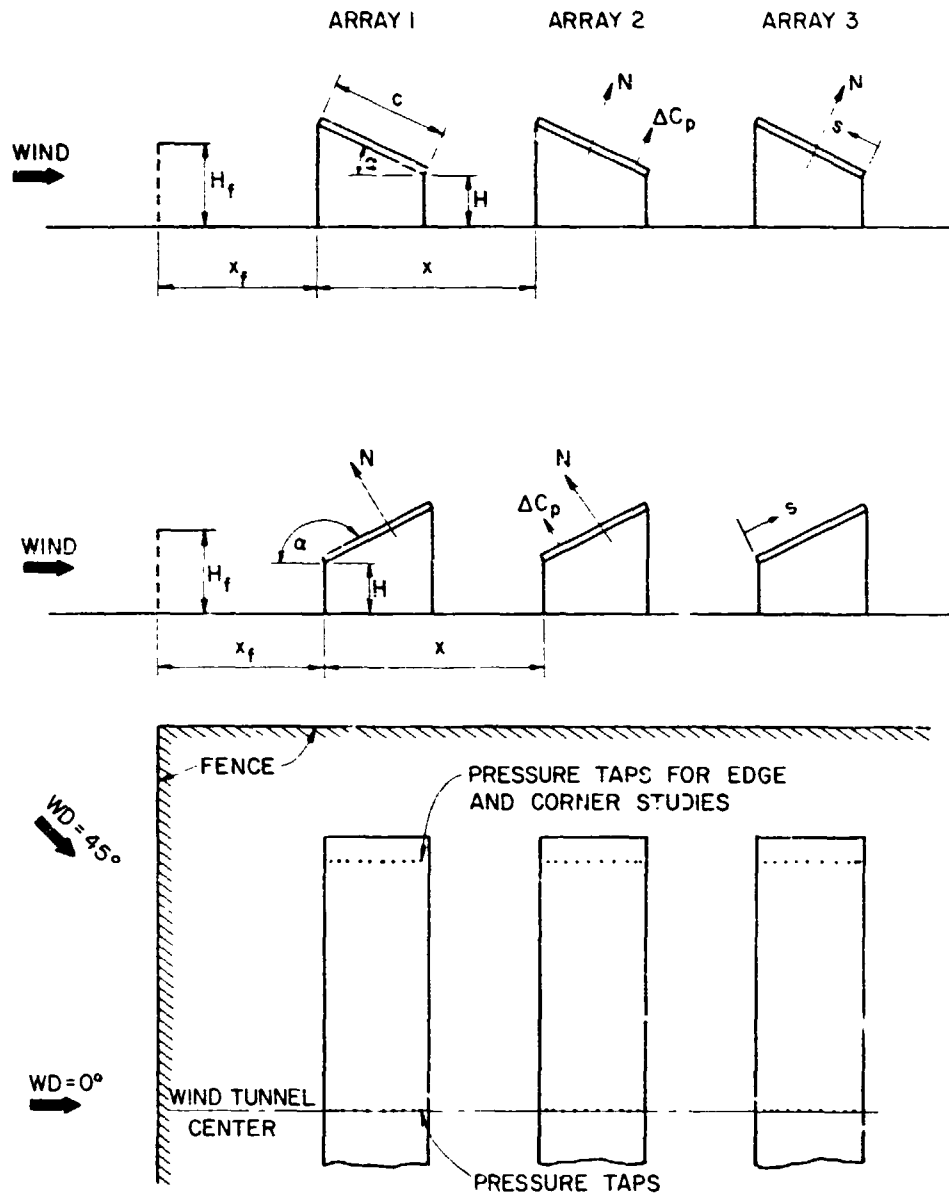


Figure 11. Schematic Description of Array Field

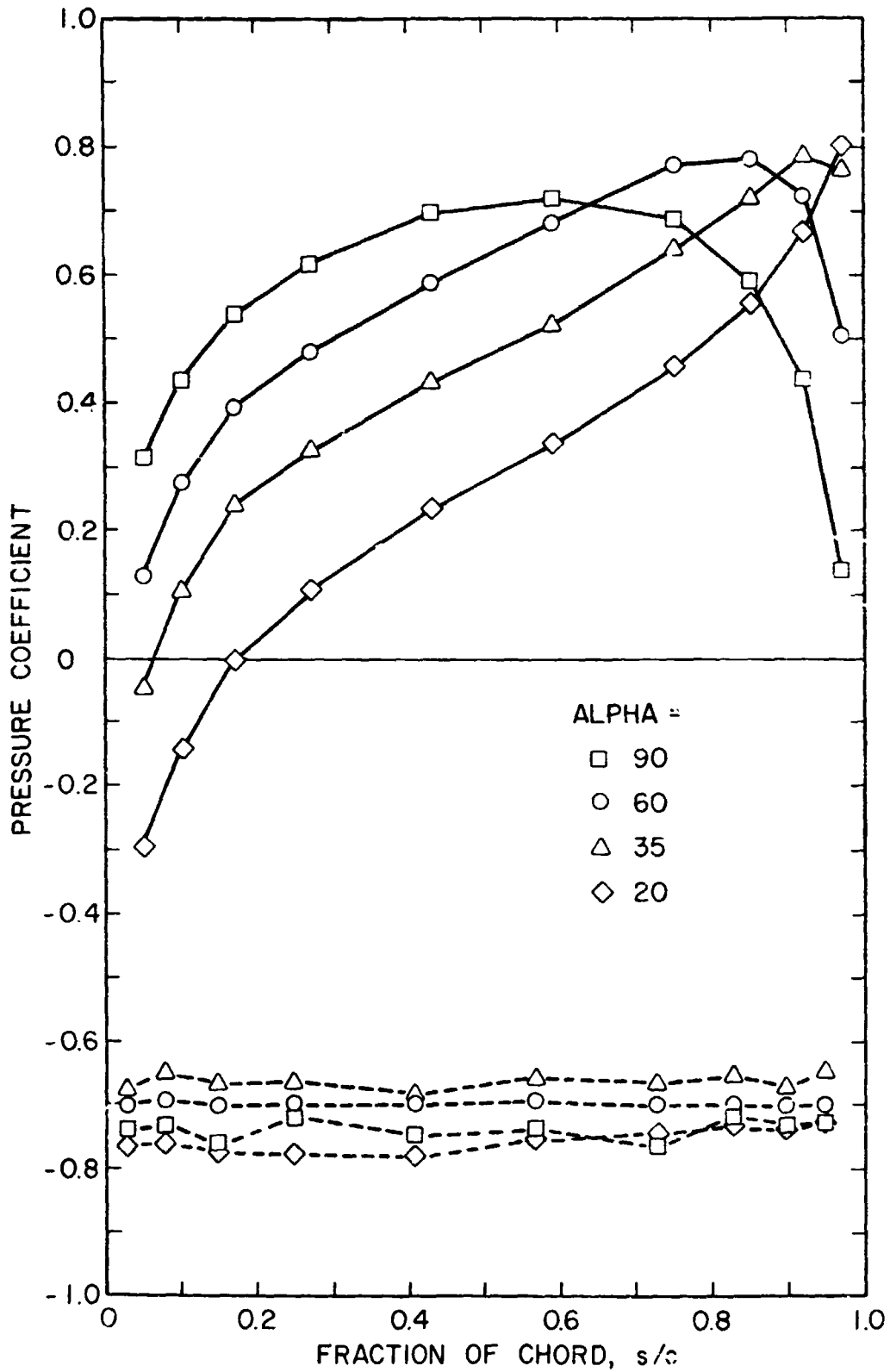


Figure 12. Front and Back Pressures on a Single Array in Uniform Flow, $WD = 0^\circ$, $H/c = 0.25$, $\alpha = 20^\circ, 35^\circ, 60^\circ$ and 90°

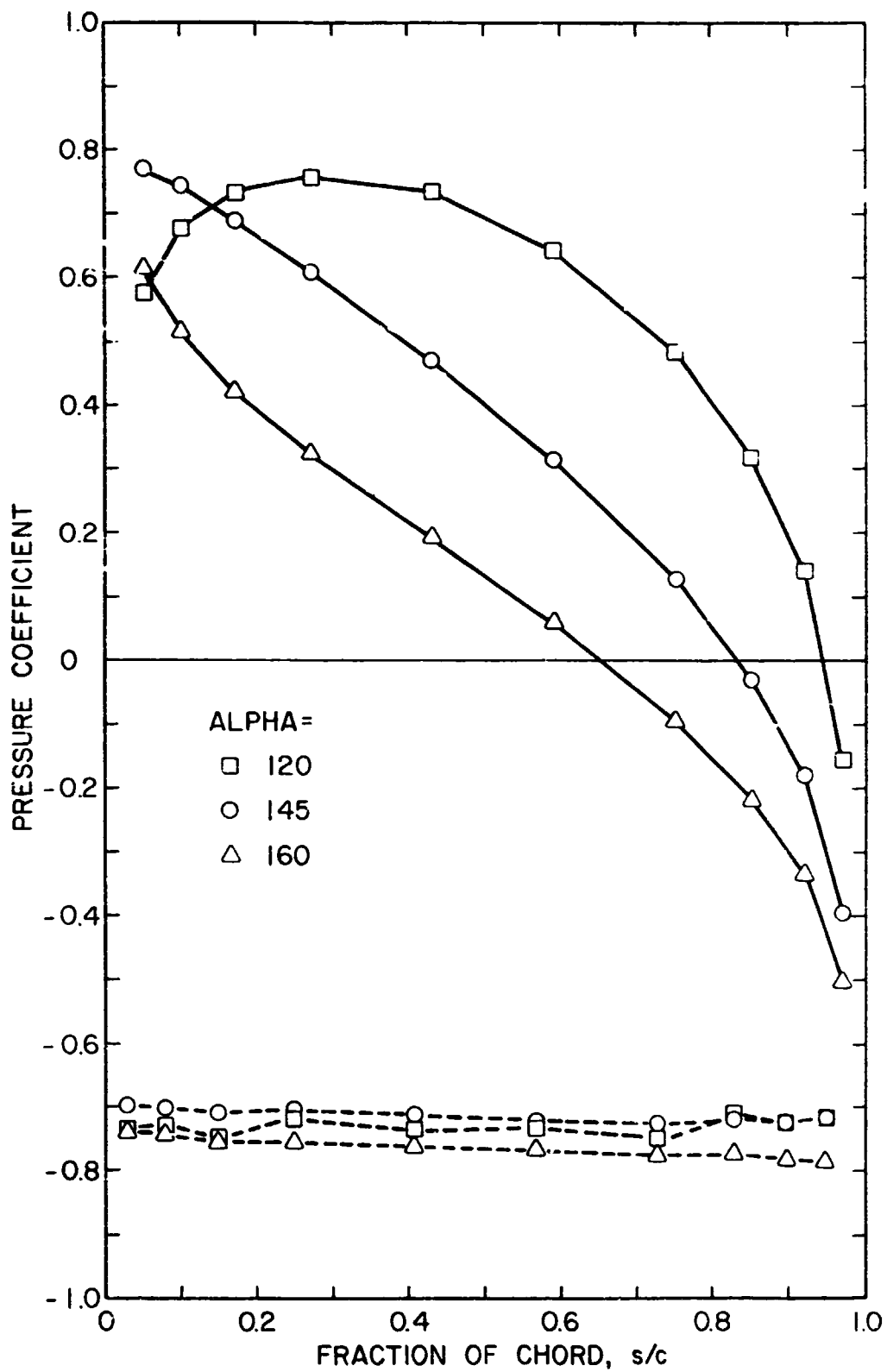


Figure 13. Front and Back Pressures on a Single Array in Uniform Flow, $WD = 0^\circ$, $H/c = 0.25$, $\alpha = 120^\circ$, 145° and 160°

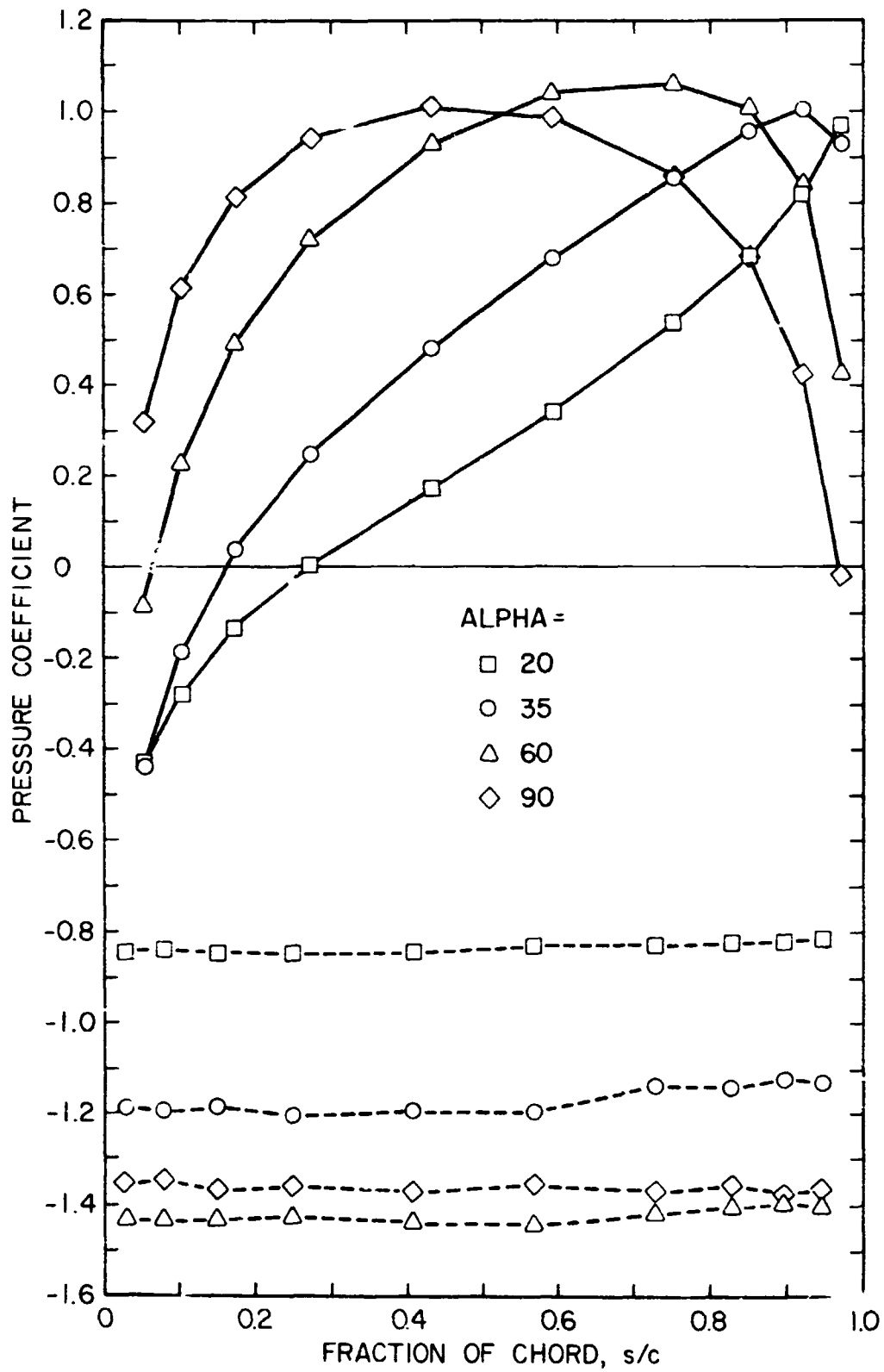


Figure 14. Front and Back Pressures on a Single Array in Uniform Flow, $WD = 0^\circ$, $H/c = \text{infinity}$, $\alpha = 20^\circ$, 30° , 60° , and 90°

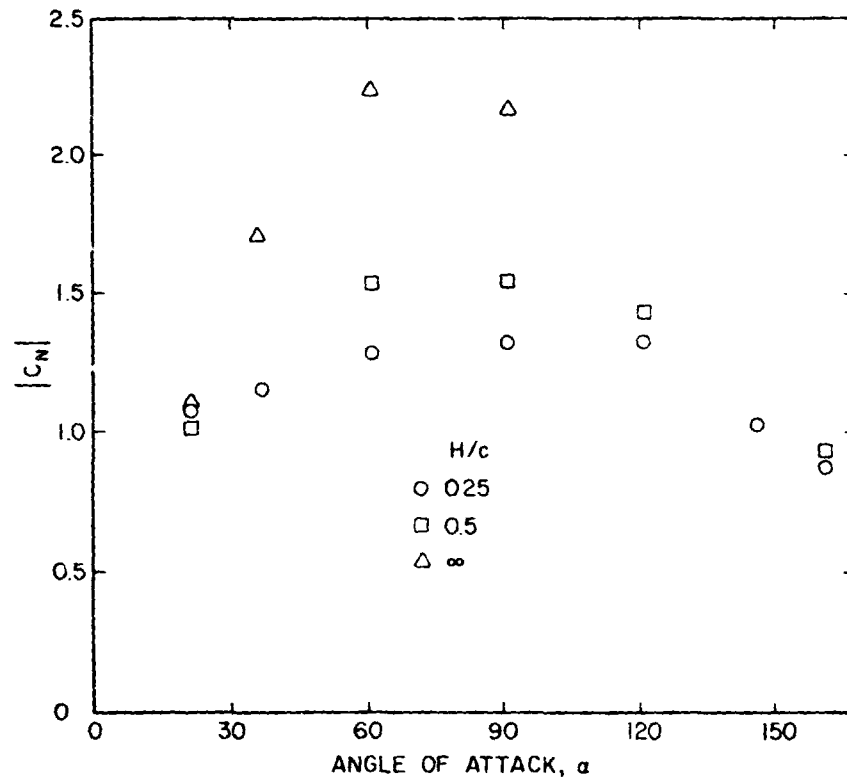


Figure 15. Absolute Values of Normal Force Coefficients on a Single Array in Uniform Flow, $WD = 0^\circ$

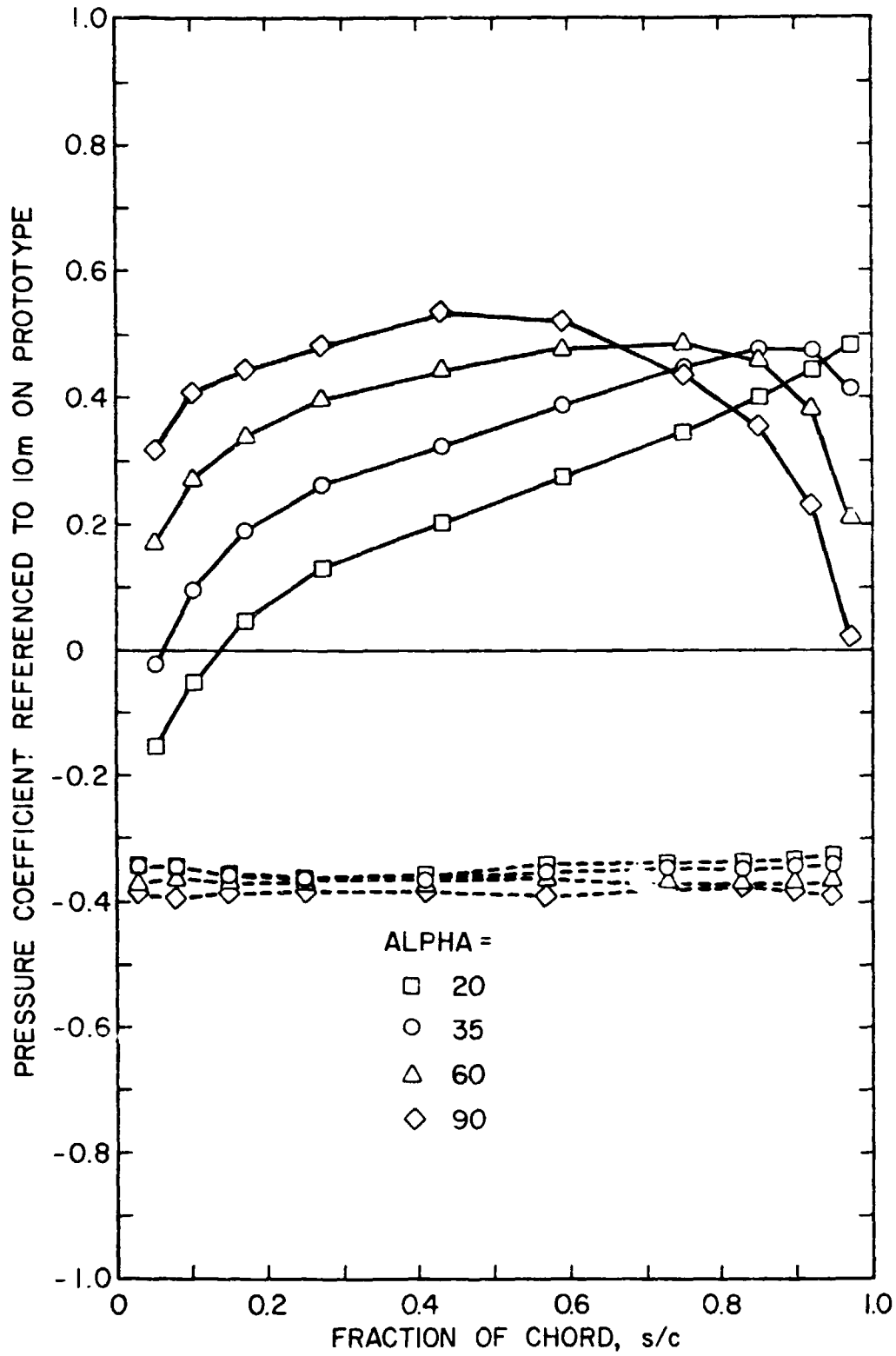


Figure 16. Front and Back Pressures on a Single Array in Nonuniform Flow, $WD = 0^\circ$, $H/c = 0.25$, $\alpha = 20^\circ$, 30° , 60° and 90°

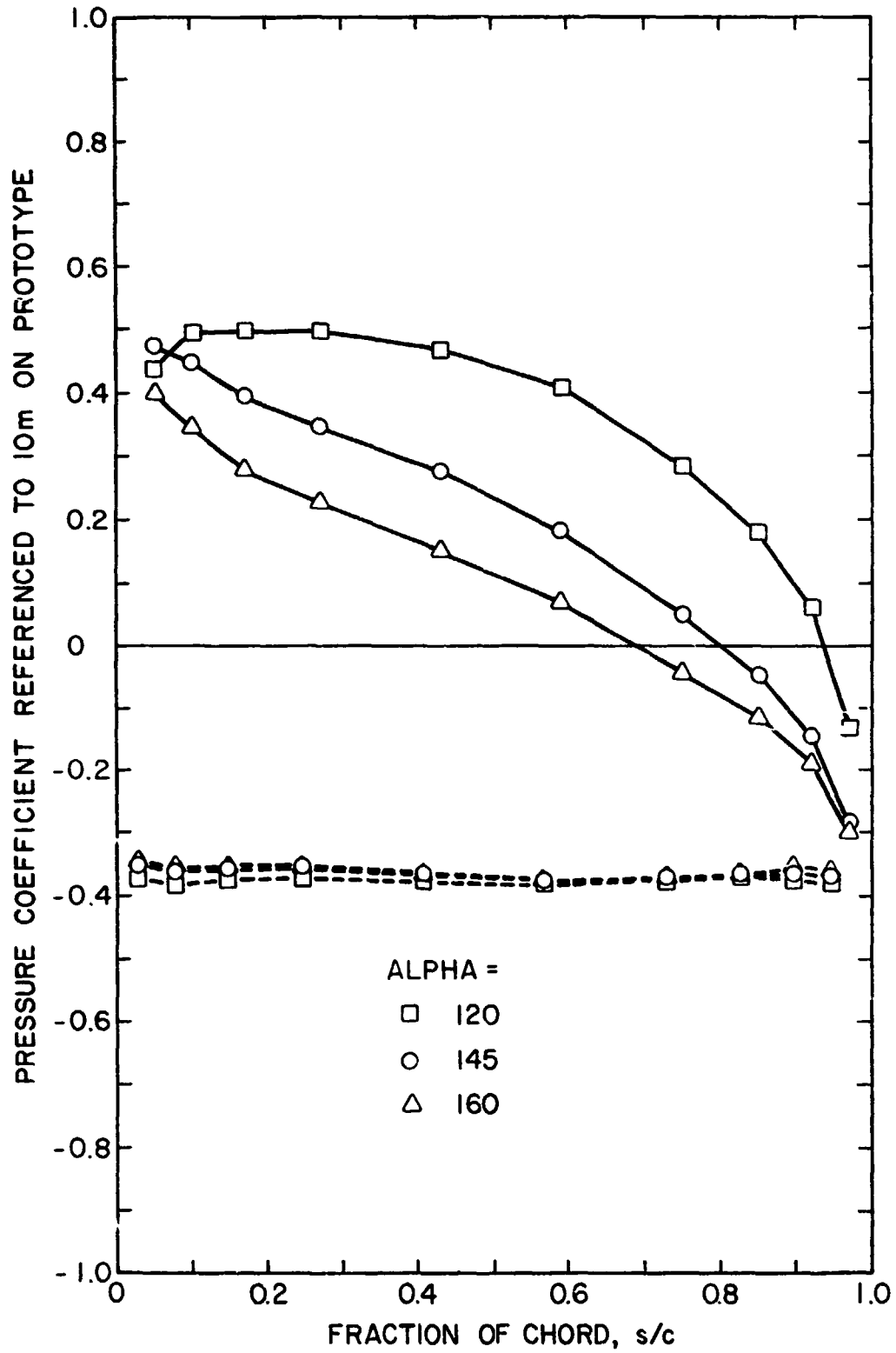


Figure 17. Front and Back Pressures on a Single Array in Nonuniform Flow, $WD = 0^\circ$, $H/c = 0.25$, $\alpha = 120^\circ$, 145° and 160°

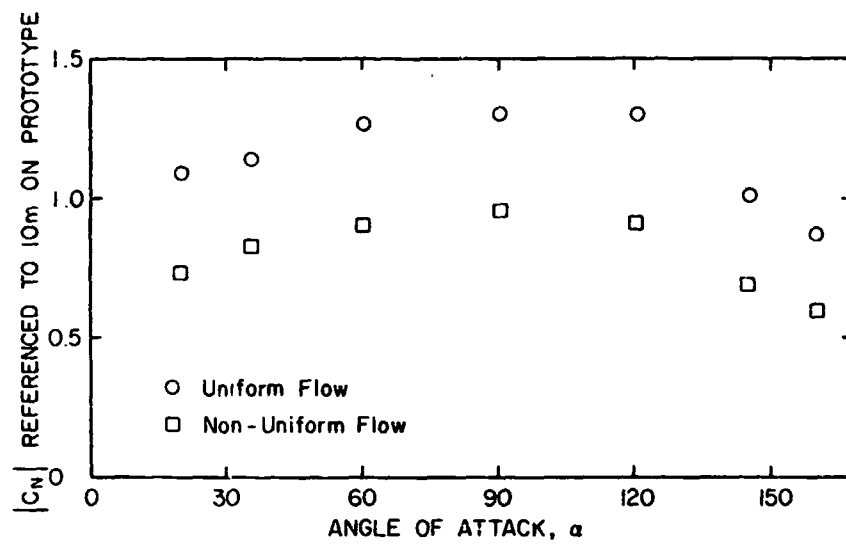


Figure 13. Absolute Values of Normal Force Coefficients on a Single Array in Nonuniform and Uniform Flows, $WD = 0^\circ$, $H/c = 0.25$

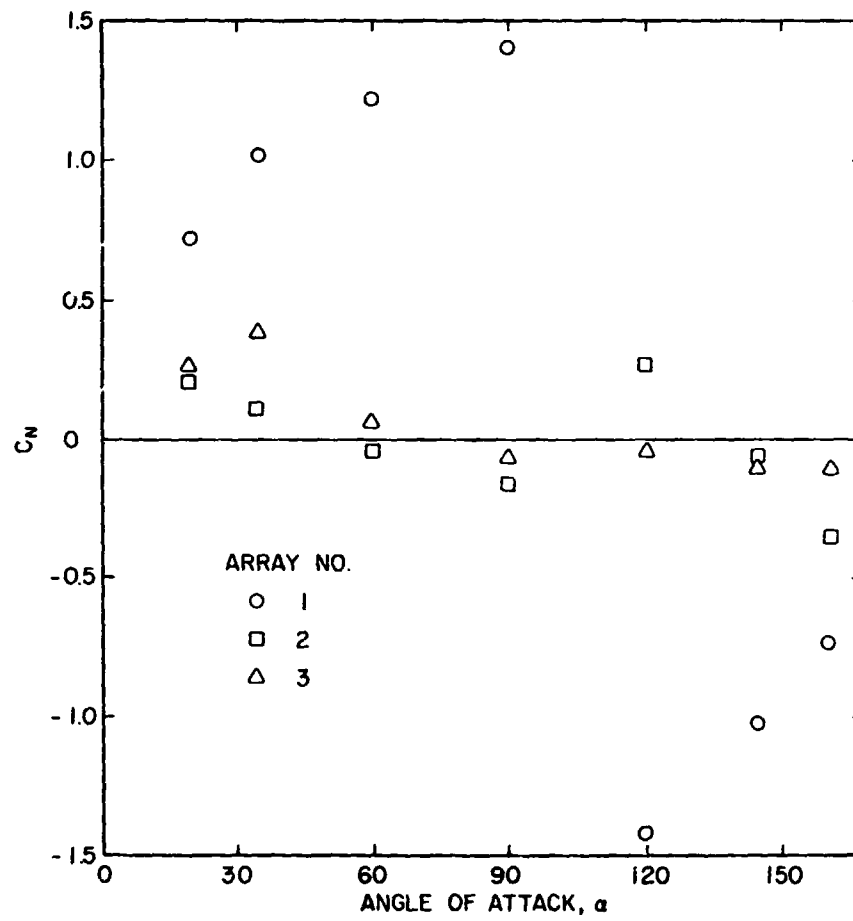


Figure 19. Normal Force Coefficients for an Array Field in Uniform Flow, $WD = 0^\circ$, $x/c = 2.0$, $H/c = 0.25$, No Fence

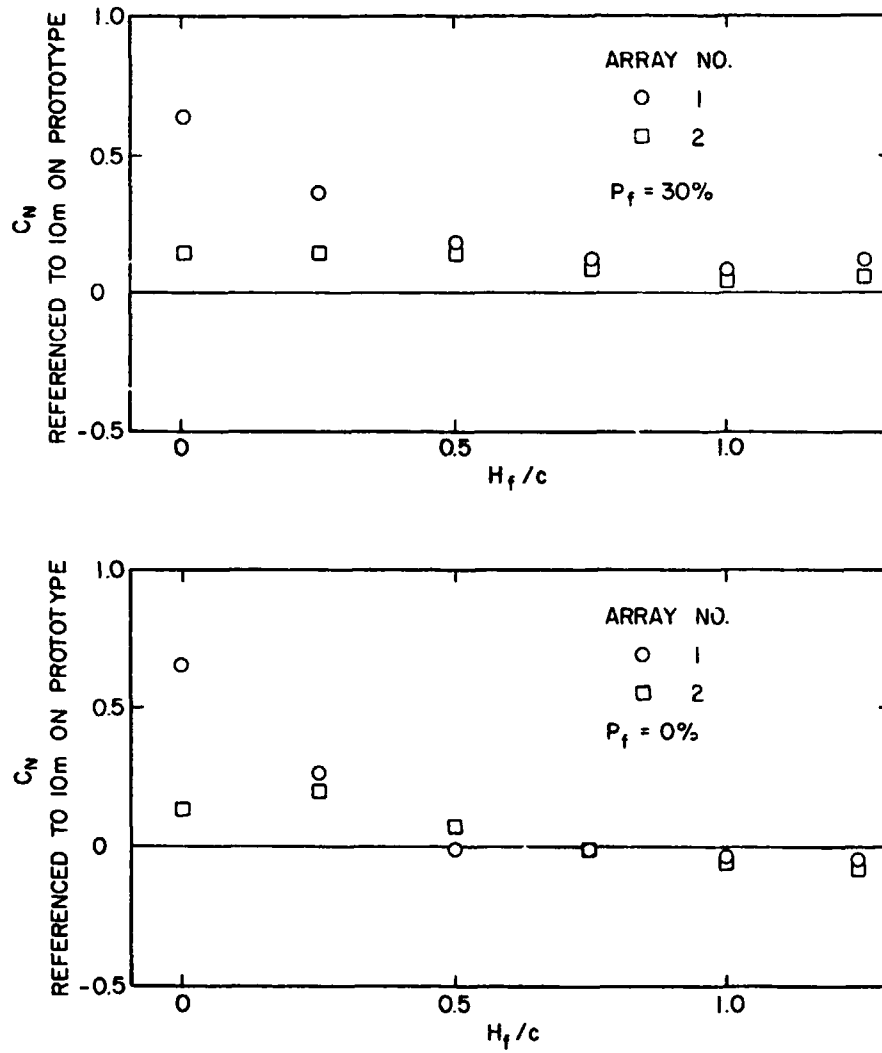


Figure 20. Normal Force Coefficients for an Array Field with a Fence of Various Height and Porosity, $WD = 0^\circ$, $x/c = 2.0$, $H/c = 0.25$, $\alpha = 35^\circ$

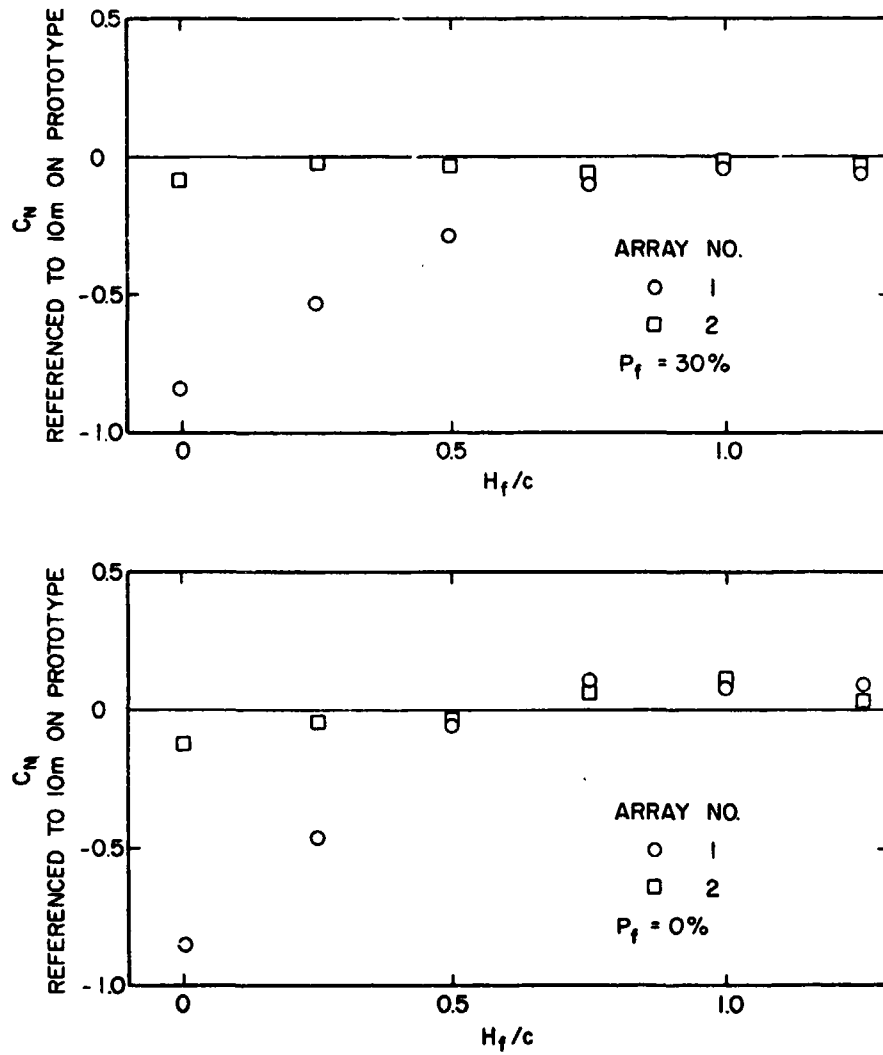


Figure 21. Normal Force Coefficients for an Array Field with a Fence of various Height and Porosity, $WD = 0^\circ$, $x/c = 2-0$, $H/c = 0.25$, $\alpha = 145^\circ$

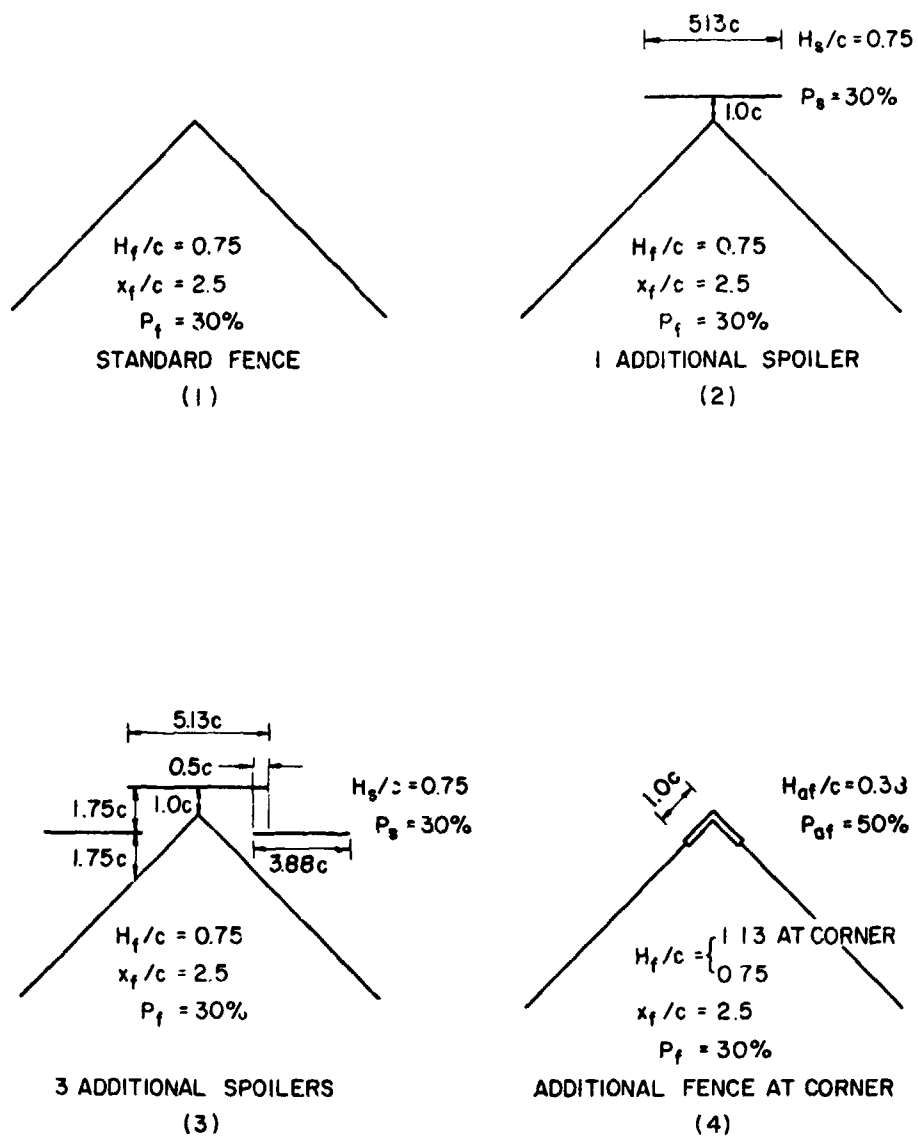


Figure 22. Corner Fence Configurations

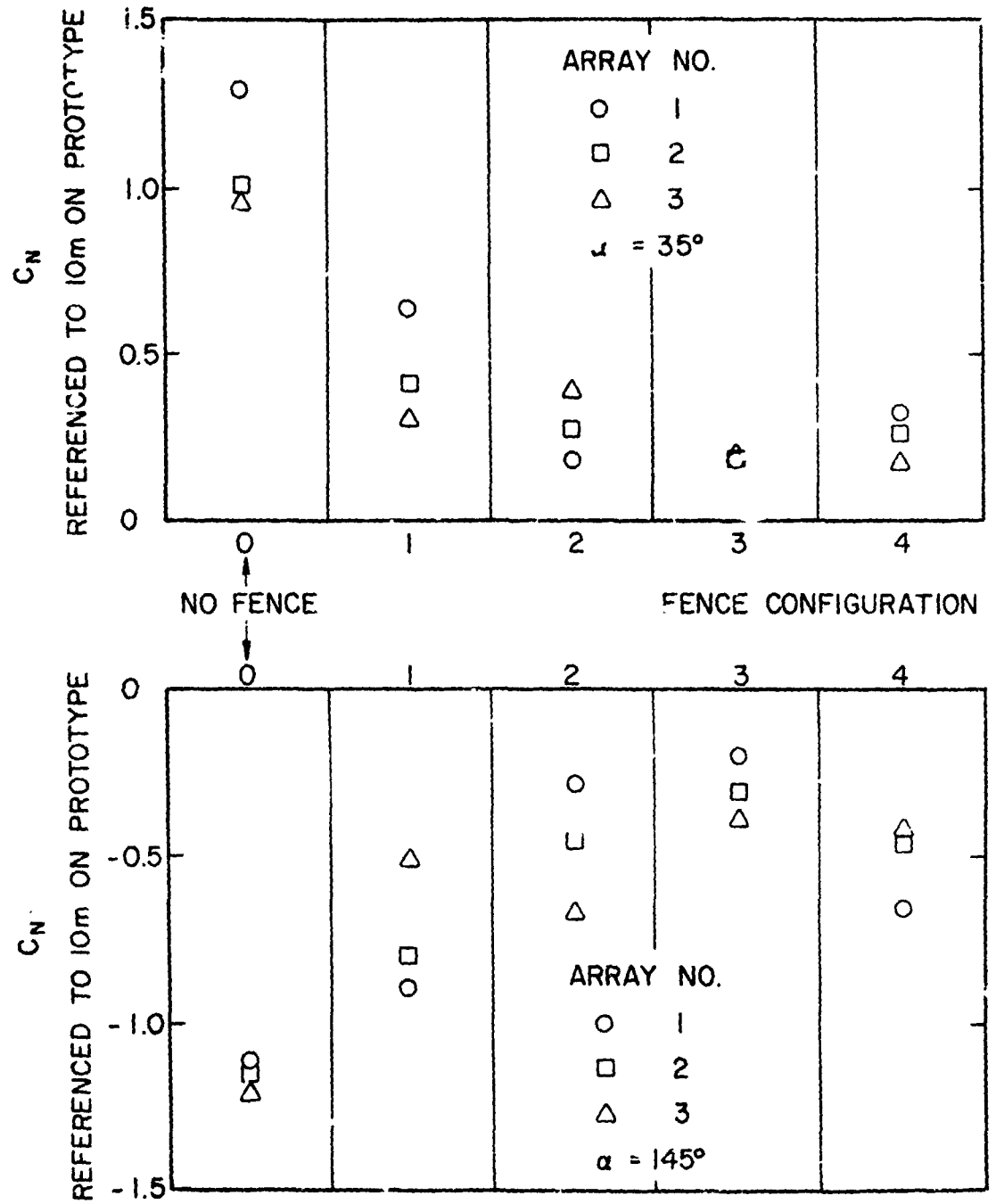


Figure 23. Normal Force Coefficients for an Array Field with Various Fence Configurations; $WD = 45^\circ$, $x/c = 2.0$, $h/c = 0.25$, $MC = 0$

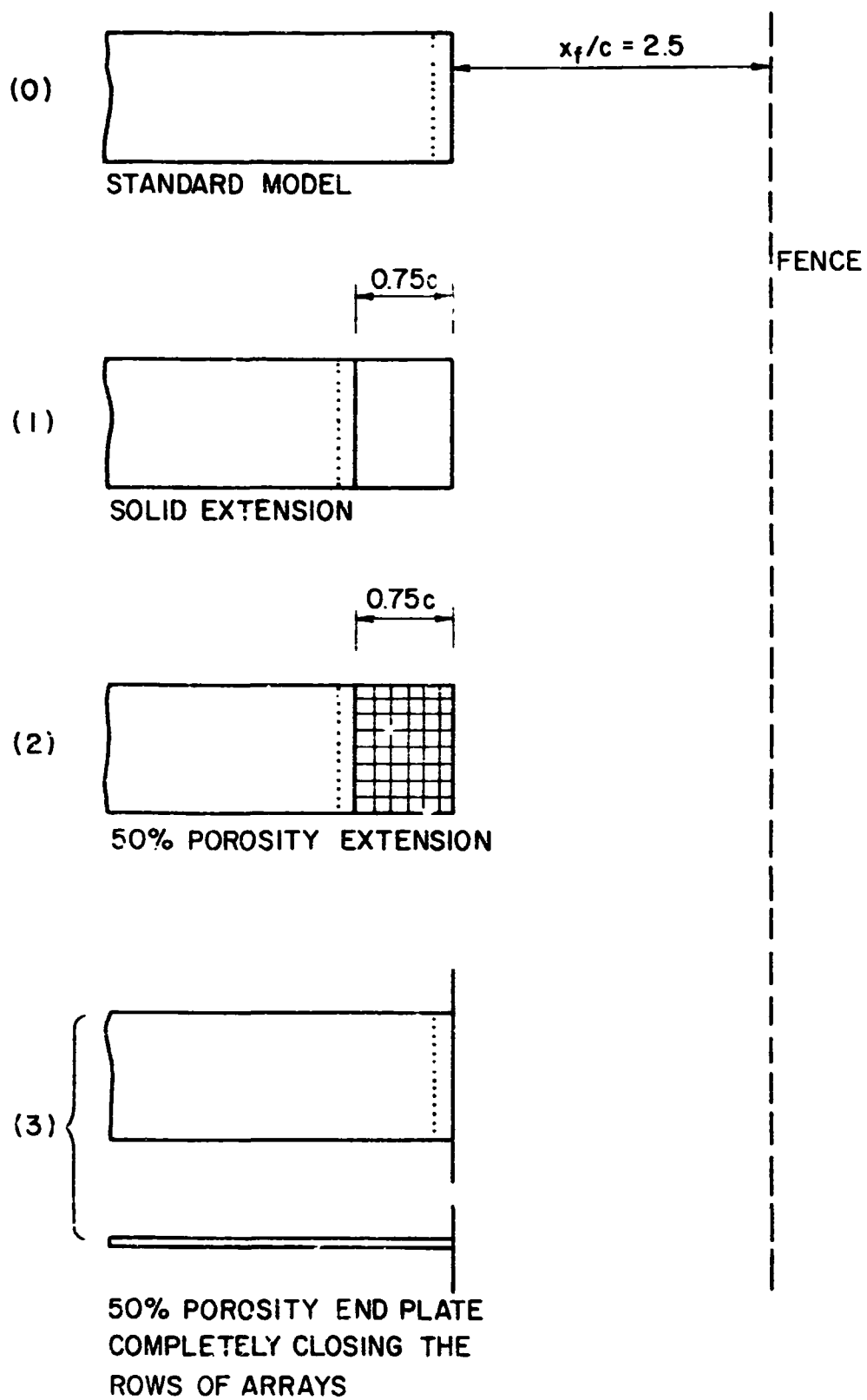


Figure 24. Model Configurations

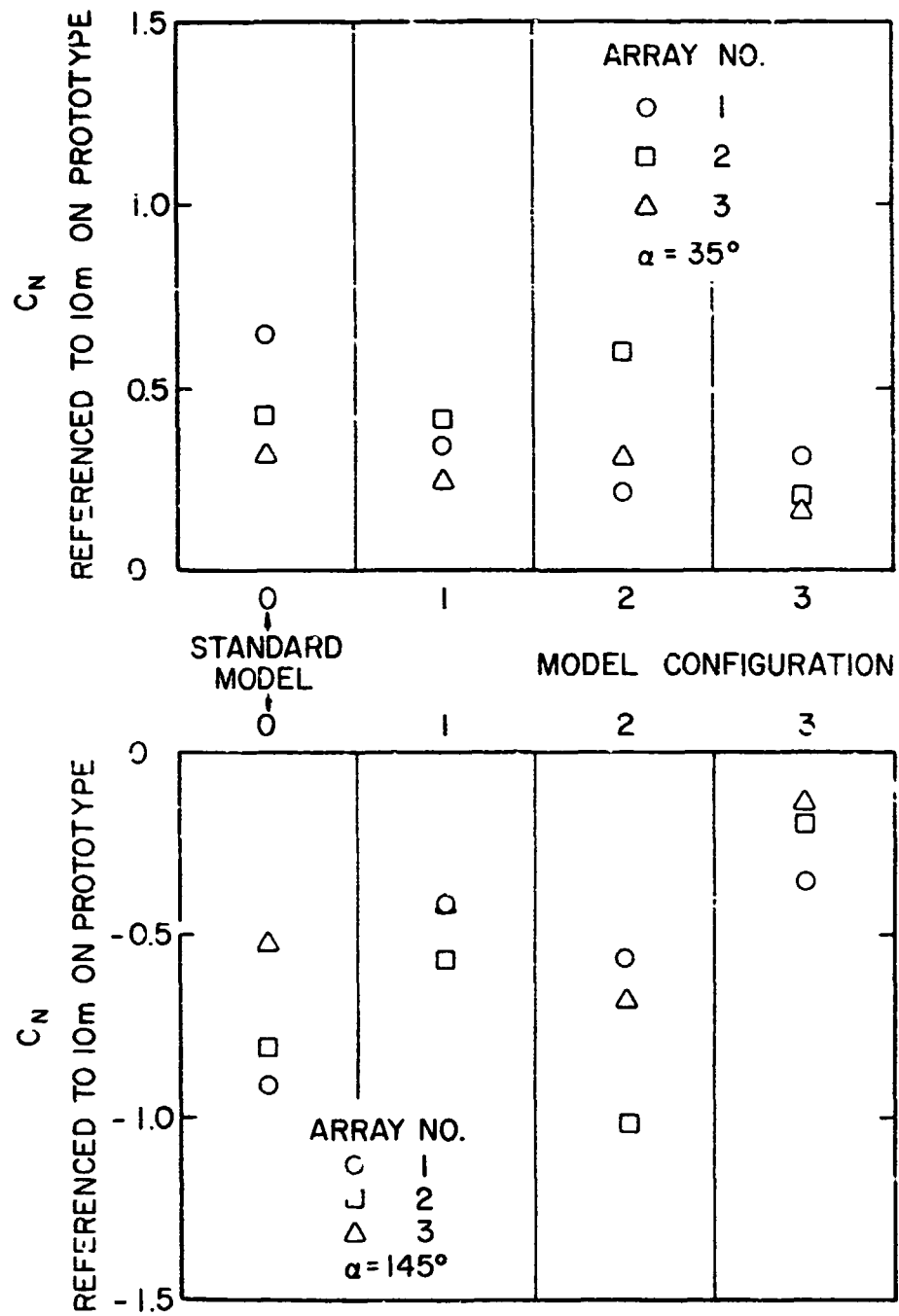


Figure 25. Normal Force Coefficients for an Array Field with Various Model Configurations, $WD = 45^\circ$, $x/c = 2.0$, $H/c = 0.25$, $FC = 1$

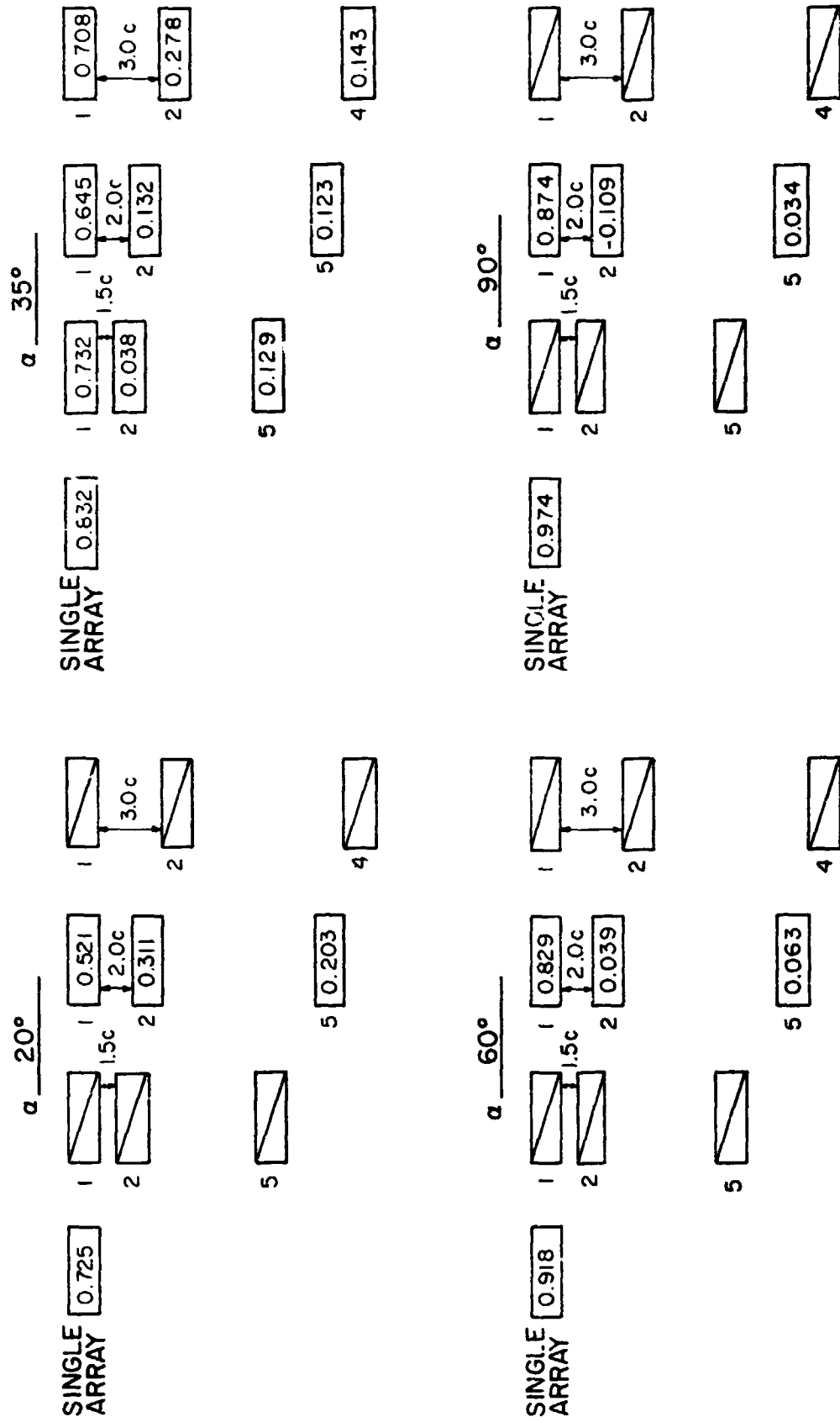


Figure 26. Normal Force Coefficients for an Array Field in Nonuniform Flow, No Fence, $WD = 0^\circ$, $H/c = 0.25$, $\alpha = 20^\circ, 35^\circ, 60^\circ$ and 90°

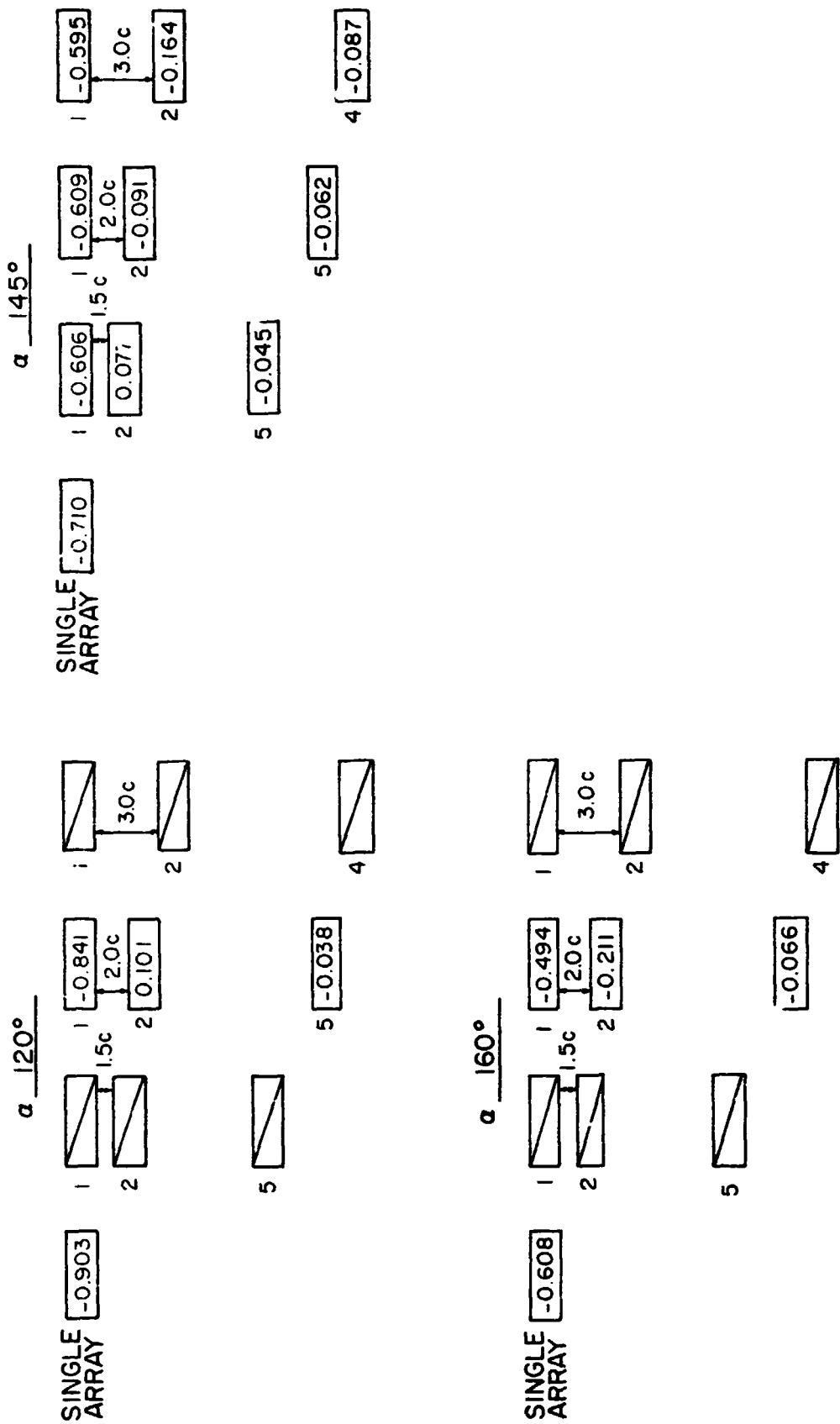


Figure 27. Normal Force Coefficients for an Array Field in Nonuniform Flow, No Fence, $WD = 0^\circ$, $H/c = 0.25$, $\alpha = 120^\circ$, 145° and 160°

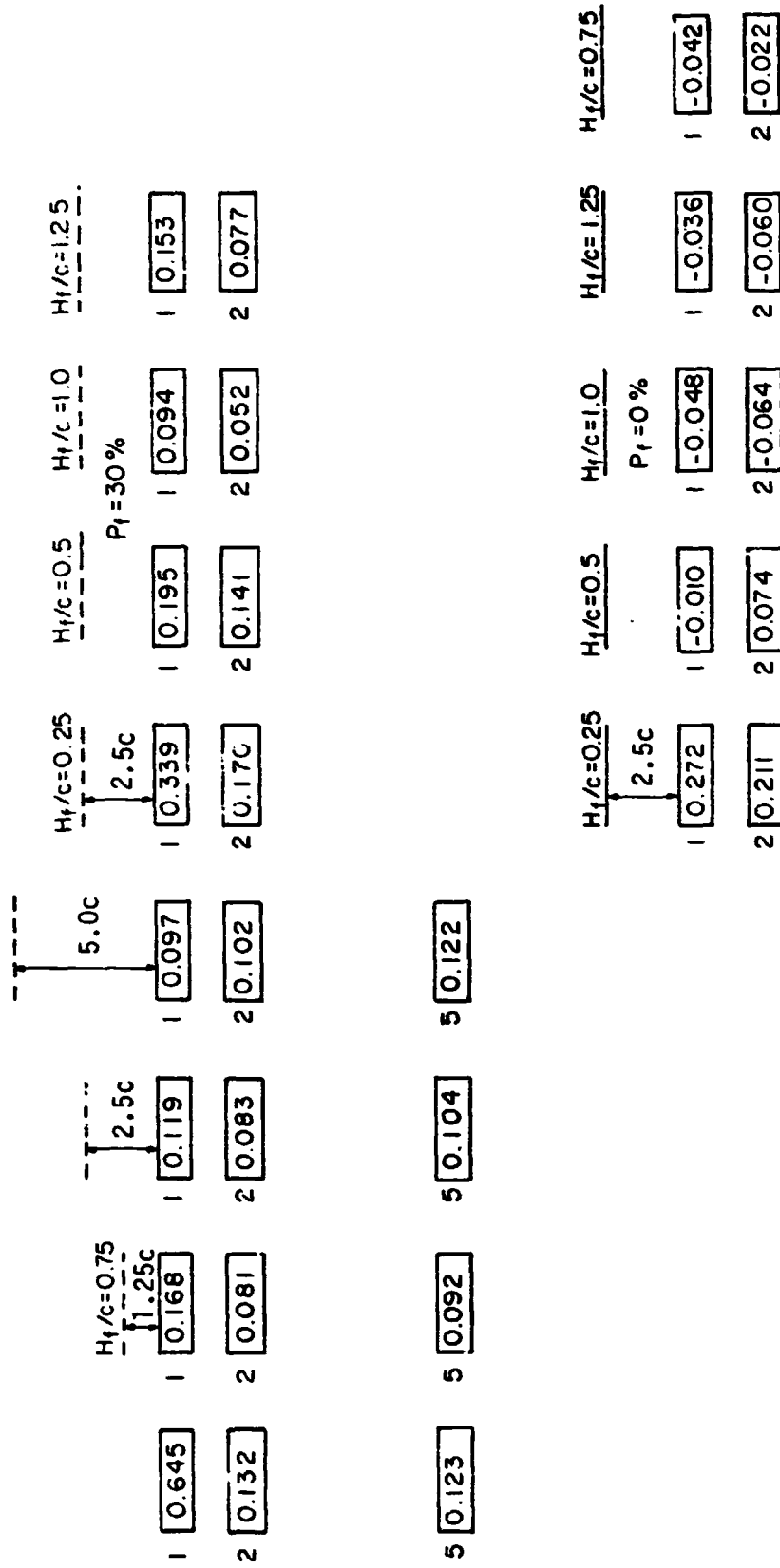


Figure 28a. Normal Force Coefficients for an Array Field with Various Fences, $WD = 0^\circ$, $x/c = 2.0$, $H/c = 0.25$, $\alpha = 35^\circ$, Nonuniform Flow

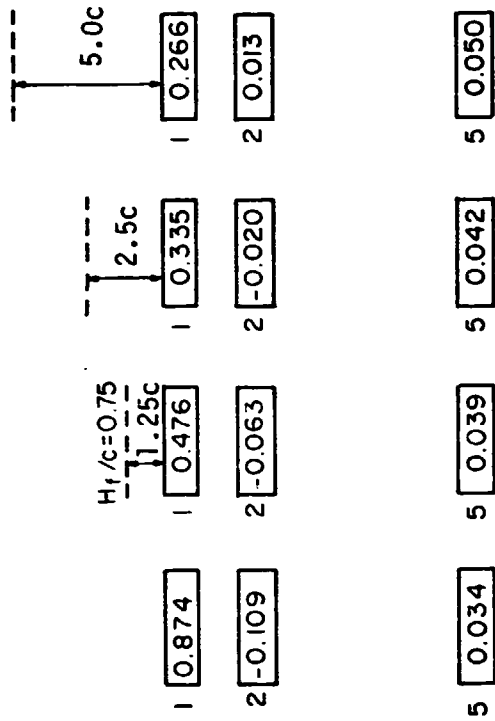


Figure 28b. Normal Force Coefficients for an Array Field with Various Fences, $WD = 0^\circ$, $x/c = 2.0$, $H/c = 0.25$, $\alpha = 90^\circ$, Nonuniform Flow

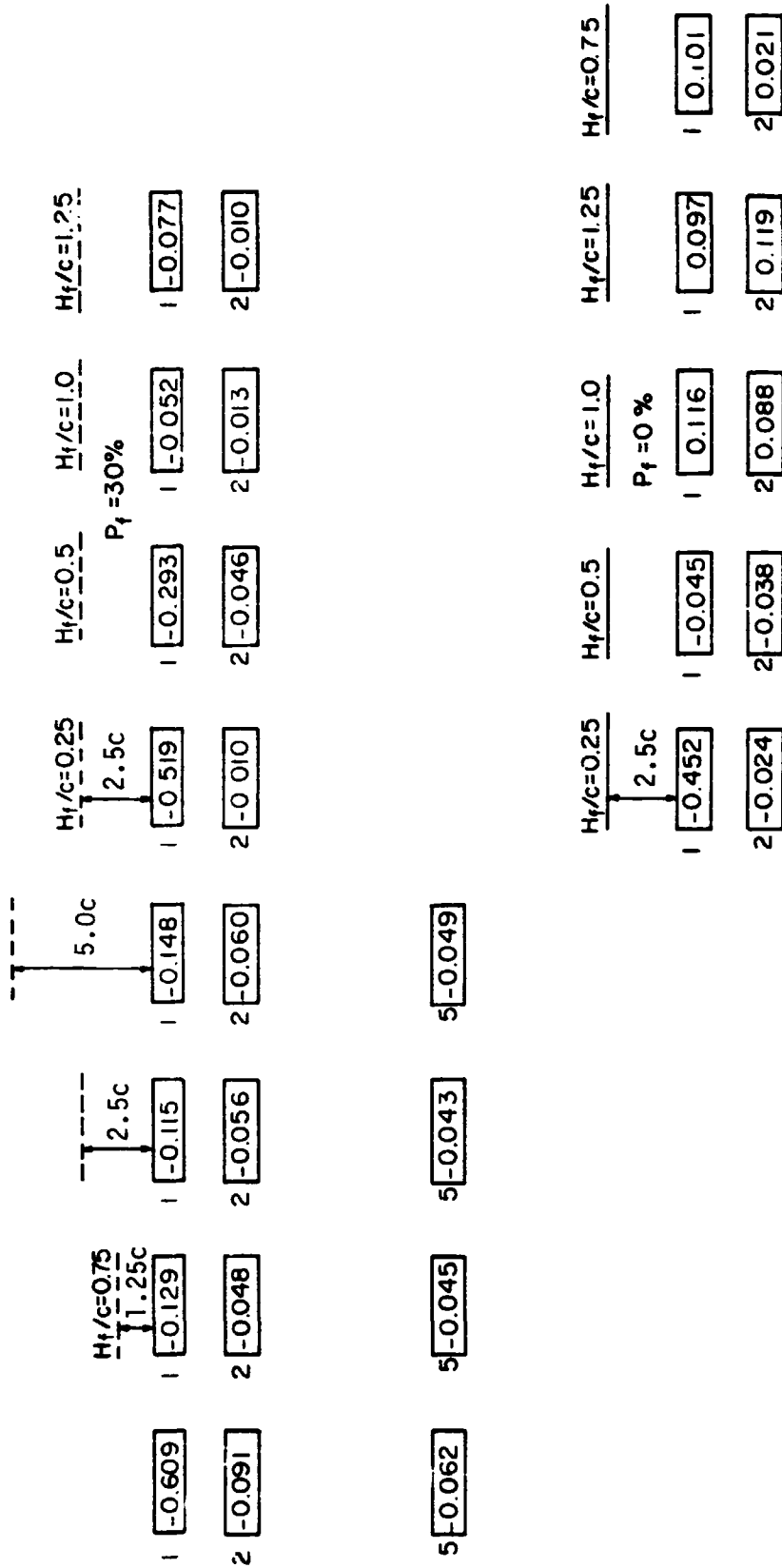


Figure 28c. Normal Force Coefficients for an Array Field with Various Fences, $WD = 0^\circ$, $x/c = 2.0$, $H/c = 0.25$, $\alpha = 145^\circ$, Nonuniform Flow

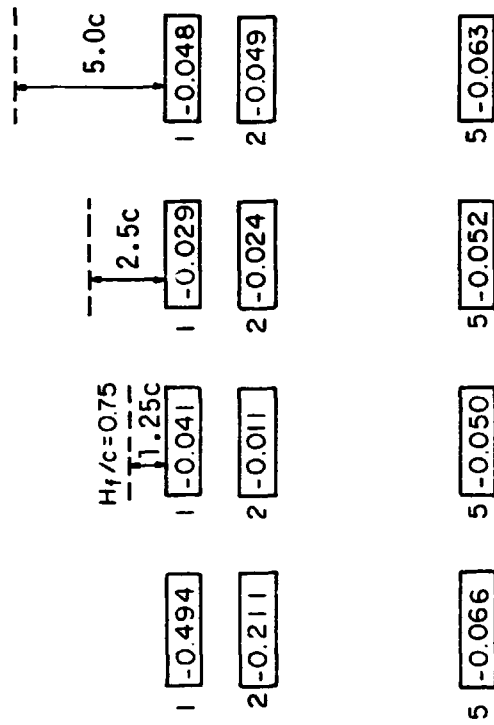


Figure 28d. Normal Force Coefficients for an Array Field with Various Fences, $\omega D = 0^\circ$, $x/c = 2.0$, $H/c = 0.25$, $\alpha = 160^\circ$, Nonuniform Flow

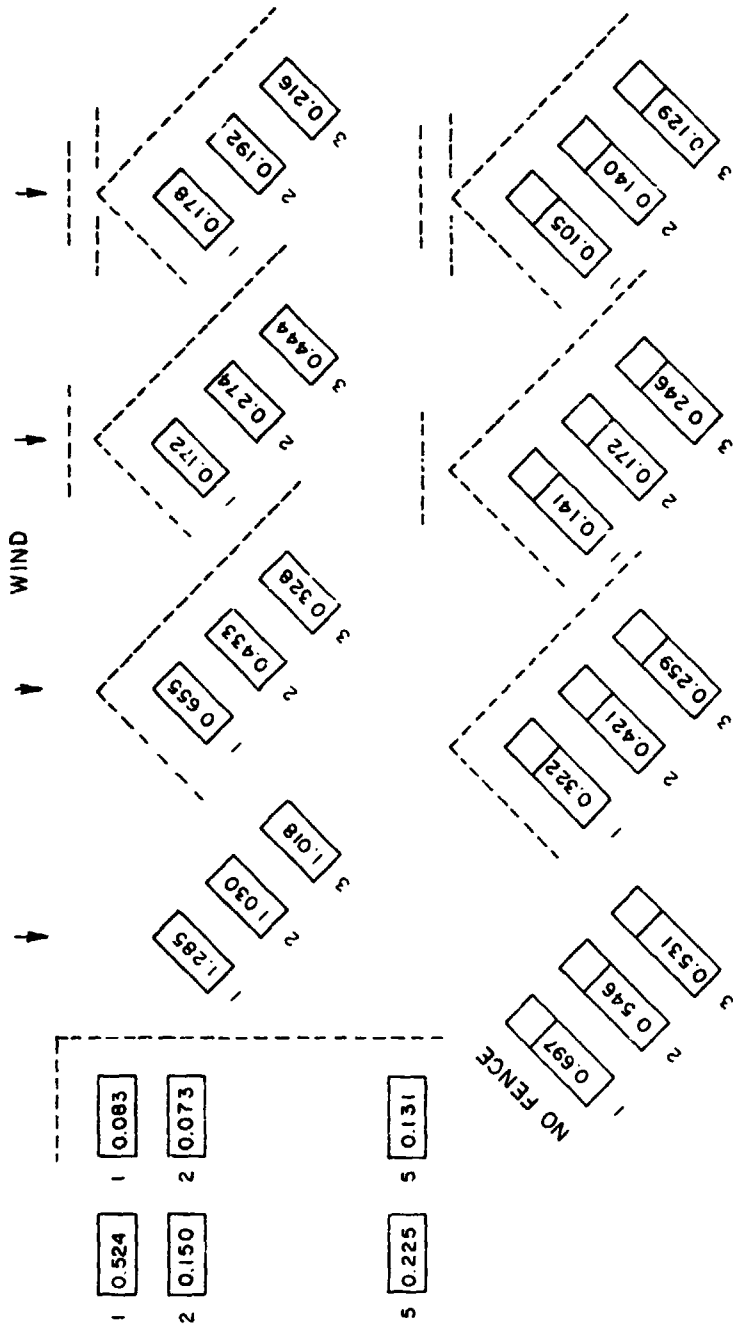


Figure 29a. Normal Force Coefficients for an Array Field, Edge and Corner Studies, $x/c = 2.0$, $H/c = 0.25$, $\alpha = 35^\circ$, Nonuniform Flow

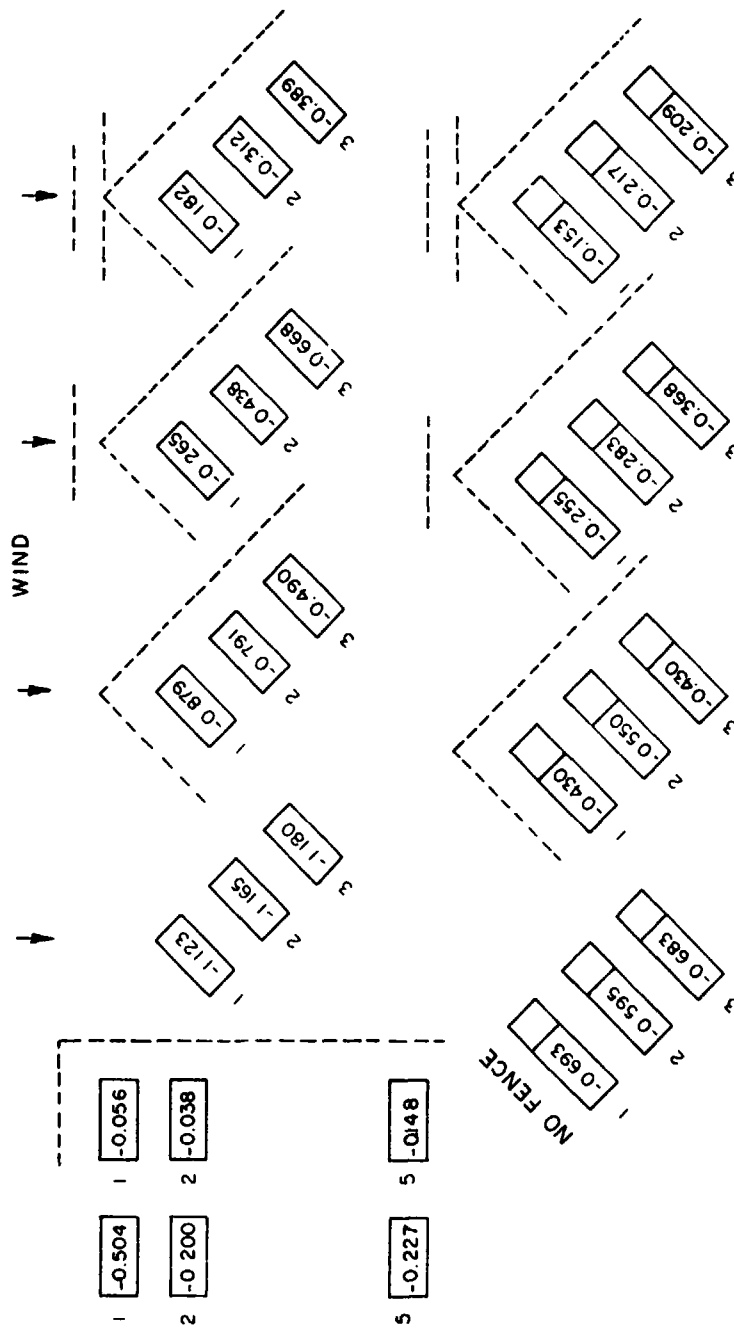


Figure 29b. Normal Force Coefficients for an Array Field, Edge and Corner Studies, $x/c = 2.0$, $H/c = 0.25$, $\alpha = 145^\circ$, Nonuniform Flow

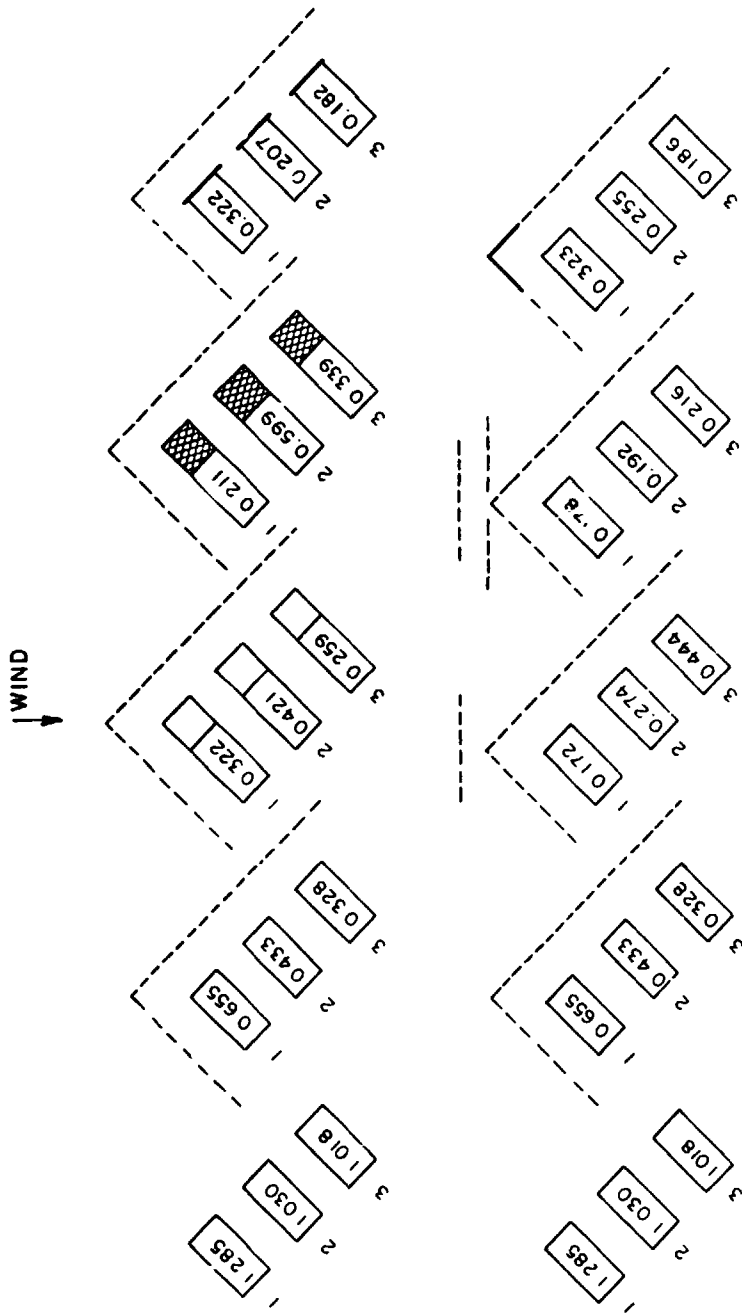


Figure 30a. Normal Force Coefficients for an Array Field, Corner Study with Various Fence and Model Configurations, $x/c = 2.0$, $H/c = 0.25$, $\alpha = 35^\circ$, Nonuniform Flow

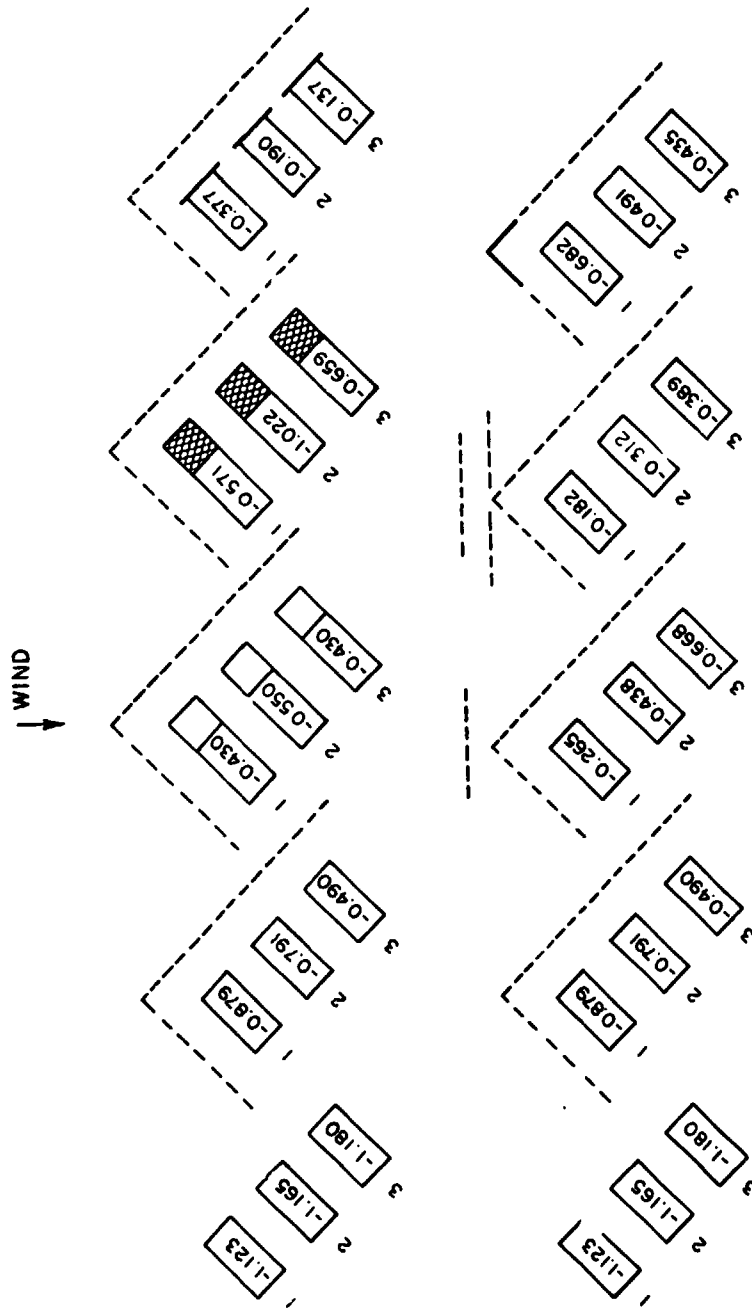


Figure 30b. Normal Force Coefficients for an Array Field, Corner Study with Various Fence and Model Configurations, $x/c = 2.0$, $H/c = 0.25$, $\alpha = 145^\circ$, Nonuniform flow

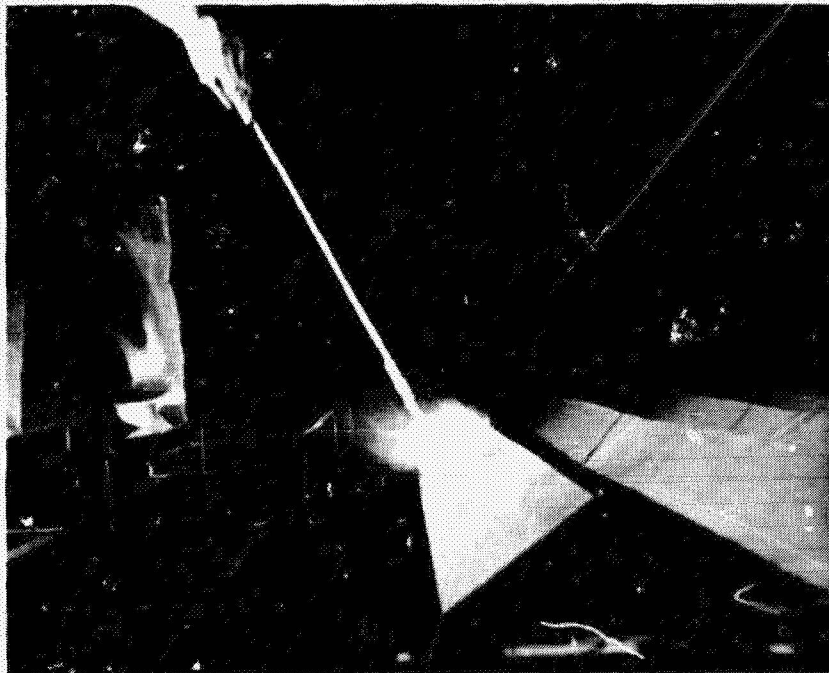
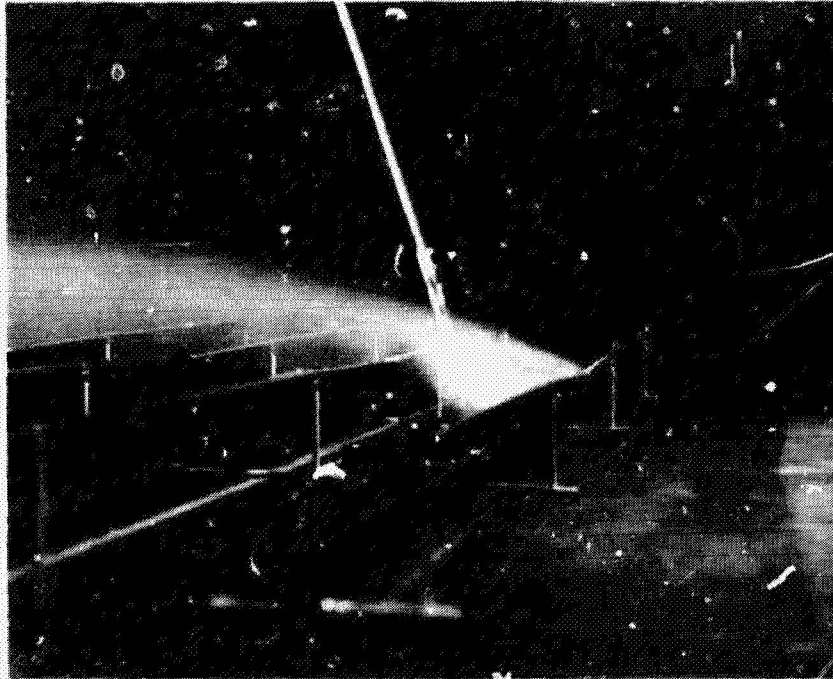


Figure 31a. Flow visualization for an Array Field, $WD = 0^\circ$

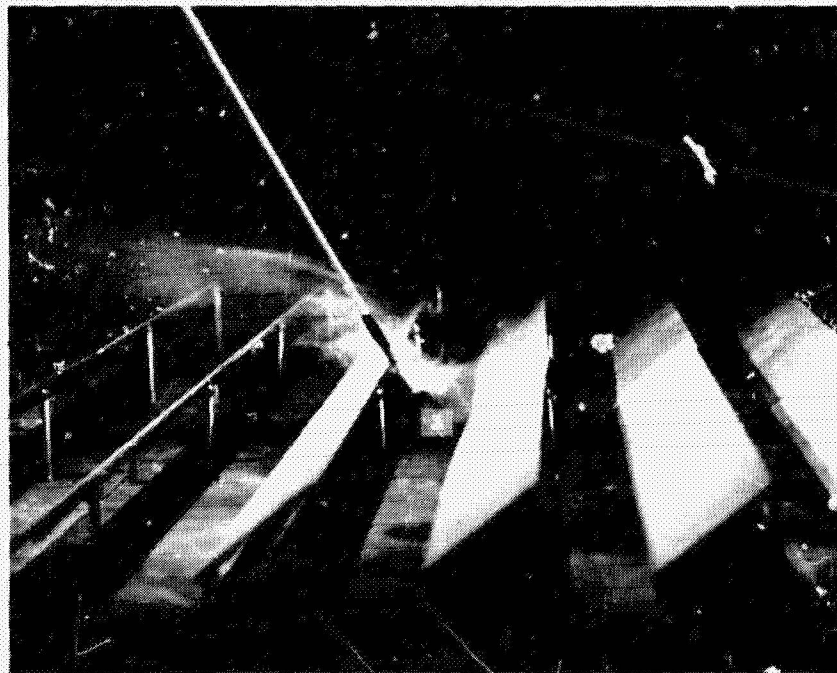
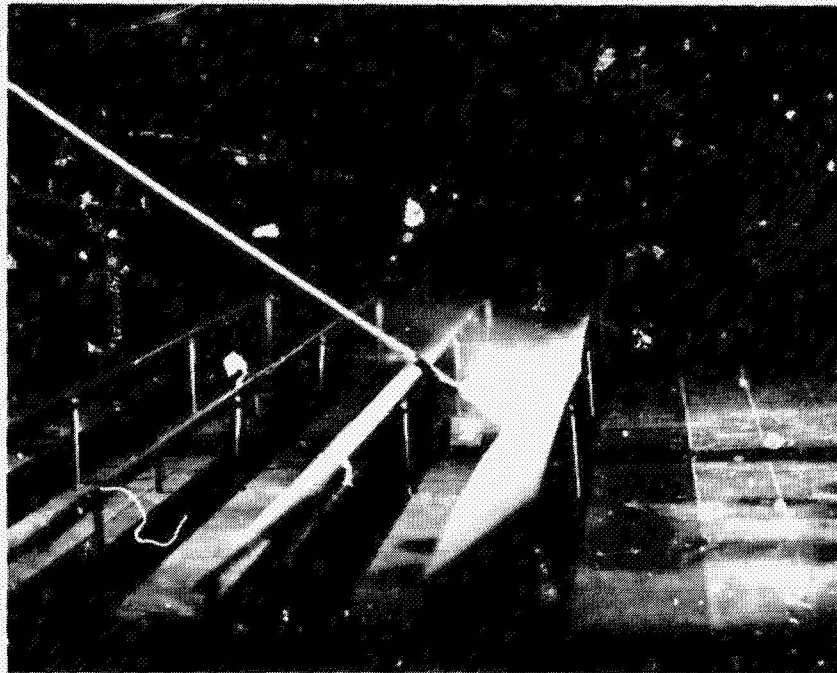


Figure 31b. Flow Visualization for an Array Field, $WD = 0^\circ$

ORIGINAL PAGE IS
OF POOR QUALITY



Figure 31c. Flow Visualization for an Array Field, $WD = 0^\circ$

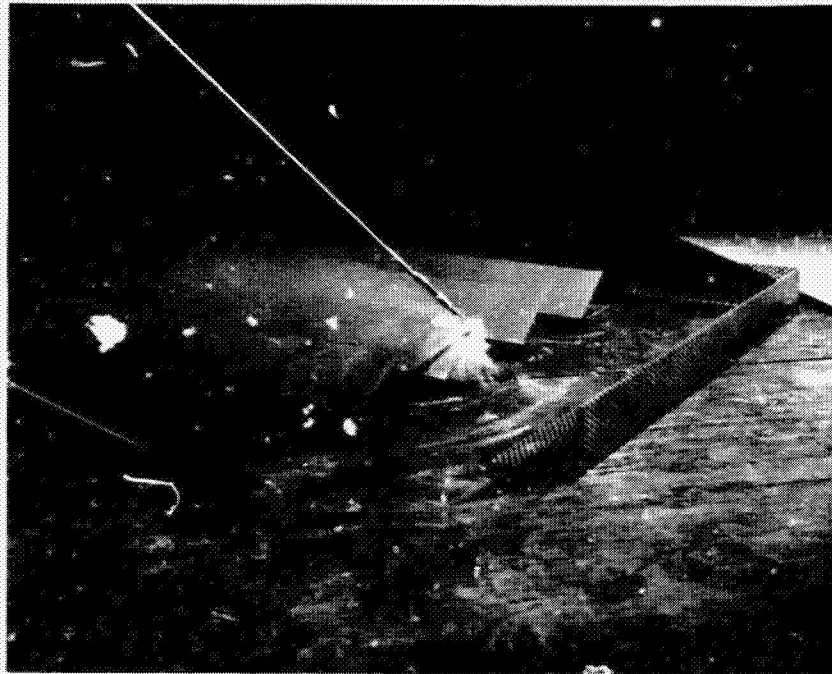


Figure 32. Flow Visualization for an Array Field, $WD = 45^\circ$

ORIGINAL PAGE IS
OF POOR QUALITY

A-58

TABLES

Table 1. Normal Force and Maximum Pressure Difference
for a Single Array in Uniform Flow

File Name	H/c	α	C_N	$\Delta C_{p \max}$	s_{\max}/c
A02001	0.25	20	1.086	1.53	0.98
A03501	0.25	35	1.145	1.45	0.89
A06001	0.25	60	1.283	1.48	0.83
A09001	0.25	90	1.320	1.46	0.59
A12001	0.25	120	-1.320	-1.48	0.29
A14501	0.25	145	-1.024	-1.46	0.06
A16001	0.25	160	-0.885	-1.37	0.05
B02001	0.5	20	1.015	1.66	0.96
B06001	0.5	60	1.523	1.76	0.74
B09001	0.5	90	1.534	1.74	0.42
B12001	0.5	120	-1.440	-1.73	0.18
B16001	0.5	160	-0.936	-1.49	0.04
C02001	∞	20	1.133	1.79	0.97
C03501	∞	35	1.715	2.13	0.91
C06001	∞	60	2.228	2.48	0.71
C09001	∞	90	2.168	2.35	0.42

Table 2. Normal Force and Maximum Pressure Difference
for an Array Field in Uniform Flow, $x/c = 2.0$

File Name	Array #	α	C_N	$\Delta C_{p \max}$	s_{\max}/c
E02001	1	20	0.717	1.06	0.96
E02101	2	20	0.210	0.82	0.73
E02201	5	20	0.267	0.91	0.86
E03501	1	35	1.006	1.24	0.91
E03601	2	35	0.383	0.75	0.26
E03701	5	35	0.100	0.20	0.45
E06001	1	60	1.220	1.39	0.84
E06101	2	60	-0.055	0.32	0.05
E06201	5	60	0.011	-0.04	0.46
E09001	1	90	1.400	1.56	0.58
E09101	2	90	-0.156	-0.28	0.59
E09201	5	90	-0.056	-0.07	0.42
E12001	1	120	-1.419	-1.60	0.27
E12101	2	120	0.277	0.38	0.28
E12201	5	120	-0.026	-0.10	0.92
E14501	1	145	-1.021	-1.38	0.04
E14601	2	145	-0.031	-0.11	0.74
E14701	5	145	-0.072	-0.10	0.83
E16001	1	160	-0.734	-1.10	0.05
E16101	2	160	-0.348	-0.48	0.05
E16201	5	160	-0.084	-0.10	0.59

Table 3. Normal Force and Maximum Pressure Difference
for an Array Field in Uniform Flow,
 $x/c = 1.5$ and 3.0

File Name	x/c	Array #	α	C_N	$\Delta C_{p \max}$	s_{\max}/c
D03501	1.5	1	35	1.065	1.32	0.92
D03601	1.5	2	35	0.034	0.43	0.97
D03701	1.5	5	35	0.123	0.25	0.19
D14501	1.5	1	145	-1.076	-1.44	0.05
D14601	1.5	2	145	0.168	0.30	0.08
F03501	3.0	1	35	0.925	1.13	0.97
F03601	3.0	2	35	0.326	0.48	0.26
F03701	3.0	4	35	0.081	0.12	0.95
F14501	3.0	1	145	-0.937	-1.38	0.06
F14601	3.0	2	145	-0.063	-0.08	0.56
F14701	3.0	4	145	-0.116	-0.14	0.74

Table 4. Normal Force and Maximum Pressure Difference for a Single Array in Nonuniform Flow

File Name	H_f/c	α	C_N^*	$\Delta C_{p \max}^*$	s_{\max}/c
G02001	---	20	0.725	0.96	0.96
G03501	---	35	0.832	0.98	0.85
G06001	---	60	0.918	1.02	0.74
G09001	---	90	0.974	1.05	0.44
G12001	---	120	-0.903	-1.04	0.16
G14501	---	145	-0.710	-0.99	0.05
G16001	---	160	-0.608	-0.87	0.05
G01101	0.25	35	0.504	0.71	0.96
G01201	0.5	35	0.295	0.41	0.96
G01301	0.75	35	0.143	0.18	0.82
G01401	1.0	35	0.099	0.11	0.81
G01501	1.25	35	0.286	0.34	0.85
G02101	0.25	145	-0.577	-0.66	0.32
G02201	0.5	145	-0.309	-0.38	0.56
G02301	0.75	145	-0.120	-0.14	0.54
G02401	1.0	145	-0.066	-0.08	0.08
G02501	1.25	145	-0.196	-0.28	0.06

*referenced to 10 m on prototype

Table 5. Normal Force and Maximum Pressure Difference
for an Array Field in Nonuniform Flow,
 $x/c = 2.0$

File Name	Array #	α	C_N^*	$\Delta C_{p \max}^*$	s_{\max}/c
I02001	1	20	0.521	0.73	0.95
I02101	2	20	0.311	0.38	0.74
I02201	5	20	0.203	0.31	0.90
I03501	1	35	0.645	0.76	0.91
I03601	2	35	0.132	0.29	0.20
I03701	5	35	0.123	0.15	0.74
I06001	1	60	0.829	0.90	0.75
I06101	2	60	0.039	0.34	0.06
I06201	5	60	0.063	0.08	0.83
I09001	1	90	0.874	0.97	0.28
I09101	2	90	-0.109	-0.20	0.57
I09201	5	90	0.034	0.08	0.96
I12001	1	120	-0.841	-0.94	0.17
I12101	2	120	0.101	0.17	0.42
I12201	5	120	-0.031	-0.08	0.92
I14501	1	145	-0.609	-0.83	0.05
I14601	2	145	-0.091	-0.11	0.13
I14701	5	145	-0.062	-0.08	0.78
I16001	1	150	-0.494	-0.71	0.05
I16101	2	160	-0.211	-0.32	0.05
I16201	5	160	-0.066	-0.08	0.59

*referenced to 10 m on prototype

Table 6. Normal Force and Maximum Pressure Difference
for an Array Field in Nonuniform Flow,
 $x/c = 1.5$ and 3.0

File Name	x/c	Array #	α	C_N^*	$\wedge C_{p \max}^*$	s_{\max}/c
H03501	1.5	1	35	0.732	0.85	0.93
H03601	1.5	2	35	0.038	0.29	0.16
H03701	1.5	5	35	0.129	0.18	0.43
H14501	1.5	1	145	-0.606	-0.81	0.05
H14601	1.5	2	145	0.077	0.17	0.05
H14701	1.5	5	145	-0.045	-0.11	0.82
J03501	3.0	1	35	0.708	0.83	0.93
J03601	3.0	2	35	0.278	0.42	0.40
J03701	3.0	4	35	0.143	0.21	0.82
J14501	3.0	1	145	-0.595	-0.78	0.05
J14601	3.0	2	145	-0.164	-0.18	0.56
J14701	3.0	4	145	-0.087	-0.10	0.63

*referenced to 10 m on prototype

Table 7. Normal Force and Maximum Pressure Difference
for an Array Field with a Fence, $H_f/c = 0.75$,
 $P_f = 30\%$, $x_f/c = 1.25$

File Name	Array #	α	C_N^*	$\Delta C_{p \max}^*$	s_{\max}'/c
K03501	1	35	0.168	0.20	0.82
K03601	2	35	0.081	0.10	0.53
K03701	5	35	0.092	0.14	0.90
K09001	1	90	0.476	0.53	0.84
K09101	2	90	-0.063	-0.13	0.46
K09201	5	90	0.039	0.08	0.86
K14501	1	145	-0.129	-0.15	0.17
K14601	2	145	-0.048	-0.06	0.76
K14701	5	145	-0.045	-0.07	0.77
K16001	1	160	-0.041	-0.06	0.11
K16101	2	160	-0.011	-0.03	0.82
K16201	5	160	-0.050	-0.07	0.61

*referenced to 10 m on prototype

Table 8. Normal Force and Maximum Pressure Difference
for an Array Field with a Fence, $H_f/c = 0.75$,
 $P_f = 30\%$, $x_f/c = 2.5$

File Name	Array #	α	C_N^*	$\Delta C_{p \max}^*$	s_{\max}/c
L03501	1	35	0.119	0.13	0.58
L03601	2	35	0.083	0.11	0.83
L03701	5	35	0.104	0.13	0.84
L09001	1	90	0.335	0.38	0.83
L09101	2	90	-0.020	-0.04	0.44
L09201	5	90	0.042	0.08	0.92
L14501	1	145	-0.115	-0.13	0.73
L14601	2	145	-0.056	-0.08	0.77
L14701	5	145	-0.043	-0.08	0.85
L16001	1	160	-0.029	-0.06	0.12
L16101	2	160	-0.024	-0.03	0.58
L16201	5	160	-0.052	-0.08	0.58

*referenced to 10 m on prototype

Table 9. Normal Force and Maximum Pressure Difference
for an Array Field with a Fence, $H_f/c = 0.75$,
 $P_f = 30\%$, $x_f/c = 5.0$

File Name	Array #	α	C_N^*	$\Delta C_{P \max}^*$	s_{\max}/c
M03501	1	35	0.097	0.13	0.83
M03601	2	35	0.102	0.14	0.84
M03701	5	35	0.122	0.17	0.95
M09001	1	90	0.266	0.34	0.82
M09101	2	90	0.013	0.03	0.24
M09201	5	90	0.050	0.08	0.96
M14501	1	145	-0.148	-0.27	0.44
M14601	2	145	-0.060	-0.10	0.77
M14701	5	145	-0.049	-0.08	0.76
M16001	1	160	-0.048	-0.06	0.28
M16101	2	160	-0.049	-0.07	0.60
M16201	5	160	-0.063	-0.08	0.55

*referenced to 10 m on prototype

Table 10. Normal Force and Maximum Pressure Difference for an Array Field with a Fence of Various Height and Porosity

File Name	P_f	H_f/c	Array #	α	C_N	$\Delta C_p^*_{max}$	s_{max}/c
N11101	30%	0.25	1	35	0.339	0.49	0.96
O11101	30%	0.25	2	35	0.170	0.22	0.41
N11201	30%	0.5	1	35	0.195	0.27	0.95
O11201	30%	0.5	2	35	0.141	0.20	0.89
N11401	30%	1.0	1	35	0.094	0.11	0.42
O11401	30%	1.0	2	35	0.052	0.08	0.43
N11501	30%	1.25	1	35	0.153	0.20	0.91
O11501	30%	1.25	2	35	0.077	0.13	0.42
N12101	30%	0.25	1	145	-0.519	-0.64	0.15
O12101	30%	0.25	2	145	-0.010	-0.06	0.76
N12201	30%	0.5	1	145	-0.293	-0.34	0.71
O12201	30%	0.5	2	145	-0.046	-0.10	0.78
N12401	30%	1.0	1	145	-0.052	-0.07	0.18
O12401	30%	1.0	2	145	-0.013	-0.06	0.74
N12501	30%	1.25	1	145	-0.077	-0.13	0.14
O12501	30%	1.25	2	145	-0.010	-0.03	0.74
N01301	0%	0.75	1	35	-0.042	-0.06	0.26
O01301	0%	0.75	2	35	-0.022	-0.04	0.26
N02301	0%	0.75	1	145	0.101	0.15	0.41
O02301	0%	0.75	2	145	0.021	0.06	0.26

*referenced to 10 m on prototype

Table 11. Normal Force and Maximum Pressure Difference for an Array Field, Edge Study

File Name	Fence	Array #	α	C_N^*	$\Delta C_{p \max}^*$	s_{\max}/c
P03501	✓	1	35	0.083	0.18	0.91
P03601	✓	2	35	0.073	0.17	0.92
P03701	✓	5	35	0.137	0.29	0.94
P14501	✓	1	145	-0.056	-0.08	0.83
P14601	✓	2	145	-0.038	-0.08	0.83
P14701	✓	5	145	-0.108	-0.17	0.73
Q03501	---	1	35	0.524	0.78	0.95
Q03601	---	2	35	0.150	0.32	0.92
Q03701	---	5	35	0.225	0.46	0.95
Q14501	---	1	145	-0.504	-0.71	0.05
Q14601	---	2	145	-0.200	-0.34	0.06
Q14701	---	5	145	-0.227	-0.36	0.06

*referenced to 10 m on prototype

Table 12. Normal Force and Maximum Pressure Difference
for an Array Field, No Fence, Corner Study

File Name	MC	Array #	α	C_N^*	$\Delta C_{p \max}^*$	s_{\max}/c
U03501	0	1	35	1.285	1.48	0.90
U03601	0	2	35	1.030	1.27	0.90
U03701	0	3	35	1.018	1.26	0.90
U14501	0	1	145	-1.123	-2.34	0.03
U14601	0	2	145	-1.165	-2.04	0.03
U14701	0	3	145	-1.180	-2.03	0.03
V03501	1	1	35	0.697	1.36	0.83
V03601	1	2	35	0.546	0.76	0.81
V03701	1	3	35	0.531	0.76	0.81
V14501	1	1	145	-0.693	-1.13	0.24
V14601	1	2	145	-0.595	-0.90	0.21
V14701	1	3	145	-0.638	-0.97	0.21

*referenced to 10 m on prototype

Table 13. Normal Force and Maximum Pressure Difference for an Array Field with Various Fences, Corner Study

File Name	FC	Array #	α	C_N^*	$\Delta C_{p \max}^*$	s_{\max}/c
R01101	1	1	35	0.655	1.93	0.96
S01101	1	2	35	0.433	1.09	0.96
T01101	1	3	35	0.328	0.62	0.96
R02101	1	1	145	0.879	-1.04	0.41
S02101	1	2	145	-0.791	-1.02	0.04
T02101	1	3	145	-0.490	-0.53	0.46
R01201	2	1	35	0.172	0.52	0.96
S01201	2	2	35	0.274	0.71	0.96
T01201	2	3	35	0.444	1.22	0.96
R02201	2	1	145	-0.265	-0.28	0.56
S02201	2	2	145	-0.438	-0.49	0.43
T02201	2	3	145	-0.668	-0.76	0.39
R01301	3	1	35	0.178	0.52	0.96
S01301	3	2	35	0.192	0.52	0.96
T01301	3	3	35	0.216	0.67	0.96
R02301	3	1	145	-0.182	-0.20	0.73
S02301	3	2	145	-0.312	-0.34	0.58
T02301	3	3	145	-0.389	-0.43	0.42

*referenced to 10 m on prototype

Table 14. Normal Force and Maximum Pressure Difference
for an Array Field with Various Fences,
MC = 1, Corner Study

File Name	FC	Array #	α	C_N^*	$\Delta C_{p \max}^*$	s_{\max}/c
R11101	1	1	35	0.322	0.77	0.96
S11101	1	2	35	0.421	0.78	0.96
T11101	1	3	35	0.259	0.34	0.84
R12101	1	1	145	-0.430	-0.50	0.43
S12101	1	2	145	-0.550	-0.64	0.40
T12101	1	3	145	-0.430	-0.50	0.27
R11201	2	1	35	0.141	0.27	0.97
S11201	2	2	35	0.172	0.31	0.97
T11201	2	3	35	0.246	0.50	0.97
R12201	2	1	145	-0.255	-0.29	0.43
S12201	2	2	145	-0.283	-0.34	0.38
T12201	2	3	145	-0.368	-0.43	0.29
R11301	3	1	35	0.105	0.20	0.96
S11301	3	2	35	0.140	0.27	0.96
T11301	3	3	35	0.129	0.22	0.96
R12301	3	1	145	-0.153	-0.17	0.43
S12301	3	2	145	-0.217	-0.27	0.43
T12301	3	3	145	-0.209	-0.25	0.43

*referenced to 10 m on prototype

Table 15. Normal Force and Maximum Pressure Difference
for an Array Field with Various Models, FC = 1
and 4, Corner Study

File Name	MC	FC	α	Array #	C_N^*	$\Delta C_{p \max}^*$	s_{\max}/c
R21101	2	1	35	1	0.211	0.67	0.96
S21101	2	1	35	2	0.599	1.64	0.96
T21101	2	1	35	3	0.339	0.53	0.96
R22101	2	1	145	1	-0.571	-0.67	0.72
S22101	2	1	145	2	-1.022	-1.19	0.16
T22101	2	1	145	3	-0.659	-0.74	0.42
R31101	3	1	35	1	0.322	0.85	0.96
S31101	3	1	35	2	0.207	0.36	0.96
T31101	3	1	35	3	0.182	0.25	0.96
R32101	3	1	145	1	-0.377	-0.45	0.04
S32101	3	1	145	2	-0.190	-0.21	0.74
T32101	3	1	145	3	-0.137	-0.15	0.61
R01401	0	4	35	1	0.323	0.14	0.82
S01401	0	4	35	2	0.255	0.13	0.83
T01401	0	4	35	3	0.186	0.15	0.83
R02401	0	4	145	1	-0.682	-0.14	0.73
S02401	0	4	145	2	-0.491	-0.10	0.77
T02401	0	4	145	3	-0.435	-0.09	0.76

*referenced to 10 m on prototype

Table 16. Normal Force and Maximum Pressure Difference
for an Array Field with a Fence, $H_f/c = 1.0$,
 $\alpha = 60^\circ$ and 120°

File Name	α	Array #	C_N^*	$\Delta C_{p \max}^*$	s_{\max}/c
N23401	60	1	0.183	0.12	0.54
N24401	60	2	0.025	0.04	0.72
N25401	60	5	0.053	0.05	0.94
N33401	120	1	-0.165	-0.10	0.18
N34401	120	2	-0.015	-0.06	0.28
N35401	120	5	-0.048	-0.05	0.79

*referenced to 10 m on prototype

Table 17. Fence Configurations

FC	H_f/c	x_f/c	P_f
1	0.75	2.5	30%
2	0.75	2.5	30%
3	0.75	2.5	30%
4	0.75	2.5	30%
5	0.75	1.25	30%
6	0.75	5.0	30%
7	0.25	2.5	30%
8	0.5	2.5	30%
9	1.0	2.5	30%
10	1.25	2.5	30%
11	0.25	2.5	0%
12	0.5	2.5	0%
13	0.75	2.5	0%
14	1.0	2.5	0%
15	1.25	2.5	0%

see Figure 22

Table 18. List of Test Configurations

File Name	Flow Profile		WD	Array		H/c	x	α	Array #	FC ¹	M ²
	Uniform	1/7 th		Single	Multiple						
A02001	✓		0	✓		0.25	-	20	-	-	0
A03501	✓		0	✓		0.25	-	35	-	-	0
A06001	✓		0	✓		0.25	-	60	-	-	0
A09001	✓		0	✓		0.25	-	90	-	-	0
A12001	✓		0	✓		0.25	-	120	-	-	0
A14501	✓		0	✓		0.25	-	145	-	-	0
A16001	✓		0	✓		0.25	-	160	-	-	0
B02001	✓		0	✓		0.5	-	20	-	-	0
B06001	✓		0	✓		0.5	-	60	-	-	0
B09001	✓		0	✓		0.5	-	90	-	-	0
B12001	✓		0	✓		0.5	-	120	-	-	0
E16001	✓		0	✓		0.5	-	160	-	-	0
C02001	✓		0	✓		-	-	20	-	-	0
C03501	✓		0	✓		-	-	35	-	-	0
C06001	✓		0	✓		-	-	60	-	-	0
C09001	✓		0	✓		-	-	90	-	-	0
D02001	✓		0		✓	0.25	1.5c	20	1	-	0
D02101	✓		0		✓	0.25	1.5c	20	2	-	0
D02201	✓		0		✓	0.25	1.5c	20	5	-	0
D03501	✓		0		✓	0.25	1.5c	35	1	-	0
D03601	✓		0		✓	0.25	1.5c	35	2	-	0
D03701	✓		0		✓	0.25	1.5c	35	5	-	0
D14501	✓		0		✓	0.25	1.5c	145	1	-	0
D14601	✓		0		✓	0.25	1.5c	145	2	-	0
D16001	✓		0		✓	0.25	1.5c	160	1	-	0
D16101	✓		0		✓	0.25	1.5c	160	2	-	0
E02001	✓		0		✓	0.25	2.0c	20	1	-	0
E02101	✓		0		✓	0.25	2.0c	20	2	-	0
E02201	✓		0		✓	0.25	2.0c	20	5	-	0
E03501	✓		0		✓	0.25	2.0c	35	1	-	0
E03601	✓		0		✓	0.25	2.0c	35	2	-	0
E03701	✓		0		✓	0.25	2.0c	35	5	-	0
E06001	✓		0		✓	0.25	2.0c	60	1	-	0
E06101	✓		0		✓	0.25	2.0c	60	2	-	0
E06201	✓		0		✓	0.25	2.0c	60	5	-	0
E09001	✓		0		✓	0.25	2.0c	90	1	-	0
E09101	✓		0		✓	0.25	2.0c	90	2	-	0
E09201	✓		0		✓	0.25	2.0c	90	5	-	0
E12001	✓		0		✓	0.25	2.0c	120	1	-	0
E12101	✓		0		✓	0.25	2.0c	120	2	-	0
E12201	✓		0		✓	0.25	2.0c	120	5	-	0
E14501	✓		0		✓	0.25	2.0c	145	1	-	0
E14601	✓		0		✓	0.25	2.0c	145	2	-	0
E14701	✓		0		✓	0.25	2.0c	145	5	-	0
E16001	✓		0		✓	0.25	2.0c	160	1	-	0
E16101	✓		0		✓	0.25	2.0c	160	2	-	0
E16201	✓		0		✓	0.25	2.0c	160	5	-	0
F03501	✓		0		✓	0.25	3.0c	35	1	-	0

¹defined in Table 17²defined in Figure 24

Table 18. (continued)

File Name	Flow Profile		WD	Array		H/c	x	a	Array #	FC	MC
	Uniform	1/7 th		Single	Multiple						
F03601	/		0		/	0.25	3.0c	35	2	-	0
F03701	/		0		/	0.25	3.0c	35	4	-	0
F06001	/		0		/	0.25	3.0c	60	1	-	0
F06101	/		0		/	0.25	3.0c	60	2	-	0
F06201	/		0		/	0.25	3.0c	60	4	-	0
F12001	/		0		/	0.25	3.0c	120	1	-	0
F12101	/		0		/	0.25	3.0c	120	2	-	0
F12201	/		0		/	0.25	3.0c	120	4	-	0
F14501	/		0		/	0.25	3.0c	145	1	-	0
F14601	/		0		/	0.25	3.0c	145	2	-	0
F14701	/		0		/	0.25	3.0c	145	4	-	0
G02001		/	0	/		0.25	-	20	-	-	0
G03501		/	0	/		0.25	-	35	-	-	0
G06001		/	0	/		0.25	-	60	-	-	0
G09001		/	0	/		0.25	-	90	-	-	0
G12001		/	0	/		0.25	-	120	-	-	0
G14501		/	0	/		0.25	-	145	-	-	0
G16001		/	0	/		0.25	-	160	-	-	0
G01101		/	0	/		0.25	-	35	-	7	0
G01201		/	0	/		0.25	-	35	-	8	0
G01301		/	0	/		0.25	-	35	-	1	0
G01401		/	0	/		0.25	-	35	-	9	0
G01501		/	0	/		0.25	-	35	-	10	0
G02101		/	0	/		0.25	-	145	-	7	0
G02201		/	0	/		0.25	-	145	-	8	0
G02301		/	0	/		0.25	-	145	-	1	0
G02401		/	0	/		0.25	-	145	-	9	0
G02501		/	0	/		0.25	-	145	-	10	0
H02001		/	0		/	0.25	1.5c	20	1	-	0
H02101		/	0		/	0.25	1.5c	20	2	-	0
H02201		/	0		/	0.25	1.5c	20	5	-	0
H03501		/	0		/	0.25	1.5c	35	1	-	0
H03601		/	0		/	0.25	1.5c	35	2	-	0
H03701		/	0		/	0.25	1.5c	35	5	-	0
H14501		/	0		/	0.25	1.5c	145	1	-	0
H14601		/	0		/	0.25	1.5c	145	2	-	0
H14701		/	0		/	0.25	1.5c	145	5	-	0
H16001		/	0		/	0.25	1.5c	160	1	-	0
H16101		/	0		/	0.25	1.5c	160	2	-	0
H16201		/	0		/	0.25	1.5c	160	5	-	0
I02001		/	0		/	0.25	2.0c	20	1	-	0
I02101		/	0		/	0.25	2.0c	20	2	-	0
I02201		/	0		/	0.25	2.0c	20	5	-	0
I03501		/	0		/	0.25	2.0c	35	1	-	0
I03601		/	0		/	0.25	2.0c	35	2	-	0
I03701		/	0		/	0.25	2.0c	35	5	-	0
I06001		/	0		/	0.25	2.0c	60	1	-	0
I06101		/	0		/	0.25	2.0c	60	2	-	0

Table 18. (continued)

File Name	Flow Profile		WD	Array		H/c	x	a	Array #	FC	NC
	Uniform	1/7 th		Single	Multiple						
I06201	✓		0	✓		0.25	2.0c	60	5	-	0
I09001	✓		0	✓		0.25	2.0c	90	1	-	0
I09101	✓		0	✓		0.25	2.0c	90	2	-	0
I09201	✓		0	✓		0.25	2.0c	90	5	-	0
I12001	✓		0	✓		0.25	2.0c	120	1	-	0
I12101	✓		0	✓		0.25	2.0c	120	2	-	0
I12201	✓		0	✓		0.25	2.0c	120	5	-	0
I14501	✓		0	✓		0.25	2.0c	145	1	-	0
I14601	✓		0	✓		0.25	2.0c	145	2	-	0
I14701	✓		0	✓		0.25	2.0c	145	5	-	0
I16001	✓		0	✓		0.25	2.0c	160	1	-	0
I16101	✓		0	✓		0.25	2.0c	160	2	-	0
I16201	✓		0	✓		0.25	2.0c	160	5	-	0
J03501	✓		0	✓		0.25	3.0c	35	1	-	0
J03601	✓		0	✓		0.25	3.0c	35	2	-	0
J03701	✓		0	✓		0.25	3.0c	35	4	-	0
J06001	✓		0	✓		0.25	3.0c	60	1	-	0
J06101	✓		0	✓		0.25	3.0c	60	2	-	0
J06201	✓		0	✓		0.25	3.0c	60	4	-	0
J12001	✓		0	✓		0.25	3.0c	120	1	-	0
J12101	✓		0	✓		0.25	3.0c	120	2	-	0
J12201	✓		0	✓		0.25	3.0c	120	4	-	0
J14501	✓		0	✓		0.25	3.0c	145	1	-	0
J14601	✓		0	✓		0.25	3.0c	145	2	-	0
J14701	✓		0	✓		0.25	3.0c	145	4	-	0
K03501	✓		0	✓		0.25	2.0c	35	1	5	0
K03601	✓		0	✓		0.25	2.0c	35	2	5	0
K03701	✓		0	✓		0.25	2.0c	35	5	5	0
K09001	✓		0	✓		0.25	2.0c	90	1	5	0
K09101	✓		0	✓		0.25	2.0c	90	2	5	0
K09201	✓		0	✓		0.25	2.0c	90	5	5	0
K14501	✓		0	✓		0.25	2.0c	145	1	5	0
K14601	✓		0	✓		0.25	2.0c	145	2	5	0
K14701	✓		0	✓		0.25	2.0c	145	5	5	0
K16001	✓		0	✓		0.25	2.0c	160	1	5	0
K16101	✓		0	✓		0.25	2.0c	160	2	5	0
K16201	✓		0	✓		0.25	2.0c	160	5	5	0
L03501	✓		0	✓		0.25	2.0c	35	1	1	0
L03601	✓		0	✓		0.25	2.0c	35	2	1	0
L03701	✓		0	✓		0.25	2.0c	35	5	1	0
L09001	✓		0	✓		0.25	2.0c	90	1	1	0
L09101	✓		0	✓		0.25	2.0c	90	2	1	0
L09201	✓		0	✓		0.25	2.0c	90	5	1	0
L14501	✓		0	✓		0.25	2.0c	145	1	1	0
L14601	✓		0	✓		0.25	2.0c	145	2	1	0
L14701	✓		0	✓		0.25	2.0c	145	5	1	0
L16001	✓		0	✓		0.25	2.0c	160	1	1	0
L16101	✓		0	✓		0.25	2.0c	160	2	1	0

Table 18. (continued)

File Name	Flow Profile		WD	Array		H/c	x	a	Array #	FC	MC
	Uniform	1/7 ch		Single	Multiple						
L16201	/		0		/	0.25	2.0c	160	5	1	0
M03501	/		0		/	0.25	2.0c	35	1	6	0
M03601	/		0		/	0.25	2.0c	35	2	6	0
M03701	/		0		/	0.25	2.0c	35	5	6	0
M09001	/		0		/	0.25	2.0c	90	1	6	0
M09101	/		0		/	0.25	2.0c	90	2	6	0
M09201	/		0		/	0.25	2.0c	90	5	6	0
M14501	/		0		/	0.25	2.0c	145	1	6	0
M14601	/		0		/	0.25	2.0c	145	2	6	0
M14701	/		0		/	0.25	2.0c	145	5	6	0
M16001	/		0		/	0.25	2.0c	160	1	6	0
M15101	/		0		/	0.25	2.0c	160	2	6	0
M16201	/		0		/	0.25	2.0c	160	5	6	0
N01101	/		0		/	0.25	2.0c	35	1	11	0
N01201	/		0		/	0.25	2.0c	35	1	12	0
N01301	/		0		/	0.25	2.0c	35	1	13	0
N01401	/		0		/	0.25	2.0c	35	1	14	0
N01501	/		0		/	0.25	2.0c	35	1	15	0
N02101	/		0		/	0.25	2.0c	145	1	11	0
N02201	/		0		/	0.25	2.0c	145	1	12	0
N02301	/		0		/	0.25	2.0c	145	1	13	0
N02401	/		0		/	0.25	2.0c	145	1	14	0
N02501	/		0		/	0.25	2.0c	145	1	15	0
N11101	/		0		/	0.25	2.0c	35	1	7	0
N11201	/		0		/	0.25	2.0c	35	1	8	0
N11401	/		0		/	0.25	2.0c	35	1	9	0
N11501	/		0		/	0.25	2.0c	35	1	10	0
N12101	/		0		/	0.25	2.0c	145	1	7	0
N12201	/		0		/	0.25	2.0c	145	1	8	0
N12401	/		0		/	0.25	2.0c	145	1	9	0
N12501	/		0		/	0.25	2.0c	145	1	10	0
N23401	/		0		/	0.25	2.0c	60	1	9	0
N24401	/		0		/	0.25	2.0c	60	2	9	0
N25401	/		0		/	0.25	2.0c	60	5	9	0
N33401	/		0		/	0.25	2.0c	120	1	9	0
N34401	/		0		/	0.25	2.0c	120	2	9	0
N35401	/		0		/	0.25	2.0c	120	5	9	0
001101	/		0		/	0.25	2.0c	35	2	11	0
001201	/		0		/	0.25	2.0c	35	2	12	0
001301	/		0		/	0.25	2.0c	35	2	13	0
001401	/		0		/	0.25	2.0c	35	2	14	0
001501	/		0		/	0.25	2.0c	35	2	15	0
002101	/		0		/	0.25	2.0c	145	2	11	0
002201	/		0		/	0.25	2.0c	145	2	12	0
002301	/		0		/	0.25	2.0c	145	2	13	0
002401	/		0		/	0.25	2.0c	145	2	14	0
002501	/		0		/	0.25	2.0c	145	2	15	0
C11101	/		0		/	0.25	2.0c	35	2	7	0

Table 18. (continued)

File Name	Flow Profile		WD	Array		H/c	x	a	Array #	FC	MC
	Uniform	1/7 th		Single	Multiple						
O11201	✓		0		✓	0.25	2.0c	35	2	8	0
O11401	✓		0		✓	0.25	2.0c	35	2	9	0
O11501	✓		0		✓	0.25	2.0c	35	2	10	0
O12101	✓		0		✓	0.25	2.0c	145	2	7	0
O12201	✓		0		✓	0.25	2.0c	145	2	8	0
O12401	✓		0		✓	0.25	2.0c	145	2	9	0
O12501	✓		0		✓	0.25	2.0c	145	2	10	0
P03501	✓		0		(edge)	0.25	2.0c	35	1	1	0
P03601	✓		0		(edge)	0.25	2.0c	35	2	1	0
P03701	✓		0		(edge)	0.25	2.0c	35	5	1	0
P14501	✓		0		(edge)	0.25	2.0c	145	1	1	0
P14601	✓		0		(edge)	0.25	2.0c	145	2	1	0
P14701	✓		0		(edge)	0.25	2.0c	145	5	1	0
Q03501	✓		0		(edge)	0.25	2.0c	35	1	-	0
Q03601	✓		0		(edge)	0.25	2.0c	35	2	-	0
Q03701	✓		0		(edge)	0.25	2.0c	35	5	-	0
Q14501	✓		0		(edge)	0.25	2.0c	145	1	-	0
Q14601	✓		0		(edge)	0.25	2.0c	145	2	-	0
Q14701	✓		0		(edge)	0.25	2.0c	145	5	-	0
R01101	✓		45		✓	0.25	2.0c	35	1	1	0
R02101	✓		45		✓	0.25	2.0c	145	1	1	0
R01201	✓		45		✓	0.25	2.0c	35	1	2	0
R02201	✓		45		✓	0.25	2.0c	145	1	2	0
R01301	✓		45		✓	0.25	2.0c	35	1	3	0
R02301	✓		45		✓	0.25	2.0c	145	1	3	0
R01401	✓		45		✓	0.25	2.0c	35	1	4	0
R02401	✓		45		✓	0.25	2.0c	145	1	4	0
R11101	✓		45		✓	0.25	2.0c	35	1	1	1
R12101	✓		45		✓	0.25	2.0c	145	1	1	1
R11201	✓		45		✓	0.25	2.0c	35	1	2	1
R12201	✓		45		✓	0.25	2.0c	145	1	2	1
R11301	✓		45		✓	0.25	2.0c	35	1	3	1
R12301	✓		45		✓	0.25	2.0c	145	1	3	1
R21101	✓		45		✓	0.25	2.0c	35	1	1	2
R22101	✓		45		✓	0.25	2.0c	145	1	1	2
R31101	✓		45		✓	0.25	2.0c	35	1	1	3
R32101	✓		45		✓	0.25	2.0c	145	1	1	3
S01101	✓		45		✓	0.25	2.0c	35	2	1	0
S02101	✓		45		✓	0.25	2.0c	145	2	1	0
S01201	✓		45		✓	0.25	2.0c	35	2	2	0
S02201	✓		45		✓	0.25	2.0c	145	2	2	0
S01301	✓		45		✓	0.25	2.0c	35	2	3	0
S02301	✓		45		✓	0.25	2.0c	145	2	3	0
S01401	✓		45		✓	0.25	2.0c	35	2	4	0
S02401	✓		45		✓	0.25	2.0c	145	2	4	0
S11101	✓		45		✓	0.25	2.0c	35	2	1	1
S12101	✓		45		✓	0.25	2.0c	145	2	1	1
S11201	✓		45		✓	0.25	2.0c	35	2	2	1

Table 18. (continued)

File Name	Flow Profile		WD	Array		H/c	x	a	Array #	FC	MC
	Uniform	1/7 th		Single	Multiple						
S12201	✓		45		✓	0.25	2.0c	145	2	2	1
S11301	✓		45		✓	0.25	2.0c	35	2	3	1
S12301	✓		45		✓	0.25	2.0c	145	2	3	1
S21101	✓		45		✓	0.25	2.0c	35	2	1	2
S22101	✓		45		✓	0.25	2.0c	145	2	1	2
S31101	✓		45		✓	0.25	2.0c	35	2	1	3
S32101	✓		45		✓	0.25	2.0c	145	2	1	3
T01101	✓		45		✓	0.25	2.0c	35	3	1	0
T02101	✓		45		✓	0.25	2.0c	145	3	1	0
T01201	✓		45		✓	0.25	2.0c	35	3	2	0
T02201	✓		45		✓	0.25	2.0c	145	3	2	0
T01301	✓		45		✓	0.25	2.0c	35	3	3	0
T02301	✓		45		✓	0.25	2.0c	145	3	3	0
T01401	✓		45		✓	0.25	2.0c	35	3	4	0
T02401	✓		45		✓	0.25	2.0c	145	3	4	0
T11101	✓		45		✓	0.25	2.0c	35	3	1	1
T12101	✓		45		✓	0.25	2.0c	145	3	1	1
T11201	✓		45		✓	0.25	2.0c	35	3	2	1
T12201	✓		45		✓	0.25	2.0c	145	3	2	1
T11301	✓		45		✓	0.25	2.0c	35	3	3	1
T12301	✓		45		✓	0.25	2.0c	145	3	3	1
T21101	✓		45		✓	0.25	2.0c	35	3	1	2
T22101	✓		45		✓	0.25	2.0c	145	3	1	2
T31101	✓		45		✓	0.25	2.0c	35	3	1	3
T32101	✓		45		✓	0.25	2.0c	145	3	1	3
U03501	✓		45		✓	0.25	2.0c	35	1	-	0
U03601	✓		45		✓	0.25	2.0c	35	2	-	0
U03701	✓		45		✓	0.25	2.0c	35	3	-	0
U14501	✓		45		✓	0.25	2.0c	145	1	-	0
U14601	✓		45		✓	0.25	2.0c	145	2	-	0
U14701	✓		45		✓	0.25	2.0c	145	3	-	0
V03501	✓		45		✓	0.25	2.0c	35	1	-	1
V03601	✓		45		✓	0.25	2.0c	35	2	-	1
V03701	✓		45		✓	0.25	2.0c	35	3	-	1
V14501	✓		45		✓	0.25	2.0c	145	1	-	1
V14601	✓		45		✓	0.25	2.0c	145	2	-	1
V14701	✓		45		✓	0.25	2.0c	145	3	-	1
W03501	✓		0		(edge)	0.25	2.0c	35	1	-	(1:12) ⁰
W03601	✓		0		(edge)	0.25	2.0c	35	2	-	(1:12) ⁰
W03701	✓		0		(edge)	0.25	2.0c	35	5	-	(1:12) ⁰
W14501	✓		0		(edge)	0.25	2.0c	145	1	-	(1:12) ⁰
W14601	✓		0		(edge)	0.25	2.0c	145	2	-	(1:12) ⁰
W14701	✓		0		(edge)	0.25	2.0c	145	5	-	(1:12) ⁰
X03501	✓		0		(edge)	0.25	2.0c	35	1	1	(1:12) ⁰
X03601	✓		0		(edge)	0.25	2.0c	35	2	1	(1:12) ⁰
X14501	✓		0		(edge)	0.25	2.0c	145	1	1	(1:12) ⁰
X14601	✓		0		(edge)	0.25	2.0c	145	2	1	(1:12) ⁰
Z03501	✓		0		✓	0.25	-	35	-	-	(1:12) ⁰

A-82



B-1

APPENDIX B

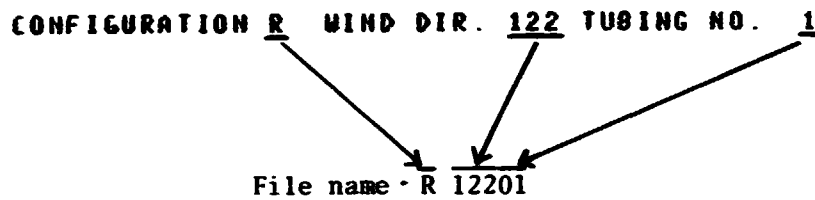
Pressure Data Referenced to 10 m on Prototype

**This Page Left
Blank Intentionally**

B-1a

This appendix presents the data supplement consisting of the velocity and turbulent profile of the nonuniform flow, the digitized pressure data referenced to 10 m on prototype and the various plots of pressure distribution along the chord of the solar array.

Pressure coefficients are defined in Section 3.2 on the main report. The pressure tap numbers shown in Appendix B are defined that; on the upstream surface of the solar array, the number runs 1 through 10 from the edge where $s/c = 0$, and on the downstream surface, 20 through 11. The file name for each test configuration is formulated as follows.



Force and model configurations are schematically explained in Figures 22 and 24 of the main report, respectively. Fence configurations are also tabulated in Table 17 of that report.

List of Run Configurations

File Name	Flow Profile		WD	Array		H/c	x	a	Array #	FC	MC
	Uniform	1/7 th		Single	Multiple						
A02001	✓		0	✓		0.25	-	20	-	-	0
A03501	✓		0	✓		0.25	-	35	-	-	0
A06001	✓		0	✓		0.25	-	60	-	-	0
A09001	✓		0	✓		0.25	-	90	-	-	0
A12001	✓		0	✓		0.25	-	120	-	-	0
A14501	✓		0	✓		0.25	-	145	-	-	0
A16001	✓		0	✓		0.25	-	160	-	-	0
B02001	✓		0	✓		0.5	-	20	-	-	0
B06001	✓		0	✓		0.5	-	60	-	-	0
B09001	✓		0	✓		0.5	-	90	-	-	0
B12001	✓		0	✓		0.5	-	120	-	-	0
B16001	✓		0	✓		0.5	-	160	-	-	0
C02001	✓		0	✓		"	-	20	-	-	0
C03501	✓		0	✓		"	-	35	-	-	0
C06001	✓		0	✓		"	-	60	-	-	0
C09001	✓		0	✓		"	-	90	-	-	0
D02001	✓		0		✓	0.25	1.5c	20	1	-	0
D02101	✓		0		✓	0.25	1.5c	20	2	-	0
D02201	✓		0		✓	0.25	1.5c	20	5	-	0
D03501	✓		0		✓	0.25	1.5c	35	1	-	0
D03601	✓		0		✓	0.25	1.5c	35	2	-	0
D03701	✓		0		✓	0.25	1.5c	35	5	-	0
D14501	✓		0		✓	0.25	1.5c	145	1	-	0
D14601	✓		0		✓	0.25	1.5c	145	2	-	0
D16001	✓		0		✓	0.25	1.5c	160	1	-	0
D16101	✓		0		✓	0.25	1.5c	160	2	-	0
E02001	✓		0		✓	0.25	2.0c	20	1	-	0
E02101	✓		0		✓	0.25	2.0c	20	2	-	0
E02201	✓		0		✓	0.25	2.0c	20	5	-	0
E03501	✓		0		✓	0.25	2.0c	35	1	-	0
E03601	✓		0		✓	0.25	2.0c	35	2	-	0
E03701	✓		0		✓	0.25	2.0c	35	5	-	0
E06001	✓		0		✓	0.25	2.0c	60	1	-	0
E06101	✓		0		✓	0.25	2.0c	60	2	-	0
E06201	✓		0		✓	0.25	2.0c	60	5	-	0
E09001	✓		0		✓	0.25	2.0c	90	1	-	0
E09101	✓		0		✓	0.25	2.0c	90	2	-	0
E09201	✓		0		✓	0.25	2.0c	90	5	-	0
E12001	✓		0		✓	0.25	2.0c	120	1	-	0
E12101	✓		0		✓	0.25	2.0c	120	2	-	0
E12201	✓		0		✓	0.25	2.0c	120	5	-	0
E14501	✓		0		✓	0.25	2.0c	145	1	-	0
E14601	✓		0		✓	0.25	2.0c	145	2	-	0
E14701	✓		0		✓	0.25	2.0c	145	5	-	0
E16001	✓		0		✓	0.25	2.0c	160	1	-	0
E16101	✓		0		✓	0.25	2.0c	160	2	-	0
E16201	✓		0		✓	0.25	2.0c	160	5	-	0
F03501	✓		0		✓	0.25	3.0c	35	1	-	0

B-3

File Name	Flow Profile		WD	Array		H/c	x	a	Array #	FC	MC
	Uniform	1/7 th		Single	Multiple						
F03601	✓		0		✓	0.25	3.0c	35	2	-	0
F03701	✓		0		✓	0.25	3.0c	35	4	-	0
F06001	✓		0		✓	0.25	3.0c	60	1	-	0
F06101	✓		0		✓	0.25	3.0c	60	2	-	0
F06201	✓		0		✓	0.25	3.0c	60	4	-	0
F12001	✓		0		✓	0.25	3.0c	120	1	-	0
F12101	✓		0		✓	0.25	3.0c	120	2	-	0
F12401	✓		0		✓	0.25	3.0c	120	4	-	0
F14501	✓		0		✓	0.25	3.0c	145	1	-	0
F14601	✓		0		✓	0.25	3.0c	145	2	-	0
F14701	✓		0		✓	0.25	3.0c	145	4	-	0
G02001		✓	0	✓		0.25	-	20	-	-	0
G03501		✓	0	✓		0.25	-	35	-	-	0
G06001		✓	0	✓		0.25	-	60	-	-	0
G09001		✓	0	✓		0.25	-	90	-	-	0
G12001		✓	0	✓		0.25	-	120	-	-	0
G14501		✓	0	✓		0.25	-	145	-	-	0
G16001		✓	0	✓		0.25	-	160	-	-	0
G01101		✓	0	✓		0.25	-	35	-	7	0
G01201		✓	0	✓		0.25	-	35	-	8	0
G01301		✓	0	✓		0.25	-	35	-	1	0
G01401		✓	0	✓		0.25	-	35	-	9	0
G01501		✓	0	✓		0.25	-	35	-	10	0
G02101		✓	0	✓		0.25	-	145	-	7	0
G02201		✓	0	✓		0.25	-	145	-	8	0
G02301		✓	0	✓		0.25	-	145	-	1	0
G02401		✓	0	✓		0.25	-	145	-	9	0
G02501		✓	0	✓		0.25	-	145	-	10	0
H02001		✓	0		✓	0.25	1.5c	20	1	-	0
H02101		✓	0		✓	0.25	1.5c	20	2	-	0
H02201		✓	0		✓	0.25	1.5c	20	5	-	0
H03501		✓	0		✓	0.25	1.5c	35	1	-	0
H03601		✓	0		✓	0.25	1.5c	35	2	-	0
H03701		✓	0		✓	0.25	1.5c	35	5	-	0
H14501		✓	0		✓	0.25	1.5c	145	1	-	0
H14601		✓	0		✓	0.25	1.5c	145	2	-	0
H14701		✓	0		✓	0.25	1.5c	145	5	-	0
H16001		✓	0		✓	0.25	1.5c	160	1	-	0
H16101		✓	0		✓	0.25	1.5c	160	2	-	0
H16201		✓	0		✓	0.25	1.5c	160	5	-	0
I02001		✓	0		✓	0.25	2.0c	20	1	-	0
I02101		✓	0		✓	0.25	2.0c	20	2	-	0
I02201		✓	0		✓	0.25	2.0c	20	5	-	0
I03501		✓	0		✓	0.25	2.0c	35	1	-	0
I03601		✓	0		✓	0.25	2.0c	35	2	-	0
I03701		✓	0		✓	0.25	2.0c	35	5	-	0
I06001		✓	0		✓	0.25	2.0c	60	1	-	0
I06101		✓	0		✓	0.25	2.0c	60	2	-	0

File Name	Flow Profile		WD	Array		H/c	x	a	Array #	FC	MC
	Uniform	1/7 th		Single	Multiple						
I06201	/		0	/		0.25	2.0c	60	5	-	0
I09001	/		0	/		0.25	2.0c	90	1	-	0
I09101	/		0	/		0.25	2.0c	90	2	-	0
I09201	/		0	/		0.25	2.0c	90	5	-	0
I12001	/		0	/		0.25	2.0c	120	1	-	0
I12101	/		0	/		0.25	2.0c	120	2	-	0
I12201	/		0	/		0.25	2.0c	120	5	-	0
I14501	/		0	/		0.25	2.0c	145	1	-	0
I14601	/		0	/		0.25	2.0c	145	2	-	0
I14701	/		0	/		0.25	2.0c	145	5	-	0
I16001	/		0	/		0.25	2.0c	160	1	-	0
I16101	/		0	/		0.25	2.0c	160	2	-	0
I16201	/		0	/		0.25	2.0c	160	5	-	0
J03501	/		0	/		0.25	3.0c	35	1	-	0
J03601	/		0	/		0.25	3.0c	35	2	-	0
J03701	/		0	/		0.25	3.0c	35	4	-	0
J06001	/		0	/		0.25	3.0c	60	1	-	0
J06101	/		0	/		0.25	3.0c	60	2	-	0
J06201	/		0	/		0.25	3.0c	60	4	-	0
J12001	/		0	/		0.25	3.0c	120	1	-	0
J12101	/		0	/		0.25	3.0c	120	2	-	0
J12201	/		0	/		0.25	3.0c	120	4	-	0
J14501	/		0	/		0.25	3.0c	145	1	-	0
J14601	/		0	/		0.25	3.0c	145	2	-	0
J14701	/		0	/		0.25	3.0c	145	4	-	0
K03501	/		0	/		0.25	2.0c	35	1	5	0
K03601	/		0	/		0.25	2.0c	35	2	5	0
K03701	/		0	/		0.25	2.0c	35	5	5	0
K09001	/		0	/		0.25	2.0c	90	1	5	0
K09101	/		0	/		0.25	2.0c	90	2	5	0
K09201	/		0	/		0.25	2.0c	90	5	5	0
K14501	/		0	/		0.25	2.0c	145	1	5	0
K14601	/		0	/		0.25	2.0c	145	2	5	0
K14701	/		0	/		0.25	2.0c	145	5	5	0
K16001	/		0	/		0.25	2.0c	160	1	5	0
K16101	/		0	/		0.25	2.0c	160	2	5	0
K16201	/		0	/		0.25	2.0c	160	5	5	0
L03501	/		0	/		0.25	2.0c	35	1	1	0
L03601	/		0	/		0.25	2.0c	35	2	1	0
L03701	/		0	/		0.25	2.0c	35	5	1	0
L09001	/		0	/		0.25	2.0c	90	1	1	0
L09101	/		0	/		0.25	2.0c	90	2	1	0
L09201	/		0	/		0.25	2.0c	90	5	1	0
L14501	/		0	/		0.25	2.0c	145	1	1	0
L14601	/		0	/		0.25	2.0c	145	2	1	0
L14701	/		0	/		0.25	2.0c	145	5	1	0
L16001	/		0	/		0.25	2.0c	160	1	1	0
L16101	/		0	/		0.25	2.0c	160	2	1	0

B-5

File Name	Flow Profile		WD	Array		H/c	x	a	Array #	FC	MC
	Uniform	1/7 th		Single	Multiple						
L16201	✓		0		✓	0.25	2.0c	160	5	1	0
M03501	✓		0		✓	0.25	2.0c	35	1	6	0
M03601	✓		0		✓	0.25	2.0c	35	2	6	0
M03701	✓		0		✓	0.25	2.0c	35	5	6	0
M09001	✓		0		✓	0.25	2.0c	90	1	6	0
M09101	✓		0		✓	0.25	2.0c	90	2	6	0
M09201	✓		0		✓	0.25	2.0c	90	5	6	0
M14501	✓		0		✓	0.25	2.0c	145	1	6	0
M14601	✓		0		✓	0.25	2.0c	145	2	6	0
M14701	✓		0		✓	0.25	2.0c	145	5	6	0
M16001	✓		0		✓	0.25	2.0c	160	1	6	0
M16101	✓		0		✓	0.25	2.0c	160	2	6	0
M16201	✓		0		✓	0.25	2.0c	160	5	6	0
N01101	✓		0		✓	0.25	2.0c	35	1	11	0
N01201	✓		0		✓	0.25	2.0c	35	1	12	0
N01301	✓		0		✓	0.25	2.0c	35	1	13	0
N01401	✓		0		✓	0.25	2.0c	35	1	14	0
N01501	✓		0		✓	0.25	2.0c	35	1	15	0
N02101	✓		0		✓	0.25	2.0c	145	1	11	0
N02201	✓		0		✓	0.25	2.0c	145	1	12	0
N02301	✓		0		✓	0.25	2.0c	145	1	13	0
N02401	✓		0		✓	0.25	2.0c	145	1	14	0
N02501	✓		0		✓	0.25	2.0c	145	1	15	0
N11101	✓		0		✓	0.25	2.0c	35	1	7	0
N11201	✓		0		✓	0.25	2.0c	35	1	8	0
N11401	✓		0		✓	0.25	2.0c	35	1	9	0
N11501	✓		0		✓	0.25	2.0c	35	1	10	0
N12101	✓		0		✓	0.25	2.0c	145	1	7	0
N12201	✓		0		✓	0.25	2.0c	145	1	8	0
N12401	✓		0		✓	0.25	2.0c	145	1	9	0
N12501	✓		0		✓	0.25	2.0c	145	1	10	0
N23401	✓		0		✓	0.25	2.0c	60	1	9	0
N24401	✓		0		✓	0.25	2.0c	60	2	9	0
N25401	✓		0		✓	0.25	2.0c	60	5	9	0
N33401	✓		0		✓	0.25	2.0c	120	1	9	0
N34401	✓		0		✓	0.25	2.0c	120	2	9	0
N35401	✓		0		✓	0.25	2.0c	120	5	9	0
O01101	✓		0		✓	0.25	2.0c	35	2	11	0
O01201	✓		0		✓	0.25	2.0c	35	2	12	0
O01301	✓		0		✓	0.25	2.0c	35	2	13	0
O01401	✓		0		✓	0.25	2.0c	35	2	14	0
O01501	✓		0		✓	0.25	2.0c	35	2	15	0
O02101	✓		0		✓	0.25	2.0c	145	2	11	0
O02201	✓		0		✓	0.25	2.0c	145	2	12	0
O02301	✓		0		✓	0.25	2.0c	145	2	13	0
O02401	✓		0		✓	0.25	2.0c	145	2	14	0
O02501	✓		0		✓	0.25	2.0c	145	2	15	0
O11101	✓		0		✓	0.25	2.0c	35	2	7	0

B-6

File Name	Flow Profile		WD	Array		H/c	x	a	Array #	FC	MC
	Uniform	1/7 ch		Single	Multiple						
O11201	✓		0		✓	0.25	2.0c	35	2	8	0
O11401	✓		0		✓	0.25	2.0c	35	2	9	0
O11501	✓		0		✓	0.25	2.0c	35	2	10	0
O12101	✓		0		✓	0.25	2.0c	145	2	7	0
O12201	✓		0		✓	0.25	2.0c	145	2	8	0
O12401	✓		0		✓	0.25	2.0c	145	2	9	0
O12501	✓		0		✓	0.25	2.0c	145	2	10	0
P03501	✓		0		(edge)	0.25	2.0c	35	1	1	0
P03601	✓		0		(edge)	0.25	2.0c	35	2	1	0
P03701	✓		0		(edge)	0.25	2.0c	35	5	1	0
P14501	✓		0		(edge)	0.25	2.0c	145	1	1	0
P14601	✓		0		(edge)	0.25	2.0c	145	2	1	0
P14701	✓		0		(edge)	0.25	2.0c	145	5	1	0
Q03501	✓		0		(edge)	0.25	2.0c	35	1	-	0
Q03601	✓		0		(edge)	0.25	2.0c	35	2	-	0
Q03701	✓		0		(edge)	0.25	2.0c	35	5	-	0
Q14501	✓		0		(edge)	0.25	2.0c	145	1	-	0
Q14601	✓		0		(edge)	0.25	2.0c	145	2	-	0
Q14701	✓		0		(edge)	0.25	2.0c	145	5	-	0
R01101	✓		45		✓	0.25	2.0c	35	1	1	0
R02101	✓		45		✓	0.25	2.0c	145	1	1	0
R01201	✓		45		✓	0.25	2.0c	35	1	2	0
R02201	✓		45		✓	0.25	2.0c	145	1	2	0
R01301	✓		45		✓	0.25	2.0c	35	1	3	0
R02301	✓		45		✓	0.25	2.0c	145	1	3	0
R01401	✓		45		✓	0.25	2.0c	35	1	4	0
R02401	✓		45		✓	0.25	2.0c	145	1	4	0
R11101	✓		45		✓	0.25	2.0c	35	1	1	1
R12101	✓		45		✓	0.25	2.0c	145	1	1	1
R11201	✓		45		✓	0.25	2.0c	35	1	2	1
R12201	✓		45		✓	0.25	2.0c	145	1	2	1
R11301	✓		45		✓	0.25	2.0c	35	1	3	1
R12301	✓		45		✓	0.25	2.0c	145	1	3	1
R21101	✓		45		✓	0.25	2.0c	35	1	1	2
R22101	✓		45		✓	0.25	2.0c	145	1	1	2
R31101	✓		45		✓	0.25	2.0c	35	1	1	3
R32101	✓		45		✓	0.25	2.0c	145	1	1	3
S1101	✓		45		✓	0.25	2.0c	35	2	1	0
S02101	✓		45		✓	0.25	2.0c	145	2	1	0
S01201	✓		45		✓	0.25	2.0c	35	2	2	0
S02201	✓		45		✓	0.25	2.0c	145	2	2	0
S01301	✓		45		✓	0.25	2.0c	35	2	3	0
S02301	✓		45		✓	0.25	2.0c	145	2	3	0
S01401	✓		45		✓	0.25	2.0c	35	2	4	0
S02401	✓		45		✓	0.25	2.0c	145	2	4	0
S11101	✓		45		✓	0.25	2.0c	35	2	1	1
S12101	✓		45		✓	0.25	2.0c	145	2	1	1
S11201	✓		45		✓	0.25	2.0c	35	2	2	1

B-7

File Name	Flow Profile		WD	Array		H/c	x	a	Array #	FC	MC
	Uniform	1/7 th		Single	Multiple						
S12201	✓		45	✓		0.25	2.0c	145	2	2	1
S11301	✓		45	✓		0.25	2.0c	35	2	3	1
S12301	✓		45	✓		0.25	2.0c	145	2	3	1
S21101	✓		45	✓		0.25	2.0c	35	2	1	2
S22101	✓		45	✓		0.25	2.0c	145	2	1	2
S31101	✓		45	✓		0.25	2.0c	35	2	1	3
S32101	✓		45	✓		0.25	2.0c	145	2	1	3
T01101	✓		45	✓		0.25	2.0c	35	3	1	0
T02101	✓		45	✓		0.25	2.0c	145	3	1	0
T01201	✓		45	✓		0.25	2.0c	35	3	2	0
TC2201	✓		45	✓		0.25	2.0c	145	3	2	0
T01301	✓		45	✓		0.25	2.0c	35	3	3	0
T02301	✓		45	✓		0.25	2.0c	145	3	3	0
T01401	✓		45	✓		0.25	2.0c	35	3	4	0
T02401	✓		45	✓		0.25	2.0c	145	3	4	0
T11101	✓		45	✓		0.25	2.0c	35	3	1	1
T12101	✓		45	✓		0.25	2.0c	145	3	1	1
T11201	✓		45	✓		0.25	2.0c	35	3	2	1
T12201	✓		45	✓		0.25	2.0c	145	3	2	1
T11301	✓		45	✓		0.25	2.0c	35	3	3	1
T12301	✓		45	✓		0.25	2.0c	145	3	3	1
T21101	✓		45	✓		0.25	2.0c	35	3	1	2
T2101	✓		45	✓		0.25	2.0c	145	3	1	2
T31101	✓		45	✓		0.25	2.0c	35	3	1	3
T32101	✓		45	✓		0.25	2.0c	145	3	1	3
U03501	✓		45	✓		0.25	2.0c	35	1	-	0
U03601	✓		45	✓		0.25	2.0c	35	2	-	0
U03701	✓		45	✓		0.25	2.0c	35	3	-	0
U14501	✓		45	✓		0.25	2.0c	145	1	-	0
U14601	✓		45	✓		0.25	2.0c	145	2	-	0
U14701	✓		45	✓		0.25	2.0c	145	3	-	0
V03501	✓		45	✓		0.25	2.0c	35	1	-	1
V03601	✓		45	✓		0.25	2.0c	35	2	-	1
V03701	✓		45	✓		0.25	2.0c	35	3	-	1
V14501	✓		45	✓		0.25	2.0c	145	1	-	1
V14601	✓		45	✓		0.25	2.0c	145	2	-	1
V14701	✓		45	✓		0.25	2.0c	145	3	-	1
W03501	✓		0	(edge)		0.25	2.0c	35	1	-	0 (1:12)
W03601	✓		0	(edge)		0.25	2.0c	35	2	-	0 (1:12)
W03701	✓		0	(edge)		0.25	2.0c	35	5	-	0 (1:12)
W14501	✓		0	(edge)		0.25	2.0c	145	1	-	0 (1:12)
W14601	✓		0	(edge)		0.25	2.0c	145	2	-	0 (1:12)
W14701	✓		0	(edge)		0.25	2.0c	145	5	-	0 (1:12)
X03501	✓		0	(edge)		0.25	2.0c	35	1	1	0 (1:12)
X03601	✓		0	(edge)		0.25	2.0c	35	2	1	0 (1:12)
X14501	✓		0	(edge)		0.25	2.0c	145	1	1	0 (1:12)
X14601	✓		0	(edge)		0.25	2.0c	145	2	1	0 (1:12)
Z03501	✓		0	✓		0.25	-	35	-	-	0 (1:12)

DATA FOR PROJECT 6022 CONFIG. 8 WIND DIR. 20 TUBING NO. 1									
TAP	MEAN	RMS	MAX	MIN	TAP	MEAN	RMS	MAX	MIN
1	379	040	150	25	1	714	039	576	879
2	248	022	110	22	2	719	027	504	885
3	104	025	109	13	3	725	029	505	879
4	153	020	119	14	4	729	032	516	875
5	298	019	141	15	5	757	035	522	898
6	615	017	169	16	6	761	040	522	898
7	759	016	159	17	7	777	047	526	891
8	929	016	159	18	8	777	060	526	891
9				19	9				
10				20	10				

DATA FOR PROJECT 6022 CONFIG. 8 WIND DIR. 90 TUBING NO. 1									
TAP	MEAN	RMS	MAX	MIN	TAP	MEAN	RMS	MAX	MIN
1	497	074	694	01	1	500	038	595	875
2	700	050	863	01	2	503	038	595	875
3	837	041	969	02	3	503	038	595	875
4	931	039	1111	02	4	503	038	595	875
5	931	035	1111	02	5	503	038	595	875
6	802	024	925	02	6	503	038	595	875
7	637	024	715	02	7	503	038	595	875
8	439	025	503	02	8	503	038	595	875
9				21	9				
10				21	10				

DATA FOR PROJECT 6022 CONFIG. 8 WIND DIR. 160 TUBING NO. 1									
TAP	MEAN	RMS	MAX	MIN	TAP	MEAN	RMS	MAX	MIN
1	887	015	159	31	1	885	074	251	875
2	657	014	159	31	2	885	020	251	875
3	477	013	159	31	3	885	020	251	875
4	477	012	159	31	4	885	020	251	875
5	134	013	159	31	5	885	020	251	875
6	157	013	159	31	6	885	020	251	875
7	156	013	159	31	7	885	020	251	875
8				31	8				
9				31	9				
10				31	10				

DATA FOR PROJECT 6022 CONFIG. C				WIND DIR. C				WIND DIR. 35 TUBING NO. 1						
TAP	MEAN	RMS	MAX	MIN	TAP	MEAN	RMS	MAX	MIN	TAP	MEAN	RMS	MAX	MIN
1	1025	0.22	1025	1025	1	123	0.17	123	123	1	123	0.17	123	123
2	1025	0.22	1025	1025	2	123	0.17	123	123	2	123	0.17	123	123
3	1025	0.22	1025	1025	3	123	0.17	123	123	3	123	0.17	123	123
4	1025	0.22	1025	1025	4	123	0.17	123	123	4	123	0.17	123	123
5	1025	0.22	1025	1025	5	123	0.17	123	123	5	123	0.17	123	123
6	1025	0.22	1025	1025	6	123	0.17	123	123	6	123	0.17	123	123
7	1025	0.22	1025	1025	7	123	0.17	123	123	7	123	0.17	123	123
8	1025	0.22	1025	1025	8	123	0.17	123	123	8	123	0.17	123	123
9	1025	0.22	1025	1025	9	123	0.17	123	123	9	123	0.17	123	123
10	1025	0.22	1025	1025	10	123	0.17	123	123	10	123	0.17	123	123

DATA FOR PROJECT 6022 CONFIG. C				WIND DIR. C				WIND DIR. 90 TUBING NO. 1						
TAP	MEAN	RMS	MAX	MIN	TAP	MEAN	RMS	MAX	MIN	TAP	MEAN	RMS	MAX	MIN
1	1025	0.22	1025	1025	1	123	0.17	123	123	1	123	0.17	123	123
2	1025	0.22	1025	1025	2	123	0.17	123	123	2	123	0.17	123	123
3	1025	0.22	1025	1025	3	123	0.17	123	123	3	123	0.17	123	123
4	1025	0.22	1025	1025	4	123	0.17	123	123	4	123	0.17	123	123
5	1025	0.22	1025	1025	5	123	0.17	123	123	5	123	0.17	123	123
6	1025	0.22	1025	1025	6	123	0.17	123	123	6	123	0.17	123	123
7	1025	0.22	1025	1025	7	123	0.17	123	123	7	123	0.17	123	123
8	1025	0.22	1025	1025	8	123	0.17	123	123	8	123	0.17	123	123
9	1025	0.22	1025	1025	9	123	0.17	123	123	9	123	0.17	123	123
10	1025	0.22	1025	1025	10	123	0.17	123	123	10	123	0.17	123	123

DATA FOR PROJECT 6022 CONFIG. D				WIND DIR. D				WIND DIR. 21 TUBING NO. 1						
TAP	MEAN	RMS	MAX	MIN	TAP	MEAN	RMS	MAX	MIN	TAP	MEAN	RMS	MAX	MIN
1	1025	0.22	1025	1025	1	123	0.17	123	123	1	123	0.17	123	123
2	1025	0.22	1025	1025	2	123	0.17	123	123	2	123	0.17	123	123
3	1025	0.22	1025	1025	3	123	0.17	123	123	3	123	0.17	123	123
4	1025	0.22	1025	1025	4	123	0.17	123	123	4	123	0.17	123	123
5	1025	0.22	1025	1025	5	123	0.17	123	123	5	123	0.17	123	123
6	1025	0.22	1025	1025	6	123	0.17	123	123	6	123	0.17	123	123
7	1025	0.22	1025	1025	7	123	0.17	123	123	7	123	0.17	123	123
8	1025	0.22	1025	1025	8	123	0.17	123	123	8	123	0.17	123	123
9	1025	0.22	1025	1025	9	123	0.17	123	123	9	123	0.17	123	123
10	1025	0.22	1025	1025	10	123	0.17	123	123	10	123	0.17	123	123

DATA FOR PROJECT 6022 CONFIG. D WIND DIR. 161 TUBING NO. 1									
TAP	MEAN	RMS	MAX	MIN	TAP	MEAN	RMS	MAX	MIN
1	594	027	44	37	1	207	041	055	387
2	400	020	31	25	2	213	043	060	374
3	314	020	21	16	3	212	040	048	369
4	202	015	10	07	4	220	048	072	426
5	097	016	00	00	5	234	055	074	526
6	157	019	00	00	6	230	051	073	524
7	255	025	00	00	7	240	050	074	524
8	357	033	00	00	8	250	051	075	524
9	457	041	00	00	9	260	051	075	524
10	557	049	00	00	10	270	051	075	524

DATA FOR PROJECT 6022 CONFIG. E WIND DIR. 21 TUBING NO. 1									
TAP	MEAN	RMS	MAX	MIN	TAP	MEAN	RMS	MAX	MIN
1	107	019	15	10	1	310	038	051	726
2	127	017	10	08	2	309	038	051	726
3	147	016	07	06	3	308	038	051	726
4	167	015	04	04	4	307	038	051	726
5	187	014	01	01	5	306	038	051	726
6	207	013	00	00	6	305	038	051	726
7	227	012	00	00	7	304	038	051	726
8	247	011	00	00	8	303	038	051	726
9	267	010	00	00	9	302	038	051	726
10	287	009	00	00	10	301	038	051	726

DATA FOR PROJECT 6022 CONFIG. E WIND DIR. 35 TUBING NO. 1									
TAP	MEAN	RMS	MAX	MIN	TAP	MEAN	RMS	MAX	MIN
1	179	028	28	21	1	499	085	111	626
2	164	027	27	20	2	497	085	111	626
3	149	026	26	19	3	495	085	111	626
4	134	025	25	18	4	493	085	111	626
5	119	024	24	17	5	491	085	111	626
6	104	023	23	16	6	489	085	111	626
7	89	022	22	15	7	487	085	111	626
8	74	021	21	14	8	485	085	111	626
9	59	020	20	13	9	483	085	111	626
10	44	019	19	12	10	481	085	111	626

DATA FOR PROJECT 6022											
E WIND DIR			WIND DIR			E WIND DIR			WIND DIR		
TAP	MEAN	RMS	MAX	MIN	TAP	MEAN	RMS	MAX	MIN	TAP	MEAN
1	112	0.00	1.00	0.00	1	112	0.00	1.00	0.00	1	112
2	112	0.00	1.00	0.00	2	112	0.00	1.00	0.00	2	112
3	112	0.00	1.00	0.00	3	112	0.00	1.00	0.00	3	112
4	112	0.00	1.00	0.00	4	112	0.00	1.00	0.00	4	112
5	112	0.00	1.00	0.00	5	112	0.00	1.00	0.00	5	112
6	112	0.00	1.00	0.00	6	112	0.00	1.00	0.00	6	112
7	112	0.00	1.00	0.00	7	112	0.00	1.00	0.00	7	112
8	112	0.00	1.00	0.00	8	112	0.00	1.00	0.00	8	112
9	112	0.00	1.00	0.00	9	112	0.00	1.00	0.00	9	112
10	112	0.00	1.00	0.00	10	112	0.00	1.00	0.00	10	112

DATA FOR PROJECT 6022											
E WIND DIR			WIND DIR			E WIND DIR			WIND DIR		
TAP	MEAN	RMS	MAX	MIN	TAP	MEAN	RMS	MAX	MIN	TAP	MEAN
1	112	0.00	1.00	0.00	1	112	0.00	1.00	0.00	1	112
2	112	0.00	1.00	0.00	2	112	0.00	1.00	0.00	2	112
3	112	0.00	1.00	0.00	3	112	0.00	1.00	0.00	3	112
4	112	0.00	1.00	0.00	4	112	0.00	1.00	0.00	4	112
5	112	0.00	1.00	0.00	5	112	0.00	1.00	0.00	5	112
6	112	0.00	1.00	0.00	6	112	0.00	1.00	0.00	6	112
7	112	0.00	1.00	0.00	7	112	0.00	1.00	0.00	7	112
8	112	0.00	1.00	0.00	8	112	0.00	1.00	0.00	8	112
9	112	0.00	1.00	0.00	9	112	0.00	1.00	0.00	9	112
10	112	0.00	1.00	0.00	10	112	0.00	1.00	0.00	10	112

DATA FOR PROJECT 6022											
E WIND DIR			WIND DIR			E WIND DIR			WIND DIR		
TAP	MEAN	RMS	MAX	MIN	TAP	MEAN	RMS	MAX	MIN	TAP	MEAN
1	112	0.00	1.00	0.00	1	112	0.00	1.00	0.00	1	112
2	112	0.00	1.00	0.00	2	112	0.00	1.00	0.00	2	112
3	112	0.00	1.00	0.00	3	112	0.00	1.00	0.00	3	112
4	112	0.00	1.00	0.00	4	112	0.00	1.00	0.00	4	112
5	112	0.00	1.00	0.00	5	112	0.00	1.00	0.00	5	112
6	112	0.00	1.00	0.00	6	112	0.00	1.00	0.00	6	112
7	112	0.00	1.00	0.00	7	112	0.00	1.00	0.00	7	112
8	112	0.00	1.00	0.00	8	112	0.00	1.00	0.00	8	112
9	112	0.00	1.00	0.00	9	112	0.00	1.00	0.00	9	112
10	112	0.00	1.00	0.00	10	112	0.00	1.00	0.00	10	112

DATA FOR PROJECT 6022 CONFIG. E WIND DIR 147 TUBING NO. 1									
TAP	MEAN	PMS	MAX	MIN	TAP	MEAN	PMS	MAX	MIN
1	1.4	0.0	1.5	1.3	1	0.0	0.0	0.0	0.0
2	1.4	0.0	1.5	1.3	2	0.0	0.0	0.0	0.0
3	1.4	0.0	1.5	1.3	3	0.0	0.0	0.0	0.0
4	1.4	0.0	1.5	1.3	4	0.0	0.0	0.0	0.0
5	1.4	0.0	1.5	1.3	5	0.0	0.0	0.0	0.0
6	1.4	0.0	1.5	1.3	6	0.0	0.0	0.0	0.0
7	1.4	0.0	1.5	1.3	7	0.0	0.0	0.0	0.0
8	1.4	0.0	1.5	1.3	8	0.0	0.0	0.0	0.0
9	1.4	0.0	1.5	1.3	9	0.0	0.0	0.0	0.0
10	1.4	0.0	1.5	1.3	10	0.0	0.0	0.0	0.0

DATA FOR PROJECT 6022 CONFIG. E WIND DIR 161 TUBING NO. 1									
TAP	MEAN	PMS	MAX	MIN	TAP	MEAN	PMS	MAX	MIN
1	1.4	0.0	1.5	1.3	1	0.0	0.0	0.0	0.0
2	1.4	0.0	1.5	1.3	2	0.0	0.0	0.0	0.0
3	1.4	0.0	1.5	1.3	3	0.0	0.0	0.0	0.0
4	1.4	0.0	1.5	1.3	4	0.0	0.0	0.0	0.0
5	1.4	0.0	1.5	1.3	5	0.0	0.0	0.0	0.0
6	1.4	0.0	1.5	1.3	6	0.0	0.0	0.0	0.0
7	1.4	0.0	1.5	1.3	7	0.0	0.0	0.0	0.0
8	1.4	0.0	1.5	1.3	8	0.0	0.0	0.0	0.0
9	1.4	0.0	1.5	1.3	9	0.0	0.0	0.0	0.0
10	1.4	0.0	1.5	1.3	10	0.0	0.0	0.0	0.0

DATA FOR PROJECT 6022 CONFIG. F WIND DIR 35 TUBING NO. 1									
TAP	MEAN	PMS	MAX	MIN	TAP	MEAN	PMS	MAX	MIN
1	1.4	0.0	1.5	1.3	1	0.0	0.0	0.0	0.0
2	1.4	0.0	1.5	1.3	2	0.0	0.0	0.0	0.0
3	1.4	0.0	1.5	1.3	3	0.0	0.0	0.0	0.0
4	1.4	0.0	1.5	1.3	4	0.0	0.0	0.0	0.0
5	1.4	0.0	1.5	1.3	5	0.0	0.0	0.0	0.0
6	1.4	0.0	1.5	1.3	6	0.0	0.0	0.0	0.0
7	1.4	0.0	1.5	1.3	7	0.0	0.0	0.0	0.0
8	1.4	0.0	1.5	1.3	8	0.0	0.0	0.0	0.0
9	1.4	0.0	1.5	1.3	9	0.0	0.0	0.0	0.0
10	1.4	0.0	1.5	1.3	10	0.0	0.0	0.0	0.0

DATA FOR PROJECT 6022 CONFIG. F WIND DIR. 147 TUBING NO. 1										DATA FOR PROJECT 6022 CONFIG. G WIND DIR. 20 TUBING NO. 1									
TAP	MEAN	RMS	MAX	MIN	TAP	MEAN	RMS	MAX	MIN	TAP	MEAN	RMS	MAX	MIN	TAP	MEAN	RMS	MAX	MIN
1	107	0.69	147	427	120	222	0.27	120	394	1	107	0.69	147	427	1	107	0.69	147	427
2	107	0.87	147	227	120	222	0.27	120	394	2	107	0.87	147	227	2	107	0.87	147	227
3	107	1.07	147	227	120	222	0.27	120	394	3	107	1.07	147	227	3	107	1.07	147	227
4	107	1.16	147	227	120	222	0.27	120	394	4	107	1.16	147	227	4	107	1.16	147	227
5	107	1.16	147	227	120	222	0.27	120	394	5	107	1.16	147	227	5	107	1.16	147	227
6	107	1.16	147	227	120	222	0.27	120	394	6	107	1.16	147	227	6	107	1.16	147	227
7	107	1.16	147	227	120	222	0.27	120	394	7	107	1.16	147	227	7	107	1.16	147	227
8	107	1.16	147	227	120	222	0.27	120	394	8	107	1.16	147	227	8	107	1.16	147	227
9	107	1.16	147	227	120	222	0.27	120	394	9	107	1.16	147	227	9	107	1.16	147	227
10	107	1.16	147	227	120	222	0.27	120	394	10	107	1.16	147	227	10	107	1.16	147	227

DATA FOR PROJECT 6022 CONFIG. G WIND DIR. 35 TUBING NO. 1										DATA FOR PROJECT 6022 CONFIG. G WIND DIR. 60 TUBING NO. 1									
TAP	MEAN	RMS	MAX	MIN	TAP	MEAN	RMS	MAX	MIN	TAP	MEAN	RMS	MAX	MIN	TAP	MEAN	RMS	MAX	MIN
1	107	0.51	156	208	112	222	0.27	120	394	1	107	0.51	156	208	1	107	0.51	156	208
2	107	0.57	156	208	112	222	0.27	120	394	2	107	0.57	156	208	2	107	0.57	156	208
3	107	0.65	156	208	112	222	0.27	120	394	3	107	0.65	156	208	3	107	0.65	156	208
4	107	0.65	156	208	112	222	0.27	120	394	4	107	0.65	156	208	4	107	0.65	156	208
5	107	0.65	156	208	112	222	0.27	120	394	5	107	0.65	156	208	5	107	0.65	156	208
6	107	0.65	156	208	112	222	0.27	120	394	6	107	0.65	156	208	6	107	0.65	156	208
7	107	0.65	156	208	112	222	0.27	120	394	7	107	0.65	156	208	7	107	0.65	156	208
8	107	0.65	156	208	112	222	0.27	120	394	8	107	0.65	156	208	8	107	0.65	156	208
9	107	0.65	156	208	112	222	0.27	120	394	9	107	0.65	156	208	9	107	0.65	156	208
10	107	0.65	156	208	112	222	0.27	120	394	10	107	0.65	156	208	10	107	0.65	156	208

DATA FOR PROJECT 6022 CONFIG. G WIND DIR. 90 TUBING NO. 1										DATA FOR PROJECT 6022 CONFIG. G WIND DIR. 120 TUBING NO. 1									
TAP	MEAN	RMS	MAX	MIN	TAP	MEAN	RMS	MAX	MIN	TAP	MEAN	RMS	MAX	MIN	TAP	MEAN	RMS	MAX	MIN
1	107	0.96	186	267	112	222	0.27	120	394	1	107	0.96	186	267	1	107	0.96	186	267
2	107	1.05	186	267	112	222	0.27	120	394	2	107	1.05	186	267	2	107	1.05	186	267
3	107	1.15	186	267	112	222	0.27	120	394	3	107	1.15	186	267	3	107	1.15	186	267
4	107	1.17	186	267	112	222	0.27	120	394	4	107	1.17	186	267	4	107	1.17	186	267
5	107	1.17	186	267	112	222	0.27	120	394	5	107	1.17	186	267	5	107	1.17	186	267
6	107	1.17	186	267	112	222	0.27	120	394	6	107	1.17	186	267	6	107	1.17	186	267
7	107	1.17	186	267	112	222	0.27	120	394	7	107	1.17	186	267	7	107	1.17	186	267
8	107	1.17	186	267	112	222	0.27	120	394	8	107	1.17	186	267	8	107	1.17	186	267
9	107	1.17	186	267	112	222	0.27	120	394	9	107	1.17	186	267	9	107	1.17	186	267
10	107	1.17	186	267	112	222	0.27	120	394	10	107	1.17	186	267	10	107	1.17	186	267

DATA FOR PROJECT 6022 CONFIG. G WIND DIR. 145 TUBING NO. 1											
TAP	MEAN	RMS	MAX	MIN	TAP	MEAN	RMS	MAX	MIN	TAP	MEAN
1	12.4	0.73	9.0	1.5	1	12.4	0.73	9.0	1.5	1	12.4
2	13.5	0.73	9.0	1.5	2	13.5	0.73	9.0	1.5	2	13.5
3	14.6	0.73	9.0	1.5	3	14.6	0.73	9.0	1.5	3	14.6
4	15.7	0.73	9.0	1.5	4	15.7	0.73	9.0	1.5	4	15.7
5	16.8	0.73	9.0	1.5	5	16.8	0.73	9.0	1.5	5	16.8
6	17.9	0.73	9.0	1.5	6	17.9	0.73	9.0	1.5	6	17.9
7	19.0	0.73	9.0	1.5	7	19.0	0.73	9.0	1.5	7	19.0
8	20.1	0.73	9.0	1.5	8	20.1	0.73	9.0	1.5	8	20.1
9	21.2	0.73	9.0	1.5	9	21.2	0.73	9.0	1.5	9	21.2
10	22.3	0.73	9.0	1.5	10	22.3	0.73	9.0	1.5	10	22.3

DATA FOR PROJECT 6022 CONFIG. G WIND DIR. 12 TUBING NO. 1											
TAP	MEAN	RMS	MAX	MIN	TAP	MEAN	RMS	MAX	MIN	TAP	MEAN
1	12.4	0.83	9.5	1.5	1	12.4	0.83	9.5	1.5	1	12.4
2	13.5	0.83	9.5	1.5	2	13.5	0.83	9.5	1.5	2	13.5
3	14.6	0.83	9.5	1.5	3	14.6	0.83	9.5	1.5	3	14.6
4	15.7	0.83	9.5	1.5	4	15.7	0.83	9.5	1.5	4	15.7
5	16.8	0.83	9.5	1.5	5	16.8	0.83	9.5	1.5	5	16.8
6	17.9	0.83	9.5	1.5	6	17.9	0.83	9.5	1.5	6	17.9
7	19.0	0.83	9.5	1.5	7	19.0	0.83	9.5	1.5	7	19.0
8	20.1	0.83	9.5	1.5	8	20.1	0.83	9.5	1.5	8	20.1
9	21.2	0.83	9.5	1.5	9	21.2	0.83	9.5	1.5	9	21.2
10	22.3	0.83	9.5	1.5	10	22.3	0.83	9.5	1.5	10	22.3

DATA FOR PROJECT 6022 CONFIG. G WIND DIR. 14 TUBING NO. 1											
TAP	MEAN	RMS	MAX	MIN	TAP	MEAN	RMS	MAX	MIN	TAP	MEAN
1	12.4	0.61	8.5	1.5	1	12.4	0.61	8.5	1.5	1	12.4
2	13.5	0.61	8.5	1.5	2	13.5	0.61	8.5	1.5	2	13.5
3	14.6	0.61	8.5	1.5	3	14.6	0.61	8.5	1.5	3	14.6
4	15.7	0.61	8.5	1.5	4	15.7	0.61	8.5	1.5	4	15.7
5	16.8	0.61	8.5	1.5	5	16.8	0.61	8.5	1.5	5	16.8
6	17.9	0.61	8.5	1.5	6	17.9	0.61	8.5	1.5	6	17.9
7	19.0	0.61	8.5	1.5	7	19.0	0.61	8.5	1.5	7	19.0
8	20.1	0.61	8.5	1.5	8	20.1	0.61	8.5	1.5	8	20.1
9	21.2	0.61	8.5	1.5	9	21.2	0.61	8.5	1.5	9	21.2
10	22.3	0.61	8.5	1.5	10	22.3	0.61	8.5	1.5	10	22.3

DATA FOR PROJECT 6022										DATA FOR PROJECT 6022																			
CONFIG. H					WIND DIR.					TUBING NO. 1					CONFIG. H					WIND DIR.					TUBING NO. 1				
TAP	MEAN	RMS	MAX	MIN	TAP	MEAN	RMS	MAX	MIN	TAP	MEAN	RMS	MAX	MIN	TAP	MEAN	RMS	MAX	MIN	TAP	MEAN	RMS	MAX	MIN					
1	002	002	171	52	1	002	002	002	002	1	002	002	002	002	1	002	002	002	002	1	002	002	002	002					
2	003	003	200	53	2	003	003	003	003	2	003	003	003	003	2	003	003	003	003	2	003	003	003	003					
3	004	004	220	54	3	004	004	004	004	3	004	004	004	004	3	004	004	004	004	3	004	004	004	004					
4	005	005	240	55	4	005	005	005	005	4	005	005	005	005	4	005	005	005	005	4	005	005	005	005					
5	006	006	260	56	5	006	006	006	006	5	006	006	006	006	5	006	006	006	006	5	006	006	006	006					
6	007	007	280	57	6	007	007	007	007	6	007	007	007	007	6	007	007	007	007	6	007	007	007	007					
7	008	008	300	58	7	008	008	008	008	7	008	008	008	008	7	008	008	008	008	7	008	008	008	008					
8	009	009	320	59	8	009	009	009	009	8	009	009	009	009	8	009	009	009	009	8	009	009	009	009					
9	010	010	340	60	9	010	010	010	010	9	010	010	010	010	9	010	010	010	010	9	010	010	010	010					
10	011	011	360	61	10	011	011	011	011	10	011	011	011	011	10	011	011	011	011	10	011	011	011	011					

DATA FOR PROJECT 6022										DATA FOR PROJECT 6022																			
CONFIG. H					WIND DIR.					TUBING NO. 1					CONFIG. H					WIND DIR.					TUBING NO. 1				
TAP	MEAN	RMS	MAX	MIN	TAP	MEAN	RMS	MAX	MIN	TAP	MEAN	RMS	MAX	MIN	TAP	MEAN	RMS	MAX	MIN	TAP	MEAN	RMS	MAX	MIN					
1	025	025	025	025	1	025	025	025	025	1	025	025	025	025	1	025	025	025	025	1	025	025	025	025					
2	026	026	026	026	2	026	026	026	026	2	026	026	026	026	2	026	026	026	026	2	026	026	026	026					
3	027	027	027	027	3	027	027	027	027	3	027	027	027	027	3	027	027	027	027	3	027	027	027	027					
4	028	028	028	028	4	028	028	028	028	4	028	028	028	028	4	028	028	028	028	4	028	028	028	028					
5	029	029	029	029	5	029	029	029	029	5	029	029	029	029	5	029	029	029	029	5	029	029	029	029					
6	030	030	030	030	6	030	030	030	030	6	030	030	030	030	6	030	030	030	030	6	030	030	030	030					
7	031	031	031	031	7	031	031	031	031	7	031	031	031	031	7	031	031	031	031	7	031	031	031	031					
8	032	032	032	032	8	032	032	032	032	8	032	032	032	032	8	032	032	032	032	8	032	032	032	032					
9	033	033	033	033	9	033	033	033	033	9	033	033	033	033	9	033	033	033	033	9	033	033	033	033					
10	034	034	034	034	10	034	034	034	034	10	034	034	034	034	10	034	034	034	034	10	034	034	034	034					

DATA FOR PROJECT 6022										DATA FOR PROJECT 6022																			
CONFIG. H					WIND DIR.					TUBING NO. 1					CONFIG. H					WIND DIR.					TUBING NO. 1				
TAP	MEAN	RMS	MAX	MIN	TAP	MEAN	RMS	MAX	MIN	TAP	MEAN	RMS	MAX	MIN	TAP	MEAN	RMS	MAX	MIN	TAP	MEAN	RMS	MAX	MIN					
1	035	035	035	035	1	035	035	035	035	1	035	035	035	035	1	035	035	035	035	1	035	035	035	035					
2	036	036	036	036	2	036	036	036	036	2	036	036	036	036	2	036	036	036	036	2	036	036	036	036					
3	037	037	037	037	3	037	037	037	037	3	037	037	037	037	3	037	037	037	037	3	037	037	037	037					
4	038	038	038	038	4	038	038	038	038	4	038	038	038	038	4	038	038	038	038	4	038	038	038	038					
5	039	039	039	039	5	039	039	039	039	5	039	039	039	039	5	039	039	039	039	5	039	039	039	039					
6	040	040	040	040	6	040	040	040	040	6	040	040	040	040	6	040	040	040	040	6	040	040	040	040					
7	041	041	041	041	7	041	041	041	041	7	041	041	041	041	7	041	041	041	041	7	041	041	041	041					
8	042	042	042	042	8	042	042	042	042	8	042	042	042	042	8	042	042	042	042	8	042	042	042	042					
9	043	043	043	043	9	043	043	043	043	9	043	043	043	043	9	043	043	043	043	9	043	043	043	043					
10	044	044	044	044	10	044	044	044	044	10	044	044	044	044	10	044	044	044	044	10	044	044	044	044					

DATA FOR PROJECT 6022 CONFIG. H WIND DIR. 146 TUBING NO. 1									
TAP	MEAN	RMS	MAX	MIN	TAP	MEAN	RMS	MAX	MIN
10M456789	42	106	620	13	12	42	106	620	13
1	41622	1091	6251	14	14	41622	1091	6251	14
	3727	823	525	0	15	3727	823	525	0
	287	664	388	0	16	287	664	388	0
	104	495	280	0	17	104	495	280	0
	21	105	60	0	18	21	105	60	0
					19				
					20				
					21				
					22				
					23				
					24				
					25				
					26				
					27				
					28				
					29				
					30				

DATA FOR PROJECT 6022 CONFIG. H WIND DIR. 147 TUBING NO. 1									
TAP	MEAN	RMS	MAX	MIN	TAP	MEAN	RMS	MAX	MIN
10M456789	110	49	280	7	12	110	49	280	7
1	1035	105	620	15	14	1035	105	620	15
	1075	105	620	15	15	1075	105	620	15
	950	66	388	0	16	950	66	388	0
	525	49	280	0	17	525	49	280	0
	155	105	620	15	18	155	105	620	15
					19				
					20				
					21				
					22				
					23				
					24				
					25				
					26				
					27				
					28				
					29				
					30				

DATA FOR PROJECT 6022 CONFIG. H WIND DIR. 162 TUBING NO. 1									
TAP	MEAN	RMS	MAX	MIN	TAP	MEAN	RMS	MAX	MIN
10M456789	164	26	160	5	12	164	26	160	5
1	117	26	160	5	14	117	26	160	5
	117	26	160	5	15	117	26	160	5
	106	26	160	5	16	106	26	160	5
	104	26	160	5	17	104	26	160	5
	107	26	160	5	18	107	26	160	5
	107	26	160	5	19	107	26	160	5
	107	26	160	5	20	107	26	160	5
	107	26	160	5	21	107	26	160	5
	107	26	160	5	22	107	26	160	5
	107	26	160	5	23	107	26	160	5
	107	26	160	5	24	107	26	160	5
	107	26	160	5	25	107	26	160	5
	107	26	160	5	26	107	26	160	5
	107	26	160	5	27	107	26	160	5
	107	26	160	5	28	107	26	160	5
	107	26	160	5	29	107	26	160	5
	107	26	160	5	30	107	26	160	5

DATA FOR PROJECT 6022 CONFIG. 1 WIND DIR. 1 WIND DIR. 1 WIND DIR. 1														
DATA FOR PROJECT 6022 CONFIG. 1			DATA FOR PROJECT 6022 CONFIG. 1			DATA FOR PROJECT 6022 CONFIG. 1			DATA FOR PROJECT 6022 CONFIG. 1					
TAP	MEAN	RMS	MAX	MIN	TAP	MEAN	RMS	MAX	MIN	TAP	MEAN	RMS	MAX	MIN
1	0.37	0.64	1.97	2.60	1	0.09	0.29	0.95	1.25	1	0.09	0.29	0.95	1.25
2	0.37	0.64	1.97	2.60	2	0.09	0.29	0.95	1.25	2	0.09	0.29	0.95	1.25
3	0.37	0.64	1.97	2.60	3	0.09	0.29	0.95	1.25	3	0.09	0.29	0.95	1.25
4	0.37	0.64	1.97	2.60	4	0.09	0.29	0.95	1.25	4	0.09	0.29	0.95	1.25
5	0.37	0.64	1.97	2.60	5	0.09	0.29	0.95	1.25	5	0.09	0.29	0.95	1.25
6	0.37	0.64	1.97	2.60	6	0.09	0.29	0.95	1.25	6	0.09	0.29	0.95	1.25
7	0.37	0.64	1.97	2.60	7	0.09	0.29	0.95	1.25	7	0.09	0.29	0.95	1.25
8	0.37	0.64	1.97	2.60	8	0.09	0.29	0.95	1.25	8	0.09	0.29	0.95	1.25
9	0.37	0.64	1.97	2.60	9	0.09	0.29	0.95	1.25	9	0.09	0.29	0.95	1.25
10	0.37	0.64	1.97	2.60	10	0.09	0.29	0.95	1.25	10	0.09	0.29	0.95	1.25

DATA FOR PROJECT 6022 CONFIG. 1 WIND DIR. 1 WIND DIR. 1 WIND DIR. 1														
DATA FOR PROJECT 6022 CONFIG. 1			DATA FOR PROJECT 6022 CONFIG. 1			DATA FOR PROJECT 6022 CONFIG. 1			DATA FOR PROJECT 6022 CONFIG. 1					
TAP	MEAN	RMS	MAX	MIN	TAP	MEAN	RMS	MAX	MIN	TAP	MEAN	RMS	MAX	MIN
1	0.19	0.52	1.59	2.15	1	0.16	0.52	1.59	2.15	1	0.16	0.52	1.59	2.15
2	0.19	0.52	1.59	2.15	2	0.16	0.52	1.59	2.15	2	0.16	0.52	1.59	2.15
3	0.19	0.52	1.59	2.15	3	0.16	0.52	1.59	2.15	3	0.16	0.52	1.59	2.15
4	0.19	0.52	1.59	2.15	4	0.16	0.52	1.59	2.15	4	0.16	0.52	1.59	2.15
5	0.19	0.52	1.59	2.15	5	0.16	0.52	1.59	2.15	5	0.16	0.52	1.59	2.15
6	0.19	0.52	1.59	2.15	6	0.16	0.52	1.59	2.15	6	0.16	0.52	1.59	2.15
7	0.19	0.52	1.59	2.15	7	0.16	0.52	1.59	2.15	7	0.16	0.52	1.59	2.15
8	0.19	0.52	1.59	2.15	8	0.16	0.52	1.59	2.15	8	0.16	0.52	1.59	2.15
9	0.19	0.52	1.59	2.15	9	0.16	0.52	1.59	2.15	9	0.16	0.52	1.59	2.15
10	0.19	0.52	1.59	2.15	10	0.16	0.52	1.59	2.15	10	0.16	0.52	1.59	2.15

DATA FOR PROJECT 6022 CONFIG. 1 WIND DIR. 1 WIND DIR. 1 WIND DIR. 1														
DATA FOR PROJECT 6022 CONFIG. 1			DATA FOR PROJECT 6022 CONFIG. 1			DATA FOR PROJECT 6022 CONFIG. 1			DATA FOR PROJECT 6022 CONFIG. 1					
TAP	MEAN	RMS	MAX	MIN	TAP	MEAN	RMS	MAX	MIN	TAP	MEAN	RMS	MAX	MIN
1	0.09	0.29	0.95	1.25	1	0.09	0.29	0.95	1.25	1	0.09	0.29	0.95	1.25
2	0.09	0.29	0.95	1.25	2	0.09	0.29	0.95	1.25	2	0.09	0.29	0.95	1.25
3	0.09	0.29	0.95	1.25	3	0.09	0.29	0.95	1.25	3	0.09	0.29	0.95	1.25
4	0.09	0.29	0.95	1.25	4	0.09	0.29	0.95	1.25	4	0.09	0.29	0.95	1.25
5	0.09	0.29	0.95	1.25	5	0.09	0.29	0.95	1.25	5	0.09	0.29	0.95	1.25
6	0.09	0.29	0.95	1.25	6	0.09	0.29	0.95	1.25	6	0.09	0.29	0.95	1.25
7	0.09	0.29	0.95	1.25	7	0.09	0.29	0.95	1.25	7	0.09	0.29	0.95	1.25
8	0.09	0.29	0.95	1.25	8	0.09	0.29	0.95	1.25	8	0.09	0.29	0.95	1.25
9	0.09	0.29	0.95	1.25	9	0.09	0.29	0.95	1.25	9	0.09	0.29	0.95	1.25
10	0.09	0.29	0.95	1.25	10	0.09	0.29	0.95	1.25	10	0.09	0.29	0.95	1.25

DATA FOR PROJECT 6022 CONFIG. 1 WIND DIR. 1 WIND DIR. 61 TUBING NO. 1									
TAP	MEAN	RMS	MAX	MIN	TAP	MEAN	RMS	MAX	MIN
1	1275	072	427	023	1	3296	106	968	012
2	3395	087	1271	045	2	2286	083	000	116
3	4742	096	824	138	3	2286	087	000	116
4	4850	096	824	138	4	2286	087	000	116
5	4850	096	824	138	5	2286	087	000	116
6	4850	096	824	138	6	2286	087	000	116
7	4850	096	824	138	7	2286	087	000	116
8	4850	096	824	138	8	2286	087	000	116
9	4850	096	824	138	9	2286	087	000	116
10	4850	096	824	138	10	2286	087	000	116

DATA FOR PROJECT 6022 CONFIG. 1 WIND DIR. 1 WIND DIR. 90 TUBING NO. 1									
TAP	MEAN	RMS	MAX	MIN	TAP	MEAN	RMS	MAX	MIN
1	0288	078	159	028	1	4239	054	3887	009
2	0684	087	159	045	2	4239	054	3887	009
3	0684	087	159	045	3	4239	054	3887	009
4	0684	087	159	045	4	4239	054	3887	009
5	0684	087	159	045	5	4239	054	3887	009
6	0684	087	159	045	6	4239	054	3887	009
7	0684	087	159	045	7	4239	054	3887	009
8	0684	087	159	045	8	4239	054	3887	009
9	0684	087	159	045	9	4239	054	3887	009
10	0684	087	159	045	10	4239	054	3887	009

DATA FOR PROJECT 6022 CONFIG. 1 WIND DIR. 1 WIND DIR. 92 TUBING NO. 1									
TAP	MEAN	RMS	MAX	MIN	TAP	MEAN	RMS	MAX	MIN
1	0708	072	027	023	1	0652	055	022	000
2	0708	072	027	023	2	0652	055	022	000
3	0708	072	027	023	3	0652	055	022	000
4	0708	072	027	023	4	0652	055	022	000
5	0708	072	027	023	5	0652	055	022	000
6	0708	072	027	023	6	0652	055	022	000
7	0708	072	027	023	7	0652	055	022	000
8	0708	072	027	023	8	0652	055	022	000
9	0708	072	027	023	9	0652	055	022	000
10	0708	072	027	023	10	0652	055	022	000

DATA FOR PROJECT 6022 CONFIG. I WIND DIR. 120 TUBING NO. 1									
TAP	MEAN	RMS	MAX	MIN	TAP	MEAN	RMS	MAX	MIN
1	297	116	60	136	1	127	054	277	557
2	477	111	82	170	2	128	055	287	557
3	477	111	82	170	3	129	055	294	557
4	477	111	82	170	4	129	055	294	557
5	477	111	82	170	5	129	055	294	557
6	477	111	82	170	6	129	055	294	557
7	477	111	82	170	7	129	055	294	557
8	477	111	82	170	8	129	055	294	557
9	477	111	82	170	9	129	055	294	557
10	477	111	82	170	10	129	055	294	557

DATA FOR PROJECT 6022 CONFIG. I WIND DIR. 145 TUBING NO. 1									
TAP	MEAN	RMS	MAX	MIN	TAP	MEAN	RMS	MAX	MIN
1	627	107	110	220	1	127	054	277	557
2	100	107	110	220	2	128	055	287	557
3	100	107	110	220	3	129	055	294	557
4	100	107	110	220	4	129	055	294	557
5	100	107	110	220	5	129	055	294	557
6	100	107	110	220	6	129	055	294	557
7	100	107	110	220	7	129	055	294	557
8	100	107	110	220	8	129	055	294	557
9	100	107	110	220	9	129	055	294	557
10	100	107	110	220	10	129	055	294	557

DATA FOR PROJECT 6022 CONFIG. I WIND DIR. 147 TUBING NO. 1									
TAP	MEAN	RMS	MAX	MIN	TAP	MEAN	RMS	MAX	MIN
1	627	107	110	220	1	127	054	277	557
2	100	107	110	220	2	128	055	287	557
3	100	107	110	220	3	129	055	294	557
4	100	107	110	220	4	129	055	294	557
5	100	107	110	220	5	129	055	294	557
6	100	107	110	220	6	129	055	294	557
7	100	107	110	220	7	129	055	294	557
8	100	107	110	220	8	129	055	294	557
9	100	107	110	220	9	129	055	294	557
10	100	107	110	220	10	129	055	294	557

DATA FOR PROJECT 6022 CONFIG. I WIND DIR. 161 TUBING NO. 1

TAP	MEAN	RMS	MAX	MIN	TAP	MEAN	RMS	MAX	MIN
1	0.000	0.000	0.000	0.000	1	0.000	0.000	0.000	0.000
2	0.000	0.000	0.000	0.000	2	0.000	0.000	0.000	0.000
3	0.000	0.000	0.000	0.000	3	0.000	0.000	0.000	0.000
4	0.000	0.000	0.000	0.000	4	0.000	0.000	0.000	0.000
5	0.000	0.000	0.000	0.000	5	0.000	0.000	0.000	0.000
6	0.000	0.000	0.000	0.000	6	0.000	0.000	0.000	0.000
7	0.000	0.000	0.000	0.000	7	0.000	0.000	0.000	0.000
8	0.000	0.000	0.000	0.000	8	0.000	0.000	0.000	0.000
9	0.000	0.000	0.000	0.000	9	0.000	0.000	0.000	0.000
10	0.000	0.000	0.000	0.000	10	0.000	0.000	0.000	0.000

DATA FOR PROJECT 6022 CONFIG. J WIND DIR. 35 TUBING NO. 1

TAP	MEAN	RMS	MAX	MIN	TAP	MEAN	RMS	MAX	MIN
1	0.000	0.000	0.000	0.000	1	0.000	0.000	0.000	0.000
2	0.000	0.000	0.000	0.000	2	0.000	0.000	0.000	0.000
3	0.000	0.000	0.000	0.000	3	0.000	0.000	0.000	0.000
4	0.000	0.000	0.000	0.000	4	0.000	0.000	0.000	0.000
5	0.000	0.000	0.000	0.000	5	0.000	0.000	0.000	0.000
6	0.000	0.000	0.000	0.000	6	0.000	0.000	0.000	0.000
7	0.000	0.000	0.000	0.000	7	0.000	0.000	0.000	0.000
8	0.000	0.000	0.000	0.000	8	0.000	0.000	0.000	0.000
9	0.000	0.000	0.000	0.000	9	0.000	0.000	0.000	0.000
10	0.000	0.000	0.000	0.000	10	0.000	0.000	0.000	0.000

DATA FOR PROJECT 6022 CONFIG. J WIND DIR. 37 TUBING NO. 1

TAP	MEAN	RMS	MAX	MIN	TAP	MEAN	RMS	MAX	MIN
1	0.000	0.000	0.000	0.000	1	0.000	0.000	0.000	0.000
2	0.000	0.000	0.000	0.000	2	0.000	0.000	0.000	0.000
3	0.000	0.000	0.000	0.000	3	0.000	0.000	0.000	0.000
4	0.000	0.000	0.000	0.000	4	0.000	0.000	0.000	0.000
5	0.000	0.000	0.000	0.000	5	0.000	0.000	0.000	0.000
6	0.000	0.000	0.000	0.000	6	0.000	0.000	0.000	0.000
7	0.000	0.000	0.000	0.000	7	0.000	0.000	0.000	0.000
8	0.000	0.000	0.000	0.000	8	0.000	0.000	0.000	0.000
9	0.000	0.000	0.000	0.000	9	0.000	0.000	0.000	0.000
10	0.000	0.000	0.000	0.000	10	0.000	0.000	0.000	0.000

DATA FOR PROJECT 6022 CONFIG. L WIND DIR. 91 TUBING NO. 1									
TAP	MEAN	RMS	MAX	MIN	TAP	MEAN	RMS	MAX	MIN
1	078	056	245	000	1	123	065	523	000
2	074	054	245	000	2	123	065	523	000
3	074	054	245	000	3	123	065	523	000
4	087	054	245	000	4	123	065	523	000
5	106	054	245	000	5	123	065	523	000
6	107	054	245	000	6	123	065	523	000
7	107	054	245	000	7	123	065	523	000
8	107	054	245	000	8	123	065	523	000
9	107	054	245	000	9	123	065	523	000
10	107	054	245	000	10	123	065	523	000

DATA FOR PROJECT 6022 CONFIG. L WIND DIR. 145 TUBING NO. 1									
TAP	MEAN	RMS	MAX	MIN	TAP	MEAN	RMS	MAX	MIN
1	078	056	245	000	1	123	065	523	000
2	074	054	245	000	2	123	065	523	000
3	074	054	245	000	3	123	065	523	000
4	087	054	245	000	4	123	065	523	000
5	106	054	245	000	5	123	065	523	000
6	107	054	245	000	6	123	065	523	000
7	107	054	245	000	7	123	065	523	000
8	107	054	245	000	8	123	065	523	000
9	107	054	245	000	9	123	065	523	000
10	107	054	245	000	10	123	065	523	000

DATA FOR PROJECT 6022 CONFIG. L WIND DIR. 147 TUBING NO. 1									
TAP	MEAN	RMS	MAX	MIN	TAP	MEAN	RMS	MAX	MIN
1	078	056	245	000	1	123	065	523	000
2	074	054	245	000	2	123	065	523	000
3	074	054	245	000	3	123	065	523	000
4	087	054	245	000	4	123	065	523	000
5	106	054	245	000	5	123	065	523	000
6	107	054	245	000	6	123	065	523	000
7	107	054	245	000	7	123	065	523	000
8	107	054	245	000	8	123	065	523	000
9	107	054	245	000	9	123	065	523	000
10	107	054	245	000	10	123	065	523	000

DATA FOR PROJECT 6022 CONFIG. L WIND DIR. 161 TUBING NO. 1									
TAP	MEAN	RMS	MAX	MIN	TAP	MEAN	RMS	MAX	MIN
1	0.02	0.32	0.8	0.1	1	0.73	0.39	0.93	0.29
2	0.02	0.32	0.8	0.1	2	0.81	0.39	0.93	0.29
3	0.02	0.32	0.8	0.1	3	0.78	0.39	0.93	0.29
4	0.02	0.32	0.8	0.1	4	0.78	0.39	0.93	0.29
5	0.02	0.32	0.8	0.1	5	0.78	0.39	0.93	0.29
6	0.02	0.32	0.8	0.1	6	0.78	0.39	0.93	0.29
7	0.02	0.32	0.8	0.1	7	0.78	0.39	0.93	0.29
8	0.02	0.32	0.8	0.1	8	0.78	0.39	0.93	0.29
9	0.02	0.32	0.8	0.1	9	0.78	0.39	0.93	0.29
10	0.02	0.32	0.8	0.1	10	0.78	0.39	0.93	0.29

DATA FOR PROJECT 6022 CONFIG. M WIND DIR. 35 TUBING NO. 1									
TAP	MEAN	RMS	MAX	MIN	TAP	MEAN	RMS	MAX	MIN
1	0.02	0.32	0.8	0.1	1	0.73	0.39	0.93	0.29
2	0.02	0.32	0.8	0.1	2	0.81	0.39	0.93	0.29
3	0.02	0.32	0.8	0.1	3	0.78	0.39	0.93	0.29
4	0.02	0.32	0.8	0.1	4	0.78	0.39	0.93	0.29
5	0.02	0.32	0.8	0.1	5	0.78	0.39	0.93	0.29
6	0.02	0.32	0.8	0.1	6	0.78	0.39	0.93	0.29
7	0.02	0.32	0.8	0.1	7	0.78	0.39	0.93	0.29
8	0.02	0.32	0.8	0.1	8	0.78	0.39	0.93	0.29
9	0.02	0.32	0.8	0.1	9	0.78	0.39	0.93	0.29
10	0.02	0.32	0.8	0.1	10	0.78	0.39	0.93	0.29

DATA FOR PROJECT 6022 CONFIG. N WIND DIR. 37 TUBING NO. 1									
TAP	MEAN	RMS	MAX	MIN	TAP	MEAN	RMS	MAX	MIN
1	0.02	0.32	0.8	0.1	1	0.73	0.39	0.93	0.29
2	0.02	0.32	0.8	0.1	2	0.81	0.39	0.93	0.29
3	0.02	0.32	0.8	0.1	3	0.78	0.39	0.93	0.29
4	0.02	0.32	0.8	0.1	4	0.78	0.39	0.93	0.29
5	0.02	0.32	0.8	0.1	5	0.78	0.39	0.93	0.29
6	0.02	0.32	0.8	0.1	6	0.78	0.39	0.93	0.29
7	0.02	0.32	0.8	0.1	7	0.78	0.39	0.93	0.29
8	0.02	0.32	0.8	0.1	8	0.78	0.39	0.93	0.29
9	0.02	0.32	0.8	0.1	9	0.78	0.39	0.93	0.29
10	0.02	0.32	0.8	0.1	10	0.78	0.39	0.93	0.29

DATA FOR PROJECT 6022 CONFIG. H WIND DIR. 91 TUBING NO. 1									
TAP	MEAN	RMS	MAX	MIN	TAP	MEAN	RMS	MAX	MIN
1	0.22	0.61	2.15	0.71	1	0.95	0.58	1.74	0.70
2	0.26	0.62	2.22	0.77	2	0.99	0.55	1.81	0.95
3	0.45	0.74	2.39	0.99	3	1.02	0.51	1.81	1.02
4	0.28	0.72	2.59	0.85	4	1.05	0.46	1.82	1.04
5	0.98	0.92	2.87	1.29	5	1.08	0.38	1.82	1.09
6	1.16	1.13	3.11	1.59	6	1.16	0.35	1.82	1.16
7	1.15	1.16	3.31	1.59	7	1.16	0.38	1.82	1.16
8	0.85	0.85	3.41	1.34	8	1.08	0.44	1.82	1.08
9	0.85	0.85	3.41	1.34	9	1.08	0.44	1.82	1.08
10	0.85	0.85	3.41	1.34	10	1.08	0.44	1.82	1.08

DATA FOR PROJECT 6022 CONFIG. H WIND DIR. 145 TUBING NO. 1									
TAP	MEAN	RMS	MAX	MIN	TAP	MEAN	RMS	MAX	MIN
1	0.55	0.47	1.62	0.26	1	0.28	0.28	0.67	0.28
2	0.62	0.49	1.72	0.26	2	0.28	0.28	0.67	0.28
3	0.45	0.44	1.72	0.26	3	0.28	0.28	0.67	0.28
4	0.28	0.42	1.72	0.26	4	0.28	0.28	0.67	0.28
5	0.28	0.42	1.72	0.26	5	0.28	0.28	0.67	0.28
6	0.28	0.42	1.72	0.26	6	0.28	0.28	0.67	0.28
7	0.28	0.42	1.72	0.26	7	0.28	0.28	0.67	0.28
8	0.28	0.42	1.72	0.26	8	0.28	0.28	0.67	0.28
9	0.28	0.42	1.72	0.26	9	0.28	0.28	0.67	0.28
10	0.28	0.42	1.72	0.26	10	0.28	0.28	0.67	0.28

DATA FOR PROJECT 6022 CONFIG. H WIND DIR. 147 TUBING NO. 1									
TAP	MEAN	RMS	MAX	MIN	TAP	MEAN	RMS	MAX	MIN
1	0.25	0.35	1.02	0.05	1	0.28	0.28	0.67	0.28
2	0.31	0.35	1.02	0.05	2	0.28	0.28	0.67	0.28
3	0.33	0.35	1.02	0.05	3	0.28	0.28	0.67	0.28
4	0.33	0.35	1.02	0.05	4	0.28	0.28	0.67	0.28
5	0.33	0.35	1.02	0.05	5	0.28	0.28	0.67	0.28
6	0.33	0.35	1.02	0.05	6	0.28	0.28	0.67	0.28
7	0.33	0.35	1.02	0.05	7	0.28	0.28	0.67	0.28
8	0.33	0.35	1.02	0.05	8	0.28	0.28	0.67	0.28
9	0.33	0.35	1.02	0.05	9	0.28	0.28	0.67	0.28
10	0.33	0.35	1.02	0.05	10	0.28	0.28	0.67	0.28

DATA FOR PROJECT 6022 CONFIG. N WIND DIR. 14 TUBING NO. 1										DATA FOR PROJECT 6022 CONFIG. N WIND DIR. 15 TUBING NO. 1									
TAP	MEAN	RMS	MAX	MIN	TAP	MEAN	RMS	MAX	MIN	TAP	MEAN	RMS	MAX	MIN	TAP	MEAN	RMS	MAX	MIN
1	326	065	146	887	123	311	044	055	604	1	390	063	194	889	1	368	053	182	572
2	325	065	147	887	123	301	045	052	604	2	391	061	190	889	2	369	053	182	572
3	325	065	147	887	123	301	045	052	604	3	392	056	188	889	3	370	053	182	572
4	325	065	147	887	123	301	045	052	604	4	371	049	177	889	4	374	053	182	572
5	325	065	147	887	123	301	045	052	604	5	378	047	172	889	5	376	053	182	572
6	325	065	147	887	123	301	045	052	604	6	384	048	172	889	6	375	053	182	572
7	325	065	147	887	123	301	045	052	604	7	387	047	172	889	7	375	053	182	572
8	325	065	147	887	123	301	045	052	604	8	387	047	172	889	8	375	053	182	572
9	325	065	147	887	123	301	045	052	604	9	387	047	172	889	9	375	053	182	572
10	325	065	147	887	123	301	045	052	604	10	387	047	172	889	10	375	053	182	572

DATA FOR PROJECT 6022 CONFIG. N WIND DIR. 21 TUBING NO. 1										DATA FOR PROJECT 6022 CONFIG. N WIND DIR. 22 TUBING NO. 1									
TAP	MEAN	RMS	MAX	MIN	TAP	MEAN	RMS	MAX	MIN	TAP	MEAN	RMS	MAX	MIN	TAP	MEAN	RMS	MAX	MIN
1	300	076	248	210	123	209	069	129	461	1	309	043	170	330	1	309	043	170	330
2	300	076	248	210	123	209	069	129	461	2	309	043	170	330	2	309	043	170	330
3	300	076	248	210	123	209	069	129	461	3	309	043	170	330	3	309	043	170	330
4	300	076	248	210	123	209	069	129	461	4	309	043	170	330	4	309	043	170	330
5	300	076	248	210	123	209	069	129	461	5	309	043	170	330	5	309	043	170	330
6	300	076	248	210	123	209	069	129	461	6	309	043	170	330	6	309	043	170	330
7	300	076	248	210	123	209	069	129	461	7	309	043	170	330	7	309	043	170	330
8	300	076	248	210	123	209	069	129	461	8	309	043	170	330	8	309	043	170	330
9	300	076	248	210	123	209	069	129	461	9	309	043	170	330	9	309	043	170	330
10	300	076	248	210	123	209	069	129	461	10	309	043	170	330	10	309	043	170	330

DATA FOR PROJECT 6022 CONFIG. N WIND DIR. 23 TUBING NO. 1										DATA FOR PROJECT 6022 CONFIG. N WIND DIR. 24 TUBING NO. 1									
TAP	MEAN	RMS	MAX	MIN	TAP	MEAN	RMS	MAX	MIN	TAP	MEAN	RMS	MAX	MIN	TAP	MEAN	RMS	MAX	MIN
1	327	057	205	623	123	407	052	195	688	1	410	052	195	688	1	326	057	195	688
2	327	057	205	623	123	408	054	195	688	2	408	054	195	688	2	326	057	195	688
3	327	057	205	623	123	408	054	195	688	3	408	054	195	688	3	326	057	195	688
4	327	057	205	623	123	408	054	195	688	4	408	054	195	688	4	326	057	195	688
5	327	057	205	623	123	408	054	195	688	5	408	054	195	688	5	326	057	195	688
6	327	057	205	623	123	408	054	195	688	6	408	054	195	688	6	326	057	195	688
7	327	057	205	623	123	408	054	195	688	7	408	054	195	688	7	326	057	195	688
8	327	057	205	623	123	408	054	195	688	8	408	054	195	688	8	326	057	195	688
9	327	057	205	623	123	408	054	195	688	9	408	054	195	688	9	326	057	195	688
10	327	057	205	623	123	408	054	195	688	10	408	054	195	688	10	326	057	195	688

DATA FOR PROJECT 6022 CONFIG. N WIND DIR. 111 TUBING NO. 1									
TAP	MEAN	RMS	MAX	MIN	TAP	MEAN	RMS	MAX	MIN
1	151	047	229	147	1	173	050	050	499
2	092	055	232	108	2	188	046	046	513
3	141	057	239	107	3	185	039	039	489
4	148	057	239	107	4	185	004	004	453
5	192	057	239	107	5	207	007	007	472
6	227	057	239	107	6	184	002	002	397
7	227	057	239	107	7	185	002	002	397
8	227	057	239	107	8	185	002	002	397
9	227	057	239	107	9	185	002	002	397
10	227	057	239	107	10	185	002	002	397

DATA FOR PROJECT 6022 CONFIG. N WIND DIR. 114 TUBING NO. 1									
TAP	MEAN	RMS	MAX	MIN	TAP	MEAN	RMS	MAX	MIN
1	113	046	239	05	1	182	040	040	907
2	107	045	239	258	2	182	046	046	831
3	099	044	239	258	3	182	038	038	673
4	074	044	239	258	4	187	044	044	691
5	079	044	239	258	5	177	035	035	455
6	085	044	239	258	6	177	035	035	455
7	084	044	239	258	7	177	035	035	455
8	084	044	239	258	8	190	004	004	499
9	088	044	239	258	9	190	004	004	499
10	088	044	239	258	10	190	004	004	499

DATA FOR PROJECT 6022 CONFIG. N WIND DIR. 121 TUBING NO. 1									
TAP	MEAN	RMS	MAX	MIN	TAP	MEAN	RMS	MAX	MIN
1	209	055	239	103	1	295	059	059	4
2	209	055	239	103	2	302	045	045	552
3	209	055	239	103	3	302	045	045	552
4	209	055	239	103	4	302	045	045	552
5	209	055	239	103	5	302	045	045	552
6	209	055	239	103	6	302	045	045	552
7	209	055	239	103	7	302	045	045	552
8	209	055	239	103	8	302	045	045	552
9	209	055	239	103	9	302	045	045	552
10	209	055	239	103	10	302	045	045	552

DATA FOR PROJECT 6022										WIND DIR. 122 TUBING NO. 1										WIND DIR. 124 TUBING NO. 1									
TAP	MEAN	RMS	MAX	CONFIG.	H	TAP	MEAN	RMS	MAX	MIN	TAP	MEAN	RMS	MAX	CONFIG.	H	TAP	MEAN	RMS	MAX	MIN								
1	0.4	0.81	5.72	1	1	1	0.1	0.41	0.72	3.52	1	1.5	0.49	0.88	3	1	1	1.8	0.40	0.70	21								
2	0.7	0.91	6.72	1	2	1	0.3	0.45	0.84	3.59	1	1.3	0.49	0.88	3	1	1	1.8	0.40	0.70	21								
3	0.7	0.91	6.72	1	3	1	0.3	0.45	0.84	3.59	1	1.3	0.49	0.88	3	1	1	1.8	0.40	0.70	21								
4	0.9	1.08	6.80	1	4	1	0.4	0.47	0.86	3.68	1	1.4	0.52	0.94	4	1	1	1.9	0.40	0.70	21								
5	0.9	1.08	6.80	1	5	1	0.4	0.47	0.86	3.68	1	1.4	0.52	0.94	4	1	1	1.9	0.40	0.70	21								
6	0.9	1.08	6.80	1	6	1	0.4	0.47	0.86	3.68	1	1.4	0.52	0.94	4	1	1	1.9	0.40	0.70	21								
7	0.9	1.08	6.80	1	7	1	0.4	0.47	0.86	3.68	1	1.4	0.52	0.94	4	1	1	1.9	0.40	0.70	21								
8	0.9	1.08	6.80	1	8	1	0.4	0.47	0.86	3.68	1	1.4	0.52	0.94	4	1	1	1.9	0.40	0.70	21								
9	0.9	1.08	6.80	1	9	1	0.4	0.47	0.86	3.68	1	1.4	0.52	0.94	4	1	1	1.9	0.40	0.70	21								
10	0.9	1.08	6.80	1	10	1	0.4	0.47	0.86	3.68	1	1.4	0.52	0.94	4	1	1	1.9	0.40	0.70	21								

DATA FOR PROJECT 6022										WIND DIR. 125 TUBING NO. 1										WIND DIR. 234 TUBING NO. 1									
TAP	MEAN	RMS	MAX	CONFIG.	H	TAP	MEAN	RMS	MAX	MIN	TAP	MEAN	RMS	MAX	CONFIG.	H	TAP	MEAN	RMS	MAX	MIN								
1	0.4	0.81	5.72	1	1	1	0.1	0.41	0.72	3.52	1	1.5	0.49	0.88	3	1	1	1.8	0.40	0.70	21								
2	0.7	0.91	6.72	1	2	1	0.3	0.45	0.84	3.59	1	1.3	0.49	0.88	3	1	1	1.8	0.40	0.70	21								
3	0.7	0.91	6.72	1	3	1	0.3	0.45	0.84	3.59	1	1.3	0.49	0.88	3	1	1	1.8	0.40	0.70	21								
4	0.9	1.08	6.80	1	4	1	0.4	0.47	0.86	3.68	1	1.4	0.52	0.94	4	1	1	1.9	0.40	0.70	21								
5	0.9	1.08	6.80	1	5	1	0.4	0.47	0.86	3.68	1	1.4	0.52	0.94	4	1	1	1.9	0.40	0.70	21								
6	0.9	1.08	6.80	1	6	1	0.4	0.47	0.86	3.68	1	1.4	0.52	0.94	4	1	1	1.9	0.40	0.70	21								
7	0.9	1.08	6.80	1	7	1	0.4	0.47	0.86	3.68	1	1.4	0.52	0.94	4	1	1	1.9	0.40	0.70	21								
8	0.9	1.08	6.80	1	8	1	0.4	0.47	0.86	3.68	1	1.4	0.52	0.94	4	1	1	1.9	0.40	0.70	21								
9	0.9	1.08	6.80	1	9	1	0.4	0.47	0.86	3.68	1	1.4	0.52	0.94	4	1	1	1.9	0.40	0.70	21								
10	0.9	1.08	6.80	1	10	1	0.4	0.47	0.86	3.68	1	1.4	0.52	0.94	4	1	1	1.9	0.40	0.70	21								

DATA FOR PROJECT 6022										WIND DIR. 244 TUBING NO. 1										WIND DIR. 254 TUBING NO. 1									
TAP	MEAN	RMS	MAX	CONFIG.	H	TAP	MEAN	RMS	MAX	MIN	TAP	MEAN	RMS	MAX	CONFIG.	H	TAP	MEAN	RMS	MAX	MIN								
1	0.4	0.81	5.72	1	1	1	0.1	0.41	0.72	3.52	1	1.5	0.49	0.88	3	1	1	1.8	0.40	0.70	21								
2	0.7	0.91	6.72	1	2	1	0.3	0.45	0.84	3.59	1	1.3	0.49	0.88	3	1	1	1.8	0.40	0.70	21								
3	0.7	0.91	6.72	1	3	1	0.3	0.45	0.84	3.59	1	1.3	0.49	0.88	3	1	1	1.8	0.40	0.70	21								
4	0.9	1.08	6.80	1	4	1	0.4	0.47	0.86	3.68	1	1.4	0.52	0.94	4	1	1	1.9	0.40	0.70	21								
5	0.9	1.08	6.80	1	5	1	0.4	0.47	0.86	3.68	1	1.4	0.52	0.94	4	1	1	1.9	0.40	0.70	21								
6	0.9	1.08	6.80	1	6	1	0.4	0.47	0.86	3.68	1	1.4	0.52	0.94	4	1	1	1.9	0.40	0.70	21								
7	0.9	1.08	6.80	1	7	1	0.4	0.47	0.86	3.68	1	1.4	0.52	0.94	4	1	1	1.9	0.40	0.70	21								
8	0.9	1.08	6.80	1	8	1	0.4	0.47	0.86	3.68	1	1.4	0.52	0.94	4	1	1	1.9	0.40	0.70	21								
9	0.9	1.08	6.80	1	9	1	0.4	0.47	0.86	3.68	1	1.4	0.52	0.94	4	1	1	1.9	0.40	0.70	21								
10	0.9	1.08	6.80	1	10	1	0.4	0.47	0.86	3.68	1	1.4	0.52	0.94	4	1	1	1.9	0.40	0.70	21								

DATA FOR PROJECT 6022 CONFIG. 0 WIND DIR. 0 WIND DIR. 344 TUBING NO. 1

TAP	MEAN	RMS	MAX	MIN	TAP	MEAN	RMS	MAX	MIN
1	105	048	039	287	1	197	049	028	18
2	106	050	039	287	2	201	047	027	18
3	106	050	039	287	3	201	047	027	18
4	115	050	039	287	4	205	058	027	18
5	115	050	039	287	5	205	058	027	18
6	131	077	050	287	6	198	067	027	18
7	131	077	050	287	7	188	091	027	18
8	131	077	050	287	8	188	091	027	18
9	131	077	050	287	9	188	091	027	18
10	131	077	050	287	10	188	091	027	18

DATA FOR PROJECT 6022 CONFIG. 0 WIND DIR. 0 WIND DIR. 11 TUBING NO. 1

TAP	MEAN	RMS	MAX	MIN	TAP	MEAN	RMS	MAX	MIN
1	97	035	048	257	1	024	062	356	259
2	98	045	045	257	2	066	067	386	259
3	98	045	045	257	3	066	067	386	259
4	98	045	045	257	4	066	067	386	259
5	98	045	045	257	5	066	067	386	259
6	98	045	045	257	6	066	067	386	259
7	98	045	045	257	7	066	067	386	259
8	98	045	045	257	8	066	067	386	259
9	98	045	045	257	9	066	067	386	259
10	98	045	045	257	10	066	067	386	259

DATA FOR PROJECT 6022 CONFIG. 0 WIND DIR. 0 WIND DIR. 13 TUBING NO. 1

TAP	MEAN	RMS	MAX	MIN	TAP	MEAN	RMS	MAX	MIN
1	116	055	023	222	1	148	070	084	234
2	113	055	023	222	2	148	062	084	234
3	113	055	023	222	3	148	062	084	234
4	113	055	023	222	4	148	062	084	234
5	113	055	023	222	5	148	062	084	234
6	113	055	023	222	6	148	062	084	234
7	113	055	023	222	7	148	062	084	234
8	113	055	023	222	8	148	062	084	234
9	113	055	023	222	9	148	062	084	234
10	113	055	023	222	10	148	062	084	234

DATA FOR PROJECT 6022 CONFIG. 0 WIND DIR. 15 TUBING NO. 1									
TAP	MEAN	RMS	MAX	MIN	TAP	MEAN	RMS	MAX	MIN
1	277	091	050	746	1	289	070	062	686
2	280	082	041	736	2	291	072	060	690
3	285	082	042	736	3	273	072	062	690
4	282	087	042	736	4	267	073	062	693
5	286	087	042	736	5	253	070	062	693
6	282	087	042	736	6	240	067	062	692
7	282	087	042	736	7	236	065	062	692
8	282	087	042	736	8	227	063	062	696
9	283	083	041	736	9	224	063	062	696
10	283	083	041	736	10	224	063	062	696

DATA FOR PROJECT 6022 CONFIG. 0 WIND DIR. 22 TUBING NO. 1									
TAP	MEAN	RMS	MAX	MIN	TAP	MEAN	RMS	MAX	MIN
1	124	088	038	322	1	081	088	034	225
2	125	087	037	322	2	082	088	034	225
3	112	087	037	322	3	082	088	034	225
4	114	087	037	322	4	082	088	034	225
5	114	087	037	322	5	082	088	034	225
6	104	087	037	322	6	082	088	034	225
7	056	087	037	322	7	082	088	034	225
8	044	087	037	322	8	082	088	034	225
9	069	087	037	322	9	082	088	034	225
10	069	087	037	322	10	082	088	034	225

DATA FOR PROJECT 6022 CONFIG. 0 WIND DIR. 24 TUBING NO. 1									
TAP	MEAN	RMS	MAX	MIN	TAP	MEAN	RMS	MAX	MIN
1	178	074	048	383	1	158	054	036	250
2	175	074	048	383	2	155	052	036	250
3	165	074	048	383	3	155	052	036	250
4	162	074	048	383	4	155	052	036	250
5	162	074	048	383	5	155	052	036	250
6	162	074	048	383	6	155	052	036	250
7	162	074	048	383	7	155	052	036	250
8	162	074	048	383	8	155	052	036	250
9	162	074	048	383	9	155	052	036	250
10	162	074	048	383	10	155	052	036	250

DATA FOR PROJECT 6022										DATA FOR PROJECT 6022																			
CONFIG. 0					WIND DIR. 1					TUBING NO. 1					CONFIG. 0					WIND DIR. 1					TUBING NO. 1				
TAP	MEAN	RMS	MAX	MIN	TAP	MEAN	RMS	MAX	MIN	TAP	MEAN	RMS	MAX	MIN	TAP	MEAN	RMS	MAX	MIN	TAP	MEAN	RMS	MAX	MIN					
1	332	0.55	120	60	1	250	0.55	0.80	0.2	1	123	0.65	369	204	1	176	0.75	295	175	1	154	0.85	252	971					
2	332	0.55	120	60	2	250	0.55	0.80	0.2	2	123	0.65	369	204	2	176	0.75	295	175	2	154	0.85	252	146					
3	332	0.55	120	60	3	250	0.55	0.80	0.2	3	123	0.65	369	204	3	176	0.75	295	175	3	154	0.85	252	700					
4	332	0.55	120	60	4	250	0.55	0.80	0.2	4	123	0.65	369	204	4	176	0.75	295	175	4	154	0.85	252	585					
5	332	0.55	120	60	5	250	0.55	0.80	0.2	5	123	0.65	369	204	5	176	0.75	295	175	5	154	0.85	252	464					
6	332	0.55	120	60	6	250	0.55	0.80	0.2	6	123	0.65	369	204	6	176	0.75	295	175	6	154	0.85	252	464					
7	332	0.55	120	60	7	250	0.55	0.80	0.2	7	123	0.65	369	204	7	176	0.75	295	175	7	154	0.85	252	464					
8	332	0.55	120	60	8	250	0.55	0.80	0.2	8	123	0.65	369	204	8	176	0.75	295	175	8	154	0.85	252	464					
9	332	0.55	120	60	9	250	0.55	0.80	0.2	9	123	0.65	369	204	9	176	0.75	295	175	9	154	0.85	252	464					
10	332	0.55	120	60	10	250	0.55	0.80	0.2	10	123	0.65	369	204	10	176	0.75	295	175	10	154	0.85	252	464					

DATA FOR PROJECT 6022										DATA FOR PROJECT 6022																			
CONFIG. 0					WIND DIR. 1					TUBING NO. 1					CONFIG. 0					WIND DIR. 1					TUBING NO. 1				
TAP	MEAN	RMS	MAX	MIN	TAP	MEAN	RMS	MAX	MIN	TAP	MEAN	RMS	MAX	MIN	TAP	MEAN	RMS	MAX	MIN	TAP	MEAN	RMS	MAX	MIN					
1	021	0.43	200	100	1	180	0.43	0.60	0.2	1	123	0.43	0.60	0.2	1	150	0.43	0.60	0.2	1	130	0.43	0.60	0.2					
2	021	0.43	200	100	2	180	0.43	0.60	0.2	2	123	0.43	0.60	0.2	2	150	0.43	0.60	0.2	2	130	0.43	0.60	0.2					
3	021	0.43	200	100	3	180	0.43	0.60	0.2	3	123	0.43	0.60	0.2	3	150	0.43	0.60	0.2	3	130	0.43	0.60	0.2					
4	021	0.43	200	100	4	180	0.43	0.60	0.2	4	123	0.43	0.60	0.2	4	150	0.43	0.60	0.2	4	130	0.43	0.60	0.2					
5	021	0.43	200	100	5	180	0.43	0.60	0.2	5	123	0.43	0.60	0.2	5	150	0.43	0.60	0.2	5	130	0.43	0.60	0.2					
6	021	0.43	200	100	6	180	0.43	0.60	0.2	6	123	0.43	0.60	0.2	6	150	0.43	0.60	0.2	6	130	0.43	0.60	0.2					
7	021	0.43	200	100	7	180	0.43	0.60	0.2	7	123	0.43	0.60	0.2	7	150	0.43	0.60	0.2	7	130	0.43	0.60	0.2					
8	021	0.43	200	100	8	180	0.43	0.60	0.2	8	123	0.43	0.60	0.2	8	150	0.43	0.60	0.2	8	130	0.43	0.60	0.2					
9	021	0.43	200	100	9	180	0.43	0.60	0.2	9	123	0.43	0.60	0.2	9	150	0.43	0.60	0.2	9	130	0.43	0.60	0.2					
10	021	0.43	200	100	10	180	0.43	0.60	0.2	10	123	0.43	0.60	0.2	10	150	0.43	0.60	0.2	10	130	0.43	0.60	0.2					

DATA FOR PROJECT 6022										DATA FOR PROJECT 6022																			
CONFIG. 0					WIND DIR. 1					TUBING NO. 1					CONFIG. 0					WIND DIR. 1					TUBING NO. 1				
TAP	MEAN	RMS	MAX	MIN	TAP	MEAN	RMS	MAX	MIN	TAP	MEAN	RMS	MAX	MIN	TAP	MEAN	RMS	MAX	MIN	TAP	MEAN	RMS	MAX	MIN					
1	021	0.43	200	100	1	180	0.43	0.60	0.2	1	123	0.43	0.60	0.2	1	150	0.43	0.60	0.2	1	130	0.43	0.60	0.2					
2	021	0.43	200	100	2	180	0.43	0.60	0.2	2	123	0.43	0.60	0.2	2	150	0.43	0.60	0.2	2	130	0.43	0.60	0.2					
3	021	0.43	200	100	3	180	0.43	0.60	0.2	3	123	0.43	0.60	0.2	3	150	0.43	0.60	0.2	3	130	0.43	0.60	0.2					
4	021	0.43	200	100	4	180	0.43	0.60	0.2	4	123	0.43	0.60	0.2	4	150	0.43	0.60	0.2	4	130	0.43	0.60	0.2					
5	021	0.43	200	100	5	180	0.43	0.60	0.2	5	123	0.43	0.60	0.2	5	150	0.43	0.60	0.2	5	130	0.43	0.60	0.2					
6	021	0.43	200	100	6	180	0.43	0.60	0.2	6	123	0.43	0.60	0.2	6	150	0.43	0.60	0.2	6	130	0.43	0.60	0.2					
7	021	0.43	200	100	7	180	0.43	0.60	0.2	7	123	0.43	0.60	0.2	7	150	0.43	0.60	0.2	7	130	0.43	0.60	0.2					
8	021	0.43	200	100	8	180	0.43	0.60	0.2	8	123	0.43	0.60	0.2	8	150	0.43	0.60	0.2	8	130	0.43	0.60	0.2					
9	021	0.43	200	100	9	180	0.43	0.60	0.2	9	123	0.43	0.60	0.2	9	150	0.43	0.60	0.2	9	130	0.43	0.60	0.2					
10	021	0.43	200	100	10	180	0.43	0.60	0.2	10	123	0.43	0.60	0.2	10	150	0.43	0.60	0.2	10	130	0.43	0.60	0.2					

DATA FOR PROJECT 6022 CONFIG. P WIND DIR. 146 TUBING NO. 1

TAP	MEAN	RMS	MAX	MIN	TAP	MEAN	RMS	MAX	MIN
1	120750	000000	050000	000000	1	120750	000000	050000	000000
2	120750	000000	050000	000000	2	120750	000000	050000	000000
3	120750	000000	050000	000000	3	120750	000000	050000	000000
4	120750	000000	050000	000000	4	120750	000000	050000	000000
5	120750	000000	050000	000000	5	120750	000000	050000	000000
6	120750	000000	050000	000000	6	120750	000000	050000	000000
7	120750	000000	050000	000000	7	120750	000000	050000	000000
8	120750	000000	050000	000000	8	120750	000000	050000	000000
9	120750	000000	050000	000000	9	120750	000000	050000	000000
10	120750	000000	050000	000000	10	120750	000000	050000	000000

DATA FOR PROJECT 6022 CONFIG. 0 WIND DIR. 35 TUBING NO. 1

TAP	MEAN	RMS	MAX	MIN	TAP	MEAN	RMS	MAX	MIN
1	120750	000000	050000	000000	1	120750	000000	050000	000000
2	120750	000000	050000	000000	2	120750	000000	050000	000000
3	120750	000000	050000	000000	3	120750	000000	050000	000000
4	120750	000000	050000	000000	4	120750	000000	050000	000000
5	120750	000000	050000	000000	5	120750	000000	050000	000000
6	120750	000000	050000	000000	6	120750	000000	050000	000000
7	120750	000000	050000	000000	7	120750	000000	050000	000000
8	120750	000000	050000	000000	8	120750	000000	050000	000000
9	120750	000000	050000	000000	9	120750	000000	050000	000000
10	120750	000000	050000	000000	10	120750	000000	050000	000000

DATA FOR PROJECT 6022 CONFIG. 0 WIND DIR. 37 TUBING NO. 1

TAP	MEAN	RMS	MAX	MIN	TAP	MEAN	RMS	MAX	MIN
1	120750	000000	050000	000000	1	120750	000000	050000	000000
2	120750	000000	050000	000000	2	120750	000000	050000	000000
3	120750	000000	050000	000000	3	120750	000000	050000	000000
4	120750	000000	050000	000000	4	120750	000000	050000	000000
5	120750	000000	050000	000000	5	120750	000000	050000	000000
6	120750	000000	050000	000000	6	120750	000000	050000	000000
7	120750	000000	050000	000000	7	120750	000000	050000	000000
8	120750	000000	050000	000000	8	120750	000000	050000	000000
9	120750	000000	050000	000000	9	120750	000000	050000	000000
10	120750	000000	050000	000000	10	120750	000000	050000	000000

DATA FOR PROJECT 6022 CONFIG. 0 WIND DIR. 146 TUBING NO. 1									
TAP	MEAN	RMS	MAX	MIN	TAP	MEAN	RMS	MAX	MIN
1	2266	1217	8788	0208	1	1588	2443	31	451
2	2266	1217	8788	0208	2	1588	2443	31	451
3	2266	1217	8788	0208	3	1588	2443	31	451
4	2266	1217	8788	0208	4	1588	2443	31	451
5	2266	1217	8788	0208	5	1588	2443	31	451
6	2266	1217	8788	0208	6	1588	2443	31	451
7	2266	1217	8788	0208	7	1588	2443	31	451
8	2266	1217	8788	0208	8	1588	2443	31	451
9	2266	1217	8788	0208	9	1588	2443	31	451
10	2266	1217	8788	0208	10	1588	2443	31	451

DATA FOR PROJECT 6022 CONFIG. 0 WIND DIR. 147 TUBING NO. 1									
TAP	MEAN	RMS	MAX	MIN	TAP	MEAN	RMS	MAX	MIN
1	1024	455	2702	0000	1	657	88	67	269
2	1024	455	2702	0000	2	657	88	67	269
3	1024	455	2702	0000	3	657	88	67	269
4	1024	455	2702	0000	4	657	88	67	269
5	1024	455	2702	0000	5	657	88	67	269
6	1024	455	2702	0000	6	657	88	67	269
7	1024	455	2702	0000	7	657	88	67	269
8	1024	455	2702	0000	8	657	88	67	269
9	1024	455	2702	0000	9	657	88	67	269
10	1024	455	2702	0000	10	657	88	67	269

DATA FOR PROJECT 6022 CONFIG. 0 WIND DIR. 12 TUBING NO. 1									
TAP	MEAN	RMS	MAX	MIN	TAP	MEAN	RMS	MAX	MIN
1	2266	1217	8788	0208	1	1588	2443	31	451
2	2266	1217	8788	0208	2	1588	2443	31	451
3	2266	1217	8788	0208	3	1588	2443	31	451
4	2266	1217	8788	0208	4	1588	2443	31	451
5	2266	1217	8788	0208	5	1588	2443	31	451
6	2266	1217	8788	0208	6	1588	2443	31	451
7	2266	1217	8788	0208	7	1588	2443	31	451
8	2266	1217	8788	0208	8	1588	2443	31	451
9	2266	1217	8788	0208	9	1588	2443	31	451
10	2266	1217	8788	0208	10	1588	2443	31	451

DATA FOR PROJECT 6022 CONFIG. R WIND DIR. 221 TUBING NO. 1									
TAP	MEAN	RMS	MAX	MIN	TAP	MEAN	RMS	MAX	MIN
1	0.2	0.8	3.8	0.1	1	0.2	0.8	3.8	0.1
2	0.2	0.8	4.0	0.1	2	0.2	0.8	4.0	0.1
3	0.2	0.8	4.0	0.1	3	0.2	0.8	4.0	0.1
4	0.2	0.8	4.0	0.1	4	0.2	0.8	4.0	0.1
5	0.2	0.8	4.0	0.1	5	0.2	0.8	4.0	0.1
6	0.2	0.8	4.0	0.1	6	0.2	0.8	4.0	0.1
7	0.2	0.8	4.0	0.1	7	0.2	0.8	4.0	0.1
8	0.2	0.8	4.0	0.1	8	0.2	0.8	4.0	0.1
9	0.2	0.8	4.0	0.1	9	0.2	0.8	4.0	0.1
10	0.2	0.8	4.0	0.1	10	0.2	0.8	4.0	0.1

DATA FOR PROJECT 6022 CONFIG. S WIND DIR. 321 TUBING NO. 1									
TAP	MEAN	RMS	MAX	MIN	TAP	MEAN	RMS	MAX	MIN
1	0.2	0.8	3.8	0.1	1	0.2	0.8	3.8	0.1
2	0.2	0.8	4.0	0.1	2	0.2	0.8	4.0	0.1
3	0.2	0.8	4.0	0.1	3	0.2	0.8	4.0	0.1
4	0.2	0.8	4.0	0.1	4	0.2	0.8	4.0	0.1
5	0.2	0.8	4.0	0.1	5	0.2	0.8	4.0	0.1
6	0.2	0.8	4.0	0.1	6	0.2	0.8	4.0	0.1
7	0.2	0.8	4.0	0.1	7	0.2	0.8	4.0	0.1
8	0.2	0.8	4.0	0.1	8	0.2	0.8	4.0	0.1
9	0.2	0.8	4.0	0.1	9	0.2	0.8	4.0	0.1
10	0.2	0.8	4.0	0.1	10	0.2	0.8	4.0	0.1

DATA FOR PROJECT 6022 CONFIG. S WIND DIR. 311 TUBING NO. 1									
TAP	MEAN	RMS	MAX	MIN	TAP	MEAN	RMS	MAX	MIN
1	0.2	0.8	3.8	0.1	1	0.2	0.8	3.8	0.1
2	0.2	0.8	4.0	0.1	2	0.2	0.8	4.0	0.1
3	0.2	0.8	4.0	0.1	3	0.2	0.8	4.0	0.1
4	0.2	0.8	4.0	0.1	4	0.2	0.8	4.0	0.1
5	0.2	0.8	4.0	0.1	5	0.2	0.8	4.0	0.1
6	0.2	0.8	4.0	0.1	6	0.2	0.8	4.0	0.1
7	0.2	0.8	4.0	0.1	7	0.2	0.8	4.0	0.1
8	0.2	0.8	4.0	0.1	8	0.2	0.8	4.0	0.1
9	0.2	0.8	4.0	0.1	9	0.2	0.8	4.0	0.1
10	0.2	0.8	4.0	0.1	10	0.2	0.8	4.0	0.1

DATA FOR PROJECT 6022 CONFIG. 8 WIND DIR. 13 TUBING NO. 1									
TAP	MEAN	RMS	MAX	MIN	TAP	MEAN	RMS	MAX	MIN
1	0620	1113	709	0	1	2922	0327	1305	0
2	1005	1128	729	2384	2	2060	0270	1652	432
3	1355	1131	709	1928	3	2222	0270	1592	332
4	1357	1138	709	1928	4	2222	0270	1592	332
5	1115	1134	709	1928	5	2222	0270	1592	332
6	1115	1134	709	1928	6	2222	0270	1592	332
7	1115	1134	709	1928	7	2222	0270	1592	332
8	1115	1134	709	1928	8	2222	0270	1592	332
9	1115	1134	709	1928	9	2222	0270	1592	332
10	1115	1134	709	1928	10	2222	0270	1592	332

DATA FOR PROJECT 6022 CONFIG. 9 WIND DIR. 14 TUBING NO. 1									
TAP	MEAN	RMS	MAX	MIN	TAP	MEAN	RMS	MAX	MIN
1	0423	1109	735	0	1	2196	0523	1305	0
2	0645	1109	735	0	2	2196	0523	1305	0
3	0725	1109	735	0	3	2196	0523	1305	0
4	0945	1109	735	0	4	2196	0523	1305	0
5	0545	1109	735	0	5	2196	0523	1305	0
6	0545	1109	735	0	6	2196	0523	1305	0
7	0545	1109	735	0	7	2196	0523	1305	0
8	0545	1109	735	0	8	2196	0523	1305	0
9	0545	1109	735	0	9	2196	0523	1305	0
10	0545	1109	735	0	10	2196	0523	1305	0

DATA FOR PROJECT 6022 CONFIG. 5 WIND DIR. 111 TUBING NO. 1									
TAP	MEAN	RMS	MAX	MIN	TAP	MEAN	RMS	MAX	MIN
1	0908	1284	820	0	1	2541	0259	1305	0
2	1105	1284	820	0	2	2541	0259	1305	0
3	1116	1284	820	0	3	2541	0259	1305	0
4	1144	1284	820	0	4	2541	0259	1305	0
5	1144	1284	820	0	5	2541	0259	1305	0
6	1144	1284	820	0	6	2541	0259	1305	0
7	1144	1284	820	0	7	2541	0259	1305	0
8	1144	1284	820	0	8	2541	0259	1305	0
9	1144	1284	820	0	9	2541	0259	1305	0
10	1144	1284	820	0	10	2541	0259	1305	0

DATA FOR PROJECT 6022 CONFIG. 5 WIND DIR. 121 TUBING NO. 1									
TAP	MEAN	RMS	MAX	MIN	TAP	MEAN	RMS	MAX	MIN
1	126	116	607	276	1	042	08	042	587
2	126	114	622	276	2	024	085	024	587
3	126	114	622	276	3	024	085	024	587
4	126	114	622	276	4	024	085	024	587
5	126	114	622	276	5	024	085	024	587
6	126	114	622	276	6	024	085	024	587
7	126	114	622	276	7	024	085	024	587
8	126	114	622	276	8	024	085	024	587
9	126	114	622	276	9	024	085	024	587
10	126	114	622	276	10	024	085	024	587

DATA FOR PROJECT 6022 CONFIG. 5 WIND DIR. 122 TUBING NO. 1									
TAP	MEAN	RMS	MAX	MIN	TAP	MEAN	RMS	MAX	MIN
1	105	105	459	244	1	170	90	170	222
2	105	105	459	244	2	070	83	070	222
3	105	105	459	244	3	067	83	067	222
4	105	105	459	244	4	067	83	067	222
5	105	105	459	244	5	067	83	067	222
6	105	105	459	244	6	067	83	067	222
7	105	105	459	244	7	067	83	067	222
8	105	105	459	244	8	067	83	067	222
9	105	105	459	244	9	067	83	067	222
10	105	105	459	244	10	067	83	067	222

DATA FOR PROJECT 6022 CONFIG. 5 WIND DIR. 123 TUBING NO. 1									
TAP	MEAN	RMS	MAX	MIN	TAP	MEAN	RMS	MAX	MIN
1	105	105	459	244	1	024	085	024	587
2	105	105	459	244	2	024	085	024	587
3	105	105	459	244	3	024	085	024	587
4	105	105	459	244	4	024	085	024	587
5	105	105	459	244	5	024	085	024	587
6	105	105	459	244	6	024	085	024	587
7	105	105	459	244	7	024	085	024	587
8	105	105	459	244	8	024	085	024	587
9	105	105	459	244	9	024	085	024	587
10	105	105	459	244	10	024	085	024	587

DATA FOR PROJECT 6022 CONFIG. 5 WIND DIR. 112 TUBING NO. 1									
TAP	MEAN	RMS	MAX	MIN	TAP	MEAN	RMS	MAX	MIN
1	041	059	259	157	1	274	130	274	35
2	041	059	259	157	2	257	125	257	35
3	041	059	259	157	3	257	125	257	35
4	041	059	259	157	4	257	125	257	35
5	041	059	259	157	5	257	125	257	35
6	041	059	259	157	6	257	125	257	35
7	041	059	259	157	7	257	125	257	35
8	041	059	259	157	8	257	125	257	35
9	041	059	259	157	9	257	125	257	35
10	041	059	259	157	10	257	125	257	35

DATA FOR PROJECT 6022 CONFIG. 5 WIND DIR. 113 TUBING NO. 1									
TAP	MEAN	RMS	MAX	MIN	TAP	MEAN	RMS	MAX	MIN
1	041	059	259	157	1	274	130	274	35
2	041	059	259	157	2	257	125	257	35
3	041	059	259	157	3	257	125	257	35
4	041	059	259	157	4	257	125	257	35
5	041	059	259	157	5	257	125	257	35
6	041	059	259	157	6	257	125	257	35
7	041	059	259	157	7	257	125	257	35
8	041	059	259	157	8	257	125	257	35
9	041	059	259	157	9	257	125	257	35
10	041	059	259	157	10	257	125	257	35

DATA FOR PROJECT 6022 CONFIG. 5 WIND DIR. 211 TUBING NO. 1									
TAP	MEAN	RMS	MAX	MIN	TAP	MEAN	RMS	MAX	MIN
1	041	059	259	157	1	274	130	274	35
2	041	059	259	157	2	257	125	257	35
3	041	059	259	157	3	257	125	257	35
4	041	059	259	157	4	257	125	257	35
5	041	059	259	157	5	257	125	257	35
6	041	059	259	157	6	257	125	257	35
7	041	059	259	157	7	257	125	257	35
8	041	059	259	157	8	257	125	257	35
9	041	059	259	157	9	257	125	257	35
10	041	059	259	157	10	257	125	257	35

DATA FOR PROJECT 6022 CONFIG. S WIND DIR. 221 TUBING NO. 1									
TAP	MEAN	RMS	MAX	MIN	TAP	MEAN	RMS	MAX	MIN
1	407	135	922	477	1	624	124	928	236
2	493	139	927	477	2	629	118	928	236
3	432	116	940	477	3	620	122	928	236
4	386	116	942	477	4	609	134	928	236
5	380	110	939	477	5	625	129	928	236
6	165	104	934	477	6	726	120	928	236
7	160	106	944	477	7	713	117	928	236
8	160	106	944	477	8	713	117	928	236
9	160	106	944	477	9	713	117	928	236
10	160	106	944	477	10	713	117	928	236

DATA FOR PROJECT 6022 CONFIG. S WIND DIR. 311 TUBING NO. 1									
TAP	MEAN	RMS	MAX	MIN	TAP	MEAN	RMS	MAX	MIN
1	137	041	023	206	1	123	026	128	685
2	105	041	023	206	2	123	026	128	685
3	089	041	023	206	3	123	026	128	685
4	089	041	023	206	4	123	026	128	685
5	089	041	023	206	5	123	026	128	685
6	089	041	023	206	6	123	026	128	685
7	089	041	023	206	7	123	026	128	685
8	089	041	023	206	8	123	026	128	685
9	089	041	023	206	9	123	026	128	685
10	089	041	023	206	10	123	026	128	685

DATA FOR PROJECT 6022 CONFIG. T WIND DIR. 321 TUBING NO. 1									
TAP	MEAN	RMS	MAX	MIN	TAP	MEAN	RMS	MAX	MIN
1	102	049	078	232	1	173	047	125	394
2	081	049	078	232	2	173	047	125	394
3	067	049	078	232	3	173	047	125	394
4	067	049	078	232	4	173	047	125	394
5	057	049	078	232	5	173	047	125	394
6	057	049	078	232	6	173	047	125	394
7	057	049	078	232	7	173	047	125	394
8	057	049	078	232	8	173	047	125	394
9	057	049	078	232	9	173	047	125	394
10	057	049	078	232	10	173	047	125	394

DATA FOR PROJECT 6022 CONFIG. T WIND DIR. 11 TUBING NO. 1									
TAP	MEAN	RMS	MAX	MIN	TAP	MEAN	RMS	MAX	MIN
1	120	029	170	487	1	123	026	128	685
2	108	029	170	487	2	123	026	128	685
3	108	029	170	487	3	123	026	128	685
4	108	029	170	487	4	123	026	128	685
5	108	029	170	487	5	123	026	128	685
6	108	029	170	487	6	123	026	128	685
7	108	029	170	487	7	123	026	128	685
8	108	029	170	487	8	123	026	128	685
9	108	029	170	487	9	123	026	128	685
10	108	029	170	487	10	123	026	128	685

DATA FOR PROJECT 6022 CONFIG. T WIND DIR. 21 TUBING NO. 1									
TAP	MEAN	RMS	MAX	MIN	TAP	MEAN	RMS	MAX	MIN
1	137	049	078	232	1	123	026	128	685
2	137	049	078	232	2	123	026	128	685
3	137	049	078	232	3	123	026	128	685
4	137	049	078	232	4	123	026	128	685
5	137	049	078	232	5	123	026	128	685
6	137	049	078	232	6	123	026	128	685
7	137	049	078	232	7	123	026	128	685
8	137	049	078	232	8	123	026	128	685
9	137	049	078	232	9	123	026	128	685
10	137	049	078	232	10	123	026	128	685

DATA FOR PROJECT 6022 CONFIG. T WIND DIR. 12 TUBING NO. 1									
TAP	MEAN	RMS	MAX	MIN	TAP	MEAN	RMS	MAX	MIN
1	137	049	078	232	1	123	026	128	685
2	137	049	078	232	2	123	026	128	685
3	137	049	078	232	3	123	026	128	685
4	137	049	078	232	4	123	026	128	685
5	137	049	078	232	5	123	026	128	685
6	137	049	078	232	6	123	026	128	685
7	137	049	078	232	7	123	026	128	685
8	137	049	078	232	8	123	026	128	685
9	137	049	078	232	9	123	026	128	685
10	137	049	078	232	10	123	026	128	685

DATA FOR PROJECT 6022 CONFIG. T WIND DIR. 22 TUBING NO. 1

TAP	MEAN	RMS	MAX	MIN	TAP	MEAN	RMS	MAX	MIN
1	168	140	783	40	1	326	82	520	75
2	216	142	772	506	2	361	99	520	75
3	227	144	829	375	3	374	103	520	75
4	220	144	847	183	4	489	168	520	75
5	224	142	827	199	5	443	171	520	75
6	224	121	755	124	6	419	170	520	75
7	234	119	585	33	7	548	105	520	75
8	24	89	401	33	8	548	105	520	75
10					10				

DATA FOR PROJECT 6022 CONFIG. T WIND DIR. 13 TUBING NO. 1

TAP	MEAN	RMS	MAX	MIN	TAP	MEAN	RMS	MAX	MIN
1	93	66	164	93	1	634	385	166	592
2	97	67	222	233	2	622	176	166	592
3	65	64	222	233	3	622	176	166	592
4	59	64	222	233	4	622	176	166	592
5	59	64	222	233	5	622	176	166	592
6	47	64	222	233	6	622	176	166	592
7	32	64	222	233	7	622	176	166	592
8	29	64	222	233	8	622	176	166	592
9	19	64	222	233	9	622	176	166	592
10	19	64	222	233	10	622	176	166	592

DATA FOR PROJECT 6022 CONFIG. T WIND DIR. 23 TUBING NO. 1

TAP	MEAN	RMS	MAX	MIN	TAP	MEAN	RMS	MAX	MIN
1	42	112	843	93	1	127	178	178	873
2	75	112	843	93	2	149	178	178	873
3	75	112	843	93	3	158	178	178	873
4	75	112	843	93	4	158	178	178	873
5	75	112	843	93	5	158	178	178	873
6	75	112	843	93	6	158	178	178	873
7	75	112	843	93	7	158	178	178	873
8	75	112	843	93	8	158	178	178	873
9	75	112	843	93	9	158	178	178	873
10	75	112	843	93	10	158	178	178	873

DATA FOR PROJECT 6022 CONFIG. T WIND DIR. 14 TUBING NO. 1

TAP	MEAN	RMS	MAX	MIN	TAP	MEAN	RMS	MAX	MIN
1	167	66	40	43	1	827	178	178	873
2	145	66	40	43	2	827	178	178	873
3	125	66	40	43	3	827	178	178	873
4	125	66	40	43	4	827	178	178	873
5	125	66	40	43	5	827	178	178	873
6	125	66	40	43	6	827	178	178	873
7	125	66	40	43	7	827	178	178	873
8	125	66	40	43	8	827	178	178	873
9	125	66	40	43	9	827	178	178	873
10	125	66	40	43	10	827	178	178	873

DATA FOR PROJECT 6022 CONFIG. T WIND DIR. 24 TUBING NO. 1

TAP	MEAN	RMS	MAX	MIN	TAP	MEAN	RMS	MAX	MIN
1	175	112	783	25	1	282	178	178	873
2	175	112	783	25	2	282	178	178	873
3	175	112	783	25	3	282	178	178	873
4	175	112	783	25	4	282	178	178	873
5	175	112	783	25	5	282	178	178	873
6	175	112	783	25	6	282	178	178	873
7	175	112	783	25	7	282	178	178	873
8	175	112	783	25	8	282	178	178	873
9	175	112	783	25	9	282	178	178	873
10	175	112	783	25	10	282	178	178	873

DATA FOR PROJECT 6022 CONFIG. T WIND DIR. 111 TUBING NO. 1

TAP	MEAN	RMS	MAX	MIN	TAP	MEAN	RMS	MAX	MIN
1	175	112	783	25	1	282	178	178	873
2	175	112	783	25	2	282	178	178	873
3	175	112	783	25	3	282	178	178	873
4	175	112	783	25	4	282	178	178	873
5	175	112	783	25	5	282	178	178	873
6	175	112	783	25	6	282	178	178	873
7	175	112	783	25	7	282	178	178	873
8	175	112	783	25	8	282	178	178	873
9	175	112	783	25	9	282	178	178	873
10	175	112	783	25	10	282	178	178	873

DATA FOR PROJECT 6022 CONFIG. T WIND DIR. 221 TUBING NO. 1									
TAP	MEAN	RMS	MAX	MIN	TAP	MEAN	RMS	MAX	MIN
1	167	145	776	305	1	357	078	093	706
2	227	160	868	250	2	390	079	124	734
3	273	162	908	138	3	397	075	120	727
4	299	141	934	148	4	401	065	120	627
5	204	125	742	178	5	438	068	166	574
6	225	100	525	189	6	493	121	114	133
7	144	100	414	277	7	489	145	100	124
8	186	83	271	390	8	519	151	041	148
10	-	-	-	-	10	-	-	-	-

DATA FOR PROJECT 6022 CONFIG. U WIND DIR. 321 TUBING NO. 1									
TAP	MEAN	RMS	MAX	MIN	TAP	MEAN	RMS	MAX	MIN
1	114	041	012	310	1	267	049	133	403
2	138	042	015	275	2	264	039	109	380
3	133	045	023	310	3	261	039	127	386
4	133	048	022	290	4	264	040	112	384
5	133	058	029	296	5	269	041	096	420
6	136	057	024	374	6	271	041	146	413
7	136	054	025	371	7	273	041	150	413
8	130	054	000	413	8	-	-	-	-
10	-	-	-	-	10	-	-	-	-

DATA FOR PROJECT 6022 CONFIG. U WIND DIR. 36 TUBING NO. 1									
TAP	MEAN	RMS	MAX	MIN	TAP	MEAN	RMS	MAX	MIN
1	97	067	234	244	1	827	295	168	308
2	100	069	250	208	2	815	224	170	347
3	100	072	255	208	3	809	226	189	349
4	100	085	272	155	4	724	190	181	258
5	100	092	272	155	5	652	180	220	229
6	100	098	289	155	6	571	180	195	229
7	100	108	308	155	7	571	200	195	229
8	100	108	308	155	8	571	200	195	229
10	-	-	-	-	10	-	-	-	-

DATA FOR PROJECT 6022 CONFIG. T WIND DIR. 311 TUBING NO. 1									
TAP	MEAN	RMS	MAX	MIN	TAP	MEAN	RMS	MAX	MIN
1	113	043	104	99	1	369	076	126	767
2	103	044	102	225	2	357	065	126	587
3	084	042	047	225	3	321	058	127	508
4	075	042	027	225	4	290	056	061	465
5	079	047	040	225	5	265	047	031	379
6	093	049	040	225	6	219	047	039	387
7	097	051	043	225	7	219	049	056	405
8	132	058	093	225	8	232	050	056	472
10	-	-	-	-	10	-	-	-	-

DATA FOR PROJECT 6022 CONFIG. U WIND DIR. 35 TUBING NO. 1									
TAP	MEAN	RMS	MAX	MIN	TAP	MEAN	RMS	MAX	MIN
1	007	074	26	368	1	983	404	141	94
2	127	078	23	278	2	974	378	237	000
3	282	088	33	007	3	954	350	257	000
4	398	096	34	081	4	935	325	255	000
5	449	108	31	109	5	893	314	269	000
6	485	123	31	124	6	834	323	188	000
7	509	136	30	132	7	834	323	188	000
8	471	146	11	104	8	798	326	193	000
10	-	-	-	-	10	-	-	-	-

DATA FOR PROJECT 6022 CONFIG. U WIND DIR. 37 TUBING NO. 1									
TAP	MEAN	RMS	MAX	MIN	TAP	MEAN	RMS	MAX	MIN
1	006	057	00	222	1	829	292	181	44
2	193	071	13	222	2	819	222	191	68
3	224	082	33	222	3	806	222	226	25
4	259	100	39	222	4	777	164	181	00
5	391	102	37	222	5	677	189	188	00
6	443	120	10	222	6	624	221	189	00
7	409	146	10	222	7	624	221	189	00
10	-	-	-	-	10	-	-	-	-

DATA FOR PROJECT 6022 CONFIG. U WIND DIR. 145 TUBING NO. 1										DATA FOR PROJECT 6022 CONFIG. U WIND DIR. 146 TUBING NO. 1									
TAP	MEAN	RMS	MAX	MIN	TAP	MEAN	RMS	MAX	MIN	TAP	MEAN	RMS	MAX	MIN	TAP	MEAN	RMS	MAX	MIN
1	16	1260	9699	090	1	572	147	97	0	1	581	1527	97	0	1	581	1527	97	0
2	3267	1260	9699	180	2	606	170	97	0	2	557	1527	97	0	2	557	1527	97	0
3	3267	1260	9699	074	3	626	182	97	0	3	574	1527	97	0	3	574	1527	97	0
4	3267	1260	9699	020	4	749	217	97	0	4	584	1527	97	0	4	584	1527	97	0
5	3267	1260	9699	075	5	849	243	97	0	5	583	1527	97	0	5	583	1527	97	0
6	3267	1260	9699	075	6	929	259	97	0	6	583	1527	97	0	6	583	1527	97	0
7	3267	1260	9699	157	7	910	259	97	0	7	583	1527	97	0	7	583	1527	97	0
8	3267	1260	9699	157	8	910	259	97	0	8	583	1527	97	0	8	583	1527	97	0
9	3267	1260	9699	157	9	910	259	97	0	9	583	1527	97	0	9	583	1527	97	0
10	3267	1260	9699	157	10	910	259	97	0	10	583	1527	97	0	10	583	1527	97	0

DATA FOR PROJECT 6022 CONFIG. V WIND DIR. 147 TUBING NO. 1										DATA FOR PROJECT 6022 CONFIG. V WIND DIR. 147 TUBING NO. 1									
TAP	MEAN	RMS	MAX	MIN	TAP	MEAN	RMS	MAX	MIN	TAP	MEAN	RMS	MAX	MIN	TAP	MEAN	RMS	MAX	MIN
1	235	146	949	025	1	596	155	94	0	1	827	227	94	0	1	827	227	94	0
2	3267	146	949	044	2	691	162	94	0	2	800	227	94	0	2	800	227	94	0
3	3267	146	949	052	3	725	172	94	0	3	800	227	94	0	3	800	227	94	0
4	3267	146	949	052	4	857	182	94	0	4	800	227	94	0	4	800	227	94	0
5	3267	146	949	052	5	957	195	94	0	5	800	227	94	0	5	800	227	94	0
6	3267	146	949	125	6	1260	224	94	0	6	800	227	94	0	6	800	227	94	0
7	3267	146	949	125	7	1260	224	94	0	7	800	227	94	0	7	800	227	94	0
8	3267	146	949	125	8	1260	224	94	0	8	800	227	94	0	8	800	227	94	0
9	3267	146	949	125	9	1260	224	94	0	9	800	227	94	0	9	800	227	94	0
10	3267	146	949	125	10	1260	224	94	0	10	800	227	94	0	10	800	227	94	0

DATA FOR PROJECT 6022 CONFIG. V WIND DIR. 147 TUBING NO. 1										DATA FOR PROJECT 6022 CONFIG. V WIND DIR. 37 TUBING NO. 1									
TAP	MEAN	RMS	MAX	MIN	TAP	MEAN	RMS	MAX	MIN	TAP	MEAN	RMS	MAX	MIN	TAP	MEAN	RMS	MAX	MIN
1	140	66	433	085	1	457	147	94	0	1	467	147	94	0	1	467	147	94	0
2	125	66	433	281	2	485	150	94	0	2	452	147	94	0	2	452	147	94	0
3	250	66	433	152	3	485	150	94	0	3	452	147	94	0	3	452	147	94	0
4	250	66	433	152	4	485	150	94	0	4	452	147	94	0	4	452	147	94	0
5	250	66	433	152	5	485	150	94	0	5	452	147	94	0	5	452	147	94	0
6	250	66	433	152	6	485	150	94	0	6	452	147	94	0	6	452	147	94	0
7	250	66	433	152	7	485	150	94	0	7	452	147	94	0	7	452	147	94	0
8	250	66	433	152	8	485	150	94	0	8	452	147	94	0	8	452	147	94	0
9	250	66	433	152	9	485	150	94	0	9	452	147	94	0	9	452	147	94	0
10	250	66	433	152	10	485	150	94	0	10	452	147	94	0	10	452	147	94	0

DATA FOR PROJECT 6022 CONFIG. U WIND DIR. 146 TUBING NO. 1										
TAP	MEAN	RMS	MAX	MIN	TAP	MEAN	RMS	MAX	MIN	TAP
1	103	0.08	0.23	0.02	1	123	0.08	0.23	0.02	1
2	103	0.08	0.23	0.02	2	123	0.08	0.23	0.02	2
3	103	0.08	0.23	0.02	3	123	0.08	0.23	0.02	3
4	103	0.08	0.23	0.02	4	123	0.08	0.23	0.02	4
5	103	0.08	0.23	0.02	5	123	0.08	0.23	0.02	5
6	103	0.08	0.23	0.02	6	123	0.08	0.23	0.02	6
7	103	0.08	0.23	0.02	7	123	0.08	0.23	0.02	7
8	103	0.08	0.23	0.02	8	123	0.08	0.23	0.02	8
9	103	0.08	0.23	0.02	9	123	0.08	0.23	0.02	9
10	103	0.08	0.23	0.02	10	123	0.08	0.23	0.02	10

DATA FOR PROJECT 6022 CONFIG. X WIND DIR. 35 TUBING NO. 1										
TAP	MEAN	RMS	MAX	MIN	TAP	MEAN	RMS	MAX	MIN	TAP
1	127	0.09	0.28	0.03	1	147	0.09	0.28	0.03	1
2	127	0.09	0.28	0.03	2	147	0.09	0.28	0.03	2
3	127	0.09	0.28	0.03	3	147	0.09	0.28	0.03	3
4	127	0.09	0.28	0.03	4	147	0.09	0.28	0.03	4
5	127	0.09	0.28	0.03	5	147	0.09	0.28	0.03	5
6	127	0.09	0.28	0.03	6	147	0.09	0.28	0.03	6
7	127	0.09	0.28	0.03	7	147	0.09	0.28	0.03	7
8	127	0.09	0.28	0.03	8	147	0.09	0.28	0.03	8
9	127	0.09	0.28	0.03	9	147	0.09	0.28	0.03	9
10	127	0.09	0.28	0.03	10	147	0.09	0.28	0.03	10

DATA FOR PROJECT 6022 CONFIG. X WIND DIR. 145 TUBING NO. 1										
TAP	MEAN	RMS	MAX	MIN	TAP	MEAN	RMS	MAX	MIN	TAP
1	123	0.08	0.23	0.02	1	143	0.08	0.23	0.02	1
2	123	0.08	0.23	0.02	2	143	0.08	0.23	0.02	2
3	123	0.08	0.23	0.02	3	143	0.08	0.23	0.02	3
4	123	0.08	0.23	0.02	4	143	0.08	0.23	0.02	4
5	123	0.08	0.23	0.02	5	143	0.08	0.23	0.02	5
6	123	0.08	0.23	0.02	6	143	0.08	0.23	0.02	6
7	123	0.08	0.23	0.02	7	143	0.08	0.23	0.02	7
8	123	0.08	0.23	0.02	8	143	0.08	0.23	0.02	8
9	123	0.08	0.23	0.02	9	143	0.08	0.23	0.02	9
10	123	0.08	0.23	0.02	10	143	0.08	0.23	0.02	10

DATA FOR PROJECT 6022 CONFIG X				WIND DIR.				146 TUBING NO . 1				DATA FOR PROJECT 6022 CONFIG. 2				WIND DIR.				35 TUBING NO . 1											
TAP	MEAN	RMS	MAX	TAP	MEAN	RMS	MAX	TAP	MEAN	RMS	MAX	TAP	MEAN	RMS	MAX	TAP	MEAN	RMS	MAX	TAP	MEAN	RMS	MAX	TAP	MEAN	RMS	MAX				
1	107	044	199	1	100	043	224	1	210	024	167	1	204	026	167	1	204	026	167	1	204	026	167	1	204	026	167	1	204	026	167
2	107	044	199	2	100	043	224	2	210	024	167	2	204	026	167	2	204	026	167	2	204	026	167	2	204	026	167	2	204	026	167
3	107	044	199	3	100	043	224	3	210	024	167	3	204	026	167	3	204	026	167	3	204	026	167	3	204	026	167	3	204	026	167
4	107	044	199	4	100	043	224	4	210	024	167	4	204	026	167	4	204	026	167	4	204	026	167	4	204	026	167	4	204	026	167
5	107	044	199	5	100	043	224	5	210	024	167	5	204	026	167	5	204	026	167	5	204	026	167	5	204	026	167	5	204	026	167
6	107	044	199	6	100	043	224	6	210	024	167	6	204	026	167	6	204	026	167	6	204	026	167	6	204	026	167	6	204	026	167
7	107	044	199	7	100	043	224	7	210	024	167	7	204	026	167	7	204	026	167	7	204	026	167	7	204	026	167	7	204	026	167
8	107	044	199	8	100	043	224	8	210	024	167	8	204	026	167	8	204	026	167	8	204	026	167	8	204	026	167	8	204	026	167
9	107	044	199	9	100	043	224	9	210	024	167	9	204	026	167	9	204	026	167	9	204	026	167	9	204	026	167	9	204	026	167
10	107	044	199	10	100	043	224	10	210	024	167	10	204	026	167	10	204	026	167	10	204	026	167	10	204	026	167	10	204	026	167

C-1

APPENDIX C

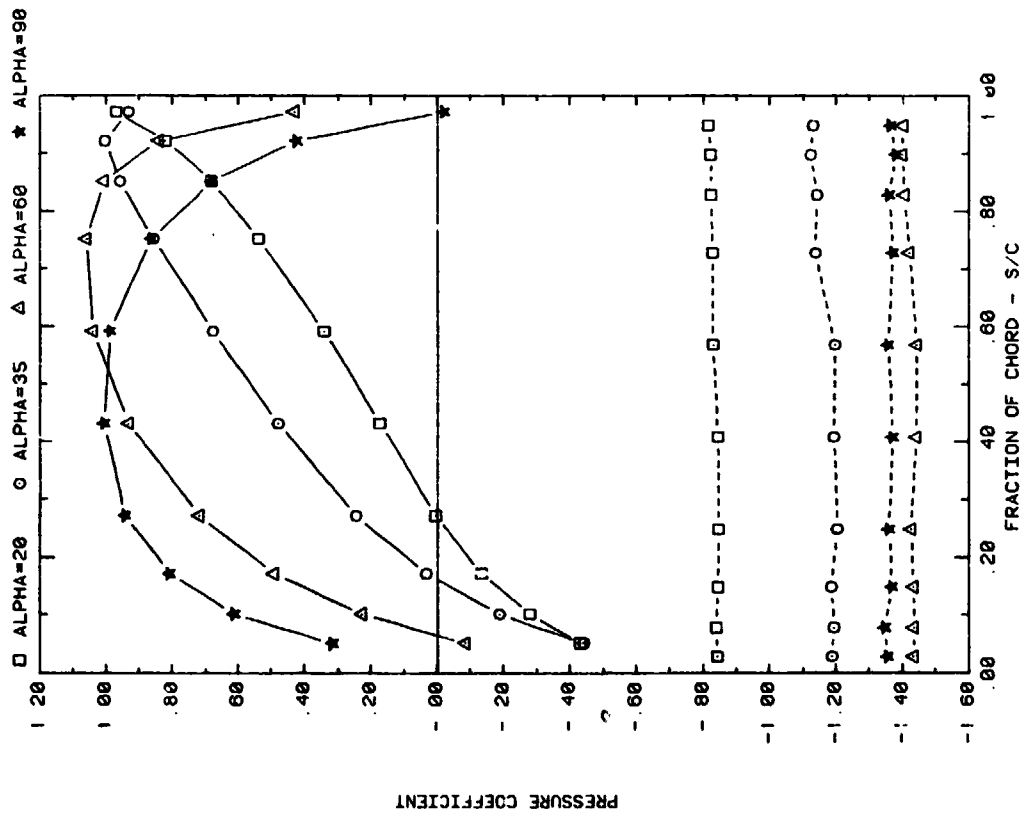
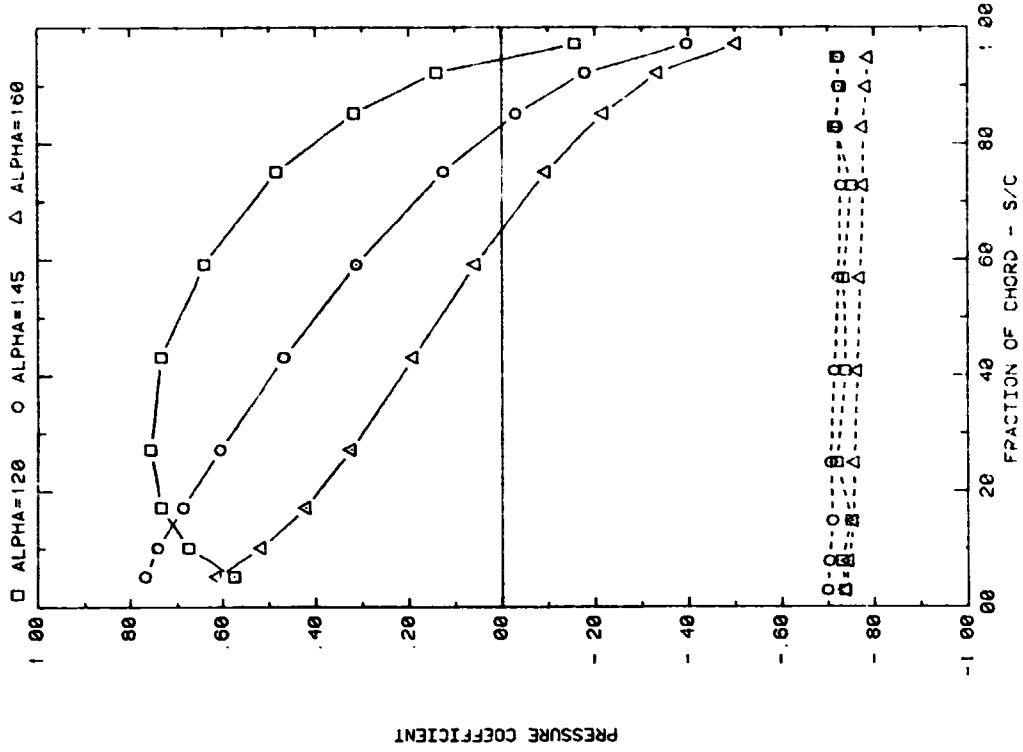
Plots of Pressure Distribution along Chord of Solar Array

LIST OF PLOTS

<u>Plot</u>	<u>Page</u>
1-1 Single Array, Uniform Flow Study Effects of Angle of Attack and Ground Clearance	C-3
1-2 Single Array, Nonuniform Flow Study Effects of Angle of Attack and Fence Height	C-9
2-1-1 Multiple Arrays without Fence, Uniform Flow Study Effect of Angle of Attack	C-11
2-1-2 Multiple Arrays without Fence, Uniform Flow Study Effect of Separation Distance	C-20
2-1-3 Multiple Arrays without Fence, Uniform Flow Study Effect of Array Position	C-31
2-2-1 Multiple Arrays without Fence, Nonuniform Flow Study Effect of Angle of Attack	C-39
2-2-2 Multiple Arrays without Fence, Nonuniform Flow Study Effect of Separation Distance	C-48
2-2-3 Multiple Arrays without Fence, Nonuniform Flow Study Effect of Array Position	C-59
3-1 Multiple Arrays with Fence, $WD = 0^\circ$ Effect of Angle of Attack.	C-67
3-2 Multiple Arrays with Fence, $WD = 0^\circ$ Effect of Array Position	C-72
3-3 Multiple Arrays with Fence, $WD = 0^\circ$ Effect of Fence Distance	C-78
3-4 Multiple Arrays with Fence, $WD = 0^\circ$ Effect of Fence Height	C-84
3-5 Multiple Arrays with Fence, $WD = 0^\circ$ Effect of Fence Porosity	C-92
4-1 Edge Study, $WD = 0^\circ$ Effect of Fence	C-93
5-1-1 Corner Study, $WD = 45^\circ$, Standard Model Effect of Array Position	C-96
5-1-2 Corner Study, $WD = 45^\circ$, Standard Model Effect of Fence Configuration	C-101
5-2-1 Corner Study, $WD = 45^\circ$, Modified Model with Solid Extension Effect of Array Position	C-104

C-2b

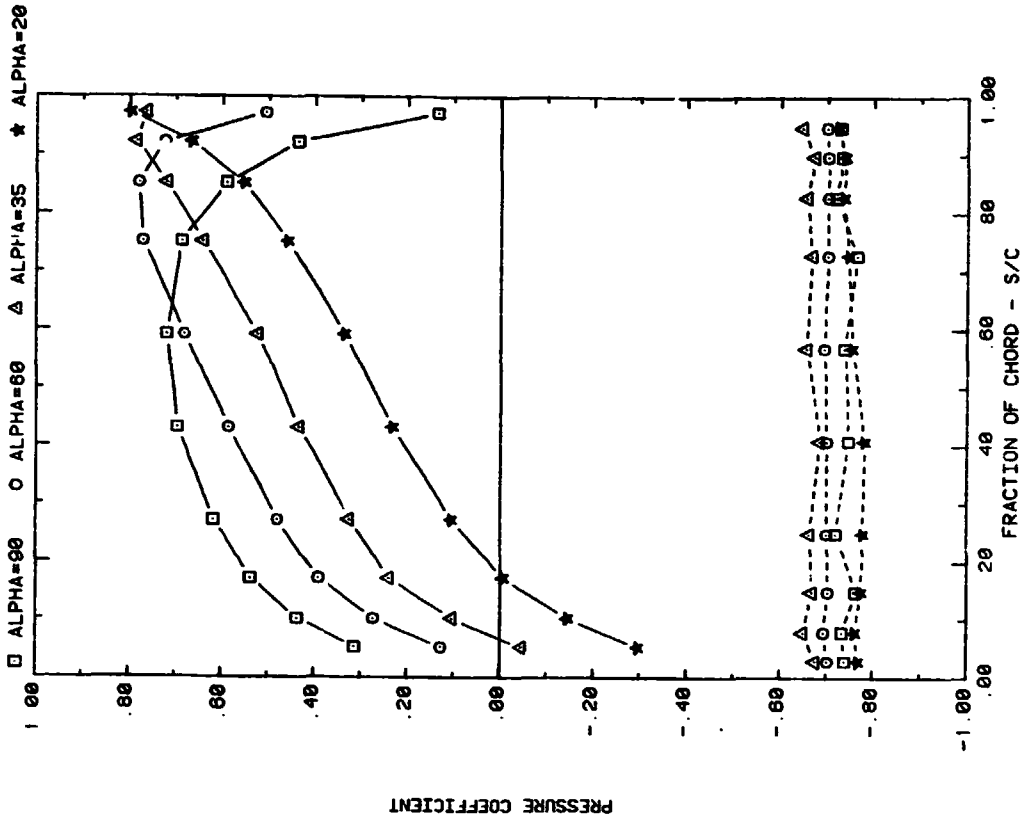
<u>Plot</u>		<u>Page</u>
5-2-2	Corner Study, WD = 45°, Modified Model with Solid Extension Effect of Model Modification	C-108
5-2-3	Corner Study, WD = 45°, Modified Model with Solid Extension Effect of Fence Configuration	C-117
5-3-1	Corner Study, WD = 45°, Modified Model with Various Extension Effect of Array Position	C-120
5-3-2	Corner Study, WD = 45°, Modified Model with Various Extension Effect of Model Configuration	C-122



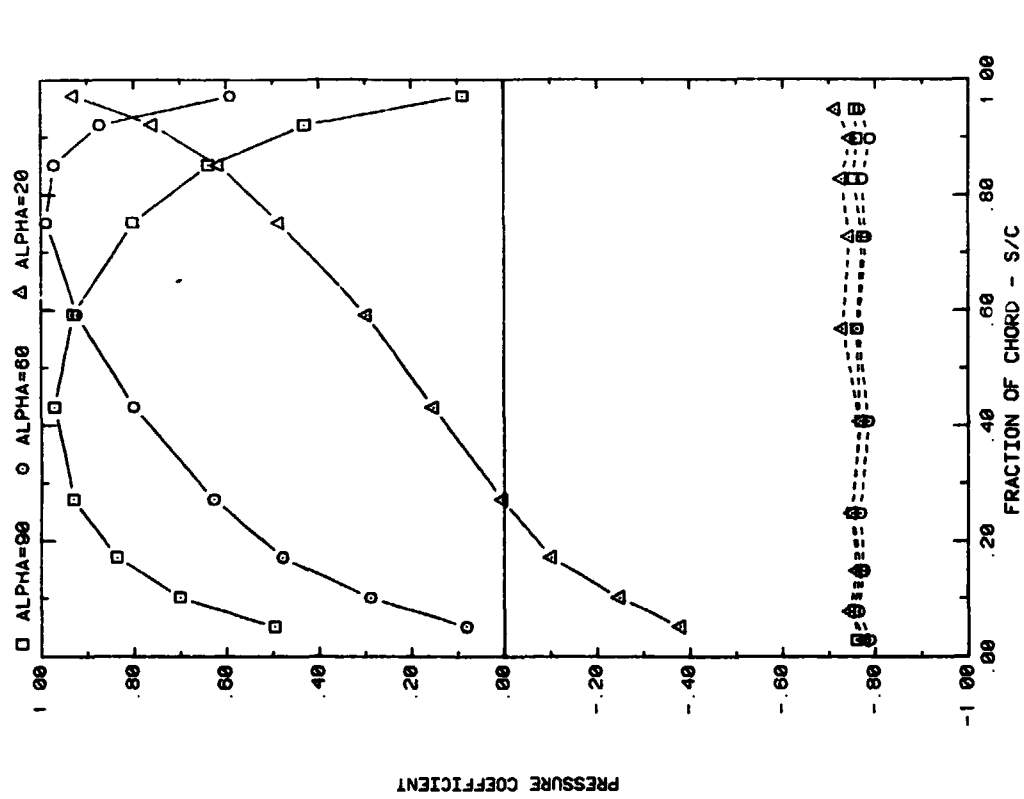
FRONT AND BACK PRESSURES ON A SINGLE ARRAY IN UNIFORM FLOW
EFFECT OF ATTACK ANGLE FOR GROUND CLEARANCE, H/C = 0.25

FRONT AND BACK PRESSURES ON A SINGLE ARRAY IN UNIFORM FLOW
EFFECT OF ATTACK ANGLE FOR GROUND CLEARANCE, H/C = INFINITY

Plot 1-1. Single Array, Uniform Flow Study Effects of
Angle of Attack and Ground Clearance

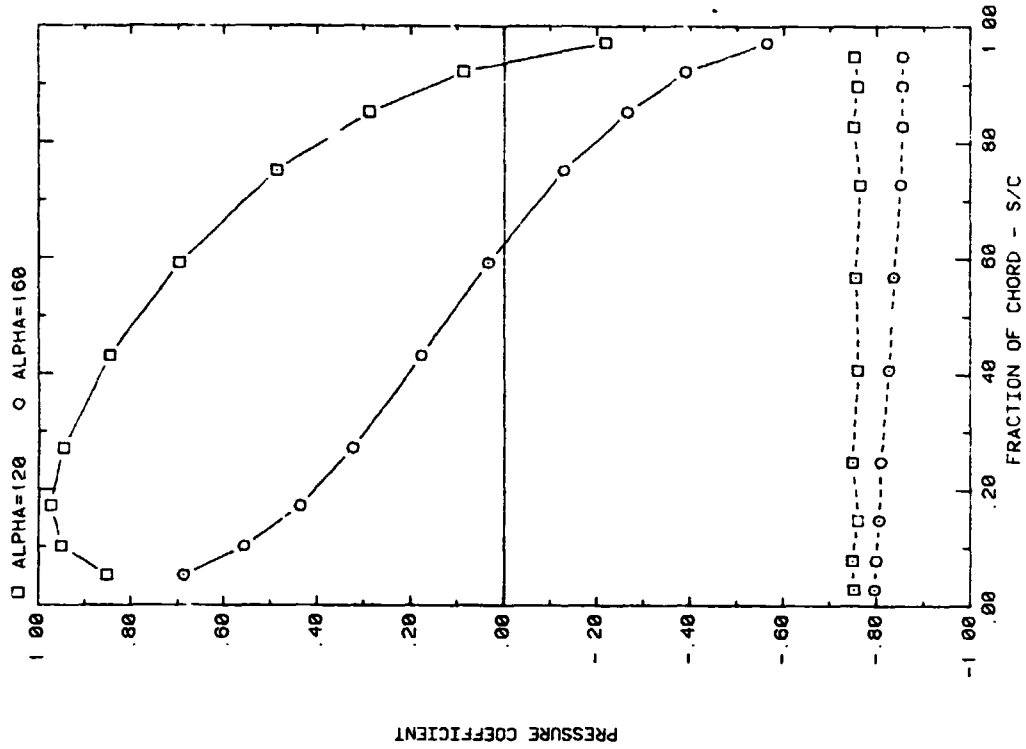


FRONT AND BACK PRESSURES ON A SINGLE ARRAY IN UNIFORM FLOW
EFFECT OF ATTACK ANGLE FOR GROUND CLEARANCE, $H/C = 0.25$

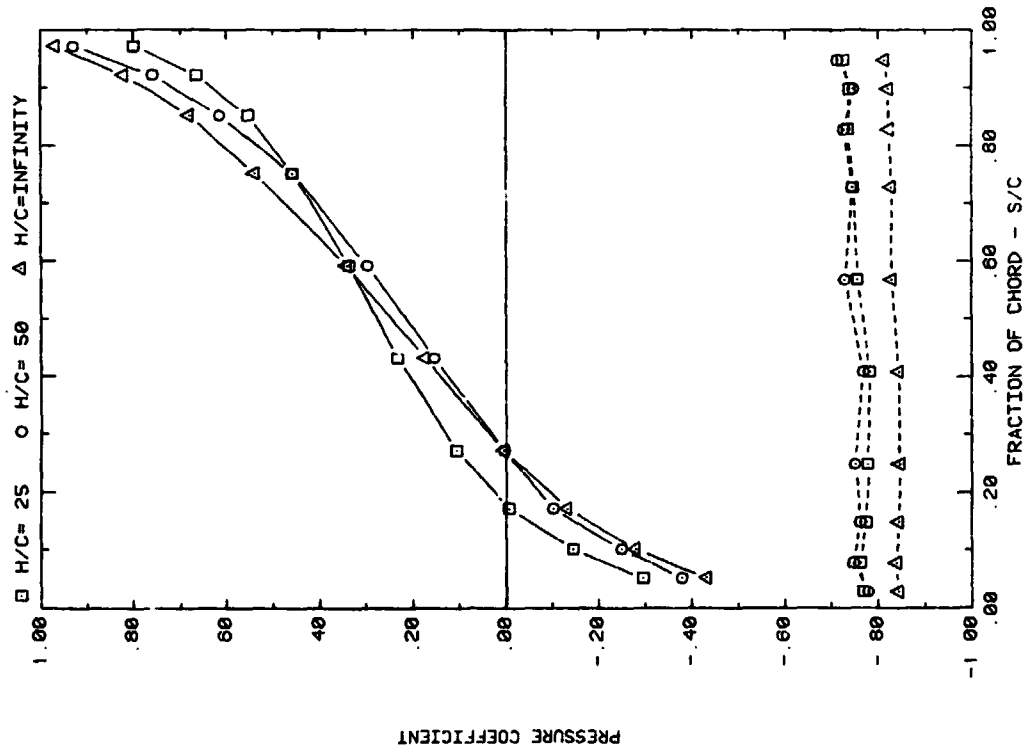


FRONT AND BACK PRESSURES ON A SINGLE ARRAY IN UNIFORM FLOW
EFFECT OF ATTACK ANGLE FOR GROUND CLEARANCE, $H/C = 0.50$

Plot 1-1. (Continued)

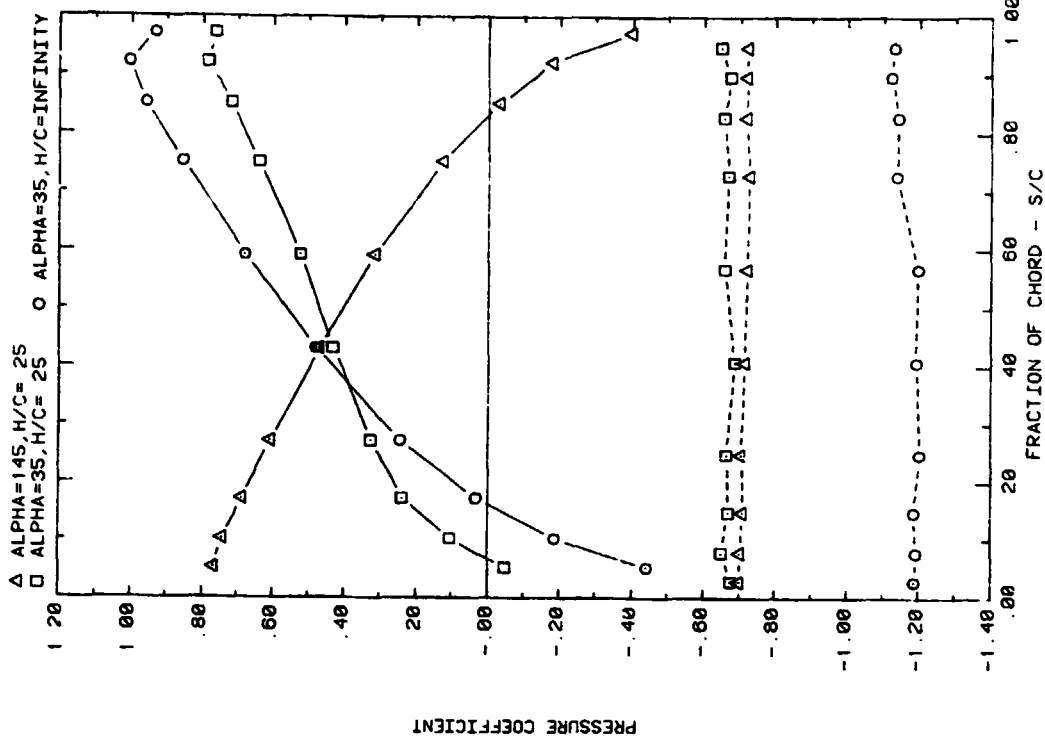


FRONT AND BACK PRESSURES ON A SINGLE ARRAY IN UNIFORM FLOW
EFFECT ON ATTACK ANGLE FOR GROUND CLEARANCE, H/C = 0.50

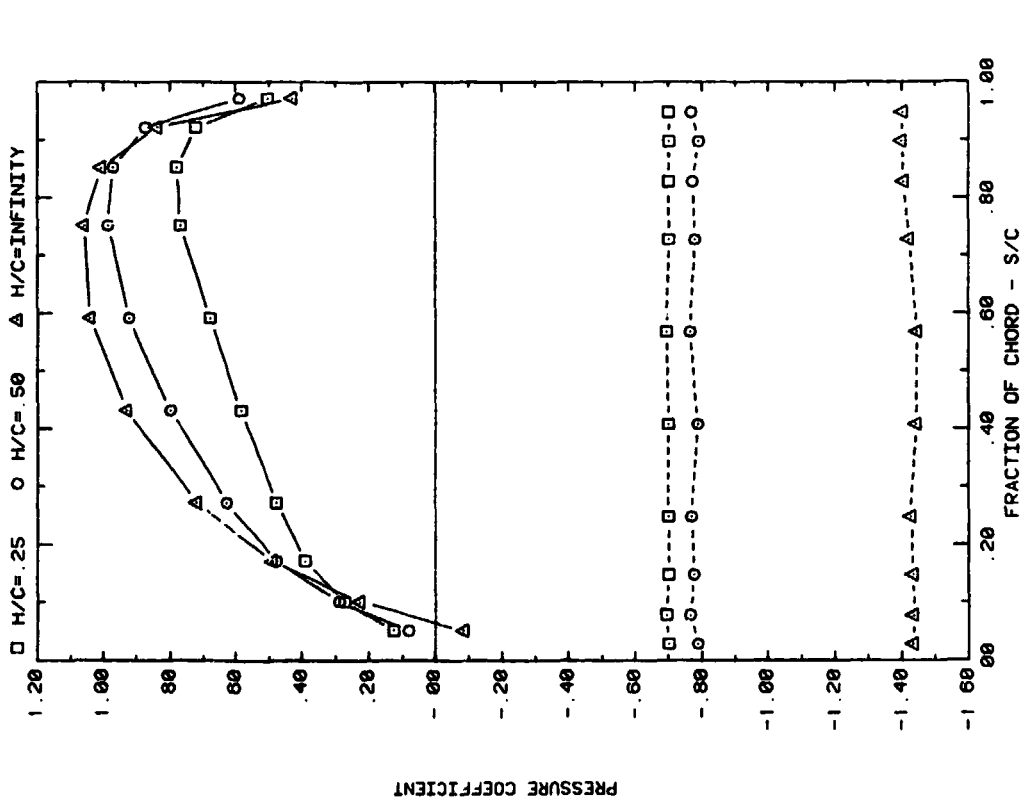


FRONT AND BACK PRESSURES ON A SINGLE ARRAY IN UNIFORM FLOW
EFFECT OF GROUND CLEARANCE FOR ATTACK ANGLE, ALPHA = 20

Plot 1-1. (Continued)

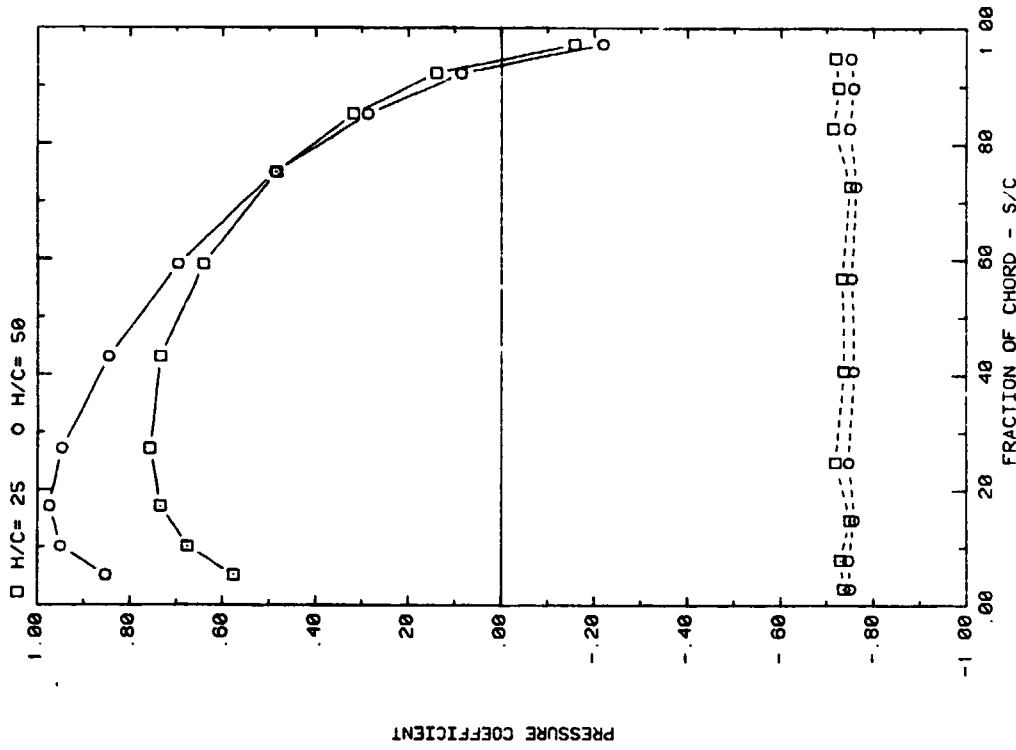


FRONT AND BACK PRESSURES ON A SINGLE ARRAY IN UNIFORM FLOW
EFFECT OF GROUND CLEARANCE FOR ATTACK ANGLES

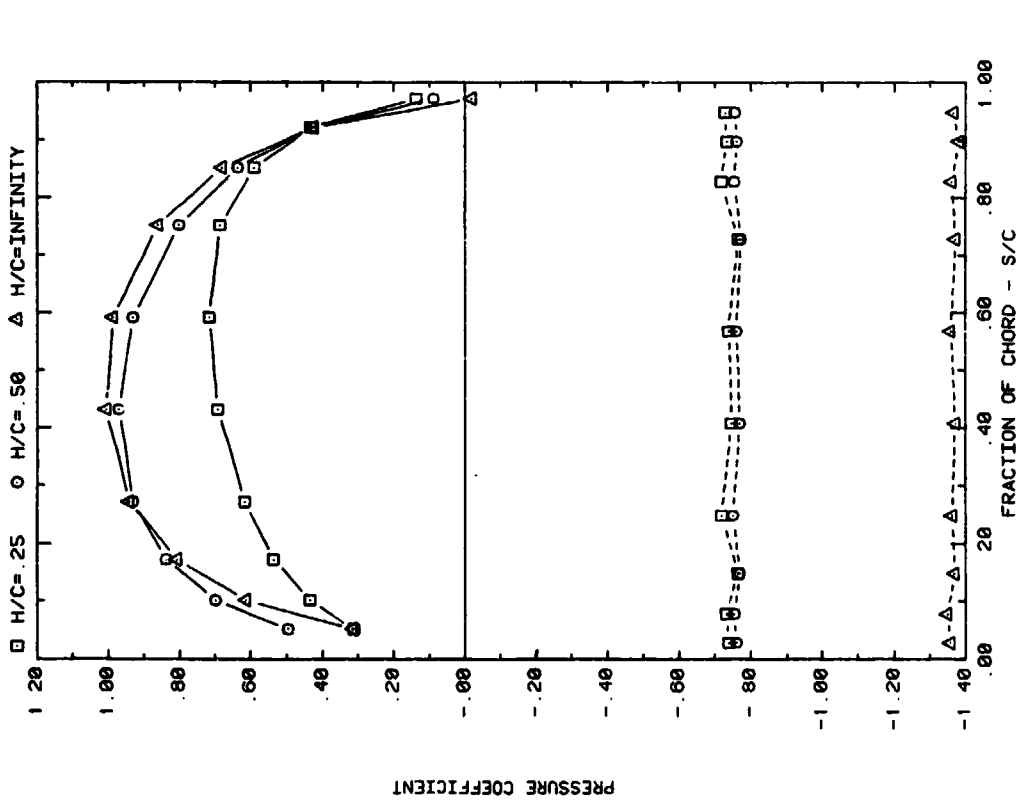


FRONT AND BACK PRESSURES ON A SINGLE ARRAY IN UNIFORM FLOW
EFFECT OF GROUND CLEARANCE FOR ATTACK ANGLE, ALPHA = 60

Plot 1-1. (Continued)

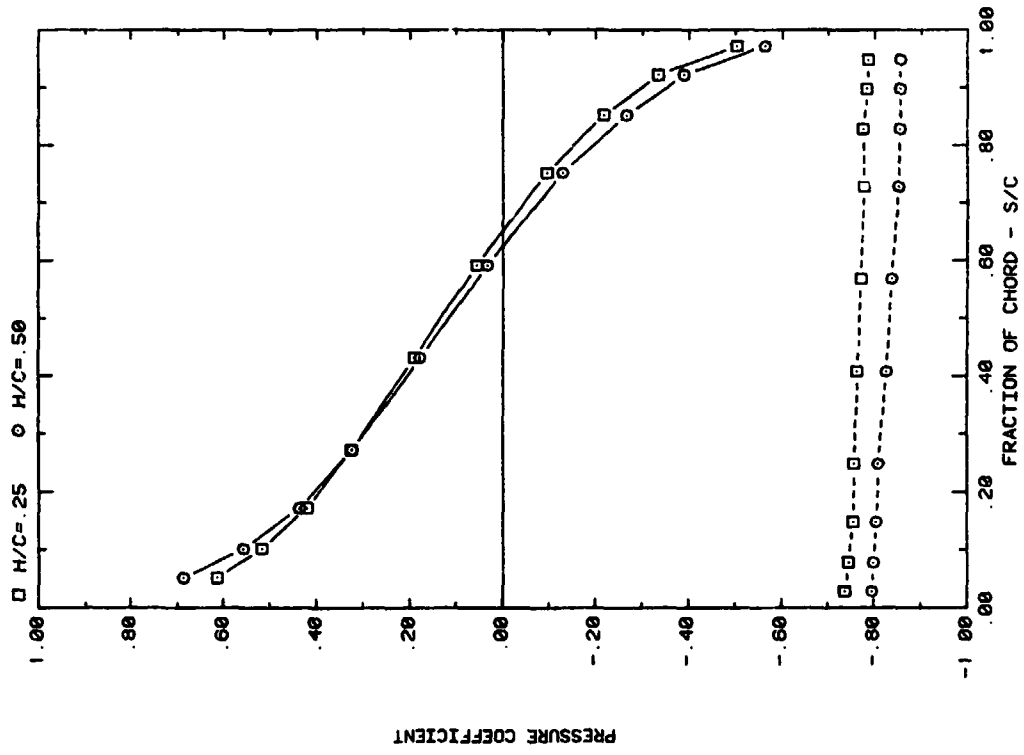


FRONT AND BACK PRESSURES ON A SINGLE ARRAY IN UNIFORM FLOW
EFFECT OF GROUND CLEARANCE FOR ATTACK ANGLE, ALPHA = 120



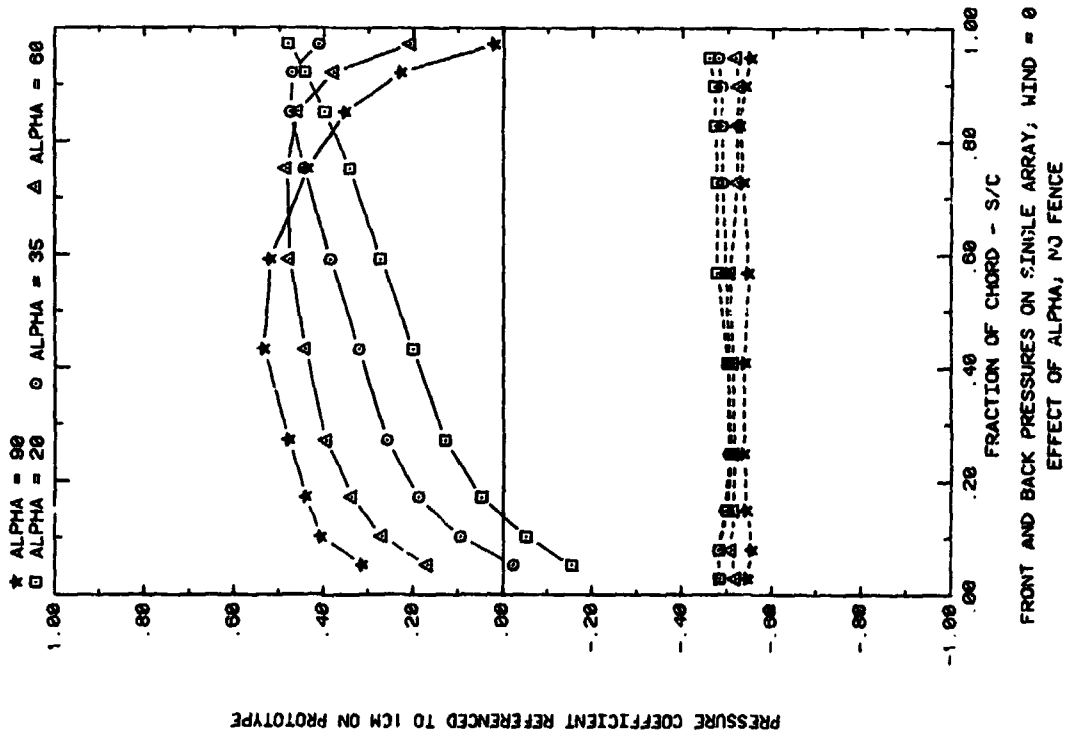
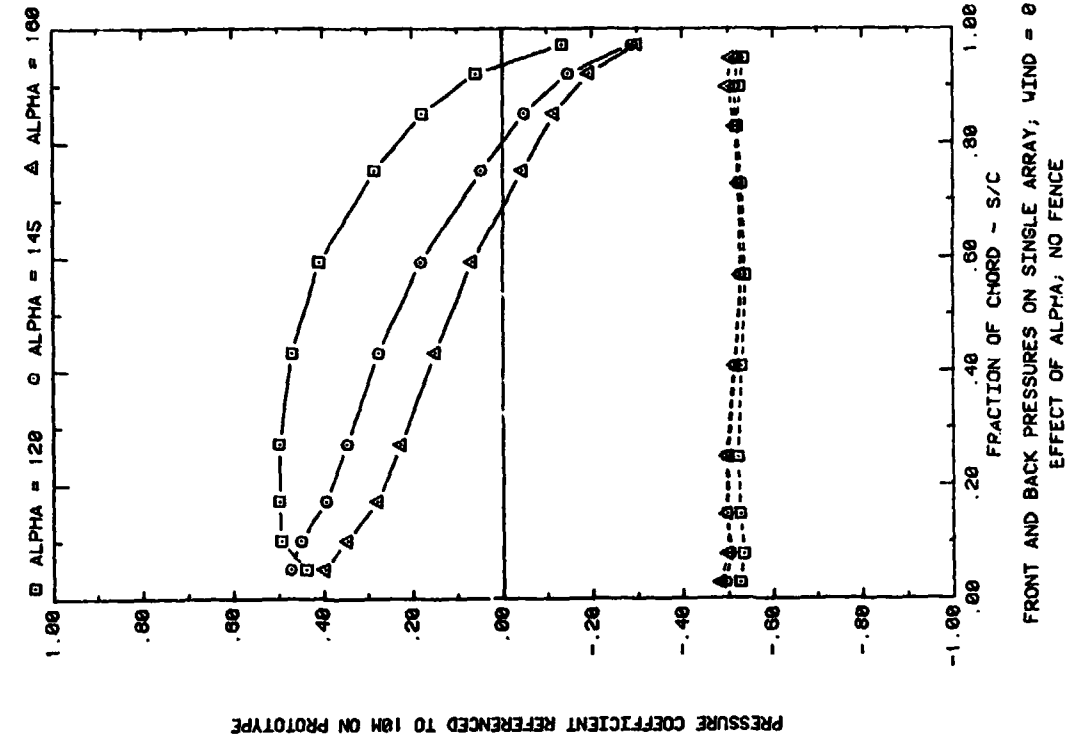
FRONT AND BACK PRESSURES ON A SINGLE ARRAY IN UNIFORM FLOW
EFFECT OF GROUND CLEARANCE FOR ATTACK ANGLE, ALPHA = 90

Plot 1-1. (Continued)

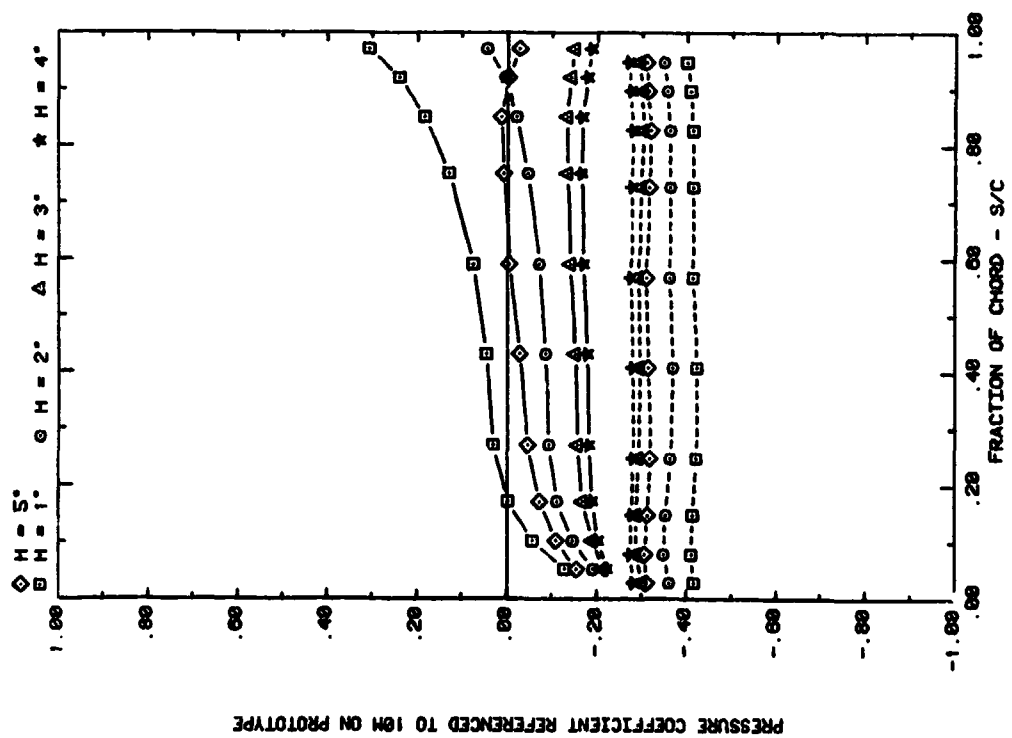
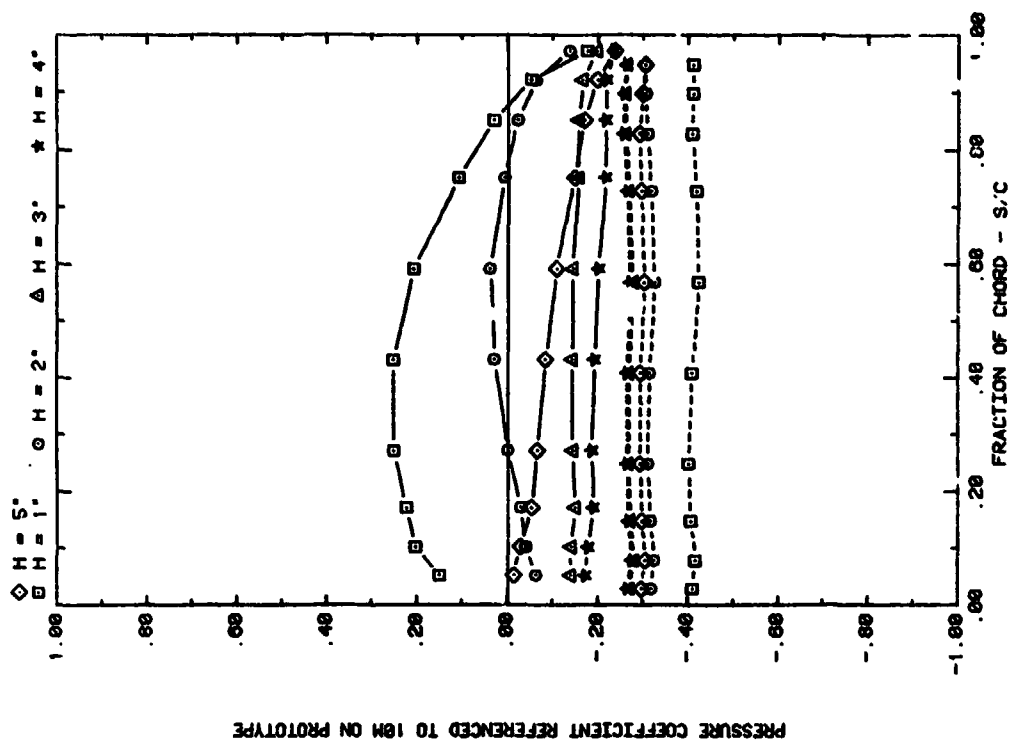


FRONT AND BACK PRESSURES ON A SINGLE ARRAY IN UNIFORM FLOW
EFFECT OF GROUND CLEARANCE FOR ATTACK ANGLE, ALPHA = 160

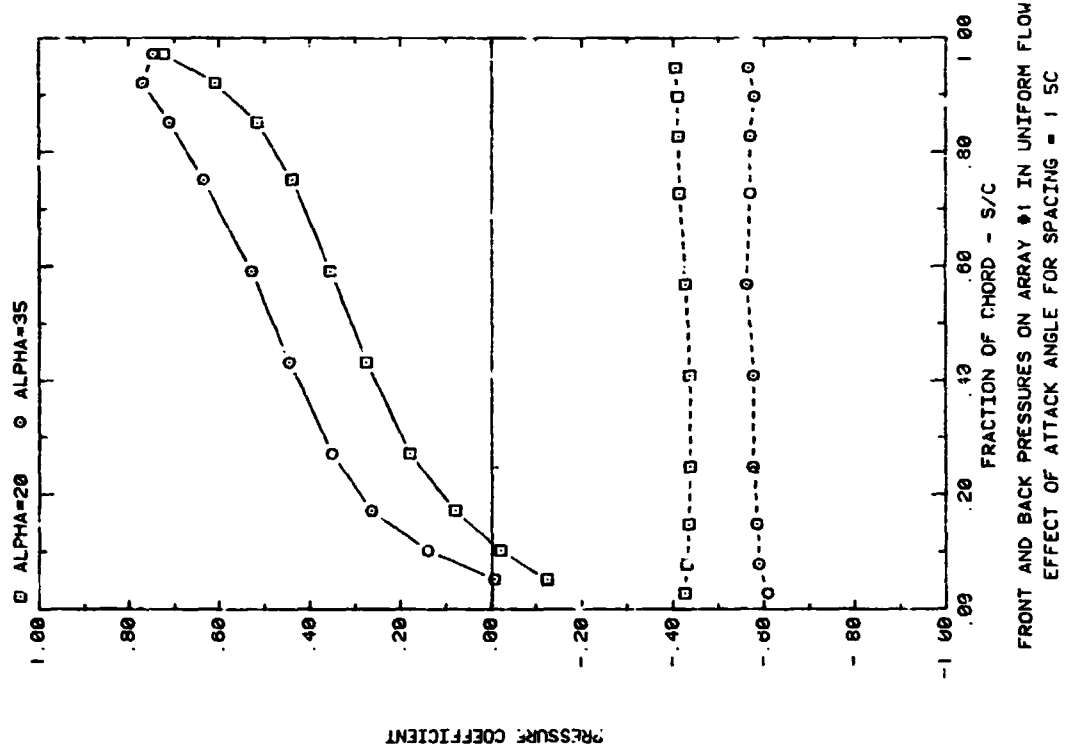
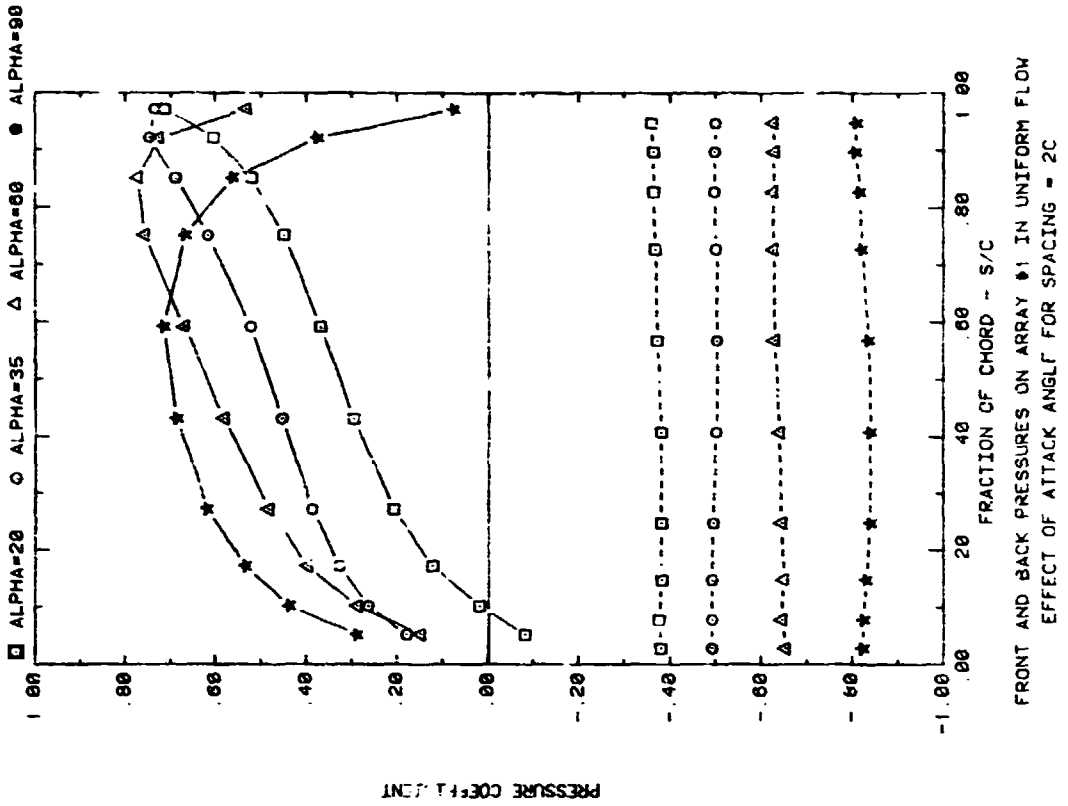
Plot 1-1. (Concluded)



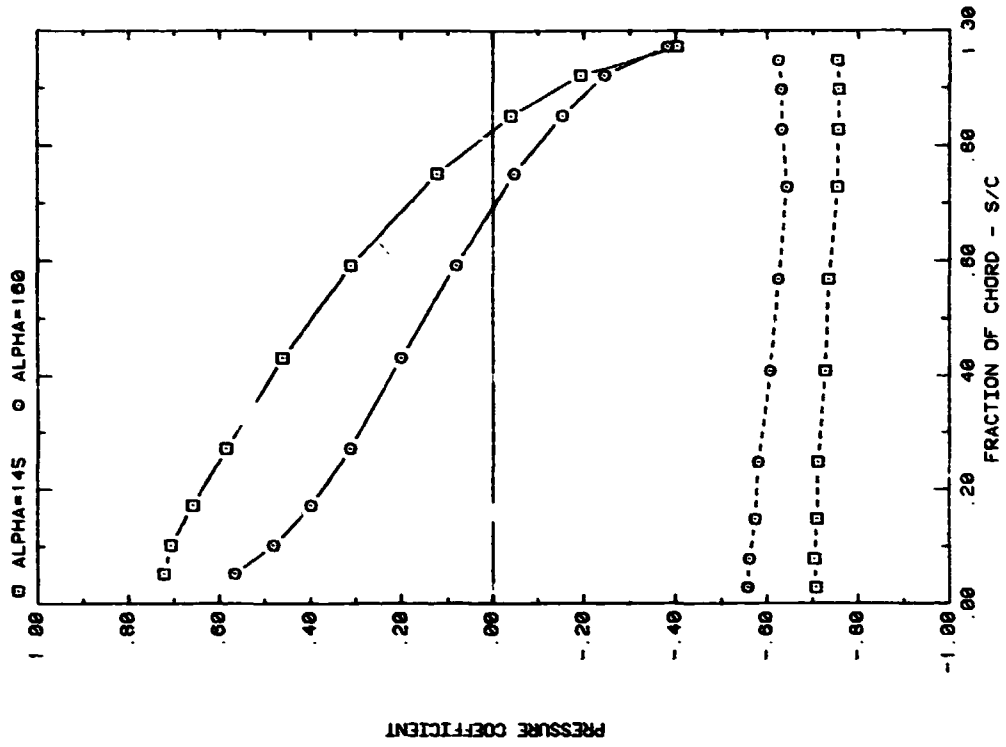
Plot 1-2. Single Array, Nonuniform Flow Study Effects of Angle of Attack and Fence Height



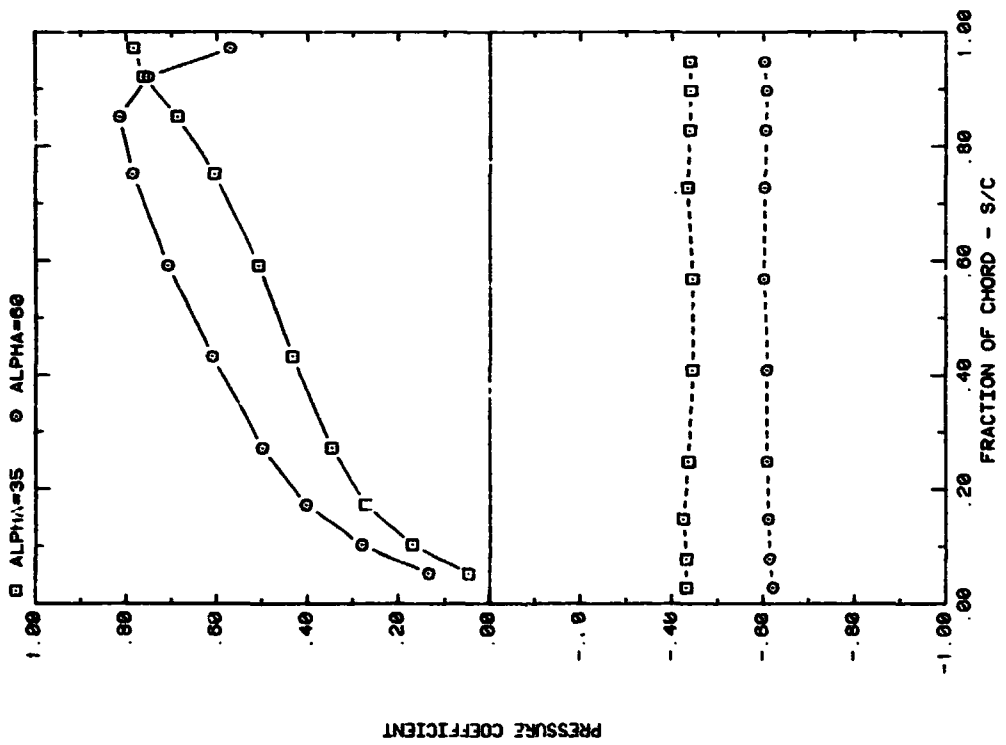
Plot 1-2. (Concluded)



Plot 2-1-1. Multiple Arrays without Fence, Uniform Flow Study
Effect of Angle of Attack

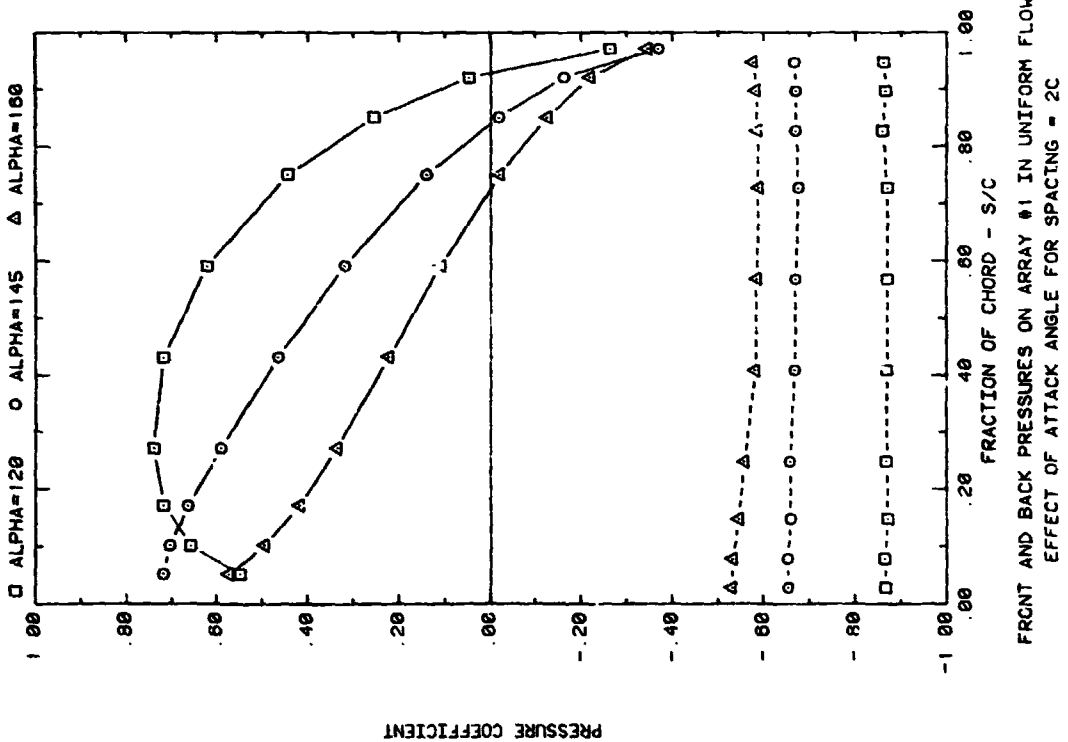
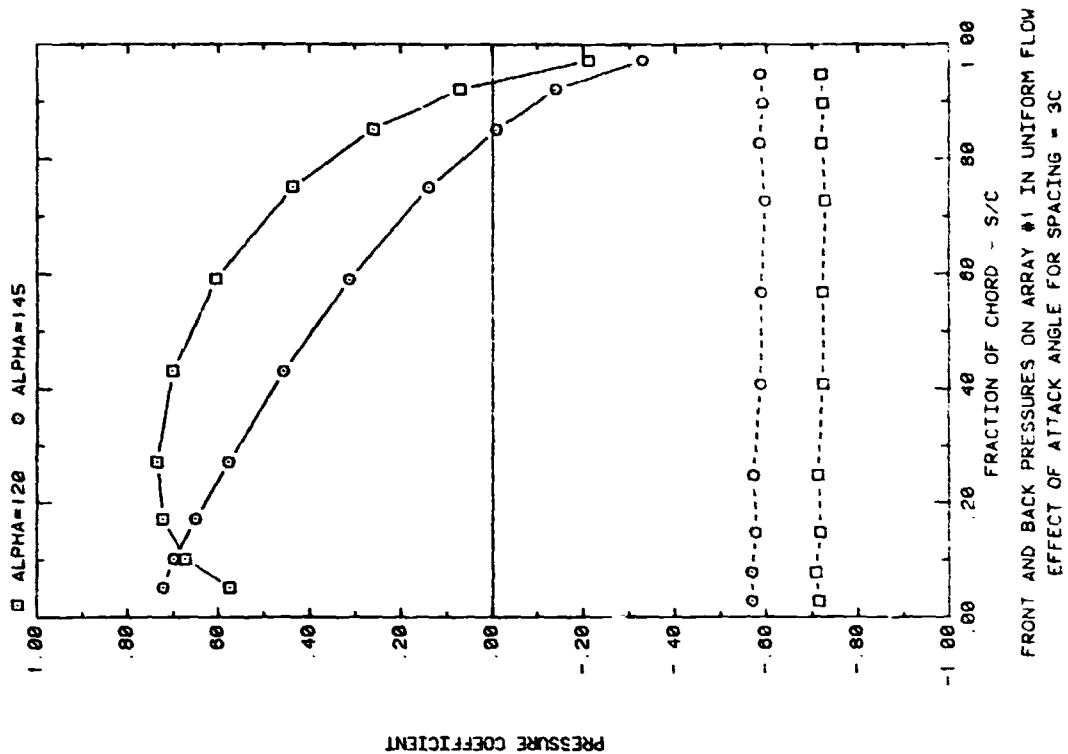


FRONT AND BACK PRESSURES ON ARRAY #1 IN UNIFORM FLOW
EFFECT OF ATTACK ANGLE FOR SPACING = 1 SC

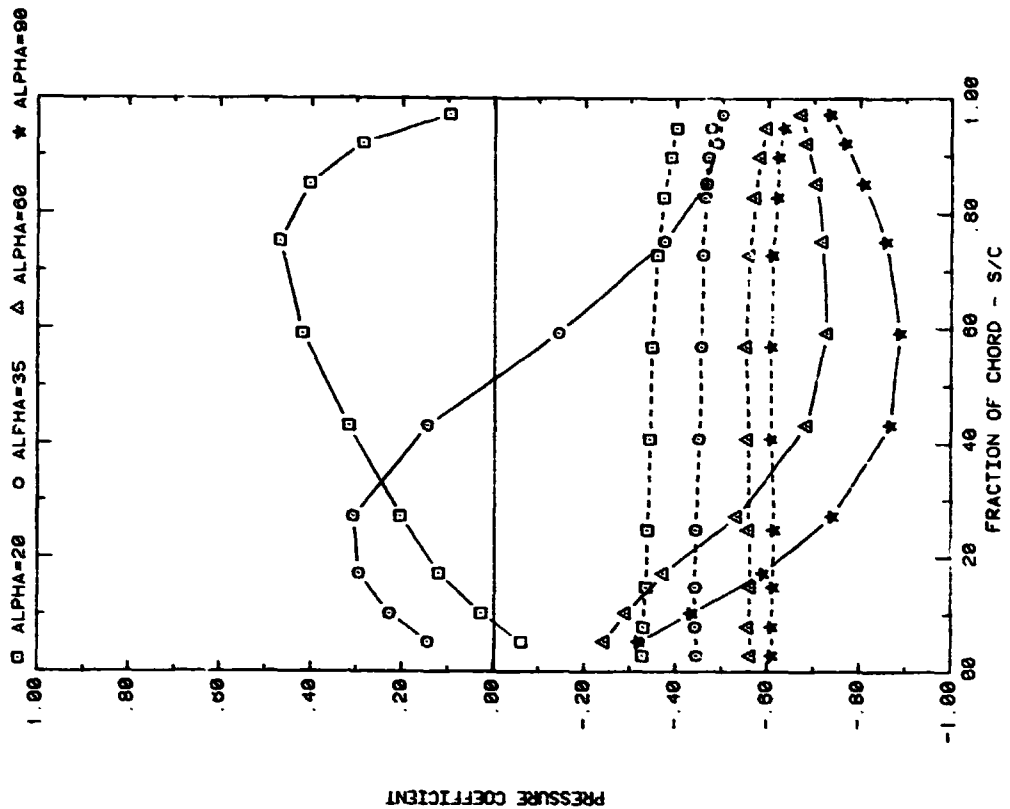


FRONT AND BACK PRESSURES ON ARRAY #1 IN UNIFORM FLOW
EFFECT OF ATTACK ANGLE FOR SPACING = 3C

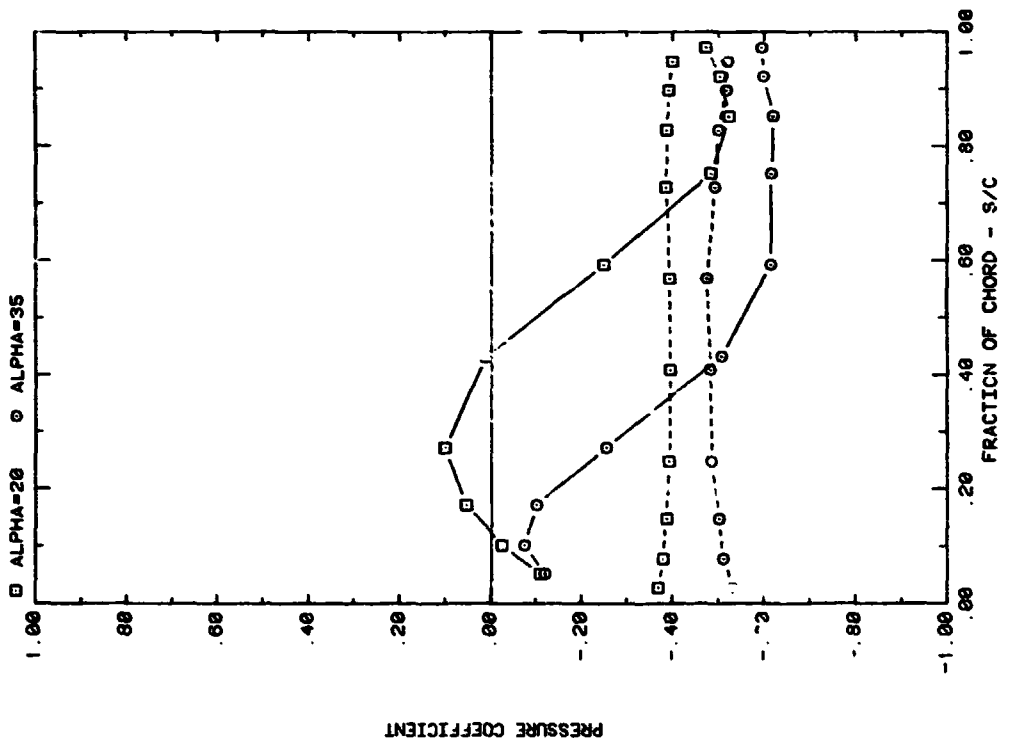
Plot 2-1-1. (Continued)



Plot 2-1-1. (Continued)

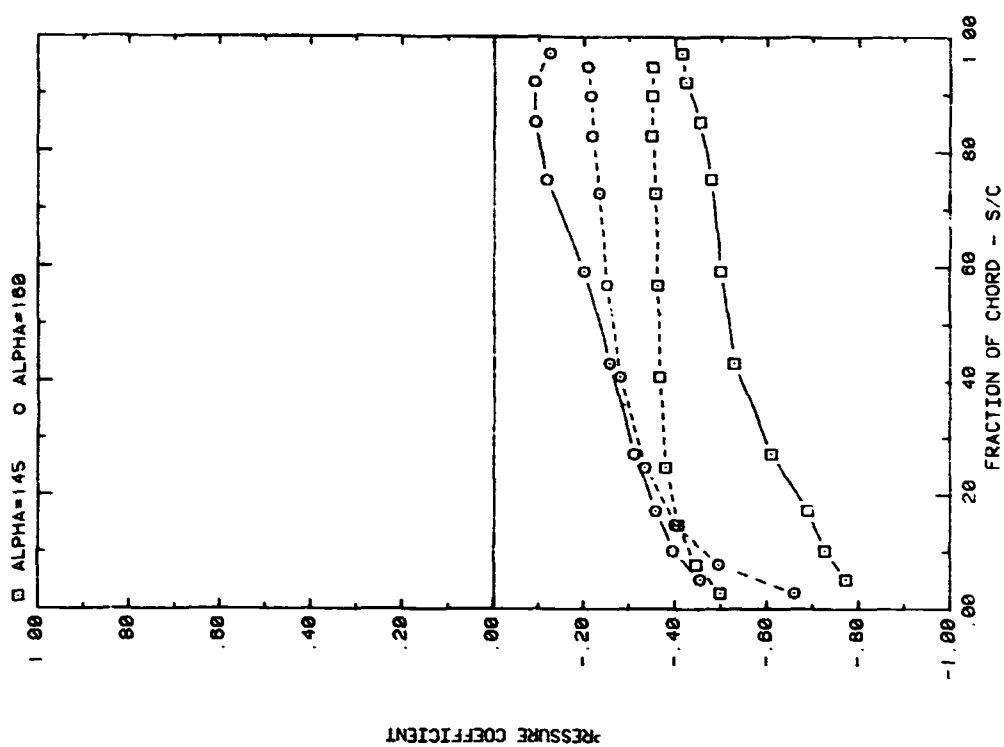


FRONT AND BACK PRESSURES ON ARRAY #2 IN UNIFORM FLOW
EFFECT OF ATTACK ANGLE FOR SPACING = 2C

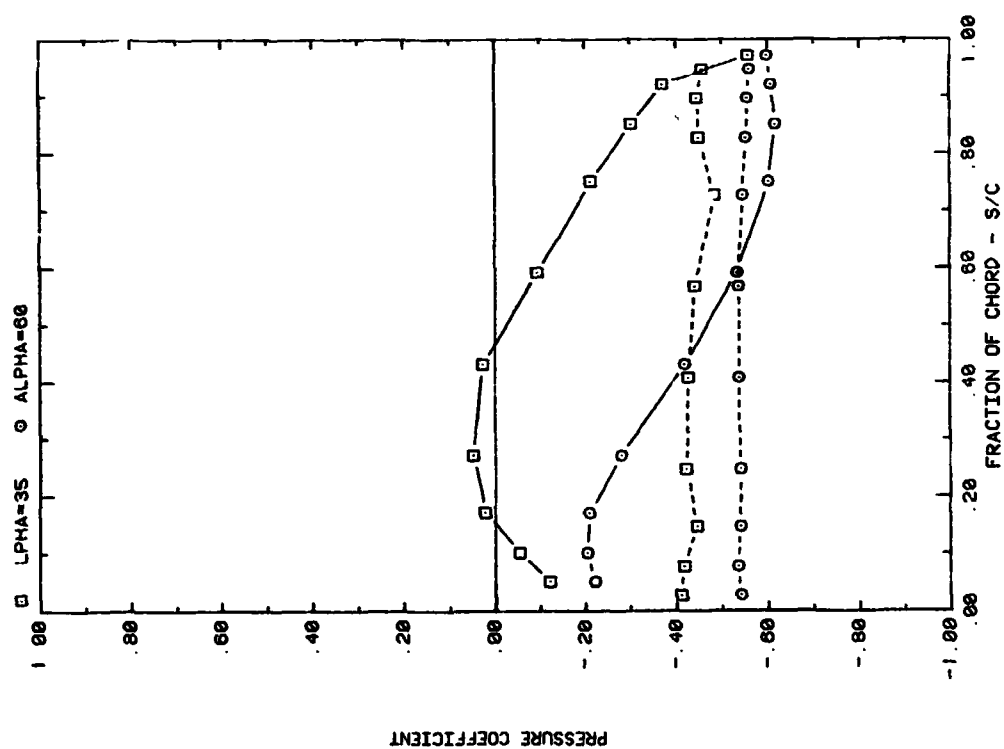


FRONT AND BACK PRESSURES ON ARRAY #2 IN UNIFORM FLOW
EFFECT OF ATTACK ANGLE FOR SPACING = 1.5C

Plot 2-1-1. (Continued)

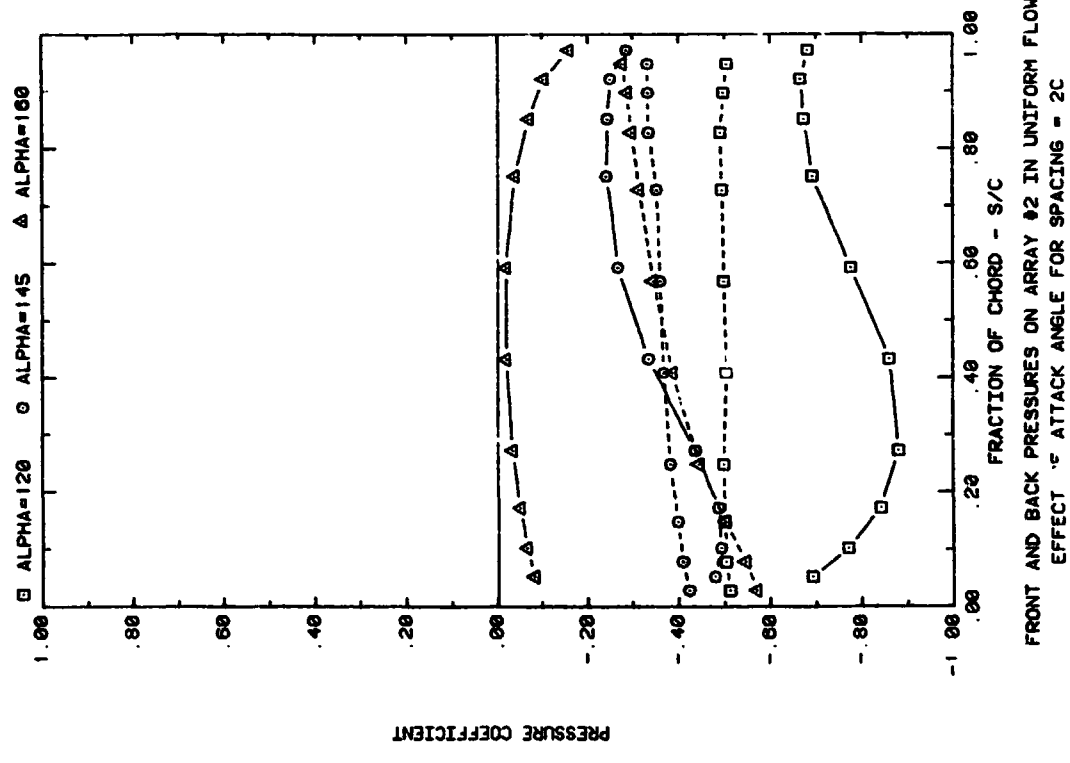
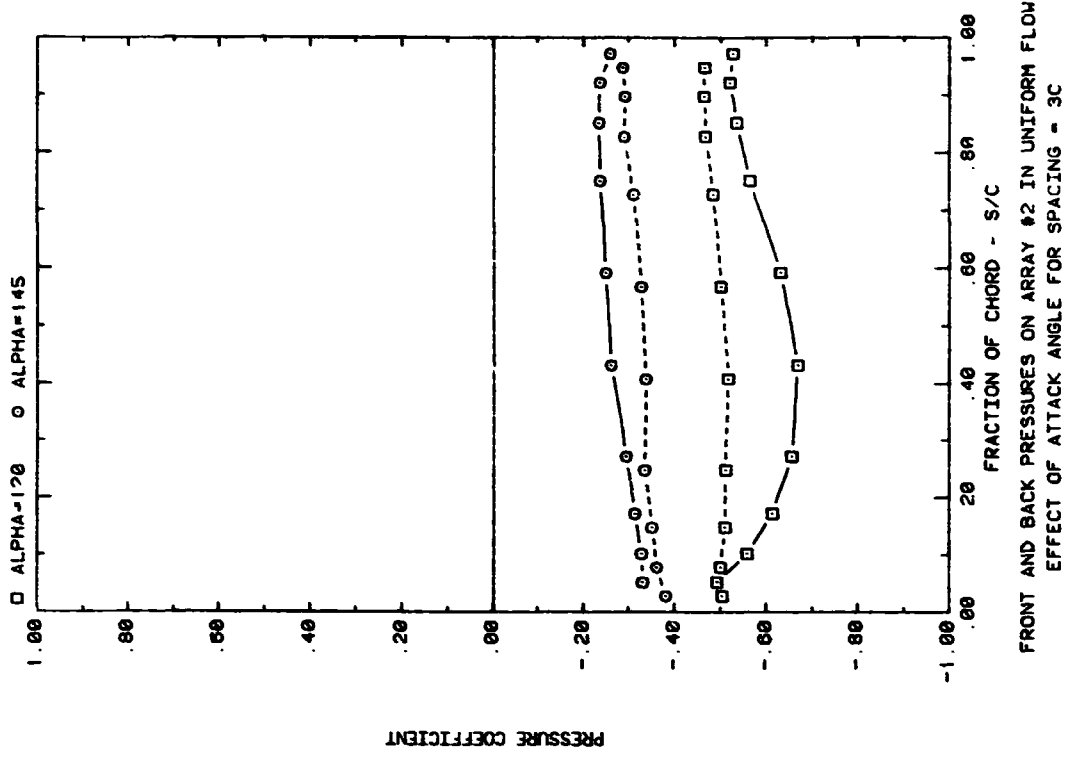


FRONT AND BACK PRESSURES ON ARRAY #2 IN UNIFORM FLOW
EFFECT OF ATTACK ANGLE FOR SPACING = 1.5C

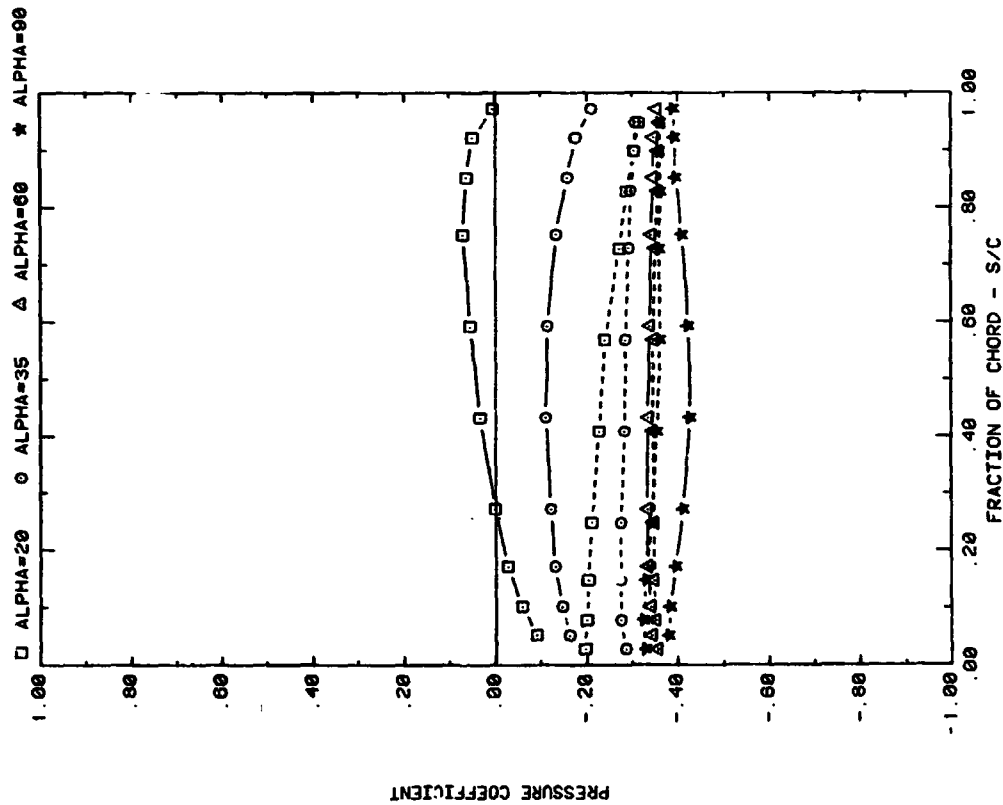
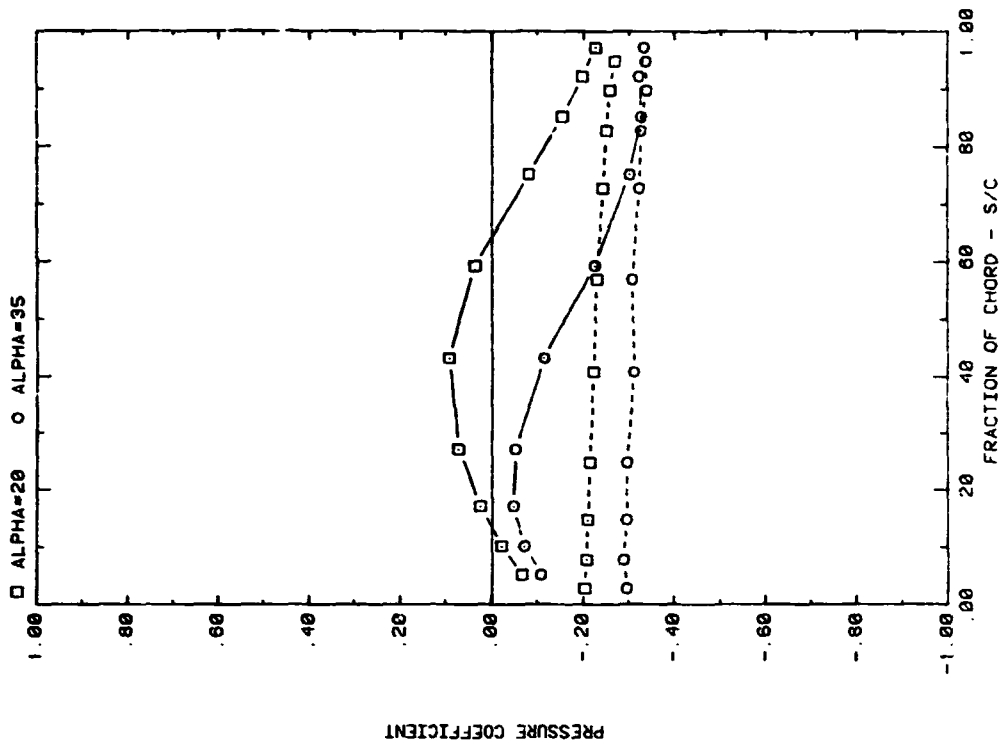


FRONT AND BACK PRESSURES ON ARRAY #2 IN UNIFORM FLOW
EFFECT OF ATTACK ANGLE FOR SPACING = 3C

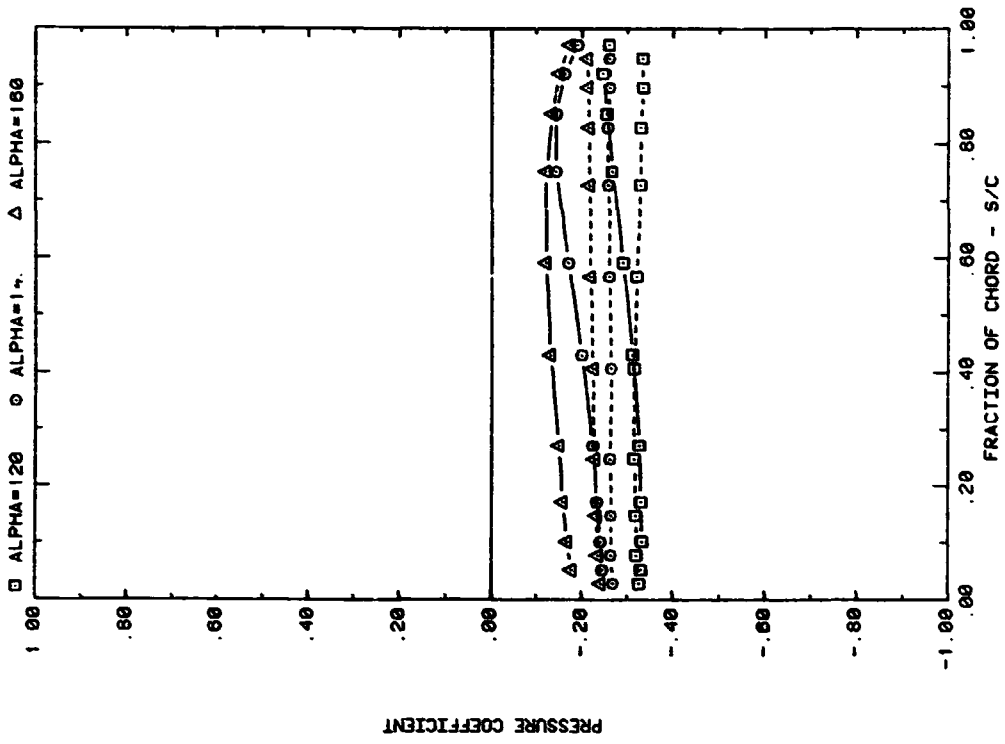
Plot 2-1-1. (Continued)



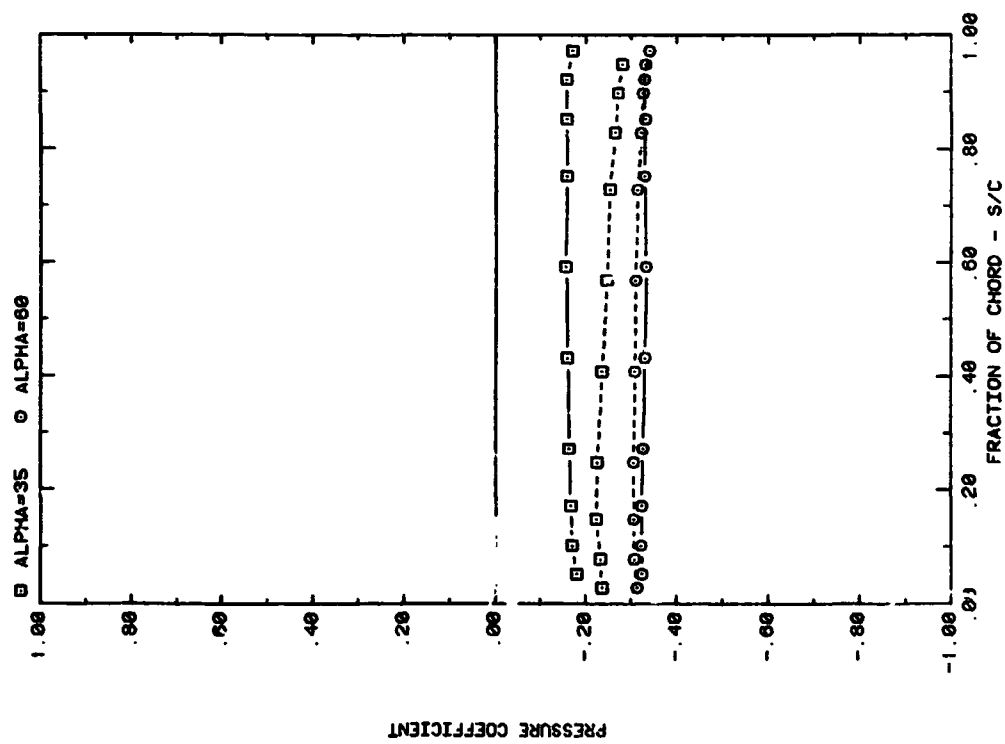
Plot 2-1-1. (Continued)



Plot 2-1-1. (Continued)

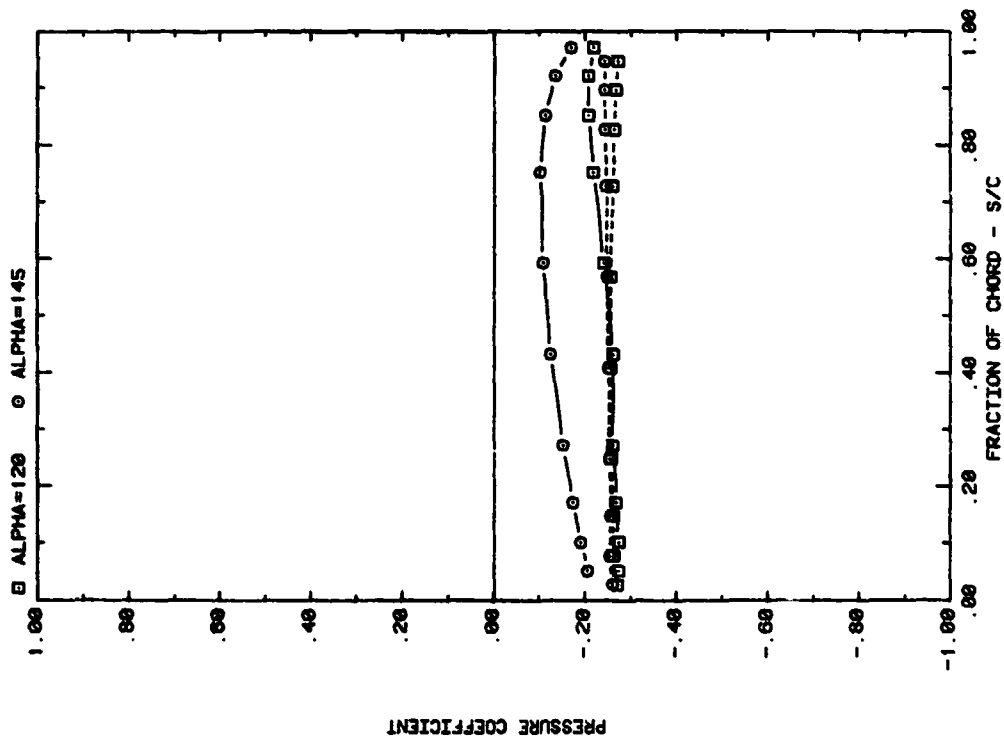


FRONT AND BACK PRESSURES ON ARRAY #5 IN UNIFORM FLOW
EFFECT OF ATTACK ANGLE FOR SPACING = 2C



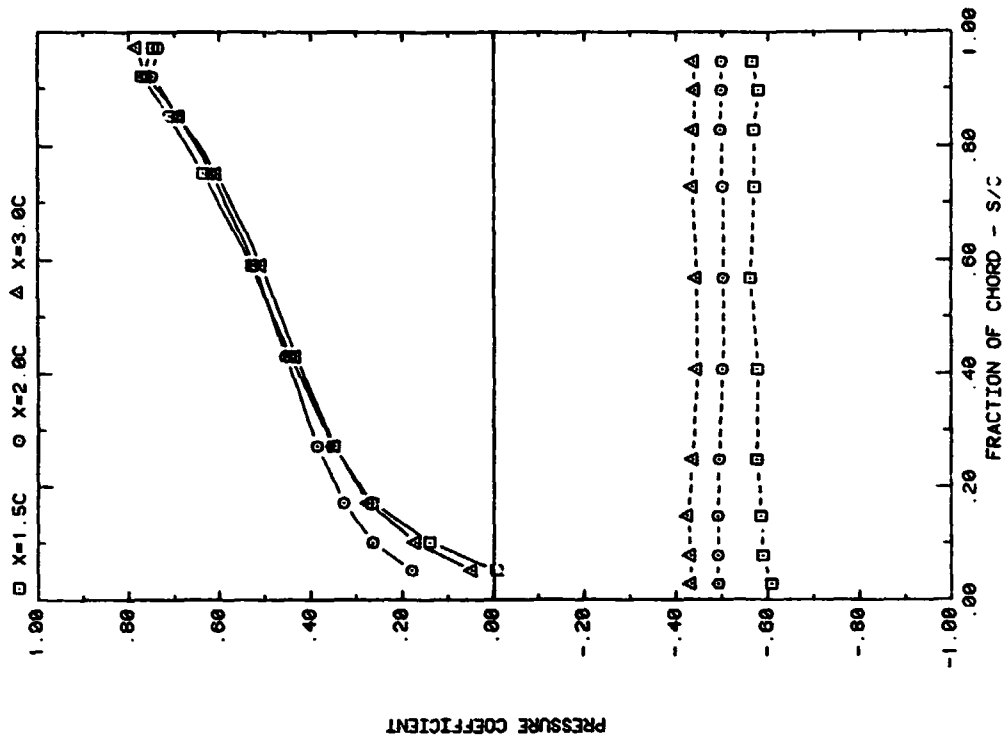
FRONT AND BACK PRESSURES ON ARRAY #4 IN UNIFORM FLOW
EFFECT OF ATTACK ANGLE FOR SPACING = 3C

Plot 2-1-1. (Continued)

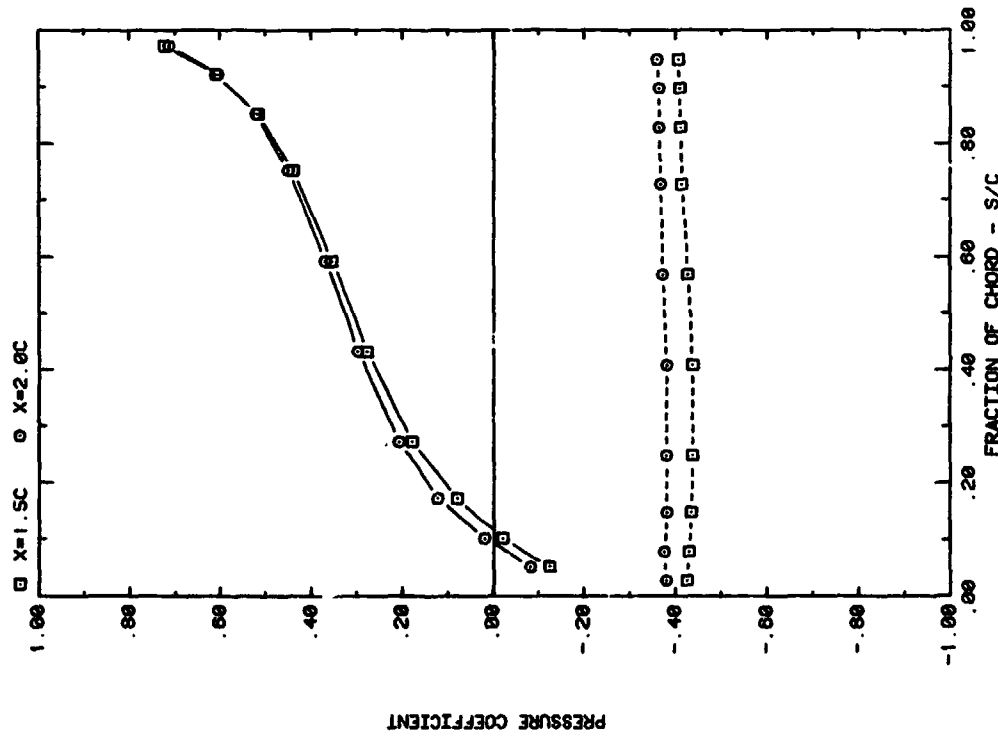


FRONT AND BACK PRESSURES ON ARRAY #4 IN UNIFORM FLOW
EFFECT OF ATTACK ANGLE FOR SPACING = 3C

Plot 2-1-1. (Concluded)

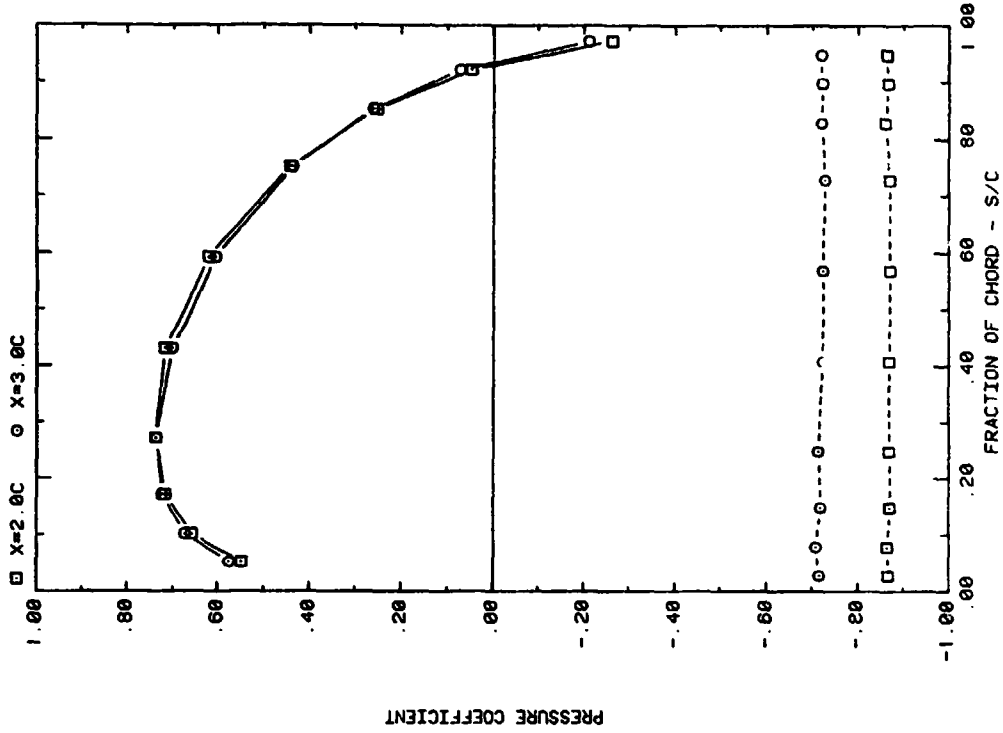


FRONT AND BACK PRESSURES ON ARRAY #1 IN UNIFORM FLOW
EFFECT OF SEPARATION (X) ON ATTACK ANGLE 35, H/C = 0.25

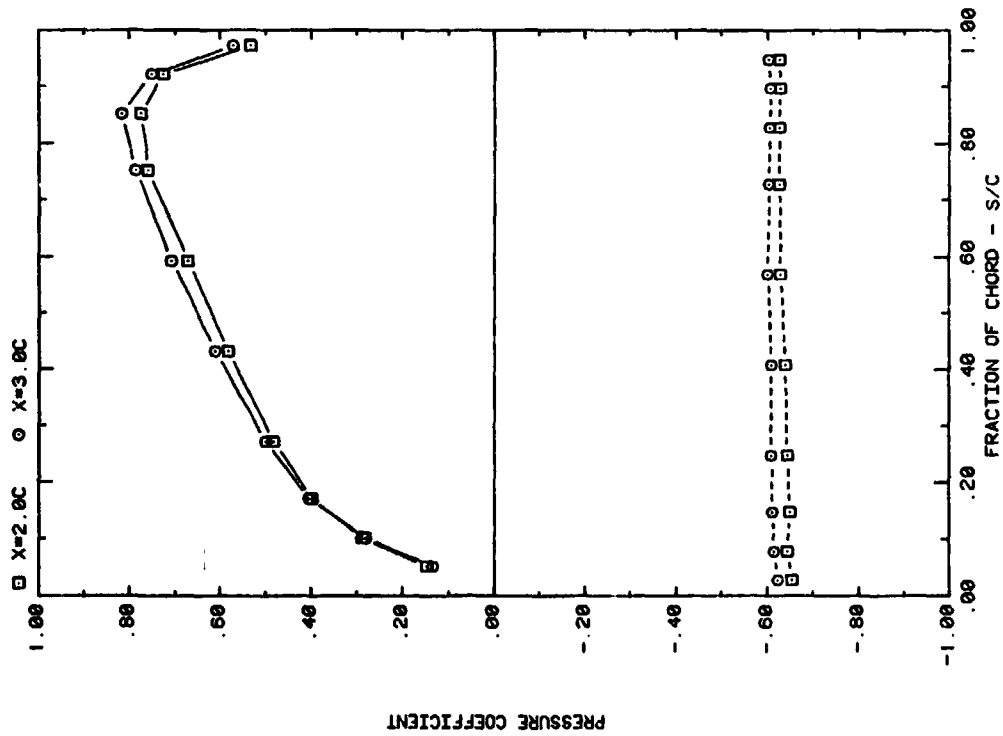


FRONT AND BACK PRESSURES ON ARRAY #1 IN UNIFORM FLOW
EFFECT OF SEPARATION (X) ON ATTACK ANGLE 20, H/C = 0.25

Plot 2-1-2. Multiple Arrays without Fence, Uniform Flow Study
Effect of Separation Distance

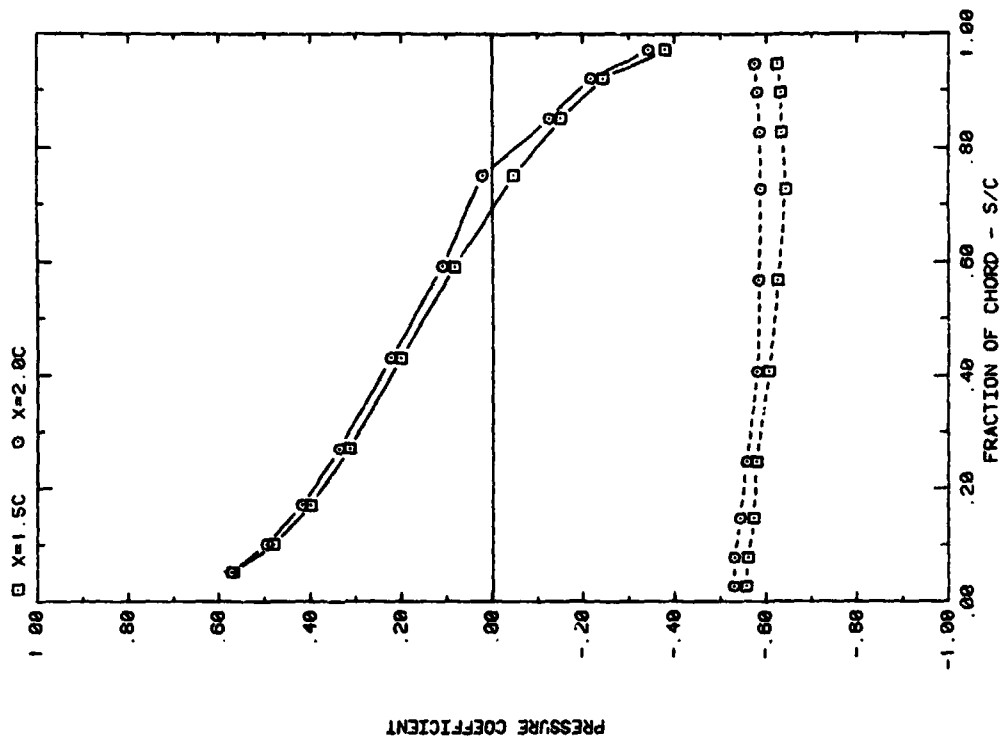


FRONT AND BACK PRESSURES ON ARRAY #1 IN UNIFORM FLOW
EFFECT OF SEPARATION (X) ON ATTACK ANGLE 120, H/C = 0.25

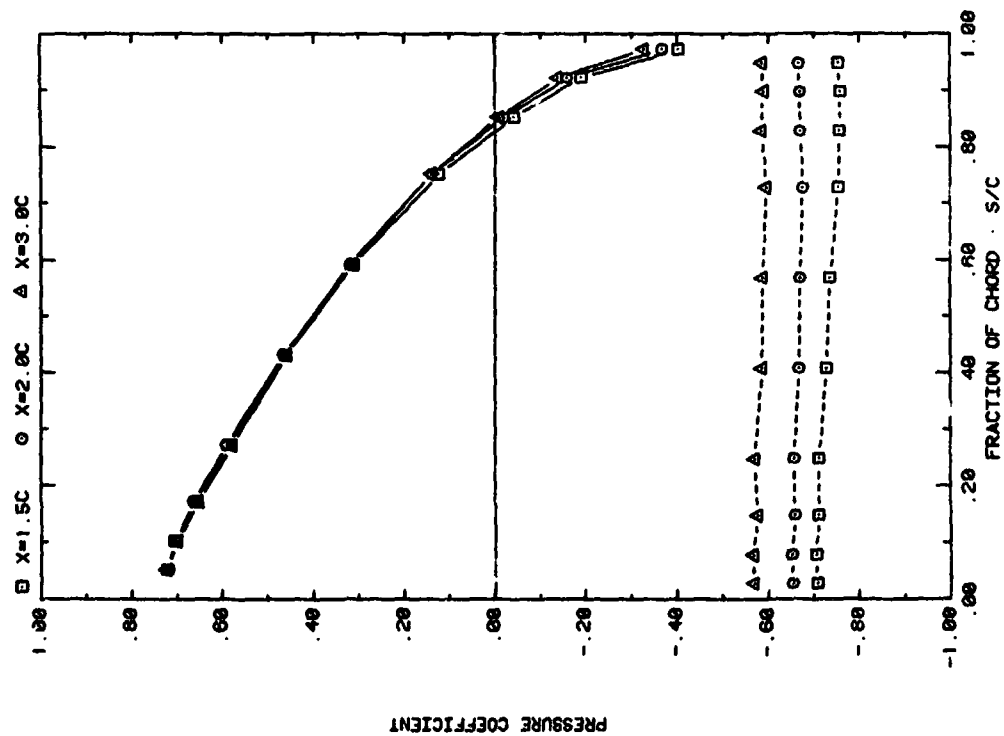


FRONT AND BACK PRESSURES ON ARRAY #1 IN UNIFORM FLOW
EFFECT OF SEPARATION (X) ON ATTACK ANGLE 60, H/C = 0.25

Plot 2-1-2. (Continued)

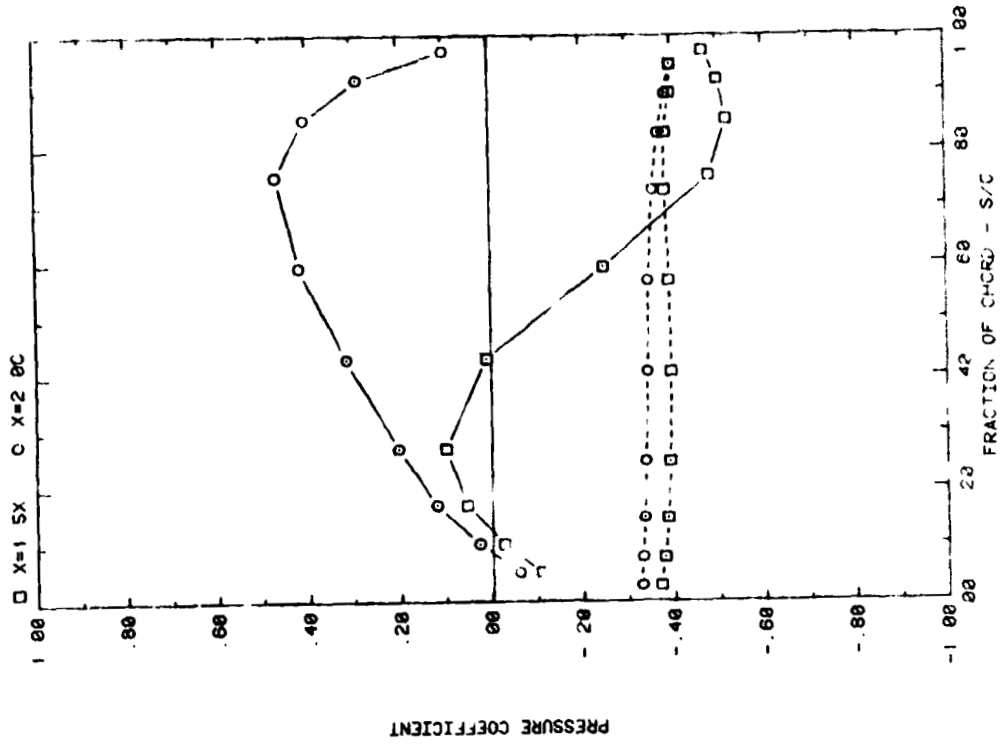


FRONT AND BACK PRESSURES ON ARRAY #1 IN UNIFORM FLOW EFFECT OF SEPARATION (X) ON ATTACK ANGLE 160, H/C = 0.25

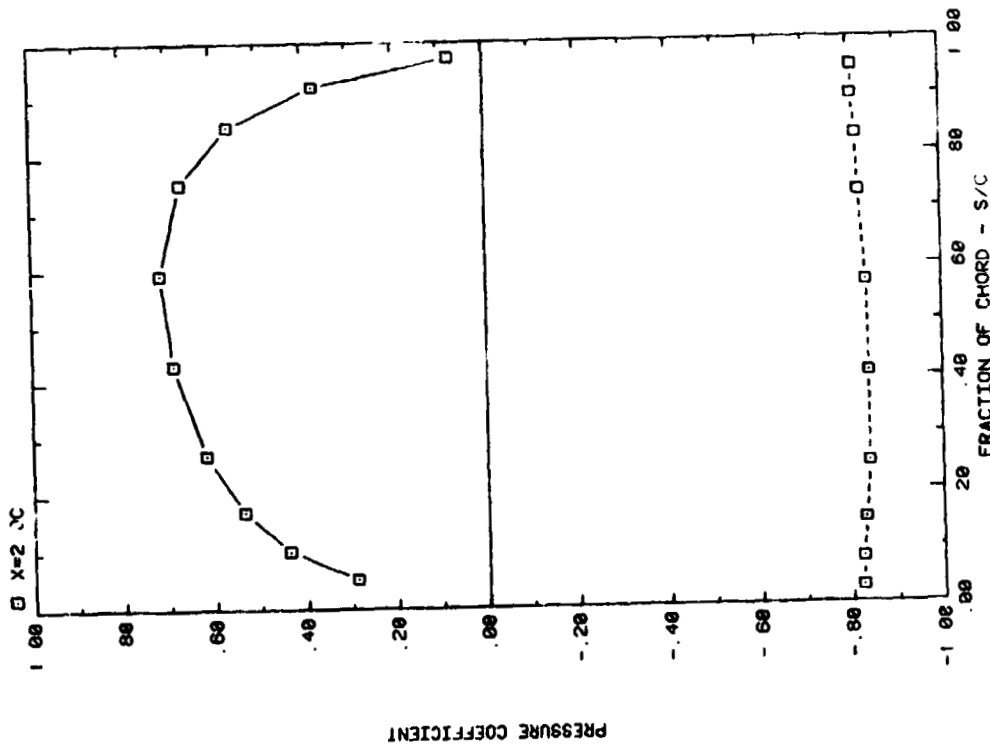


FRONT AND BACK PRESSURES ON ARRAY #1 IN UNIFORM FLOW EFFECT OF SEPARATION (X) ON ATTACK ANGLE 145, H/C = 0.25

Plot 2-1-2. (Continued)

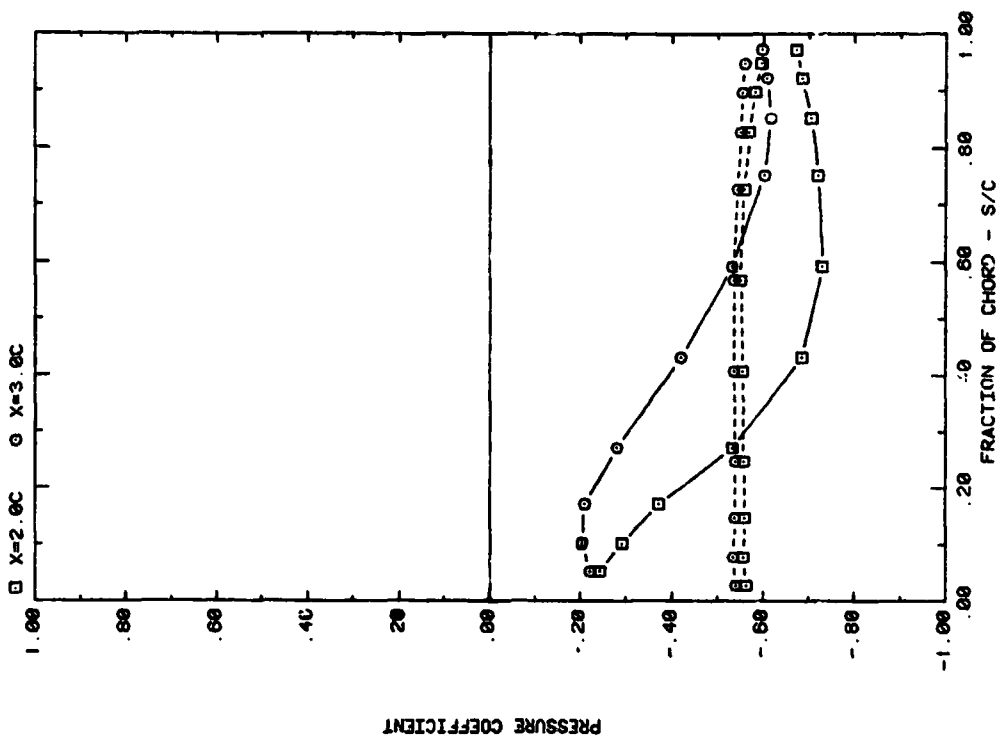


FRONT AND BACK PRESSURES ON ARRAY #2 IN UNIFORM FLOW
EFFECT OF SEPARATION (X) ON ATTACK ANGLE 90, H/C = 0.25

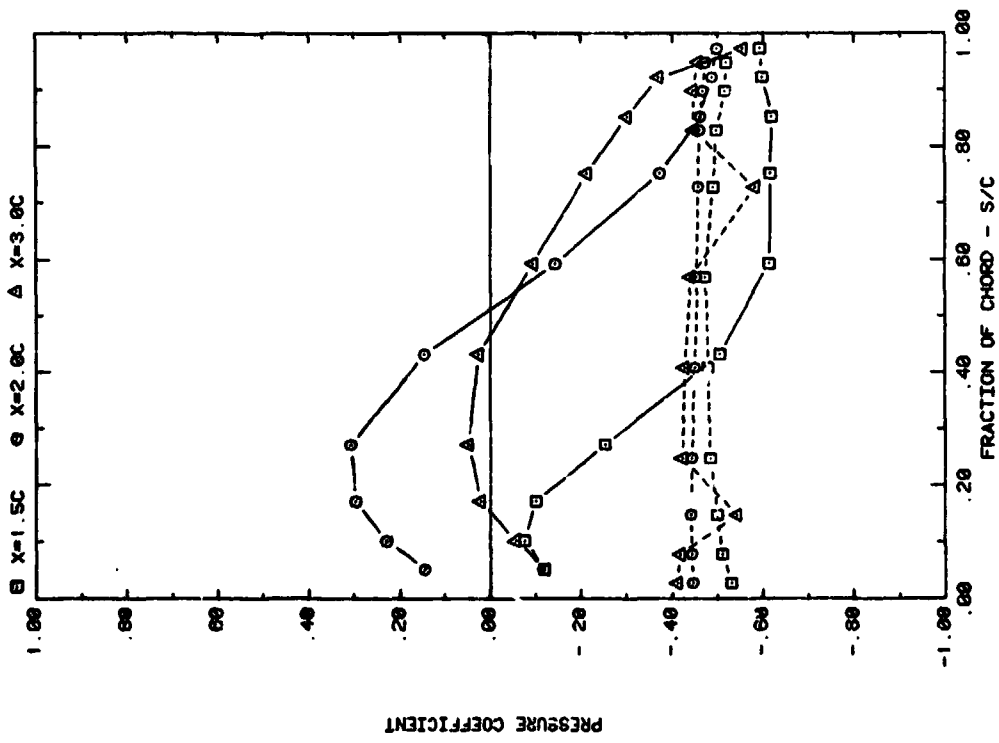


FRONT AND BACK PRESSURES ON ARRAY #1 IN UNIFORM FLOW
EFFECT OF SEPARATION (X) ON ATTACK ANGLE 90, H/C = 0.25

Plot 2-1-2. (Continued)

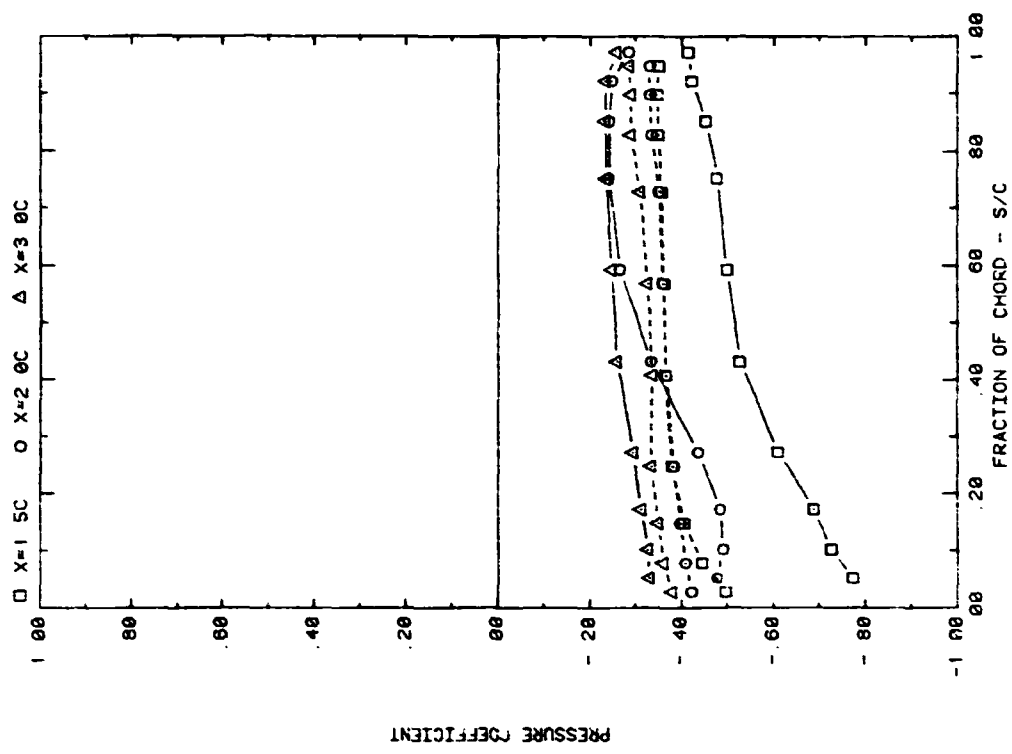


FRONT AND BACK PRESSURES ON ARRAY #2 IN UNIFORM FLOW
EFFECT OF SEPARATION ANGLE (X) ON ATTACK ANGLE 60, H/C = 0.25

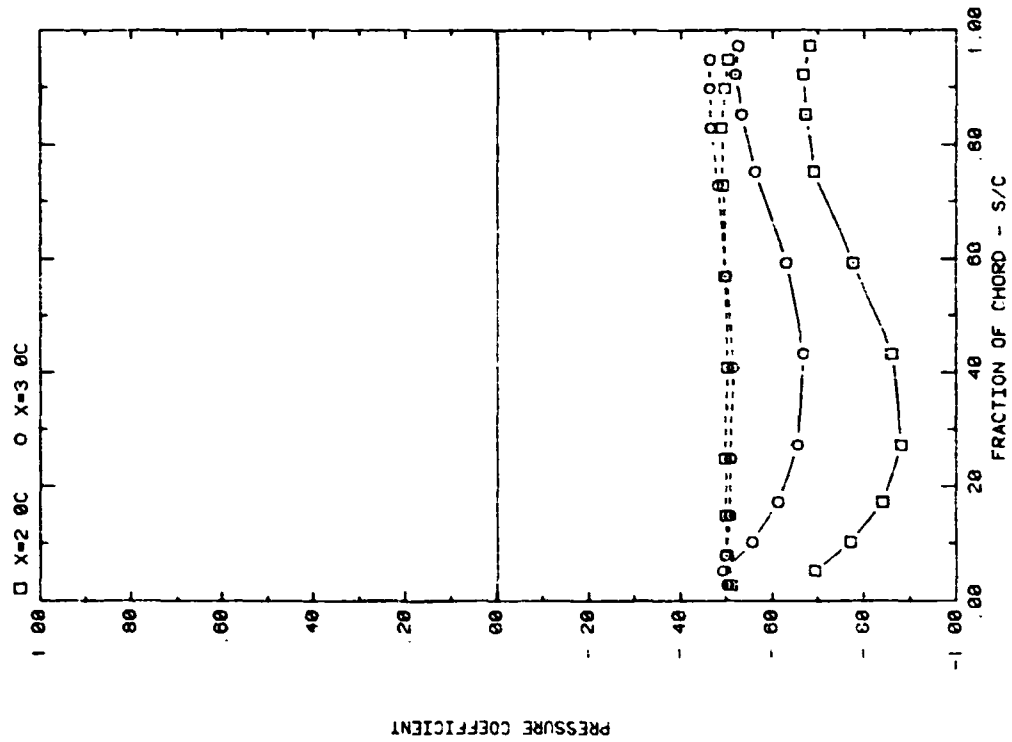


FRONT AND BACK PRESSURES ON ARRAY #2 IN UNIFORM FLOW
EFFECT OF SEPARATION ANGLE (X) ON ATTACK ANGLE 95, H/C = 0.25

Plot 2-1-2. (Continued)



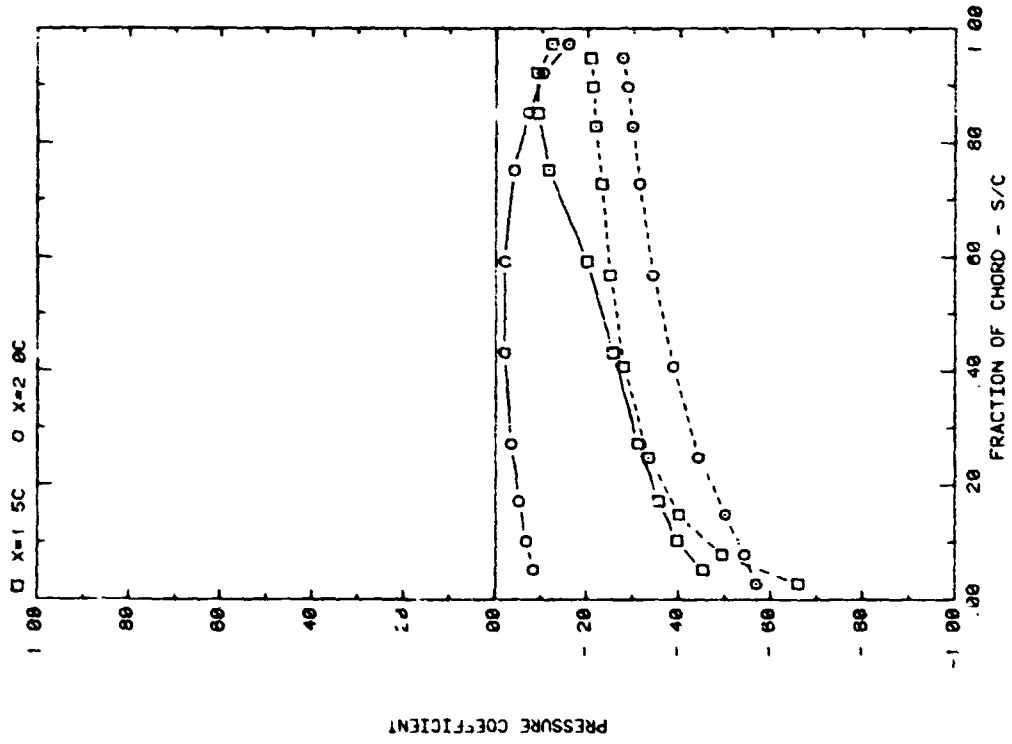
FRONT AND BACK PRESSURES ON ARRAY #2 IN UNIFORM FLOW
EFFECT OF SEPARATION (X) ON ATTACK ANGLE 145, H/C = 0.25



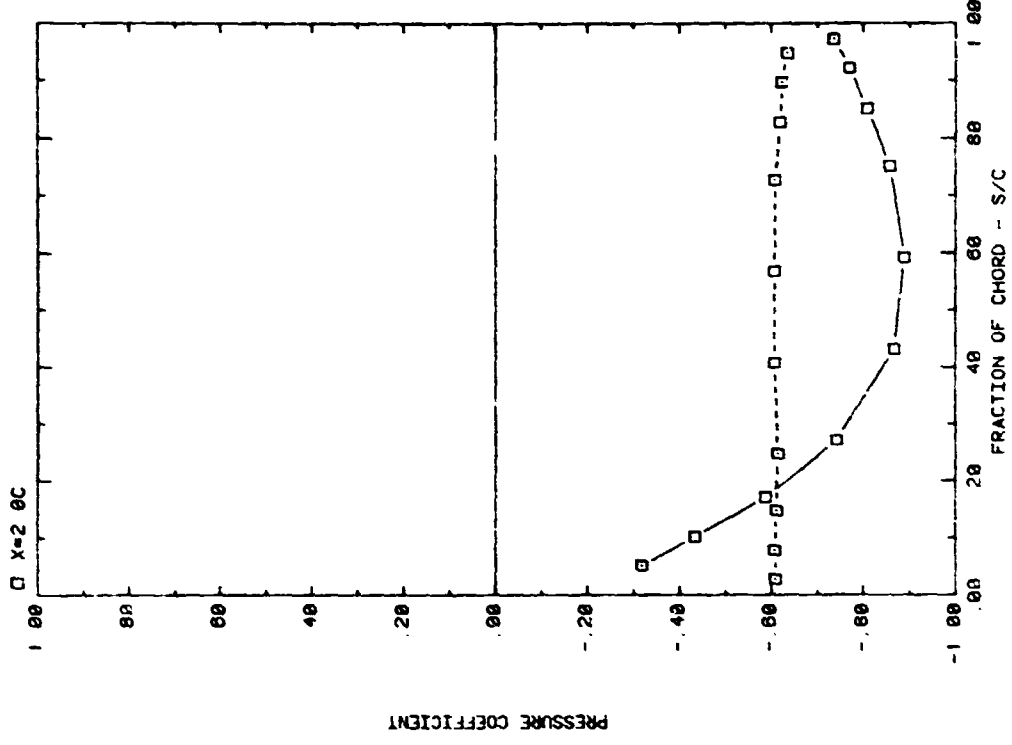
FRONT AND BACK PRESSURES ON ARRAY #2 IN UNIFORM FLOW
EFFECT OF SEPARATION (X) ON ATTACK ANGLE 120, H/C = 0.25

Plot 2-1-2. (Continued)

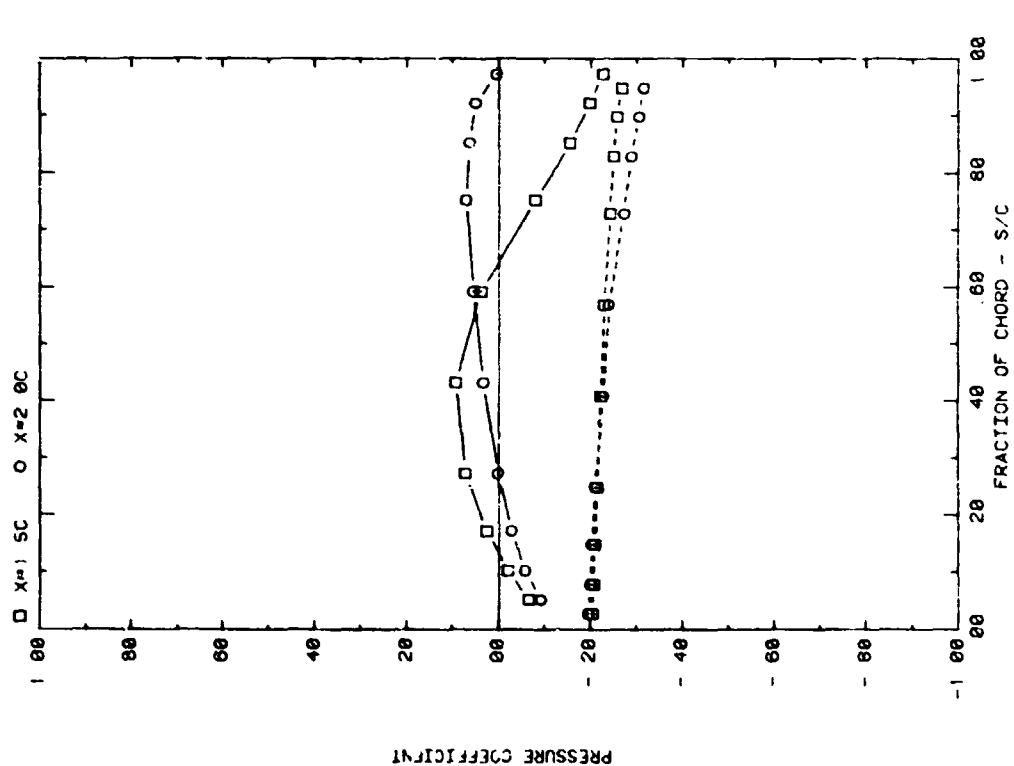
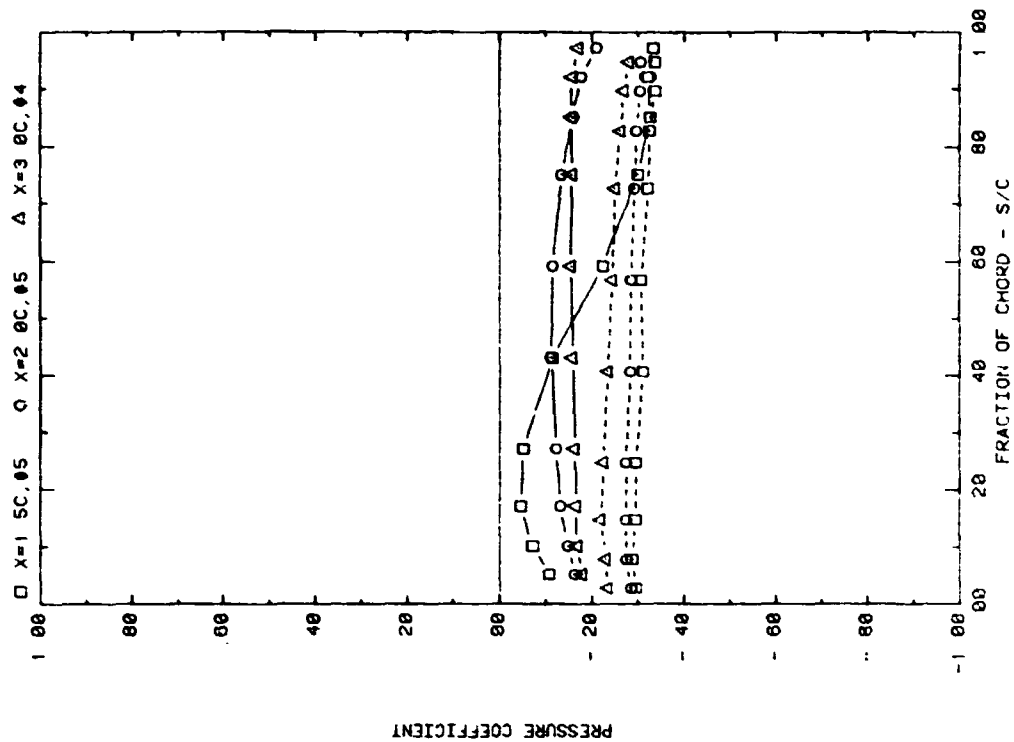
4



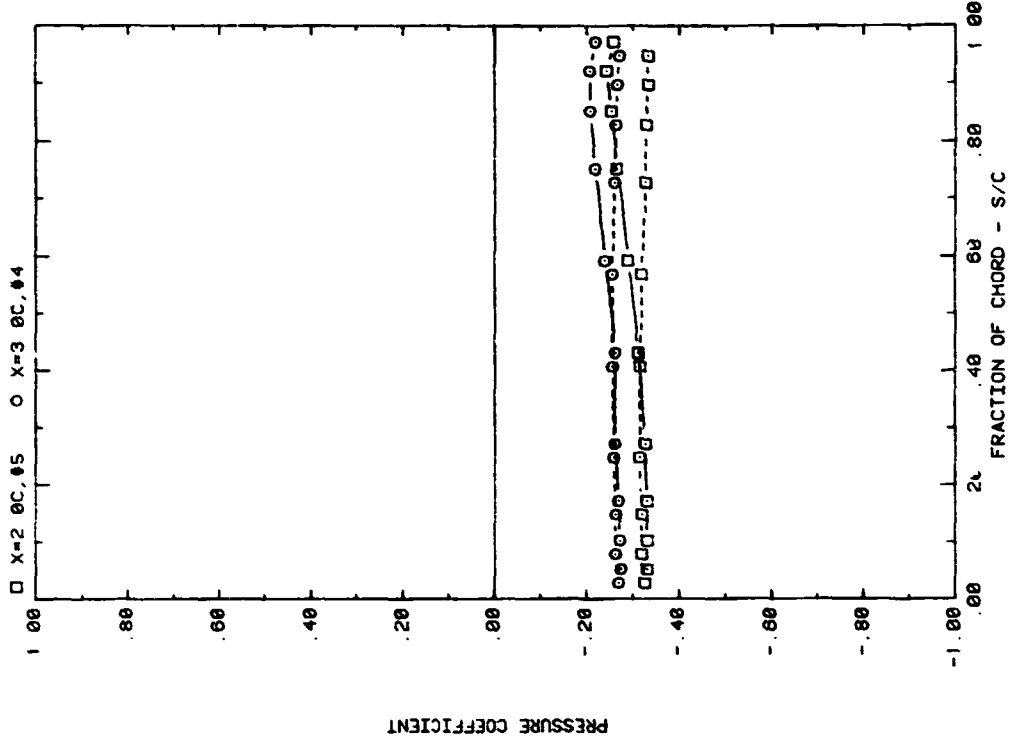
FRONT AND BACK PRESSURES ON ARRAY #2 IN UNIFORM FLOW
EFFECT OF SEPARATION (X) ON ATTACK ANGLE 160, H/C = 0.25



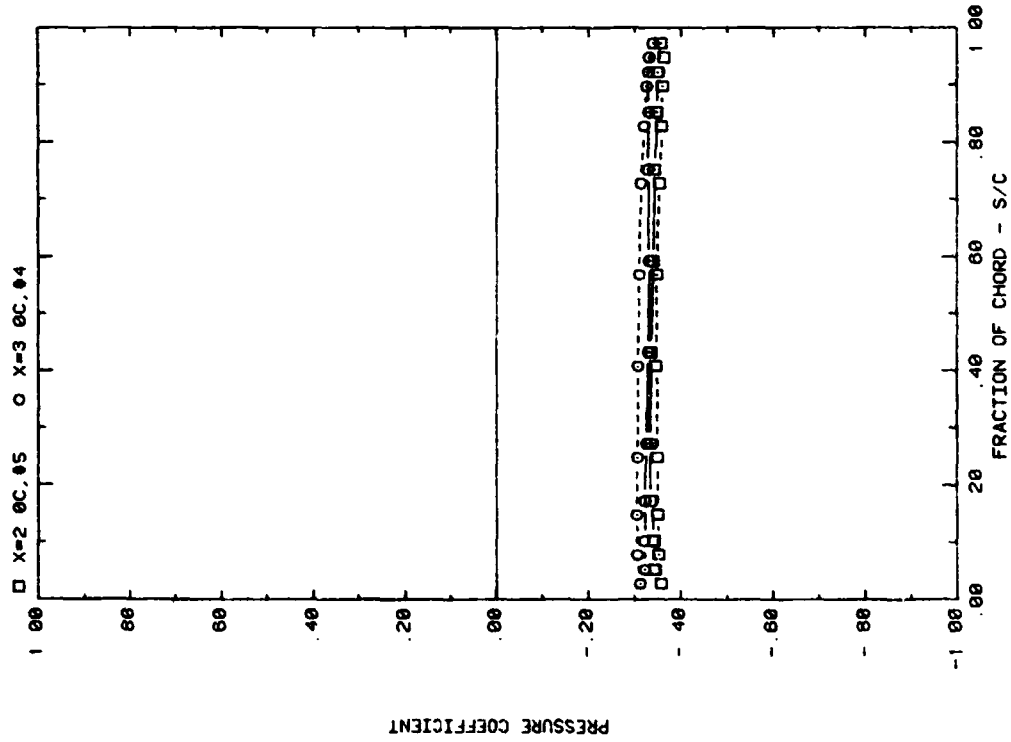
FRONT AND BACK PRESSURES ON ARRAY #2 IN UNIFORM FLOW
EFFECT OF SEPARATION (X) ON ATTACK ANGLE 90, H/C = 0.25



Plot 2-1-2. (Continued)

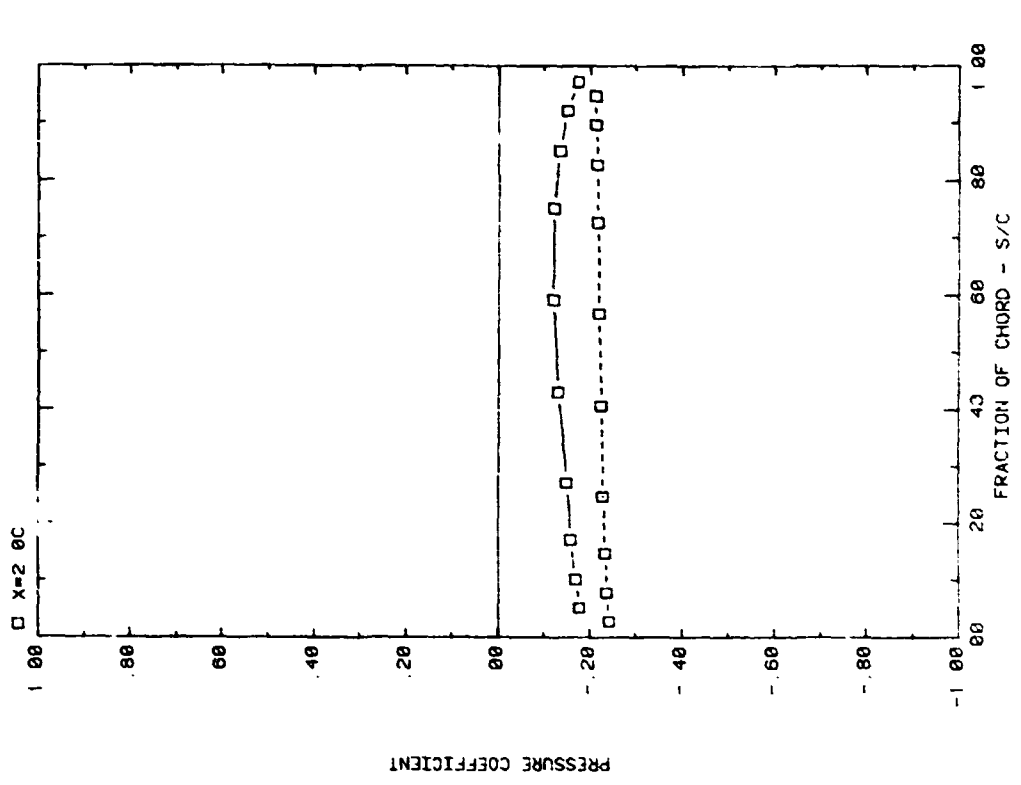


FRONT AND BACK PRESSURES ON ARRAY #4 OF #5 IN UNIFORM FLOW
EFFECT OF SEPARATION (X) ON ATTACK ANGLE 120, H/C = 0.25

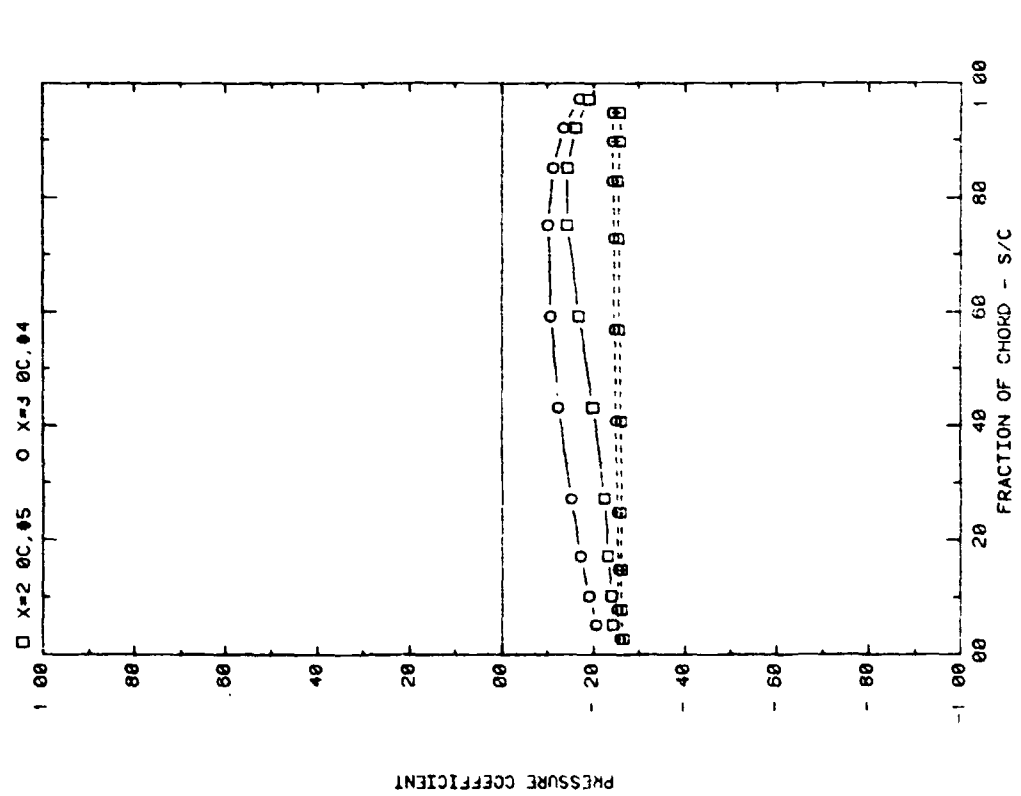


FRONT AND BACK PRESSURES ON ARRAY #4 OR #5 IN UNIFORM FLOW
EFFECT OF SEPARATION (X) ON ATTACK ANGLE 60, H/C = 0.25

Plot 2-1-2. (Continued)

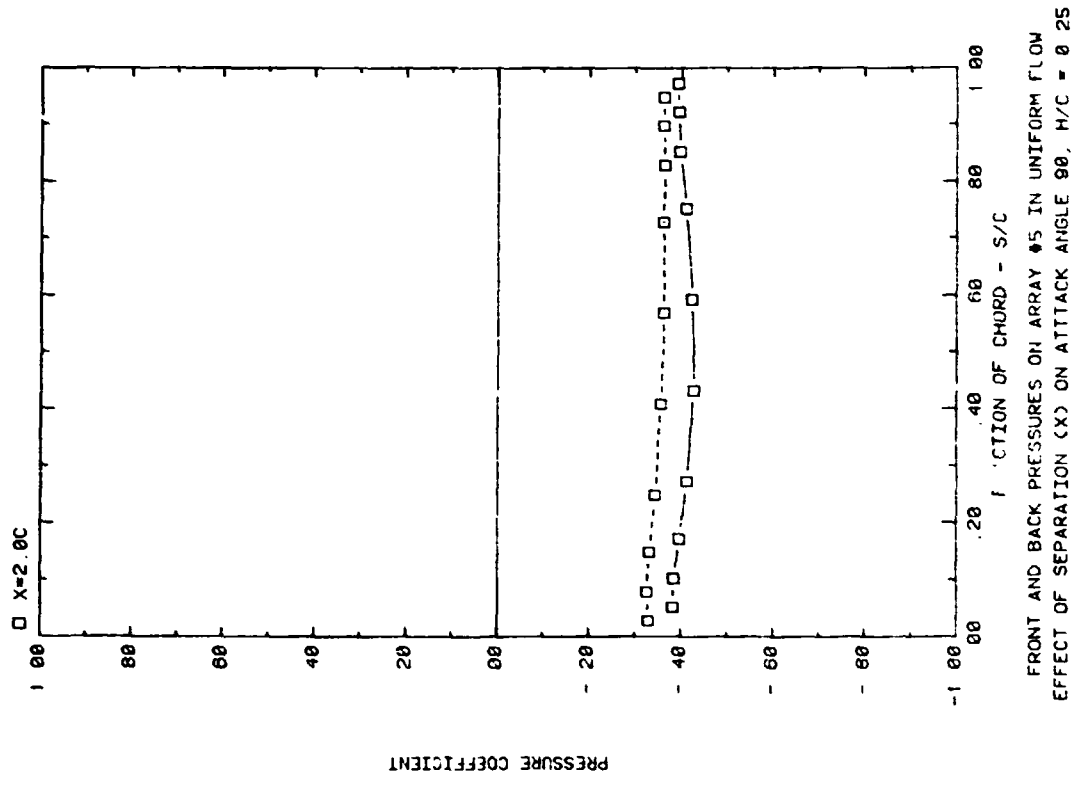


FRONT AND BACK PRESSURES ON ARRAY #5 IN UNIFORM FLOW
EFFECT OF SEPARATION (Y) ON ATTACK ANGLE 160, H/C = 0.25

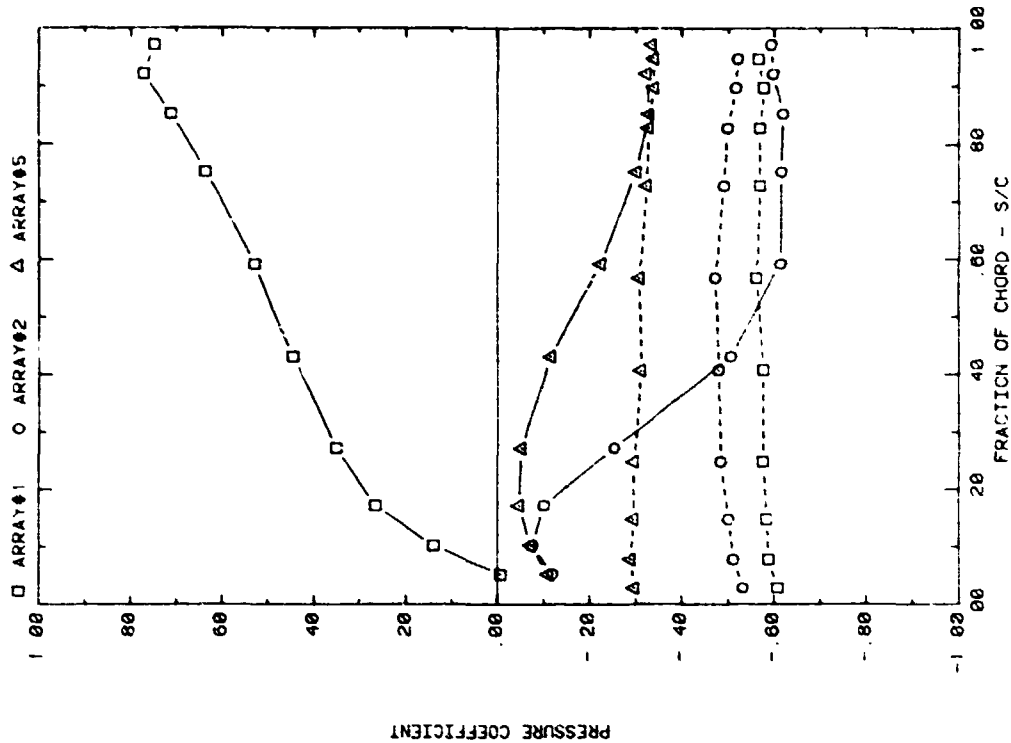


FRONT AND BACK PRESSURES ON ARRAY #4 OR #5 IN UNIFORM FLOW
EFFECT OF SEPARATION (X) ON ATTACK ANGLE 145, H/C = 0.25

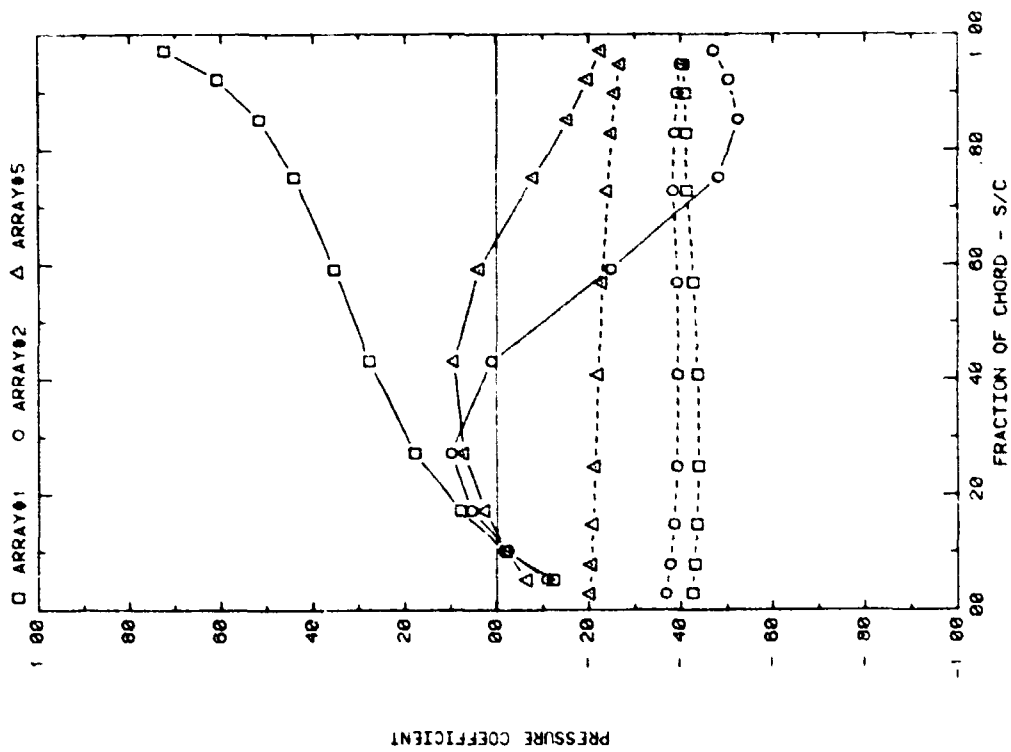
Plot 2-1-2. (Continued)



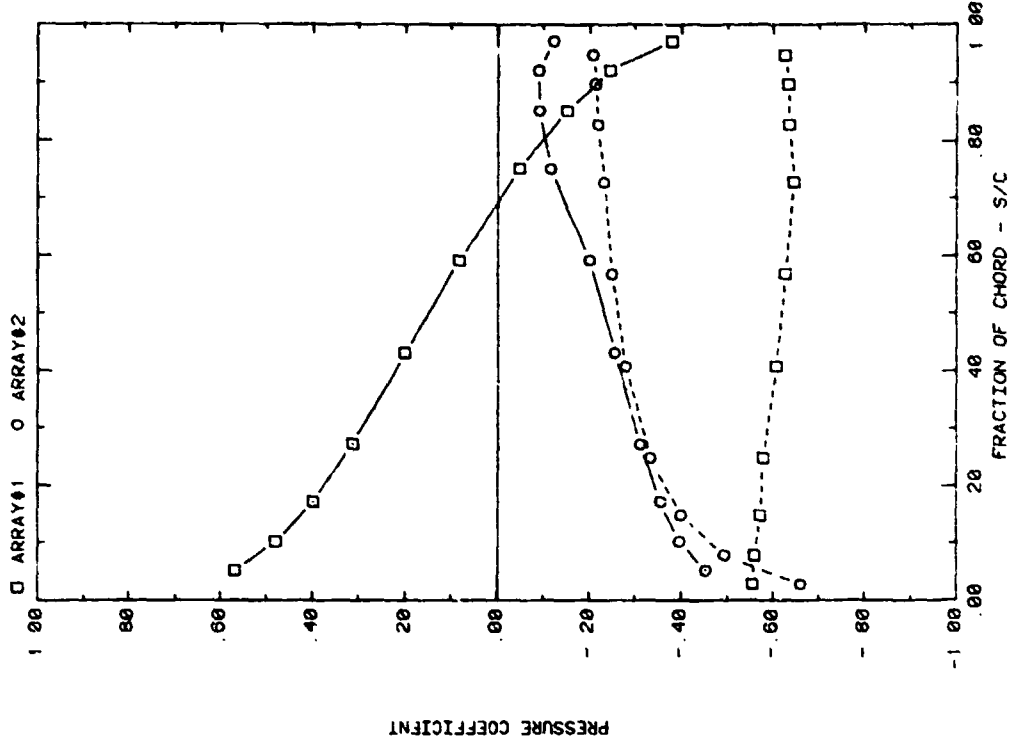
Plot 2-1-2. (Concluded)



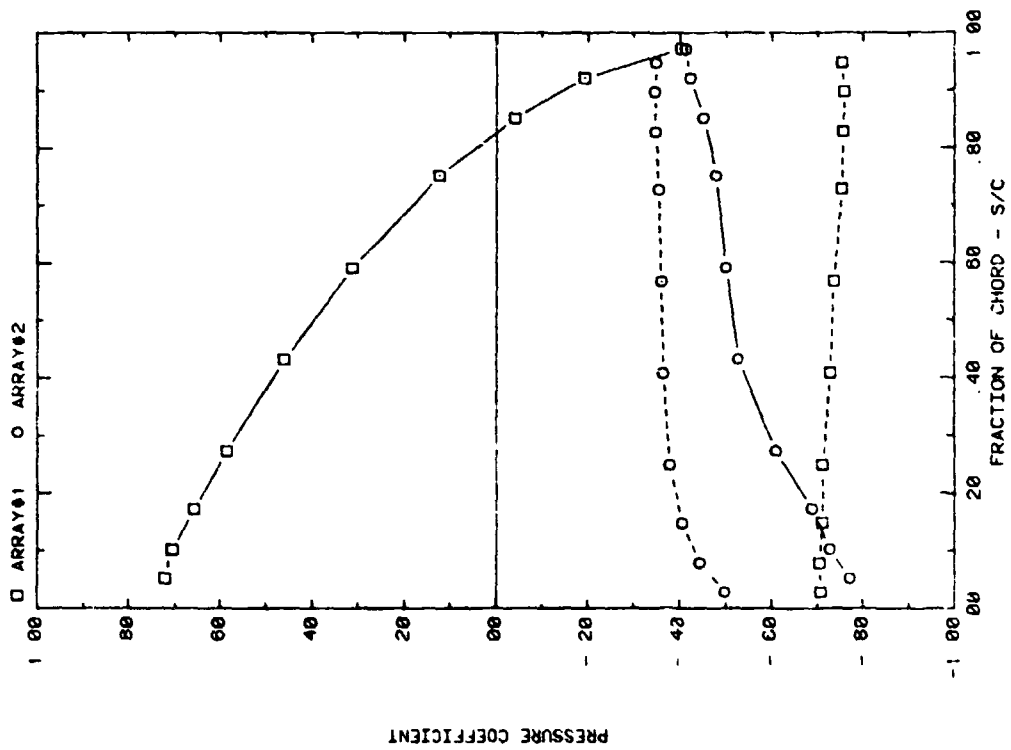
FRONT AND BACK PRESSURES ON VARIOUS ARRAYS FOR SEPARATION = 1.5C
EFFECT OF ARRAY CONFIGURATION FOR ATTACK ANGLE, ALPHA = 35



FRONT AND BACK PRESSURES ON VARIOUS ARRAYS FOR SEPARATION = 1.5C
EFFECT OF ARRAY CONFIGURATION FOR ATTACK ANGLE, ALPHA = 28
Plot 2-1-3. Multiple Arrays without Fence, Uniform Flow Study
Effect of Array Position

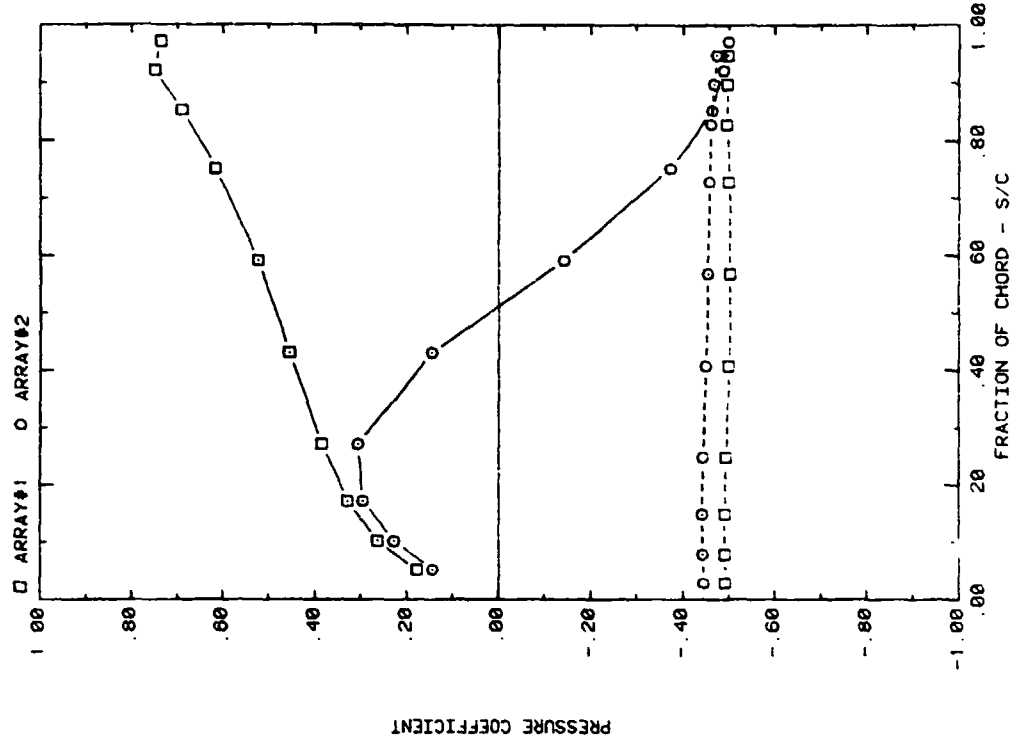


FRONT AND BACK PRESSURES ON VARIOUS ARRAYS FOR SEPARATION -1 SC
EFFECT OF ARRAY CONFIGURATION FOR ATTACK ANGLE, ALPHA = 160

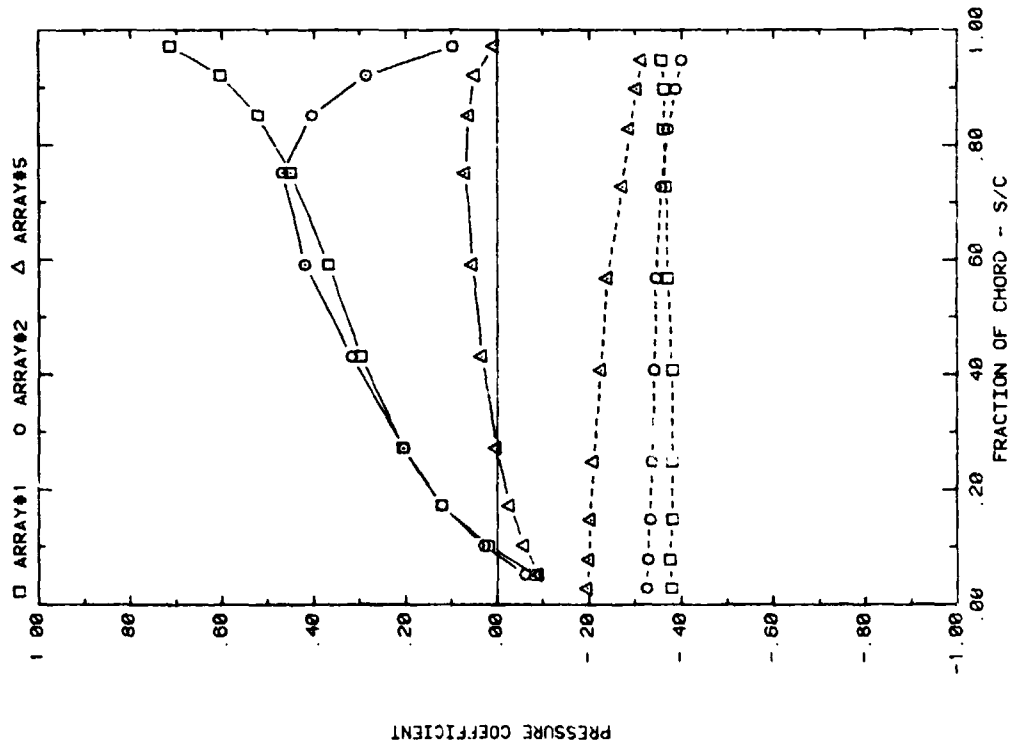


FRONT AND BACK PRESSURES ON VARIOUS ARRAYS FOR SEPARATION -1 SC
EFFECT OF ARRAY CONFIGURATION FOR ATTACK ANGLE, ALPHA = 145

Plot 2-1-3. (Continued)

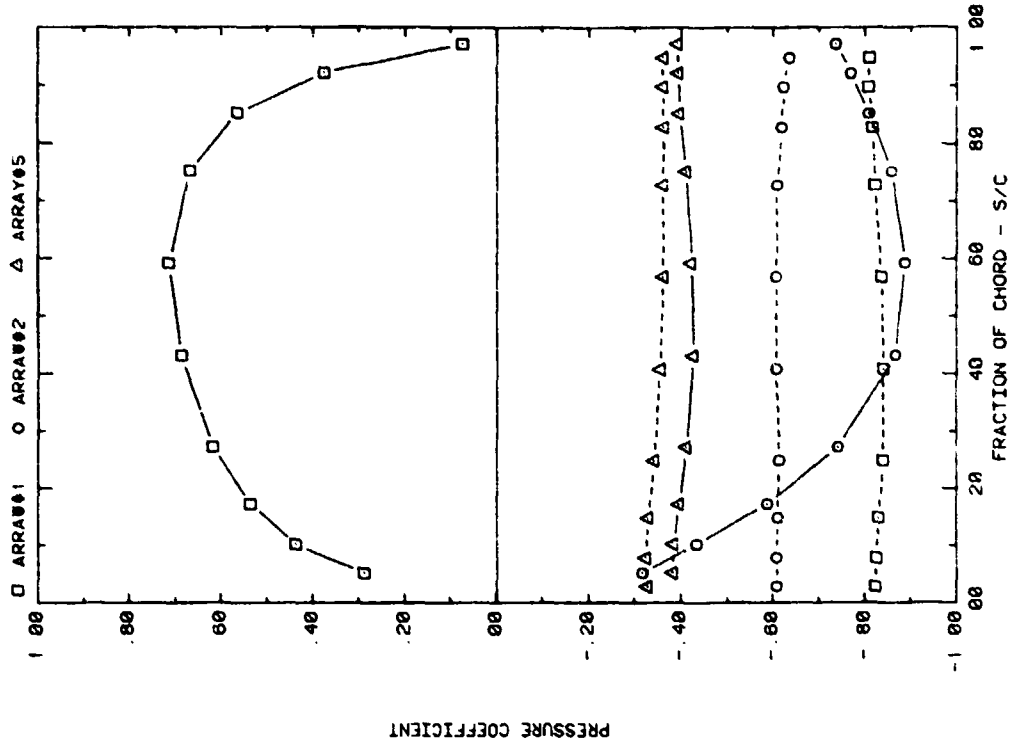


FRONT AND BACK PRESSURES ON VARIOUS ARRAYS FOR SEPARATION = 2C
EFFECT OF ARRAY CONFIGURATION FOR ATTACK ANGLE, ALPHA = 35

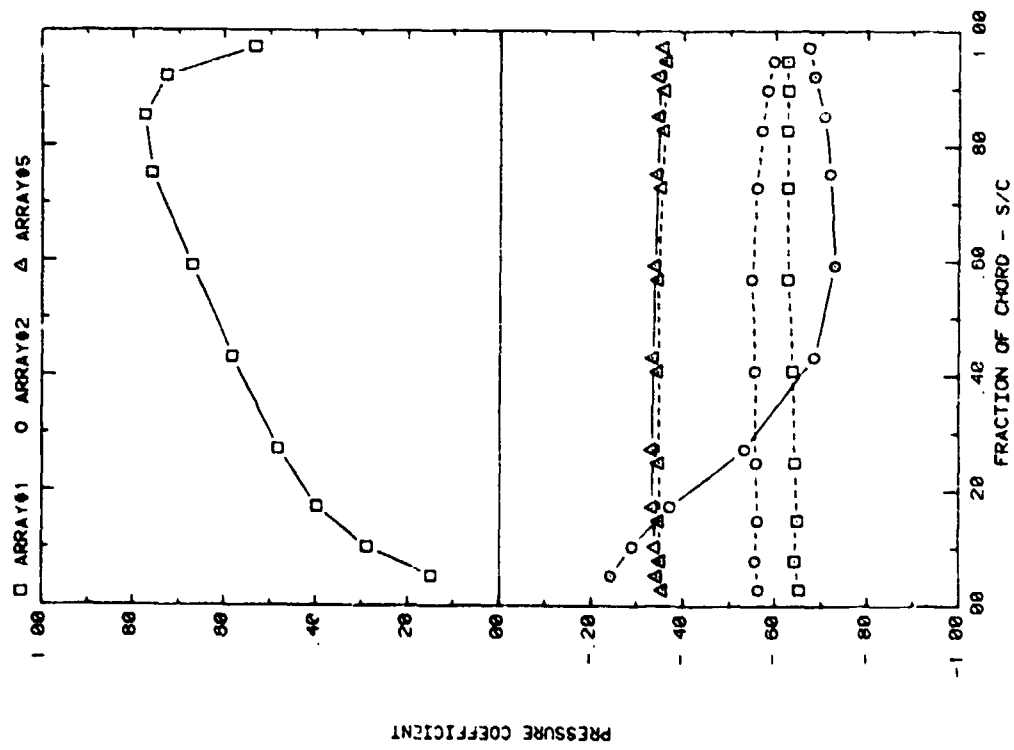


FRONT AND BACK PRESSURES ON VARIOUS ARRAYS FOR SEPARATION = 2C
EFFECT OF ARRAY CONFIGURATION FOR ATTACK ANGLE, ALPHA = 20

Plot 2-1-3. (Continued)

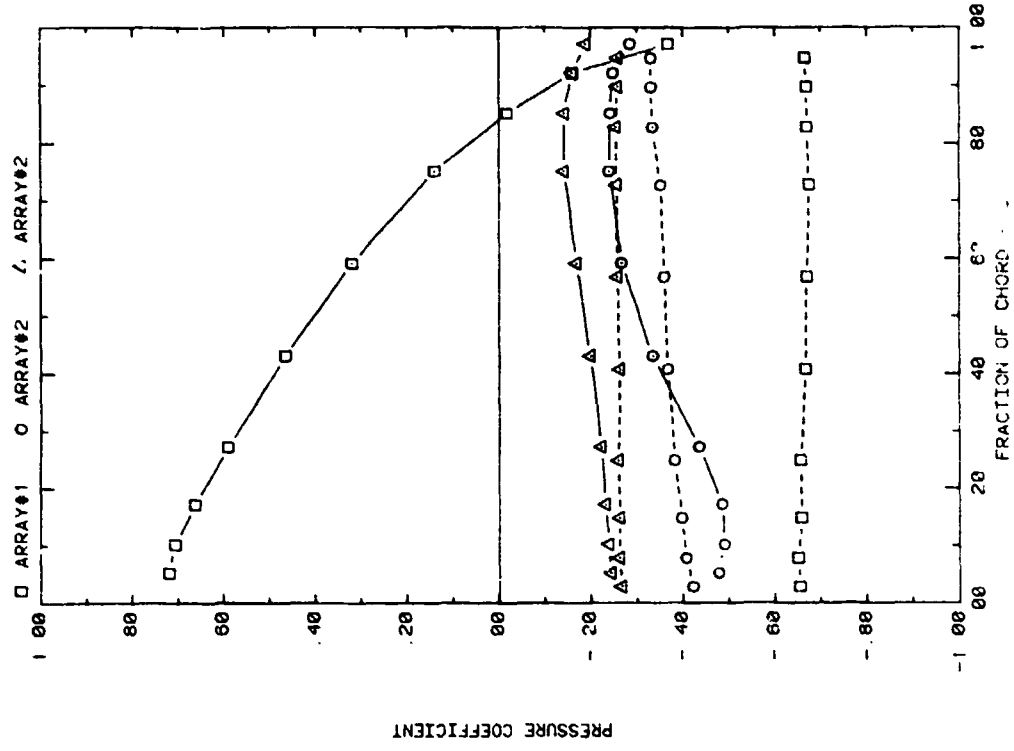


FRONT AND BACK PRESSURES ON VARIOUS ARRAYS FOR SEPARATION = 2C
EFFECT OF ARRAY CONFIGURATION FOR ATTACK ANGLE, ALPHA = 90

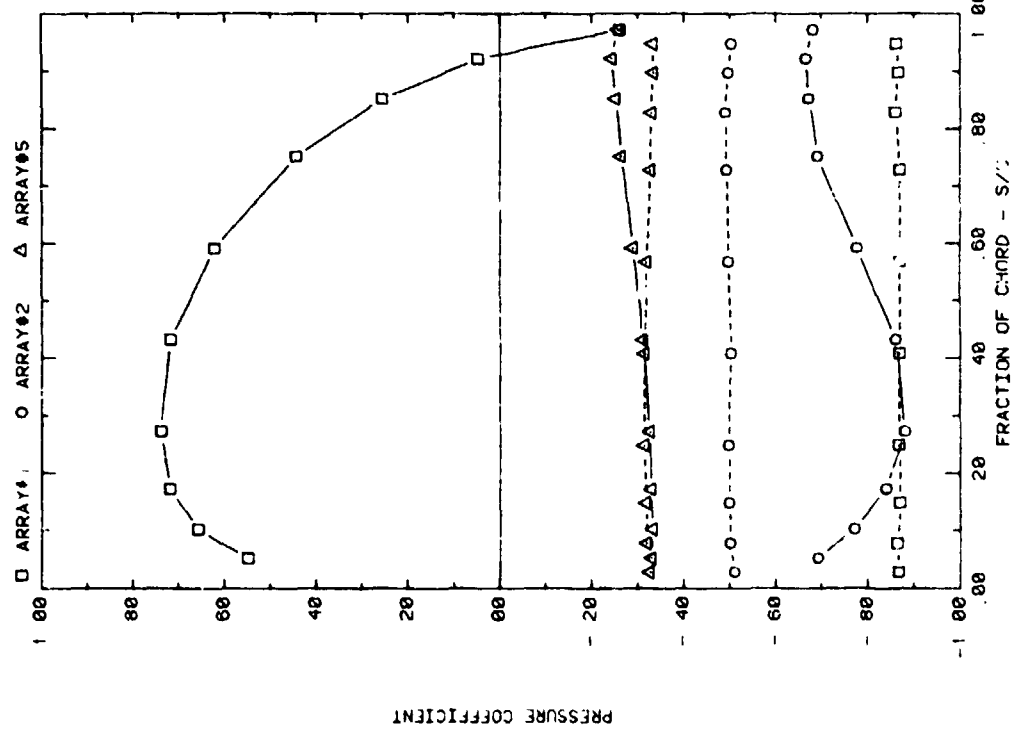


FRONT AND BACK PRESSURES ON VARIOUS ARRAYS FOR SEPARATION = 2C
EFFECT OF ARRAY CONFIGURATION FOR ATTACK ANGLE, ALPHA = 60

Plot 2-1-3. (Continued)

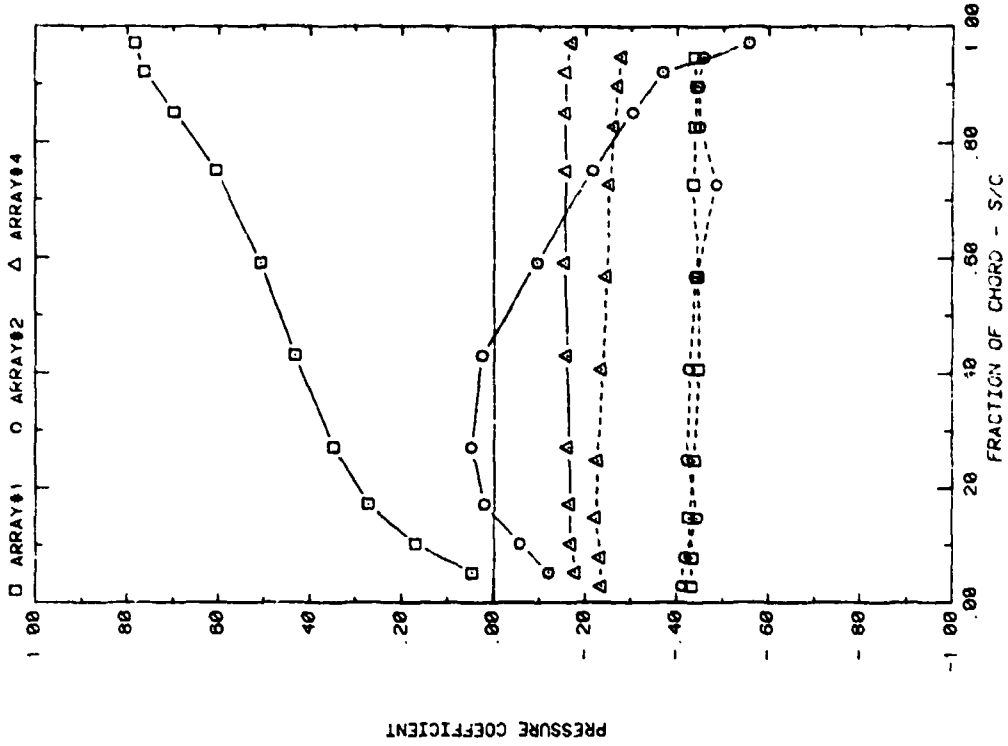


FRONT AND BACK PRESSURES ON VARIOUS ARRAYS FOR SEPARATION = 2C
EFFECT OF ARRAY CONFIGURATION FOR ATTACK ANGLE, ALPHA = 145

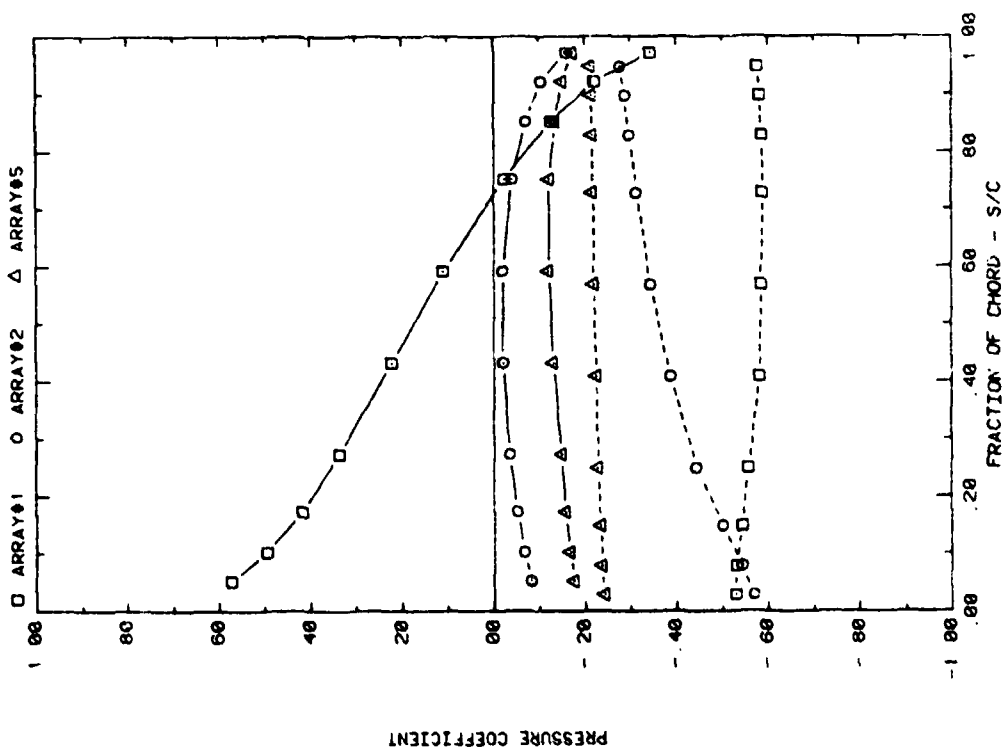


FRONT AND BACK PRESSURES ON VARIOUS ARRAYS FOR SEPARATION = 2C
EFFECT OF ARRAY CONFIGURATION FOR ATTACK ANGLE, ALPHA = 120

Plot 2-1-3. (Continued)

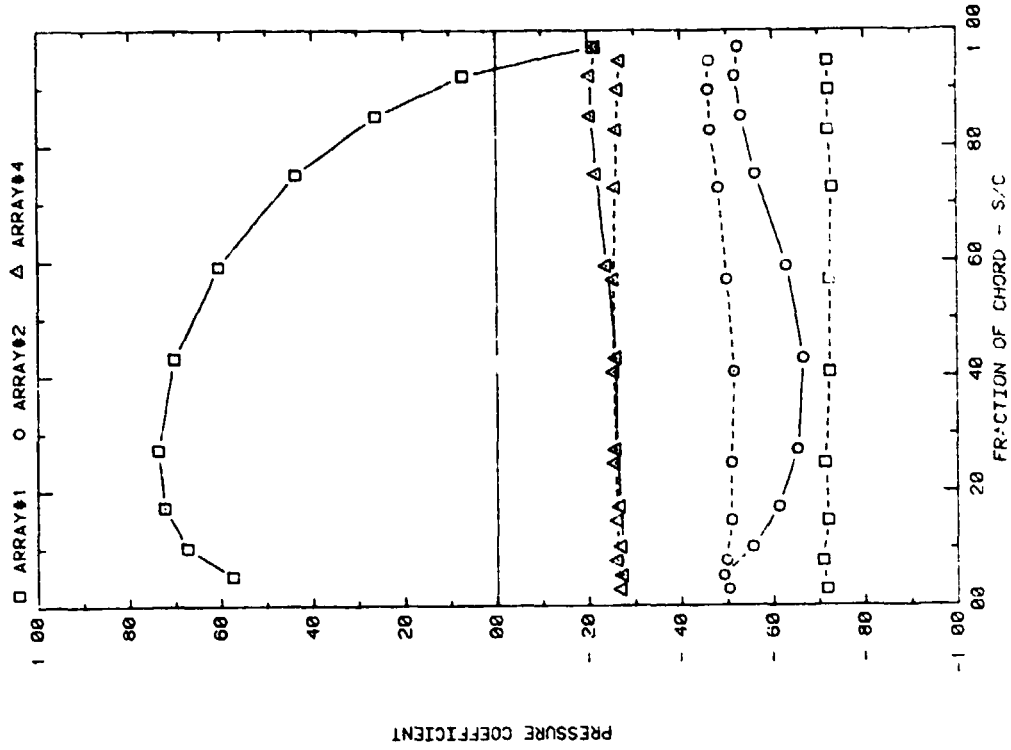


FRONT AND BACK PRESSURES ON VARIOUS ARRAYS FOR SEPARATION = 3C
EFFECT OF ARRAY CONFIGURATION FOR ATTACK ANGLE, ALPHA = 35

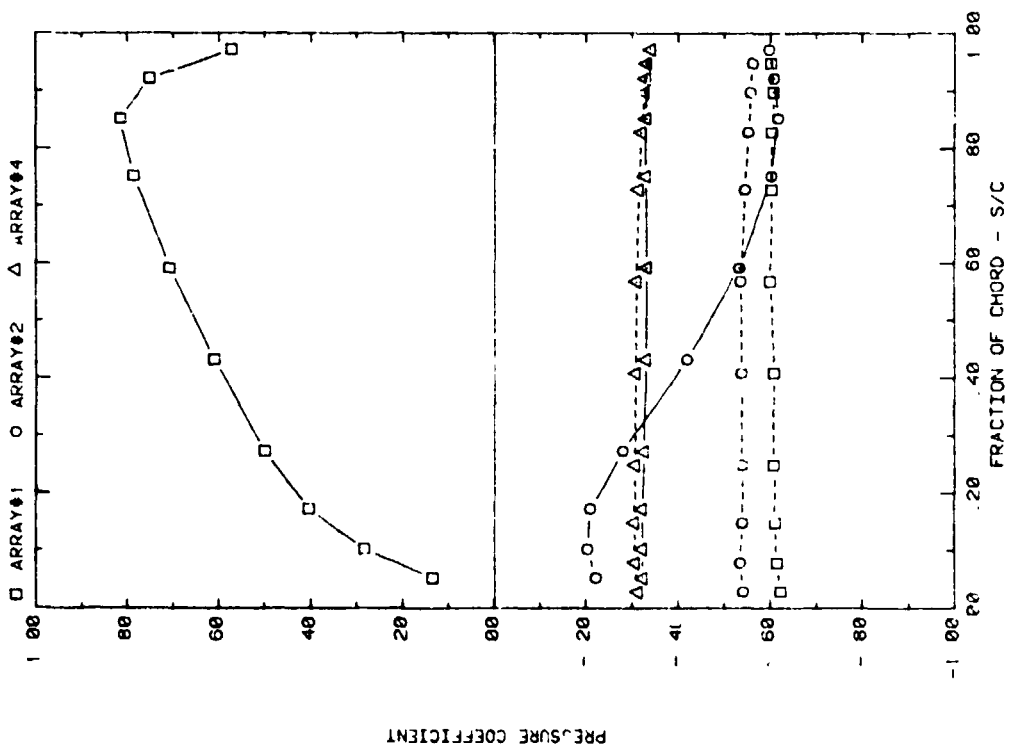


FRONT AND BACK PRESSURES ON VARIOUS ARRAYS FOR SEPARATION = 2C
EFFECT OF ARRAY CONFIGURATION FOR ATTACK ANGLE, ALPHA = 16C

Plot 1-3. (Continued)

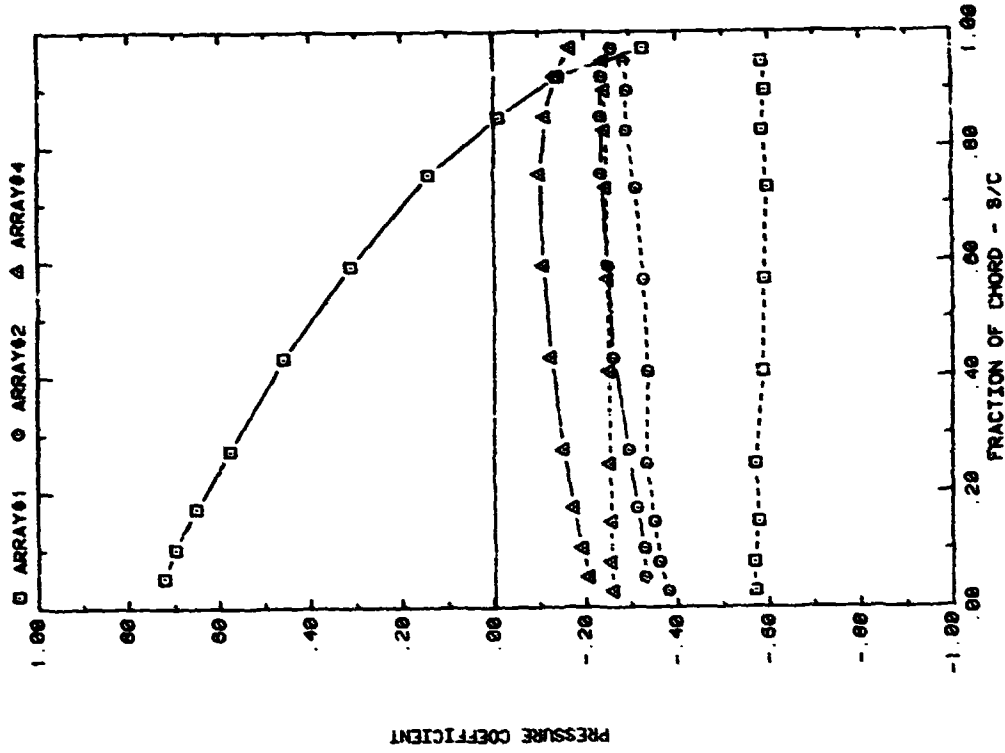


FRONT AND BACK PRESSURES ON VARIOUS ARRAYS FOR SEPARATION = 3C
EFFECT OF ARRAY CONFIGURATION FOR ATTACK ANGLE, ALPHA = 120



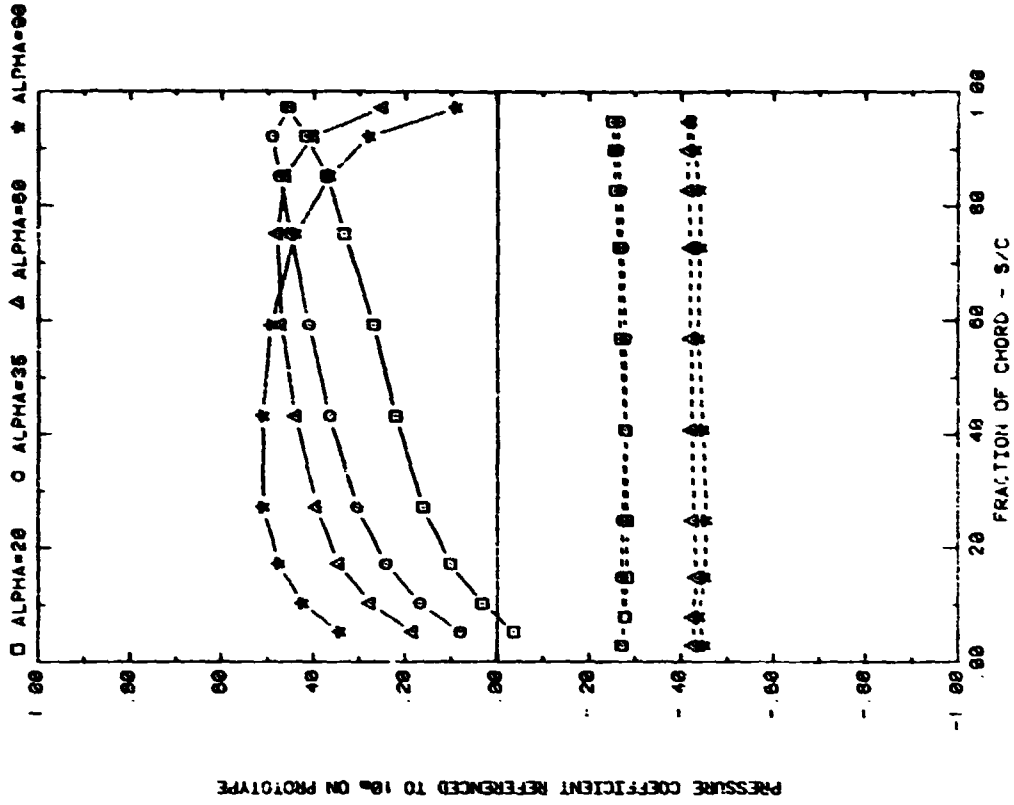
FRONT AND BACK PRESSURES ON VARIOUS ARRAYS FOR SEPARATION = 3C
EFFECT OF ARRAY CONFIGURATION FOR ATTACK ANGLE, ALPHA = 60

Plot 2-1-3. (Continued)

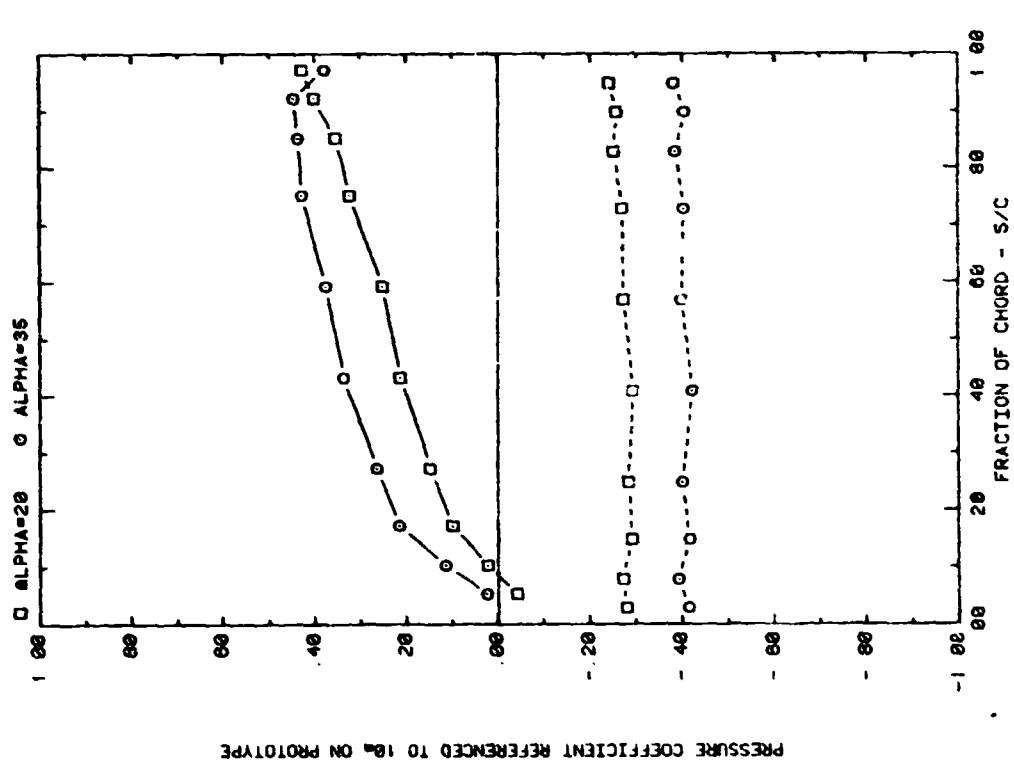


FRONT AND BACK PRESSURES ON VARIOUS ARRAYS FOR SEPARATION = 3C
EFFECT OF ARRAY CONFIGURATION FOR ATTACK ANGLE, ALPHA = 145

Plot 2-1-3. (Concluded)

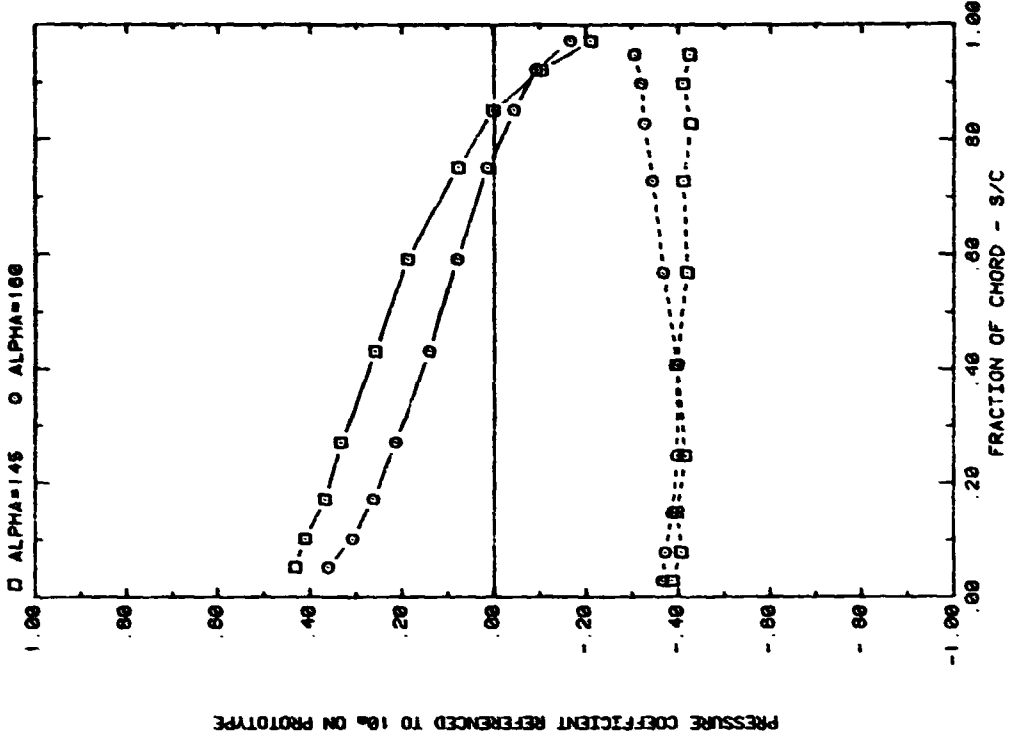


FRONT AND BACK PRESSURES ON ARRAY #1 IN BOUNDARY LAYER
EFFECT OF ATTACK ANGLE FOR SPACING = 2C

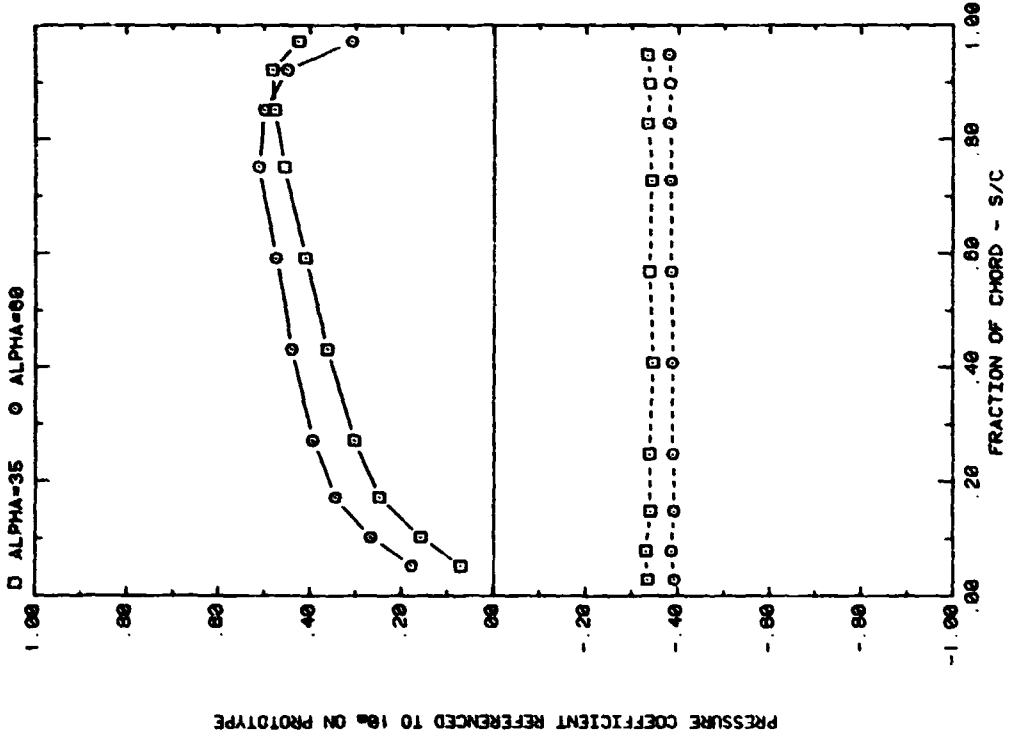


FRONT AND BACK PRESSURES ON ARRAY #1 IN BOUNDARY LAYER
EFFECT OF ATTACK ANGLE FOR SPACING = 1.5C

Plot 2-2-1. Multiple Arrays without Fence, Nonuniform Flow
Study Effect of Angle of Attack

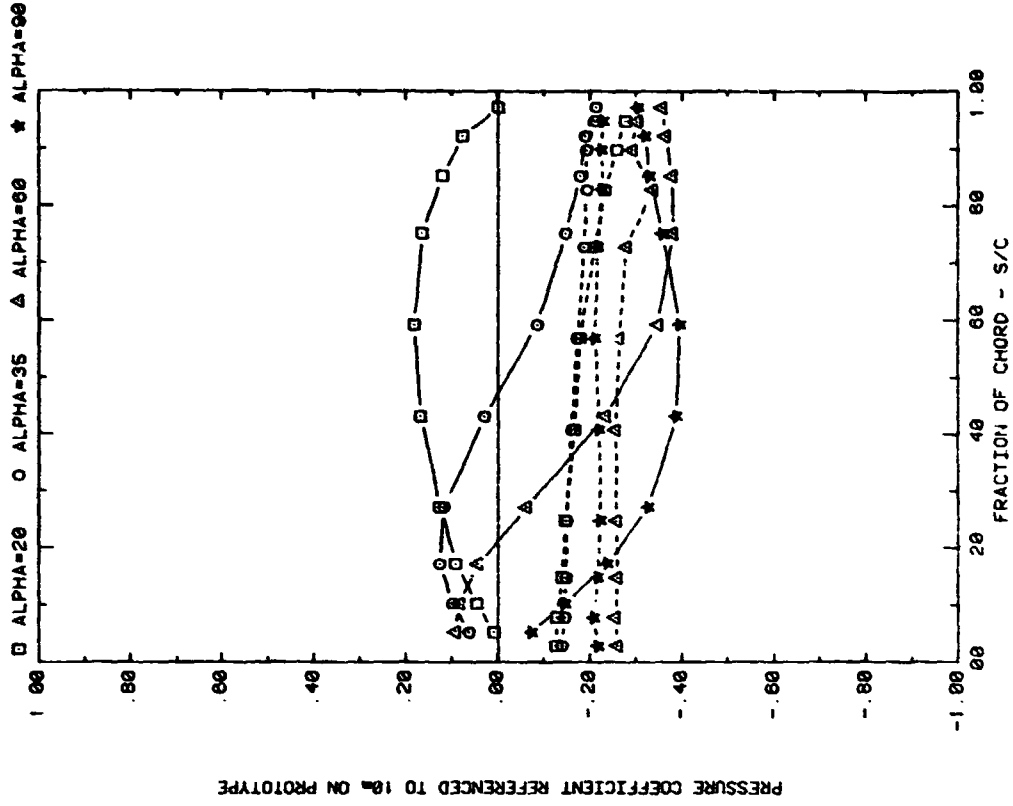


FRONT AND BACK PRESSURES ON ARRAY #1 IN BOUNDARY LAYER
EFFECT OF ATTACK ANGLE FOR SPACING = 1.5C

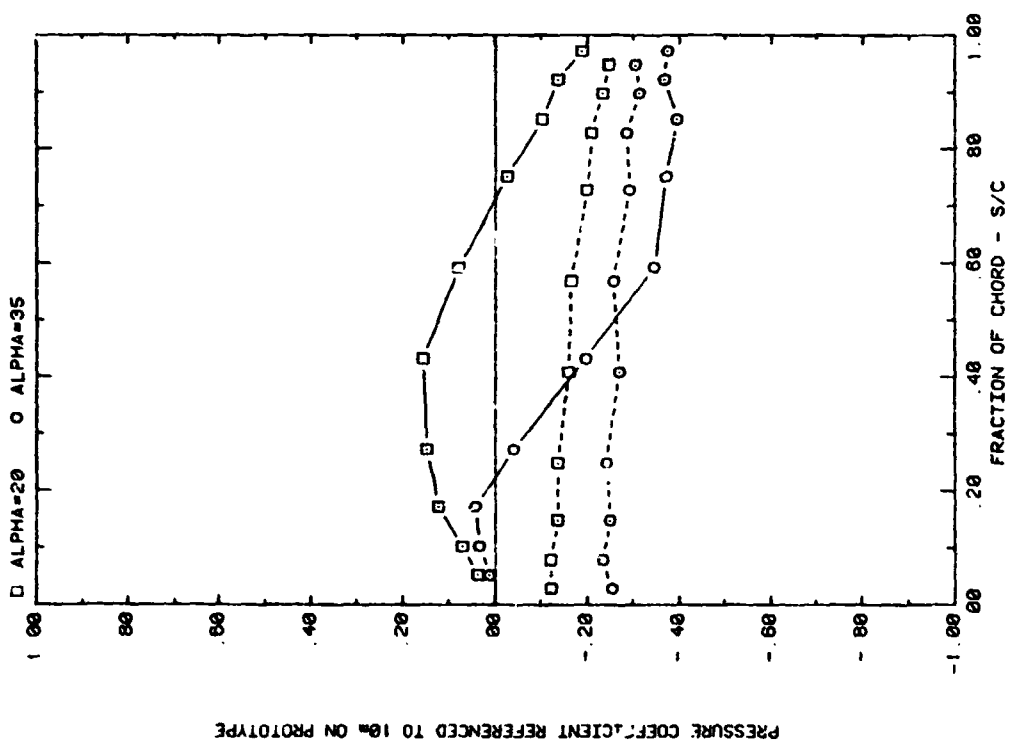


FRONT AND BACK PRESSURES ON ARRAY #1 IN BOUNDARY LAYER
EFFECT OF ATTACK ANGLE FOR SPACING = 3C

Plot 2-2-1. (Continued)

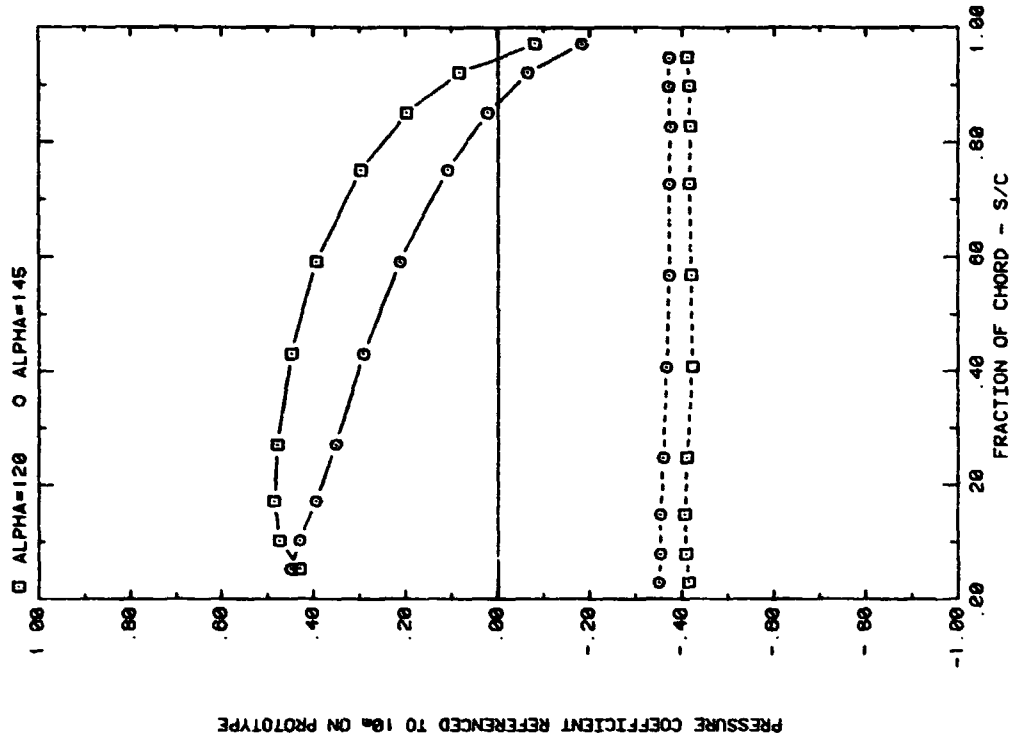


FRONT AND BACK PRESSURES ON ARRAY #2 IN BOUNDARY LAYER
EFFECT OF ATTACK ANGLE FOR SPACING = 2C

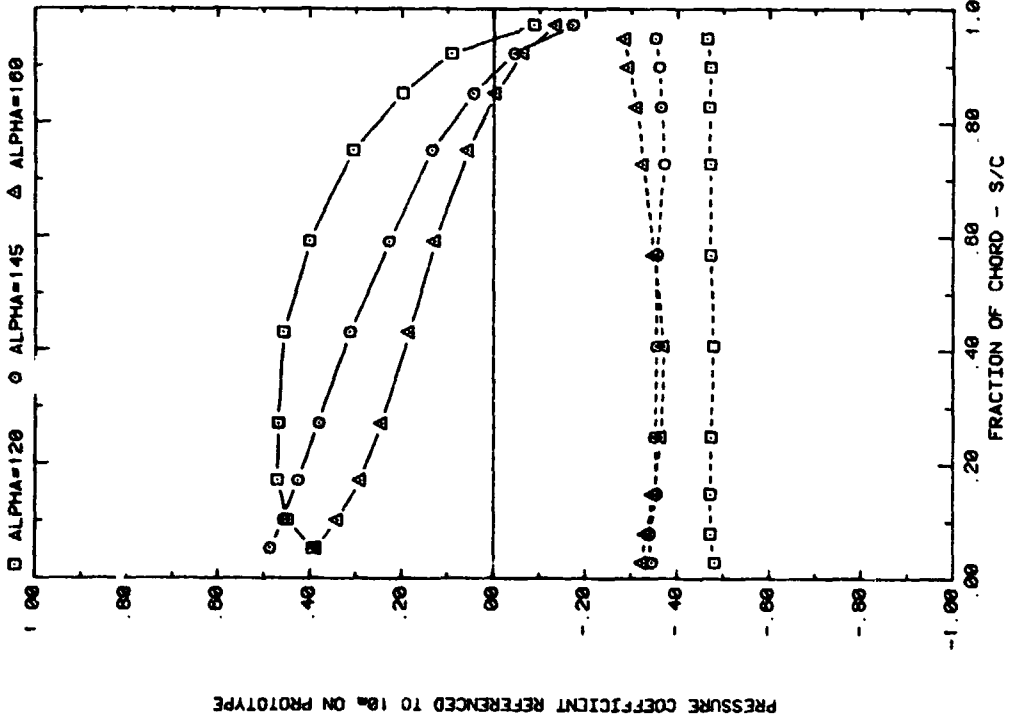


FRONT AND BACK PRESSURES ON ARRAY #2 IN BOUNDARY LAYER
EFFECT OF ATTACK ANGLE FOR SPACING = 1.5C

Plot 2-2-1. (Continued)

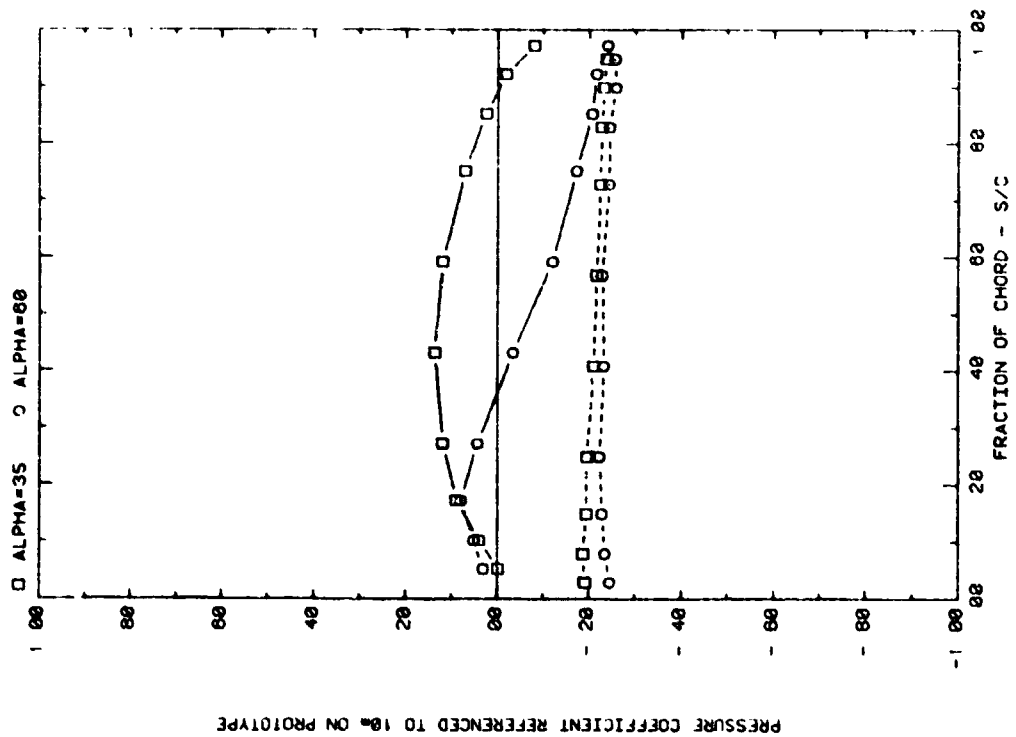


FRONT AND BACK PRESSURES ON ARRAY #1 IN BOUNDARY LAYER
EFFECT OF ATTACK ANGLE FOR SPACING = 3C

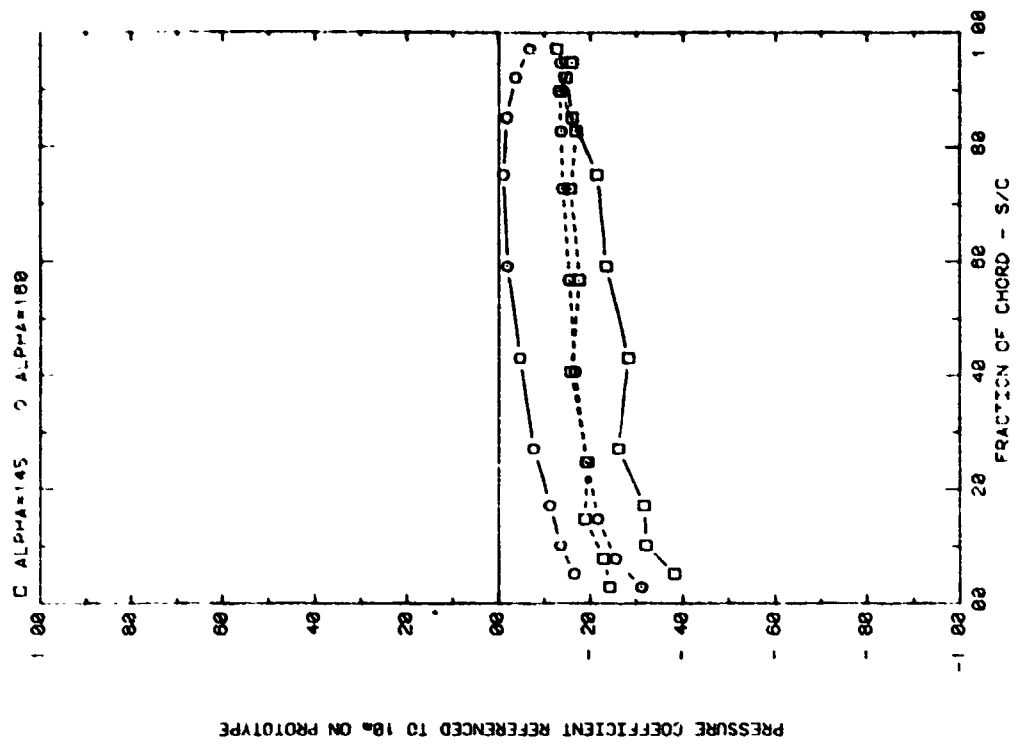


FRONT AND BACK PRESSURES ON ARRAY #1 IN BOUNDARY LAYER
EFFECT OF ATTACK ANGLE FOR SPACING = 2C

Plot 2-2-1. (Continued)

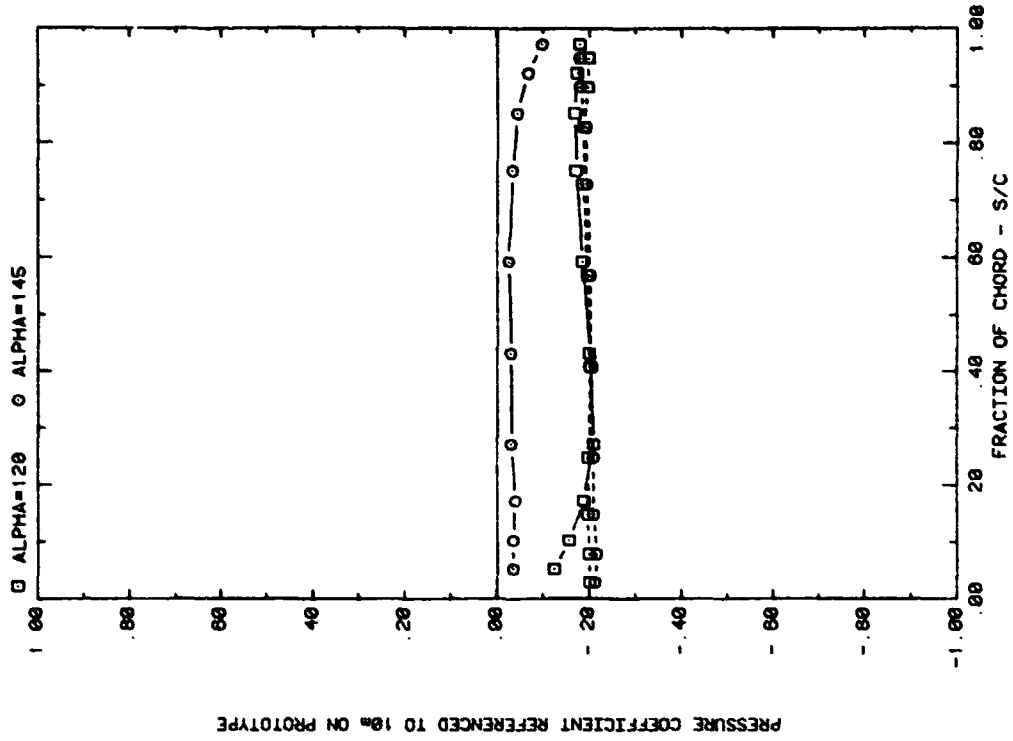


FRONT AND BACK PRESSURES ON ARRAY #2 IN BOUNDARY LAYER
EFFECT OF ATTACK ANGLE FOR SPACING = 3C

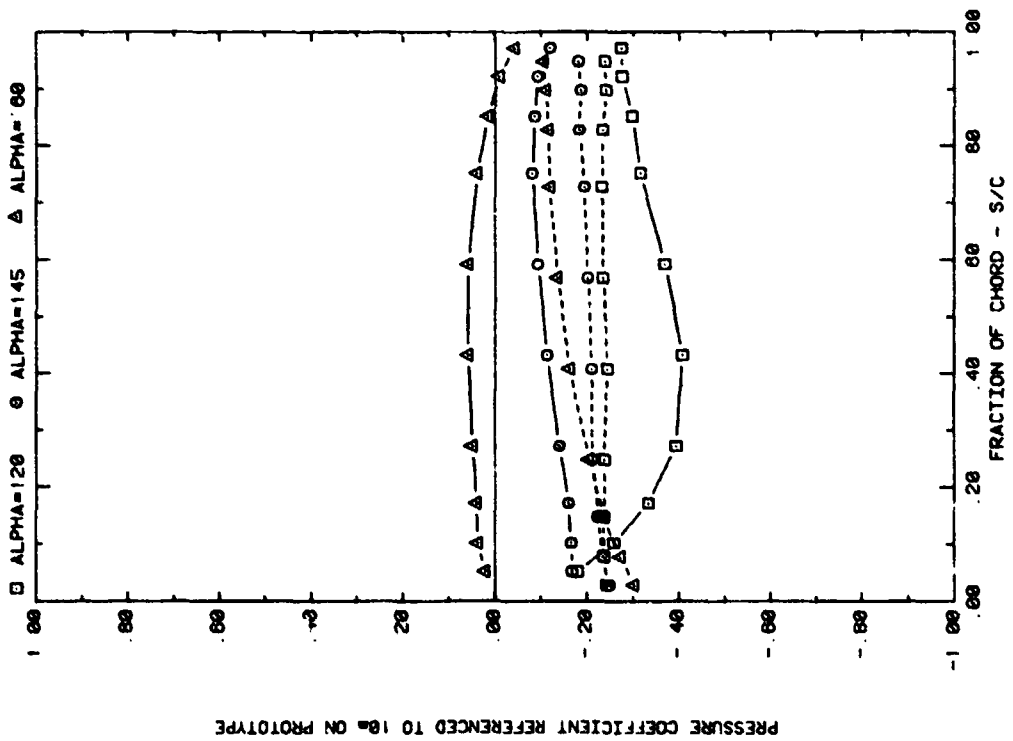


FRONT AND BACK PRESSURES ON ARRAY #2 IN BOUNDARY LAYER
EFFECT OF ATTACK ANGLE FOR SPACING = 15C

Plot 2-2-1. (Continued)

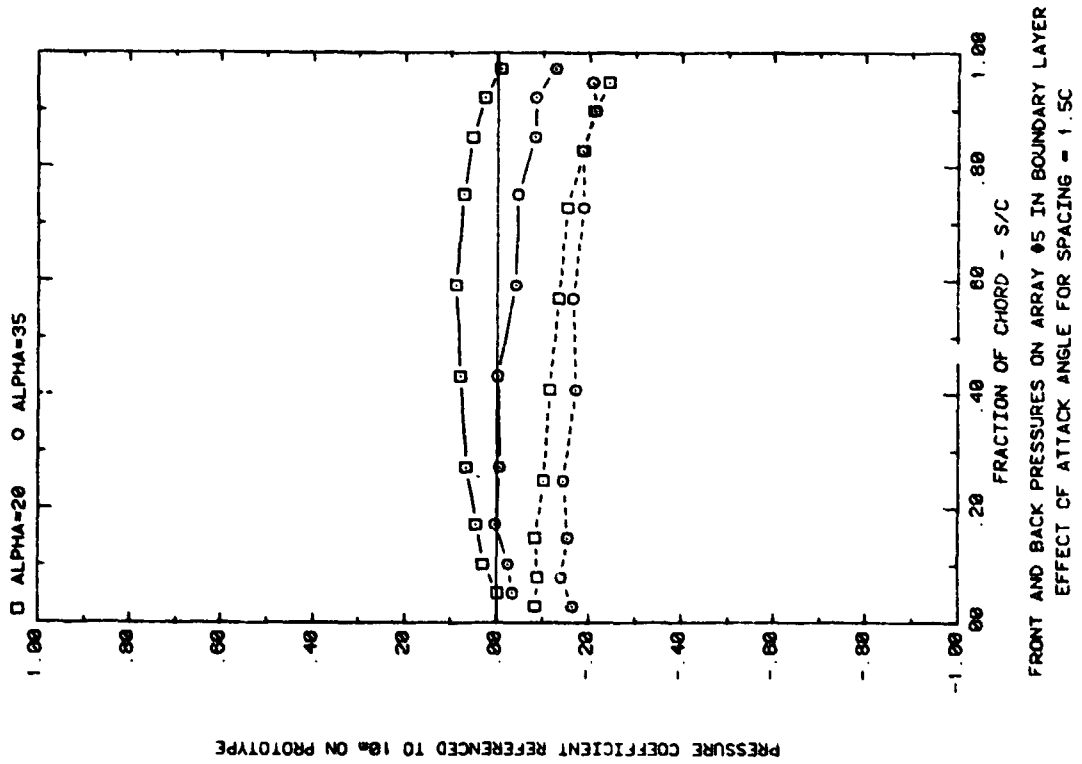
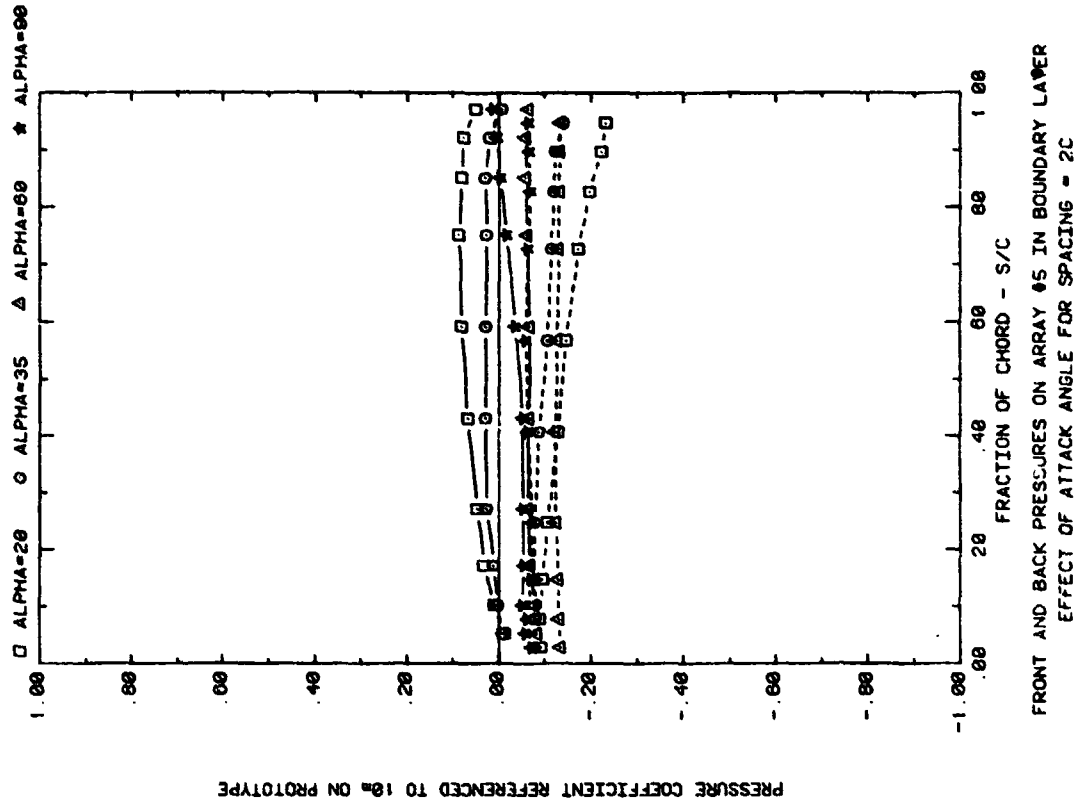


FRONT AND BACK PRESSURES ON ARRAY #2 IN BOUNDARY LAYER
EFFECT OF ATTACK ANGLE FOR SPACING = 3C

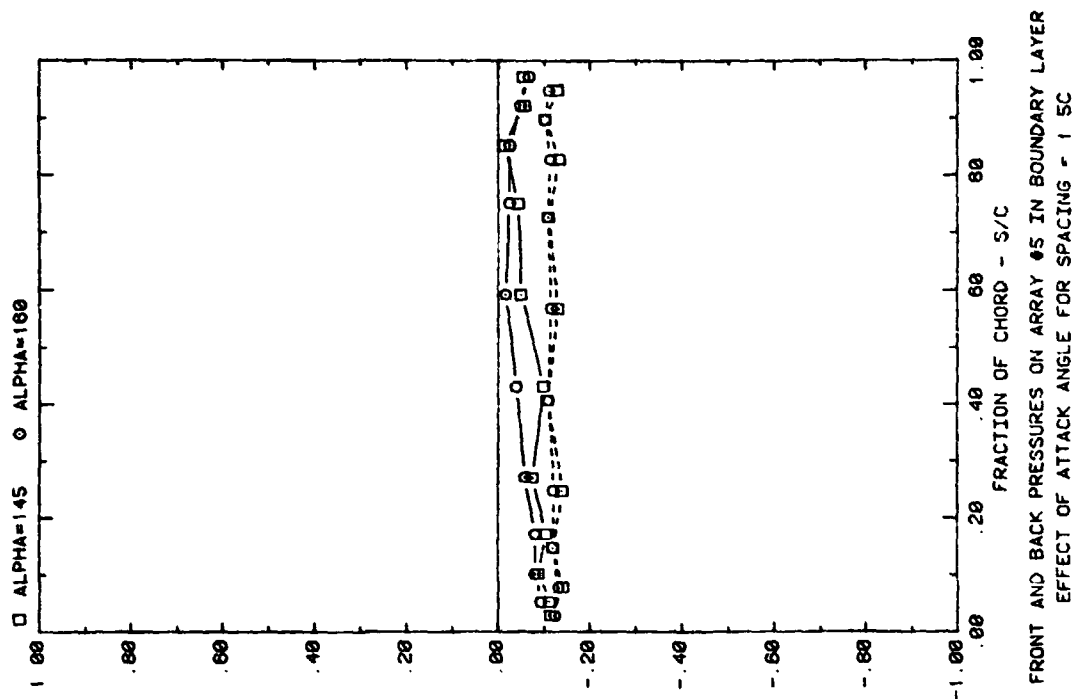


FRONT AND BACK PRESSURES ON ARRAY #2 IN BOUNDARY LAYER
EFFECT OF ATTACK ANGLE FOR SPACING = 2C

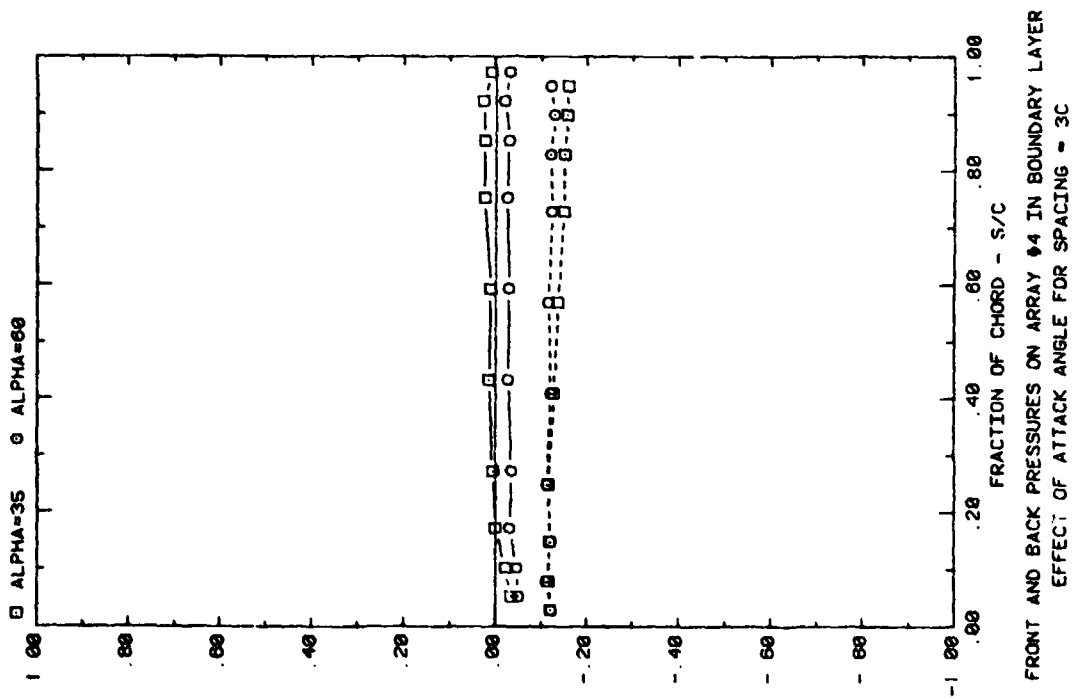
Plot 2-2-1. (Continued)



Plot 2-2-1. (Continued)

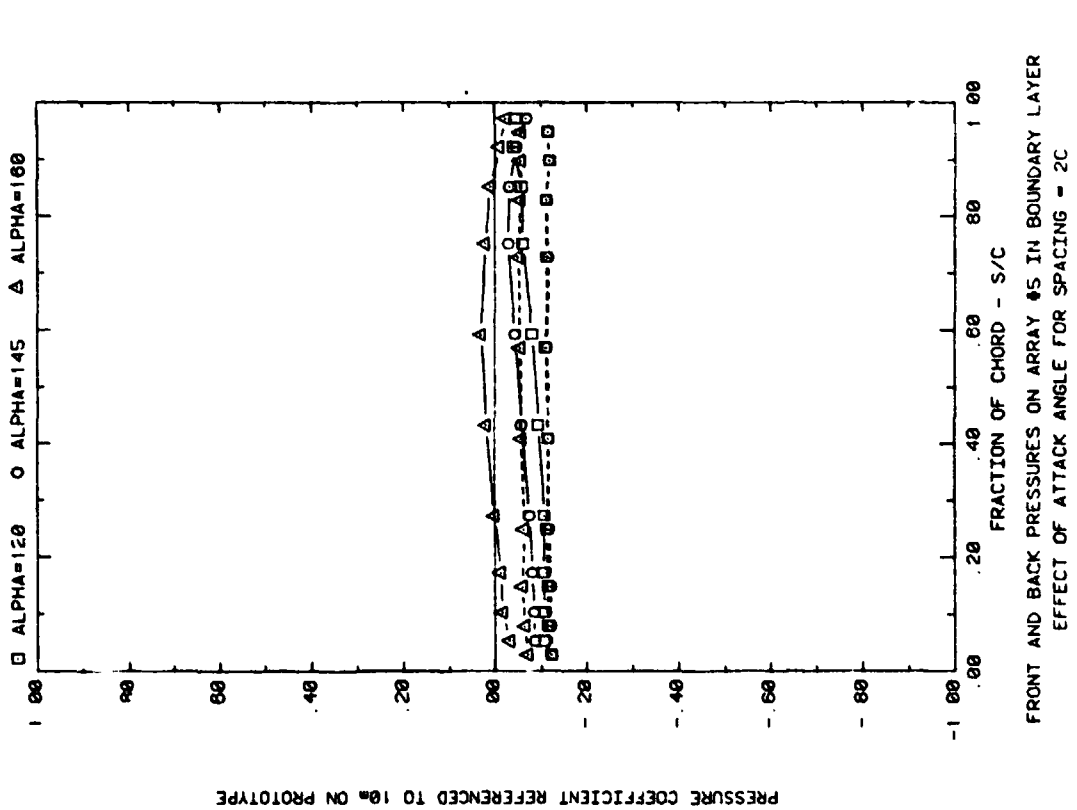
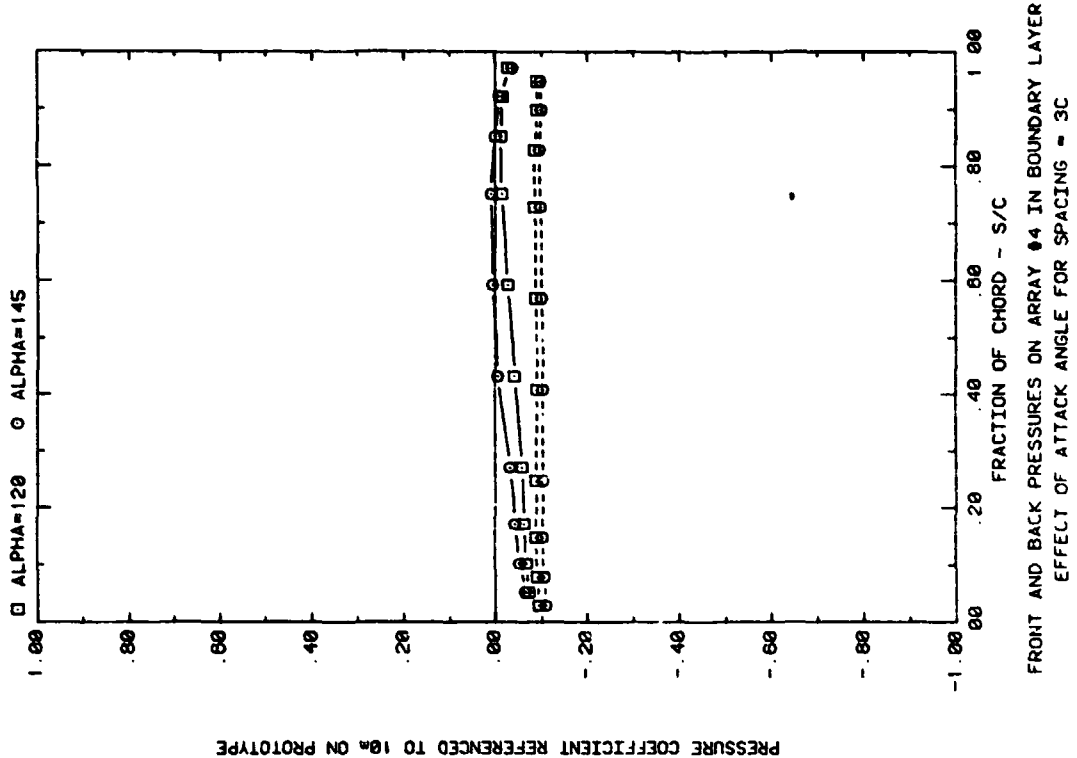


PRESSURE COEFFICIENT REFERENCED TO 10% ON PROTOTYPE

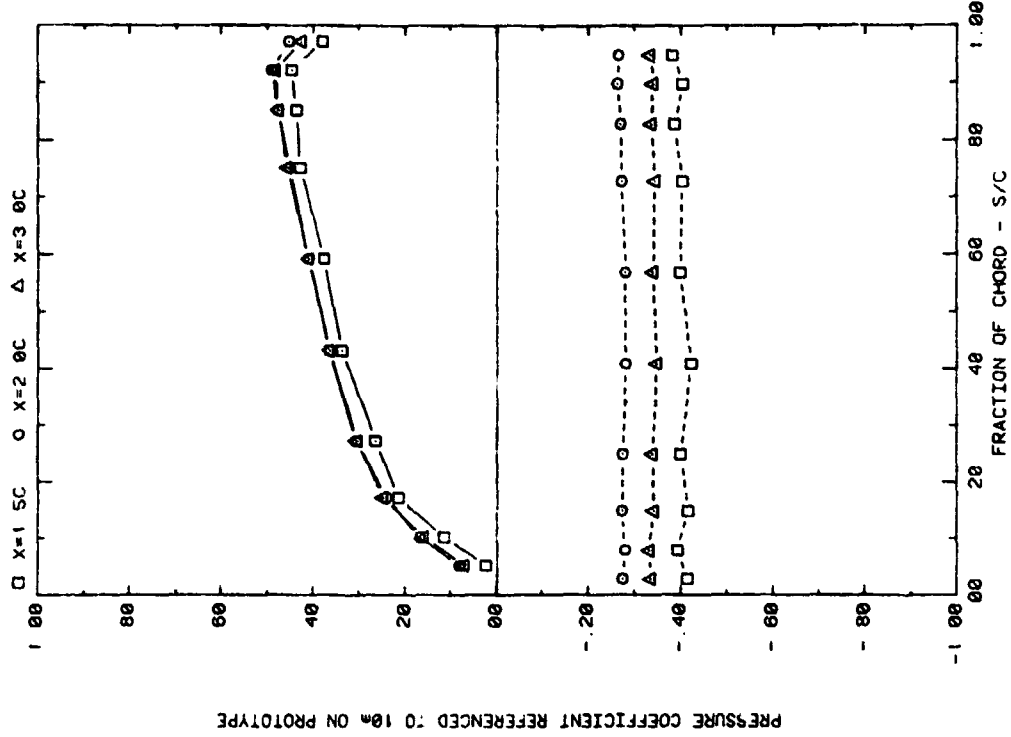


PRESSURE COEFFICIENT REFERENCED TO 10% ON PROTOTYPE

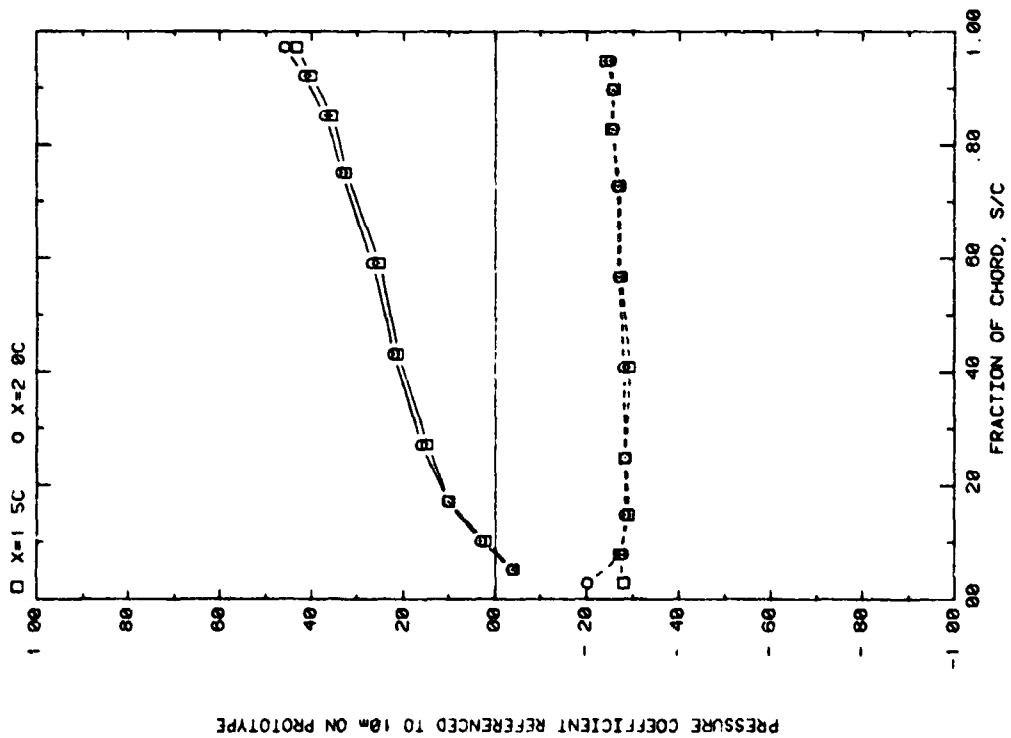
Plot 2-2-1. (Continued)



Plot 2-2-1. (Concluded)

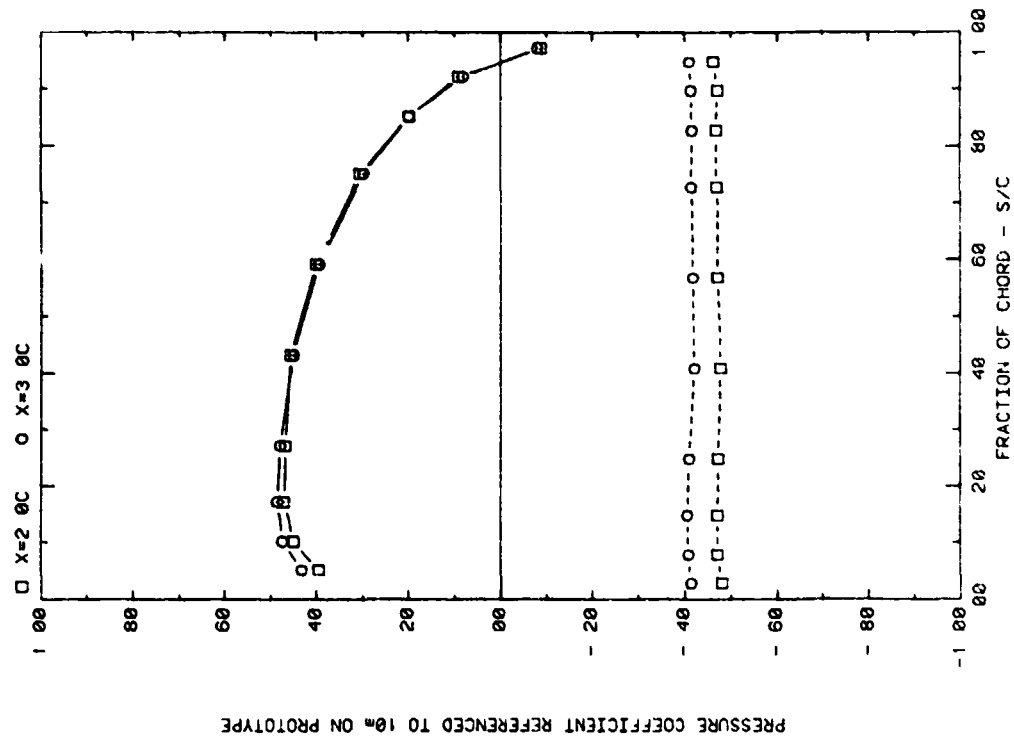


FRONT AND BACK PRESSURES ON ARRAY #1 IN BOUNDARY LAYER
EFFECT OF SEPARATION (X) ON ATTACK ANGLE 35, H/C = 0.25

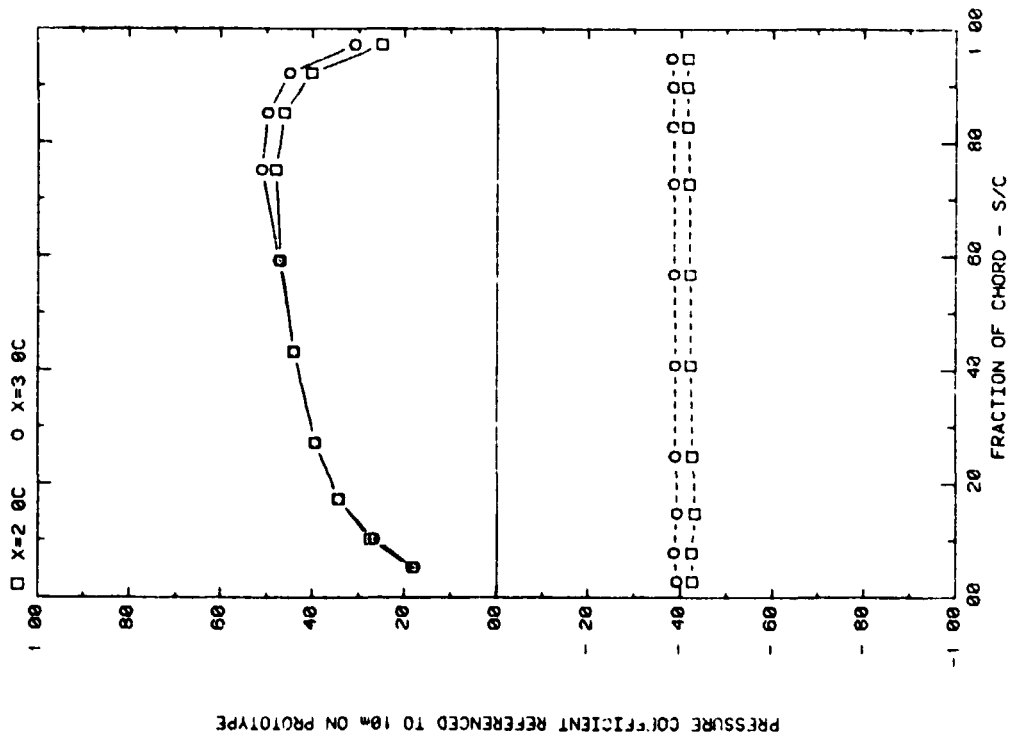


FRONT AND BACK PRESSURES ON ARRAY #1 IN BOUNDARY LAYER
EFFECT OF SEPARATION (X) ON ATTACK ANGLE 20, H/C = 0.25

Plot 2-2-2. Multiple Arrays without Fence, Nonuniform Flow Study
Effect of Separation Distance

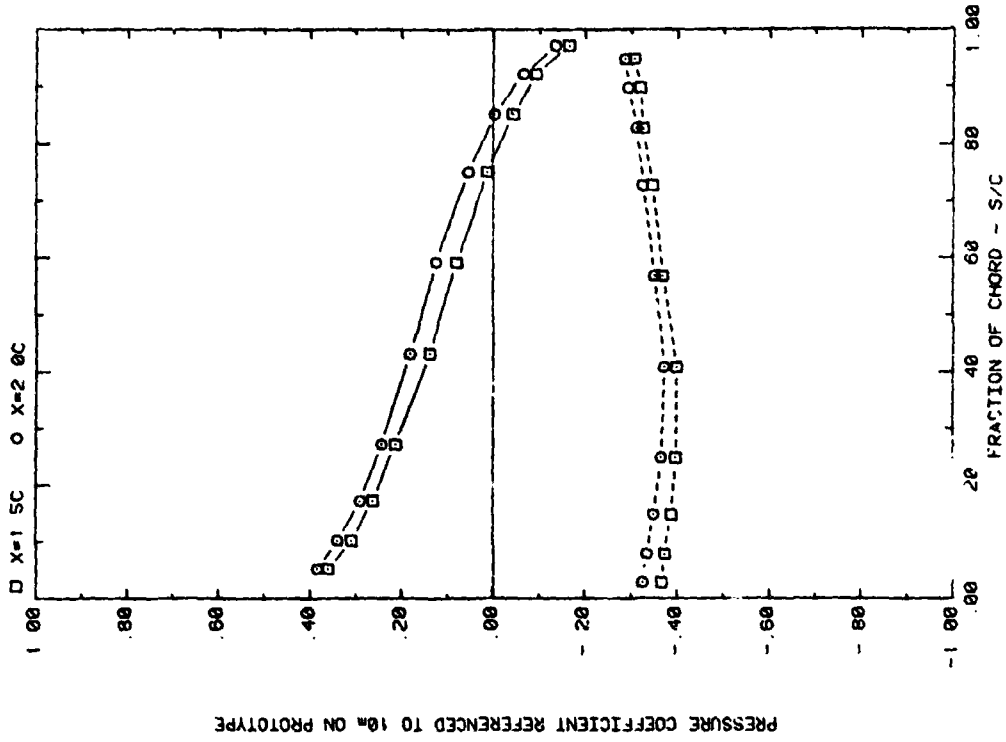


FRONT AND BACK PRESSURES ON ARRAY #1 IN BOUNDARY LAYER
EFFECT OF SEPARATION (Y) ON ATTACK ANGLE 120, H/C = 0.25

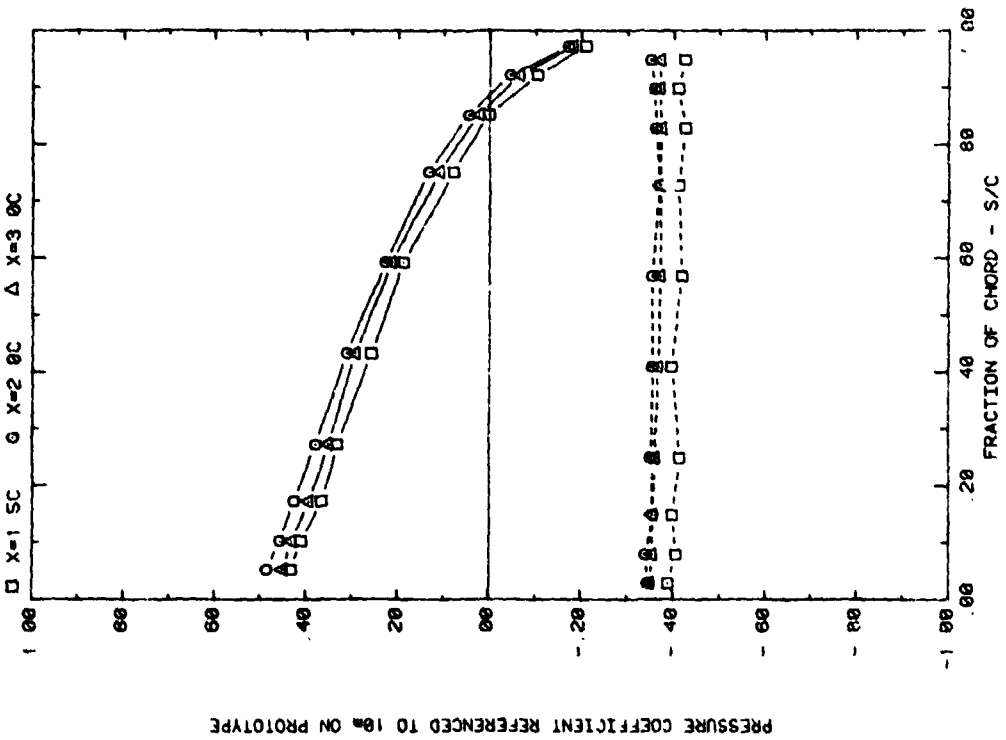


FRONT AND BACK PRESSURES ON ARRAY #1 IN BOUNDARY LAYER
EFFECT OF SEPARATION (Y) ON ATTACK ANGLE 60, H/C = 0.25

Plot 2-2-2. (Continued)

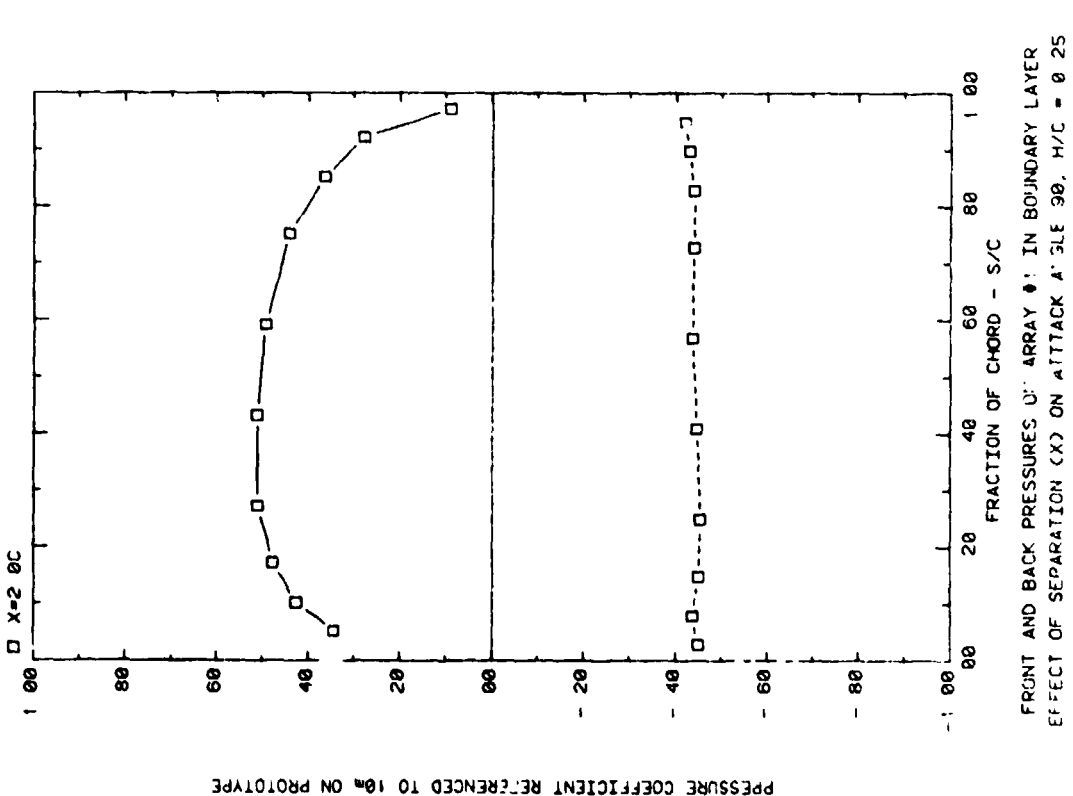
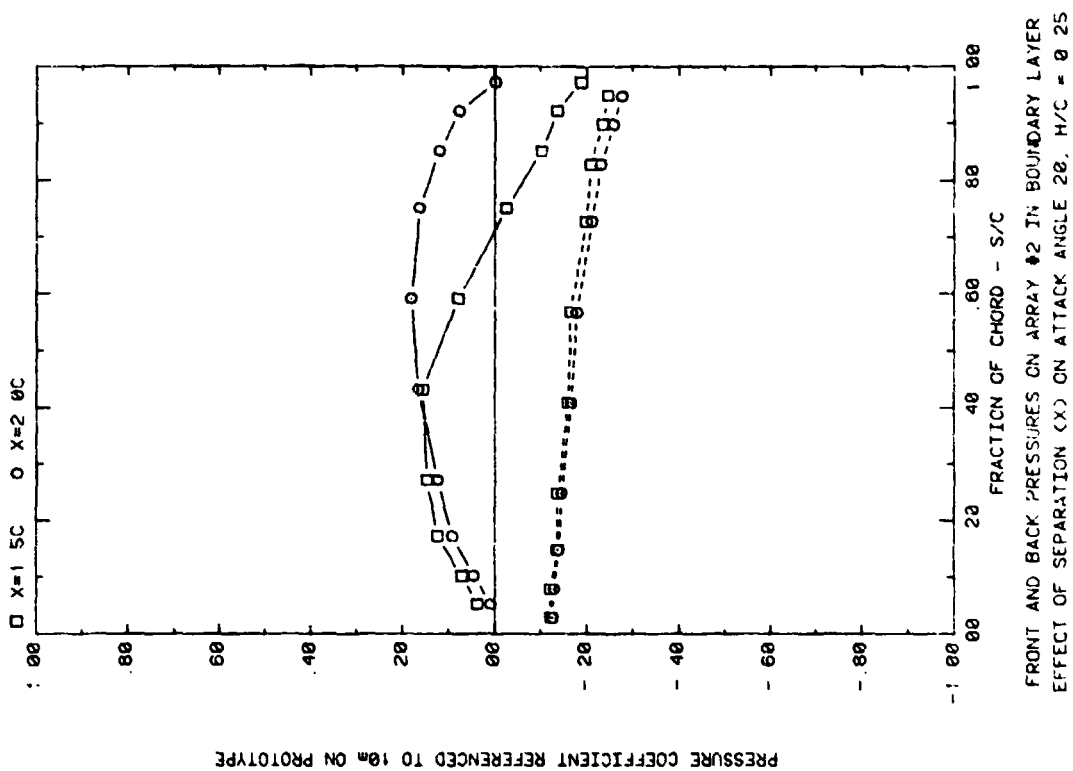


FRONT AND BACK PRESSURES ON ARRAY #1 IN BOUNDARY LAYER
EFFECT OF SEPARATION (X) ON ATTACK ANGLE 160, H/C = 0.25

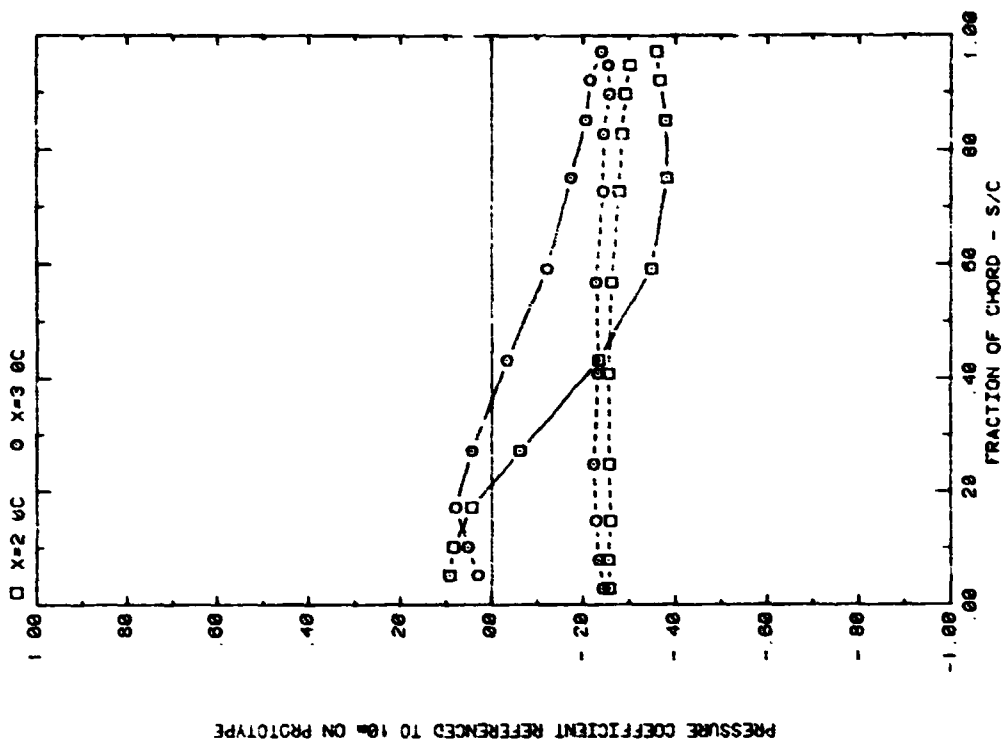


FRONT AND BACK PRESSURES ON ARRAY #1 IN BOUNDARY LAYER
EFFECT OF SEPARATION (X) ON ATTACK ANGLE 145, H/C = 0.25

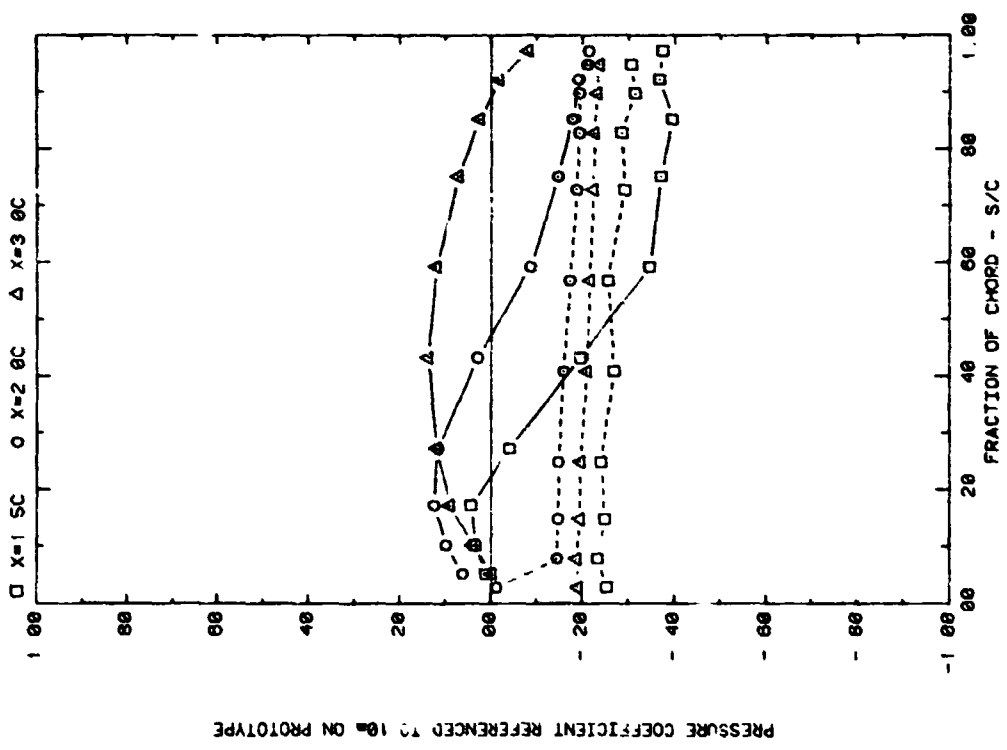
Plot 2-2-2. (Continued)



Plot 2-2-2. (Continued)

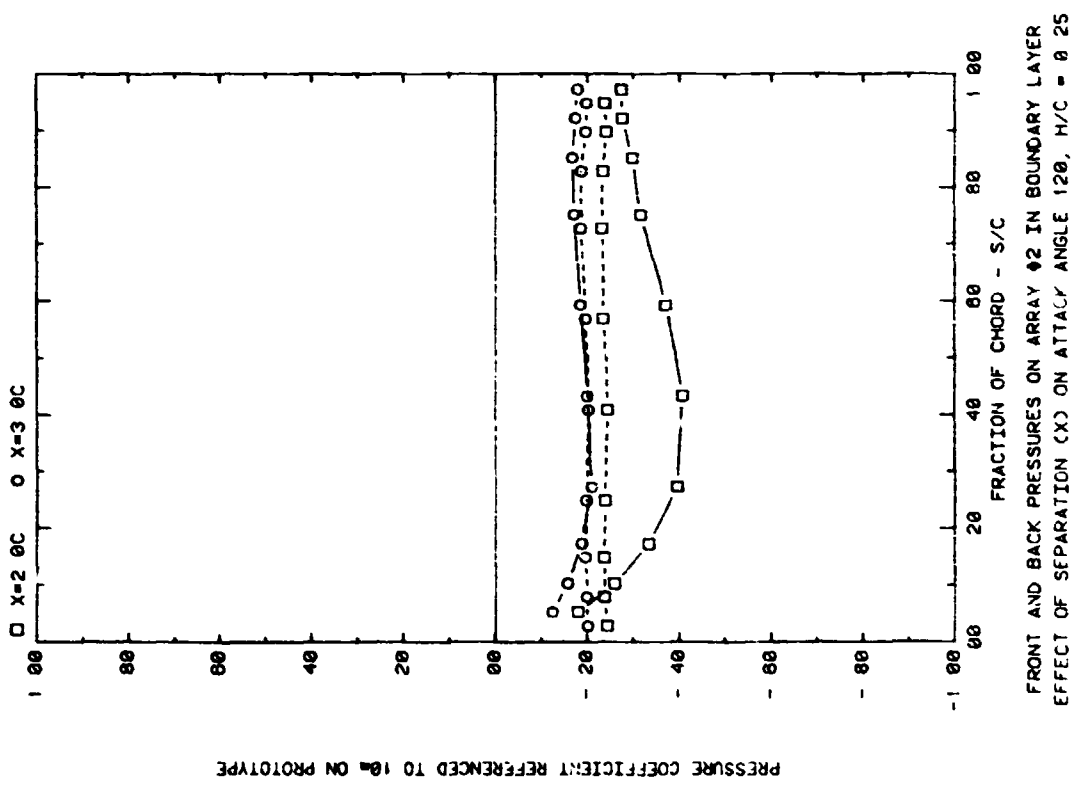
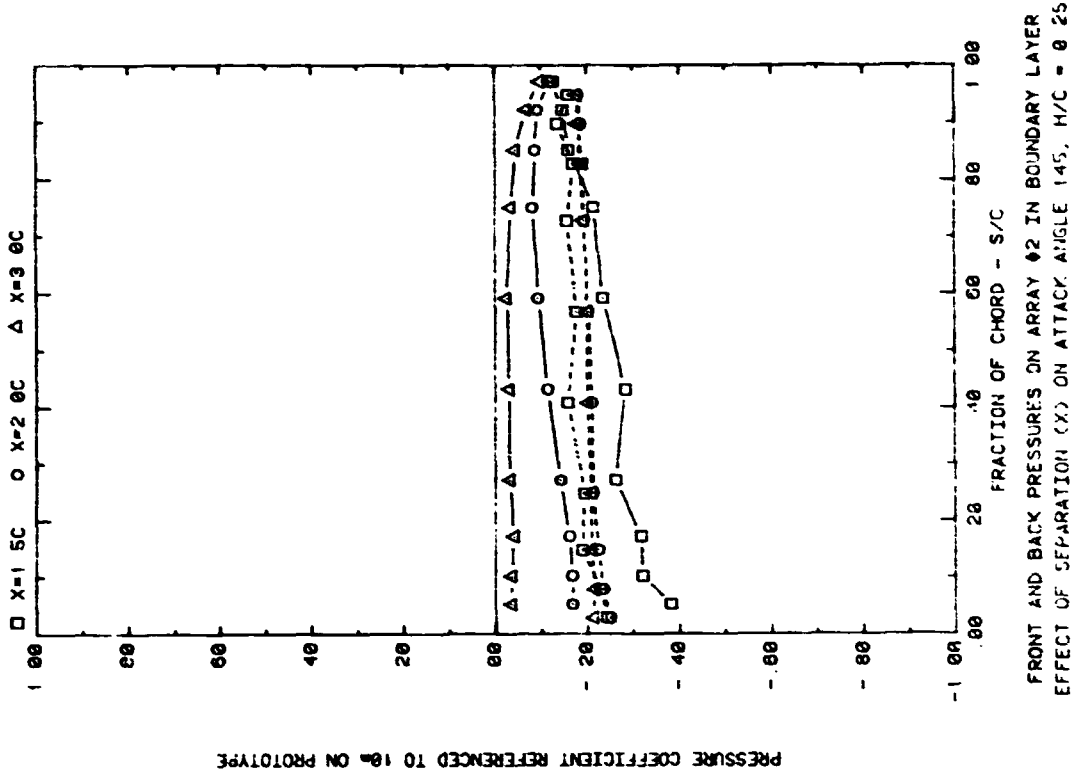


FRONT AND BACK PRESSURES ON ARRAY #2 IN BOUNDARY LAYER
EFFECT OF SEPARATION (X) ON ATTACK ANGLE 60, H/C = 0.25

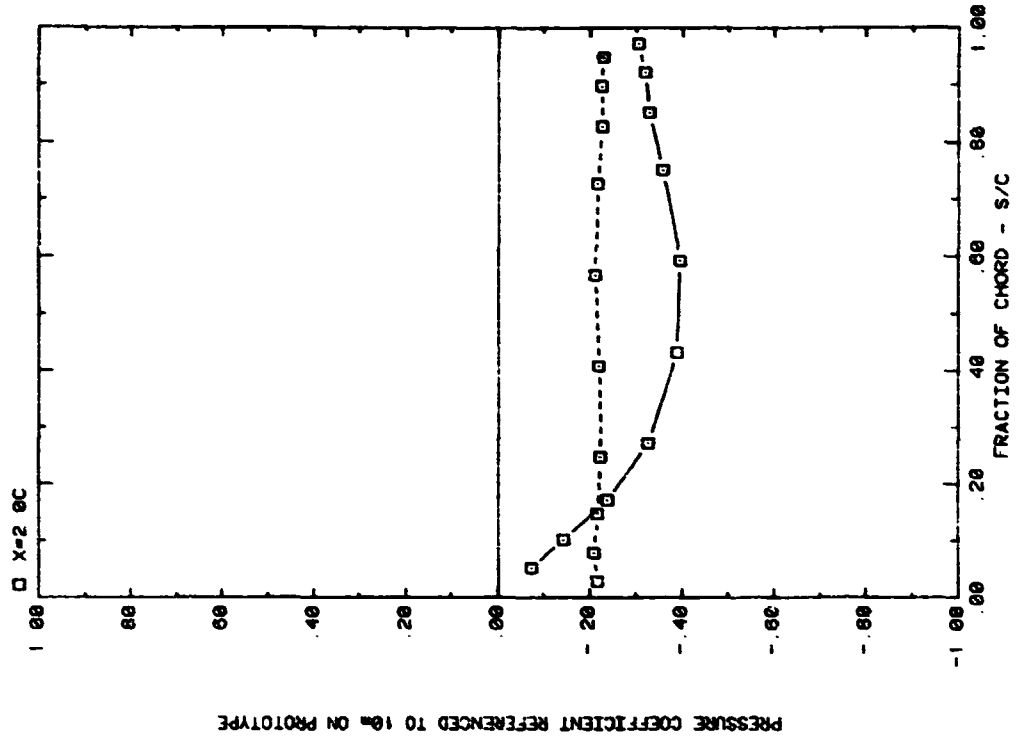


FRONT AND BACK PRESSURES ON ARRAY #2 IN BOUNDARY LAYER
EFFECT OF SEPARATION (X) ON ATTACK ANGLE 35, H/C = 0.25

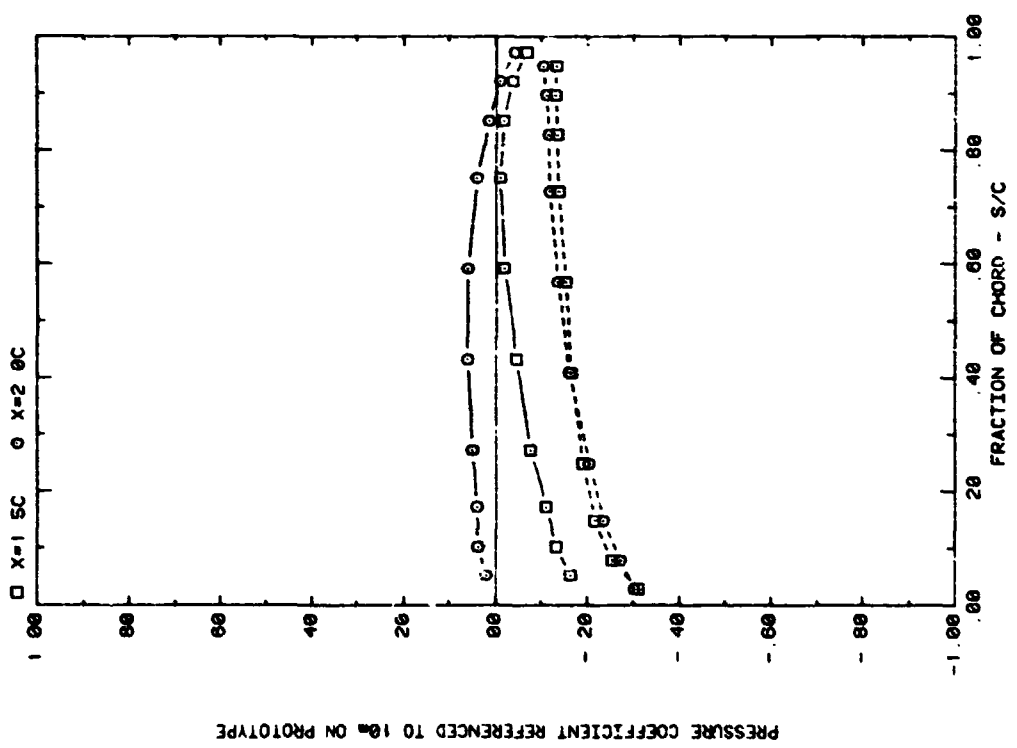
Plot 2-2-2. (Continued)



Plot 2-2-2. (Continued)

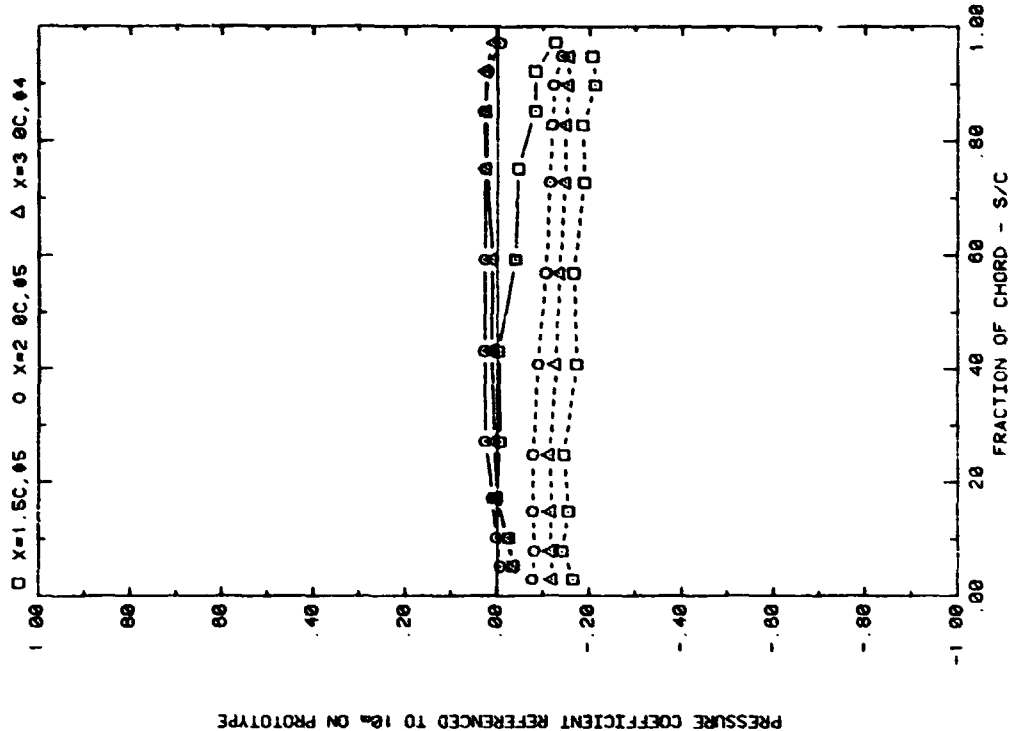


FRONT AND BACK PRESSURES ON ARRAY #2 IN BOUNDARY LAYER
EFFECT OF SEPARATION (X) ON ATTACK ANGLE 90, H/C = 0.25

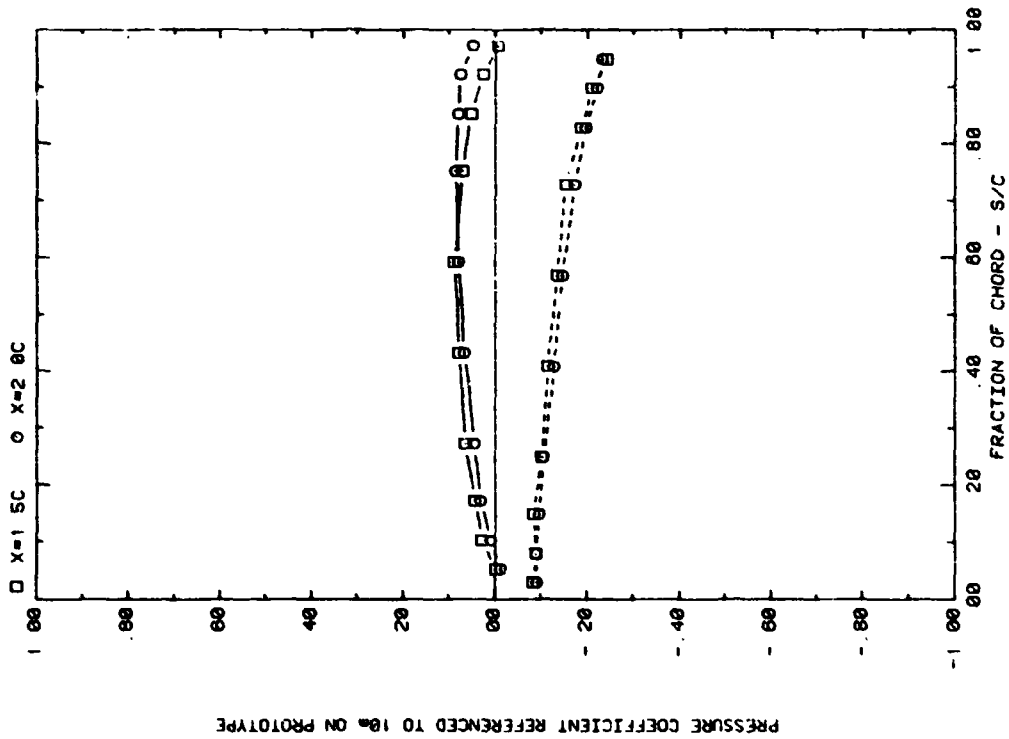


FRONT AND BACK PRESSURES ON ARRAY #2 IN BOUNDARY LAYER
EFFECT OF SEPARATION (X) ON ATTACK ANGLE 180, H/C = 0.25

Plot 2-2-2. (Continued)

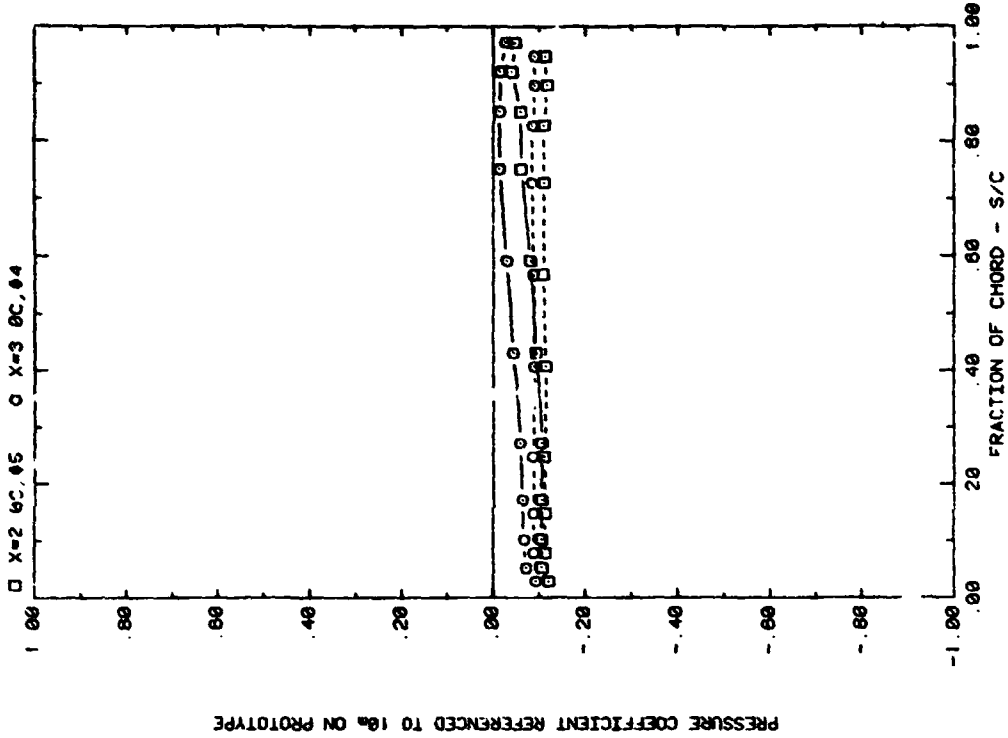


FRONT AND BACK PRESSURES ON ARRAY #5 IN BOUNDARY LAYER
EFFECT OF SEPARATION (X) ON ATTACK ANGLE 20, H/C = 0.25

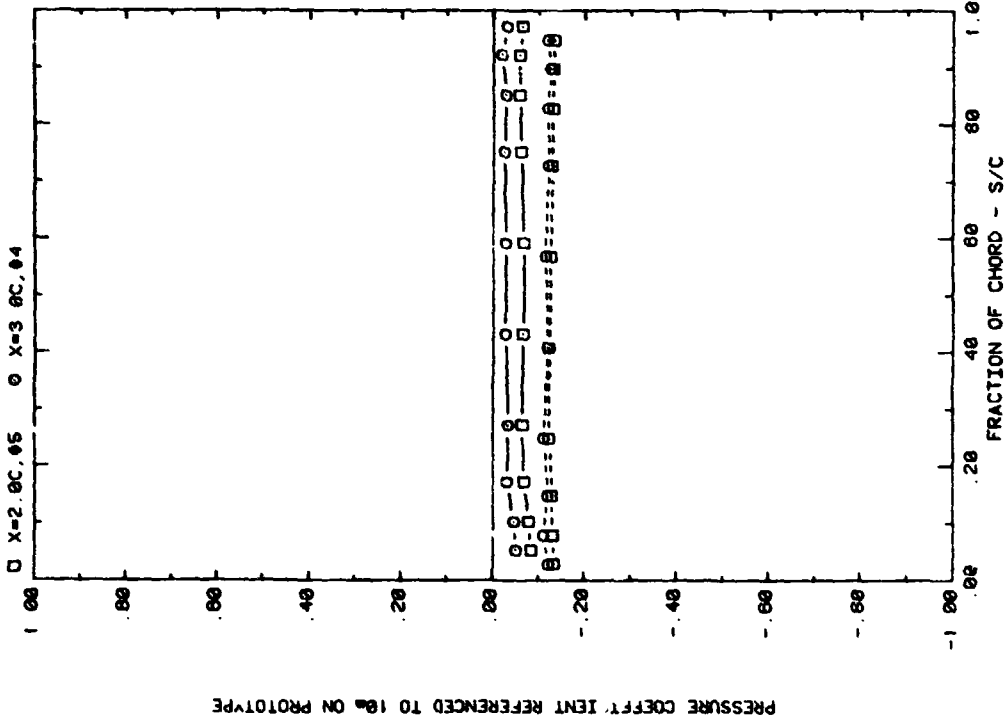


FRONT AND BACK PRESSURES ON ARRAY #5 IN BOUNDARY LAYER
EFFECT OF SEPARATION (X) ON ATTACK ANGLE 35, H/C = 0.25

Plot 2-2-2. (Continued)

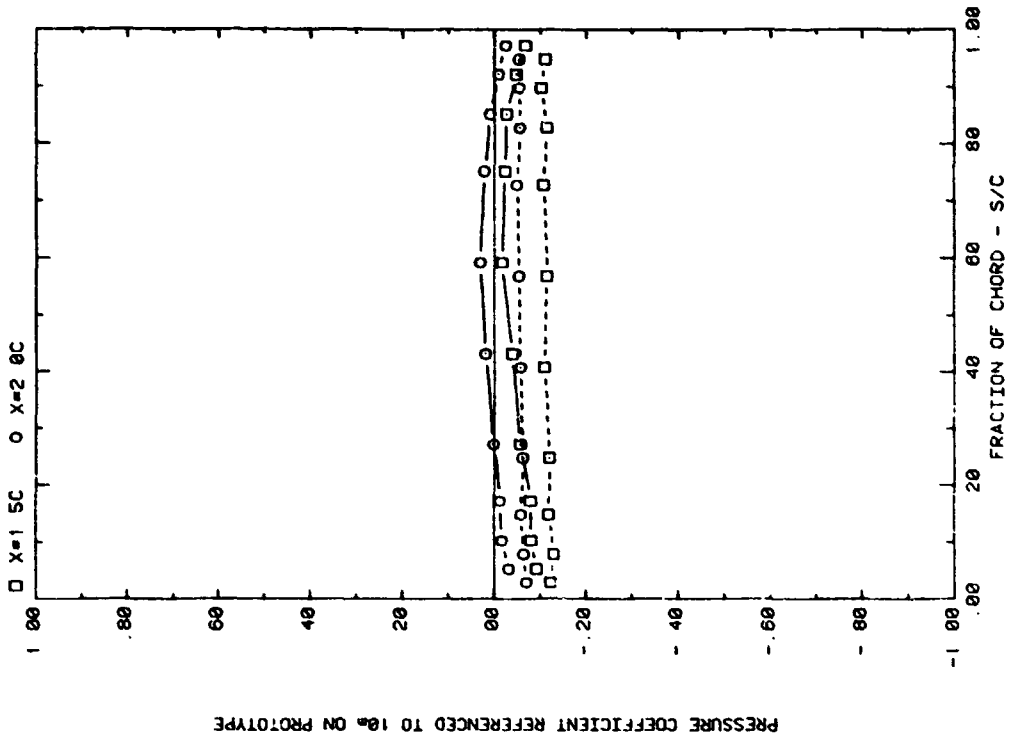


FRONT AND BACK PRESSURES ON ARRAY #4 OR #5 IN BOUNDARY LAYER
EFFECT OF SEPARATION (X) ON ATTACK ANGLE 120, H/C = 0.25

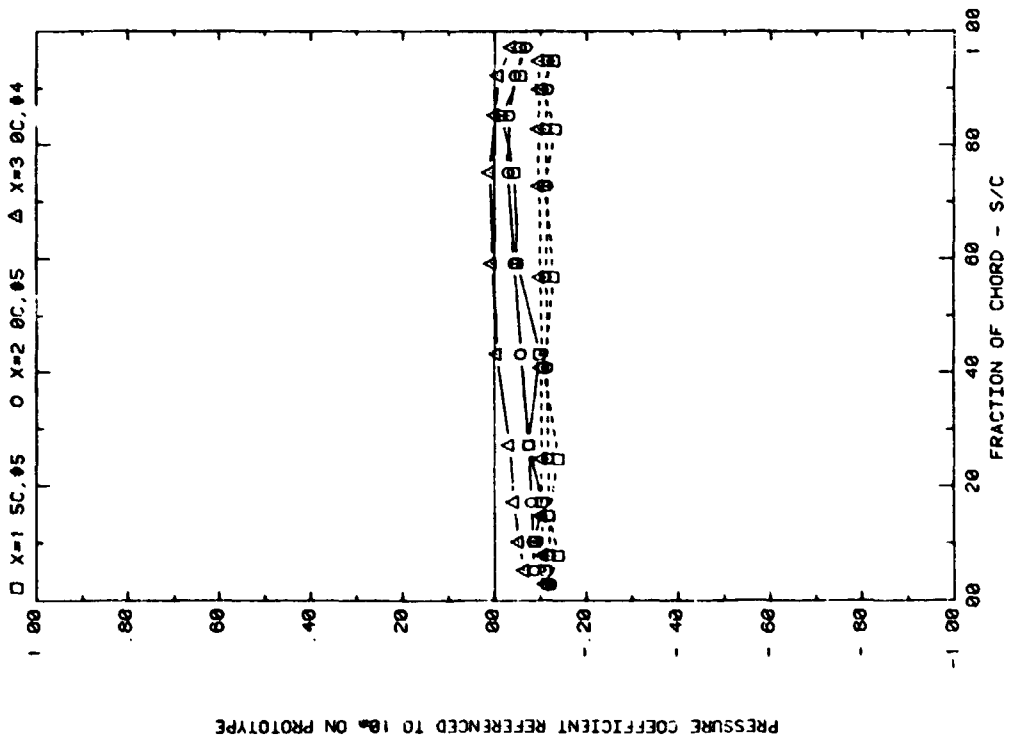


FRONT AND BACK PRESSURES ON ARRAY #4 OR #5 IN BOUNDARY LAYER
EFFECT OF SEPARATION (X) ON ATTACK ANGLE 60, H/C = 0.25

Plot 2-2-2. (Continued)

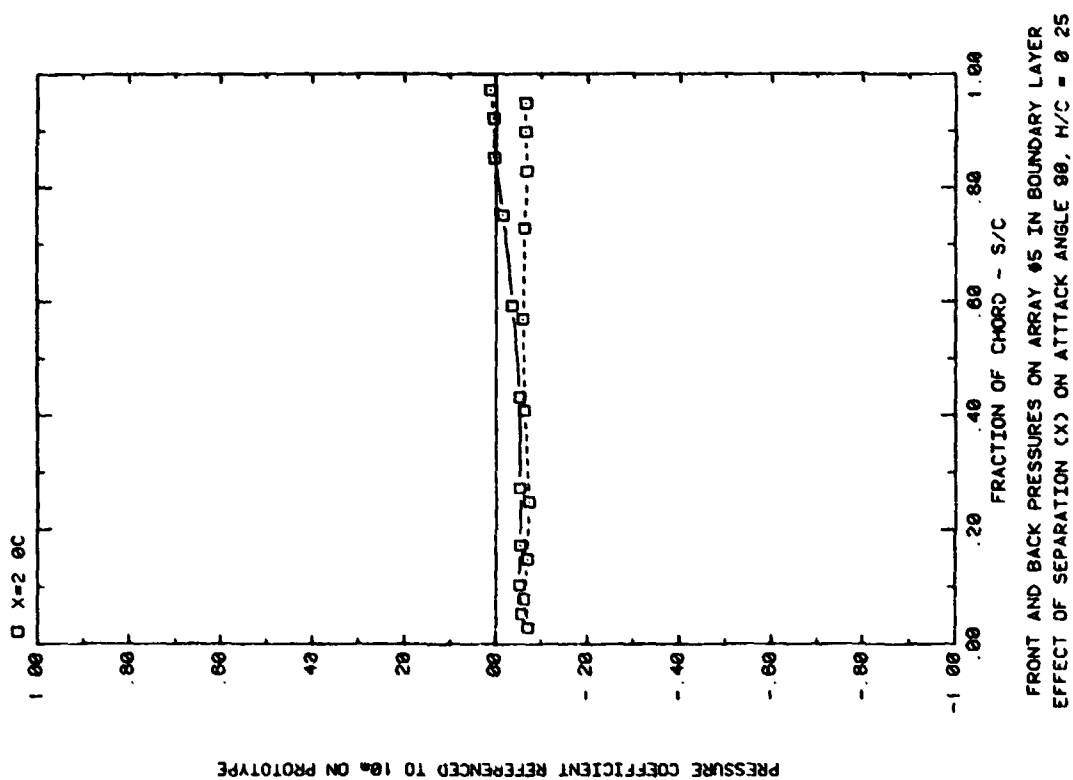


FRONT AND BACK PRESSURES ON ARRAY #5 IN BOUNDARY LAYER EFFECT OF SEPARATION (X) ON ATTACK ANGLE 160, H/C = 0.25

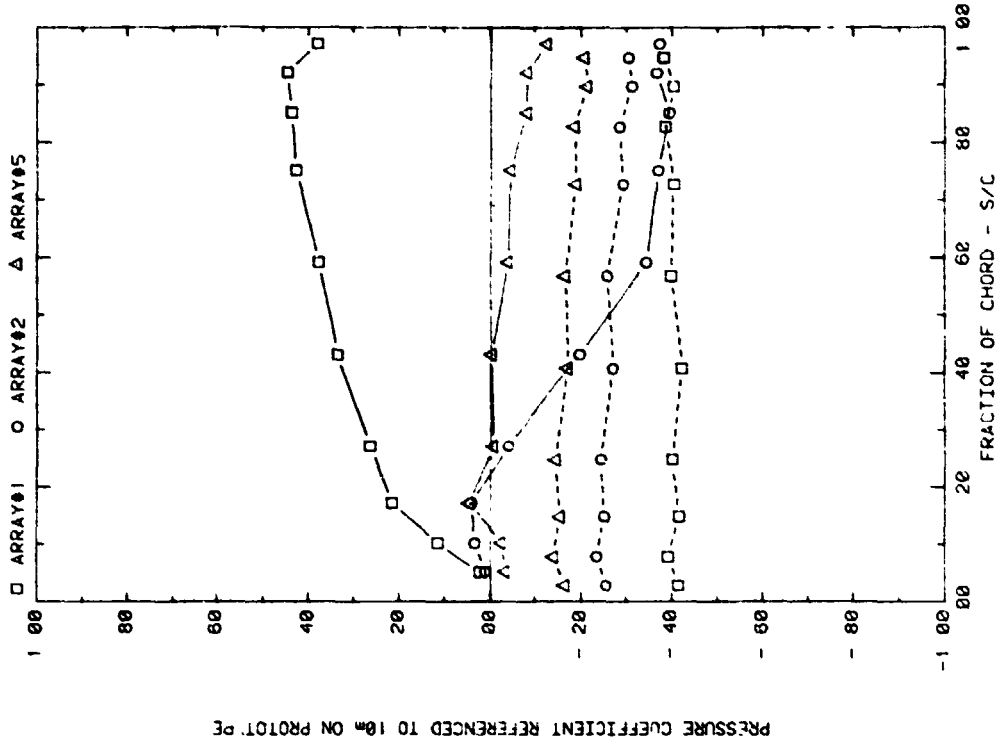


FRONT AND BACK PRESSURES ON ARRAY #4 OR #5 IN BOUNDARY LAYER EFFECT OF SEPARATION (X) ON ATTACK ANGLE 145, H/C = 0.25

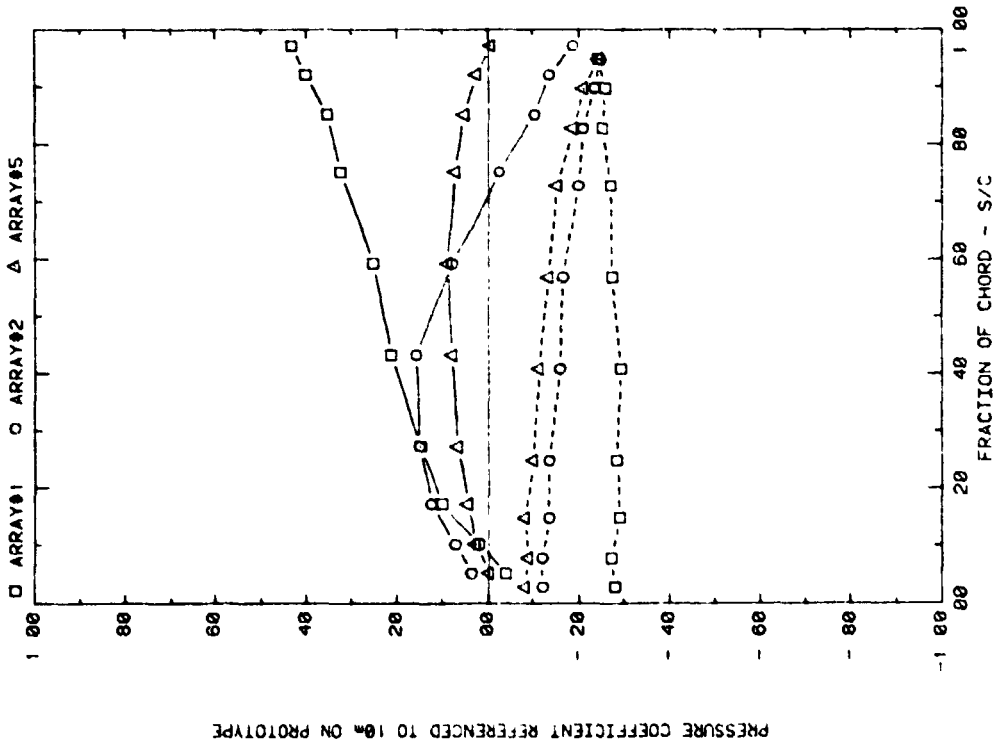
Plot 2-2-2. (Continued)



Plot 2-2-2. (Concluded)

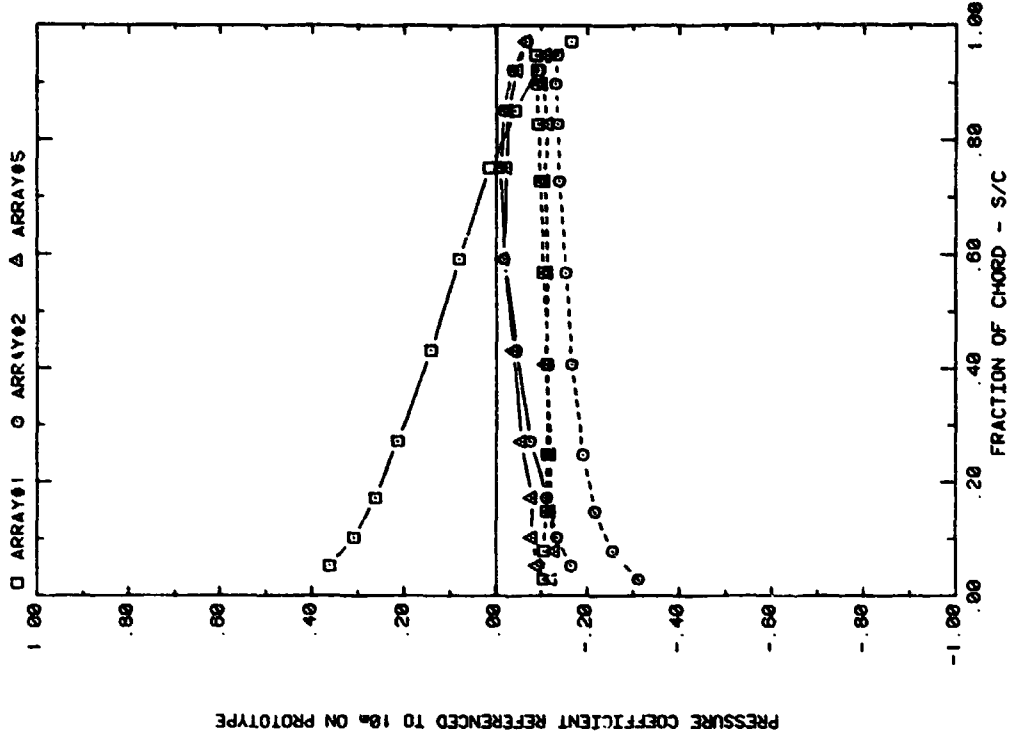


FRONT AND BACK PRESSURES ON ARRAYS IN BOUNDARY LAYER, $X = 1.5C$
EFFECT OF ARRAY CONFIGURATION ON ATTACK ANGLE 35, $H/C = 0.25$



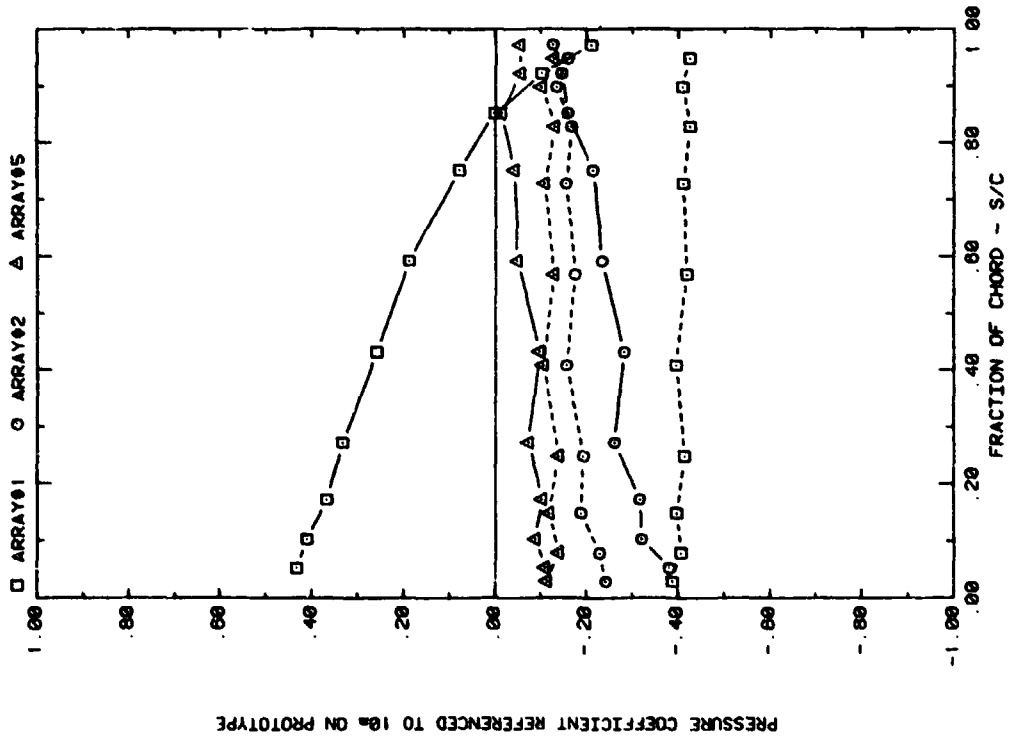
FRONT AND BACK PRESSURES ON ARRAYS IN BOUNDARY LAYER, $X = 1.5C$
EFFECT OF ARRAY CONFIGURATION ON ATTACK ANGLE 20, $H/C = 0.25$

Plot 2-2-3. Multiple Arrays without Fence, Nonuniform Flow Study
Effect of Array Position



PRESSURE COEFFICIENT REFERENCED TO 10a ON PROTOTYPE

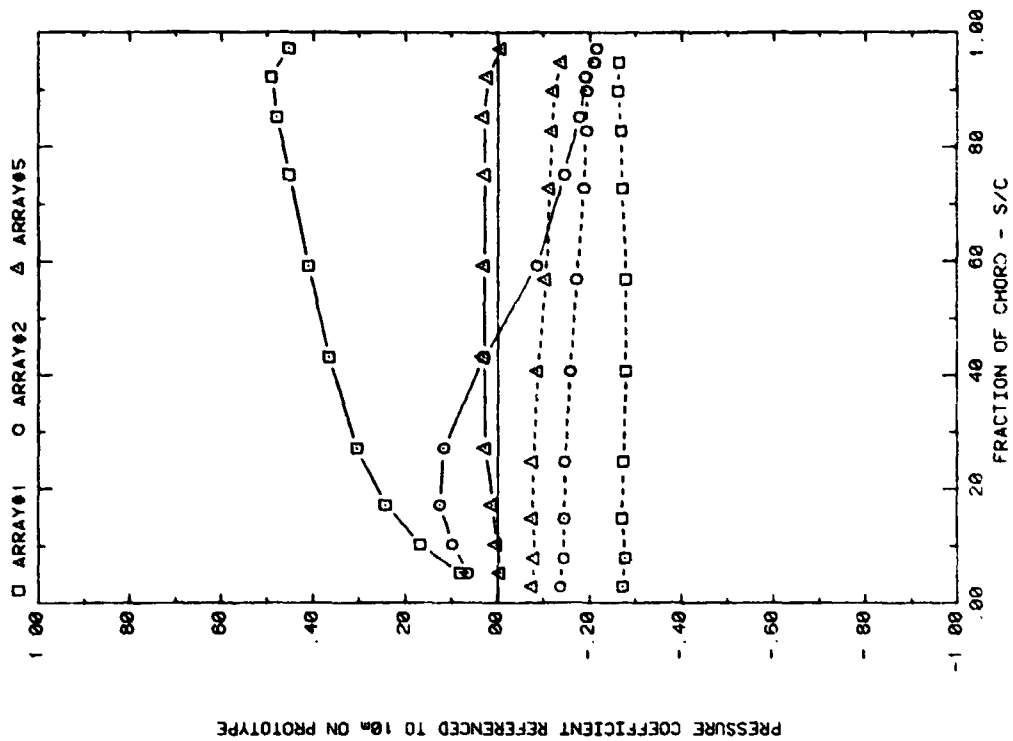
FRONT AND BACK PRESSURES ON ARRAYS IN BOUNDARY LAYER, $x = 1.5c$
EFFECT OF ARRAY CONFIGURATION ON ATTACK ANGLE 145, $H/C = 0.25$



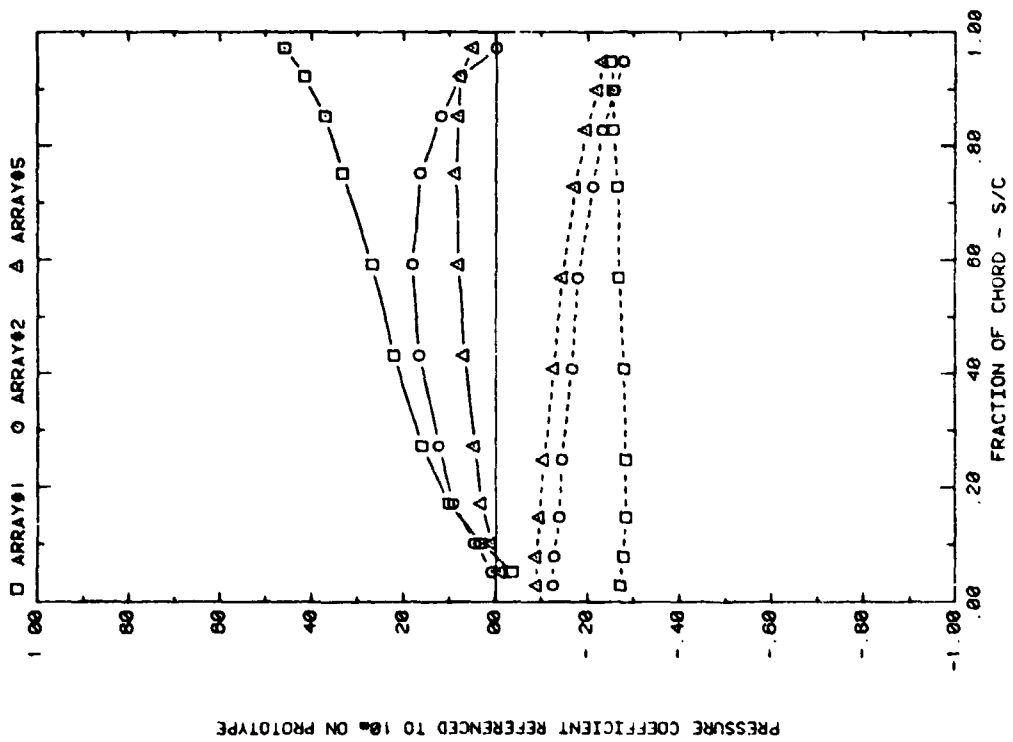
PRESSURE COEFFICIENT REFERENCED TO 10a ON PROTOTYPE

FRONT AND BACK PRESSURES ON ARRAYS IN BOUNDARY LAYER, $x = 1.5c$
EFFECT OF ARRAY CONFIGURATION ON ATTACK ANGLE 150, $H/C = 0.25$

Plot 2-2-3. (Continued)

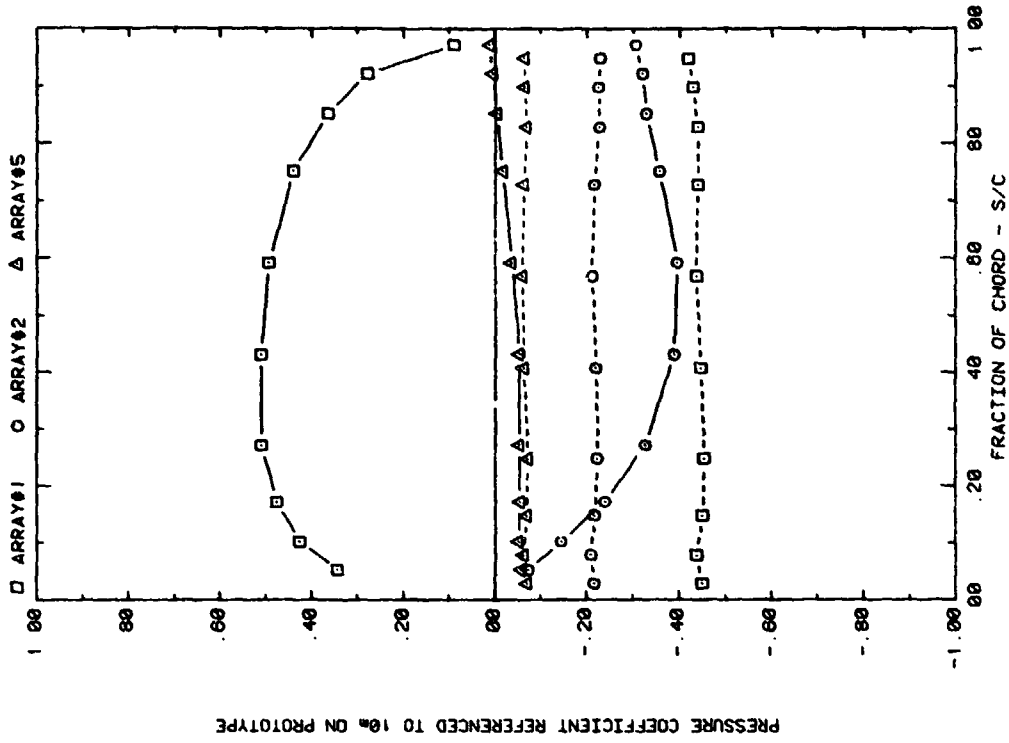


FRONT AND BACK PRESSURES ON ARRAYS IN BOUNDARY LAYER, X = 2.0C
EFFECT OF ARRAY CONFIGURATION ON ATTACK ANGLE 35, H/C = 0.25

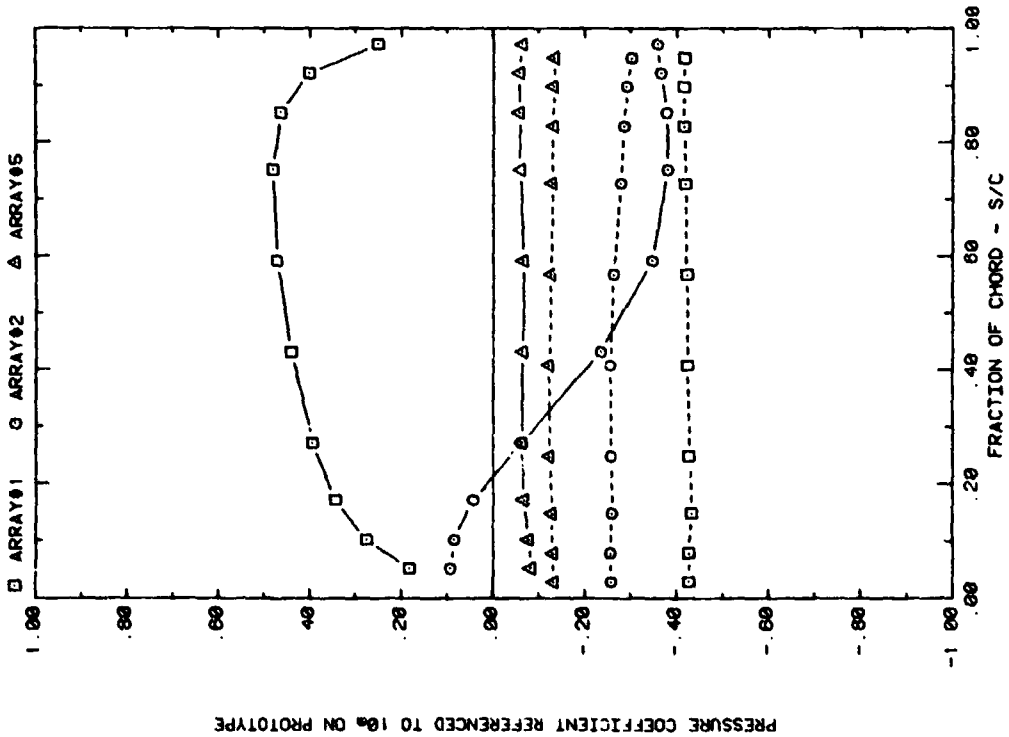


FRONT AND BACK PRESSURES ON ARRAYS IN BOUNDARY LAYER, X = 2.0C
EFFECT OF ARRAY CONFIGURATION ON ATTACK ANGLE 20, H/C = 0.25

Plot 2-2-3. (Continued)

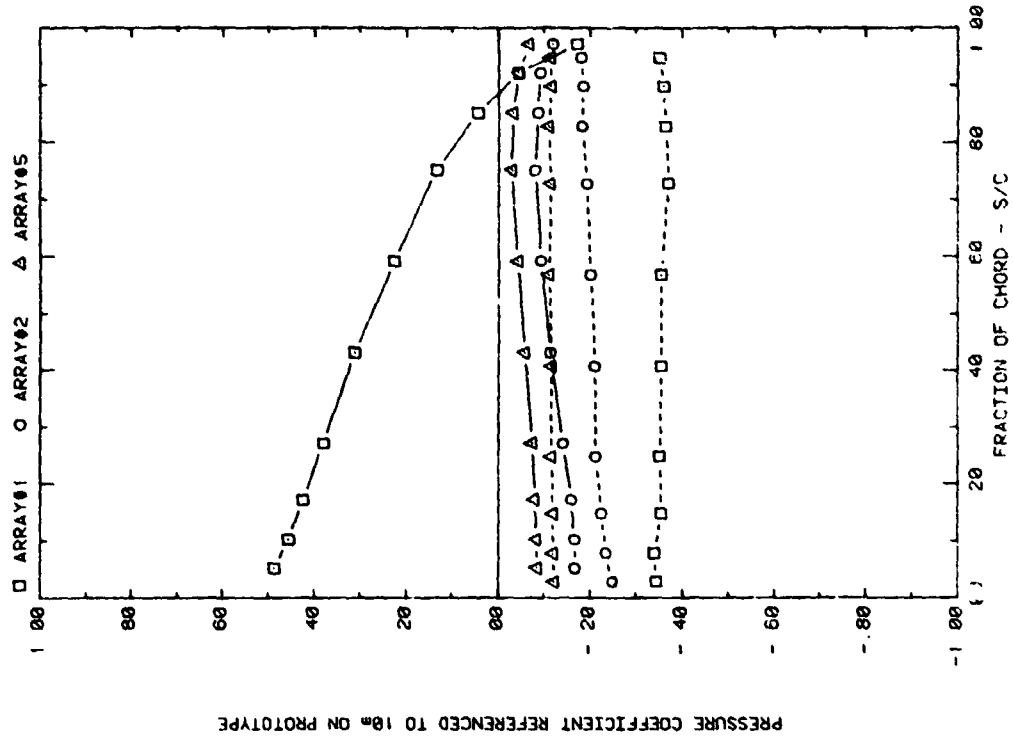


FRONT AND BACK PRESSURES ON ARRAYS IN BOUNDARY LAYER, X = 2.0
EFFECT OF ARRAY CONFIGURATION ON ATTACK ANGLE 90, H/C = 0.25

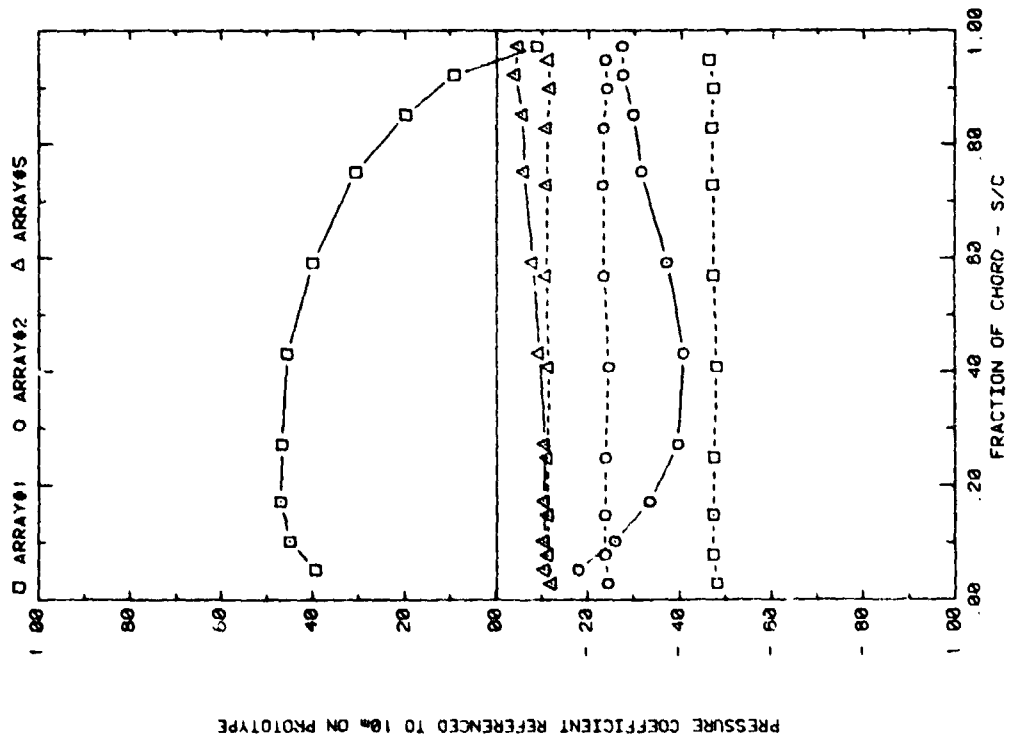


FRONT AND BACK PRESSURES ON ARRAYS IN BOUNDARY LAYER, X = 2.0
EFFECT OF ARRAY CONFIGURATION ON ATTACK ANGLE 60, H/C = 0.25

Plot 2-2-3. (Continued)

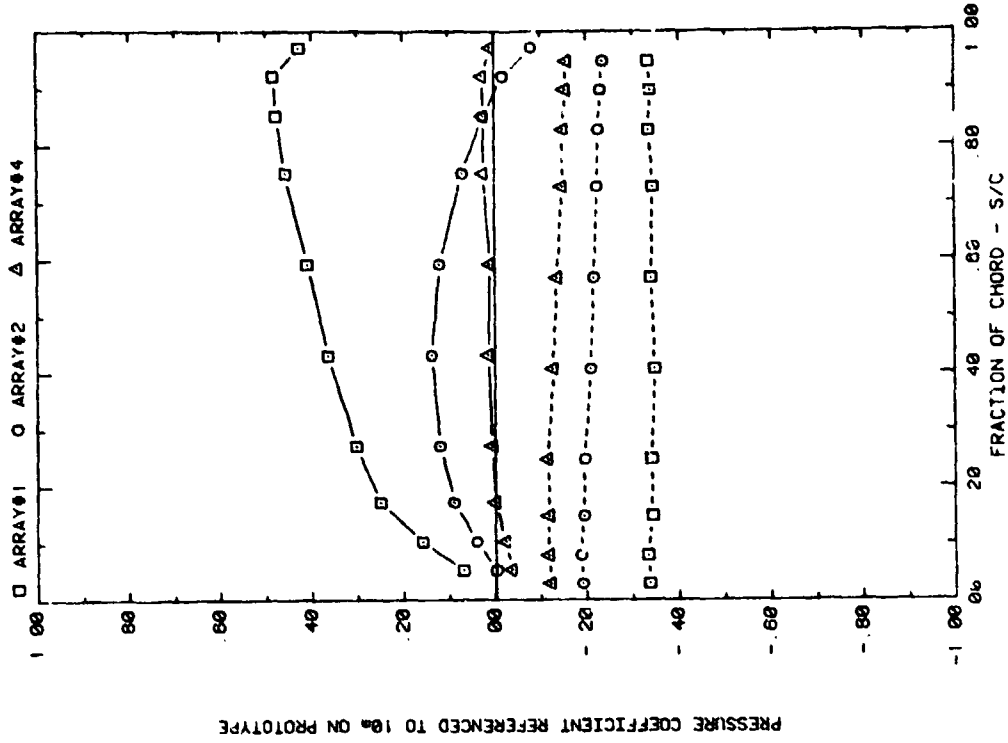


FRONT AND BACK PRESSURES ON ARRAYS IN BOUNDARY LAYER, $\alpha = 2.0^\circ$
EFFECT OF ARRAY CONFIGURATION ON ATTACK ANGLE 145° , $H/C = 0.25$

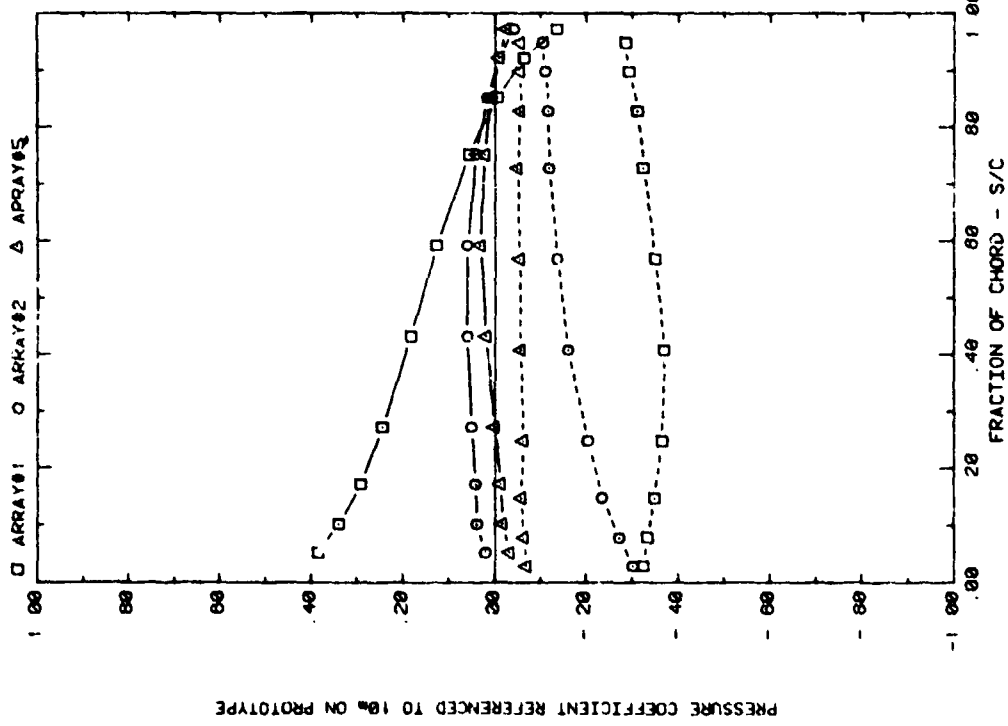


FRONT AND BACK PRESSURES ON ARRAYS IN BOUNDARY LAYER, $\alpha = 2.0^\circ$
EFFECT OF ARRAY CONFIGURATION ON ATTACK ANGLE 120° , $H/C = 0.25$

• Plot 2-2-3. (Continued)

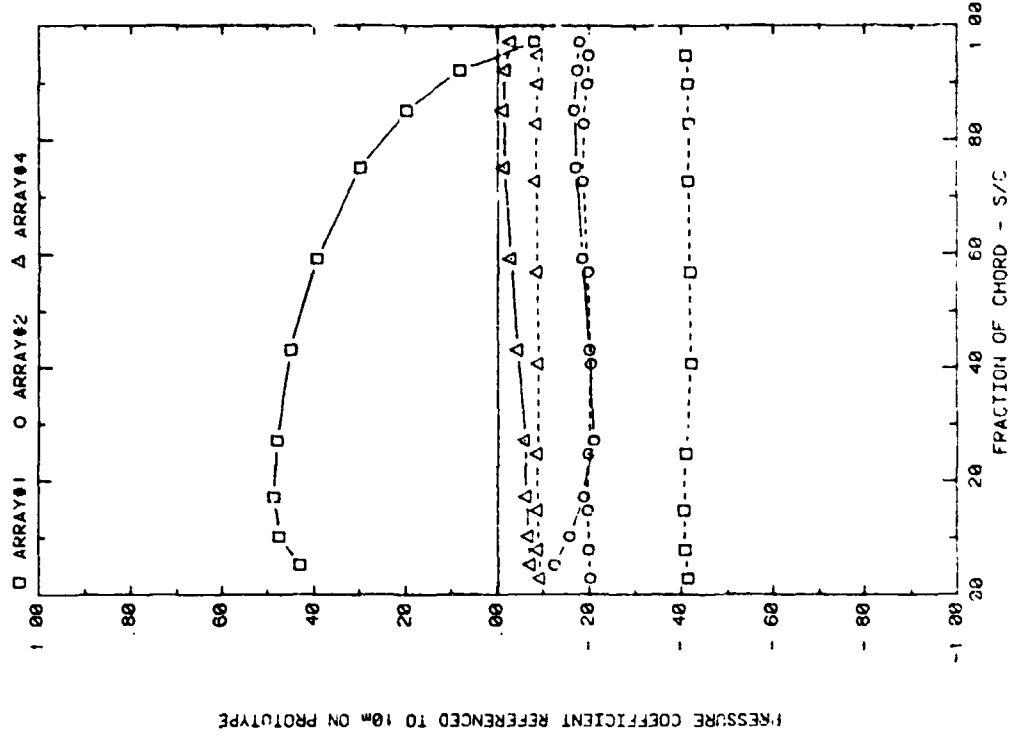


FRONT AND BACK PRESSURES ON ARRAYS IN BOUNDARY LAYER, $x = 3.0c$
EFFECT OF ARRAY CONFIGURATION ON ATTACK ANGLE 35, $H/C = 0.25$



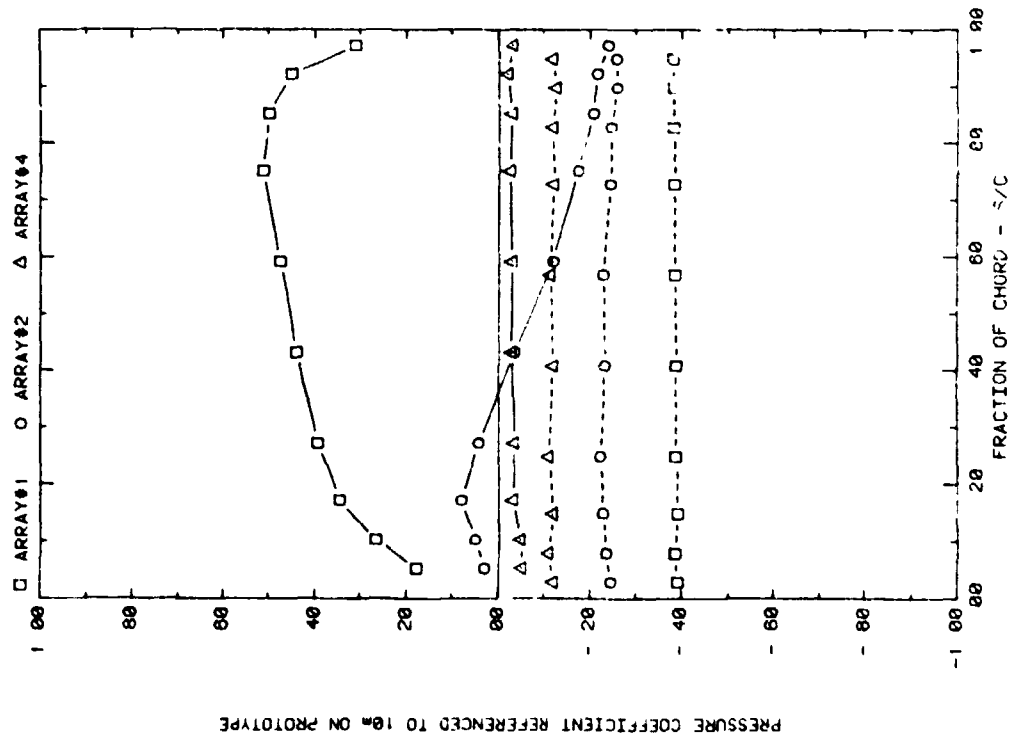
FRONT AND BACK PRESSURES ON ARRAYS IN BOUNDARY LAYER, $x = 2.0c$
EFFECT OF ARRAY CONFIGURATION ON ATTACK ANGLE 180, $H/C = 0.25$

Plot 2-2-3. (Continued)



PRESSURE COEFFICIENT REFERENCED TO 10# ON PROTOTYPE

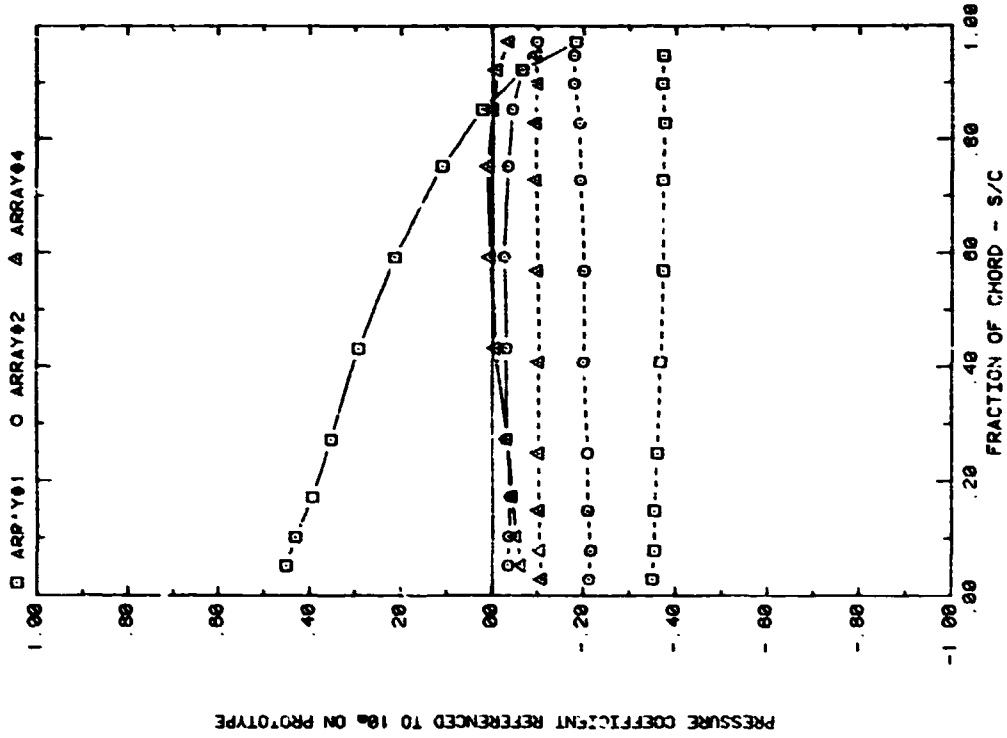
FRONT AND BACK PRESSURES OF ARRAYS IN BOUNDARY LAYER, $\alpha = 3.0^\circ$
EFFECT OF ARRAY CONFIGURATION ON ATTACK ANGLE 120, $H/C = 0.25$



PRESSURE COEFFICIENT REFERENCED TO 10# ON PROTOTYPE

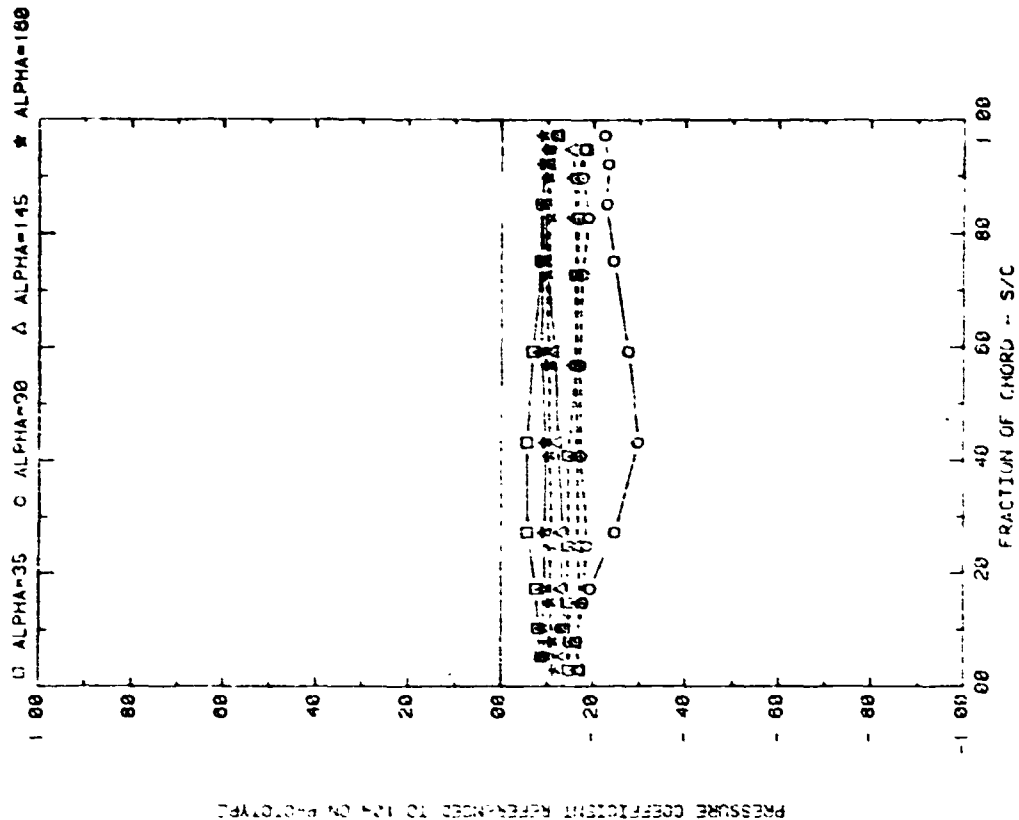
FRONT AND BACK PRESSURES ON ARRAYS IN BOUNDARY LAYER, $\alpha = 3.0^\circ$
EFFECT OF ARRAY CONFIGURATION ON ATTACK ANGLE 60, $H/C = 0.25$

Plot 2-2-3. (Continued)

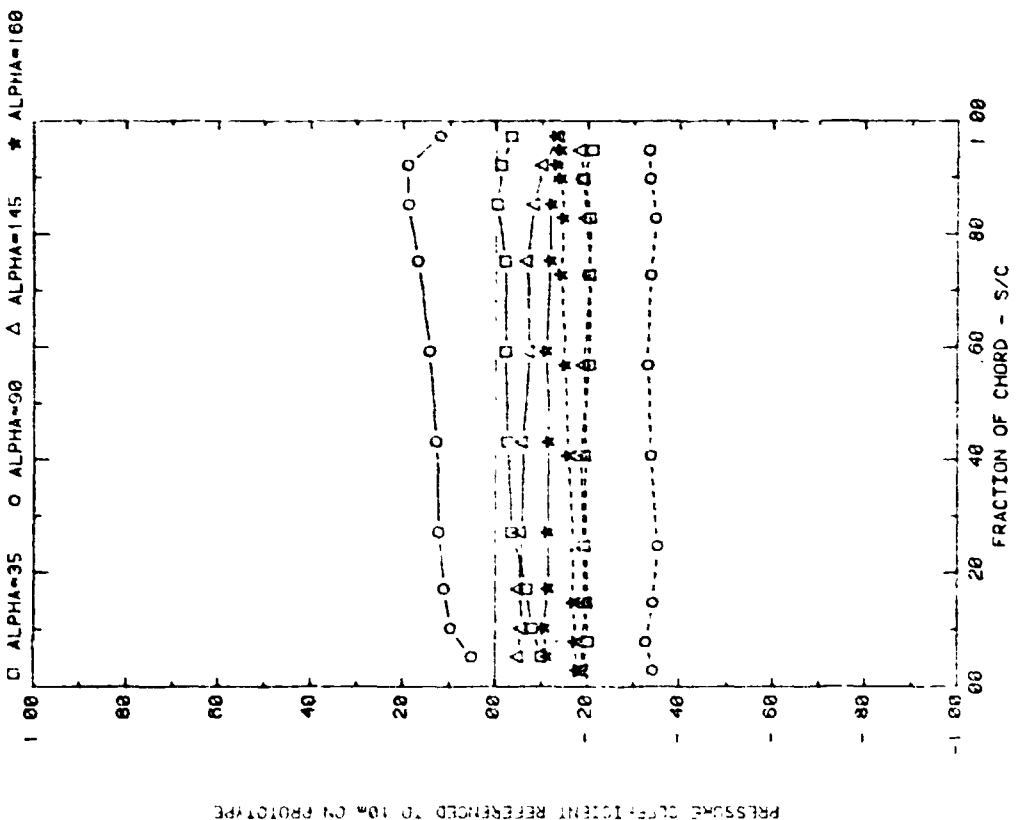


FRONT AND BACK PRESSURES ON ARRAYS IN BOUNDARY LAYER, $\alpha = 30^\circ$
EFFECT OF ARRAY CONFIGURATION ON ATTACK ANGLE 145° , $H/C = 0.25$

Plot 2-2-3. (Concluded)



FRONT AND BACK PRESSURES ON ARRAY #1 WITH SEPARATION = 2C
EFFECT OF ATTACK ANGLE WITH $M = 3^\circ$, $P = 30\%$, AND $D = 5^\circ$

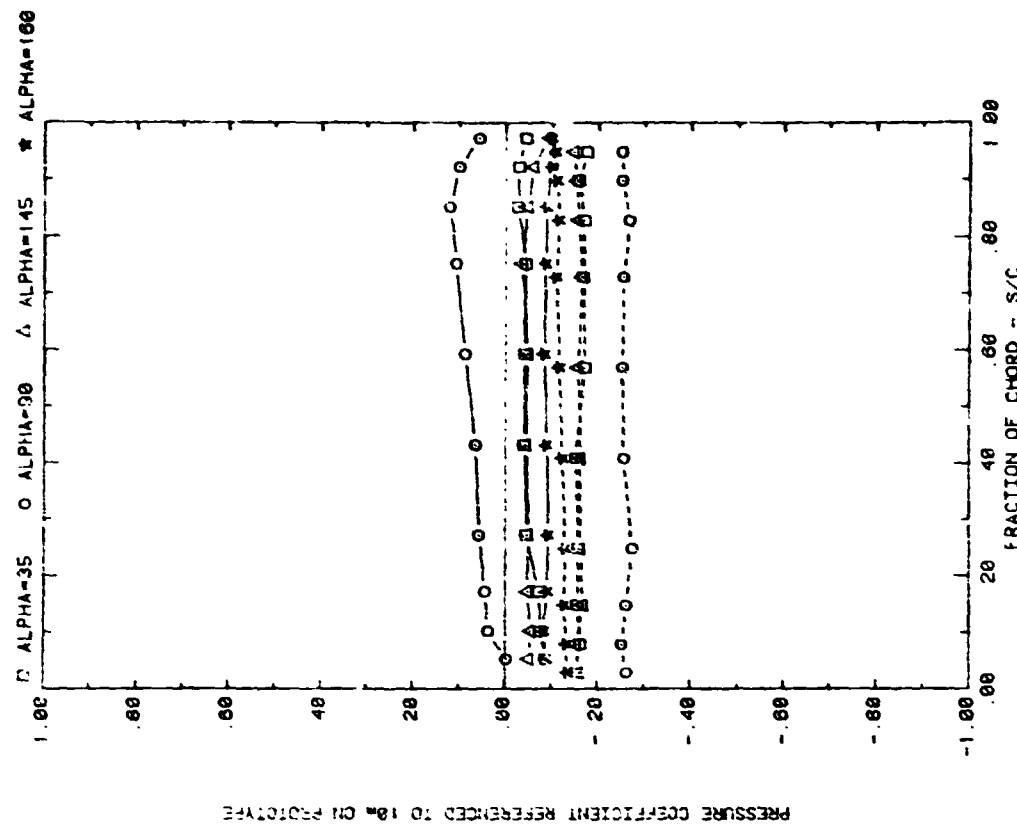


FRONT AND BACK PRESSURES ON ARRAY #1 WITH SEPARATION = 2C
EFFECT OF ATTACK ANGLE WITH $M = 3^\circ$, $P = 30\%$, AND $D = 5^\circ$

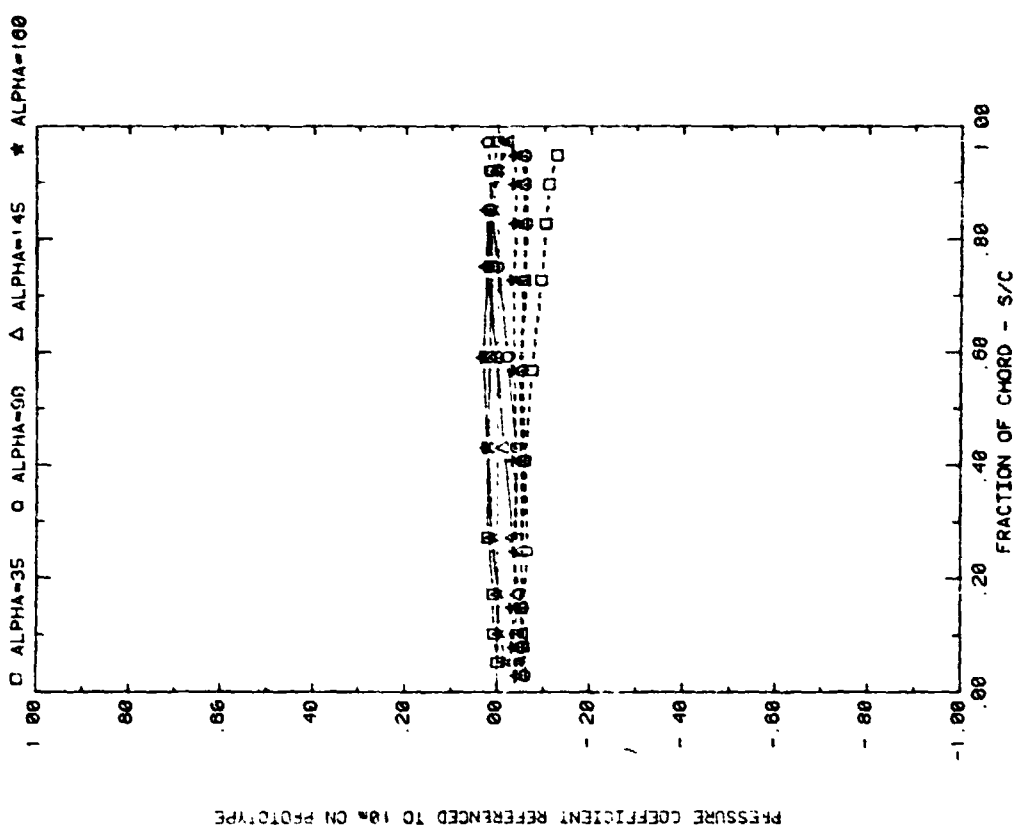
Plot 3-1. Multiple Arrays with Fence, $WD = 0^\circ$
Effect of Angle of Attack

PRESSURE COEFFICIENT REFERRED TO 1% ON PROTOTYPE

PRESSURE COEFFICIENT REFERRED TO 1% ON PROTOTYPE



FRONT AND BACK PRESSURES ON ARRAY #1 WITH SEPARATION = 2C
EFFECT OF ATTACK ANGLE WITH $M=3$, $P=30\%$, AND $D=10$.

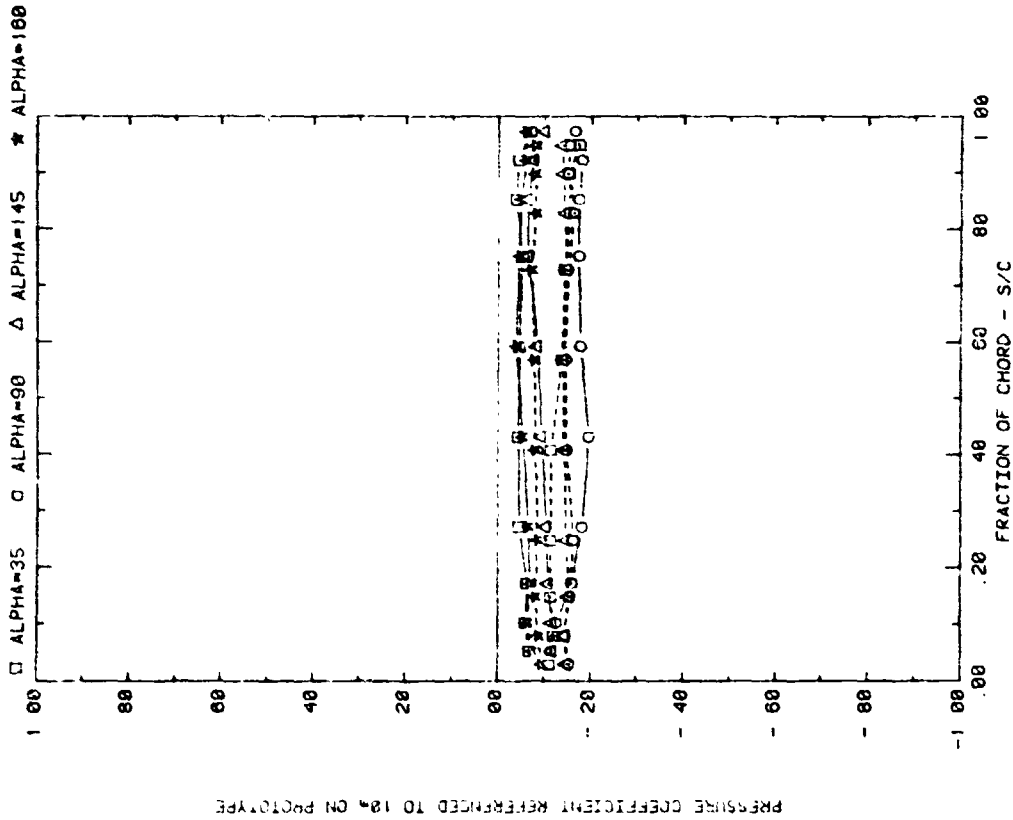
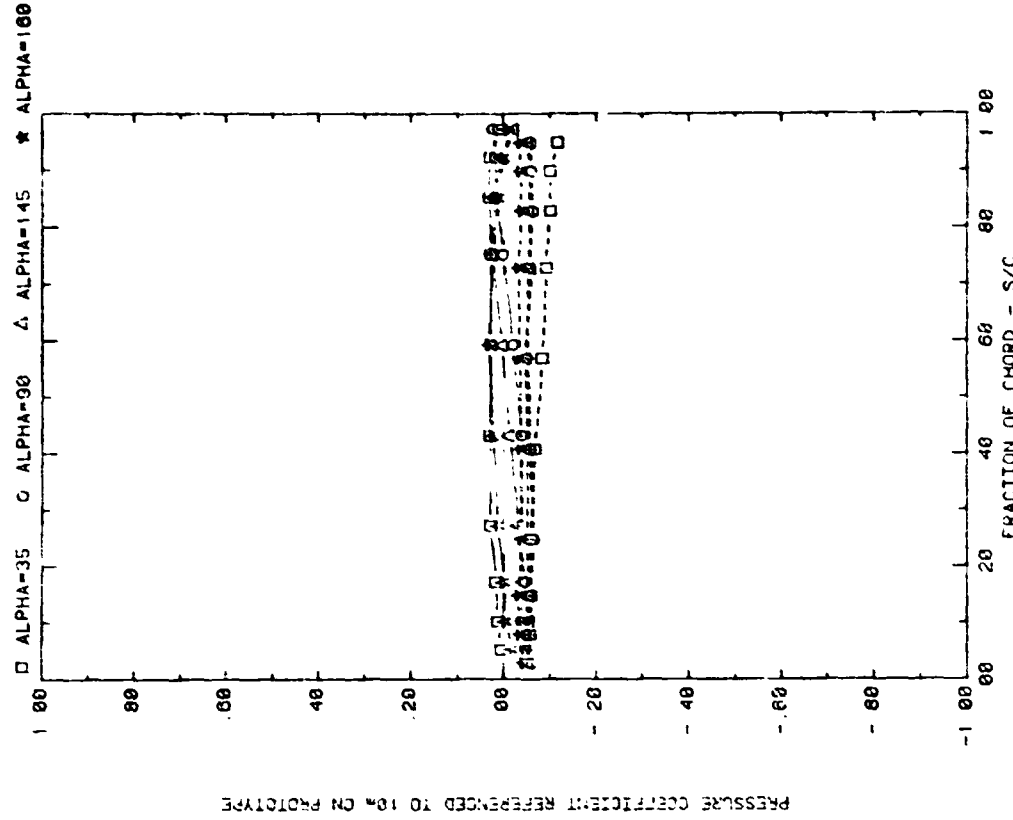


FRONT AND BACK PRESSURES ON ARRAY #5 WITH SEPARATION = 5C
EFFECT OF ATTACK ANGLE WITH $M=3$, $P=30\%$, AND $D=5$.

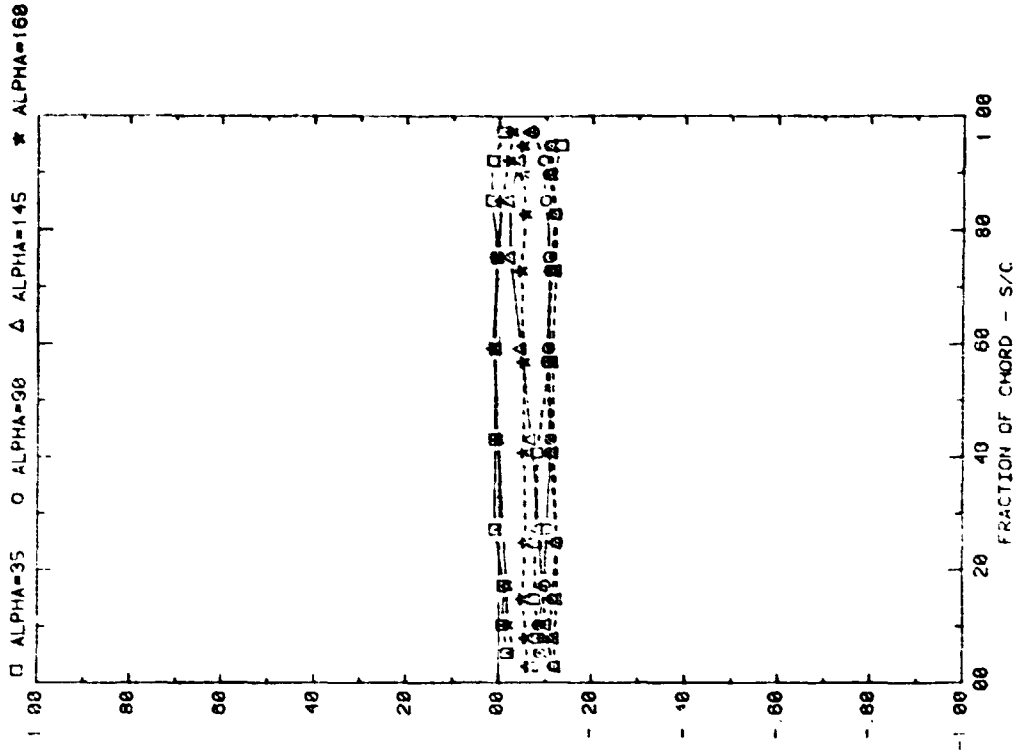
Plot 3-1. (Continued)

PRESSURE COEFFICIENT REFERENCED TO 10% ON PROTOTYPE

PRESSURE COEFFICIENT REFERENCED TO 10% ON PROTOTYPE

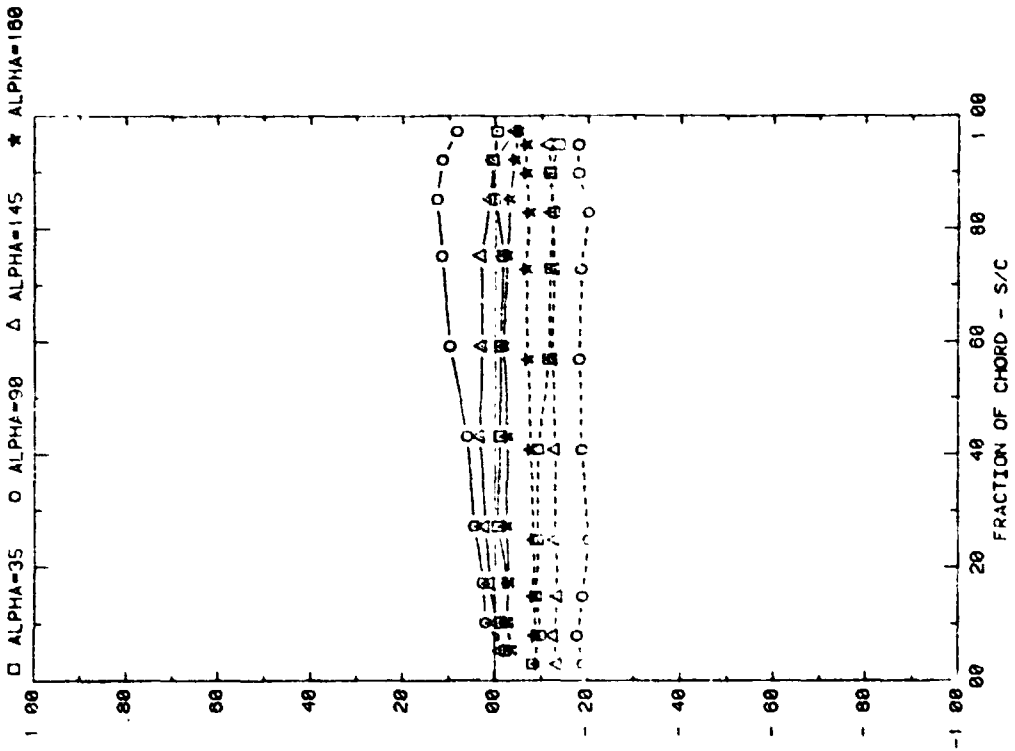


Plot 3-1. (Continued)



PRESSURE COEFFICIENT REFERENCED TO 10% ON PROTOTYPE

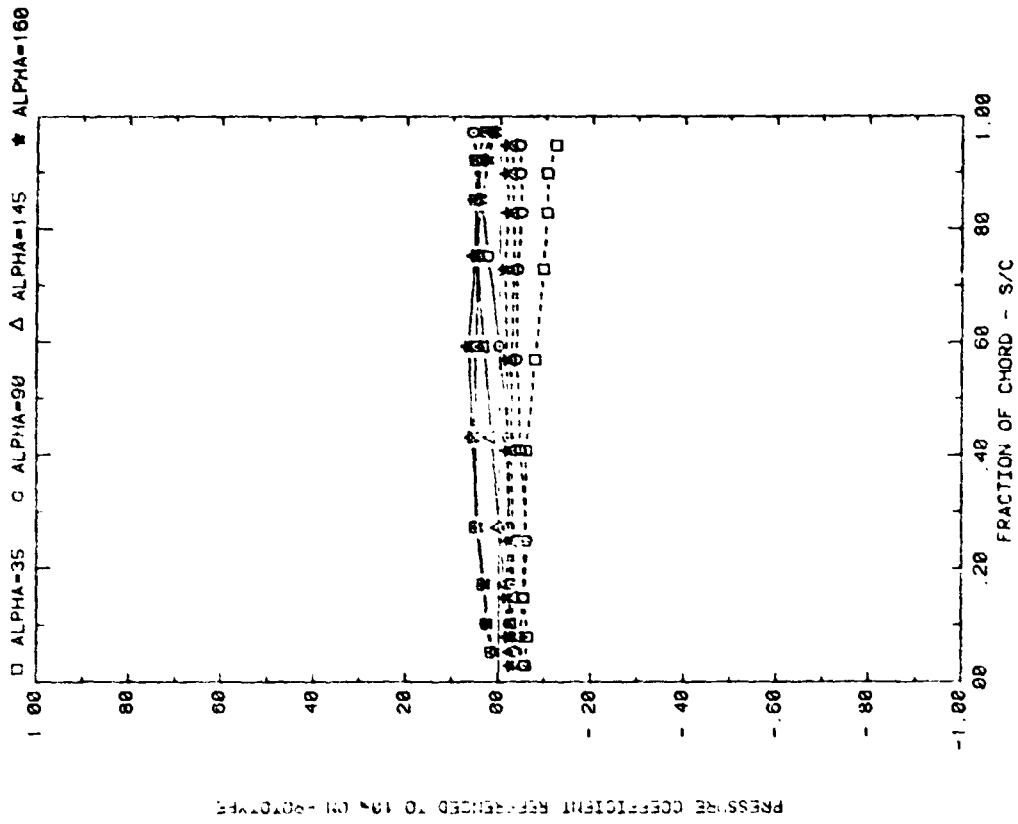
FRONT AND BACK PRESSURES ON ARRAY #2 WITH SEPARATION = 2C
EFFECT OF ATTACK ANGLE WITH H=3", P=30%, AND D=20"



PRESSURE COEFFICIENT REFERENCED TO 10% ON PROTOTYPE

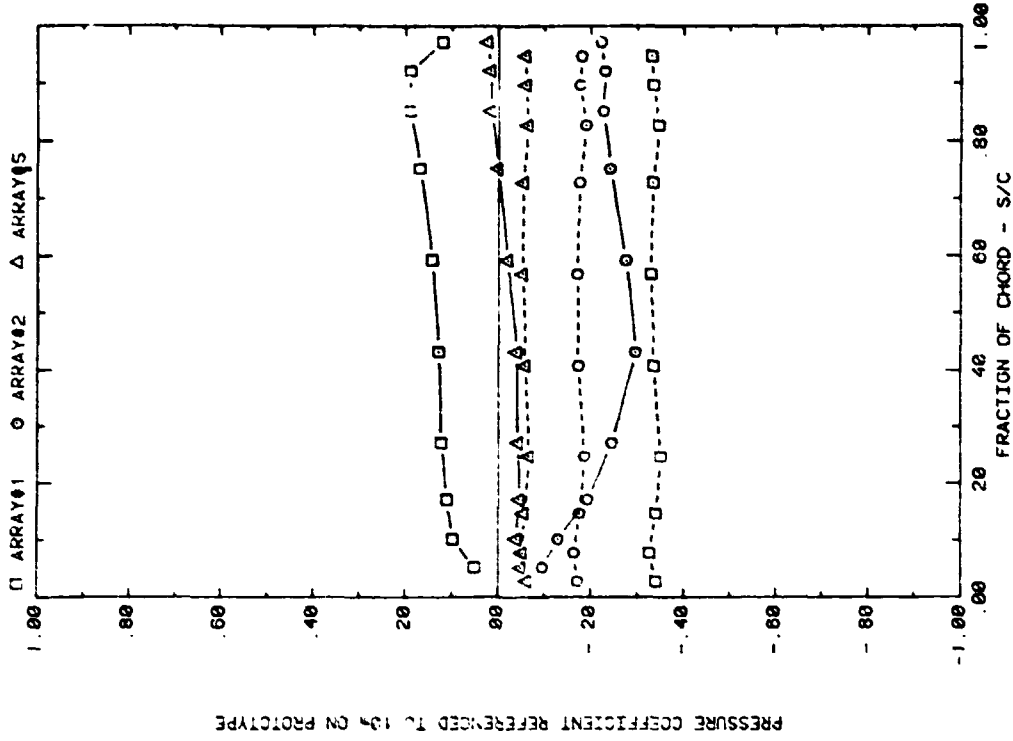
FRONT AND BACK PRESSURES ON ARRAY #1 WITH SEPARATION = 2C
EFFECT OF ATTACK ANGLE WITH H=3", P=30%, AND D=20"

Plot 3-1. (Continued)

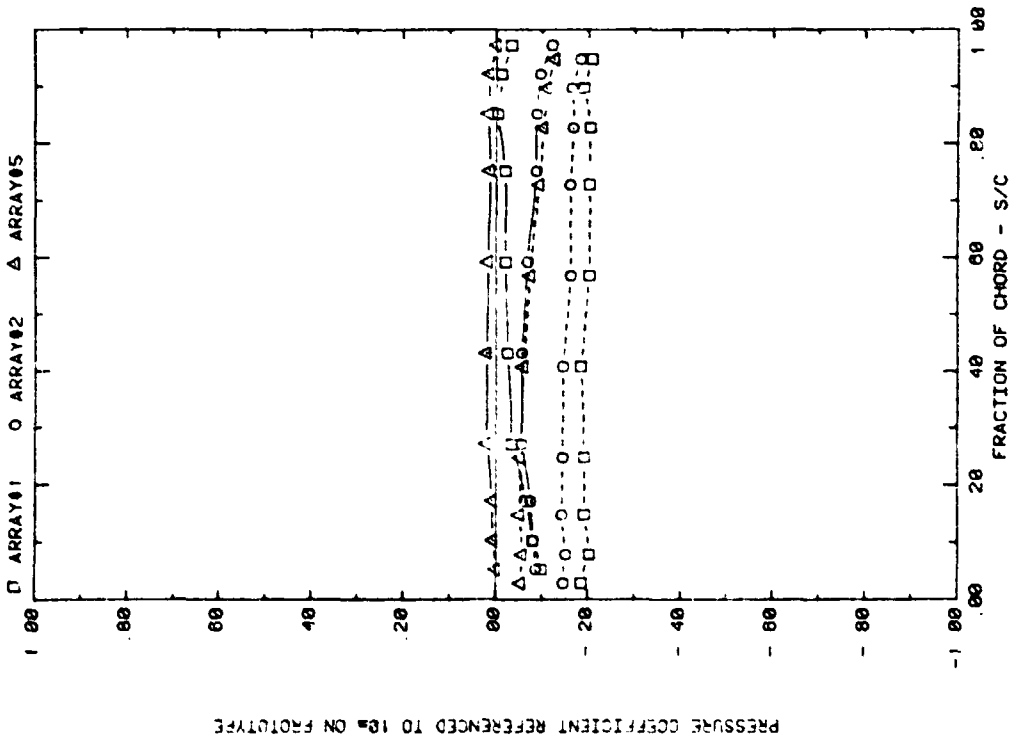


FRONT AND BACK PRESSURES ON ARRAYS WITH SEPARATION = 2C
EFFECT OF ATTACK ANGLE WITH $M=3$, $P=30\%$, AND $D=20^\circ$

Plot 3-1. (Concluded)

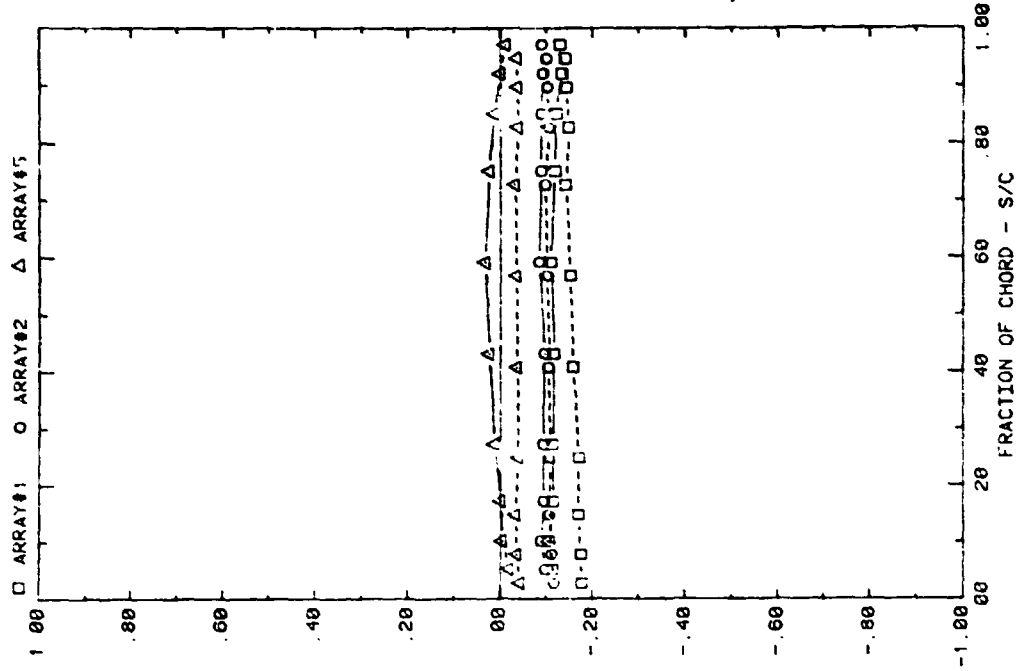


FRONT AND BACK PRESSURES ON VARIOUS ARRAYS WITH SEPARATION = 2C
EFFECT OF ARRAYS WITH ATTACK ANGLE=00, H=3°, P=30%, AND D=5°

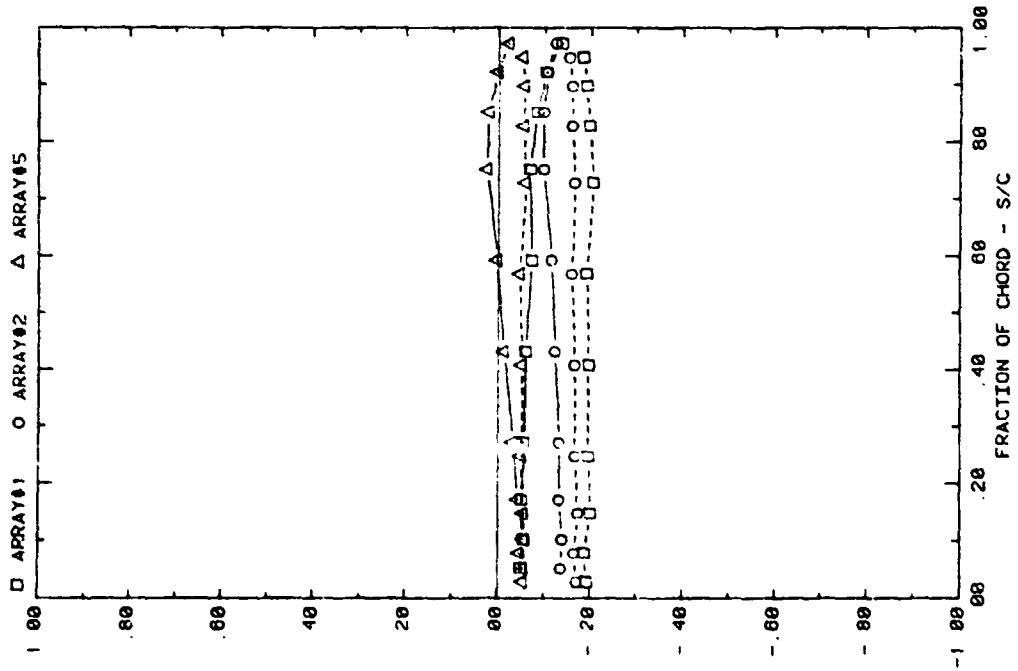


FRONT AND BACK PRESSURES ON VARIOUS ARRAYS WITH SEPARATION = 2C
EFFECT OF ARRAYS WITH ATTACK ANGLE=35, H=3°, P=30%, AND D=5°

Plot 3-2. Multiple Arrays with Fence, $WD = 0^\circ$
Effect of Array Position



PRESSURE COEFFICIENT REFERENCED TO 10% ON PROTOTYPE

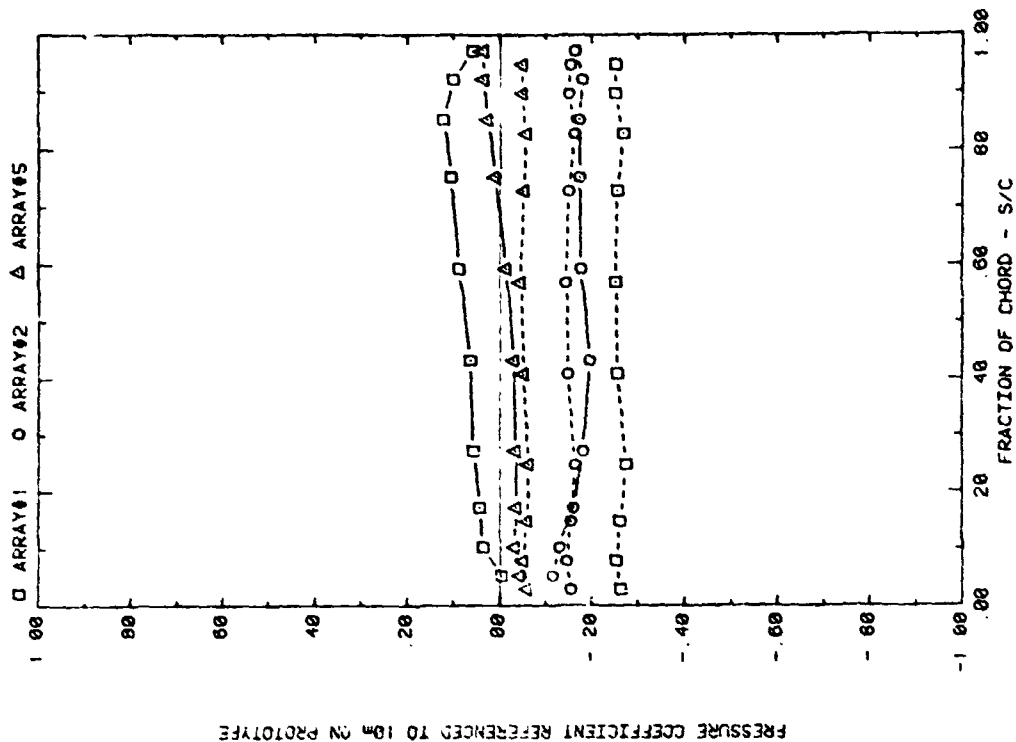


PRESSURE COEFFICIENT REFERENCED TO 10% ON PROTOTYPE

FRONT AND BACK PRESSURES ON VARIOUS ARRAYS WITH SEPARATION = 2C
EFFECT OF ARRAYS WITH ATTACK ANGLE=10°, H=3", P=30%, AND D=5"

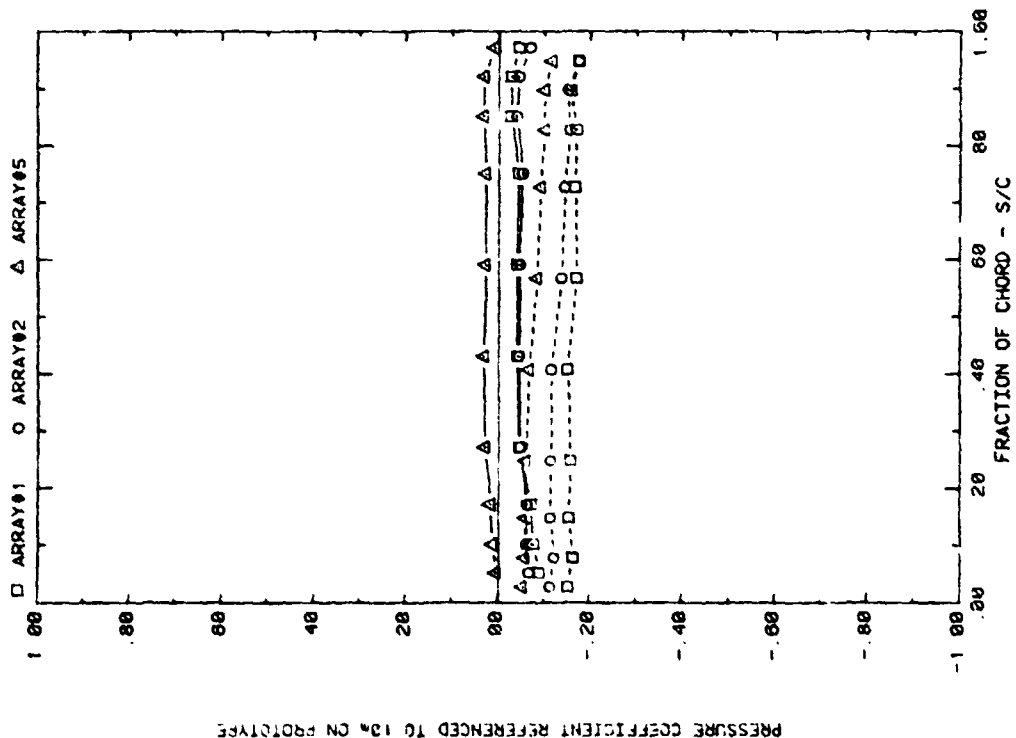
FRONT AND BACK PRESSURES ON VARIOUS ARRAYS WITH SEPARATION = 2C
EFFECT OF ARRAYS WITH ATTACK ANGLE=145°, H=3", P=30%, AND D=5"

Plot 3-2. (Continued)



PRESSURE COEFFICIENT REFERENCED TO 10% ON PROTOTYPE

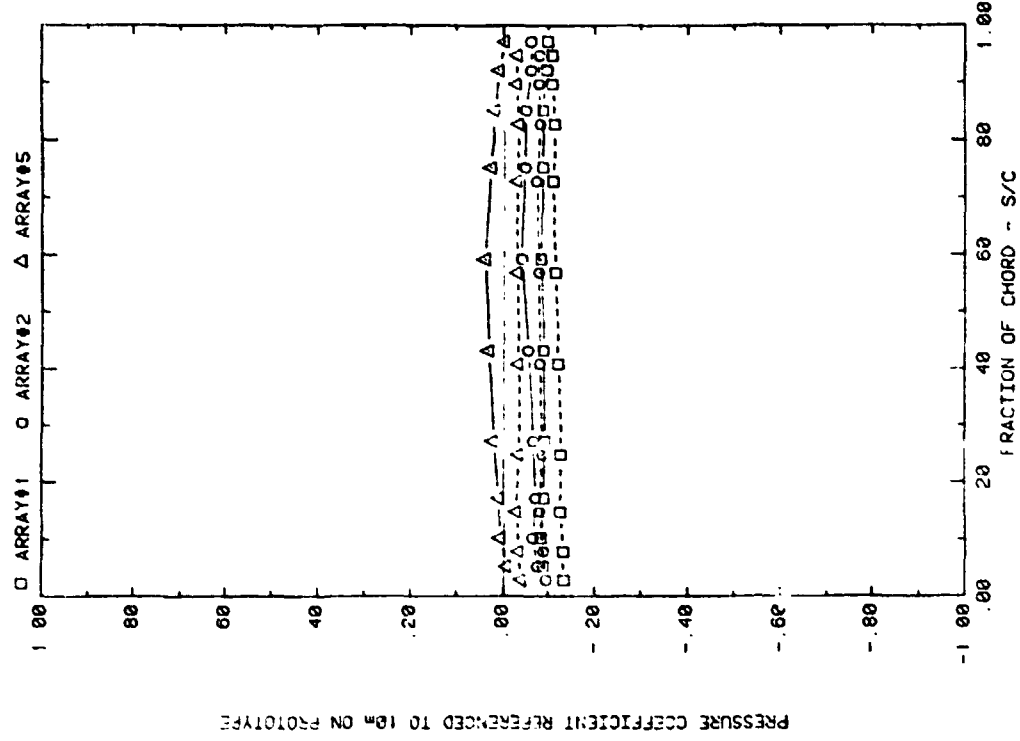
FRONT AND BACK PRESSURES ON VARIOUS ARRAYS WITH SEPARATION = 2C
EFFECT OF ARRAYS WITH ATTACK ANGLE=90, H=3", P=30%, AND D=10.



PRESSURE COEFFICIENT REFERENCED TO 10% ON PROTOTYPE

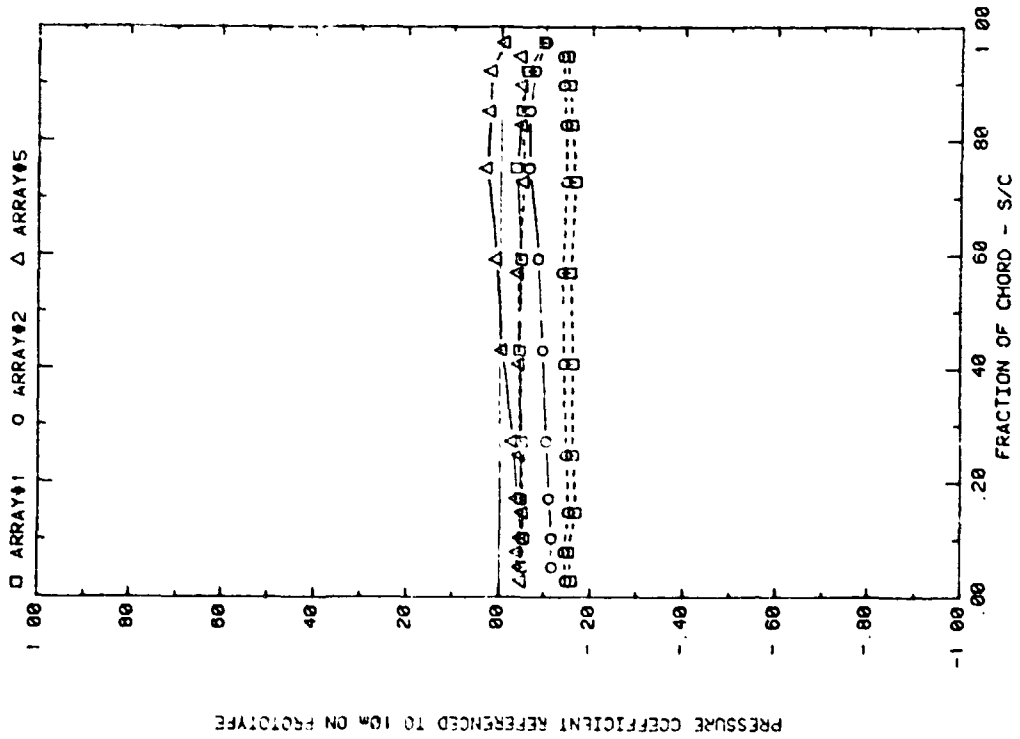
FRONT AND BACK PRESSURES ON VARIOUS ARRAYS WITH SEPARATION = 2C
EFFECT OF ARRAYS WITH ATTACK ANGLE=35, H=3", P=30%, AND D=10.

Plot 3-2. (Continued)



PRESSURE COEFFICIENT REFERENCED TO 10% ON PROTOTYPE

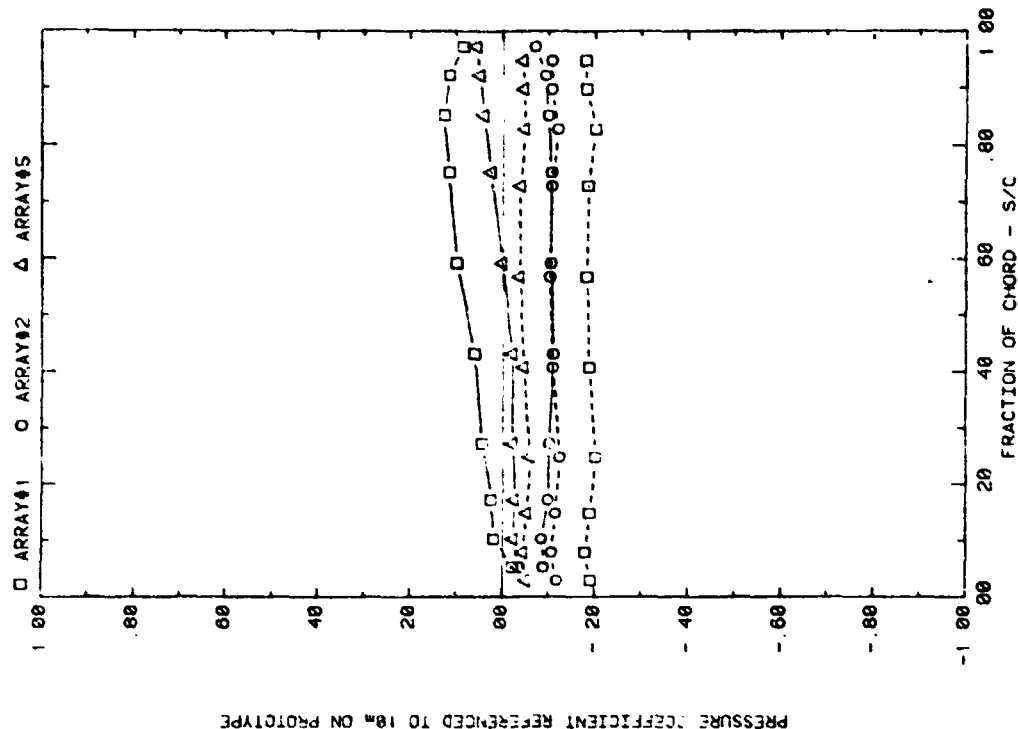
FRONT AND BACK PRESSURES ON VARIOUS ARRAYS WITH SEPARATION = 2C
EFFECT OF ARRAYS WITH ATTACK ANGLE=10°, H=3°, P=30%, AND D=10°



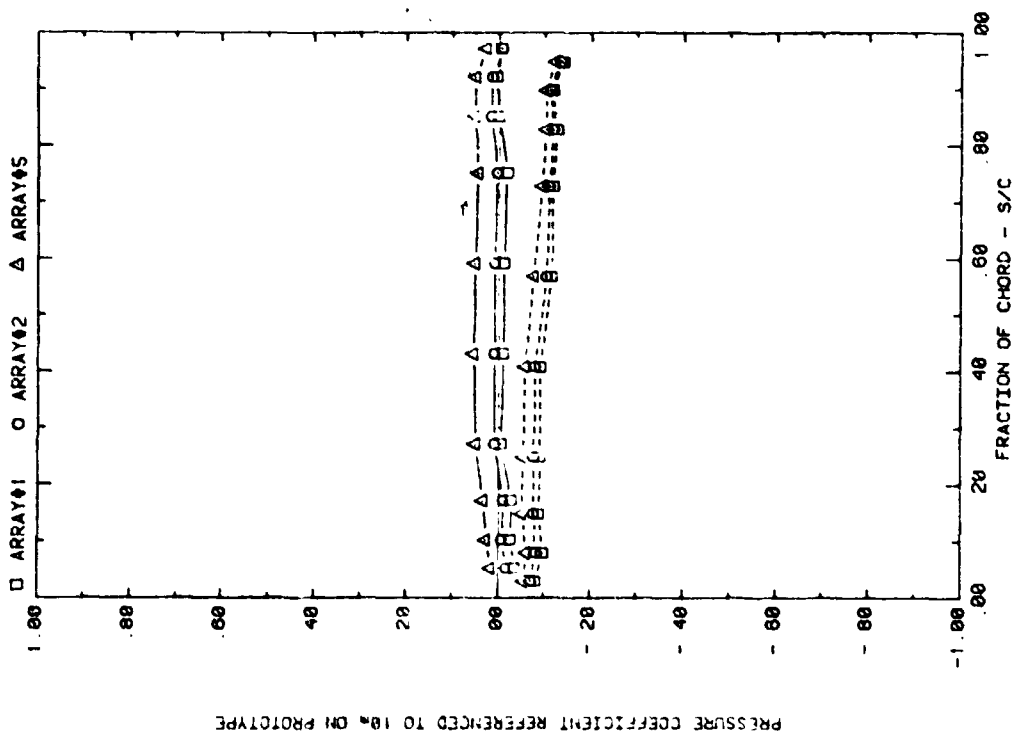
PRESSURE COEFFICIENT REFERENCED TO 10% ON PROTOTYPE

FRONT AND BACK PRESSURES ON VARIOUS ARRAYS WITH SEPARATION = 2C
EFFECT OF ARRAYS WITH ATTACK ANGLE=145°, H=3°, P=30%, AND D=10°

Plot 3-2. (Continued)

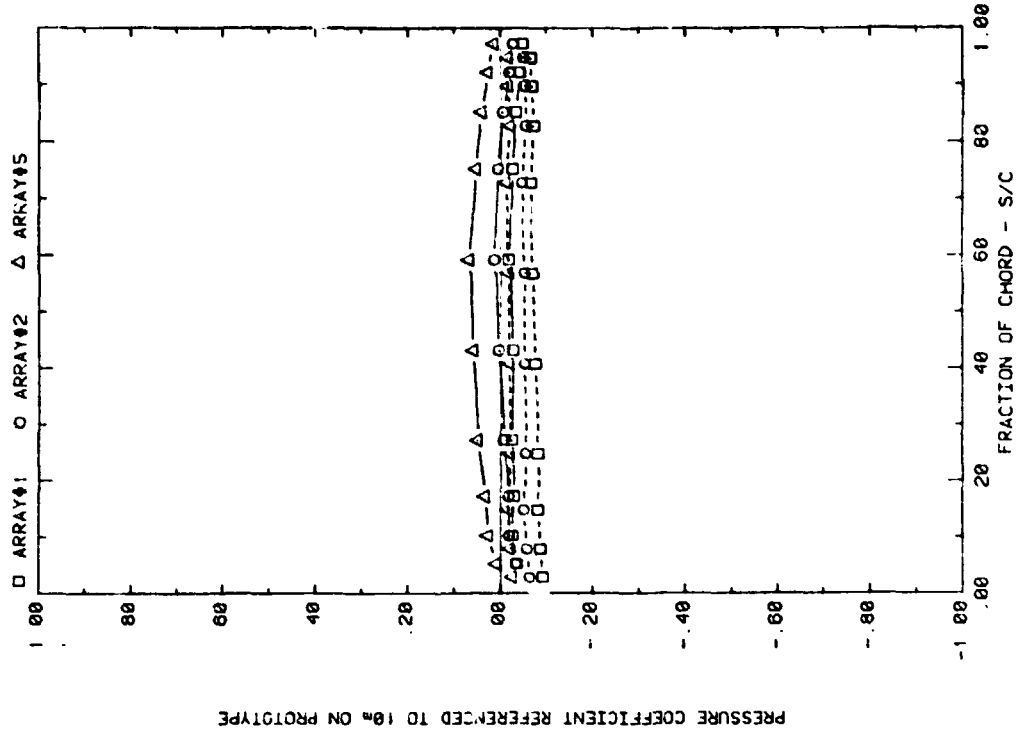


FRONT AND BACK PRESSURES ON VARIOUS ARRAYS WITH SEPARATION = 20
EFFECT OF ARRAYS WITH ATTACK ANGLE=30, M=3, P=30%, AND D=20.



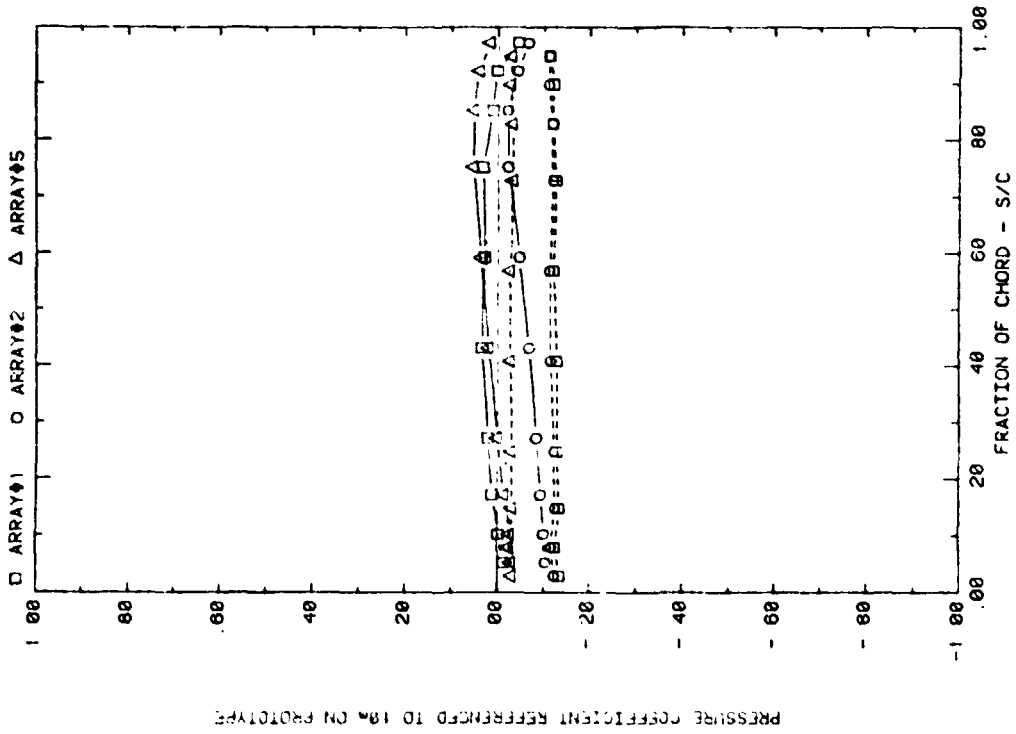
FRONT AND BACK PRESSURES ON VARIOUS ARRAYS WITH SEPARATION = 20
EFFECT OF ARRAYS WITH ATTACK ANGLE=35, M=3, P=30%, AND D=20.

Plot 3-2. (Continued)



PRESSURE COEFFICIENT REFERENCED TO 10% ON PROTOTYPE

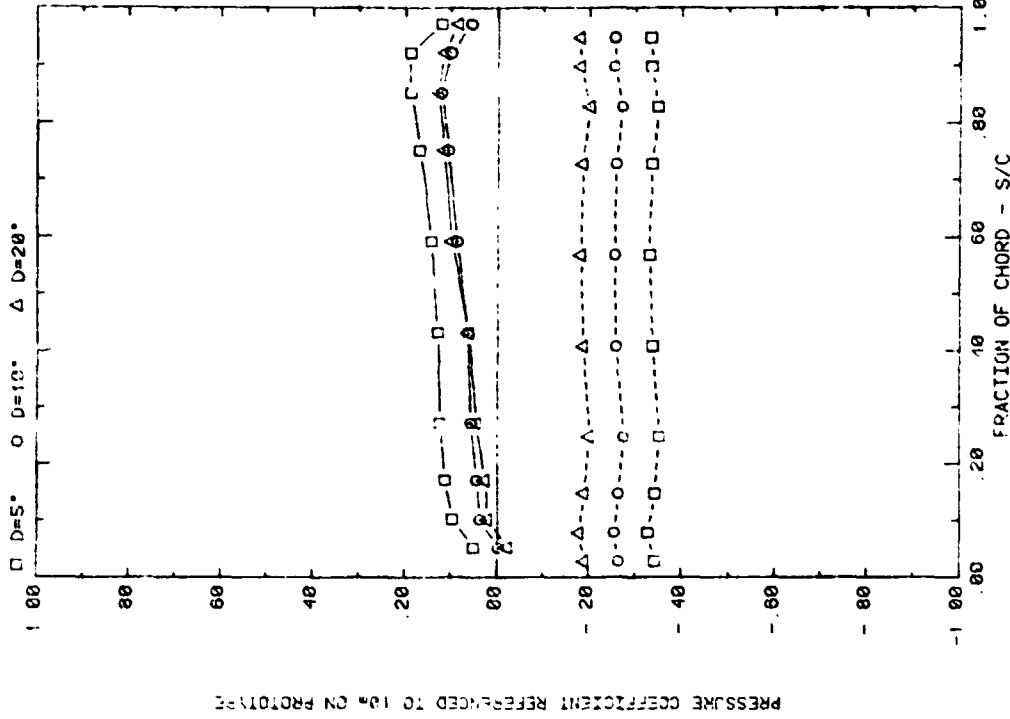
FRONT AND BACK PRESSURES ON VARIOUS ARRAYS WITH SEPARATION = 2C
EFFECT OF ARRAYS WITH ATTACK ANGLE=160, H=3', P=30%, AND D=20.



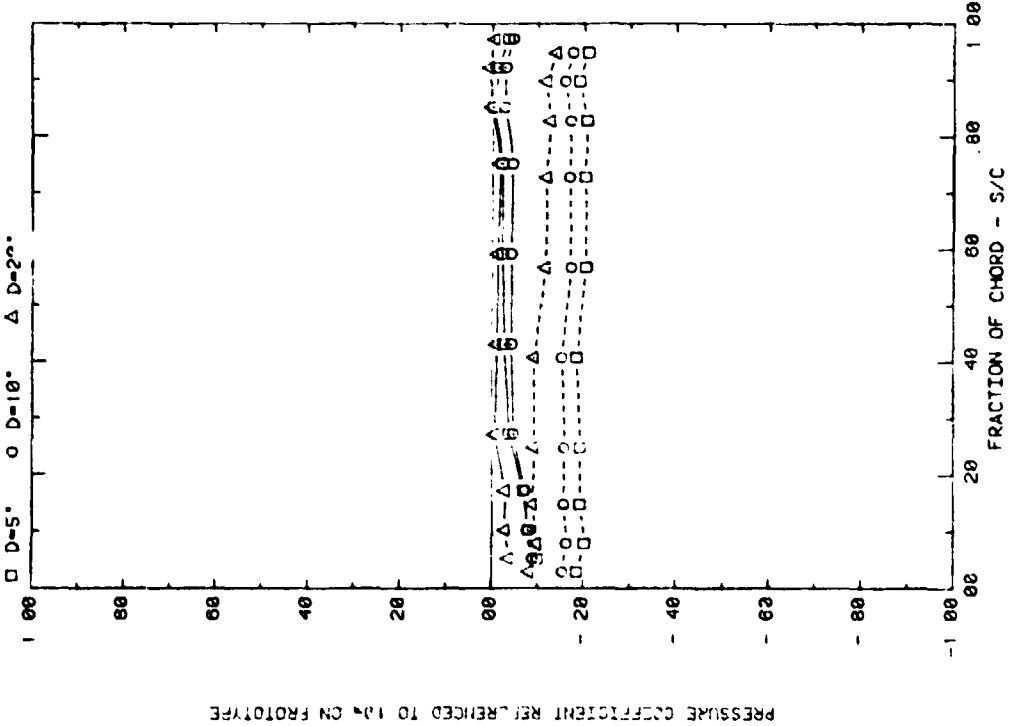
PRESSURE COEFFICIENT REFERENCED TO 10% ON PROTOTYPE

FRONT AND BACK PRESSURES ON VARIOUS ARRAYS WITH SEPARATION = 2C
EFFECT OF ARRAYS WITH ATTACK ANGLE=145, H=3', P=30%, AND D=20.

Plot 3-2. (Concluded)

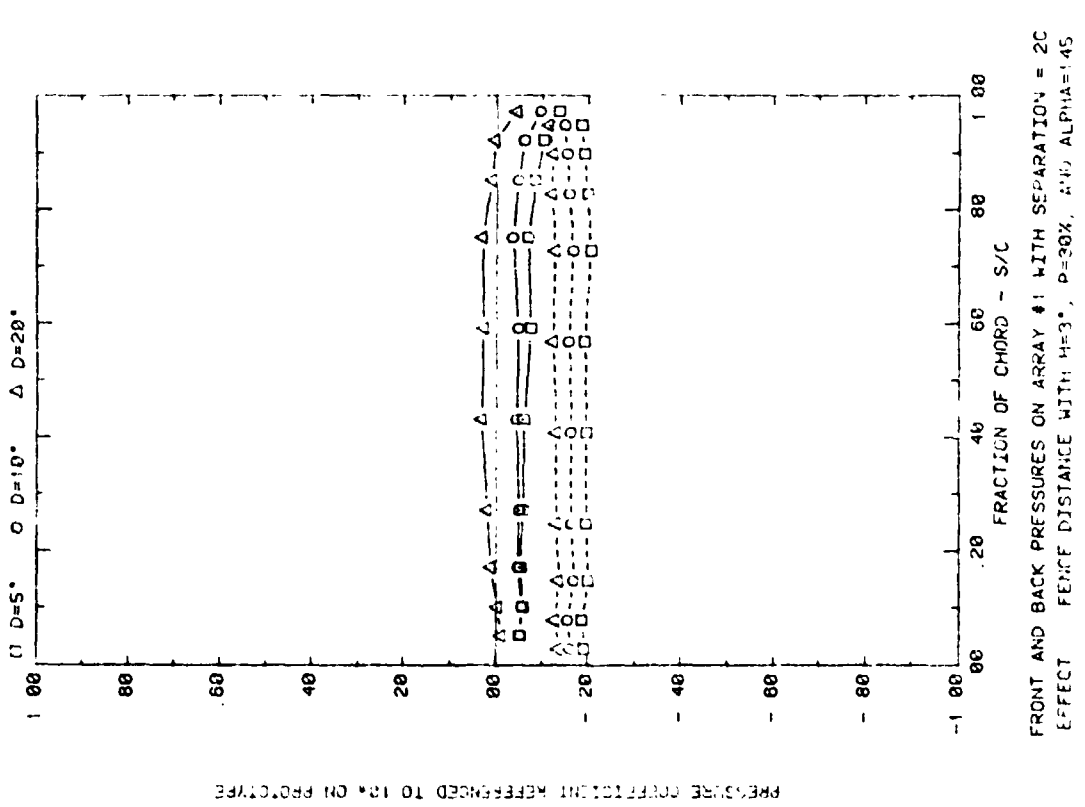
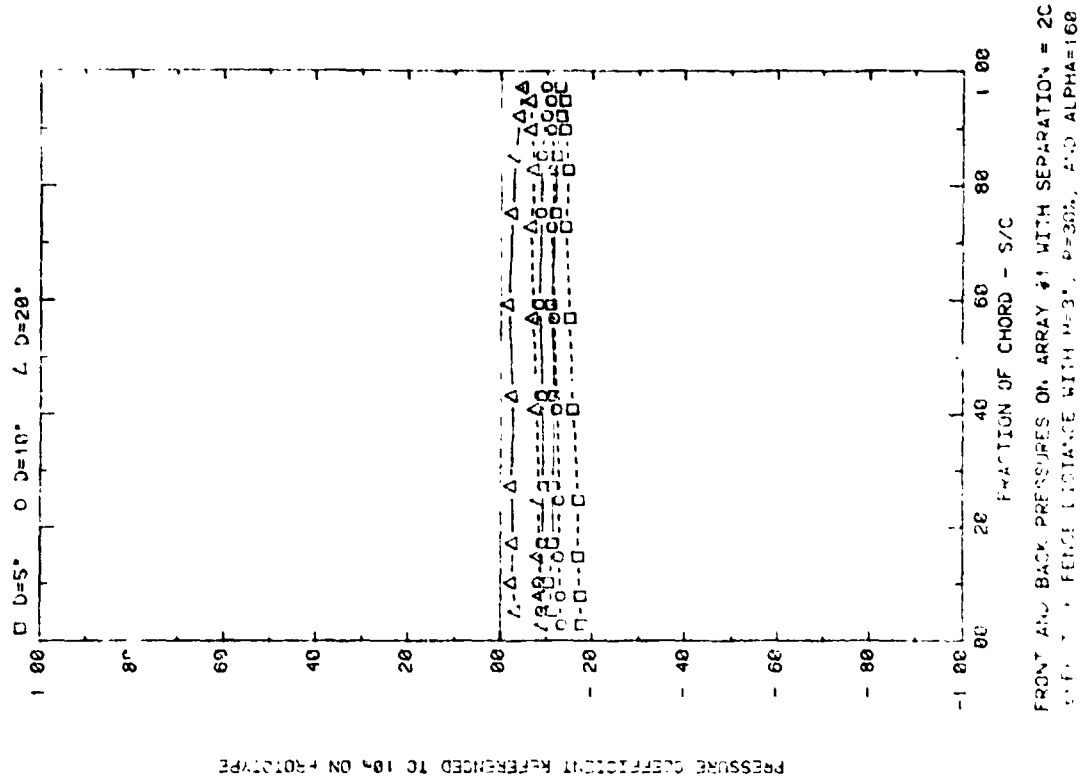


FRONT AND BACK PRESSURES ON ARRAY #1 WITH SEPARATION = 2C
EFFECT OF FENCE DISTANCE WITH H=3, P=30%, AND ALPHA=90

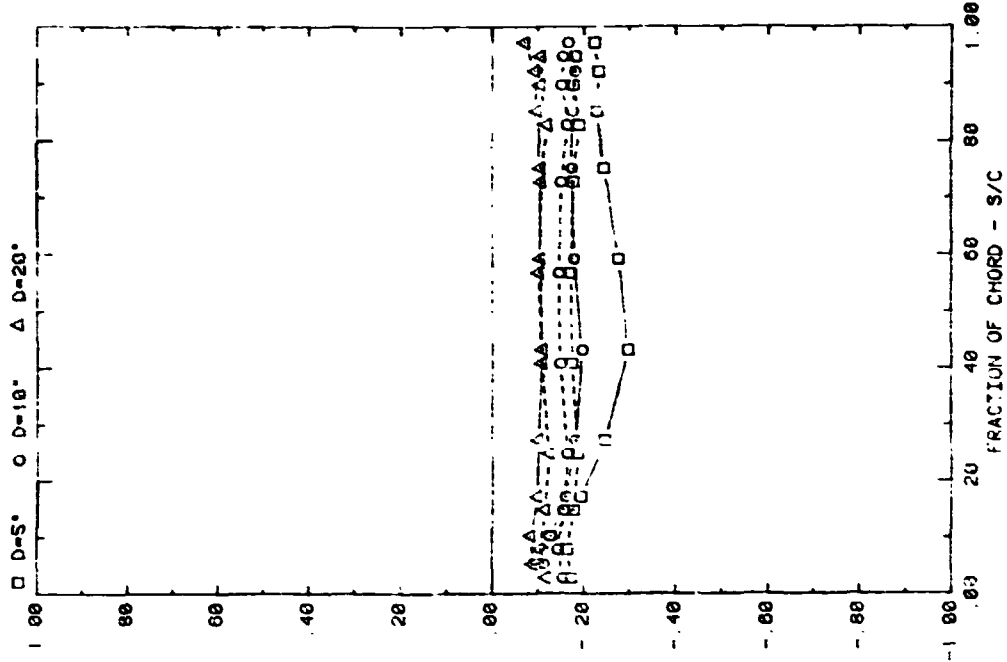


FRONT AND BACK PRESSURES ON ARRAY #1 WITH SEPARATION = 2C
EFFECT OF FENCE DISTANCE WITH H=3, P=30%, AND ALPHA=35

Plot 3-3. Multiple Arrays with Fence, WD = 0°
Effect of Fence Distance

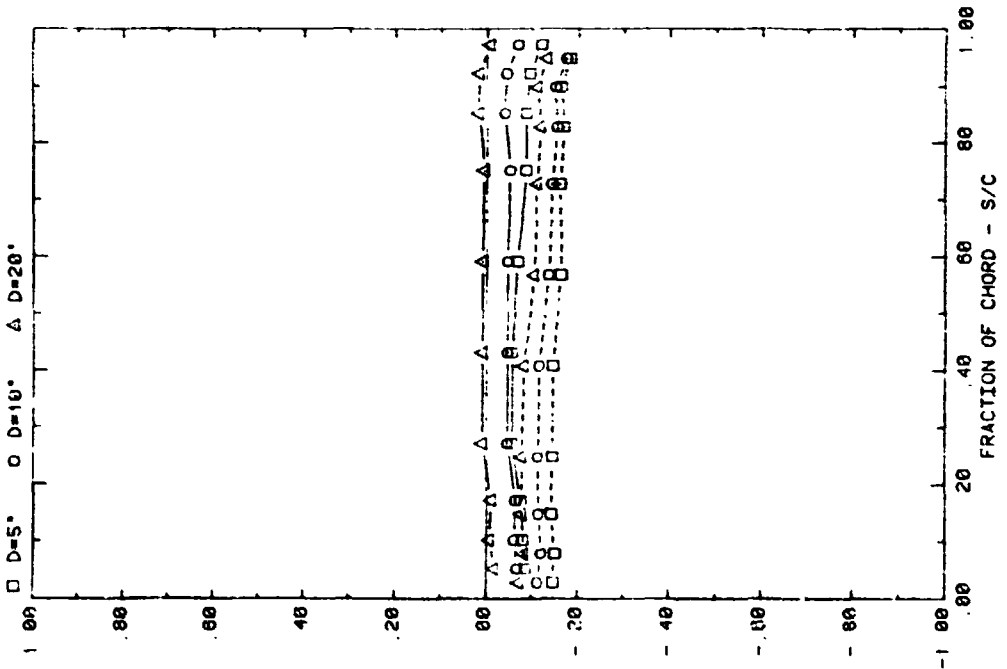


Plot 3-3. (Continued)



FRONT AND BACK PRESSURES ON ARRAY #2 WITH SEPARATION = 2C
EFFECT OF FENCE DISTANCE WITH $M=3$, $P=30\%$, AND $\alpha=90$

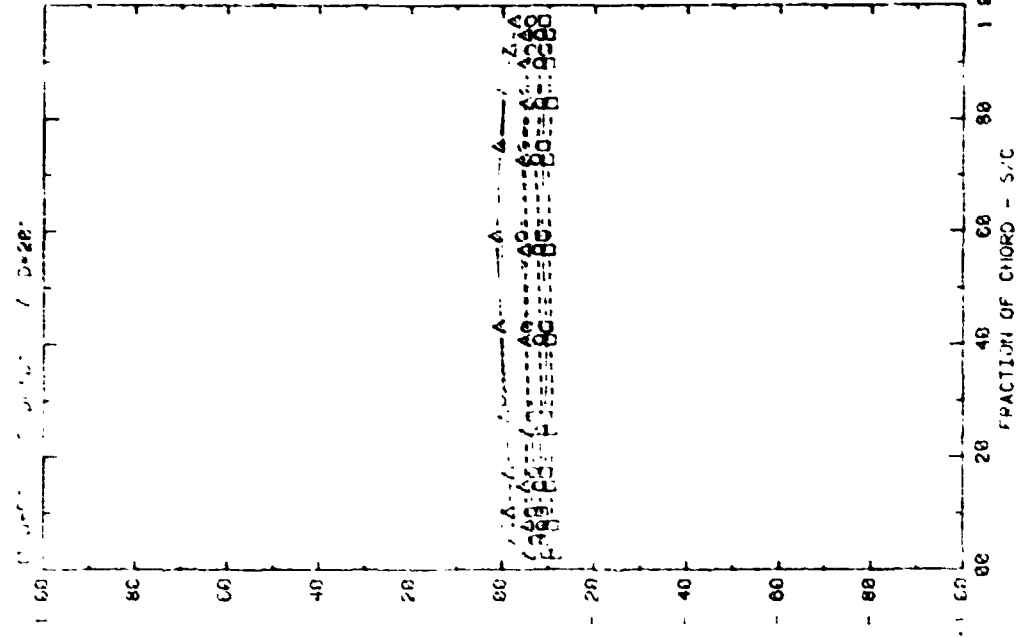
PRESSURE COEFFICIENT REFERENCED TO 1/4 IN PROTOTYPE



FRONT AND BACK PRESSURES ON ARRAY #7 WITH SEPARATION = 2C
EFFECT OF FENCE DISTANCE WITH $M=3$, $P=30\%$, AND $\alpha=95$

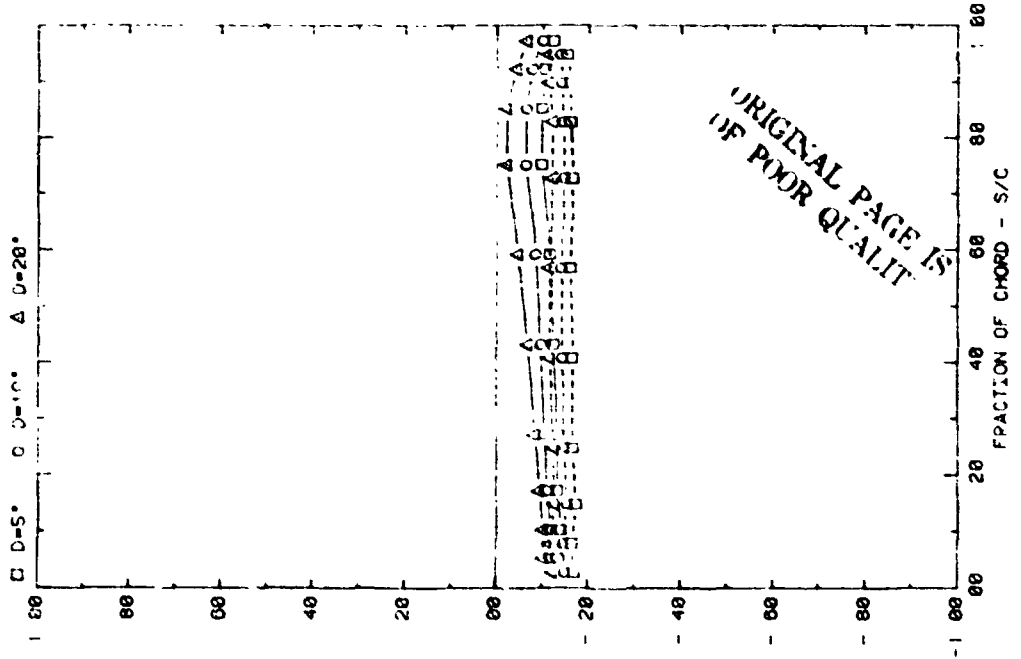
PRESSURE COEFFICIENT REFERENCED TO 1/4 IN PROTOTYPE

Plot 3-3. (Continued)



PRESSURE COEFFICIENT REFERENCED TO 1/4 IN ON PROTOTYPE

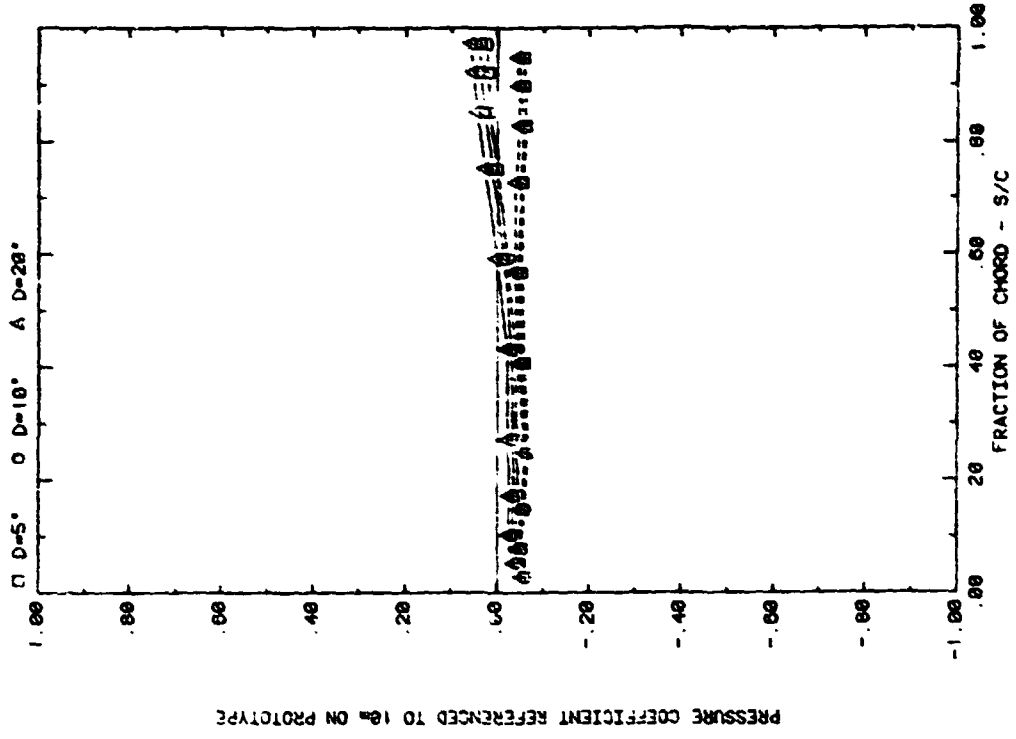
FRONT AND BACK PRESSURES ON ARRAY #2 WITH SEPARATION = 2C
EFFECT OF FEINCE DISTANCE WITH H=3*, P=30%, AND ALPHA=180



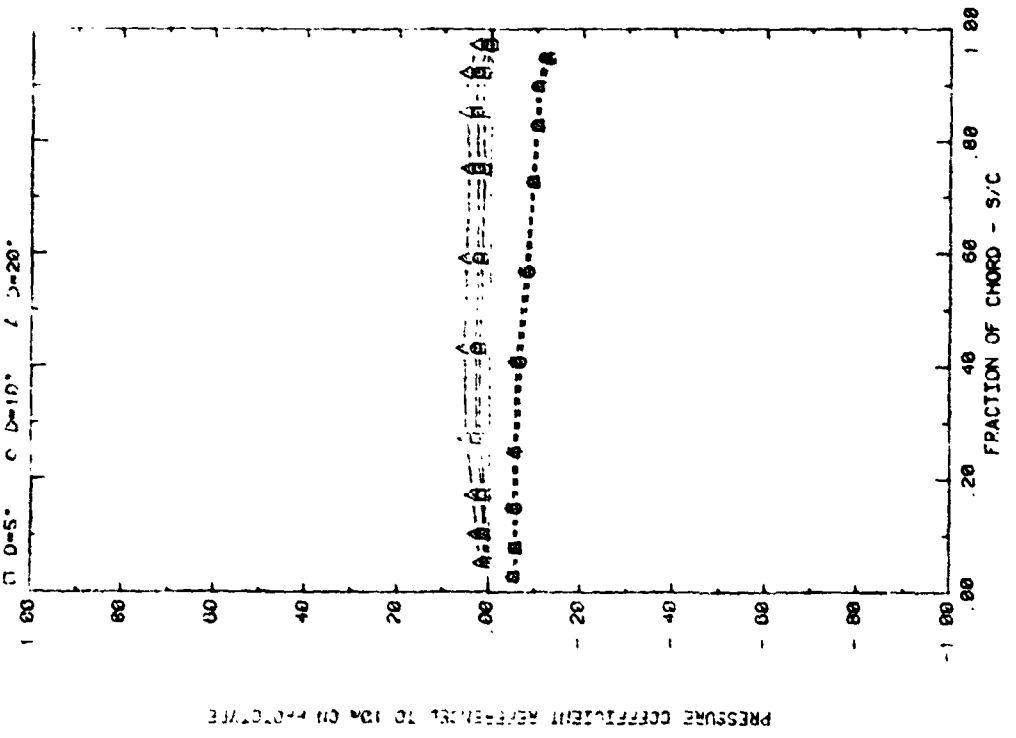
PRESSURE COEFFICIENT REFERENCED TO 1/4 IN ON PROTOTYPE

FRONT AND BACK PRESSURES ON ARRAY #2 WITH SEPARATION = 2C
EFFECT OF FEINCE DISTANCE WITH H=3*, P=30%, AND ALPHA=145

Plot 3-3. (Continued)

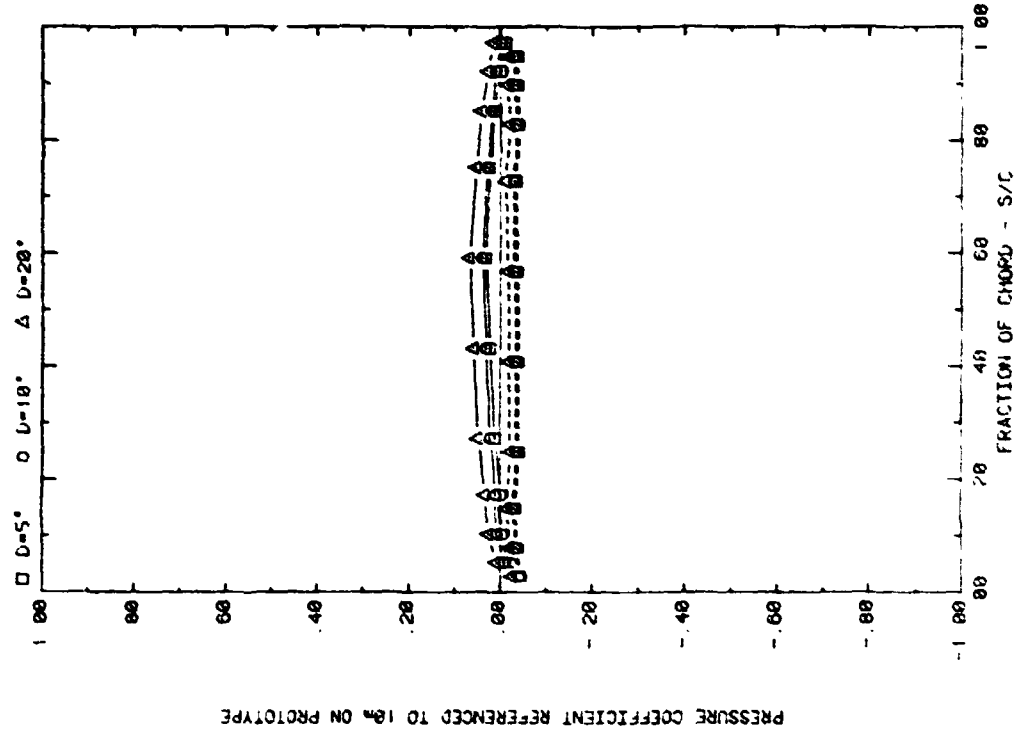


FRONT AND BACK PRESSURES ON ARRAY #5 WITH SEPARATION = 2C
EFFECT OF FENCE DISTANCE WITH H=3°, P=30%, AND ALPHA=00

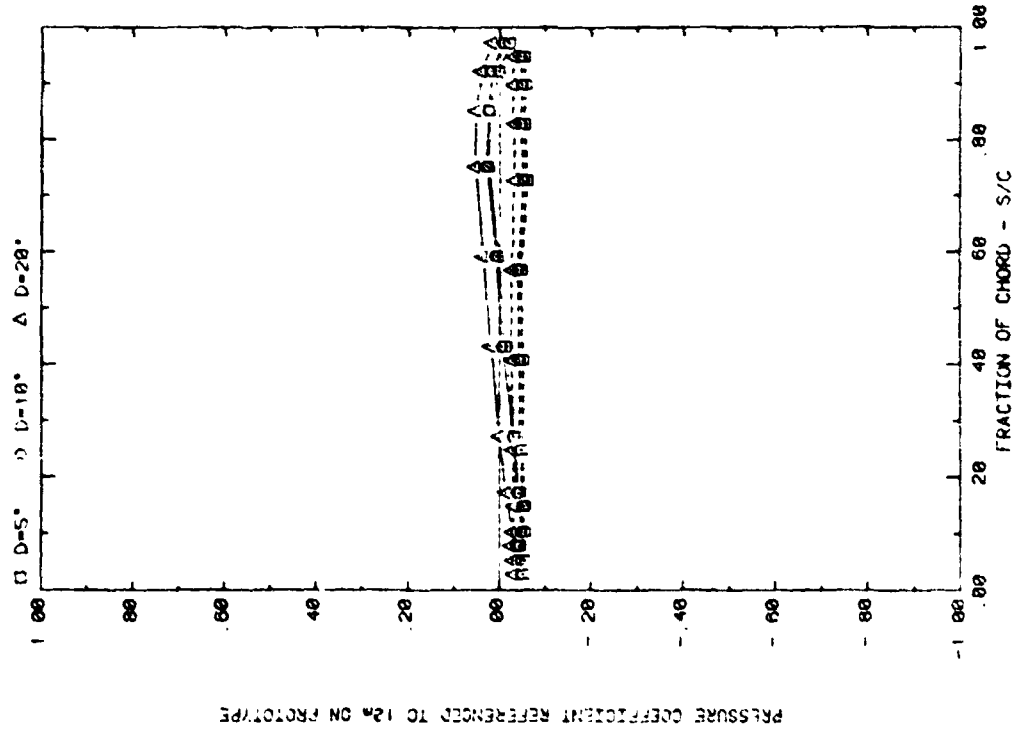


FRONT AND BACK PRESSURES ON ARRAY #5 WITH SEPARATION = 2C
EFFECT OF FENCE DISTANCE WITH H=3°, P=30%, AND ALPHA=35

Plot 3-3. (Continued)

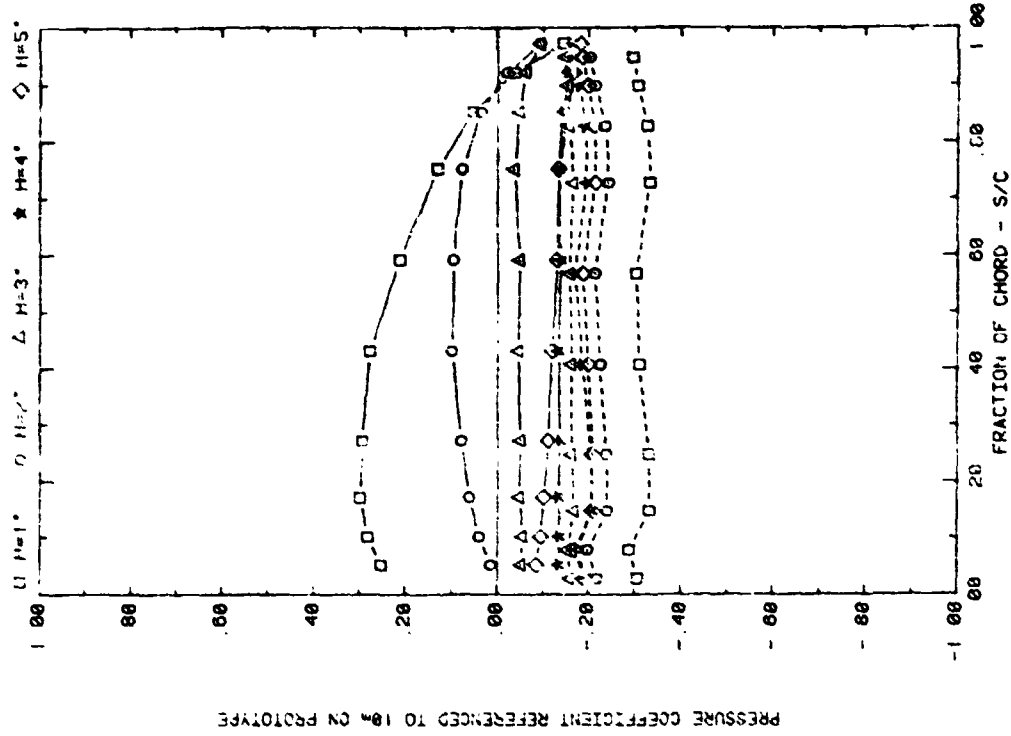


FRONT AND BACK PRESSURES ON ARRAY #5 WITH SEPARATION = 2C
EFFECT OF FENCE DISTANCE WITH M=3°, P=30%, AND ALPHA=160

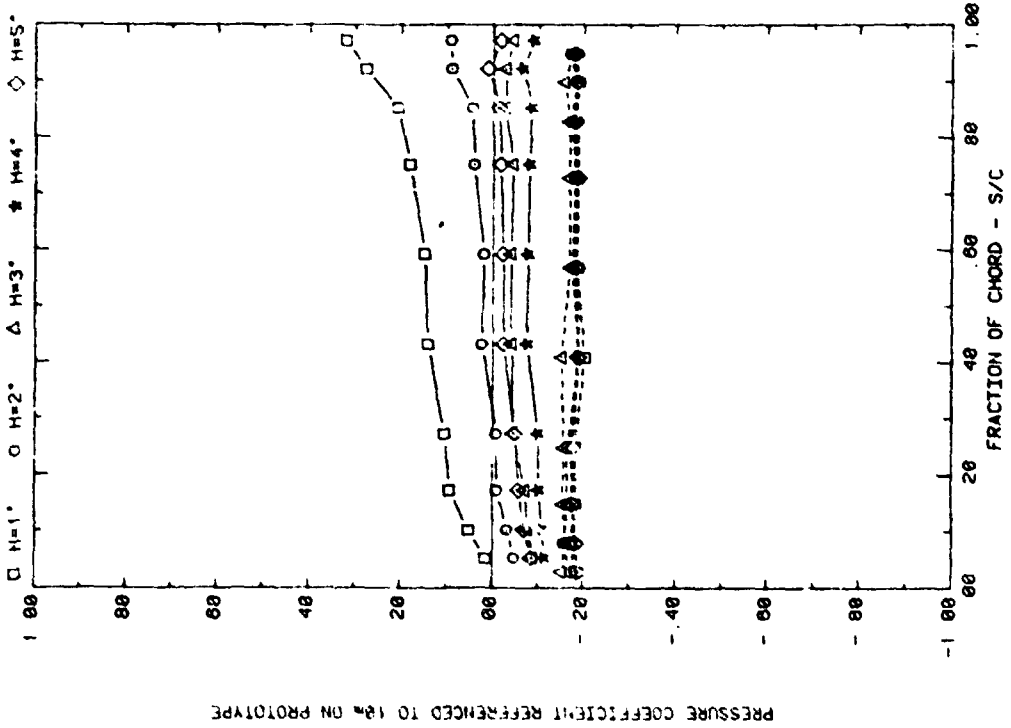


FRONT AND BACK PRESSURES ON ARRAY #5 WITH SEPARATION = 2C
EFFECT OF FENCE DISTANCE WITH M=3°, P=30%, AND ALPHA=145

Plot 3-3. (Concluded)

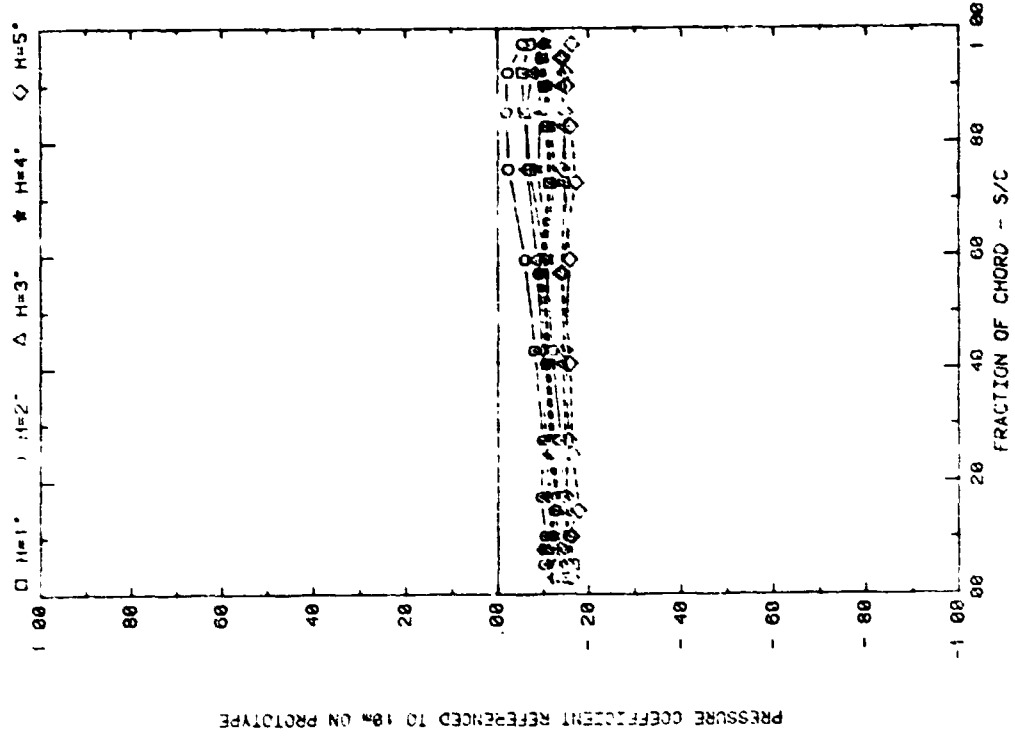


FRONT AND BACK PRESSURES ON ARRAY #1 WITH SEPARATION = 2C
EFFECT OF FENCE HEIGHT WITH ALPHA=145, D=10", AND P=30%

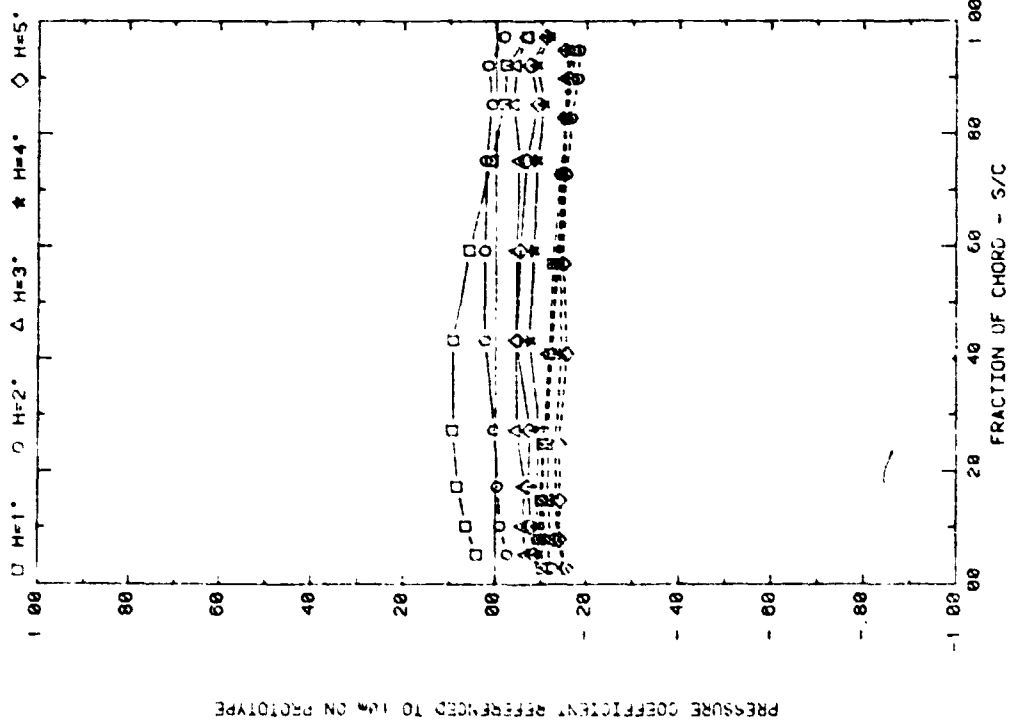


FRONT AND BACK PRESSURES ON ARRAY #1 WITH SEPARATION = 2C
EFFECT OF FENCE HEIGHT WITH ALPHA=35, D=10", AND P=30%

Plot 3-4. Multiple Arrays with Fence, $WD = 0^\circ$
Effect of Fence Height

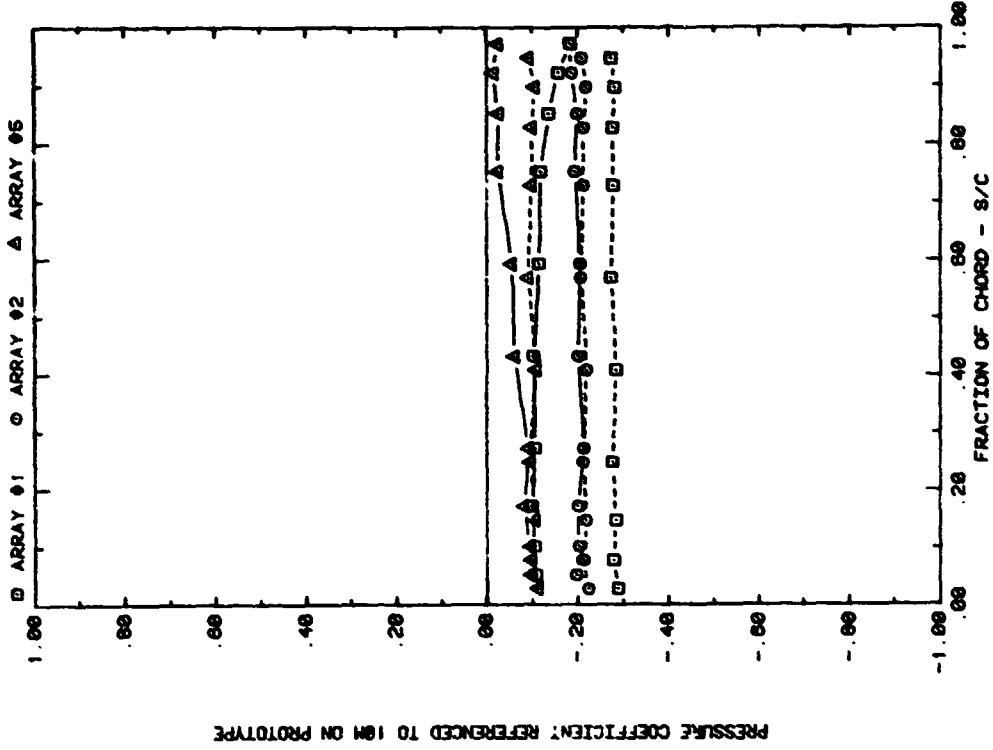


FRONT AND BACK PRESSURES ON ARRAY #2 WITH SEPARATION = 2C
EFFECT OF FENCE HEIGHT WITH ALPHA=145, D=10°, AND P=30%



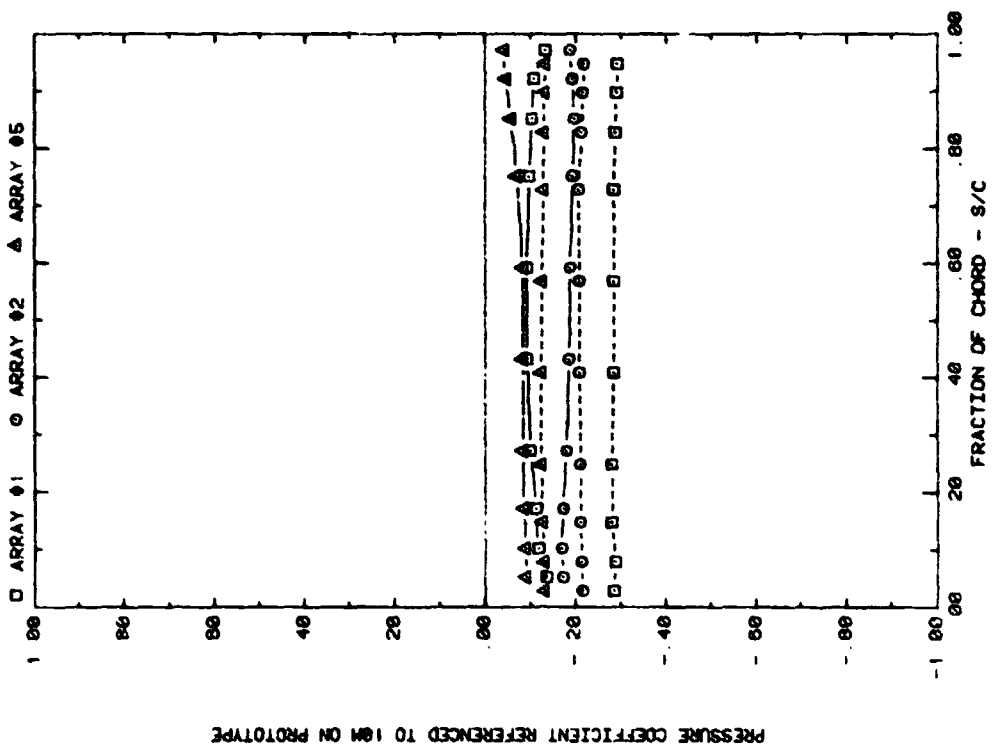
FRONT AND BACK PRESSURES ON ARRAY #2 WITH SEPARATION = 2C
EFFECT OF FENCE HEIGHT WITH ALPHA=35, D=10°, AND P=30%

Plot 3-4. (Continued)



PRESSURE COEFFICIENT REFERENCED TO 14M ON PROTOTYPE

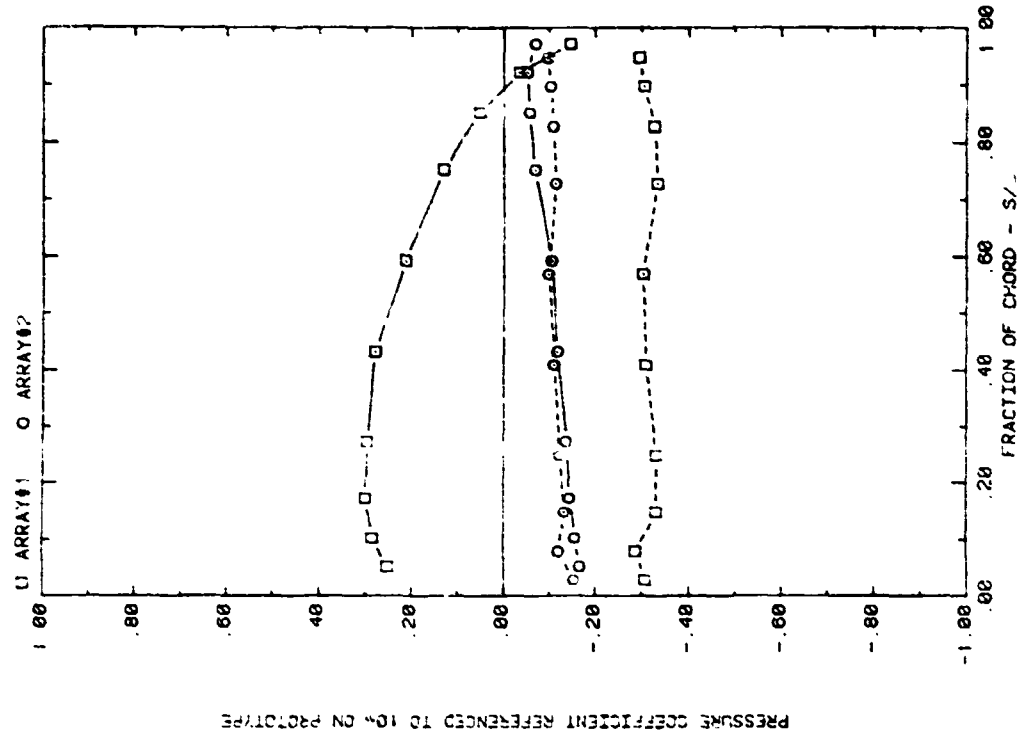
FRONT AND BACK PRESSURES ON ARRAYS #1, #2, #5 WITH SEPARATION = 2C
EFFECT OF ARRAY WITH ALPHA = 0, WIND = 0, HF = 4°



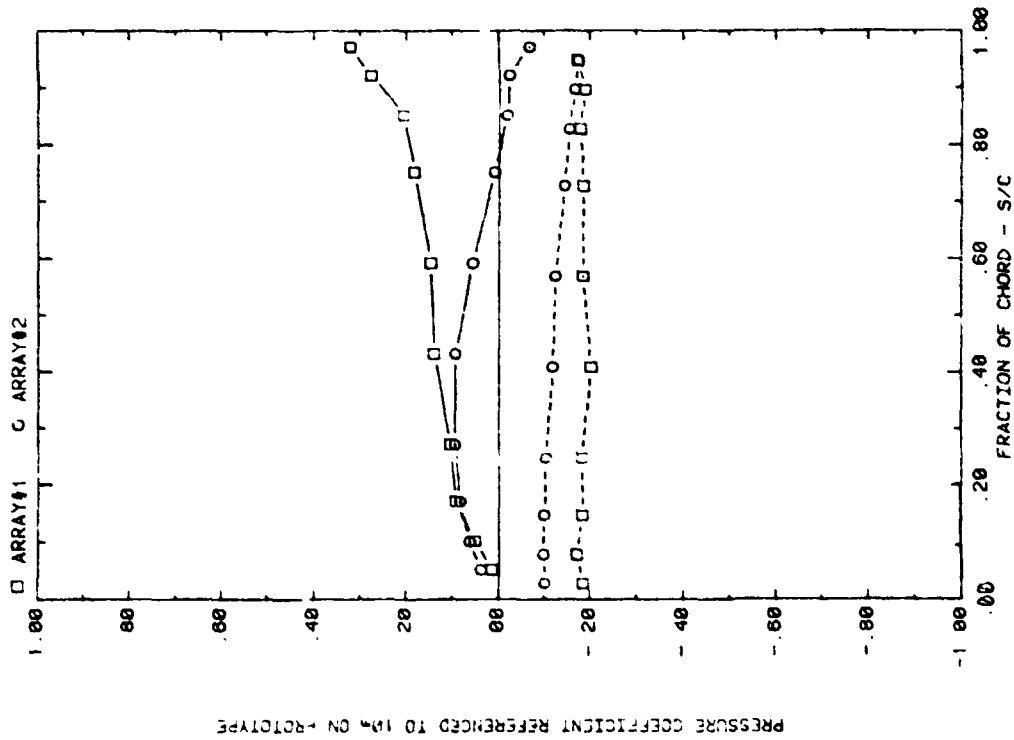
PRESSURE COEFFICIENT REFERENCED TO 14M ON PROTOTYPE

FRONT AND BACK PRESSURES ON ARRAYS #1, #2, #5 WITH SEPARATION = 2C
EFFECT OF ARRAY WITH ALPHA = 4°, WIND = 0, HF = 4°

Plot 3-4. (Continued)

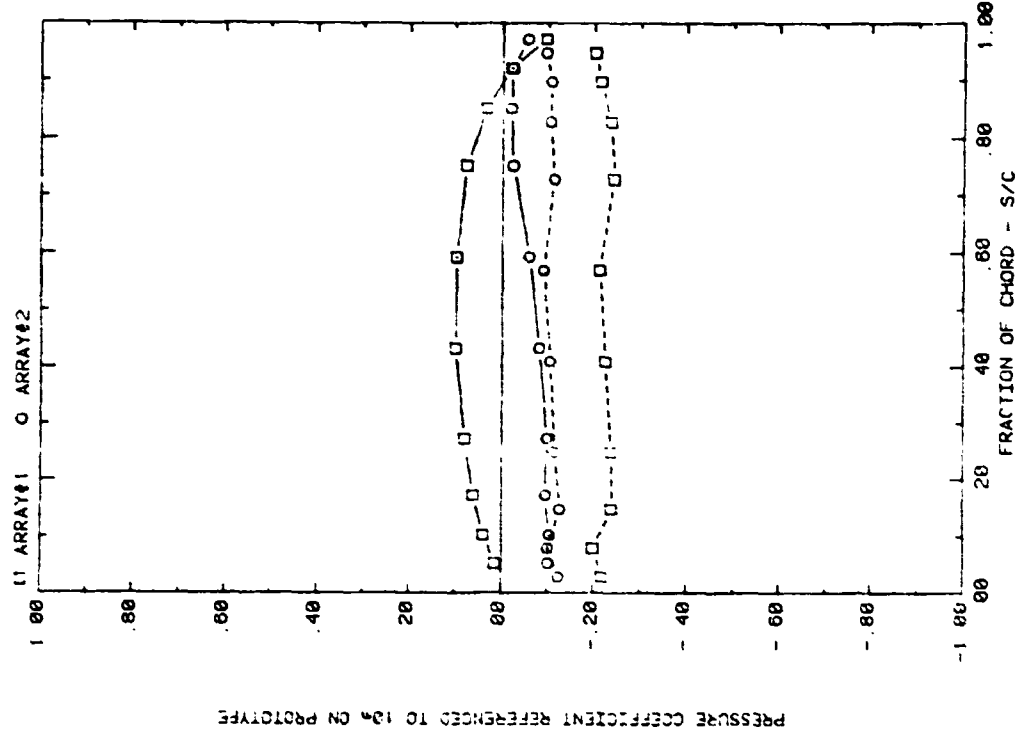


FRONT AND BACK PRESSURES ON ARRAYS #1 WITH SEPARATION = 2C
EFFECT OF ARRAY WITH ALPHA=145, H=1", D=10", AND P=30%

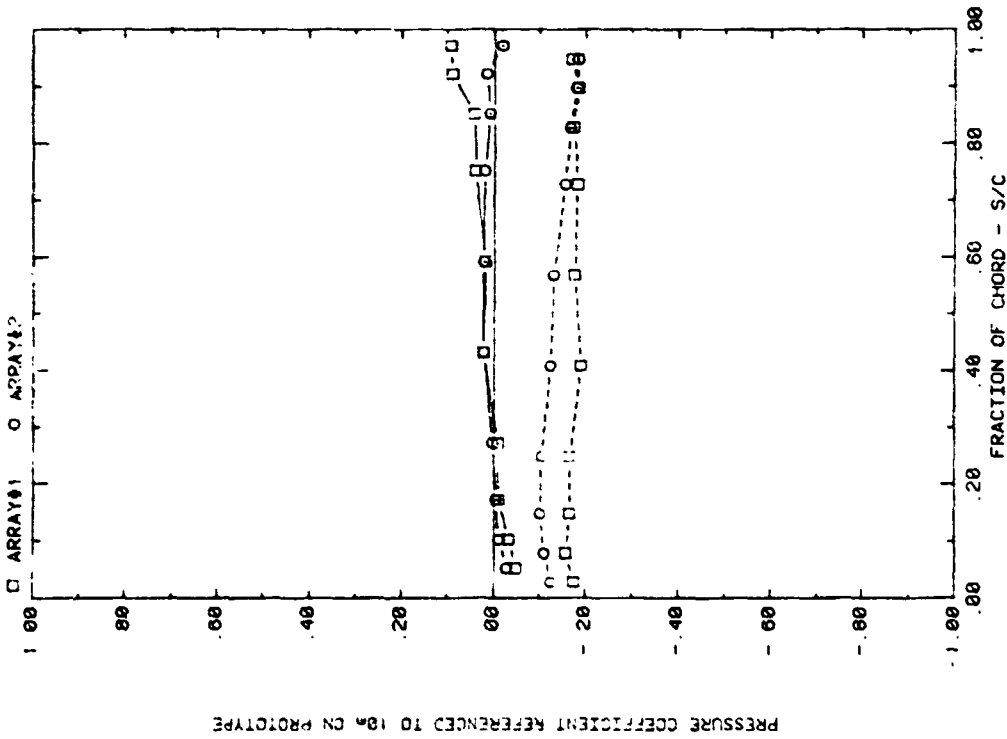


FRONT AND BACK PRESSURES ON ARRAYS #1 WITH SEPARATION = 2C
EFFECT OF ARRAY WITH ALPHA=35, H=1", D=10", AND P=30%

Plot 3-4. (Continued)

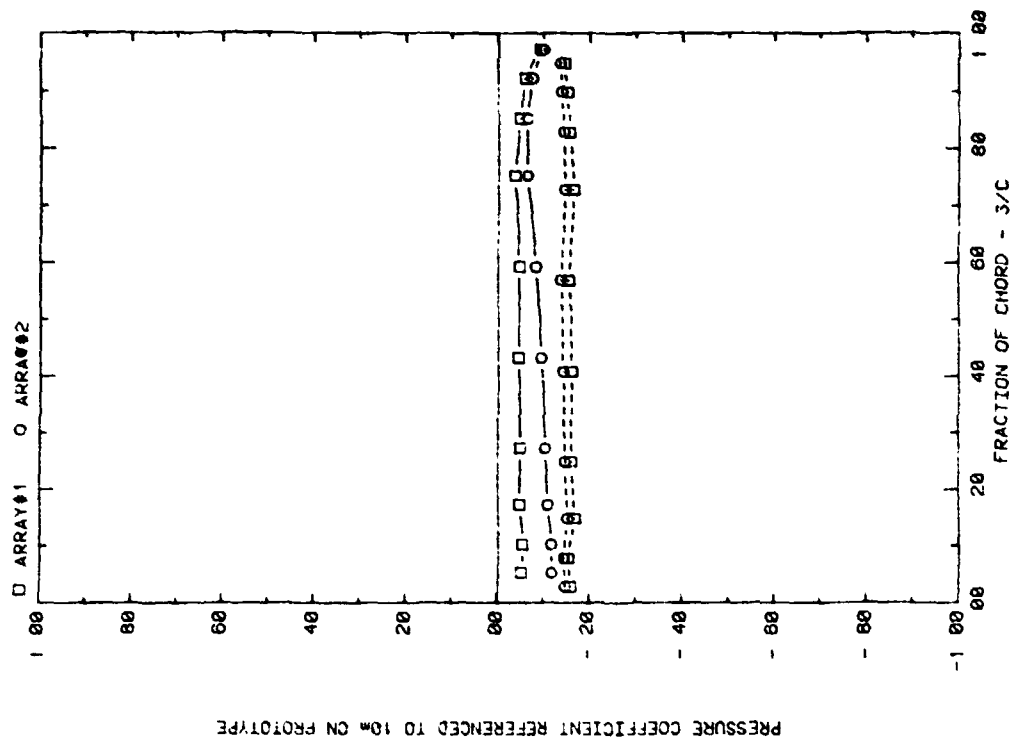


FRONT AND BACK PRESSURES ON ARRAYS #1&2 WITH SEPARATION = 2C
EFFECT OF ARRAY WITH ALPHA=145, H=2', D=10', AND P=30%

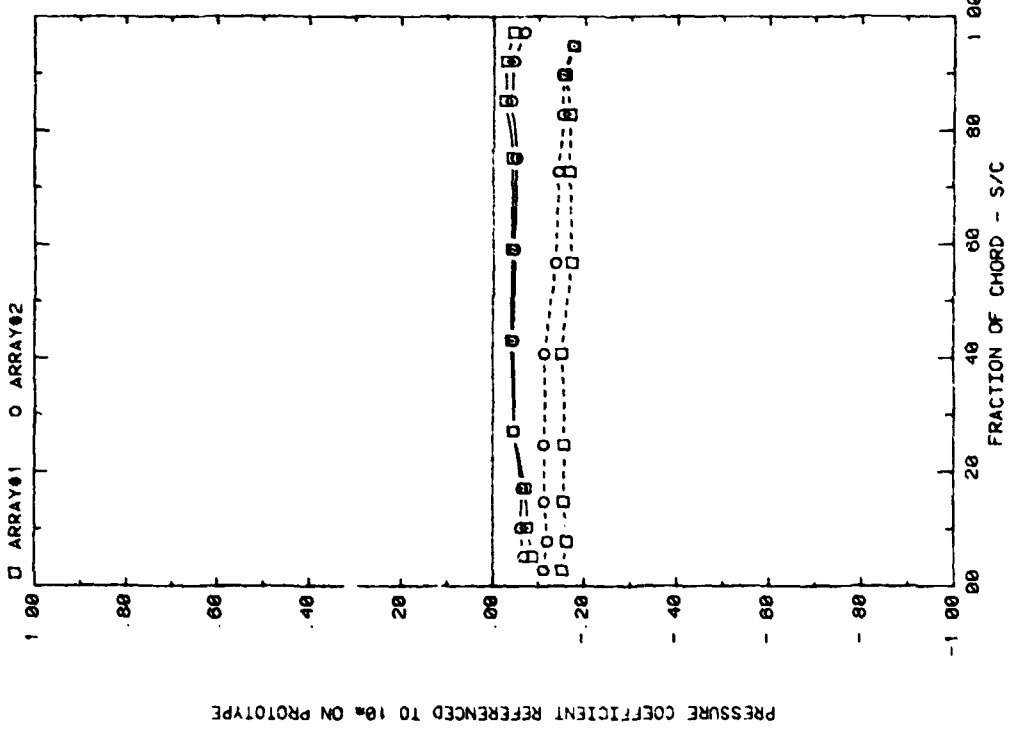


FRONT AND BACK PRESSURES ON ARRAYS #1&2 WITH SEPARATION = 2C
EFFECT OF ARRAY WITH ALPHA=35, H=2', D=10', AND P=30%

Plot 3-4. (Continued)

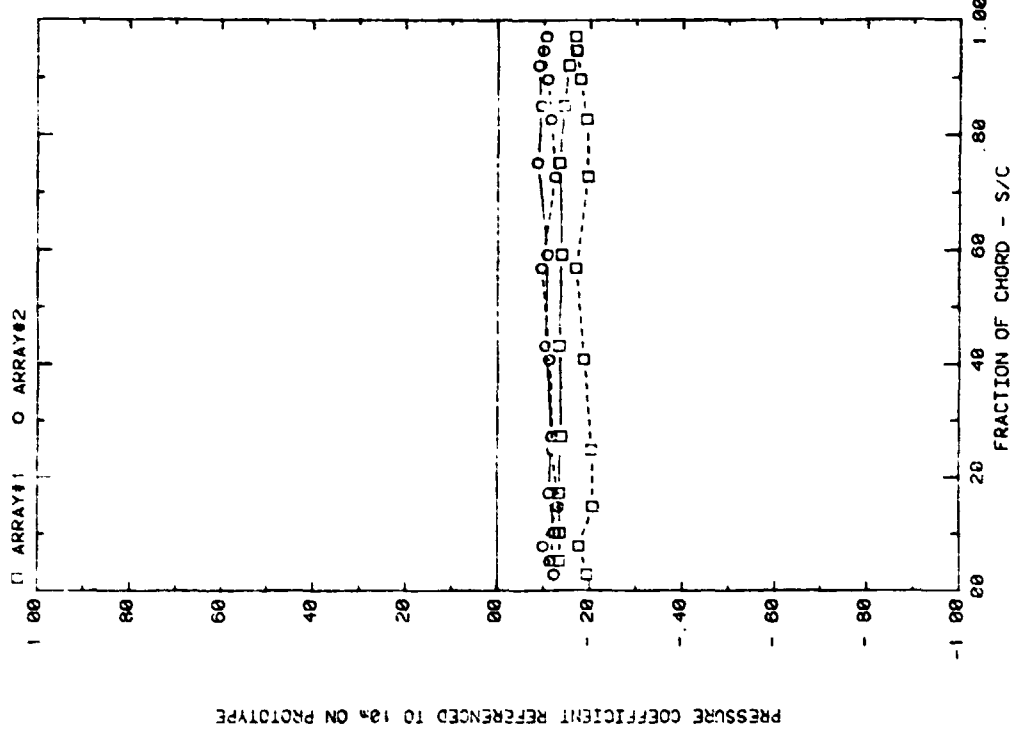


FRONT AND BACK PRESSURES ON ARRAYS #1 WITH SEPARATION = 2C
EFFECT OF ARRAY WITH ALPHA=15, H=3', D=10', AND P=30%



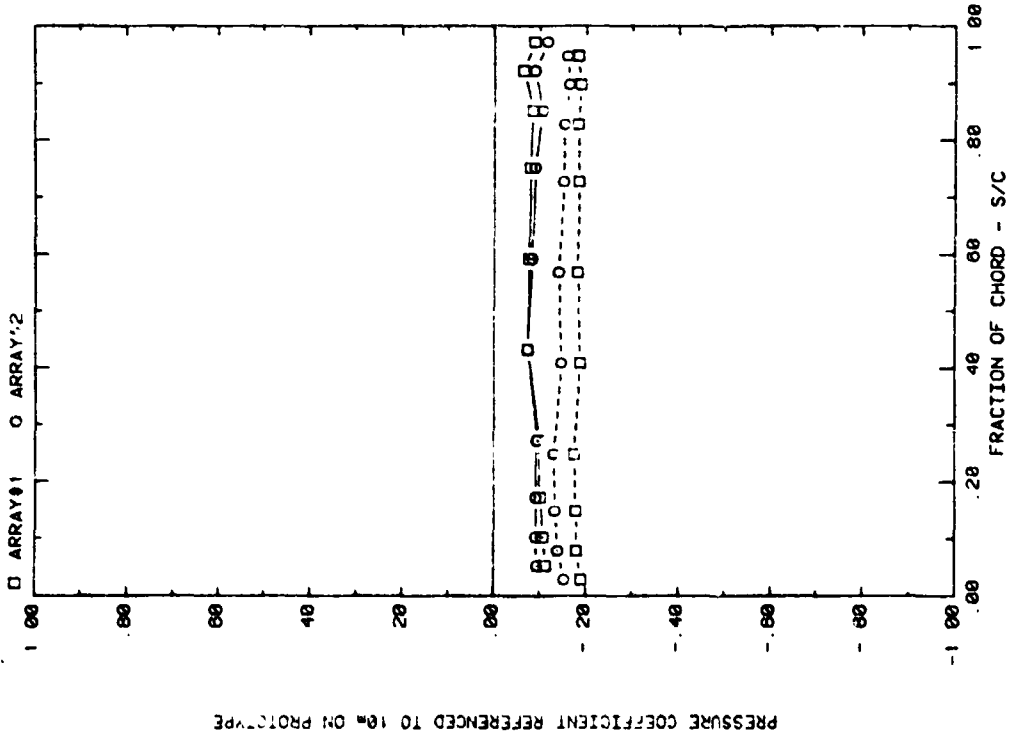
FRONT AND BACK PRESSURES ON ARRAYS #1 WITH SEPARATION = 2C
EFFECT OF ARRAY WITH ALPHA=35, H=3', D=10', AND P=30%

Plot 3-4. (Continued)



PRESSURE COEFFICIENT REFERENCED TO 12% ON PROTOTYPE

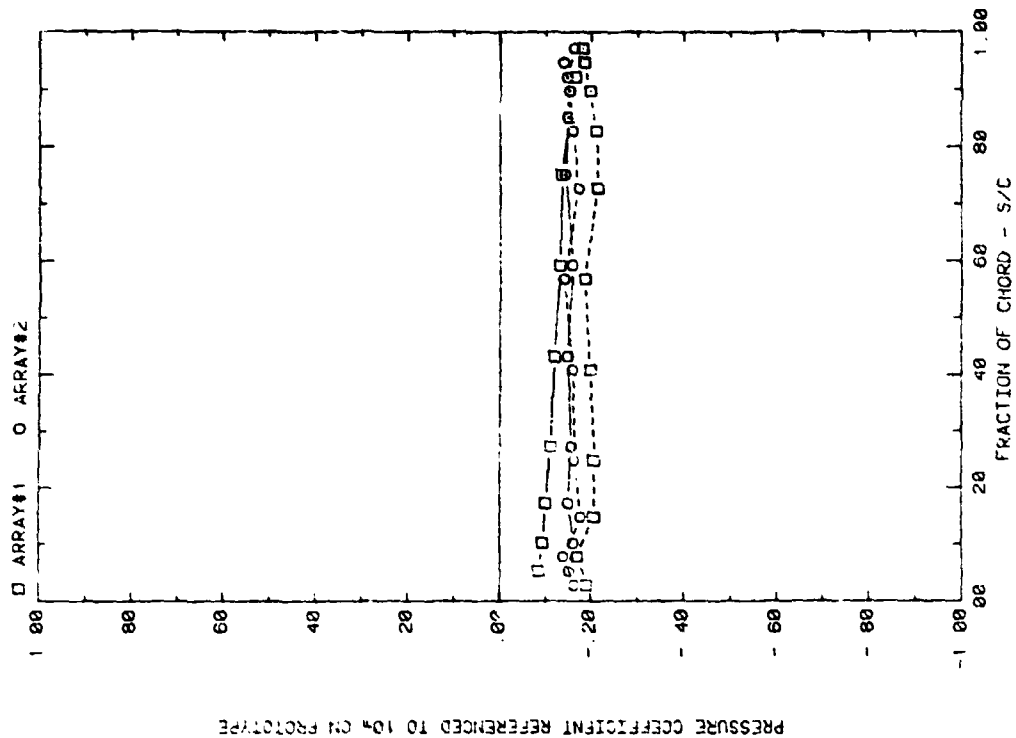
FRONT AND BACK PRESSURES ON ARRAYS #1 WITH SEPARATION = 2C
EFFECT OF ARRAY WITH ALPHA=145, H=4", D=10", AND P=30%



PRESSURE COEFFICIENT REFERENCED TO 10% ON PROTOTYPE

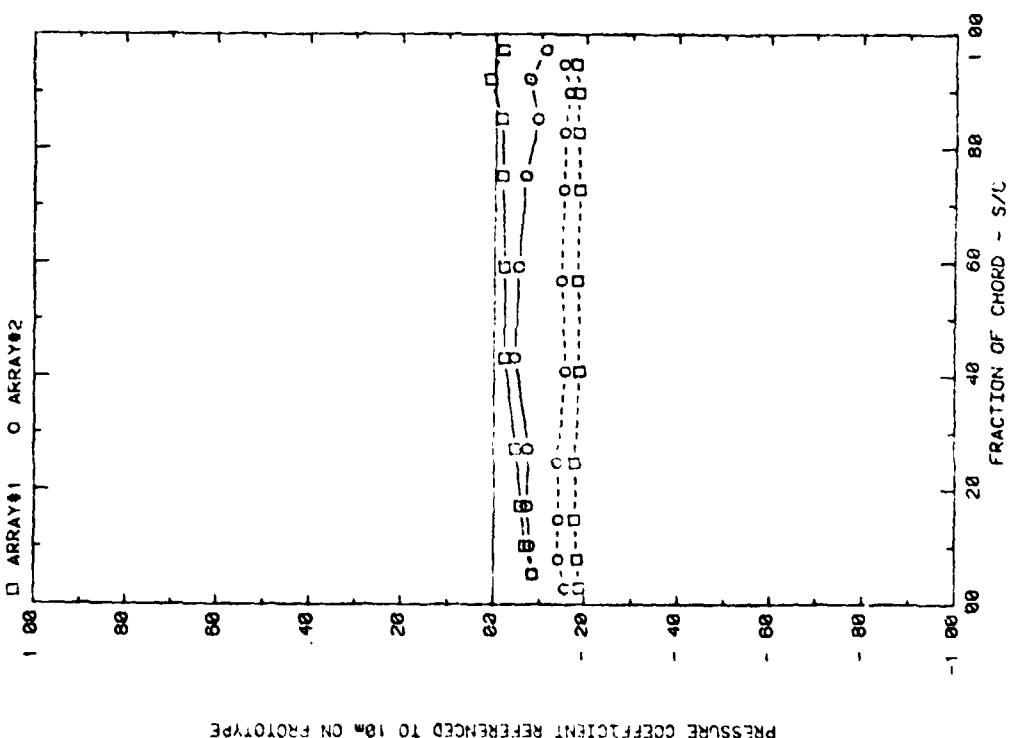
FRONT AND BACK PRESSURES ON ARRAYS #1 WITH SEPARATION = 2C
EFFECT OF ARRAY WITH ALPHA=35, H=4", D=10", AND P=30%

Plot 3-4. (Continued)



PRESSURE COEFFICIENT REFERENCED TO 10% ON PROTOTYPE

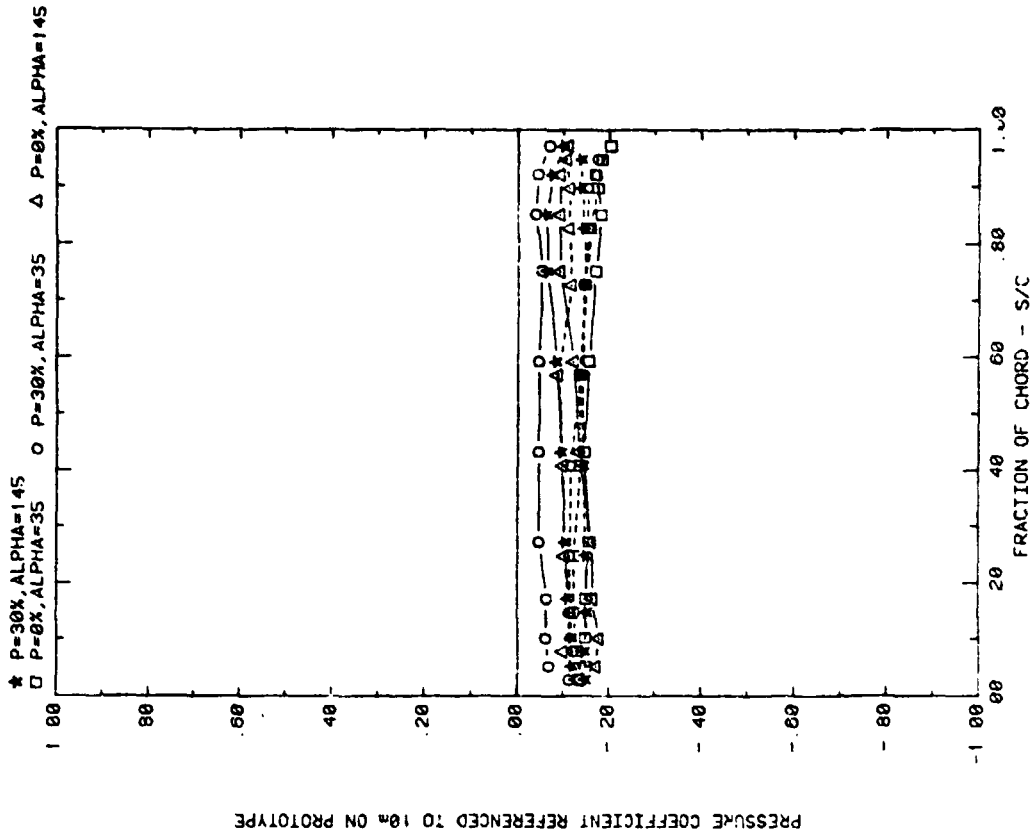
FRONT AND BACK PRESSURES ON ARRAYS #1 WITH SEPARATION = 2C
EFFECT OF ARRAY WITH ALPHA=14.5, H=5", D=10", AND P=30%



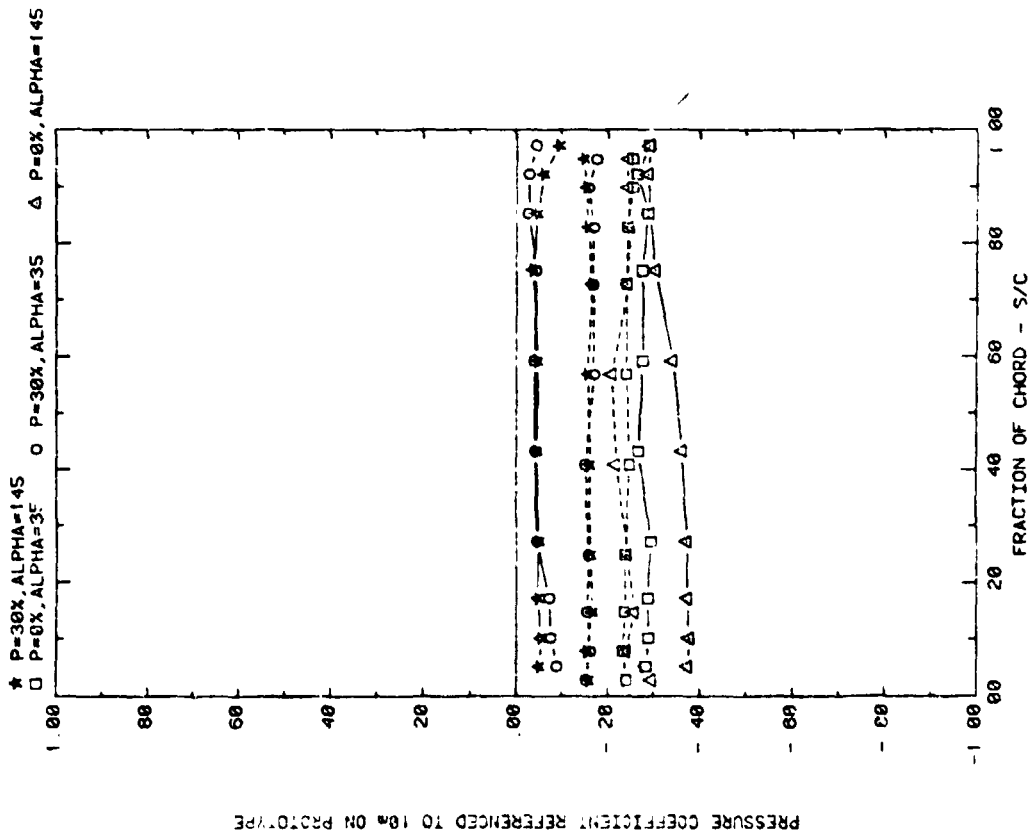
PRESSURE COEFFICIENT REFERENCED TO 10% ON PROTOTYPE

FRONT AND BACK PRESSURES ON ARRAYS #1 WITH SEPARATION = 2C
EFFECT OF ARRAY WITH ALPHA=35, H=5", D=10", AND P=30%

Plot 3-4. (Concluded)

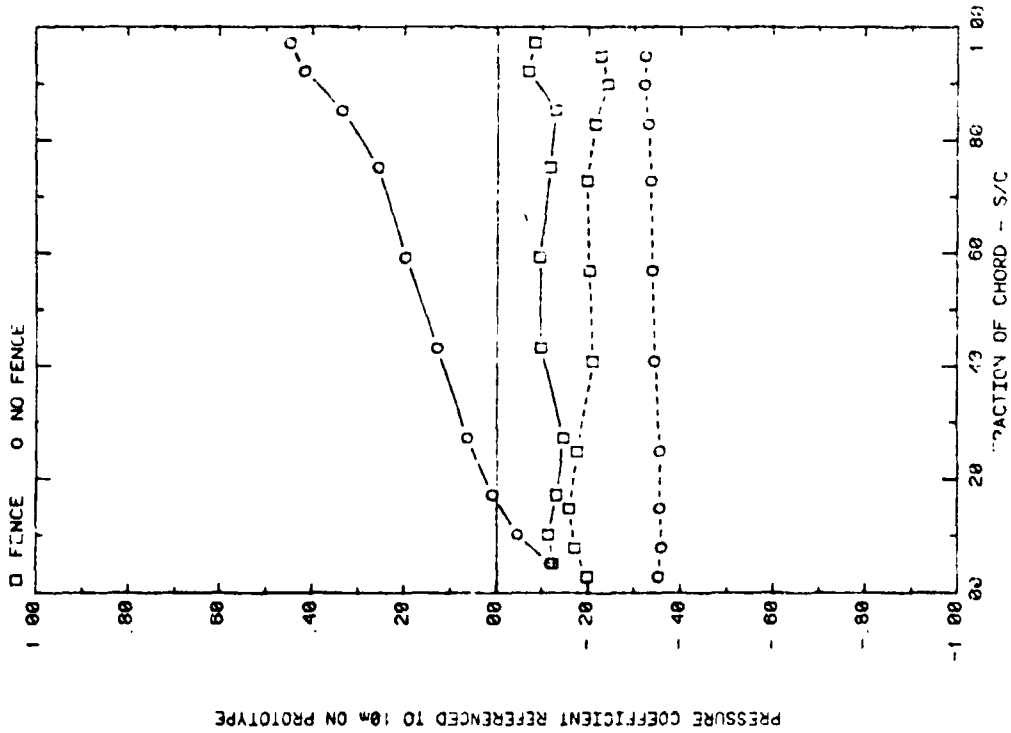
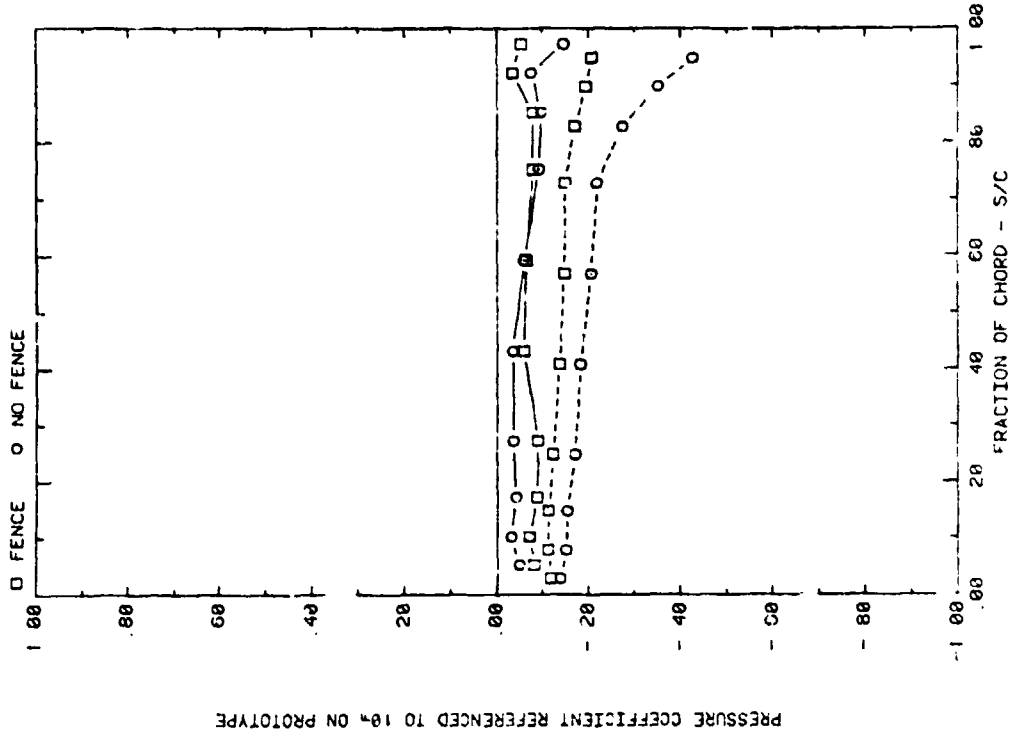


FRONT A J BACK PRESSURES ON ARRAY #2 WITH SEPARATION = 2C
 EFFECT OF FENCE POROSITY WITH ALPHA=35 OR 145, D=10', AND H=3'

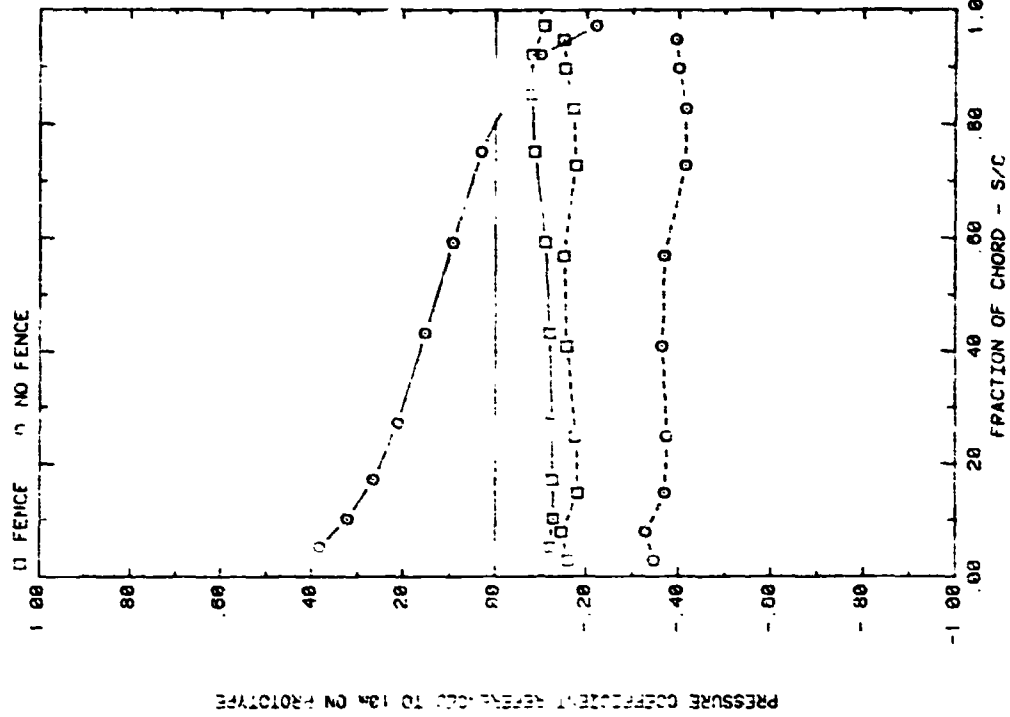


FRONT AND BACK PRESSURES ON ARRAY #1 WITH SEPARATION = 2C
 EFFECT OF FENCE POROSITY WITH ALPHA=35 OR 145, D=10', AND H=3'

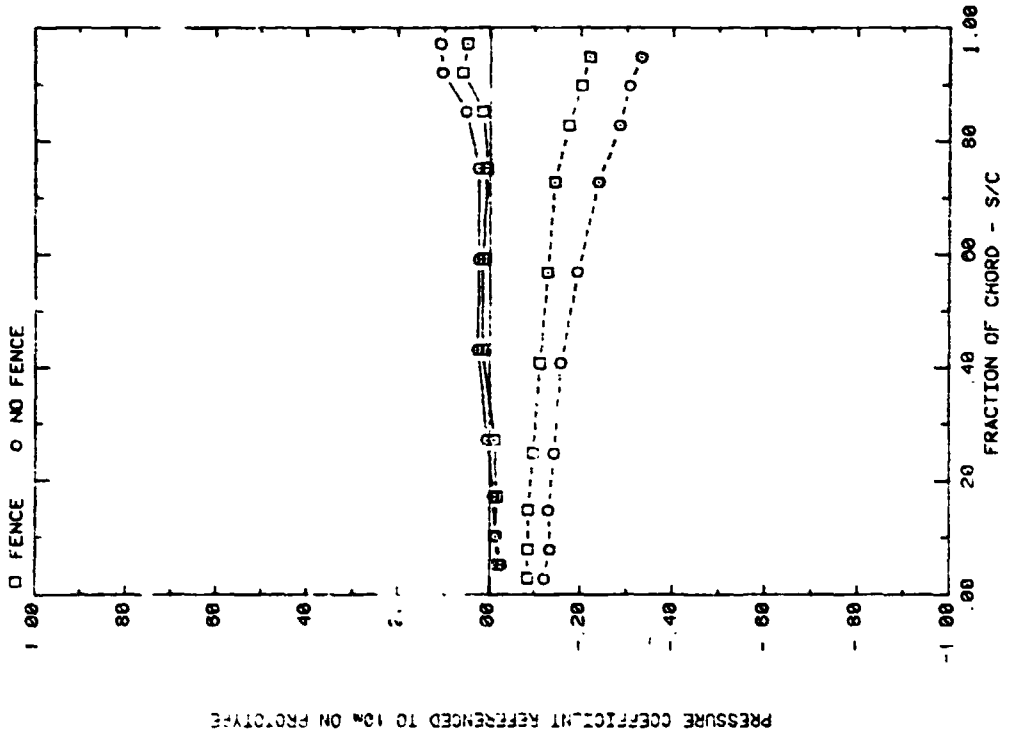
Plot 3-5. Multiple Arrays with Fence, $WD = 0^\circ$
 Effect of Fence Porosity



FRONT AND BACK PRESSURES ON ARRAY #1 WITH $X=2C$, AND WIND=0
 EFFECT OF FENCE ON APPA EDGE, ALPHA=35, H=3", D=13", AND P=30%
 FRONT AND BACK PRESSURES ON ARRAY #2 WITH $X=2C$, AND WIND=0
 EFFECT OF FENCE ON ALRAY EDGE, ALPHA=35, H=3", D=13", AND P=30%
 Plot 4-1. Edge Study, $WD = 0^\circ$
 Effect of Fence

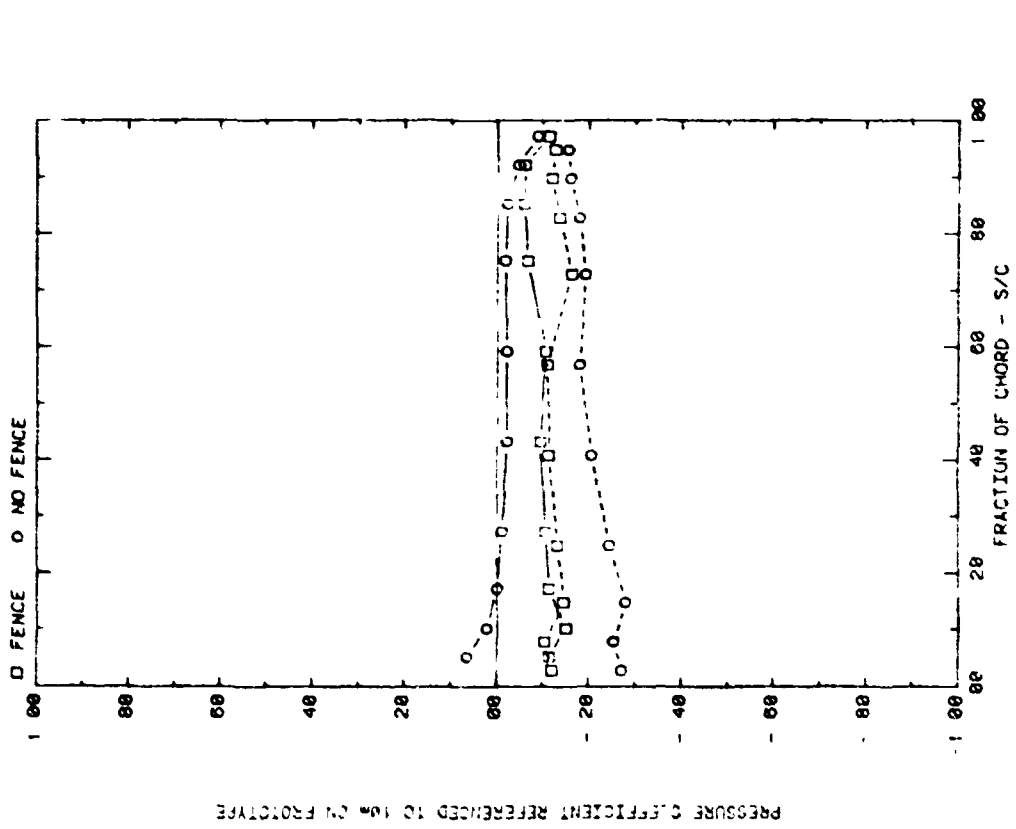
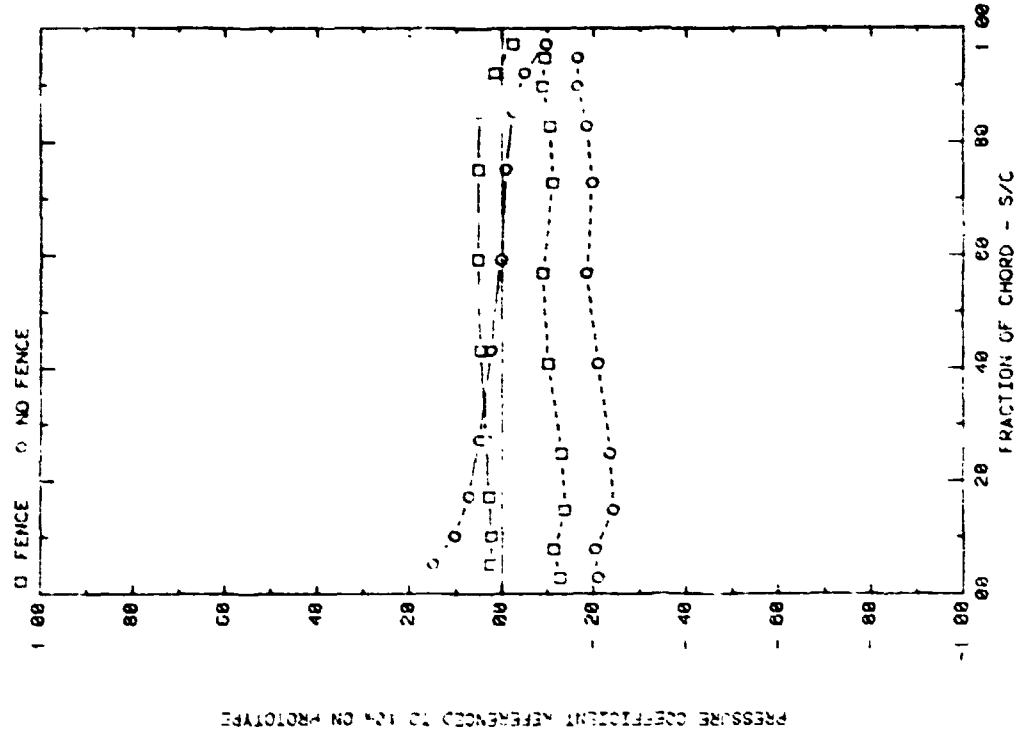


FRONT AND BACK PRESSURES ON ARRAY #1 WITH X=2C, AND WIND=0
EFFECT OF FENCE ON ARRAY EDGE, ALPHA=145, H=3, D=10, AND P=30X



FRONT AND BACK PRESSURES ON ARRAY #5 WITH X=2C, AND WIND=0
EFFECT OF FENCE ON ARRAY EDGE, ALPHA=35, H=3, D=10, AND P=30X

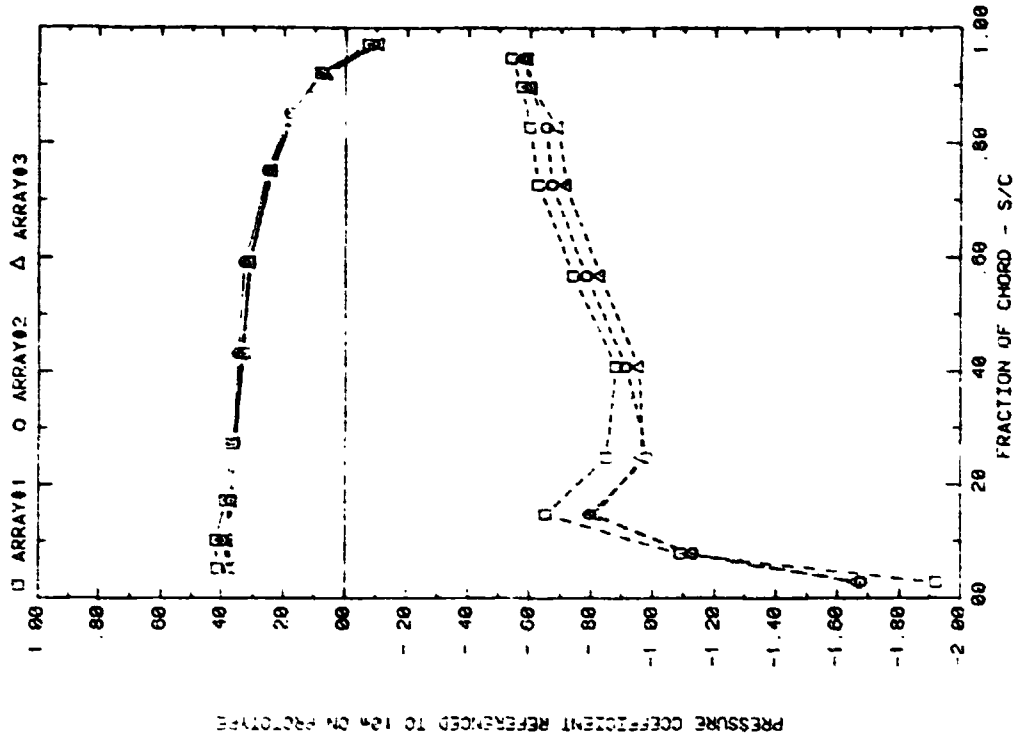
Plot 4-1. (Continued)



FRONT AND BACK PRESSURES ON ARRAY #2 WITH $\alpha=20$, AND $M=10$ EFFECT OF FENCE ON ARRAY EDGE, $\alpha=145$, $M=3$, $U=10$, AND $P=30X$

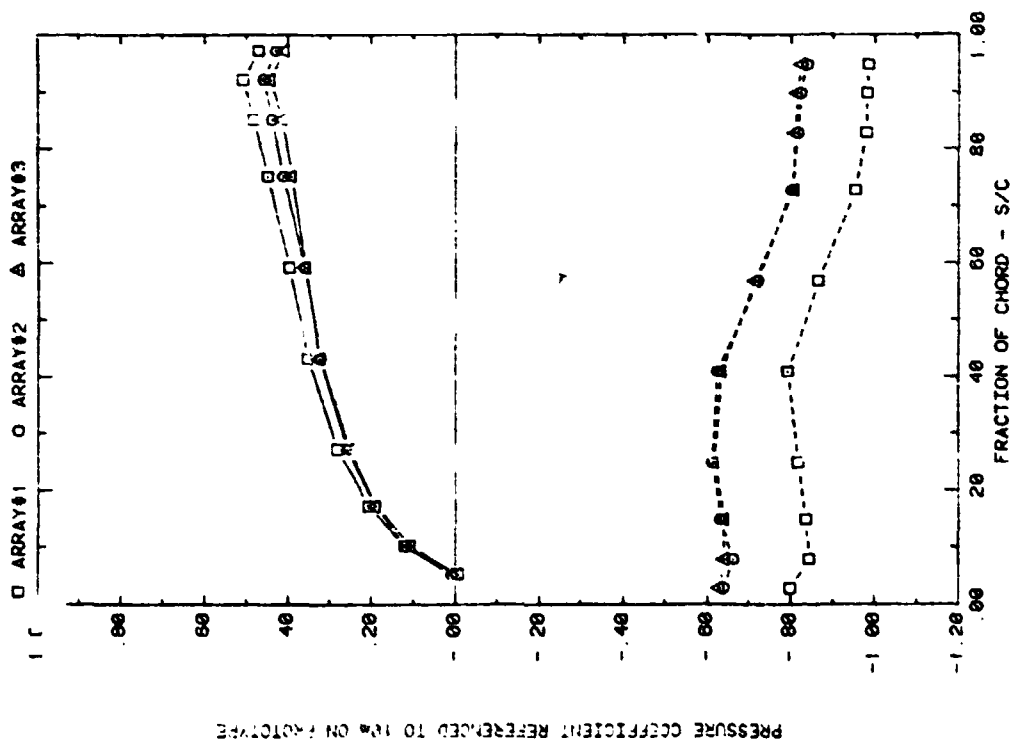
FRONT AND BACK PRESSURES ON ARRAY #2 WITH $\alpha=20$, AND $M=10$ EFFECT OF FENCE ON ARRAY EDGE, $\alpha=145$, $M=3$, $U=10$, AND $P=30X$

Plot 4-1. (Concluded)



PRESSURE COEFFICIENT REFERENCED TO 1/4 ON FACTORIVE

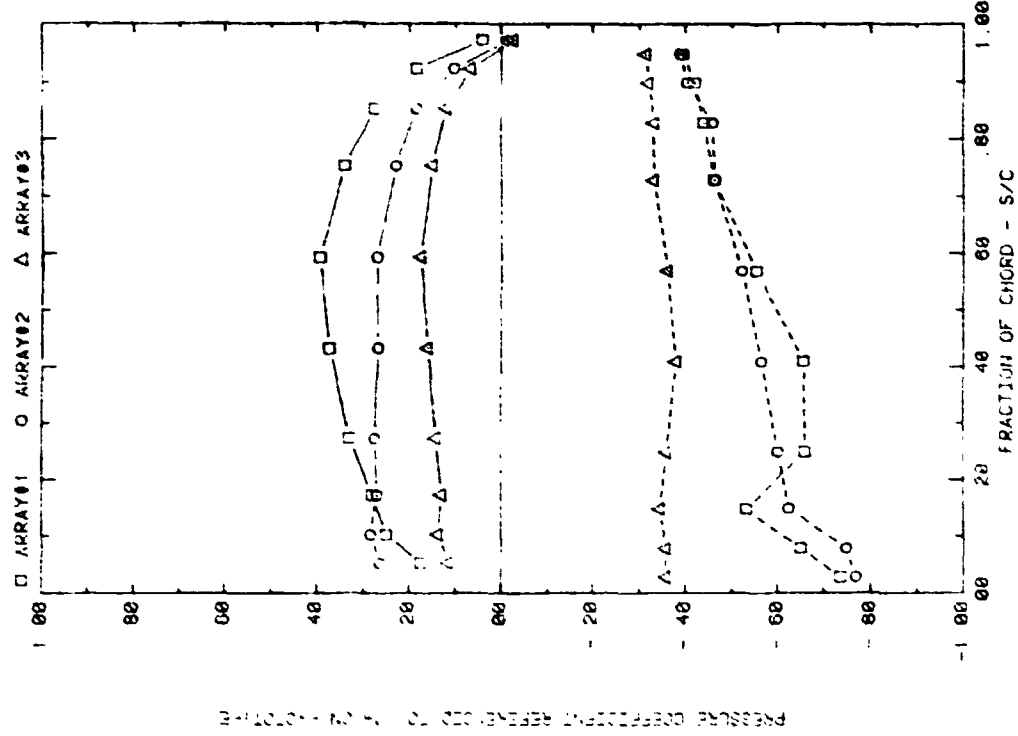
FRONT AND BACK PRESSURES 0.6" IN FROM ARRAY EDGE, $\alpha = 145^\circ$, WIND=45
EFFECT OF ARRAY WITH ALPHA=145, FC=0, H=3', D=10', AND P=30K



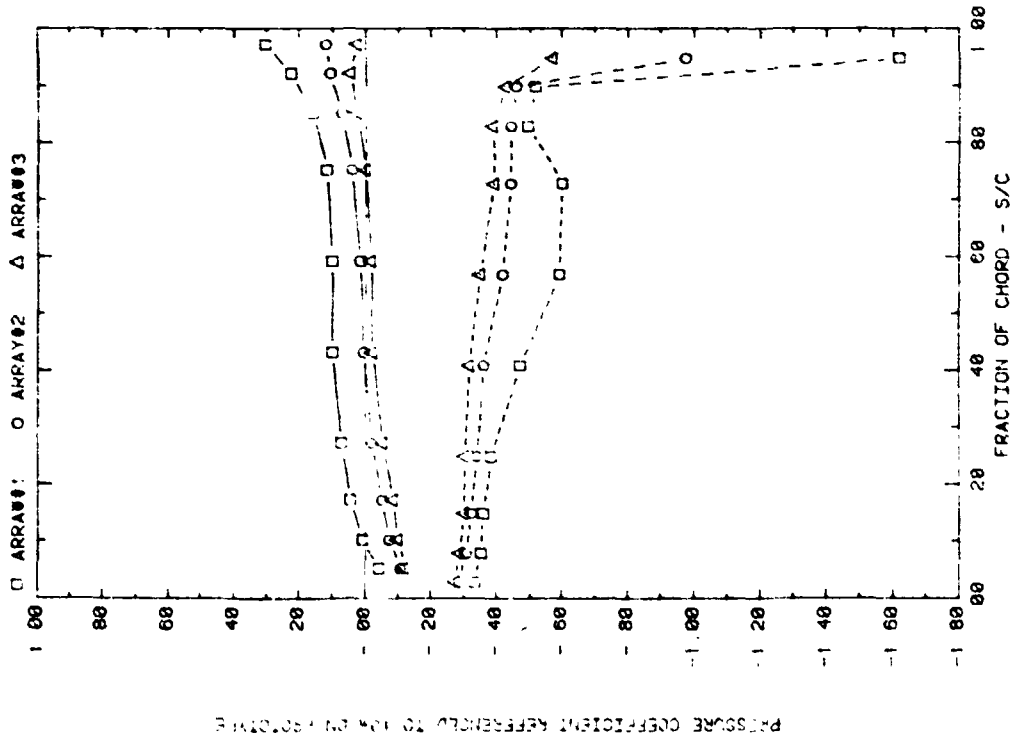
PRESSURE COEFFICIENT REFERENCED TO 1/4 ON FACTORIVE

FRONT AND BACK PRESSURES 0.6" IN FROM ARRAY EDGE, $\alpha = 35^\circ$, WIND=45
EFFECT OF ARRAY WITH ALPHA=35, FC=0, H=3', D=10', AND P=30K

Plot 5-1-1. Corner Study, $WD = 45^\circ$, Standard Model
Effect of Array Position

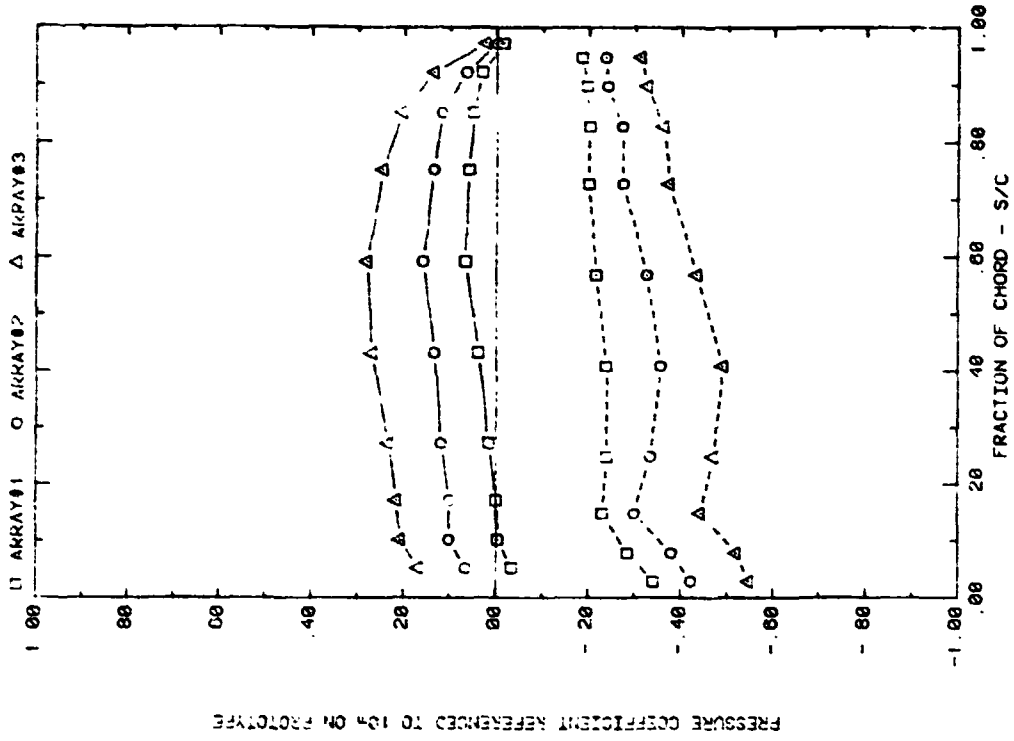


FRONT AND BACK PRESSURES 0.6" IN FROM ARRAY EDGE, X=2C, WIND=45
EFFECT OF ARRAY WITH ALPHA=45, FC=1, H=3", D=12", AND P=30X

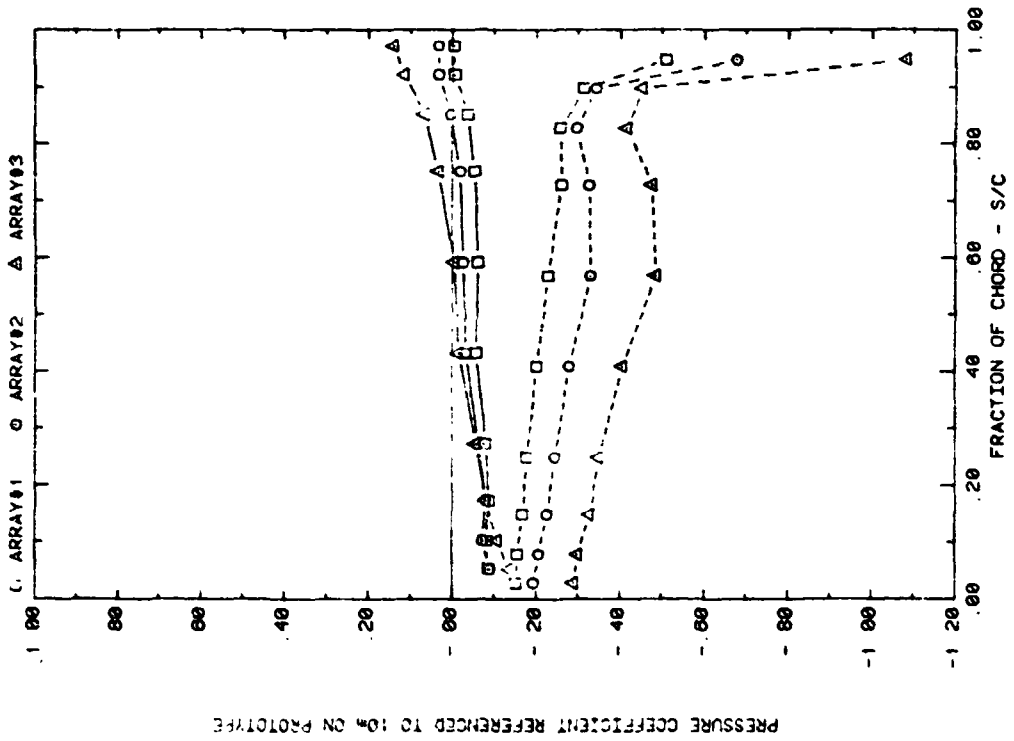


FRONT AND BACK PRESSURES 0.6" IN FROM ARRAY EDGE, X=2C, WIND=45
EFFECT OF ARRAY WITH ALPHA=30, FC=1, H=3", D=12", AND P=30X

Plot 5-1-1. (Continued)

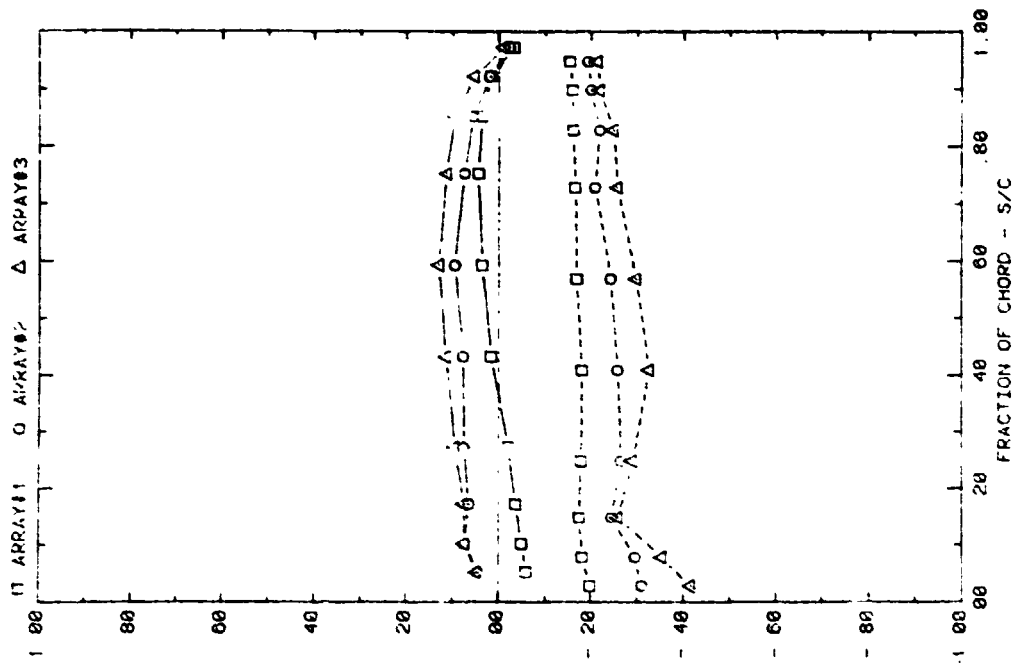


FRONT AND BACK PRESSURES $\theta = 0^\circ$ IN FROM ARRAY EDGE, $X=2C$, $WIND=45$
EFFECT OF ARRAY WITH ALPHA=145, FC=2, H=3, D=10, AND P=30%



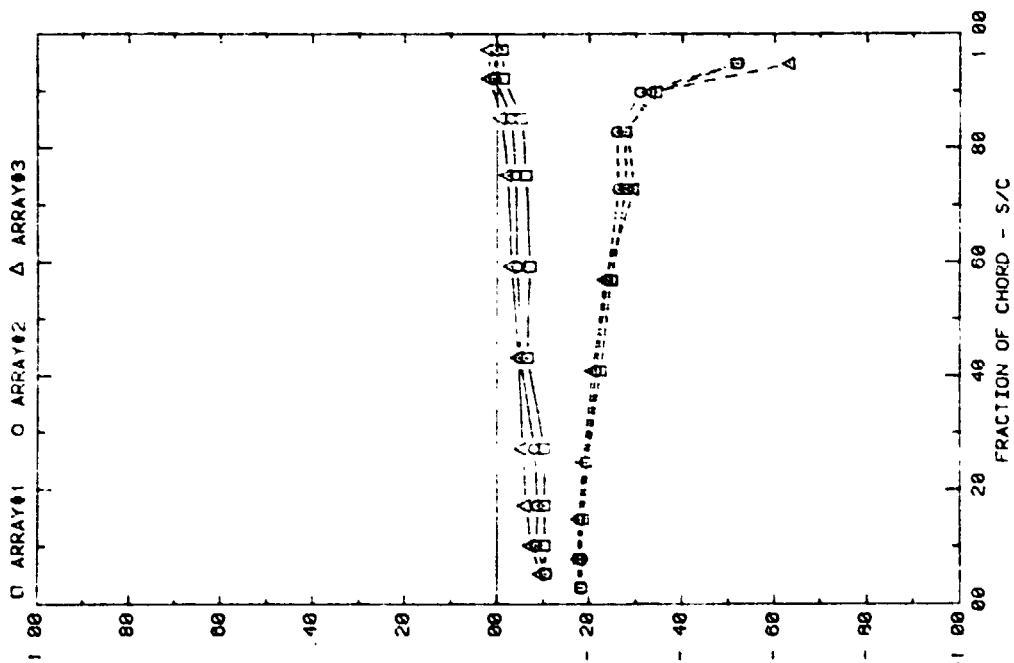
FRONT AND BACK PRESSURES $\theta = 0^\circ$ IN FROM ARRAY EDGE, $X=2C$, $WIND=45$
EFFECT OF ARRAY WITH ALPHA=35, FC=2, H=3, D=10, AND P=30%

Plot 5-1-1. (Continued)



PRESSURE COEFFICIENT REFERENCED TO 1/4 CHORD TYPE

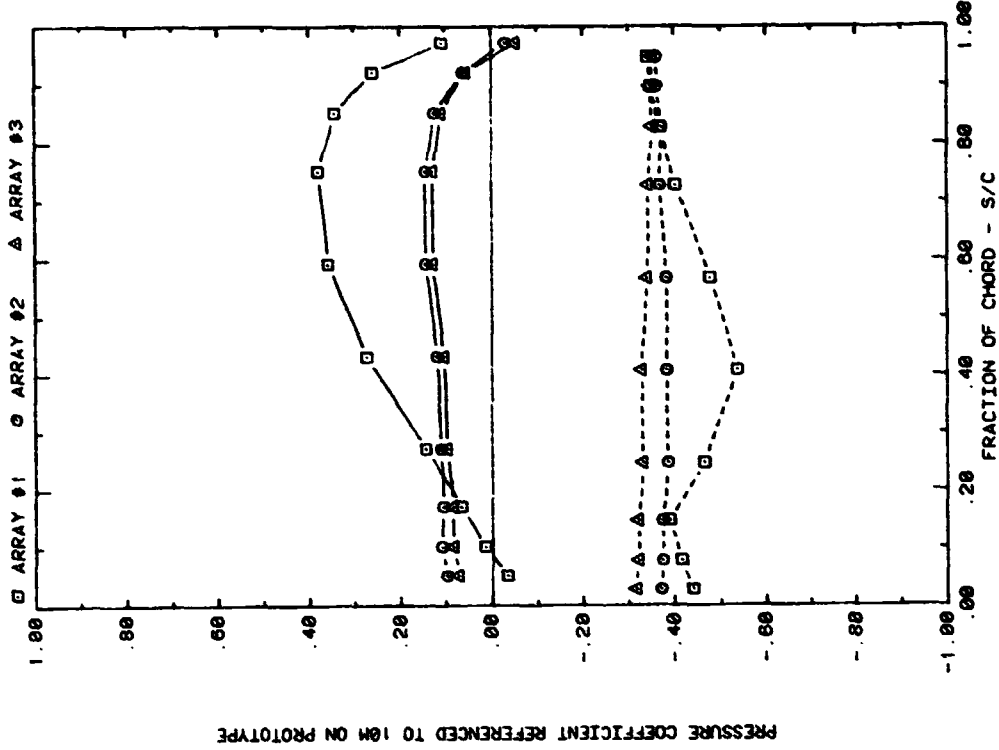
RIGHT AND BACK PRESSURES 0° IN FROM ARRAY EDGE, $X=2C$, $WIND=45$
EFFECT OF ARRAY WITH ALPHA=145, $FC=3$, $H=3^\circ$, $D=10^\circ$, AND $P=30\%$



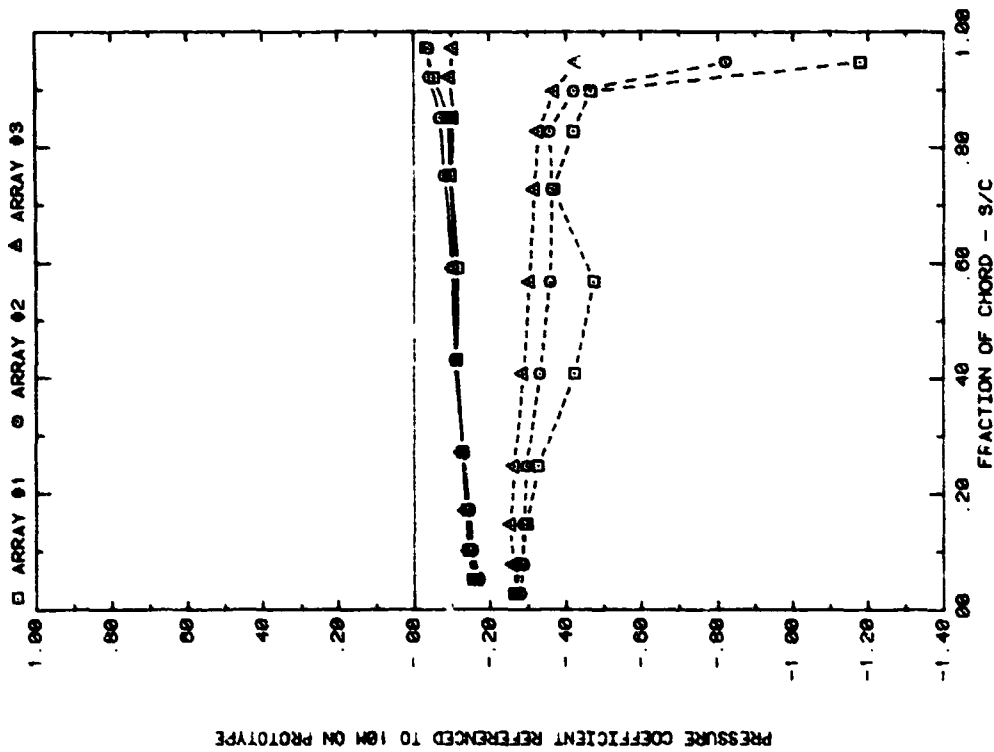
PRESSURE COEFFICIENT REFERENCED TO 1/4 CHORD TYPE

RIGHT AND BACK PRESSURES 0° IN FROM ARRAY EDGE, $X=2C$, $WIND=45$
EFFECT OF ARRAY WITH ALPHA=35, $FC=3$, $H=3^\circ$, $D=10^\circ$, AND $P=30\%$

Plot 5-1-1. (Continued)

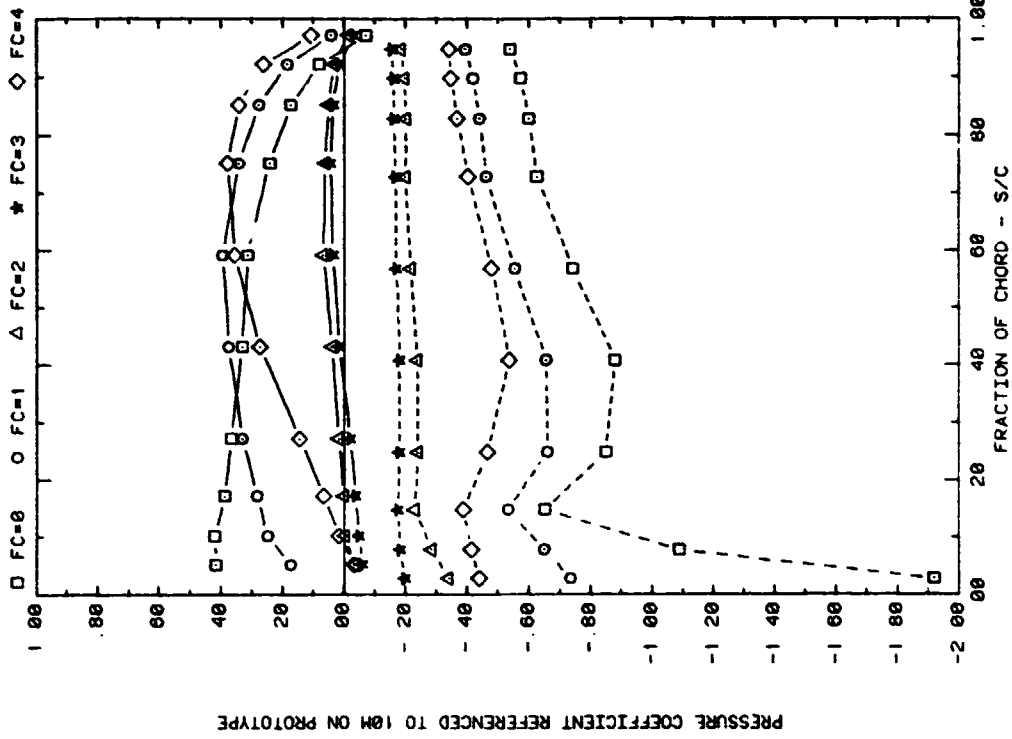


FRONT AND BACK PRESSURES ON ARRAYS #1, 2&3, WIND = 45
EFFECT OF ARRAY WITH ALPHA = 145, X = 2C, FC = 4

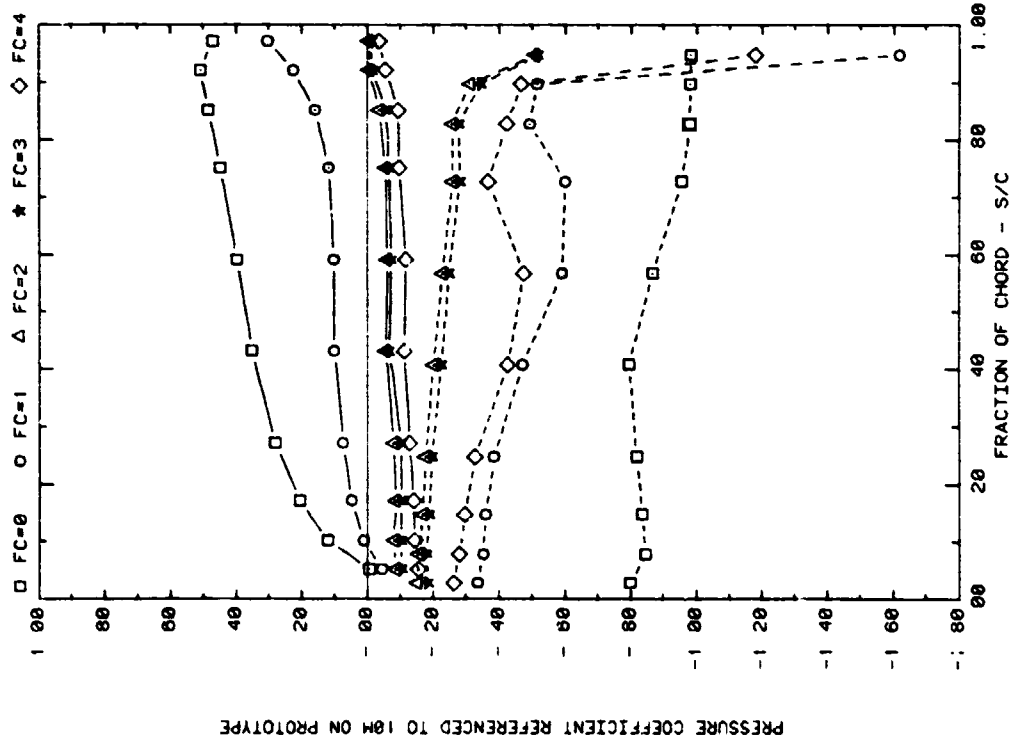


FRONT AND BACK PRESSURES ON ARRAYS #1, 2&3, WIND = 45
EFFECT OF ARRAY WITH ALPHA = 35, X = 2C, FC = 4

Plot 5-1-1. (Concluded)

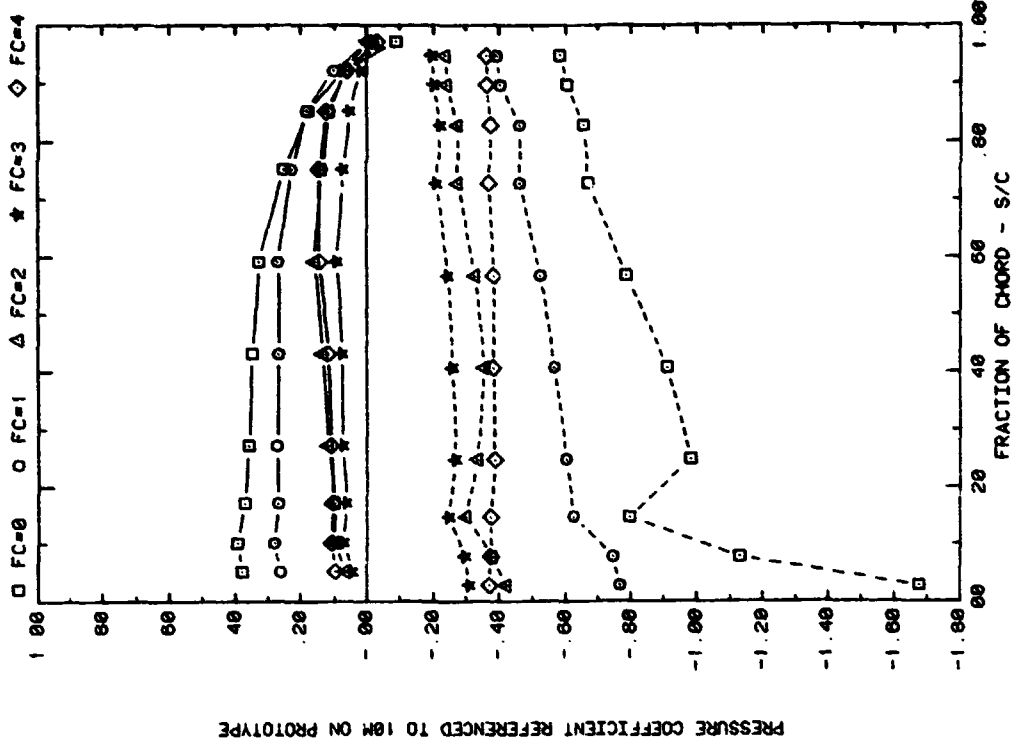


FRONT AND BACK PRESSURES 0.6" IN FROM EDGE OF ARRAY#1; WIND=45
EFFECT OF FC WITH ALPHA=145, H=3", D=10°, P=30% AND X=2C



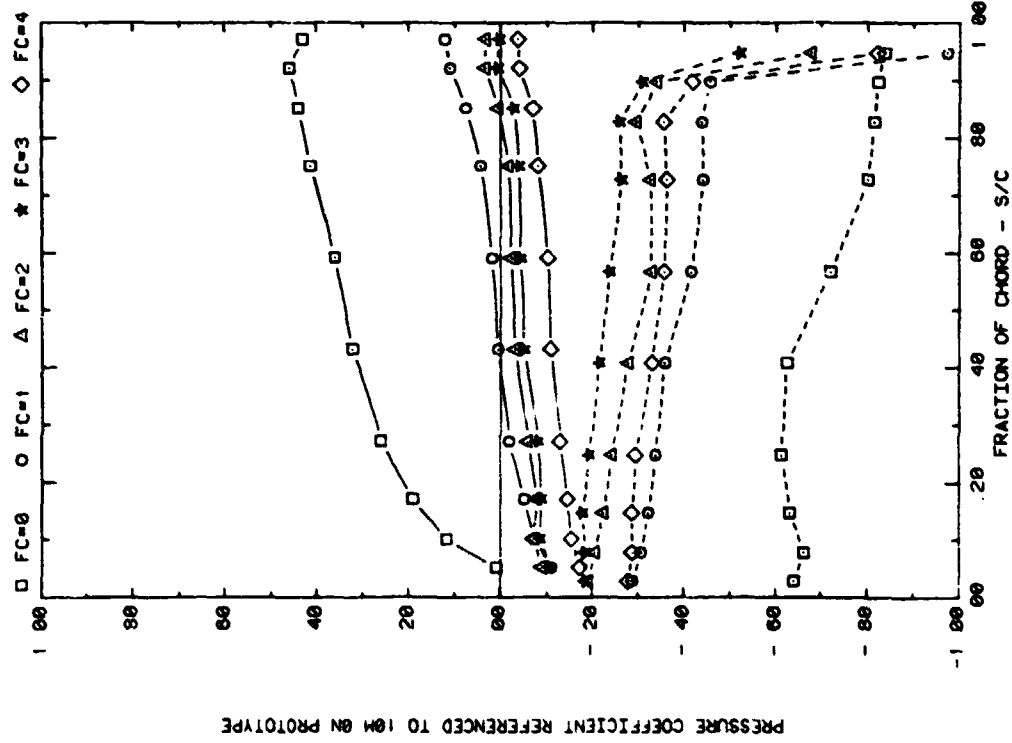
FRONT AND BACK PRESSURES 0.6" IN FROM EDGE OF ARRAY#1; WIND = 45
EFFECT OF FC WITH ALPHA=35, H=3", D=10°, P=30%, AND X=2C

Plot 5-1-2. Corner Study, WD = 45°, Standard Model
Effect of Fence Configuration



PRESSURE COEFFICIENT REFERENCED TO 10M ON PROTOTYPE

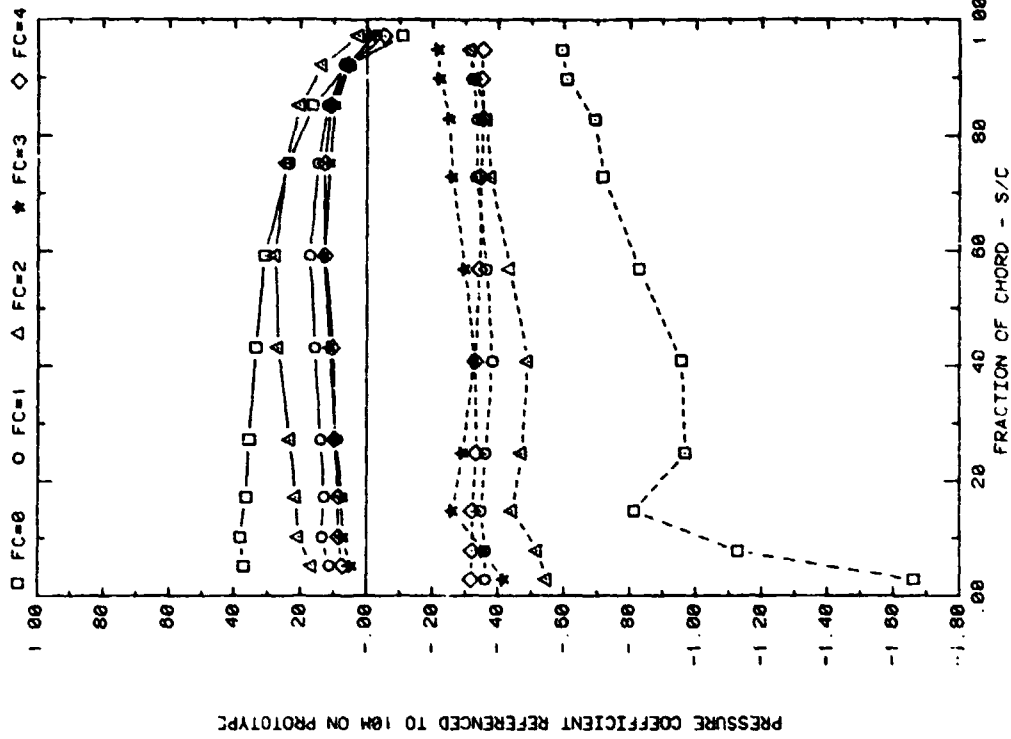
FRONT AND BACK PRESSURES θ 6° IN FROM EDGE OF ARRAY02; WIND=45
EFFECT OF FC WITH ALPHA=145, H=3', D=10', P=38% AND X=2C



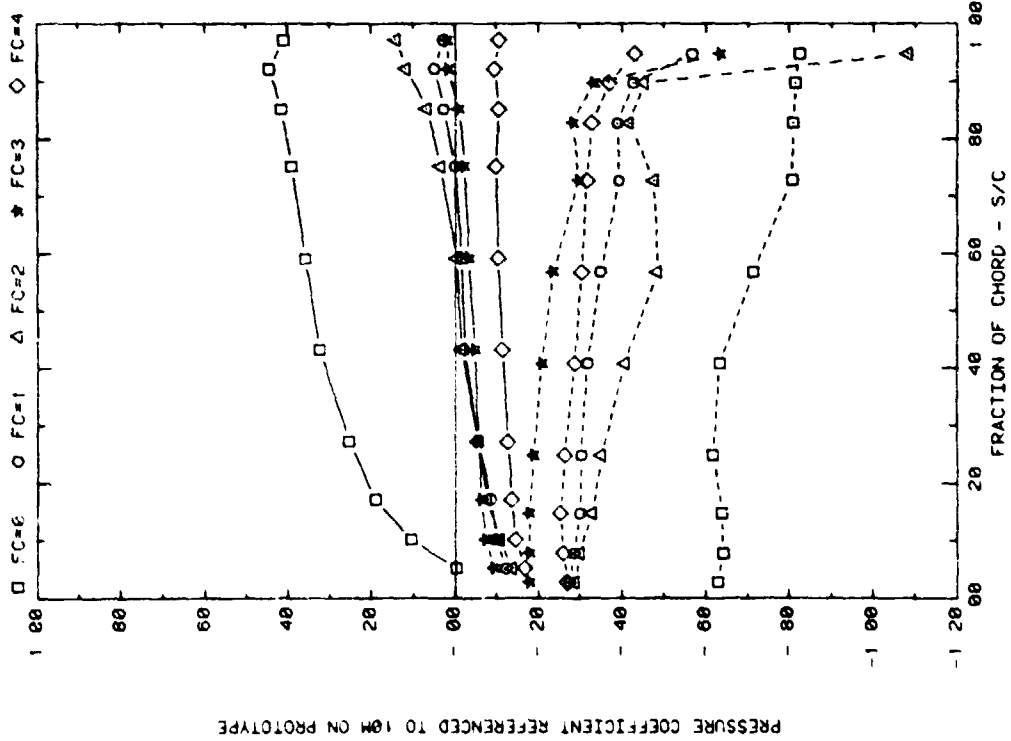
PRESSURE COEFFICIENT REFERENCED TO 10M ON PROTOTYPE

FRONT AND BACK PRESSURES θ 6° IN FROM EDGE OF ARRAY02; WIND=45
EFFECT OF FC WITH ALPHA=95, H=3', D=10', P=38% AND X=2C

Plot S-1-2. (Continued)

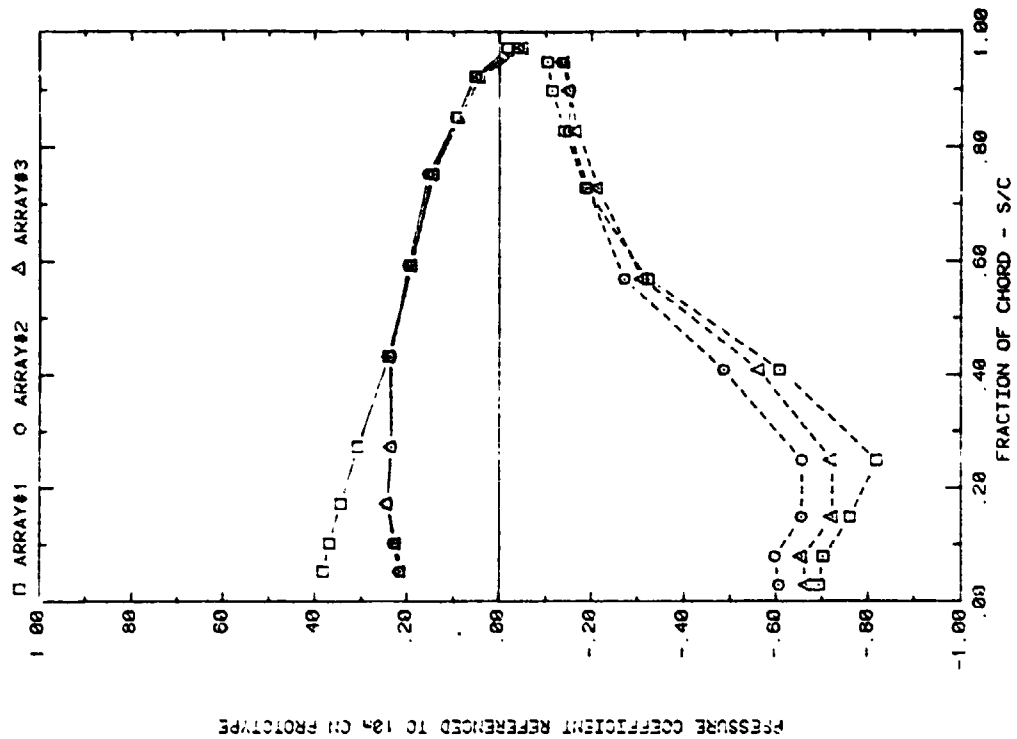


FRONT AND BACK PRESSURES θ 6° IN FROM EDGE OF ARRAY#3, WIND=45
EFFECT OF FC WITH ALPHA=145, H=3°, D=10°, P=30%, AND X=2C



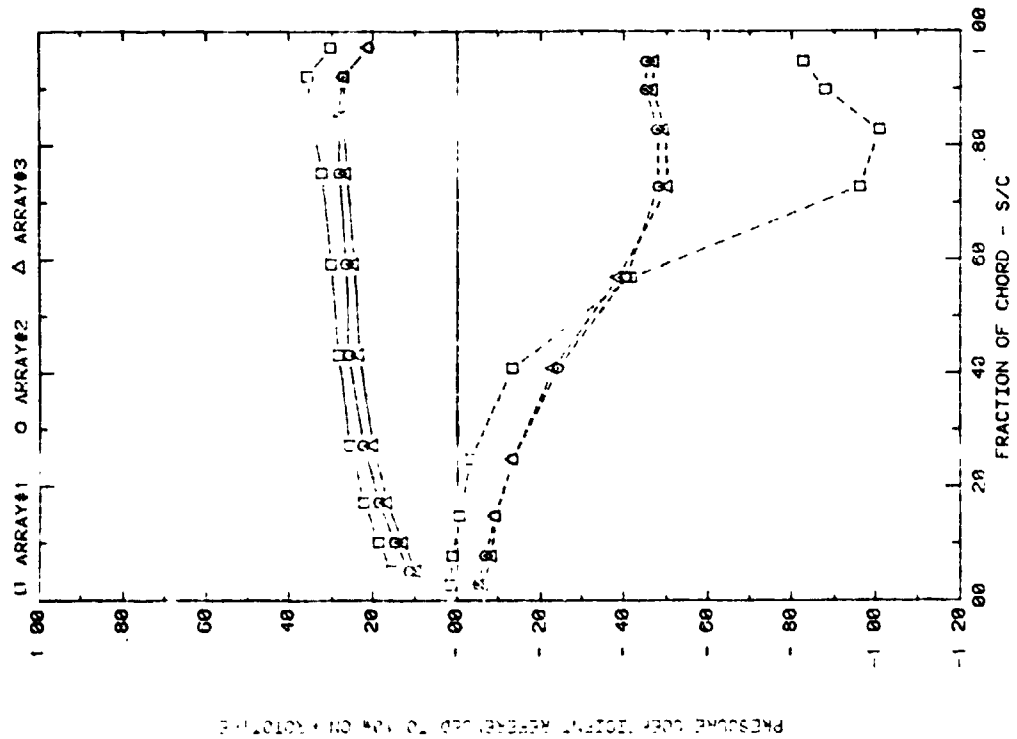
FRONT AND BACK PRESSURES θ 6° IN FROM EDGE OF ARRAY#3, WIND=45
EFFECT OF FC WITH ALPHA=35, H=3°, D=10°, P=30%, AND X=2C

Plot 5-1-2. (Concluded)



PRESSURE COEFFICIENT REFERENCED TO 1/4 CH PROTOTYPE

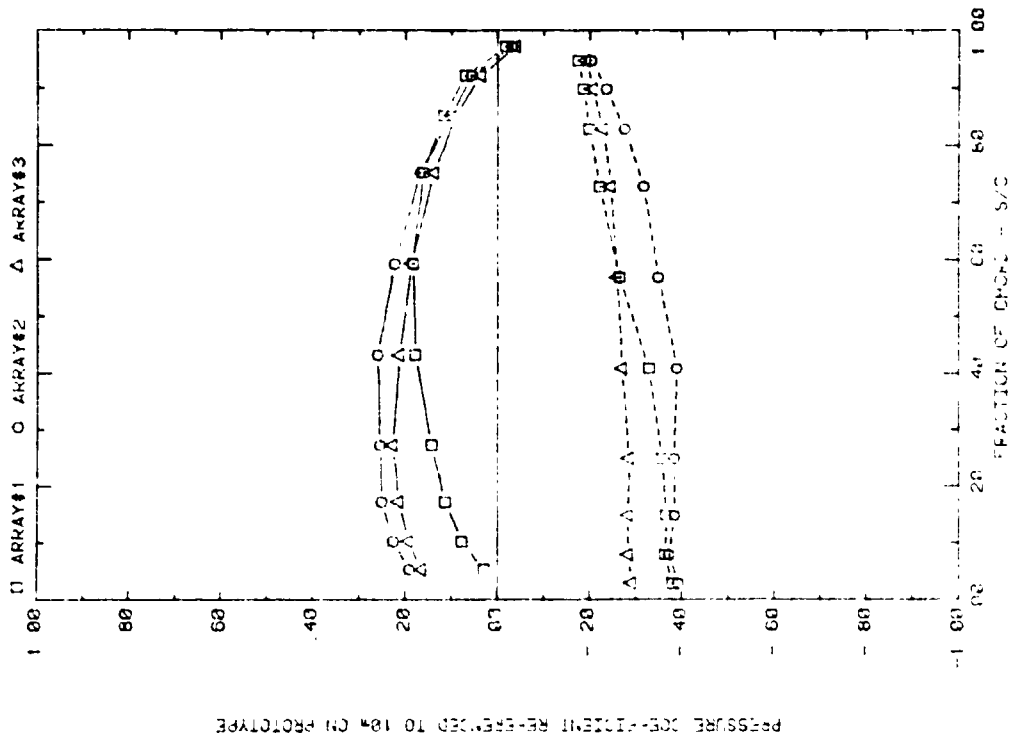
FRONT AND BACK PRESSURES 3.6° IN FROM ARRAY EDGE, X=2C, WIND=45
EFFECT OF ARRAY WITH ALPHA=145, FC=0, H=3°, D=10°, AND P=30X



PRESSURE COEFFICIENT REFERENCED TO 1/4 CH PROTOTYPE

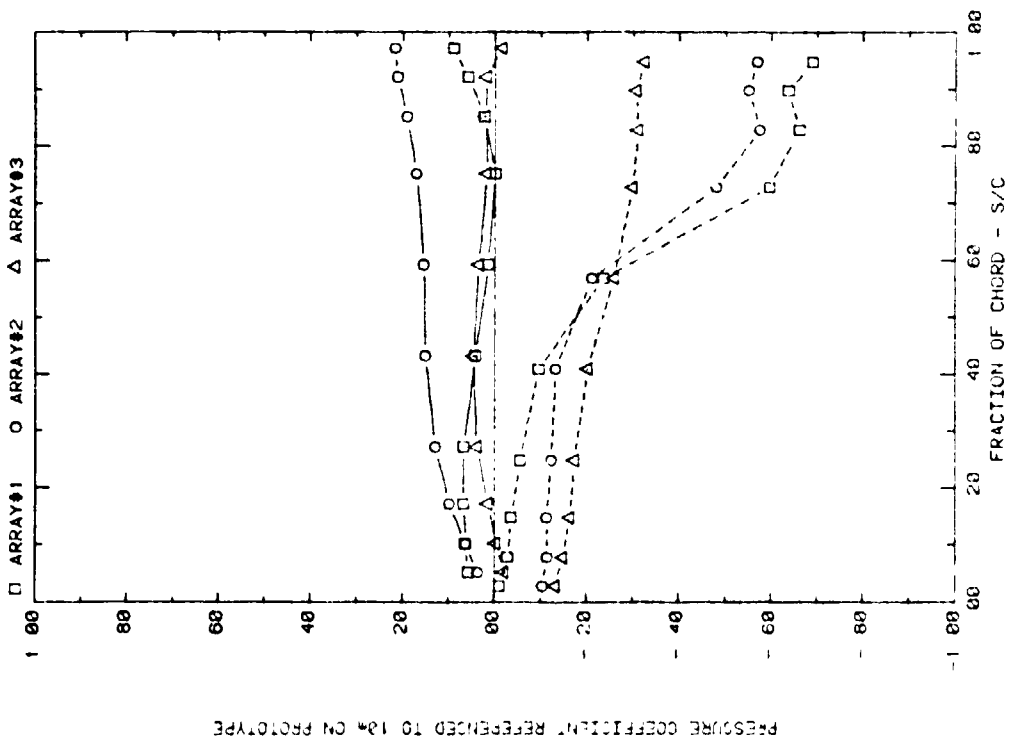
FRONT AND BACK PRESSURES 3.6° IN FROM ARRAY EDGE, X=2C, WIND=45
EFFECT OF ARRAY WITH ALPHA=35, FC=0, H=3°, D=10°, AND P=30X

Plot 5-2-1. Corner Study, WD = 45°, Modified Model with Solid Extension
Effect of Array Position



PRESSURE COEFFICIENT REFERENCED TO 10% CN PROTOTYPE

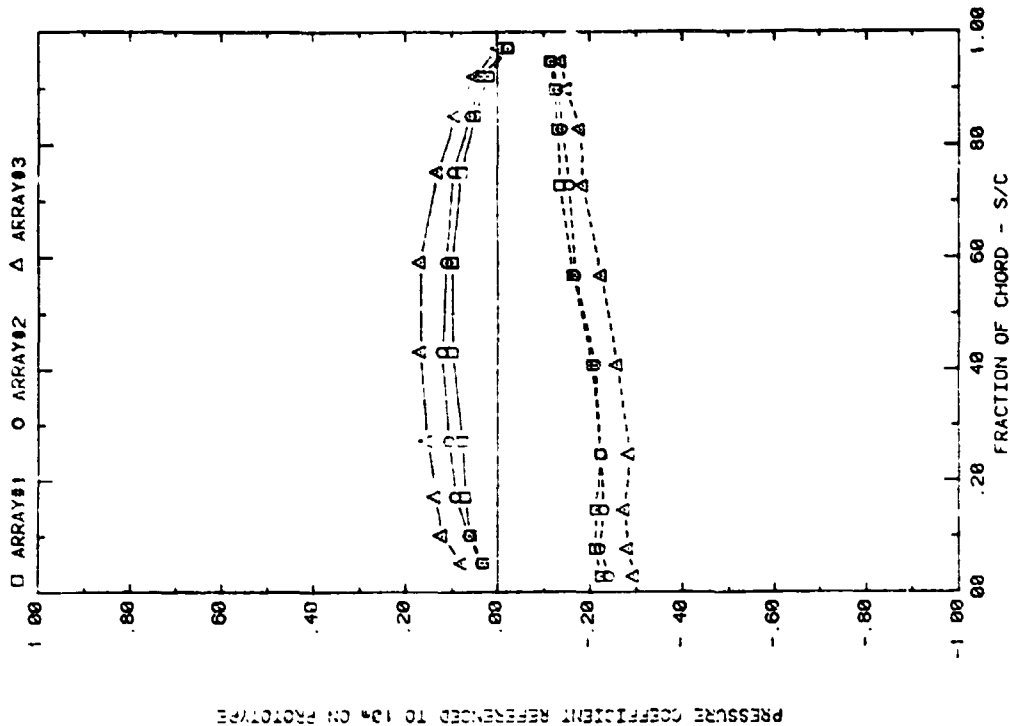
FRONT AND BACK PRESSURES 3.6" IN FROM ARRAY EDGE, X=20, WIND=45
EFFECT OF ARRAY TIP ALPHA=45, FC=1, H=3°, D=18°, AND P=30%



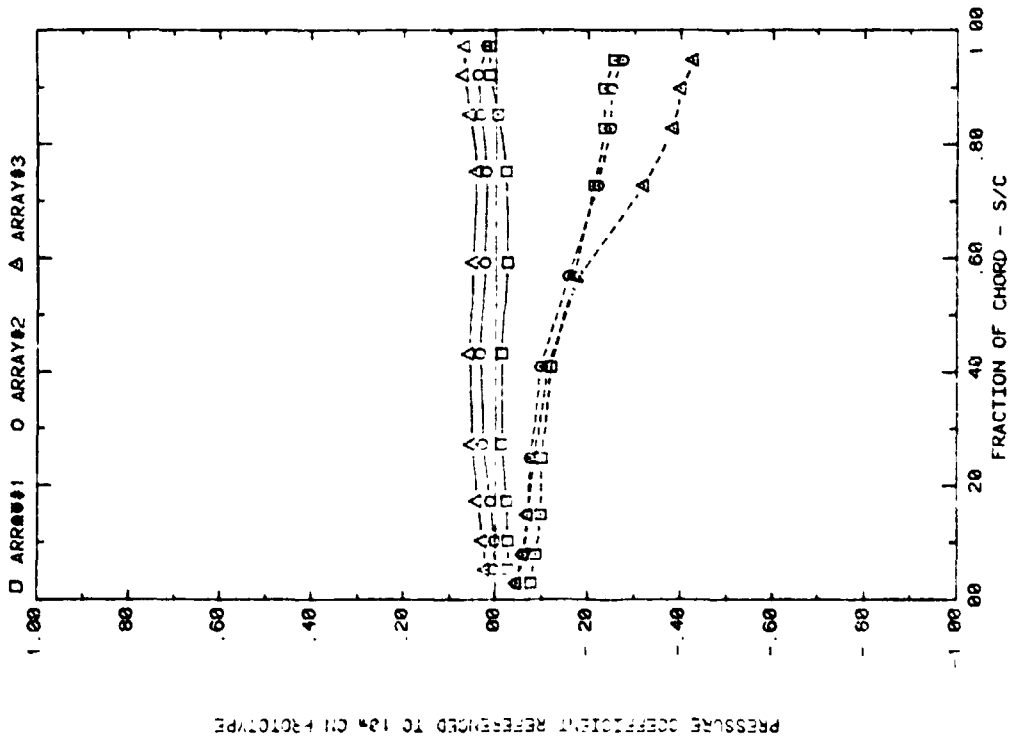
PRESSURE COEFFICIENT REFERENCED TO 10% CN PROTOTYPE

FRONT AND BACK PRESSURES 3.6" IN FROM ARRAY EDGE, X=20, WIND=45
EFFECT OF ARRAY TIP ALPHA=35, FC=1, H=3°, D=18°, AND P=30%

Plot 5-2-1. (Continued)

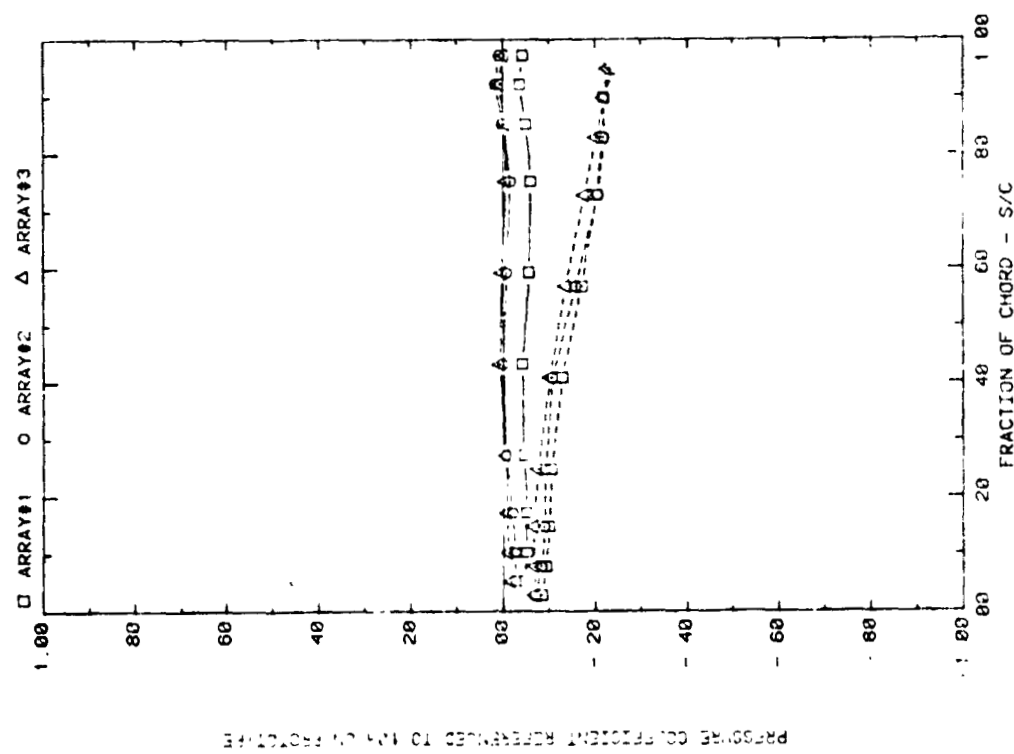
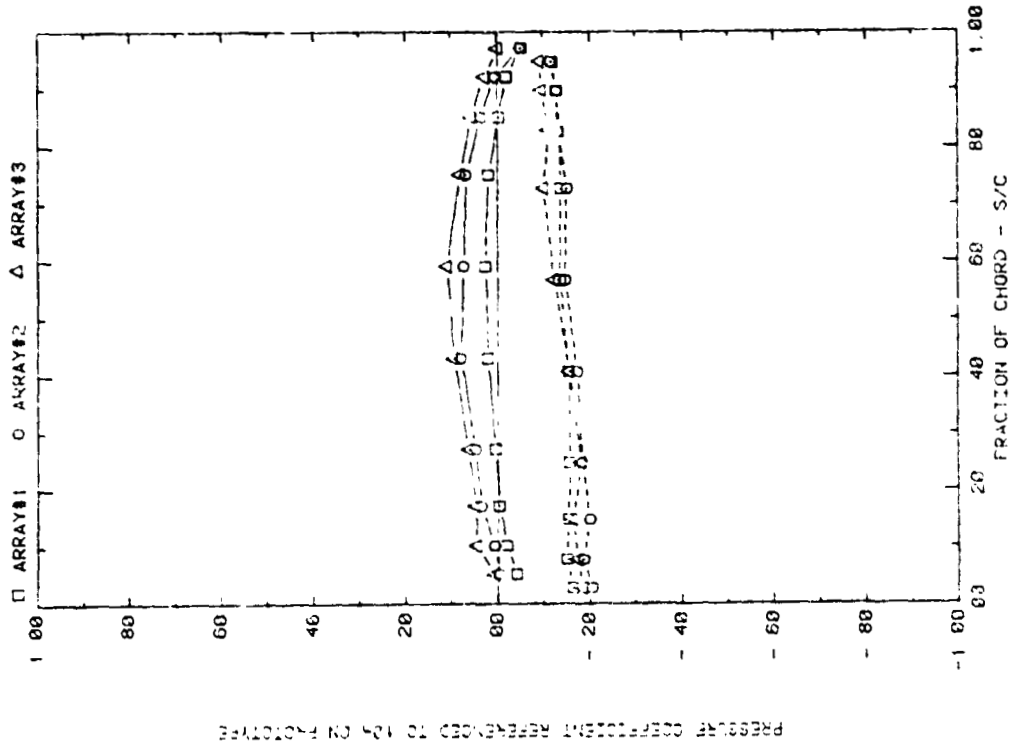


FRONT AND BACK PRESSURES 3.6° IN FROM ARRAY EDGE; X=2C, WIND=45
EFFECT OF ARRAY WITH ALPHA=35, FC=2, H=3°, D=10°, AND P=30%



FRONT AND BACK PRESSURES 3.6° IN FROM ARRAY EDGE; X=2C, WIND=45
EFFECT OF ARRAY WITH ALPHA=35, FC=2, H=3°, D=10°, AND P=30%

Plot 5-2-1. (Continued)

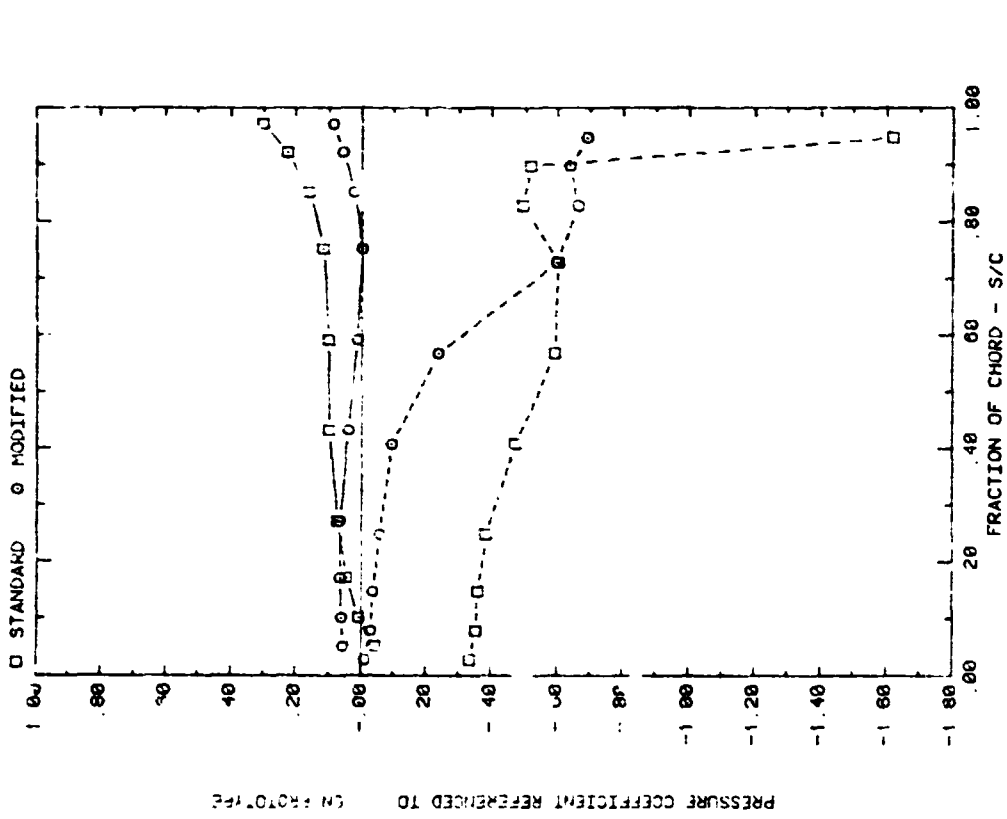
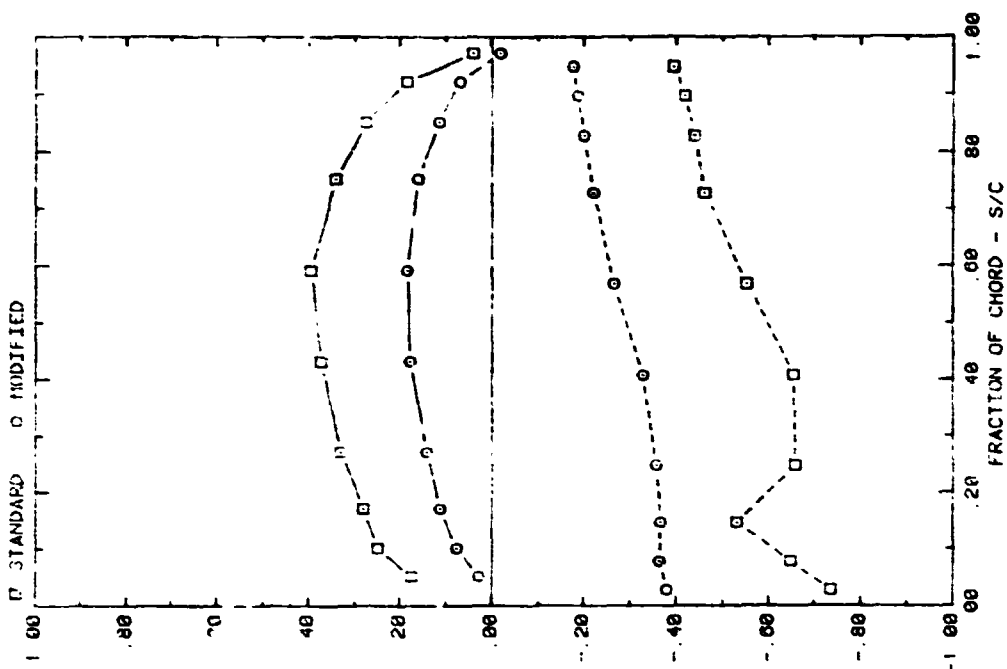


FRONT AND BACK PRESSURE COEFFICIENTS FOR ARRAY EDGE, X=2C, Y=1.4D=45
 EFFECT OF ARRAY WITH ALPHA=145, FC=3, H=3, D=10°, AND P=38%

FRONT AND BACK PRESSURE COEFFICIENTS FOR ARRAY EDGE, X=2C, WIND=45
 EFFECT OF ARRAY WITH ALPHA=145, FC=3, H=3, D=10°, AND P=38%

Plot 5-1-1. (Concluded)

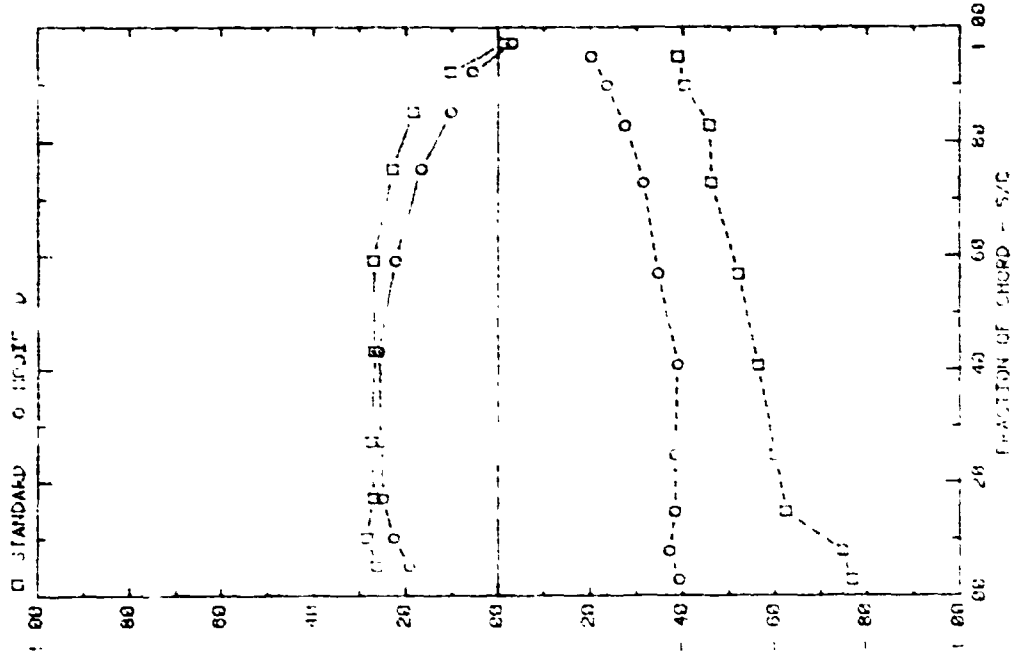
ORIGINAL PAGE IS
 OF POOR QUALITY



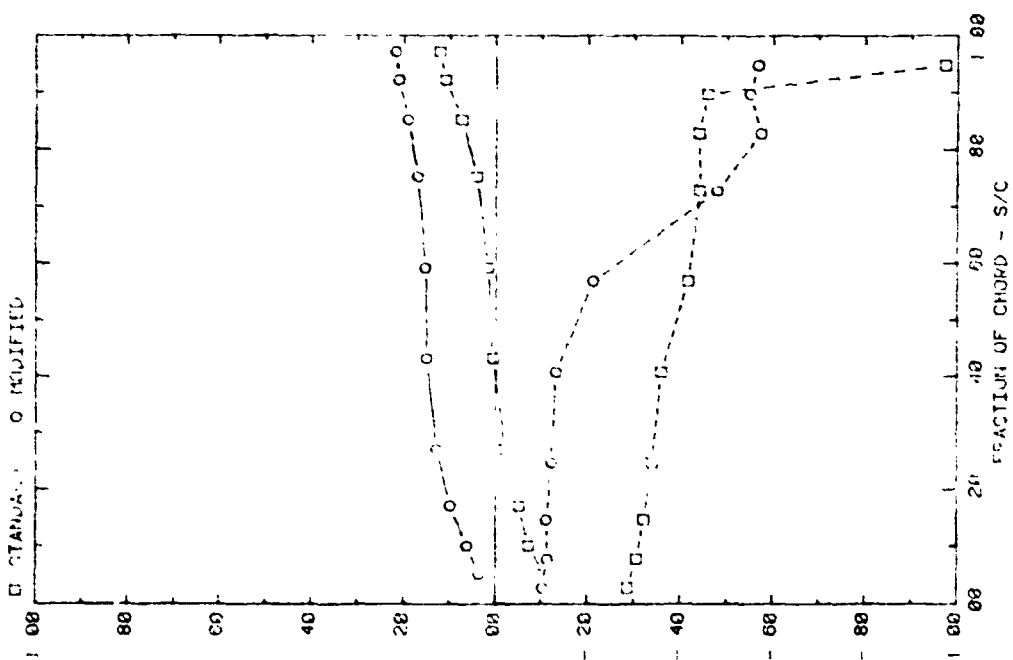
Plot 5-2-2. Corner Study, $WD = 45^\circ$, Effect of Model Modification

FRONT AND BACK PRESSURES ON ARRAY #1 WITH $X=2C$, AND $WI = 15$ EFFECT OF TAP LOCATION, $\alpha=10^\circ$, $D=3'$, $FC=1$, AND $P=30X$

FRONT AND BACK PRESSURES ON ARRAY #1 WITH $X=2C$, AND $WI=45$ EFFECT OF TAP LOCATION, $\alpha=10^\circ$, $D=3'$, $FC=1$, AND $P=30X$

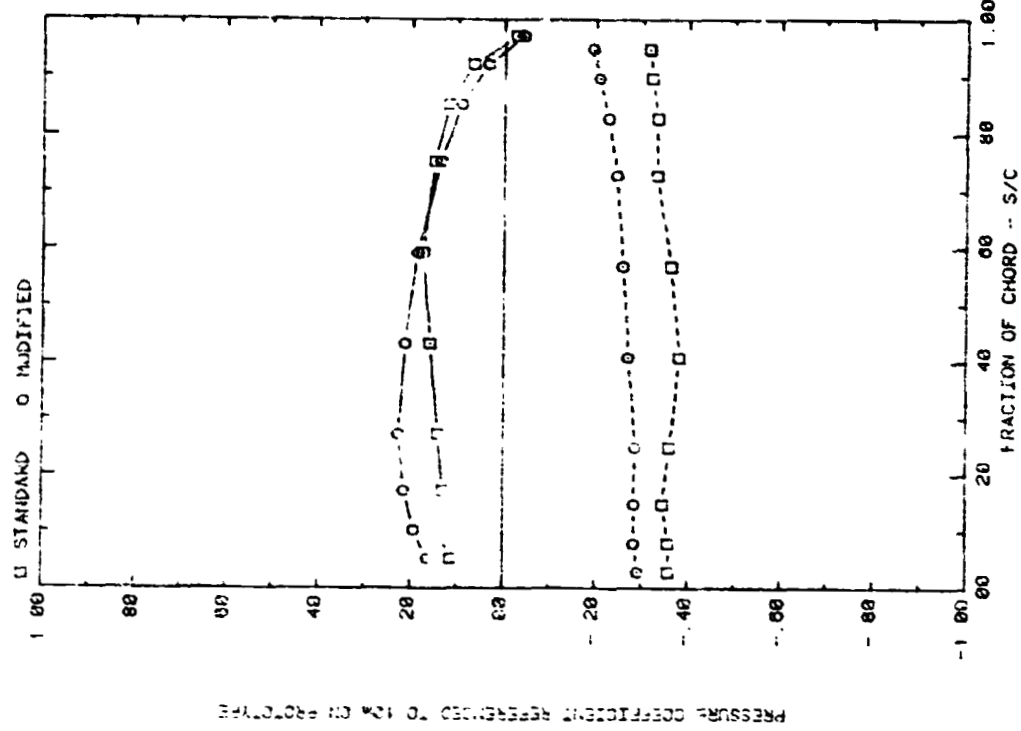


FRONT AND BACK PRESSURES ON ARRAY #2 WITH $\lambda=20$, AND $WIND=45$. EFFECT OF TAP LOCATION, ALPHA=30, 60, 90, 120, 150, 180, 210, 240, 270, 300, 330, 360.

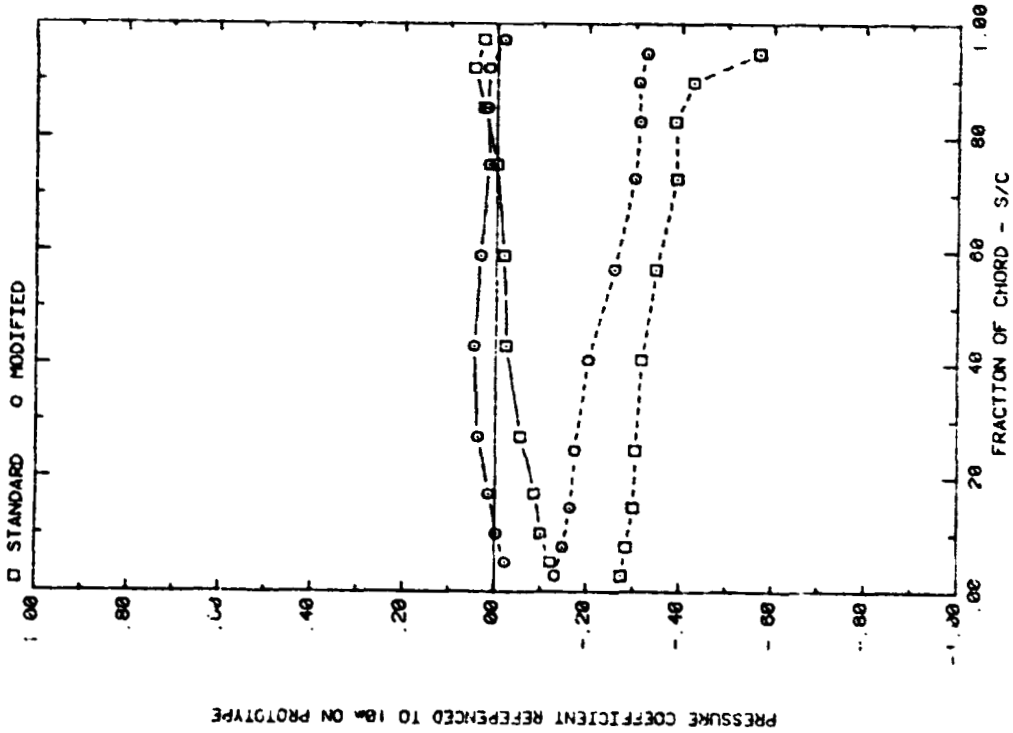


FRONT AND BACK PRESSURES ON ARRAY #2 WITH $\lambda=20$, AND $WIND=45$. EFFECT OF TAP LOCATION, ALPHA=30, 60, 90, 120, 150, 180, 210, 240, 270, 300, 330, 360.

Plot 5-2-2. (Continued)

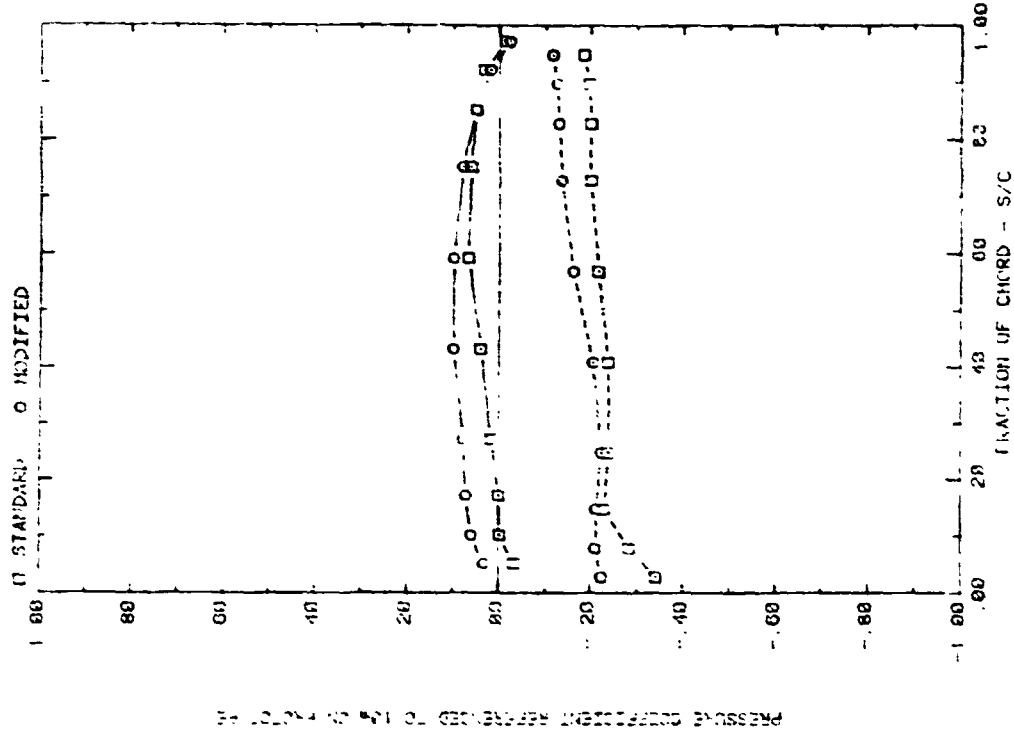


FRONT AND BACK PRESSURES ON ARRAY #3 WITH X=2C, AND WIND=45
EFFECT OF TAP LOCATION, ALPHA=145, H=3', D=10', FC=1, AND P=30%

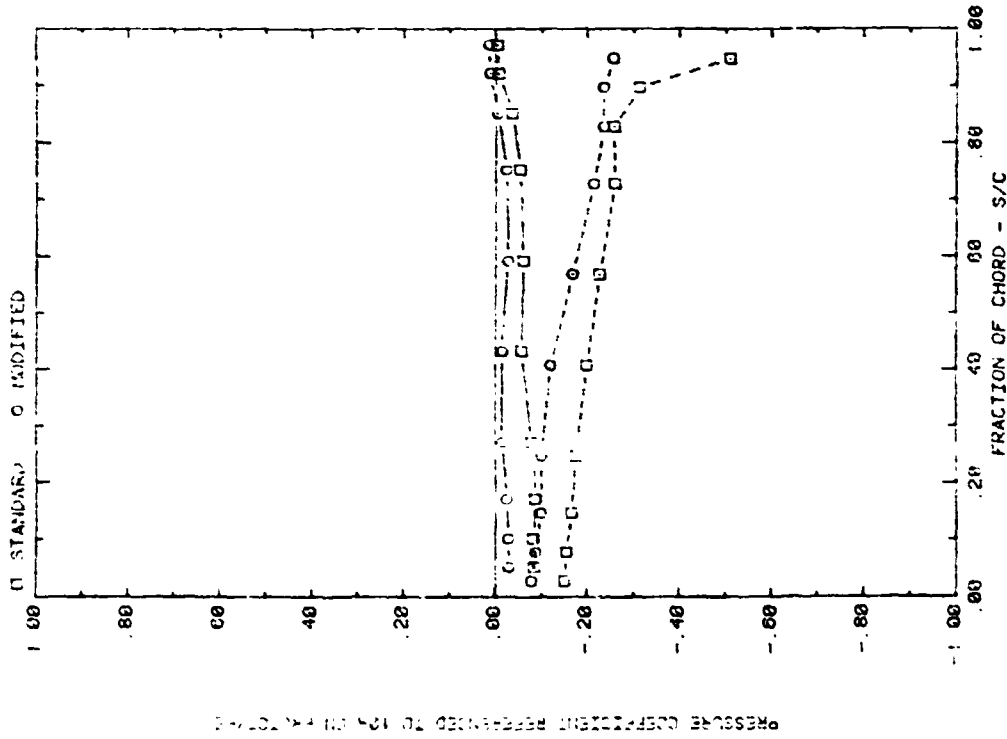


FRONT AND BACK PRESSURES ON ARRAY #3 WITH X=2C, AND WIND=45
EFFECT OF TAP LOCATION, ALPHA=35, H=3', D=10', FC=1, AND P=30%

Plot 5-2-2. (Continued)

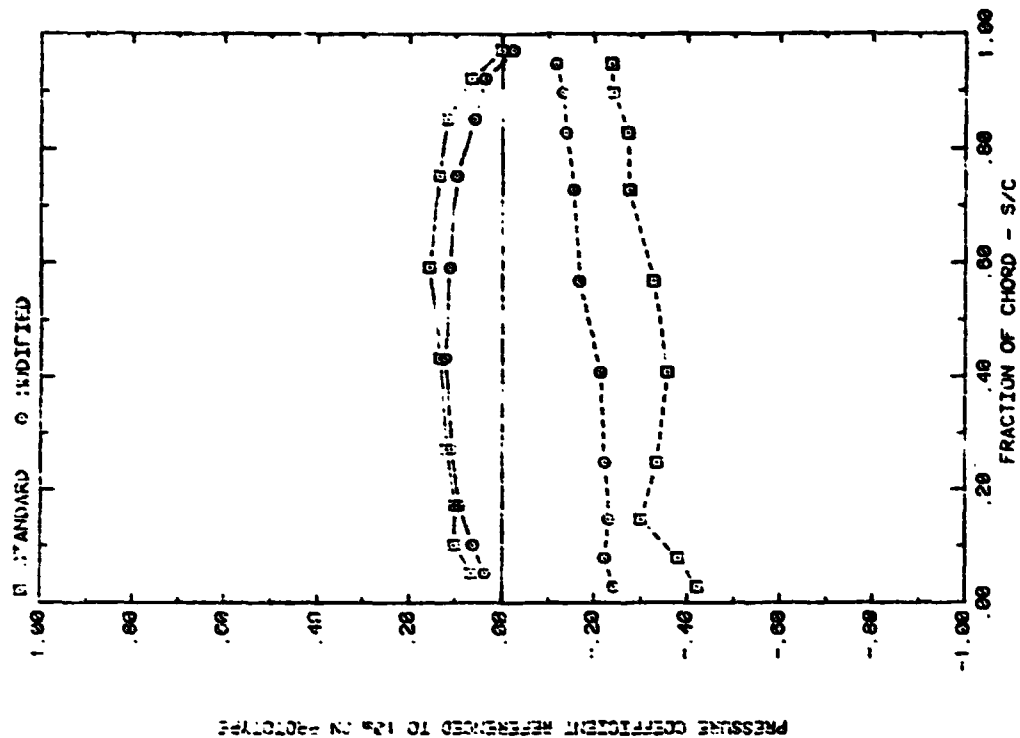


FRONT AND BACK PRESSURES ON ARRAY #1 WITH X=20, D=10, $\alpha=10^\circ$, $FC=2$, AND P=30%
EFFECT OF TAP LOCATION; ALPHA=145, H=3, D=10, $FC=2$, AND P=30X

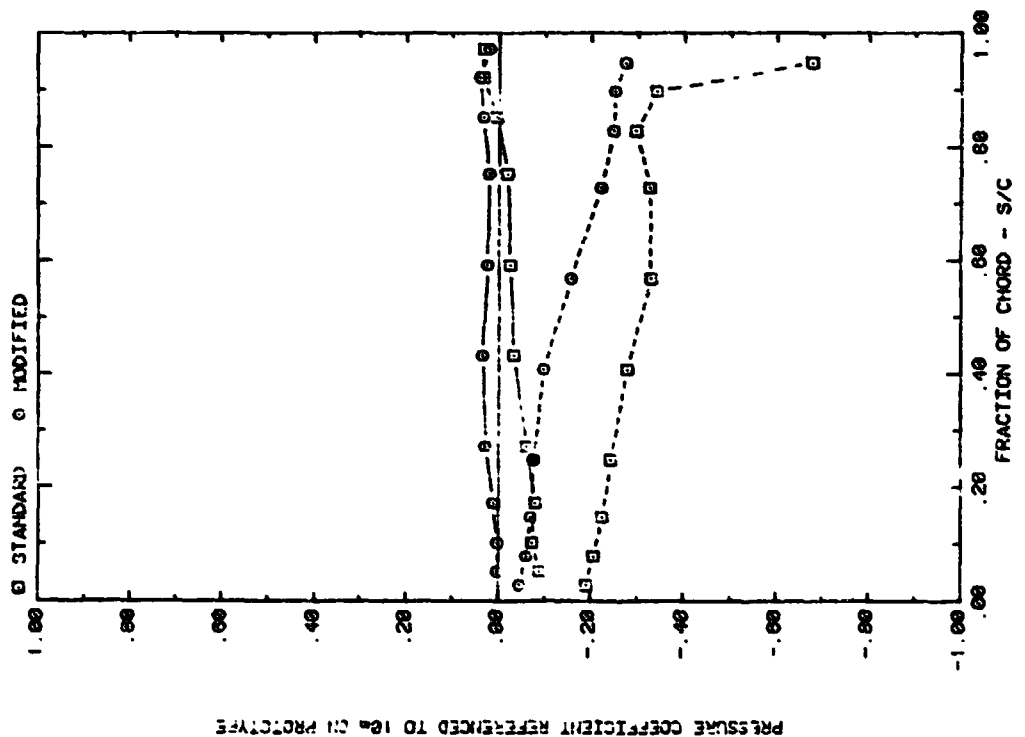


FRONT AND BACK PRESSURES ON ARRAY #1 WITH X=20, D=10, $\alpha=10^\circ$, $FC=2$, AND P=30%
EFFECT OF TAP LOCATION; ALPHA=35, H=3, D=10, $FC=2$, AND P=30X

Plot 5-2-2. (Continued)

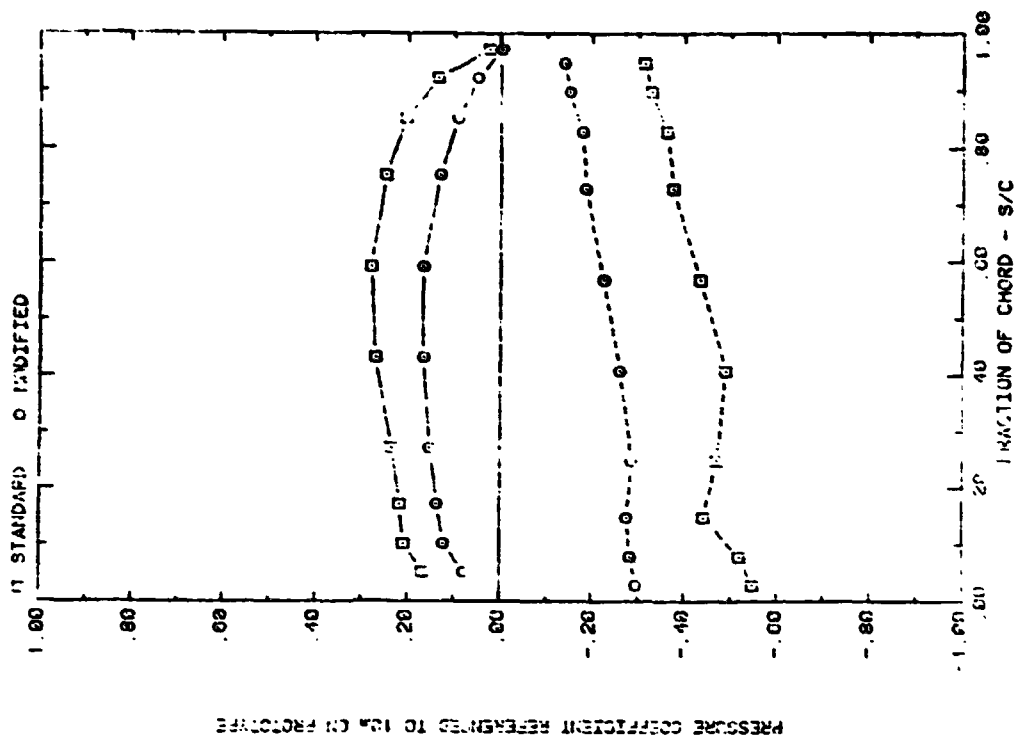


FRONT AND BACK PRESSURES ON ARRAY #2 WITH X=2C, AND WIND-45
EFFECT OF TAP LOCATION; ALPHA=2°, H=3, D=10°, FI=2°, AIJ P=30K

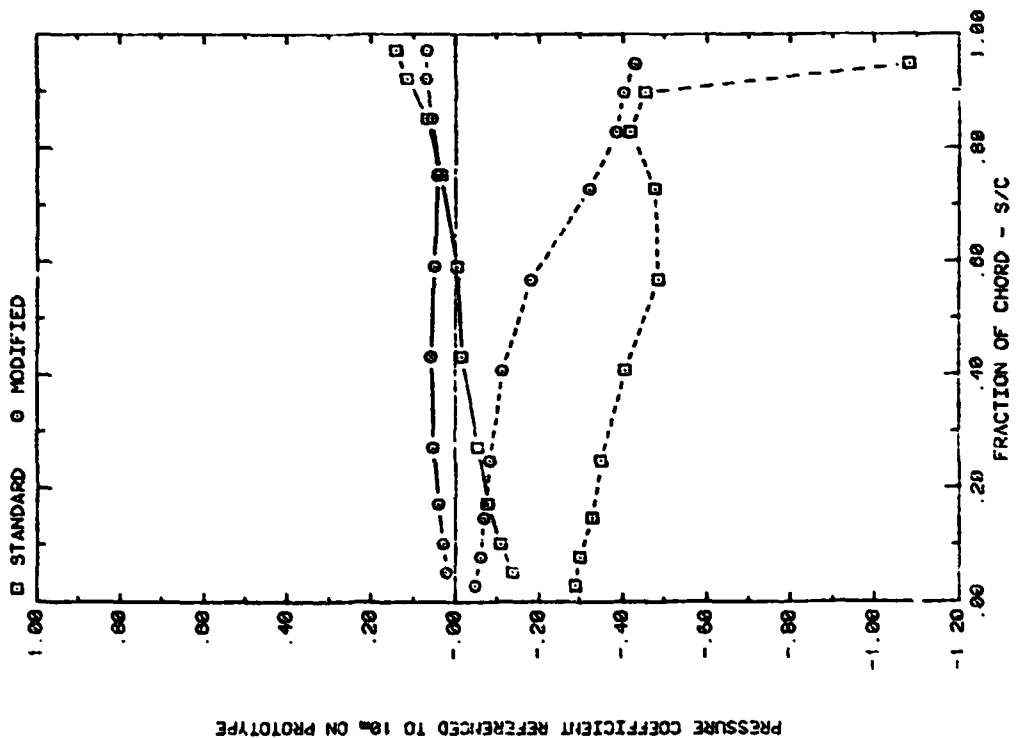


FRONT AND BACK PRESSURES ON ARRAY #2 WITH X=2C, AND WIND-45
EFFECT OF TAP LOCATION; ALPHA=2°, H=3, D=10°, FI=2°, AIJ P=30K

Plot 5-2-2. (Continued)

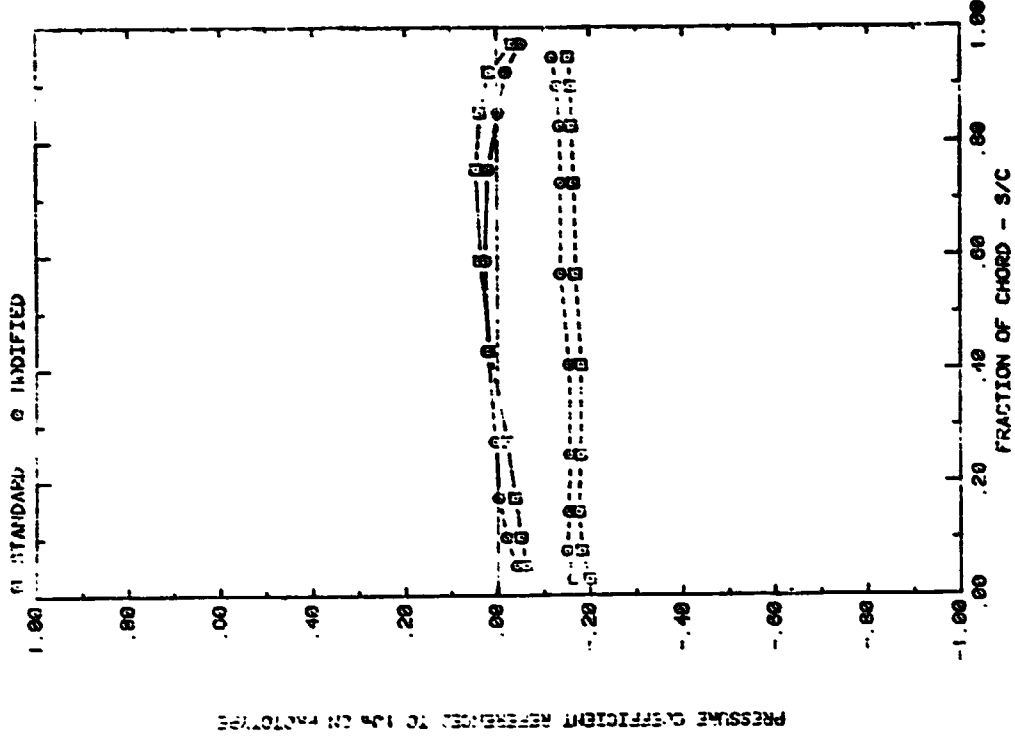


FRONT AND BACK PRESSURES ON ARRAY #3 WITH X=2C, AND WIND=45
EFFECT OF TAP LOCATION, ALPHA=15, M=3, D=10, FC=2, AND P=30K

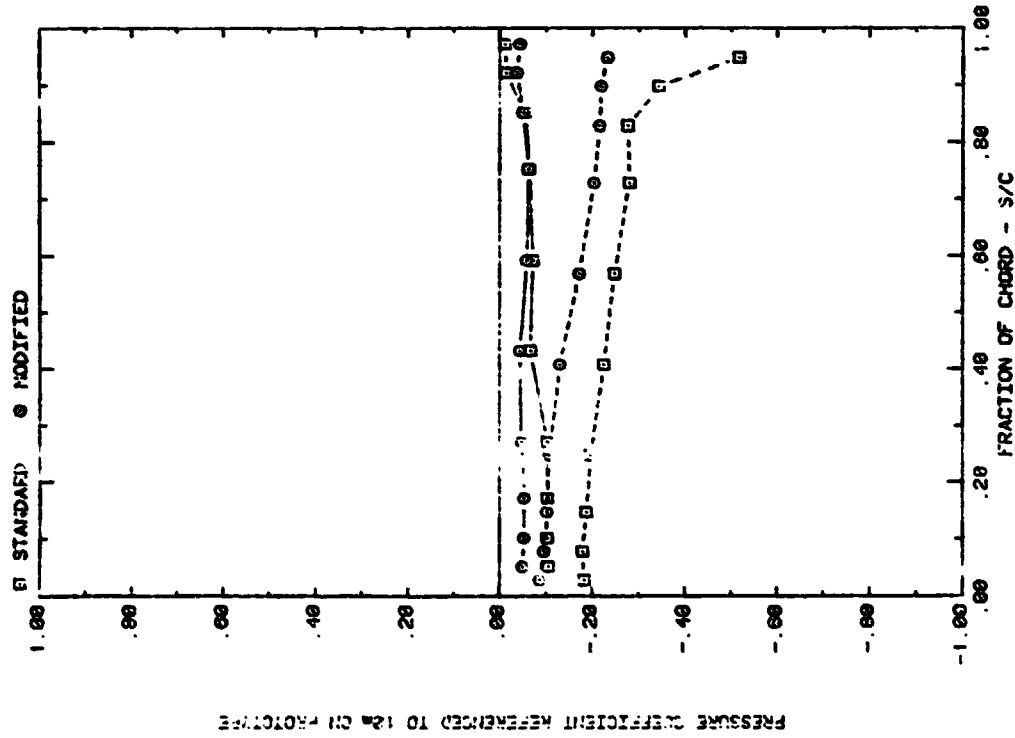


FRONT AND BACK PRESSURES ON ARRAY #3 WITH X=2C, AND WIND=45
EFFECT OF TAP LOCATION, ALPHA=15, M=3, D=10, FC=2, AND P=30K

Plot 5-2-2. (Continued)

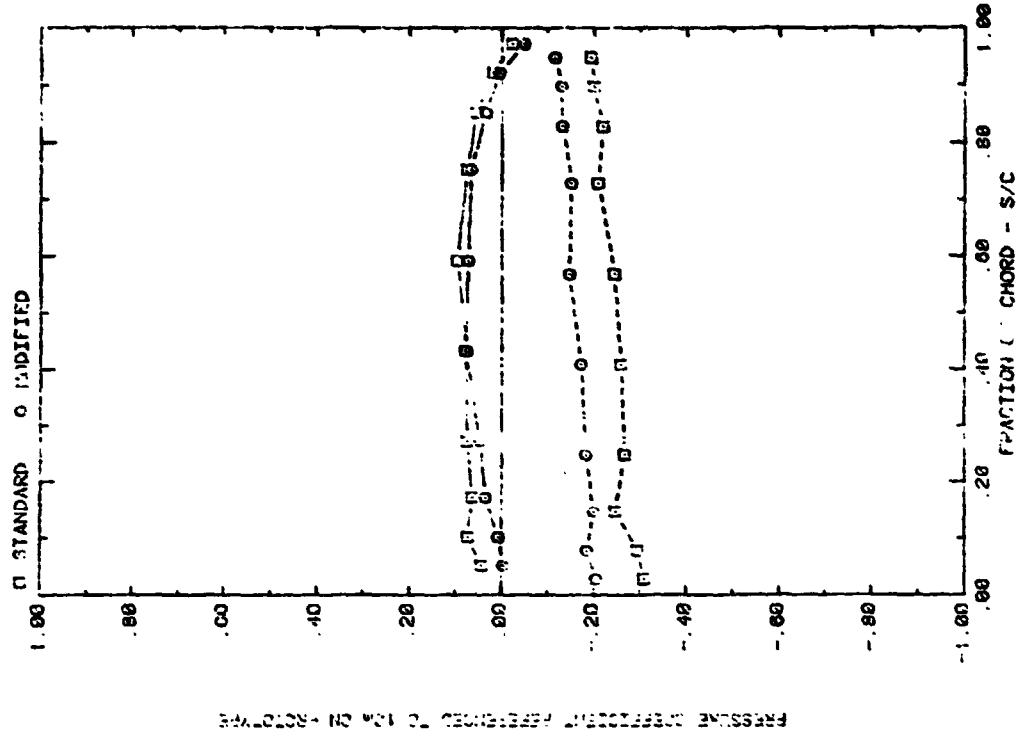


FRONT AND BACK PRESSURES ON ARRAY #1 WITH X=2C, AND WIND=45
EFFECT OF TAP LOCATION; ALPHA=145, H=3', D=10°, FC=3, AND P=30%

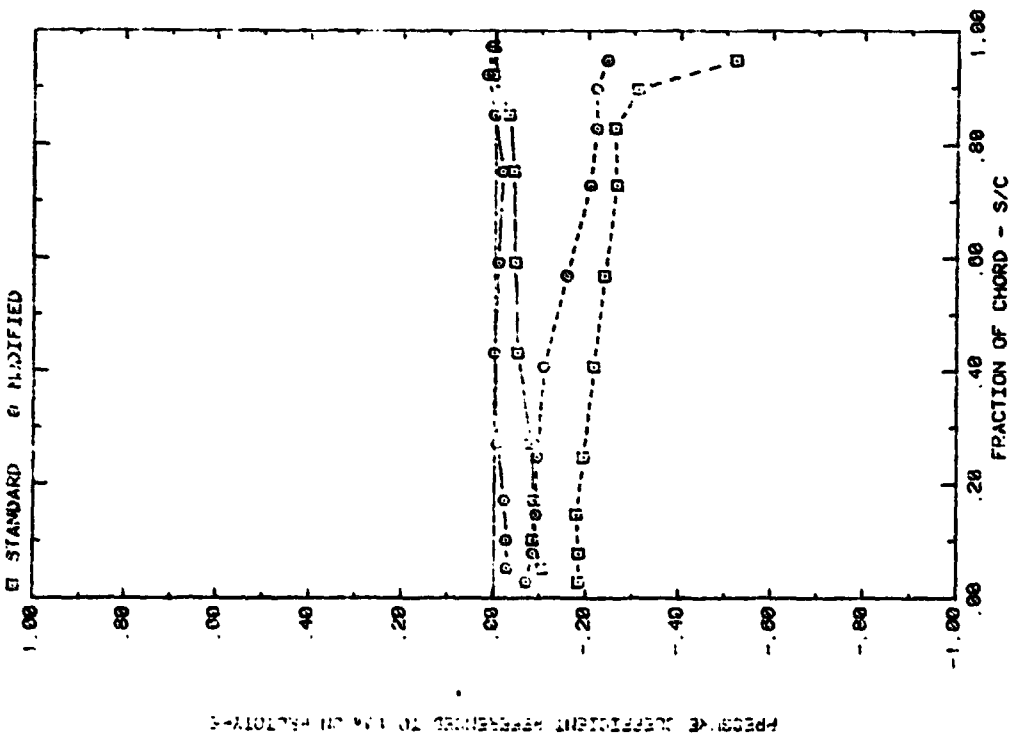


FRONT AND BACK PRESSURES ON ARRAY #1 WITH X=2C, AND WIND=45
EFFECT OF TAP LOCATION; ALPHA=35, H=3', D=10°, FC=3, AND P=30%

Plot 5-2-2. (Continued)



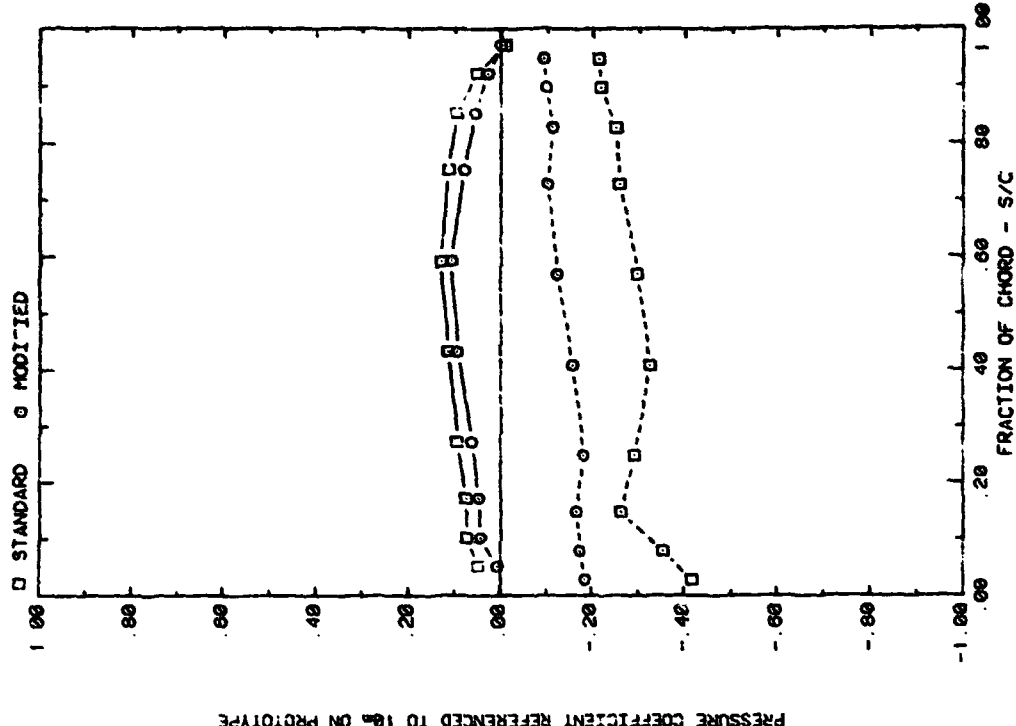
FRONT AND BACK PRESSURES ON ARRAY #2 WITH $\alpha=20^\circ$, AND WIND=45
EFFECT OF TAP LOCATION; ALPHA=20, FC-3, D=10, FC-3, AND P=30X



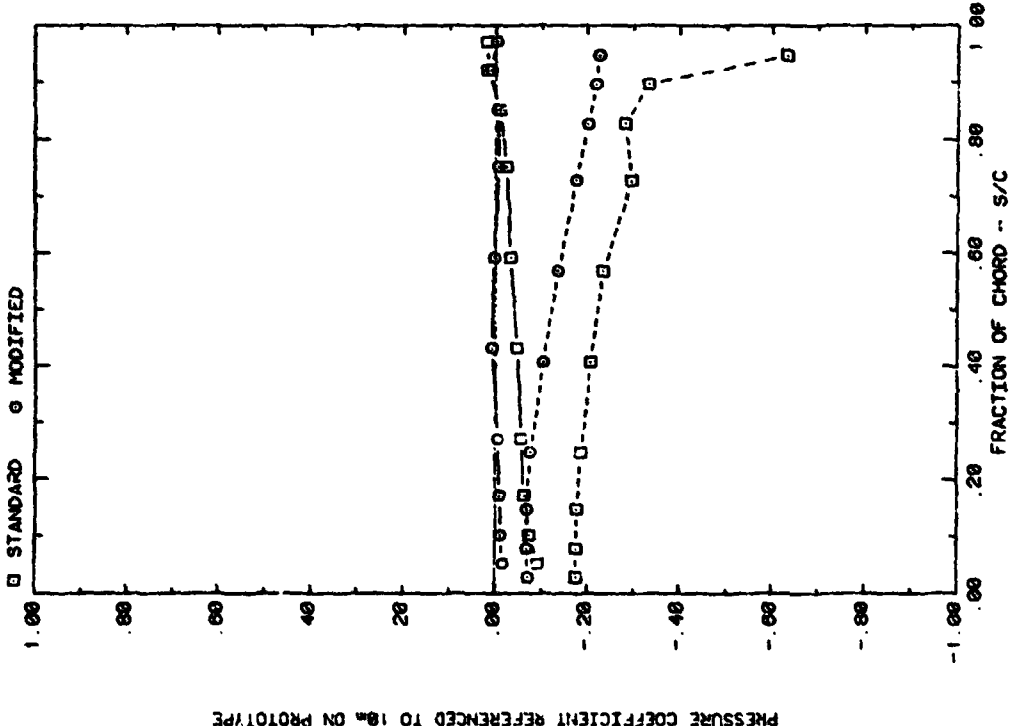
FRONT AND BACK PRESSURES ON ARRAY #2 WITH $\alpha=35^\circ$, AND WIND=45
EFFECT OF TAP LOCATION; ALPHA=35, H=3, D=10, FC-3, AND P=30X

Plot 5-2-2. (Continued)

ORIGINAL PAGE IS
OF POOR QUALITY

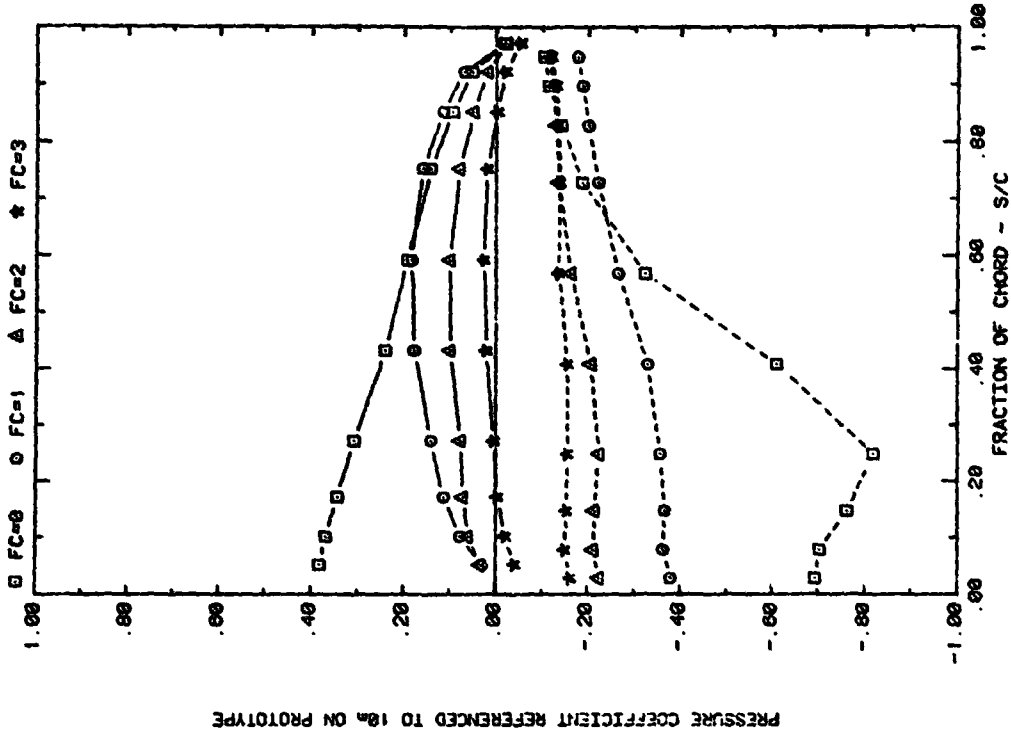


FRONT AND BACK PRESSURES ON ARRAY #3 WITH X=2C, AND WIND=45
EFFECT OF TAP LOCATION, ALPHA=145, H=3, D=10, FC=3, AND P=30X

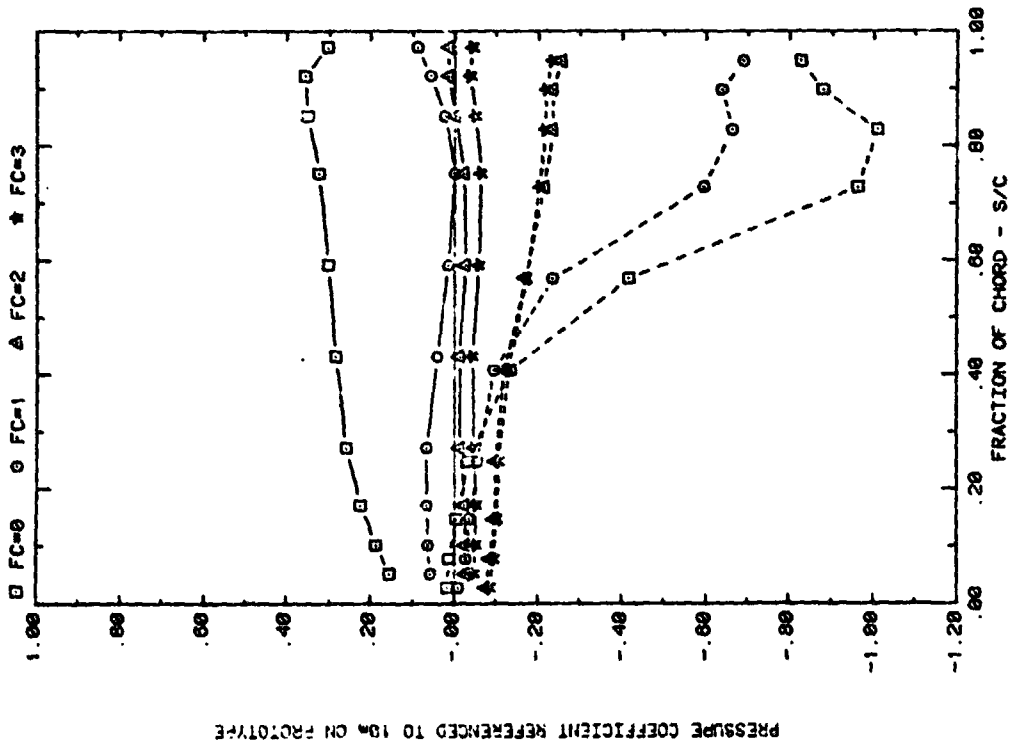


FRONT AND BACK PRESSURES ON ARRAY #3 WITH X=2C, AND WIND=45
EFFECT OF TAP LOCATION, ALPHA=35, H=3, D=10, FC=3, AND P=30X

Plot 5-2-2. (Concluded)



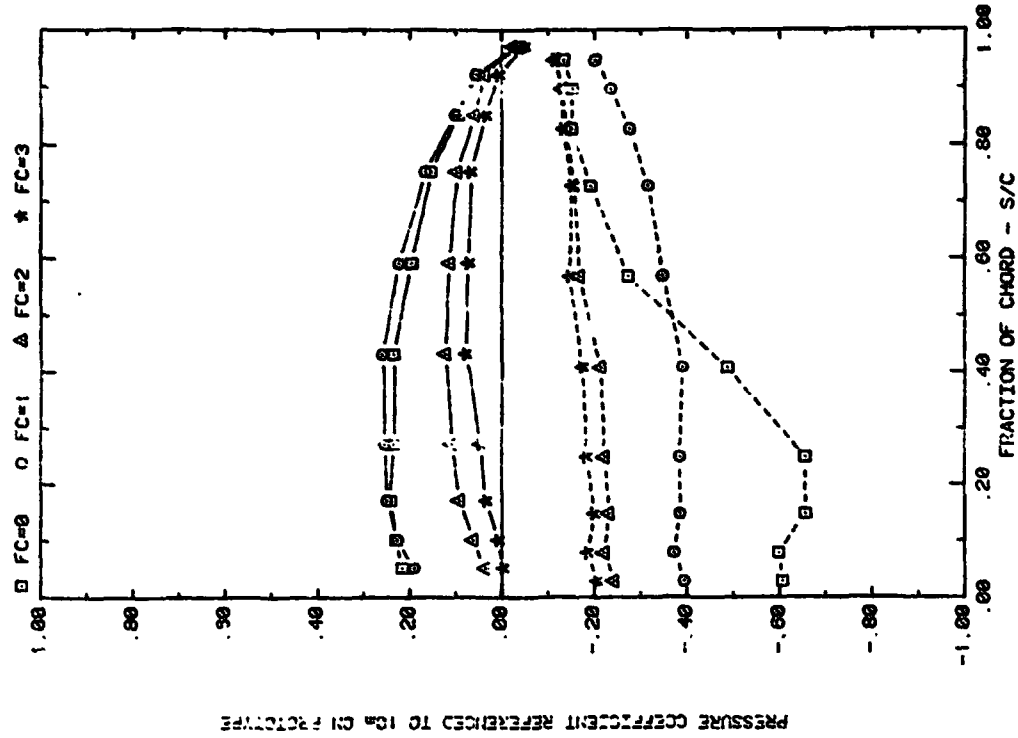
FRONT AND BACK PRESSURES 3.6° IN FROM EDGE OF ARRAY#1; WIND=45
EFFECT OF FC WITH ALPHA=145, H=3', D=18', P=30%, AND X=2C



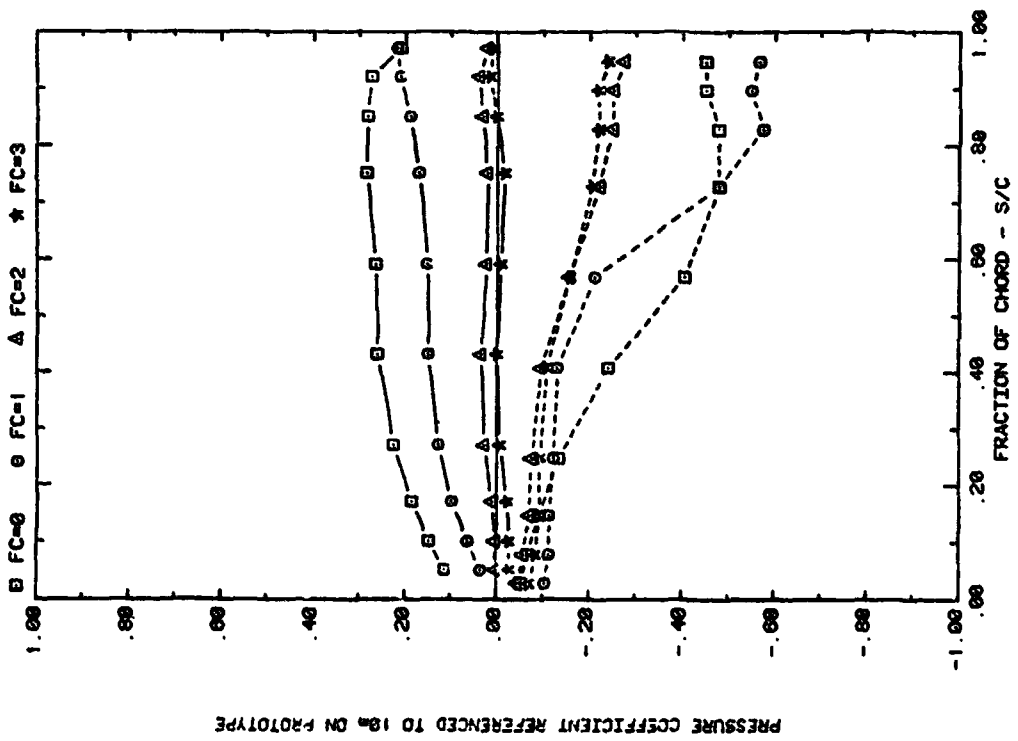
FRONT AND BACK PRESSURES 3.6° IN FROM EDGE OF ARRAY#1; WIND=45
EFFECT OF FC WITH ALPHA=35, H=3', D=18', P=30%, AND X=2C
Plot 5-2-3. Corner Study, WD = 45°, Modified Model with Solid Extension
Effect of Fence Configuration

PRESSURE COEFFICIENT REFERENCED TO 10a ON PROTOTYPE

PRESSURE COEFFICIENT REFERENCED TO 10a ON PROTOTYPE

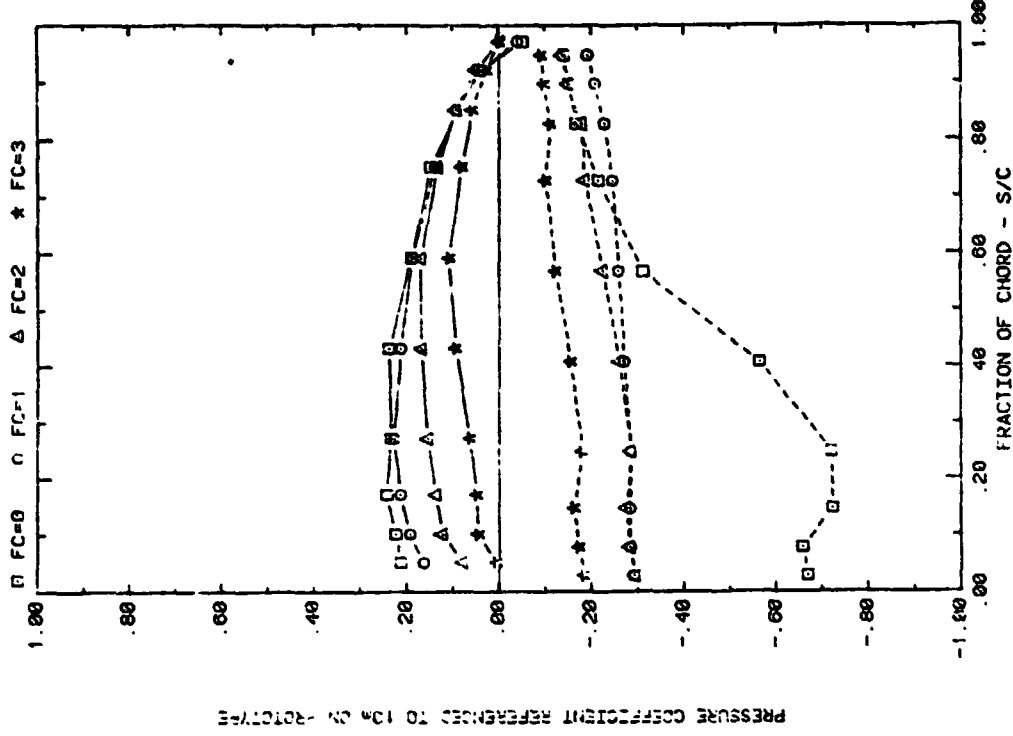


FRONT AND BACK PRESSURES 3.6" IN FROM EDGE OF ARRAY#2, WIND=45
EFFECT OF FC WITH ALPHA=145, H=3°, D=10°, P=30%, AND X=2C

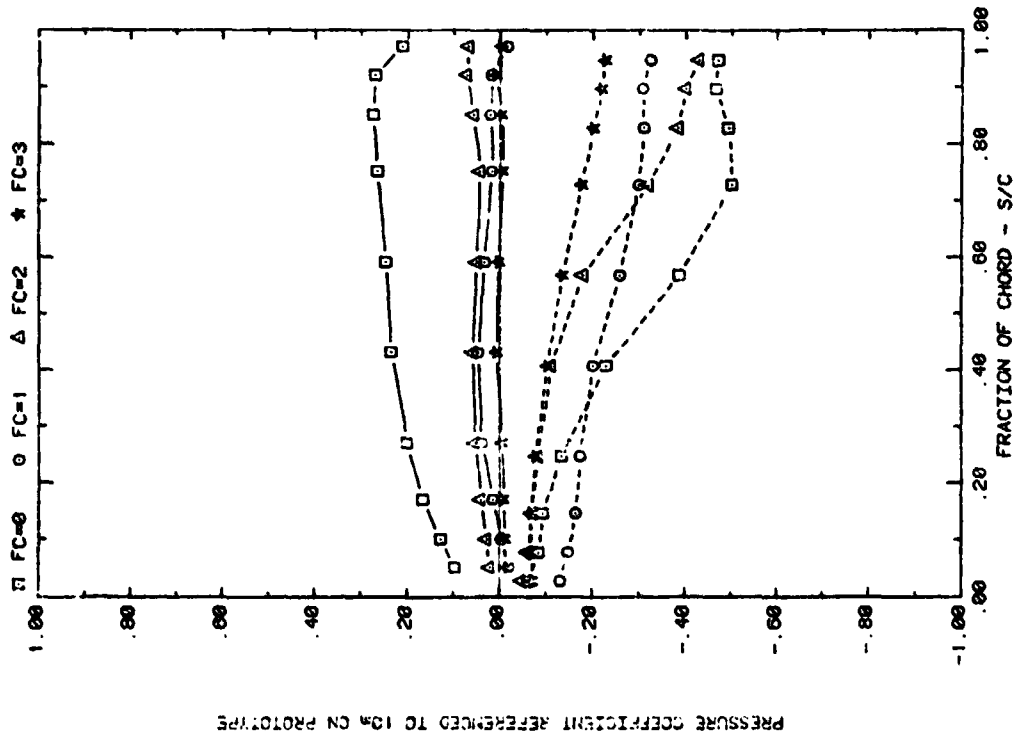


FRONT AND BACK PRESSURES 3.6" IN FROM EDGE OF ARRAY#2, WIND=45
EFFECT OF FC WITH ALPHA=35, H=3°, D=10°, P=30%, AND X=2C

Plot 5-2-3. (Continued)

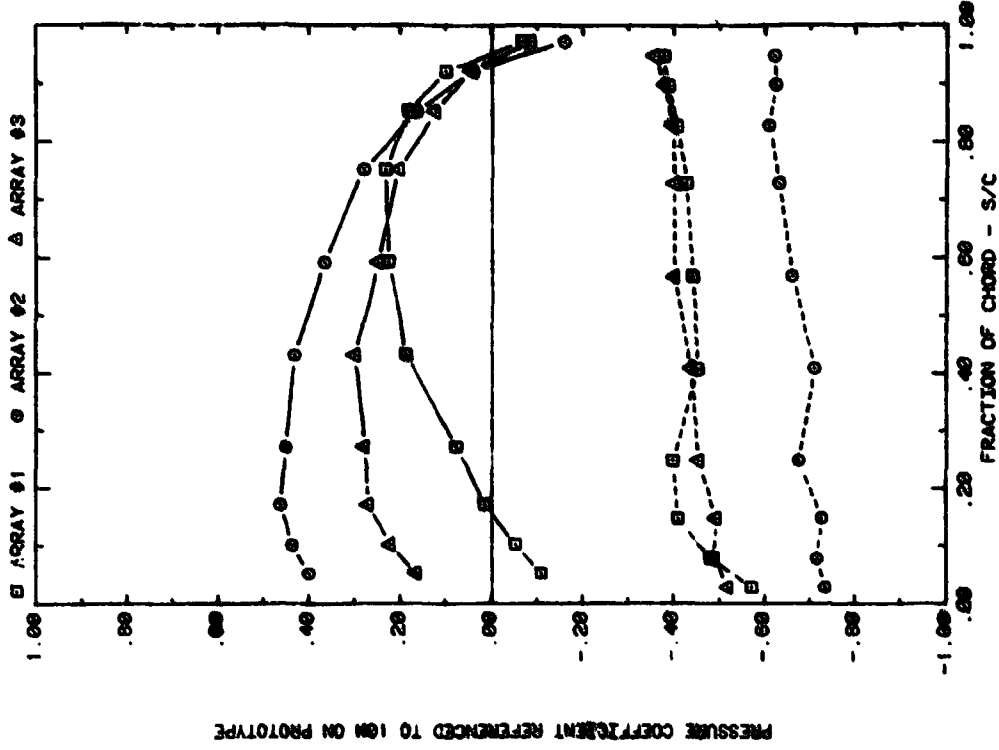


FRONT AND BACK PRESSURES 3.6° IN FROM EDGE OF ARRAY#3, WIND=45
EFFECT OF FC WITH ALPHA=145, H=3°, D=10°, P=30%, AND X=2C

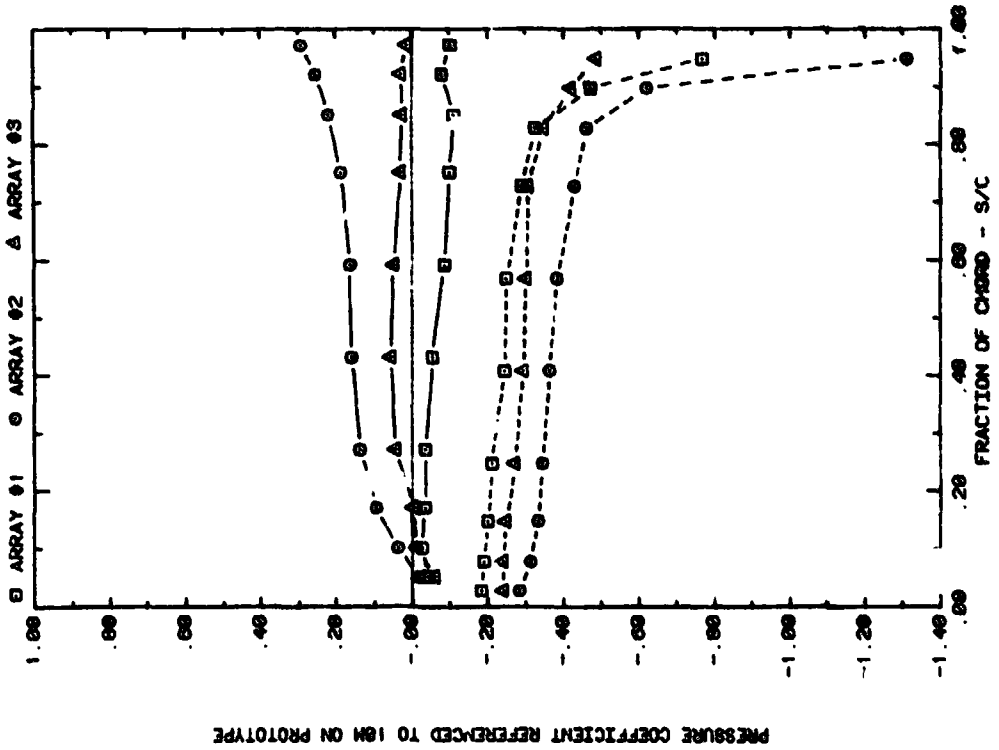


FRONT AND BACK PRESSURES 3.6° IN FROM EDGE OF ARRAY#3, WIND=45
EFFECT OF FC WITH ALPHA=35, H=3°, D=10°, P=30%, AND X=2C

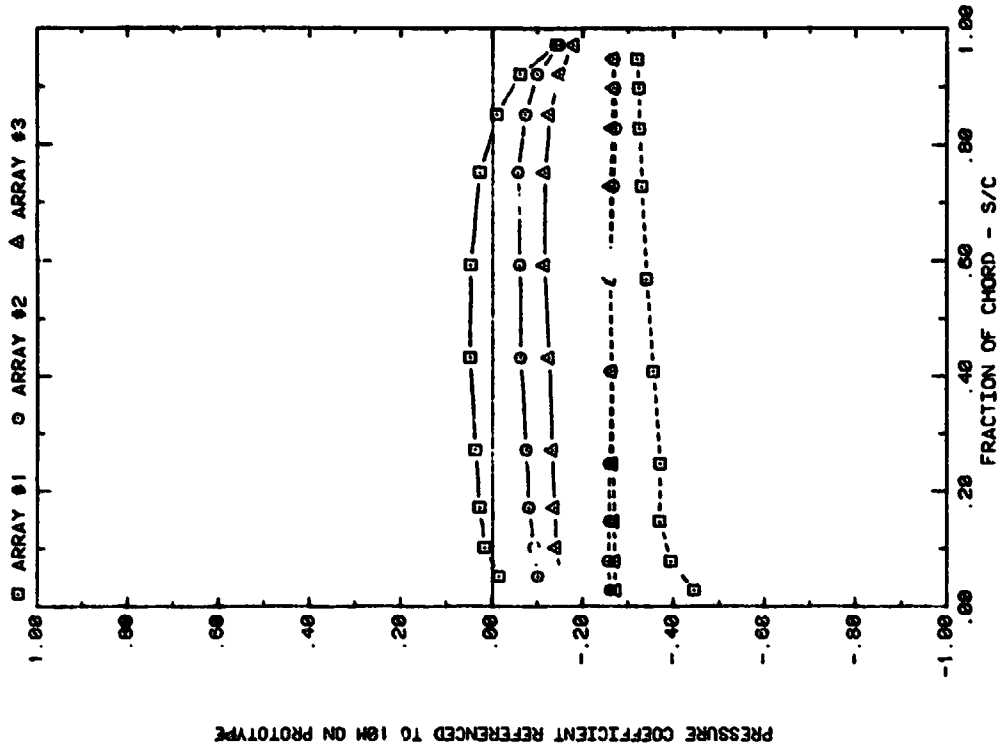
Plot 5-2-3. (Concluded)



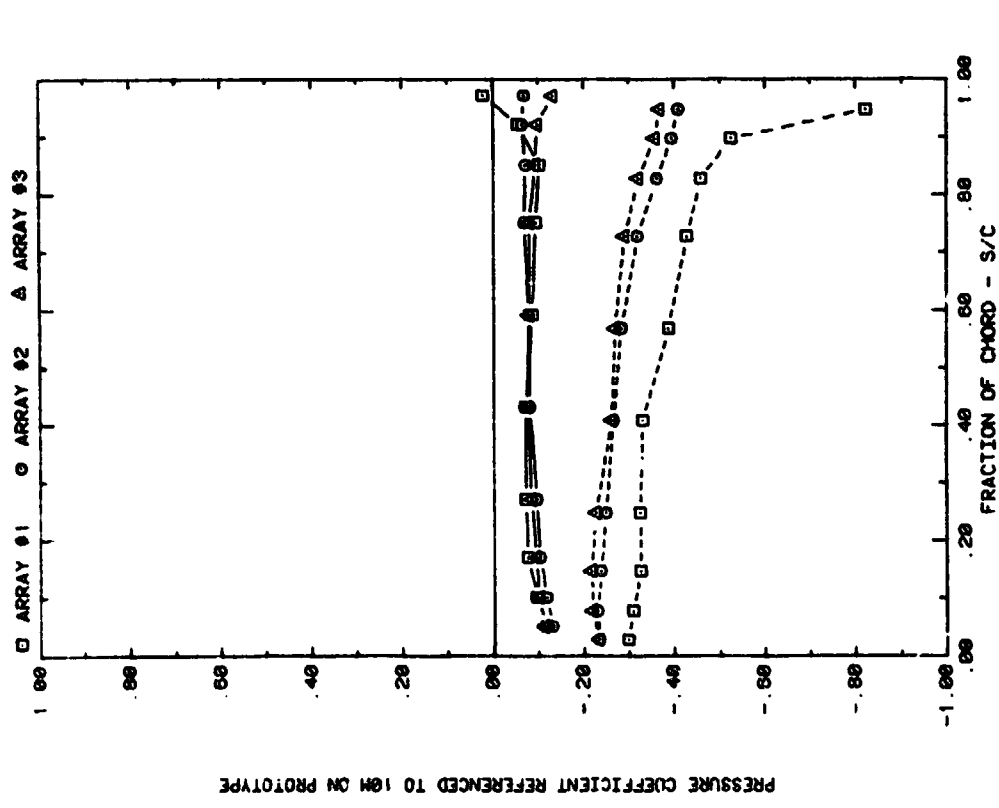
FRONT AND BACK PRESSURES ON ARRAYS #1, 2 & 3 FOR POROSITY EXTENSION EFFECT OF ARRAY WITH ALPHA = 45, WIND = 46, X = 2C, FC = 1



FRONT AND BACK PRESSURES ON ARRAYS #1, 2 & 3 FOR POROSITY EXTENSION EFFECT OF ARRAY WITH ALPHA = 45, WIND = 46, X = 2C, FC = 1
 Plot 5-3-1. Corner Study, $\alpha = 45^\circ$, Modified Model with Various Extension Effect of Array Position

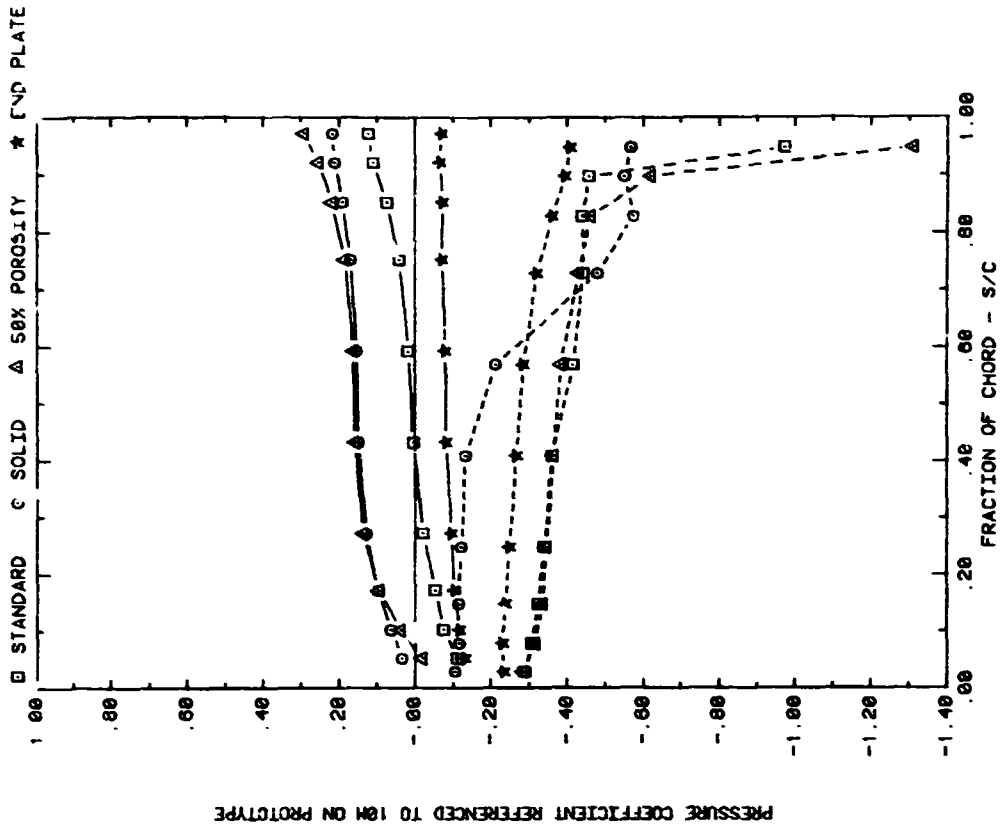


FRONT AND BACK PRESSURES ON ARRAYS #1, 2 & 3 END PLATE
EFFECT OF ARRAY WITH ALPHA = 45, X = 2C, FC = 1

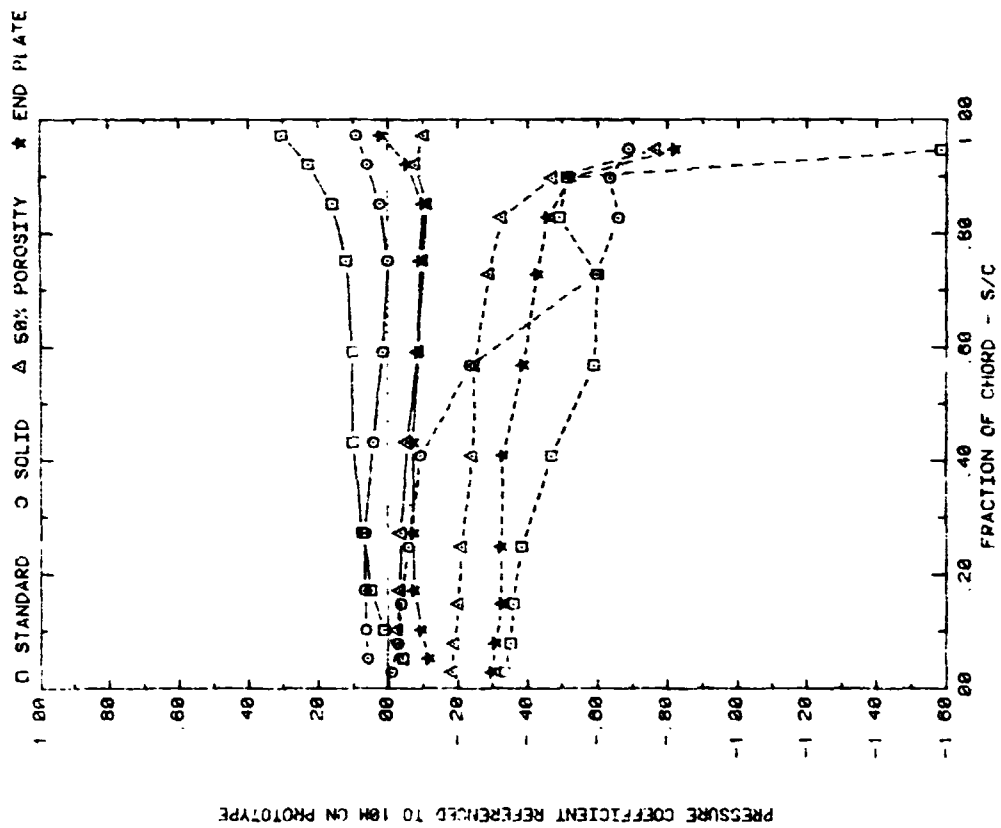


FRONT AND BACK PRESSURES ON ARRAYS #1, 2 & 3 END PLATE
EFFECT OF ARRAY WITH ALPHA = 45, X = 5, FC = 1

Plot 5-3-1. (Continued)

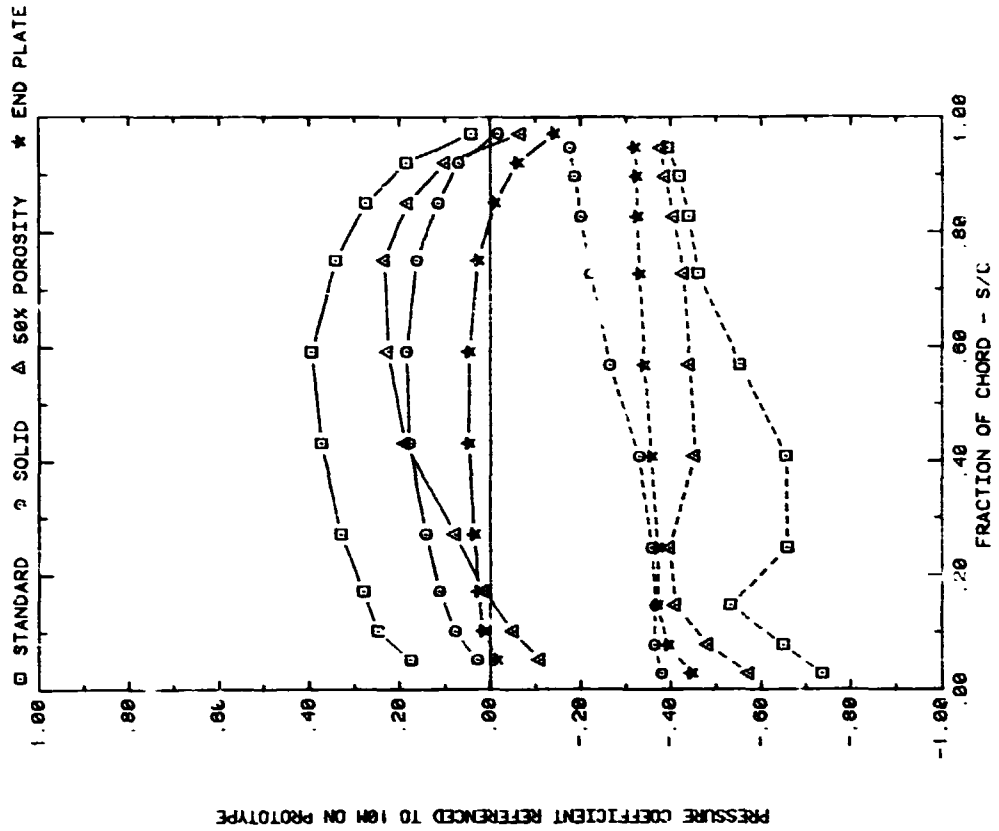


FRONT AND BACK PRESSURES ON ARRAYS; X = 2C, WIND = 45
EFFECT OF EXTENSIONS; ARRAY = 2 ALPHA = 35, FC = 1

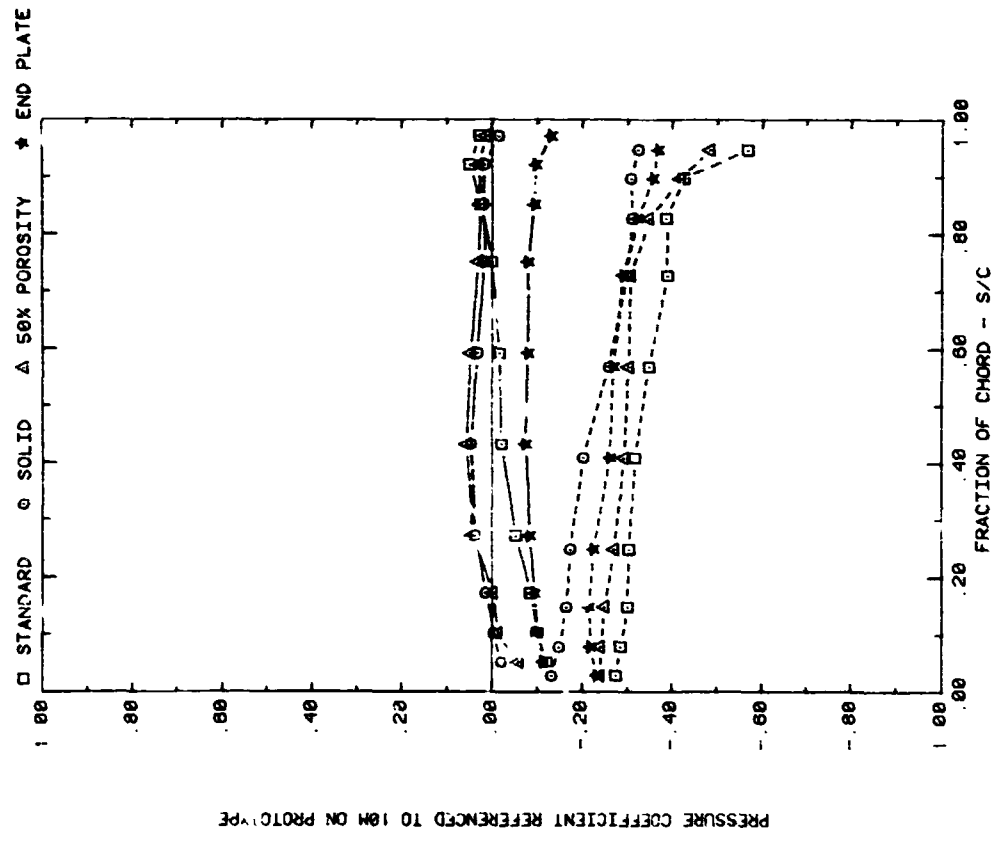


FRONT AND BACK PRESSURES ON ARRAYS; X = 2C, WIND = 45
EFFECT OF EXTENSIONS; ARRAY = 1, ALPHA = 35, FC = 1
Plot 5-3-2. Corner Study, WD = 45°, Modified Model with Various Extension
Effect of Model Configuration

C 5

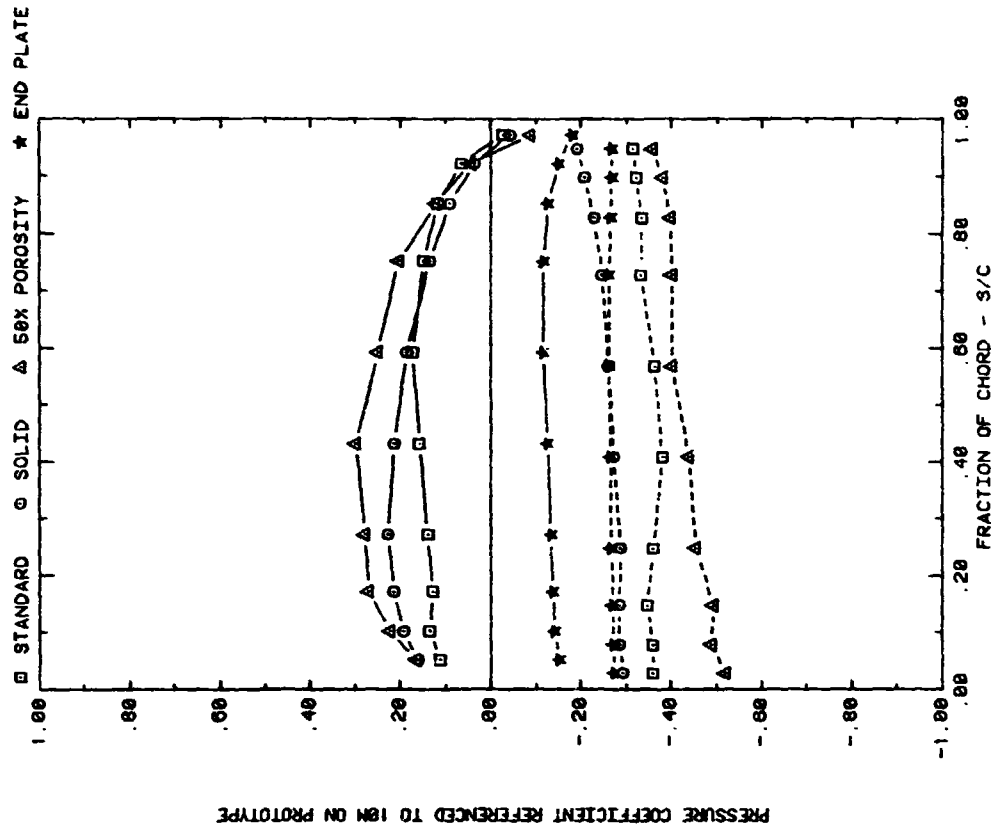


FRONT AND BACK PRESSURES ON ARRAYS; X = 2C, WIND = 45
EFFECT OF EXTENSIONS, ARRAY = 1, ALPHA = 145, FC = 1

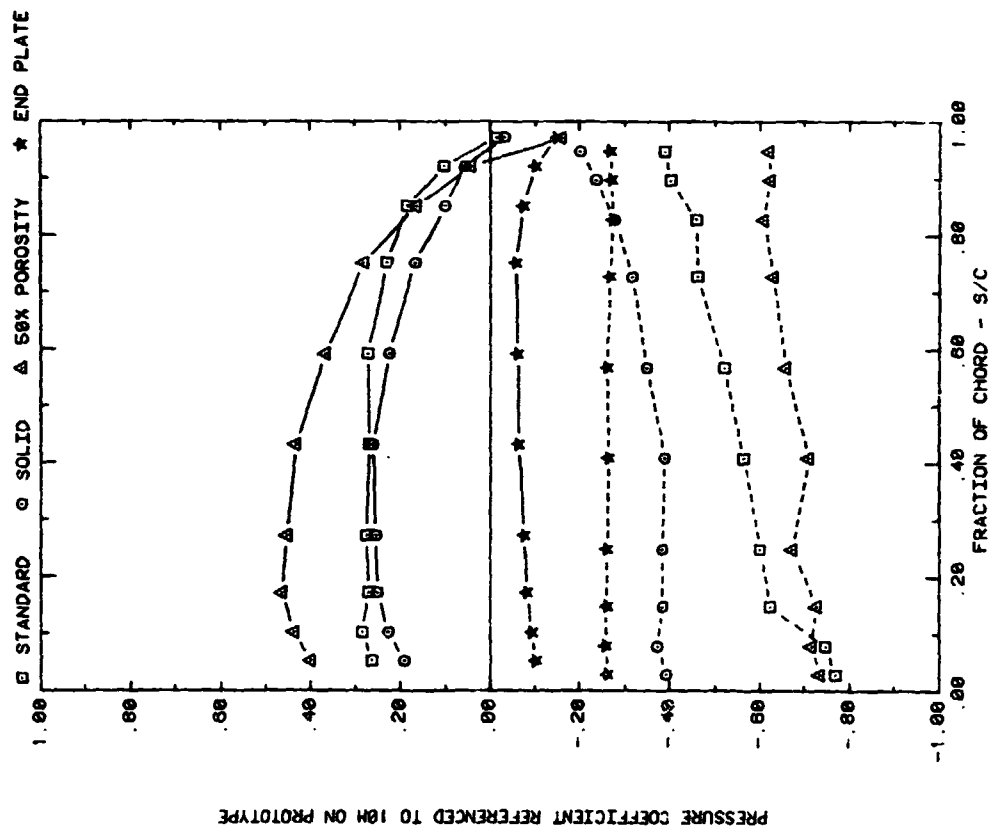


FRONT AND BACK PRESSURES ON ARRAYS; X = 2C, WIND = 45
EFFECT OF EXTENSIONS, ARRAY = 3, ALPHA = 35, FC = 1

Plot 3-3-2. (Continued)



FRONT AND BACK PRESSURES ON ARRAYS, X = 2C, WIND = 45
EFFECT OF EXTENSIONS, ARRAY = 3, ALPHA = 145, FC = 1



FRONT AND BACK PRESSURES ON ARRAYS, X = 2C, WIND = 45
EFFECT OF EXTENSIONS, ARRAY = 2, ALPHA = 145, FC = 1

Plot 5-3-2. (Concluded)